UNIVERSITÉ DE GENÈVE

Archive ouverte UNIGE
https://archive-ouverte.unige.ch

Thèse 2020

Open Access

This version of the publication is provided by the author(s) and made available in accordance with the copyright holder(s).

Epidemiological insights, cultivar resistance and natural products to control black dot (Colletotrichum coccodes) and silver scurf (Helminthosporium solani) on potato (Solanum tuberosum) tubers

Massana Codina, Josep

How to cite

MASSANA CODINA, Josep. Epidemiological insights, cultivar resistance and natural products to control black dot (Colletotrichum coccodes) and silver scurf (Helminthosporium solani) on potato (Solanum tuberosum) tubers. Doctoral Thesis, 2020. doi: 10.13097/archive-ouverte/unige:146843

This publication URL: https://archive-ouverte.unige.ch/unige:146843
Publication DOI: 10.13097/archive-ouverte/unige:146843

© This document is protected by copyright. Please refer to copyright holder(s) for terms of use.

UNIVERSITÉ DE GENÈVE
Section des Sciences Pharmaceutiques
Phytochimie et Produits Naturels Bioactifs

FACULTÉ DES SCIENCES
Professeur Jean-Luc Wolfender

AGROSCOPE
Groupe de Mycologie

PROTECTION DES VÉGÉTAUX
Dr. Katia Gindro

Epidemiological insights, cultivar resistance and natural products to control black dot (*Colletotrichum coccodes*) and silver scurf (*Helminthosporium solani*) on potato (*Solanum tuberosum*) tubers

THÈSE

présentée aux Facultés de médecine et des sciences de l'Université de Genève

pour obtenir le grade de Docteur ès sciences en sciences de la vie,

mention Sciences pharmaceutiques

par

Josep MASSANA CODINA

de Vilada (Espagne)

Thèse N° 76

GENÈVE

Centre d'Impression de l'Université de Genève

2020

LIFE SCIENCES PhD SCHOOL GENEVA

DOCTORAT ÈS SCIENCES EN SCIENCES DE LA VIE DES FACULTÉS DE MÉDECINE ET DES SCIENCES

MENTION SCIENCES PHARMACEUTIQUES

Thèse de Monsieur Josep MASSANA CODINA

intitulée :

«Epidemiological Insights, Cultivar Resistance and Natural Products to Control Black Dot (*Colletotrichum coccodes*) and Silver Scurf (*Helminthosporium solani*) On Potato (*Solanum tuberosum*) Tubers»

Les Facultés de médecine et des sciences, sur le préavis de Monsieur J.-L. WOLFENDER, professeur ordinaire et directeur de thèse (Section des sciences pharmaceutiques), Monsieur Y. KALIA, professeur associé (Section des sciences pharmaceutiques), Madame K. GINDRO, docteure (Plan Protection Division, Agroscope, Switzerland), Monsieur D. ANDRIVON, docteur (Institut de Génétique, Environnement et Protection des Plantes, Institut national de recherche pour l'agriculture, l'alimentation et l'environnement (INRAE), Bretagne, France), Monsieur Y. H. CHOI, professeur (Natural Products Laboratory, Insitute of Biology, Leiden University, Leiden, The Netherlands), autorisent l'impression de la présente thèse, sans exprimer d'opinion sur les propositions qui y sont énoncées.

Genève, le 15 octobre 2020

Thèse - 76 -

Le Doyen
Faculté de médecine

Le Doyen
Faculté des sciences

N.B. - La thèse doit porter la déclaration précédente et remplir les conditions énumérées dans les "Informations relatives aux thèses de doctorat à l'Université de Genève".

Contents

Foreword

Plant diseases caused by fungi and oomycetes are one of the main causes of food losses in the world. If these losses were mitigated in the most cultivated crops worldwide (rice, wheat, maize, potatoes and soybean), the additional food production would allow feeding approximately 8.5% of the world's population (Fisher et al., 2012). In this thesis, two fungal diseases of potatoes were studied in depth and strategies to mitigate their impact were suggested. To that end, complementary approaches combining different methodologies from the laboratory to the field were used, and involved several partners and collaborations. The main objectives of the thesis were to i) understand the factors that influence the development of both fungal diseases, ii) to characterize the biochemical, utrastructural and metabolic changes upon fungal inoculation in different potato cultivars and iii) to evaluate the efficacy of *biofungicides* as post-harvest treatments against both fungal pathogens. On one hand, the biochemical characterization of the interaction between potatoes and the fungal pathogens, as well as the isolation and structural elucidation of antifungal compounds, was carried out in the laboratory of Phytochemistry and Bioactive Natural Products of the University of Geneva under the supervision of Professor Jean-Luc Wolfender. On the other hand, field trials, greenhouse experiments, microscopical insights and antifungal assays were carried out in the Mycology group of the Plant Protection Division at Agroscope (Swiss centre of excellence for agricultural research), under the co-supervision of Dr. Katia Gindro. In addition, a collaboration with Dr. Andreas Keiser (Bern, Switzerland) was established for the quantification of fungal DNA in soil. This thesis work was part of a multidisciplinary project involving other Swiss research institutes (FiBL, HAFL) and was funded by the Swiss Commission of Technology and Innovation (CTI).

Abstract

Black dot and silver scurf are two potato blemish diseases caused by the phytopathogenic fungi *Colletotrichum coccodes* and *Helminthosporium solani*, respectively. *C. coccodes* can infect all underground parts of the plant, as well as stems and leaves, while silver scurf symptoms are only observed in tubers. In potato tubers, they both cause symptoms on the potato skin, reducing the quality of the tubers and increasing the permeability of the tuber skin, leading to water losses during storage. Furthermore, their symptoms in the potato skin are very similar, and microscopic observation of their fungal structures (microsclerotia of *C. coccodes* or conidiophores of *H. solani*) is required to confirm identification of the pathogen. Although blemish diseases had been considered of minor importance in the past, the commercialization of washed pre-packed potato tubers has led to an increase awareness of blemish diseases from consumers and they have gained attention in the past 20 years. Several partially effective control measures are available to date, but these diseases are still prevalent in commercialized potatoes, and the economic impact of black dot and silver scurf has been estimated at 5£ million losses in the UK. Since both diseases often appear in the same tuber and their symptomatology is very similar, the control strategy should take into consideration both diseases. In this thesis, black dot and silver scurf are studied at the agronomic, cytologic and metabolomic levels.

The epidemiology of black dot and silver scurf in the field and the factors that influence their development have been studied to some extent, but a comparison of the factors that impact both diseases under the same conditions had not been carried out. In this thesis, field trials and greenhouse experiments in a three-year period (2016-2018) were used to give new insights on the biotic and abiotic factors that affect the development of both diseases. The use of disease-free seed tubers was found not to be effective in the control of either disease in the field. Furthermore, humid seasons were associated with black dot disease and dry and warm seasons with silver scurf. Interestingly, *H. solani* infections appeared later in the season, and were found in tubers and, for the first time, in stolons. Finally, a severity assessment on tubers displayed differences in the susceptibility to both diseases of the potato cultivars used in Switzerland. The results obtained in these trials can contribute to elaborate a sustainable integrated pest management.

Field trials demonstrated that susceptibility to both diseases differs among potato cultivars. Five of these potato cultivars were selected for a greenhouse experiment under controlled conditions to study the structural and biochemical basis of the resistance of potato cultivars to both diseases using cytologic and metabolomics approaches. Microscopy analysis revealed that the thinnest-skin cultivar was more susceptible to both diseases. However, susceptibility to black dot or silver scurf did not correlate with skin thickness. Furthermore, suberin levels did not correlate with disease resistance. On the other hand, the metabolomics approach highlighted several resistance-related metabolites against each disease. Furthermore, some of these were highlighted in both plant-pathogen interactions, including hydroxycinnamic acid amides (HCAAs) and hydroxycoumarins, among others. Notably, some of the highlighted biomarkers of resistance showed antifungal activity *in vitro* against *C. coccodes*. These results can help understand the potato-fungal interaction and evidence biomarkers of resistance against blemish diseases in potato cultivars.

Black dot and silver scurf may be present at harvest, and both diseases develop during storage. Thus, post-harvest treatment of potato tubers may be an approach to be implemented in the integrated management strategy. An *in vitro* screening of plant extracts with antifungal activities against *C. coccodes* and *H. solani* was carried out to select crude extracts with potential antifungal properties. This *in vitro* screening led to the selection of the plant extracts of *Rheum palmatum*, *Frangula alnus* and *Curcuma longa*, which showed antifungal activity against both diseases. A chemical characterization and bio-guided isolation of the antifungal compounds of these plant extracts reveled

that anthraquinones and curcuminoids were the main antifungal compounds of these extracts. Furthermore, a new anthraquinone and two new dianthrone glycosides were isolated from *F. alnus*. The post-harvest application of the *C. longa* and the *F. alnus* plant extracts on naturally infected potato tubers resulted in the control of black dot and silver scurf under high-disease pressure conditions. Thus, the use of these plant extracts on the post-harvest control of potato blemish diseases shows potential.

Overall, this thesis gives new insights in the epidemiology, host resistance and post-harvest control of black dot and silver scurf in potatoes, and control measures against both diseases are suggested to elaborate an integrated pest management.

Résumé

La dartrose et la gale argentée sont deux maladies de flétrissement de la pomme de terre, causées respectivement par les agents pathogènes *Colletotrichum coccodes* and *Helminthosporium solani*. *C. coccodes* infecte les organes souterrains de la plante mais également les parties aériennes, tandis que les symptômes de gale argentée n'apparaissent que sur les tubercules. Ces deux maladies contaminent individuellement ou conjointement la peau des tubercules et augmentent la perméabilité de l'épiderme du tubercule, réduisant ainsi la qualité des tubercules et générant un désèchement lors du stockage des pommes de terre. Les symptômes des deux maladies étant visuellement similaires, une observation microscopique des structures fongiques (microsclérotes de *C. coccodes* et conidiophores de *H. solani*) reste nécessaire pour confirmer l'identification des pathogènes. Si ces maladies de flétrissement ont longtemps été considérées comme d'importance mineure, la commercialisation récente de pommes de terre lavées et pré-empactées a conduit depuis 20 ans à une prise de conscience grandissante des consommateurs pour cette problématique. Actuellement, plusieurs mesures de contrôle existent mais leurs efficacités restent partielles, l'impact économique de ces maladies atteignant 5 millions de £ au Royaume-Uni. Du fait de leur apparition concomittante sur un même tubercule et de la similarité de leur symptômatologie, la stratégie de recherche adoptée dans cette thèse a reposé sur la prise en compte conointe des deux maladies. Les facteurs épidémiologiques induisant la dartrose et la gale argentée de la pomme de terre ont été approchés au niveau agronomique, cytologique et métabolomique.

Des essais au champ sur une période de 3 ans (2016-2018) suppléés par des expérimentations en serre ont été mis en place pour mettre en évidence la contribution de facteurs épidémiologiques (état sanitaire du tubercule à la plantation, inoculum du sol, conditions environnementales) pilotant les deux maladies. L'utilisation de tubercules sains à la plantation ne s'est pas montrée efficace pour réduire l'incidence des maladies au champ. Globalement, les saisons végétatives humides sont associées au développement de la dartrose tandis que l'incidence de la gale argentée est associée aux périodes plus chaudes. Les infections de *H. solani* apparaissent plus tard dans la saison, et ont été observées pour la première fois sur les stolons. Parallèlement, un phénotypage des cultivars de pommes de terre exploités en Suisse a permis de mettre en évidence une large variation de sensibilité aux deux maladies. L'intégration de ces résultats dans l'élaboration d'un modèle de gestion raisonnée de ces maladies fongiques est discutée.

Sur la base des essais réalisés au champ démontrant une variation de sensibilité des cultivars étudiés, cinq d'entre eux ont été sélectionnés pour une étude structurale et biochimique du caractère de résistance aux deux maladies en environnement controlé, utilisant une approche cytologique et métabolomique. Les analyses microscopiques révèlent que les cultivars présentant une épaisseur fine de la peau sont associés à une sensibilité plus accrue. Toutefois, aucune corrélation significative a pu être mise en évidence entre l'épaisseur de l'épiderme et la sévérité des maladies fongiques. De façon similaire, l'étude qualitative et quantitative du polymère de subérine contenue dans l'épiderme ne corrèle pas avec le caractère de résistance. Parallèlement, l'approche métabolomique révèle plusieurs métabolites associés à la résistance contre chacune des maladies. Certains de ces métabolites appartenant à la famille des acides-amides hydroxycinnamiques et des hydroxycoumarines ont été mis en évidence dans les deux interactions hôte-pathogène. En outre, certains de ces biomarqueurs liés à la résistance présentent une activité antifongique *in vitro* contre *C. coccodes*. Ces résultats doivent permettrent de mieux comprendre l'interaction hôte-pathogène entre cultivar sensible et résistant aux maladies de flétrissement de la pomme de terre, notamment par le suivi des biomarqueurs liée au caractère de résistance.

La dartrose et la gale argentée peuvent être présentes discrètement à la récolte et l'incidence des maladies progressent durant le stockage. Le traitement post-récolte peut constituer une approche complémentaire à une gestion raisonnée des maladies. Un screening d'extraits de plantes, basé sur un test *in vitro* d'évaluation d'activité antifongique contre *C. coccodes* et *H. solani* a été réalisé afin de sélectionner des extraits bruts présentant un potentiel de phytoprotection. Trois extraits ont présenté des propriétés fongicides contre les deux maladies : *Rheum palmatum*, *Frangula alnus* and *Curcuma longa*. Un isolement bio-guidé et une caractérisation chimique de composés antifongiques constituant ces extraits ont révélé que des composés appartenant aux familles des anthraquinones et des curcuminoïdes étaient les principaux métabolites responsables de cette activité. De cette étude, un nouveau composé anthraquinonique et deux nouveaux glycosides dianthrone ont pu être isolés de *F. alnus*. Dans un essai miniaturisé de stockage de tubercules après un traitement post-récolte, le contrôle des deux maladies après application des extraits de plantes sur des tubercules naturellement infectés a été évalué. L'emploi de tels extraits de plantes présentant une efficacité prometeuse dans le contrôle des maladies durant le stockage constitue une piste supplémentaire de recherche.

Ce travail de doctorat a permis d'acquérir de nouvelles connaissances en matière i) d'épidémiologie, ii) d'évaluation de sensibilité variétale et iii) de traitement post-récolte à base de produits alternatifs naturels, intègrant une approche systématique de gestion raisonnée de ces maladies fongiques de flétrissement de la pomme de terre.

Abbreviations

2D	Two-dimensional
AMOPLS	Anova multiblock OPLS
ANOVA	Analysis of variance
CAD	Charged aerosol detector
COSY	Correlation Spectroscopy
CV	Coefficient of variation
DA	Discriminant Analysis
DMSO	Dimethylsulfoxide
DNP	Dictionary of Natural Products
ECD	Electronic circular dichroism
EI-MS	Electron ionization-MS
ELSD	Evaporative light scattering detector
ESI	Electrospray ionization
FA	Formic acid
FAO	Food and Agriculture Organization of the United Nations
FID	Flame ionization detector
GC	Gas chromatography
HMBC	Heteronuclear multiple-bond correlation spectroscopy
^{1}H NMR	Proton NMR
HMCQ	Heteronuclear multiple-quantum correlation spectroscopy
HPLC	High performance liquid chromatography
HRMS	High resolution mass spectrometry
HSQC	Heteronuclear single-quantum coherence spectroscopy
IS	Internal standard
ISDB	In silico database
LC	Liquid chromatography
LR	Low resolution
MN	Molecular networking
MS	Mass spectrometry
MS/MS	Tandem mass spectrometry

MS^n	Multistage mass spectrometry
m/z	mass-to-charge ratio
NI	negative ionization
NMR	Nuclear magnetic resonance
NOESY	Nuclear Overhauser enhancement spectroscopy
NPs	Natural Products
OPLS	Orthogonal projection to latent structure
PCA	Principal component analysis
PCR	Polymerase chain reaction
PDB	Potato dextrose broth
PDA	Potato dextrose agar (culture medium)
PDA	Photo diode array (detection)
PI	Positive ionization
PLS	Partial least-squares regression
QC	Quality control
qNMR	Quantitative NMR
qRT-PCR	Quantitative real-time polymerase chain reaction
QTOF MS	Quadropole time of flight MS
ROS	Reactive oxygen species
RP	Reversed phase
RT	Retention time
S/N	Signal to noise ratio
SPE	Solid phase extraction
UHPLC	Ultra high performance liquid chromnatography
UV	Ultraviolet (detection)

List of Tables

List of Figures

soil to avoid fungal infection. Half of the population is mock inoculated, while the other half is inoculated with C. coccodes. **(B)** Extraction and LC-HRMS/MS analysis. Methanolic extraction of specialized metabolites is followed by LC-HRMS/MS (data-dependent mode) analysis in both negative ionization (NI) and positive ionization (PI) modes. **(C)** Multivariate Data Analysis (AMOPLS). All features detected in full scan MS are analyzed using an AMOPLS model. ANOVA decomposition of the matrix in submatrices allows assessing the relative variability of each effect (i.e. cultivar, inoculation, interaction and residuals) by computing the sum of squares of the submatrices. This is followed by a multiblock OPLS model, the predictive components of which explain one of the effects (see Supplementary Table 2). AMOPLS separates the sources of variability related to the experimental factors with dedicated predictive score (tp) and loading values (pp) that are used for the model interpretation. Predictive scores (tp) highlight sample groupings (i.e. cultivar, see Figure 3.5)) or trends (i.e. upon inoculation, see Figure 8) and loadings (pp) highlight induced molecules with respect to the different experimental factors to evidence Resistance-Related metabolites. **(D)** Molecular Networking. Features possessing MS/MS spectra are used to build a Molecular Network (MN) based on spectral similarity. Features are then annotated by spectral comparison with experimental (GNPS) or in silico (ISDB-DNP) spectral databases. In silico annotations are re-ranked using taxonomic proximity information. Color of individual clusters of the MN are set according to the most abundant chemical class found in the cluster (consensus chemical class) or the relative intensity in resistant and susceptible cultivars (see Figure 6). **(E)** List of Resistance-Related compounds. A combination of the AMOPLS data analysis and the MN visualization is used to build a list of Resistance-Related metabolites, Constitutive (RRC) or Induced (RRI), with their annotations, and sorted according to their RRC or RRI scores (see Supplementary Table 3). **(F)** Mapping in biosynthetic pathways. A selection of Resistance-Related annotated metabolites previously reported in the Solanaceae family are placed in their biosynthetic pathways according to the Kyoto Encyclopedia of Genes and Genomes (KEGG) for *Solanum tuberosum* (or related plant species, if not available for S. tuberosum) to highlight putatively induced or repressed biochemical pathways (see Figure S7). **(G)** In vitro bioassay against *Colletotrichum coccodes*. A selection of highlighted Resistance-Related metabolites, commercially available pure compounds, are tested in an in vitro bioassay against *C. coccodes* using the food-poisoning method at decreasing concentrations from 1000 µM to 10 µM (see Figure 7 and Figure S6). 83

Figure 3.7 Global Molecular Networks (MNs) in negative ion mode of the five potato cultivars. In the global Molecular Network, color of the node is set according to the consensus chemical class across the cluster, node size is set according to the ratio of intensities between resistant and susceptible cultivars in control conditions (RRC). Molecular families of interest that include compounds confirmed by an analytical standard are highlighted in a cluster, with the structure of the standard displayed, size of the node set according to the average peak intensity (among all samples) and color of the node set as a pie-chart with the relative abundance of the metabolite in the resistant cultivars (yellow) and the susceptible cultivars (red) in control conditions. The average detected intensity (of all features in a cluster) in susceptible and resistant cultivars is shown as a histogram. The average cluster intensity

1. General introduction

This chapter introduces the main concepts of the Thesis. The plant host of this study, *Solanum tuberosum* L. is firstly introduced, followed by the two fungal pathogens that are the core subject of this work, *Colletotrichum coccodes* (Wallr.) S. Hughes (1958) and *Helminthsporium solani* Durieu & Mont. (1849), respectively the fungal agent of black dot and silver scurf, as well as a comparison of the control methods used against these two fungal diseases. In a second part of the introduction, plant-pathogen interactions and the different types of plant resistance to pathogens are reviewed, followed by a description of the different methods used to study the different aspects of fungal diseases in plants. Finally, the use of fungicides and *biofungicides*, including Natural Products (NPs), to control plant diseases is introduced, with an emphasis on post-harvest treatments of food products.

1.1. *Solanum tuberosum L.*

Potatoes are the fourth crop in the world in terms of crop production, the first non-cereal, and its worldwide cultivation makes it a pillar of nutrition around the world. Furthermore, it is usually traded locally, and unlike most cereals (which more than doubled its price in the 2000-2008 period) its price is usually determined by local production costs. In order to increase awareness of the importance of the potato crop, the Food and Agriculture Organization of the United Nations (FAO) declared 2008 the International Year of Potato (IYP). Potatoes are a global food product (produced worldwide), that can help reduce world hunger, and that are a good source of energy for human consumption (Food and Agriculture Organization of the United Nations, 2008).

1.1.1. History and genetic evolution

The origin of agriculture (cultivation of edible plants) dates from, at least, the 8th millennium BC. First domesticated plants include emmer wheat (*Triticum dicoccum*), einkorn wheat (*Triticum monoccocum*), barley (*Hordeum* vulgare) or peas (*Pisum sativum*), that were domesticated in South Asia in the 8.000-10.000 BC. Potato plants (*Solanum tuberosum*) were first domesticated in South America between 8.000 and 6.000 BC, notably in the areas of modern-day Peru (Spooner et al., 2005). They became an important food product for the establishment of ancient cultures in the highlands of Peru, Bolivia and Ecuador (Brush et al., 1981; Pearsall, 2008). They were later cultivated in other regions, such as in highland equatorial conditions and in southern latitudes, all across South America, from modern Colombia to Argentina and Chile (Hosaka, 2004; Raker and Spooner, 2002; Spooner et al., 2012). The ability of potatoes to adapt to different climatic and day length conditions allowed them to spread all over South America; these first cultivated Andean landraces were mostly tetraploids originated from autopolyploidization (Hardigan et al., 2017). The domestication of potatoes resulted in plants producing more tubers with higher nutritional value (notably, starch content) (Jansen et al., 2001; Bradshaw et al., 2006) and lower toxic glycoalkaloid content (Johns and Alonso, 1990; Friedman, 2006). This early adaptation of Andean landraces to produce eatable and nutritional tubers has followed throughout the years, also in modern bred potato cultivars. After the Spanish colonization of the Inca Empire (1532-1572), the colonizers introduced the potato crop into Europe during the second half of the 16th century, where it became a major staple crop during the 19th century. The low genetic diversity of potatoes introduced in Europe, combined with the introduction of a potato pathogen originated in Mexico (*Phytophthora infestans*), (Goss et al., 2014), led to the propagation of the late blight disease in the majority of European countries in the 1840s, resulting in the Great Irish Famine, with about a million deaths and two million emigrants in Ireland. Indeed, although there is a high genetic diversity in its original local areas, the potato varietal diversity around the world is much smaller: from the ca. 5000 potato varieties that exist worldwide, more than 3000 are found in the Andes (Hijmans and Spooner, 2001). Although late blight disease is still a major problem for potato crop production, potato production has increased during the 20th and 21st century, with over 385

million tons of potato tubers produced in 2014, being the fourth crop most cultivated worldwide (Liu et al., 2015). In 2017, more than 19 million ha of potato field area were harvested worldwide (16th crop worldwide), with a total of more than 388 million tons produced worldwide. The total area cultivated has only marginally increased in the last 30 years, but potato production has increased in 39% since 1987. Thus, this increase in total potato production is the result of an increase in yield (ca. 30% in the last 30 years), that reached more than 200 hg/ha in 2017, worldwide. The yield of potatoes differs among continents, with lowest yield in Africa (130 hg/ha) and highest in Oceania (410 hg/ha). In Europe, the yield of potatoes was, in 2017, of 227 hg/ha. Although this is not the highest yield worldwide, it is above the worldwide average yield. Factors affecting the yield include cultivar selection, abiotic stresses, and biotic stresses. Thus, a good management of the fertilization and disease control is essential for potato production. In Switzerland, the list of cultivars recommended for potato production includes 42 potato cultivars, 26 of which are for table potato production and 16 for industrial transformation (Figure 1.1).

Figure 1.1 Morphologic diversity of tubers from table potato cultivars commonly grown in Switzerland. Photos by Agroscope.

1.1.2. Plant physiology, life cycle and propagation

The potato plant is a perennial herb, but modern tetraploid (with four copies of each chromosome instead of two in traditional diploids) potato cultivars are used in agriculture as annual plants that are usually propagated by vegetative reproduction (cloning) (Struik, 2007). Potato tubers are planted as "seed-tubers" from which stems, also called sprouts, originate in order to give rise to the new plant. In some sub-tropical highlands, potatoes can be grown throughout the year, thanks to mild temperatures and high solar radiation, as well as specific cultivars (Bradshaw and Ramsay, 2009). However, in temperate zones such as in central Europe (including Switzerland), potato seed tubers are planted in early spring and grown during the warmest period of the year. Although several factors influence the morphology and physiology of the potato plant, a norm plant will be described hereafter (Struik, 2007). Seed tubers produce several shoots, since there are several eyes in each tuber seed (Figure 1.2).

Figure 1.2 Detailed picture of a germinating shoot on a potato tuber. Photo by C. Parodi, Agroscope.

Furthermore, each bud can give rise to several shoots, producing a cluster of stems per plant, often leading to short plants with many shoots (Struik, 2007). Emergence of the stems often occur 10-20 days after planting, and date of emergence is often used to compare physiologic ages of the plants. Leaves appear in every node of a shoot and will be the photosynthetically active organs of the plant, required for the general growth, but also for the tuber initiation and development. Thus, the specific leaf area will continuously increase until it reaches the maximum at about 100 days after emergence (Vos and Biemond, 1992). In addition to its vegetative reproduction, modern tetraploid cultivars can also undergo sexual reproduction. To this end, inflorescences are formed in the axil of the leaves, and a single flower has five petals and five sepals, the color and size of which depends on the cultivar (Struik, 2007). Pollinated flowers will develop berries, that can contain approximately 300 seeds per fruit (Fehr, 1987; Struik, 2007). However, the number of inflorescences and flowers depend on growing conditions, and flowering may not happen in some cultivars under specific conditions. Furthermore, sexual reproduction is not used by growers because of the genetic variability of the seeds and is only used in breeding programs. On the below-ground region, roots are essential in order to provide water and nutrients to the growing plant. The root system is developed very quickly, and sometimes roots are visible in sprouts on pre-sprouting seed tubers (Struik, 2007). However, roots are fibrous, often short, and root growth decreases upon tuber bulking (Steckel and Gray, 1979), making the root system rather weak (Struik, 2007). Thus, the efficiency of water and nutrient uptake in the potato crop is low, making it sensitive to drought and low nutrient stresses (Struik, 2007). In addition to roots, other structures found below-ground are the stolons. These are lateral shoots originating initially from the node closest to the seed tuber, at the basal nodes of the plant (Peterson et al., 1985; Struik, 2007). Stolons are stems with elongated internodes, scale leaves, and an apical recurved section also called “hook” (Peterson et al., 1985; Struik, 2007). Stolon growth is longitudinal and fast at the beginning, before shifting to radial growth during tuber initiation, a process also called tuberization (Peterson et al., 1985; Struik, 2007). Tuberization starts ca. 30-40 days after emergence, but it is regulated by several factors. Environmental conditions, such as temperature and length of the day, have been long been assumed to play a role in the induction of tuberization (Garner and Allard, 1920, 1923), since high temperatures and long days inhibit tuber formation. Interestingly, a grafting experiment using flowering tobacco shoots on potato plants grown in long day (LD) conditions (that inhibit tuberization) demonstrated that there is a graft-transmissible substance, produced in the shoot, that travels below-ground to induce tuberization (Chailakhyan et al., 1981). Similarly, both gibberellins and cytokinins have been shown to regulate stolon elongation and initiation of tuberization (Smith and Palmer, 1969, 1970; Xu et al., 1998a), which starts at the subapical region of the stolon (de Vries, 1878). Upon arrival of the signal to the elongating stolon, this will start radial expansion and thus, tuber formation (Hannapel, 2007). The stolon tip swells due to a change in the plane of cell division, inducing a radial

cell expansion of the youngest elongating internode (de Vries, 1878; Xu et al., 1998b; Vreugdenhil et al., 1999). After the initial radial expansion of this internode, other acropetally positioned internodes will follow the radial expansion. This initial step in tuberization involves both enlargement of pith cells and cell division of parenchyma cells (Peterson et al., 1985). Cell division will continue to occur in the perimedulary parenchyma and the inner cortical parenchyma during the early stages of tuber growth (Peterson et al., 1985). However, tuber size will be mainly achieved through a cell volume increase of the perimedullary parenchyma cells and the inner cortical parenchyma cells (Peterson et al., 1985). Ultimately, the stolon hook will straighten and leave the stolon apex at the rose end of the tuber (Peterson et al., 1985). After haulm destruction, potato tubers start a process called skin set that will provide resistance to mechanical and biotic damage, as well as desiccation.

1.1.3. Tuber morphology

Mature potato tubers are formed by different layers and cell types, presented in Figure 1.3. The outer layer, or periderm (2), a cortical zone that contains parenchymal tissue and the external phloem strands (3), the xylem ring (4), a perimedullary region that contains the inner phloem strands and perimedullary cells that contain starch (5), and the pith (6) (Reeve et al., 1969) (Figure 1.3). Furthermore, the periderm is formed by three layers: the phellem, the phellogen and the phelloderm (Reeve et al., 1969). The phellem is made by suberized cells that form what is often called tuber skin; the phelloderm is made by parenchyma-like cells; and the phellogen is a single-cell meristematic layer - that is also called cork cambium- between the phellem and the phelloderm (Vulavala et al., 2019). Indeed, the meristematic phellogen form the skin (phellem) by outward cell divisions and the phelloderm by inward cell divisions during tuber growth (Vulavala et al., 2017). At the end of the tuber growth period, the activity of the phellogen ceases, its cell walls become thicker, and the skin adhesion to the tuber flesh is stronger, in a process called skin-set (Vulavala et al., 2017). The phellem cells of the skin are the ones that protect the tuber to both biotic and abiotic stresses. The air contained in corky cells provide thermal insulation (Vulavala et al., 2017). The suberization of the cell walls protect the tuber against dessication, but also against microbial infection (Vaughn and Lulai, 1991). Notably, proteins involved in defense responses are abundant in skin cells, including enzymes involved in suberin polymerization (Barel and Ginzberg, 2008).

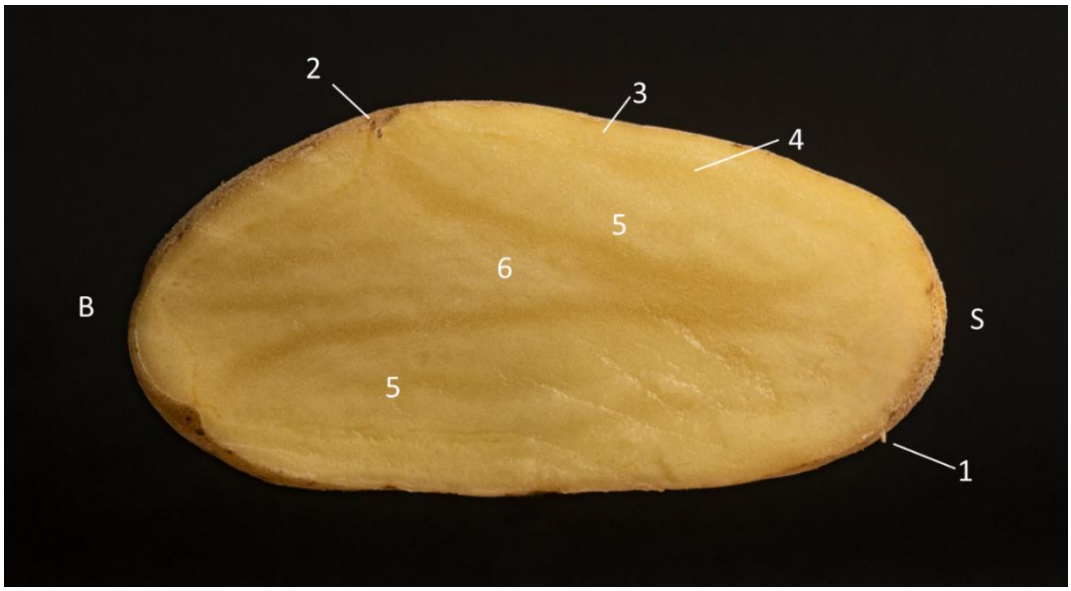

Figure 1.3 Longitudinal section of potato tuber. B. ~ bud end, S. = stem end, 1. "eyes" contaning buds in axils of scale leaves, 2. ~ periderm, 3. cortical zone containing cortical parenchyma and external phloem strands, 4. ~ xylem "ring", 5. perimedullary zone containing internal phloem and phloem parenchyma strands (darker) and perimedullary starch-storage parenchyma (lighter), 6. = pith. Adapted from *(Reeve et al., 1969)*. Photo by C. Parodi (Agroscope).

1.1.4. Main diseases of potato

Solanum tuberosum L. is susceptible to a number of pests, which can be caused by bacteria, viruses, insects or fungi.

1.1.4.1. Non-fungal diseases of potato

Several bacterial diseases cause important damages on the potato plant leading to tuber losses, the most important ones being black leg, soft rot and bacterial wilt (Charkowski et al., 2020). Black leg and soft rot are caused by the bacterial pathogens from the *Pectobacterium* and *Dickeya* genera, formerly classified as *Erwinia spp.* (Czajkowski et al., 2015). Symptoms of black leg are characterized by wilting and rotting of the stem from the mother tuber, and wilting of the leaves that may result in plant death (Czajkowski et al., 2011). In tubers, *Pectobacterium* and *Dickeya* species cause soft rot, characterized by rotting of the tuber in wet conditions which can be spread to other tubers in storage (Czajkowski et al., 2011). The most efficient control measure, in place in many countries, including Switzerland, relies on clean seed-tuber production and avoiding contamination from contaminated plants (Czajkowski et al., 2011). On the other hand, bacterial wilt is caused by *Ralstonia solanacearum*, which is also called brown rot of potato (Stead, 1999). It is an important plant disease in warm temperate and tropical climates, and has been found in some European countries, where a statutory control and eradication process is in place (Stead, 1999). Disease symptoms are characterized by a rapid wilting of the whole plant, and disease control measures focus in eradicating the pathogen from the soil and preventing further spread through surface water (Peeters et al., 2013). In Switzerland, *Ralstonia solanacearum* is a quarantine organism, and although it was first recorded in 2016, it was considered eradicated in 2018 (https://gd.eppo.int/taxon/RALSSO/distribution/CH). Other bacterial diseases of potato include the emerging zebra chip disease, caused by *Candidatus Liberibacter* spp., ring rot caused by *Clavibacter* spp. and common scab caused by *Streptomyces* spp (Charkowski et al., 2020).

Diseases caused by viruses in potato are widespread; indeed, a total of 40 viral and 2 viroid species have been shown to infect potatoes (Salazar, 1996). Among them, Potato Virus Y (PVY), Potato Virus X (PVX), Potato Leafroll Virus (PLRV) and Potato Virus S (PVS) are the most damaging, especially the former one. Yield losses due to PVY range from 10-80% (Whitworth et al., 2006), while the other viruses cause yield losses of 10-30% (Hameed et al., 2019). The symptoms of these diseases can differ from mild mosaic to chlorotic leaflets, necrotic rings in the tuber and severe necrosis in leaves and stems that can derive in plant death. Viruses such as PVY are transmitted from diseased plants to healthy plants through aphids in a non-persistent manner, so insecticide treatments are not effective in protecting plants against this spread (Torrance et al., 2020). In many regions, controlling PVY, as well as other viral diseases, is achieved by producing disease-free seed-tubers, since they are mainly seed-borne diseases. However, other strategies such as host resistance, are being used and studied (Torrance et al., 2020). Other than being transmitters of viruses, aphids and other insects can cause important diseases in potatoes through direct feeding. The most important insect pests can result in important yield losses and tuber quality reductions; this is the case of the Colorado Potato Beetle (CPB), some tuber moths or the potato leafhopper (Radcliffe and Lagnaoui, 2007). The CPB *Leptinotarsa decemlineata* can cause 30-50% of yield losses by feeding on potato leaves (Tai et al., 2014). Aphids may transmit viruses to healthy plants, but if present in great number, they can feed on the sap from the phloem. The potato leafhopper can also feed from the sap that he sucks from the leaf (Alyokhin et al., 2013). Below-ground wireworms are the main insect threat for potato production (Alyokhin et al., 2013). In general, control of insect pests if often achieved through Integrated Pest Management (IPM) strategies that help reduce the use of chemical pesticides. These strategies are varied, but usually include using resistant cultivars, cultural control measures, and the use of natural antagonists (Radcliffe and Lagnaoui, 2007).

Late blight (Phytophtora infestans)

Late blight, caused by the oomycete *Phytophthora infestans* (Mont.) de Bary (responsible of the Great Irish Famine), is the most important potato disease. It is responsible of destroying 15% of yield production worldwide, and it is specially devastating in developing countries, where the annual disease cost has been estimated at $ 3.25 billion (Arora and Khurana, 2004). Disease symptoms start as pale green lesions but quickly turn into brown and necrotic lesions. Furthermore, sporangia and spores of *P. infestans* are often observed, especially in the lower surface of infected leaves (white mildew) (Arora and Khurana, 2004). Control of late blight remains a challenge, but some control strategies are commonly used. Treatment of potatoes to avoid primary infections, as well as cultural methods that help reduce the inoculum in the field are efficient management strategies against late blight (Secor and Gudmestad, 1999; Forrer et al., 2000; Arora and Khurana, 2004). Resistant cultivars to late blight have been characterized and genetics and metabolomics studies have unraveled resistance genes and resistance-related metabolites (Ballvora et al., 2002; Kröner et al., 2011, 2012; Henriquez et al., 2012; Yogendra et al., 2015; Hamzehzarghani et al., 2016; Aguilera-Galvez et al., 2018). Finally, chemical control of late blight is a standard procedure in many countries. Furthermore, several forecast models have been developed, which help decide the best moment for a chemical treatment (Secor and Gudmestad, 1999; Arora and Khurana, 2004). The fungicide metalaxyl was shown to be very effective in controlling late blight, but resistant isolates to metalaxyl appeared soon after its introduction (Arora and Khurana, 2004). Since then, alternative control measures have been studied, including the use of antagonistic microorganisms (Eschen-Lippold et al., 2009; Guyer et al., 2015; De Vrieze et al., 2018, 2019).

1.1.4.2. Potato fungal diseases

Around 50 potato diseases are caused by phytopathogenic fungi, approximately a third of all potato diseases (Arora and Khurana, 2004). These diseases can affect the whole plant or only a specific organ, such in the case of tuber diseases (Figure 1.4).

Early blight (Alternaria sp.*)*

Early blight is caused by the fungal pathogen *Alternaria solani* (Ellis & G. Martin) L.R. Jones & Grout (Arora and Khurana, 2004). The symptoms of early blight are characterized by dark brown spots in infected leaves, and surrounding infected areas often become chlorotic (Arora and Khurana, 2004). It can also affect tubers, causing a rot characterized by a discoloration surrounding irregular lesions that can be 6 mm deep (Secor and Gudmestad, 1999). It is a major potato disease, causing 10-25% yield losses, which can be higher than losses due to late blight in some conditions (Arora and Khurana, 2004). Control of early blight is achieved by cultural methods, such as removal of diseased plants and haulms, rotation and fertilization, and chemical control measures applied depending on disease prediction systems (Secor and Gudmestad, 1999; Arora and Khurana, 2004). Furthermore, cultivar resistance can be used to help in the management of early blight (Secor and Gudmestad, 1999; Arora and Khurana, 2004).

Verticillium wilt (Verticillium sp.*)*

Verticillium wilt is caused by tow *Verticillium* species, namely *Verticillium dahliae* Kleb. and *Verticillium alboatrum* Reinke & Berthold (Secor and Gudmestad, 1999). The symptoms are characterized by wilting of the whole plant, leading to premature senescence and death. The main source of inoculum is the soil, but long rotations are not sufficient to reduce disease incidence because microsclerotia survives in the soil, as well as on weeds and plant debris (Secor and Gudmestad, 1999; Johnson and Cummings, 2015). However, seed-inoculum might be a primary source of inoculum in disease-free fields (Secor and Gudmestad, 1999; Dung et al., 2012). Control of verticillium wilt is mainly achieved through the development of resistant cultivars, which can be insensitive to *Verticillium*'s toxins or

develop mechanical barriers (Vaughn and Lulai, 1991; Secor and Gudmestad, 1999). Furthermore, biocontrol agents have been shown efficient in controlling seed-tuber inoculum (El Hadrami et al., 2011).

Dry rot (Fusarium spp.)

Several *Fusarium* species cause dry rot in potatoes (Secor and Gudmestad, 1999). Their symptoms are restricted to tubers, since infections occur after harvest. Indeed, the pathogen will penetrate the tuber through wounds or other injuries on the tuber surface (Secor and Gudmestad, 1999; Arora and Khurana, 2004). The disease will develop during storage, and symptoms will appear 2-3 months after harvest (Arora and Khurana, 2004). Infections with *Fusarium* species occur mainly from soil-borne inoculum, but planting infected seed can result in poor germination (due to seed decay) and plant wilt (Secor and Gudmestad, 1999). Management strategies rely on avoiding wounding during harvest and chemical or biological treatment of infected tubers (Secor and Gudmestad, 1999; Arora and Khurana, 2004).

Black scurf (Rhizoctonia solani)

Rhizoctonia solani J.G. Kühn causes black scurf in tubers and stem canker in stems, which are two symptoms of the same disease (Arora and Khurana, 2004). In tubers, it is a blemish disease, and symptoms are characterized by black protuberances formed by fungal sclerotia, while infected stems can show red or brown lesions, as well as other systems in the whole plant, such as poor germination, chlorosis, leave rolling or purple pigmentation (Secor and Gudmestad, 1999; Arora and Khurana, 2004). The source of infection is both the seed and the soil, and thus cultural methods such as rotation or soil solarization combined with seed treatment with fungicides or biocontrol agents has been shown to be efficient (Secor and Gudmestad, 1999; Arora and Khurana, 2004).

Powdery scab (Spongospora subterranea)

Powdery scab is a blemish disease caused by *Spongospora subterranea* (Wallr.) Lagerh, which has been traditionally regarded as a fungal pathogen (Blancard, 2012). However, it does not belong to the Fungi kingdom, but rather to the Cercozoa phylum, which is formed by microscopic single-cell eukaryotes (Gau et al., 2013) The disease is characterized by affecting all below-ground organs, especially in tubers, where symptoms appear as round scab like lesions (Arora and Khurana, 2004). The sources of inoculum are both seed and soil, as well as manure used to fertilize fields (Arora and Khurana, 2004). Thus, planting disease-free seed-tubers and long rotations are effective management strategies, as well as using resistant cultivars (Arora and Khurana, 2004).

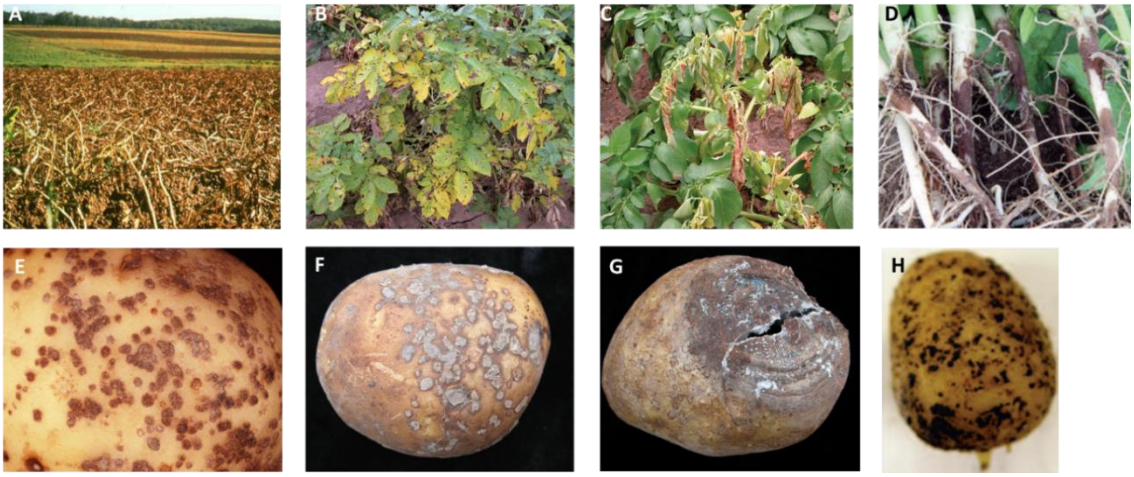

Figure 1.4 Overview of disease effects of the most common fungal diseases on potatoes. A: Late blight disease on whole plants. B: Early blight disease on whole plants. C: Verticillium wilt on whole plants. D: Stem canker on above-ground organs.

E: Common scab on tubers. F: Powdery scab on tubers.G: Dry rot on tubers. H: Black scurf on tubers. Photos: A: S.B. Goodwin (Cornell University); B, C, E, F and G: http://www.omafra.gov.on.ca/; D and H: https://www.extension.uidaho.edu/

1.2. Black dot

1.2.1. The pathogen (*Colletotrichum coccodes*)

Black dot is a potato disease caused by the anamorph *Colletotrichum coccodes* (Wallr.) S. Hughes (1958), an ascomycete that belongs to the family of the Glomerellaceae (Index Fungorum). It was first described in 1833 as *Chaetomium coccodes* (Wallroth, 1833) (Figure 1.5) and this and several other synonyms were then further grouped as *C. coccodes* in 1958 (Hughes, 1958).

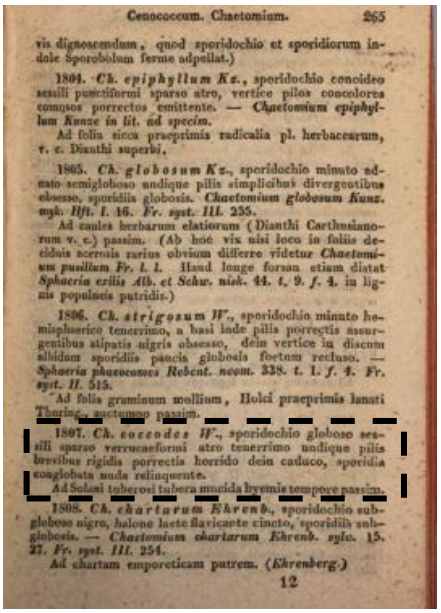

Cenococcum. Chaetomium. 265

vis dignoscendum, quod sporidochio et sporidiorum indole Sporobolum ferme adpellat.)

1804. *Ch. epiphyllum Ks.*, sporidochio concideo sessili puncti formi sparso atro, vertice pilos concolores comosos porrectos emittente. — *Chaetomium epiphyllum Kunze in lit. ad specim.*

Ad folia sicca praeprimis radicalia pl. herbacearum, v. c. Dianthi superbi.

1805. *Ch. globosum Ks.*, sporidochio minuto adnato semigloboso undique pilis simplicibus divergentibus obsesso, sporidiis globosis. *Chaetomium globosum Kunz. myk. Hft. I. 16. Fr. syst. III. 255.*

Ad caules herbarum elatiorum (Dianthi Carthusianorum v. c.) passim. (Ab hoc vix nisi loco in foliis decidua acervis rarius obvium differre videtur *Chaetomium pusillum Fr. l. l.* Haud longe forsan etiam distat *Sphaeria exilis Alb. et Schw. nisk. 44. t. 9. f. 4.* in ligneis populneis putridis.)

1806. *Ch. strigosum W.*, sporidochio minuto hemisphaerico tenerrimo, a basi inde pilis porrectis assurgentibus stipatis nigris obsesso, dein vertice in discum albidum sporidiis paucis globosis foetum recluso. — *Sphaeria phaeocomes Rebent. neom. 338. t. 1. f. 4. Fr. syst. II. 515.*

Ad folia graminum mollium, Holci praeprimis lanati Thuring., auctumno passim.

1807. *Ch. coccodes W.*, sporidochio globoso sessili sparso verrucaeformi atro tenerrimo undique pilis brevibus rigidis porrectis horrido dein caduco, sporidia conglobata nuda relinquente.

Ad Solani tuberosi tubera mucida hyemis tempore passim.

1808. *Ch. chartarum Ehrenb.*, sporidochio subgloboso nigro, halone laete flavicante cincto, sporidiis subglobosis. — *Chaetomium chartarum Ehrenb. sylv. 15. 27. Fr. syst. III. 254.*

Ad chartam emporeticam putrem. (*Ehrenberg.*)

12

Figure 1.5 First description of *C. coccodes* (as *Chaetomium coccodes*) by Wallroth *(Wallroth, 1833)*.

Cultivated in culture media, it grows quickly at warm temperatures, with growth rates of more than 0.5 cm/day at 20 to 27°C, and continue to grow, although slowly, at lower temperatures, with growth rates below 0.2 cm/day at 10 to 5°C (Nitzan and Lahkim, 2003; Glais-Varlet et al., 2004), exhibiting white mycelium at the front of growth and black microsclerotia distributed evenly throughout the mycelium (Lees and Hilton, 2003). Microsclerotia are small dense clusters of hyphae surrounded by tough melanized hyphae that provide protection against biotic and abiotic stresses, such as soil microorganisms or extreme temperatures (Money, 2016), and are used by *C. coccodes* to overwinter in the field (Lees and Hilton, 2003). Acervuli are also produced, usually together with microsclerotia, both *in vitro* and *in planta* (Lees and Hilton, 2003). They contain septate conidiophores, with fusiform conidia of 16-24 µm long and 3-4 µm wide (Sutton, 1992). A great genetic variability exists in the species *C. coccodes*, with several Vegetative Compatibility Groups (VCGs) identified, mostly isolated from potato grown in different continents (Nitzan et al., 2002, 2006; Shcolnick et al., 2007; Aqeel et al., 2008). The *Colletotrichum* genus is considered as the 8th most important fungal pathogen in plant pathology, with different species causing symptoms in almost every crop worldwide (Dean et al., 2012). Among all species of *Colletotrichum*, *C. coccodes* is the most important in economic terms (Cannon et al., 2012), invading especially potatoes and tomatoes, where it produces black dot and anthracnose, respectively. However, it has numerous hosts, mainly from the *Solanaceae*, *Cucurbitaceae* and *Fabaceae* families (Termorshuizen, 2007). These include many crop plants, including the cited potatoes and tomatoes (Byrne et al., 1997), but also others, such as peppers (Mikulic-Petkovsek et al., 2013) or onions (Rodriguez-Salamanca et al., 2012). Furthermore, several weed species can act as alternative

hosts, which are usually symptomless or show only chlorotic and necrotic flecks (Raid and Pennypacker, 1987). In some cases, *C. coccodes* is used as a biocontrol agent against unwanted weeds, such as for the case of velvetleaf, a weed particularly noxious to corn and soybean (Dauch and Jabaji-Hare, 2006).

Nonetheless, the presence of *C. coccodes* in weeds during crop rotation might be a possible reservoir for primary infections against crops such as potatoes. In potatoes, primary infections will originate from the seed-tuber or infected debris in the soil (Ducomet, 1908), or from fungal hyphae overwintering as microsclerotia. Notably, microsclerotia can survive long periods in the soil, and *C. coccodes* inoculum has been found in fields where main hosts have not been planted for up to 13 years (Cullen et al., 2002). Primary infections start at the root system, that is quickly infected by *C. coccodes*, while stolons, stems and daughter tubers develop symptoms only 8 to 10 weeks after planting (Andrivon et al., 1998; Lees and Hilton, 2003). Furthermore, acervuli can be produced from infected plant material (Lees and Hilton, 2003) and spread conidia that can produce secondary infections during plant growth, in spring and summer. Moreover, fungal colonization can continue during plant growth and storage (Lees and Hilton, 2003). Infected tubers used as seed stock can be the source of inoculum, but can also introduce the pathogen to the field in order to provide a soilborne inoculum (Read and Hide, 1988, 1995b). Microsclerotia of *C. coccodes* present on soil or brought in by infected seed-tubers are the primary inoculum for black dot disease. In contact with the plant, the pathogen is able to colonize underground and above-ground tissues, and colonization of roots is followed by colonization of stems, stolons and tubers (Andrivon et al., 1998). Conidia can be spread by wind, rain or irrigation and infect new plant tissues, including leaves, producing secondary infections (Johnson, 1994). Lesions can be observed in stems and leaves during plant growth, and infections continue to expand, especially in underground tissues. Daughter tubers can be quickly infected with *C. coccodes*, but symptoms are more important late in the season and after storage (Andrivon et al., 1998; Lees and Hilton, 2003; Johnson et al., 2018). The pathogen can survive in the soil or in plant debris for several years and be the primary inoculum for next generations of potato plants (Cullen et al., 2002).

1.2.2. The disease

Black dot can cause important yield losses in some favorable conditions (Johnson, 1994; Tsror (Lahkim) et al., 1999), although in other climatic conditions, these losses have not been observed (Read and Hide, 1995b). All underground organs are susceptible to infection by *C. coccodes* (Ducomet, 1908; Andrivon et al., 1998; Lees and Hilton, 2003), and black dot symptoms can also be observed in basal stems (Andrivon et al., 1997, 1998) and leaves (Johnson, 1994). The infection of the foliage by *C. coccodes* has led to the hypothesis that it is not only a tuber-borne and soil-borne pathogen, but also an airborne pathogen (Johnson, 1994; Tsror (Lahkim) et al., 1999). Symptoms of black dot are characterized by the presence of black microsclerotia on infected tissue, including in decaying roots and stems, stolons and daughter tubers (Read and Hide, 1988). Although all plant organs show disease symptoms, those are especially important in tubers, because they induce skin permeabilization, water losses and quality deterioration (Lees and Hilton, 2003). Lesions in tubers are brown to grey, without defined margins, and black microsclerotia may be visible to the naked eye (Read and Hide, 1988) (Figure 1.6A-C).

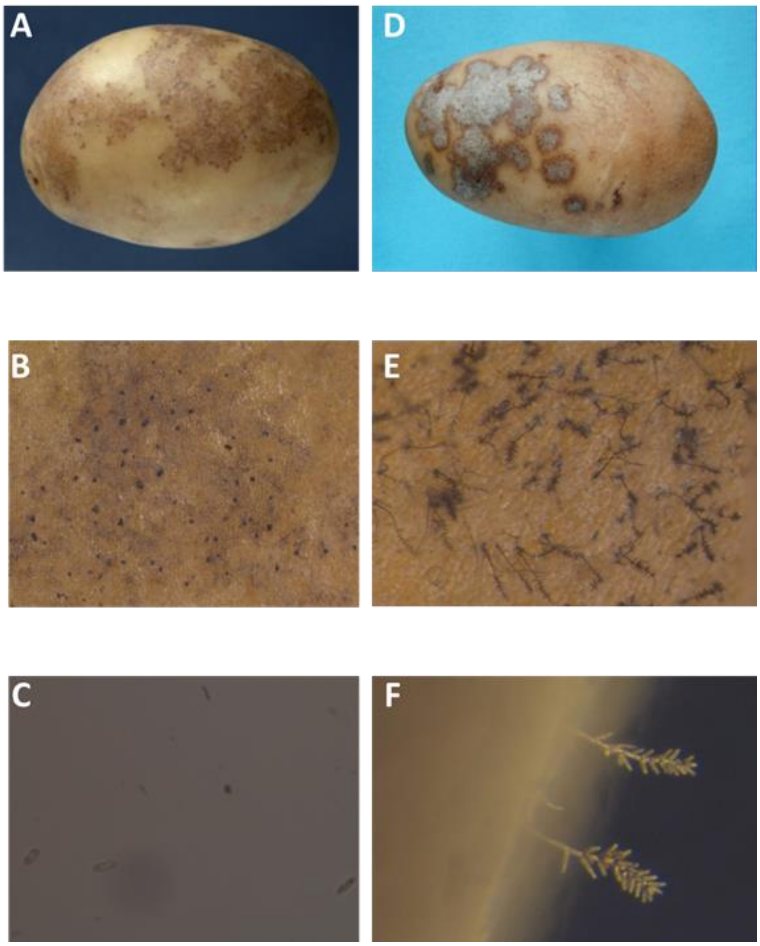

Figure 1.6 Black dot (A-C) and silver scurf (E-F) disease of potatoes. Entire tubers showing disease symptoms (A and D), observations of fungal micrisclerotia (B) and conidiophores (E and F), conidia produced by *C. coccodes* (C). Photos A and D: Agroscope. Photos B, C, E and F: F. Voinesco (Agroscope).

The development of pests, especially fungal diseases, are controlled from a long time by the use of phytosanitary products. Nonetheless, Integrated Pest Management (IPM) strategies have been developing in the recent years in order to better control plant pathogens and reduce the use of synthetic pesticides. These strategies rely on the knowledge of the epidemiology and etiology of the pathogen, its life cycle, pathogenesis factors and the environmental conditions that affect the development of the disease, in order to select the most effective methods at the right time to reduce the risk of a disease. Such information is essential for the development of preventive measures, such as cultivar choice, crop rotation or irrigation, among others. These preventive measures are at the base of an IPM. Knowing the pathogen's life cycle and the environmental conditions that favor its development can also be used to develop models of risk management, which will be essential for a correct application of other measures, such as biological or chemical control (Secor and Gudmestad, 1999; Arora and Khurana, 2004). Biological control measures (i.e. application of antagonists) or physical methods that will avoid pathogen infections are the third layer of IPMs. Finally, the last criterium of an IPM is the application of chemical control measures, which will only be applied when the risk of the disease is elevated.

One of the most efficient preventive measures in the control of fungal diseases in potatoes is to decrease the inoculum source, through crop rotation (Peters et al., 2004) and/or to produce clean seed-tubers (Frost et al., 2013). *C. coccodes* is both a tuber-borne and a soil-borne disease, and in some conditions, even an airborne disease (Johnson, 1994; Tsror (Lahkim) et al., 1999; Lees and Hilton,

2003). Thus, understanding the relative importance of each source of inoculum is important. Early work on black dot showed that planting infected tubers resulted in symptomatic plants and daughter tubers, proving it a tuber-borne disease (Dickson, 1926). On the other hand, disease-free potato cuttings developed black dot when planted using soils from potato-producing areas in France, indicating that soilborne inoculum is capable of infecting potato plants (Andrivon et al., 1997). However, the relative importance of each inoculum seems to depend on several other factors. Microsclerotia of *C. coccodes* survives for at least 8 years in the soil (Dillard and Cobb, 1998), and molecular biology techniques allowed the detection of *C. coccodes* inoculum in fields where potatoes had not been grown for 5, 8 and 13 years (Cullen et al., 2002), suggesting that once introduced in the soil, the soilborne inoculum becomes the predominant source of inoculum (Lees and Hilton, 2003). Whether the inoculum survives as microsclerotia in the field during years or reproduces in other hosts remains unclear. Few studies have actually compared the relative importance of seedborne and soilborne inoculum on the development of black dot on daughter tubers. Some reports indicated that tuberborne inoculum might be important in the development of black dot. For example, black dot incidence was higher in roots (Dashwood et al., 1992) and daughter tubers (Read and Hide, 1995a) originating from severely infected seed-tubers than from disease-free tubers, and disease-free seed-tubers planted in soils where potatoes had not been grown for 15 years resulted in disease-free daughter tubers (Read and Hide, 1995a). In Israel, black dot was found in daughter tubers of certified seed-tubers grown in fields without 7 and 12 years of potato crops, even when the soil was not inoculated (Tsror (Lahkim) et al., 1999). Long rotation was supposed to eliminate the soilborne inoculum, and infections could have been originated from asymptomatic contaminated seed-tubers (Tsror (Lahkim) et al., 1999). Alternatively, infections of control plants might have been secondary infections from conidia originated from inoculated plants and dispersed through wind or water splashes (Tsror (Lahkim) et al., 1999). Inoculated seed-tubers grown in sterilized soil develop black dot symptoms, indicating that tuberborne inoculum is important at least in disease-free soils (Andrivon et al., 1998). Indeed, the tuber progresses from the seedtuber primarily through roots and later in stolons and tubers (Andrivon et al., 1998). Furthermore, the progression of the disease is linear from the infected seed-tuber to surrounding organs, and tuberborne inoculum can be an important factor, especially during long growing seasons (Ingram and Johnson, 2010). However, tuberborne inoculum is thought to be important in introducing the pathogen in pathogen-free soils, but that soilborne inoculum is then the major factor influencing black dot (Barkdoll and Davis, 1992; Tsror (Lahkim) et al., 1999; Lees and Hilton, 2003; Nitzan et al., 2005). Indeed, other studies suggest that soilborne inoculum is the main source of inoculum of *C. coccodes*. Read and Hide (Read and Hide, 1988) compared the effect of the seed and the soil as inoculum for black dot by planting diseased seed and disease-free seeds in inoculated or non-inoculated fields, and found that black dot incidence was higher when *C. coccodes* was inoculated in the soil. However, disease-free seed tubers were selected from visual observations, and asymptomatic contaminated tubers might have been selected as disease-free. Indeed, disease-free seed-tubers grown in non-inoculated field developed black dot, suggesting that either i) they were not disease-free seed-tubers or ii) *C. coccodes* inoculum was present in uninoculated fields (Read and Hide, 1988). Furthermore, the application of *C. coccodes* inoculum in the soil was not designed to mimic soilborne inoculum, but to ensure enough disease development to study other factors (Read and Hide, 1988). Thus, the inoculum used in this experiment might not be representative of soilborne inoculum. In studies carried out in both seed areas and production areas of potato in the USA, the authors found a good correlation between soil and tuber colony forming units, suggesting that seed-tubers introduce *C. coccodes* to uninfected soils (Barkdoll and Davis, 1992). Since soil samples were taken at the same time than daughter tubers, this data suggests that seed-tubers introduce the pathogen in the soil, but does not inform about the correlation between pre-planting soil inoculum and disease severity at harvest. In a different study, artificially inoculated soil samples

showed higher disease severity than control samples, but differences in tuber black dot incidence between control and inoculated plots were not observed for all cultivars (Tsror (Lahkim) et al., 1999). Planting seed-tubers naturally infected with *C. coccodes* with different severities did not result in significant differences in black dot incidence in daughter tubers. However, fumigating the soil reduced black dot incidence of all seed-tuber lots, suggesting that soilborne inoculum is more important than seedborne inoculum (Denner et al., 1998). However, it is worth noting that daughter tubers from disease-free seed-tubers showed significantly less disease severity than all other seed-tuber lots (Denner et al., 1998), suggesting that there is also an effect of the seedborne inoculum. Furthermore, the combined effect of soil fumigation and fungicide treatment of seed-tubers results in a higher disease control than each alone (Denner et al., 1998). Unclear results were also obtained in using two generations of seed-tubers with different seed inoculum, since less contaminated seed-tubers showed higher yields but also higher disease incidence than seed-tubers with higher infections (Nitzan et al., 2005). Furthermore, these differences were observed for one of the cultivars studied, but not the other, suggesting that the inoculum source effect might be cultivar-dependent (Nitzan et al., 2005). Comparing tuber-inoculated and soil-infested as sources of inoculum was also carried out in controlled experiments (Nitzan et al., 2008). Different isolates of *C. coccodes* showed differences in the pathogenesis, but all three isolates showed higher aggressiveness as soilborne inoculum than as tuberborne inoculum (Nitzan et al., 2008). Nonetheless, tuberborne inoculum alone was also able to induce higher disease severity (Nitzan et al., 2008). Interestingly, there was a nonlinear, sigmoid response between soil inoculum and disease severity (Nitzan et al., 2008), suggesting that artificial inoculation of soils were higher than those required for a maximal expression of symptoms. Other authors found that artificial inoculations (seed, soil or foliar) do enhance black dot development under certain conditions, but no differences were observed between seed-inoculated and soil-infested samples in any field trials (Pasche et al., 2010). Seed-tuber inoculum correlated with root disease in one of the two years studied, but incidence of black dot in daughter tubers did not correlate with seedborne inoculum (Dung et al., 2012). Most epidemiological studies of black dot have relied on visual symptoms and isolation of the pathogen. The development of molecular biology techniques have allowed the quantification of fungal pathogens both in tubers and in the soil (Cullen et al., 2002; Brierley et al., 2009). These techniques are more sensitive than classical isolation methodology, although they do not differentiate between viable and dead fungal material. A correlation was observed between visual disease severity assessments in tubers and *C. coccodes* DNA in tuber sap, although fungal DNA was present in asymptomatic tubers (Lees et al., 2010). These results suggest that molecular biology techniques can complement visual observations of black dot disease, and further detect fungal DNA in visually asymptomatic tubers. Indeed, the authors selected four groups of seed-tubers with different severities, but significant differences on fungal DNA content were only observed between the two less infected lots and the two most infected lots (Lees et al., 2010). Interestingly, there were no differences on the disease development between all four lots of seed-tubers when planted in field trials or in a controlled greenhouse experiment, indicating that seedborne inoculum does not influence black dot incidence in progeny tubers (Lees et al., 2010). Nevertheless, it is worth noting that fungal DNA was detected in asymptomatic tubers, and that asymptomatic tubers grown in uncontaminated soil developed the disease (Lees et al., 2010). Altogether, these results suggest that seedborne inoculum is sufficient to induce black dot in daughter tubers, but that the amount of inoculum in the seed-tuber does not correlate with the disease severity in progeny tubers. On the other hand, planting PCR-confirmed disease-free seed-tubers in soils infested with *C. coccodes* resulted in a good correlation between soil infestation and disease severity in progeny tubers, suggesting that soilborne inoculum correlates with black dot disease development. Furthermore, a survey involving 122 crop fields showed that black dot disease in progeny tubers correlate with natural soil inoculum (Lees et al., 2010). However, the variance explained by the soil inoculum was relatively low, probably

because other factors, such as cultivar resistance, irrigation or fungicide treatment differed among field sites (Lees et al., 2010). In general, data available on black dot development suggests that soilborne inoculum is the main source of black dot in potatoes, and that soil inoculum correlates with black dot disease severity. Seedborne inoculum can also be important, especially by introducing the pathogen in *C. coccodes*-free fields. However, no correlation between visually assessed seedborne inoculum and progeny tubers disease symptoms is usually observed. Recent studies have shown that separating seed-tubers in categories according to their seed inoculum is not precise enough, and that asymptomatic tubers infected with *C. coccodes* could be selected wrongly as disease-free tubers (Lees et al., 2010). Thus, only selecting disease-free tubers would reduce the risk of introducing the pathogen in pathogen-free fields and reduce the risk of black dot in progeny tubers (Lees et al., 2010). Crop rotation could reduce the soil inoculum, but alternative hosts, as well as reintroduction of the pathogen from diseased seed-tubers, limit the effect of crop rotation (Lees and Hilton, 2003). Other cultural methods designed to reduce soil inoculum can be used to control black dot. Pre-plant solarization, which consists in covering the soil with plastic to increase the temperature of the soil, and mouldboard ploughing, which consists in turning the soil from various depths, have been shown effective to reduce the incidence of black dot (Denner et al., 2000). Furthermore, quantitative PCR can be used to determine the soil inoculum in order to select fields with low soil inoculum, or to implement solarization or mouldboard ploughing in heavily-contaminated soils. However, routine analysis of *C. coccodes* soil inoculum do not exist to date.

Other cultural methods can be applied during plant growth to limit disease contamination or expansion. Cultivar choice is used to control many diseases, including potato diseases. Resistant cultivars to black dot that do not express symptoms are not currently available, but differences in disease expression of black dot are observed among commercial cultivars (Brierley et al., 2015). Other studies have shown that disease severity is influenced by the cultivar (Read, 1991b; Tsror (Lahkim) et al., 1999; Brierley et al., 2015). Thus, planting cultivars relatively resistant to black dot can reduce the risk of disease in progeny tubers, especially under conditions where black dot is expected (i.e. in heavily contaminated soils) (Brierley et al., 2015). Studies in the USA showed that thick-skinned (Russet-type) cultivars appear to be more resistant to black dot than thin-skinned cultivars (Hunger and McIntyre, 1979), but Russet-type cultivars are not popular in Europe (Lees and Hilton, 2003). Russet-type thick-skin cultivars usually possess periderms of more than 150 µm, while medium skin thickness cultivars have ca. 130 µm and thin skin cultivars have periderms of 100-125 µm (Artschwager, 1924). In general, early-maturing cultivars are more resistant to black dot than late-maturing cultivars (Read, 1991b; Andrivon et al., 1997, 1998), probably because they spent more time in the soil with the inoculum (Lees and Hilton, 2003). Early-harvest results in lower incidence of black dot in daughter tubers, especially in fields with high soil inoculum (Hide and Boorer, 1991; Hide et al., 1994b; Brierley et al., 2015). Indeed, there is a relationship between crop duration and soil inoculum, and early harvest (short crop duration) can help reduce the risk of black dot in highly contaminated fields (Peters et al., 2016). Numerous environmental conditions also affect the development of plant diseases. Damp conditions during plant growth favor the incidence of black dot in progeny tubers (Lees et al., 2010), and watering before harvest also induces higher disease severity (Hide et al., 1994b). In field conditions, irrigation generally increases the incidence of black dot in progeny tubers (Olanya et al., 2010; Brierley et al., 2015). Furthermore, warmer temperatures (22°C vs 18°C) favor disease expression in progeny tubers, but only in damp conditions (Lees et al., 2010). Potatoes might be stored after harvest for long periods before consumption. Thus, storage conditions can also be adapted to limit the spread of the disease between potato tubers during storage. Curing is a process that takes place after harvest and before the final storage conditions, and that allows tubers to suberize and heal wounds that may be produced during harvest (Errampalli et al., 2001b; Avis et al., 2010). Curing usually takes from 10 to 21 days at

10-15 °C and 95% relative humidity (Errampalli et al., 2001b). It has been shown that drying the tubers for two weeks after harvest reduces the severity of black dot, but reducing the relative humidity from 95% to 75% in the storage room is not efficient (Hide and Boorer, 1991), suggesting that the condensation of water on the tuber surface favors the development of *C. coccodes*. Thus, dry curing before storage is another practice that can help reducing the risk of black dot. Notably, curing should be reduced to the minimum (5 days), since extended cure (12 days) favors the development of black dot, especially in potatoes grown in highly contaminated soils for a relatively long duration (Peters et al., 2016). The post-harvest application of fungicides prior to storage might also be a control method in tuber lots expected to be highly contaminated with *C. coccodes* or expected to be stored for long periods. However, biological control and other physical methods are rarely used to control black dot, and post-harvest application of fungicides, especially on table potatoes, would not be accepted by consumers. Recently, the use of essential oils has been suggested promising in controlling fungal diseases during storage, notably in fruits, against anthracnose caused by *Colletotrichum* species (Palhano et al., 2004; Lee et al., 2007; Anaruma et al., 2010). The antagonistic effect of microorganisms on *C. coccodes* has been studied to some extent (Okhovat and Zafari, 1996; Palaniyandi et al., 2013; Lee et al., 2017), but the use of biological control against black dot is not common practice among potato growers. In Switzerland, post-harvest applications on table potatoes are rare, i.e. only one biological control agent is authorized as post-harvest treatment of table potatoes. The last layer of crop protection in IPMs is the chemical control. For black dot, the efficiency of fungicide application on seed-tuber has been studied for a number of compounds, with different efficiencies (Hide and Read, 1991; Read and Hide, 1995a, 1995b; Andrivon et al., 1997). In many European countries, including Switzerland, azoxystrobin application as in-furrow fungicide during planting is approved. In-furrow application of azoxystrobin in fields with high soil inoculum can help reduce black dot severity in progeny tubers (Brierley et al., 2015). Other studies have shown the efficiency of azoxystrobin treatments in reducing black dot, but those were carried out at planting and during plant growth (Nitzan et al., 2005; Pasche et al., 2010), which is not authorized in many countries, including Switzerland, due to the possible development of resistance against strobilurin fungicides (Johnson et al., 2018). Treating seed tubers with prochloraz decreases black dot incidence in progeny tubers, but in these trials seed-tubers were planted in disease-free soils, and these treatments might not be efficient when planting in a heavily infected soil (Denner et al., 1997). The factors influencing black dot development in potatoes are summarized in Figure 1.7.

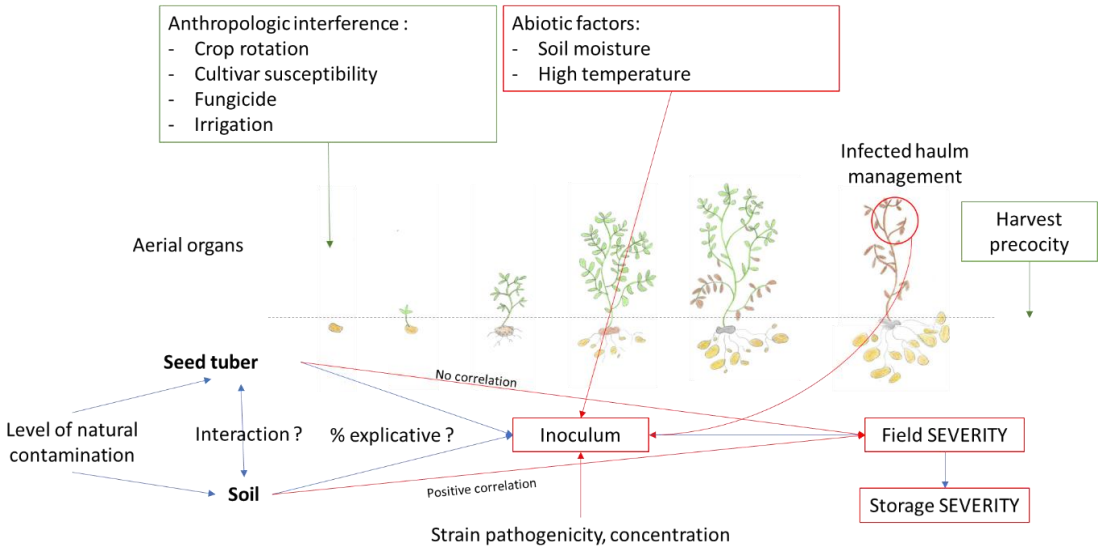

Figure 1.7 Epidemiological parameters involved in the control management of black dot. Drawing adapted from the "Crop Stages of potatoes plant" by @Ilyakalinin from Dreamstime.com.

1.3. Silver scurf

1.3.1. The pathogen (*Helminthosporium solani*)

Silver scurf is a potato blemish disease caused by *Helminthsporium solani* Durieu & Mont. (1849) is an ascomycetous fungus that belongs to the order of the Pleosporales (Termorshuizen, 2007), although it has also been suggested to belong to the order of the Moniliales, its phylogenetic position remaining unclear to date (Errampalli et al., 2001b). Hyphae are dark, but conidiophores that bear conidia arise from stromata giving a grey color to the fungus (Luttrell, 1964; Barnett and Hunter, 1998). Septate conidiophores give rise to several large and cylindrical thick wall conidia (from 5 to 30 conidia per conidiophore), that can be from 15 µm to 64 µm long, and from 4 µm to 8 µm in width (Hunger and McIntyre, 1979; Errampalli et al., 2001b). Warm temperatures (20 to 24°C) and high humidity (95% RH) favor sporulation and conidial germination *in planta*, which takes place 16 hours after inoculation (Heiny and Mclntyre, 1983; Errampalli et al., 2001b). *H. solani* is pathogenic to *Solanum tuberosum* and other tuber-bearing *Solanum* species (Rodriguez et al., 1995), but no other hosts are known. Indeed, *H. solani* was not pathogenic to other crops, such as carrots or sweet potatoes (Burke, 1938; Kamara and Hugelet, 1972). However, *H. solani* colonized senescent leaf tissue of several crops, including alfalfa, corn, wheat, or rapeseed, among others, indicating its saprophytic ability (Mérida and Loria, 1994b). Nonetheless, *H. solani* was not able to infect potato leaves, supporting that symptoms of silver scurf are limited to tubers (Mérida and Loria, 1994b). Furthermore, *H. solani* is able to overwinter in the soil, since disease-free tubers planted in natural soil became infected (Mérida and Loria, 1994b). However, detecting *H. solani* in the field by conventional methods has been proven challenging, mainly because it is a slow-growing fungus (Errampalli et al., 2001b). However, recent advances in molecular biology techniques might be useful in detecting the pathogen both in the soil and in infected plant material. PCR-based methods for the detection of *H. solani* have been developed, including quantitative PCR that allows detection of low amounts of soil inoculum (Olivier and Loria, 1998; Cullen et al., 2001; Errampalli et al., 2001a). Primary infections of *H. solani* occur in the field, mainly from infected seed-tuber (Burke, 1938; Jellis and Taylor, 1977), although overwintering of *H. solani* in the field has also been found to be a source of inoculum (Mérida and Loria, 1994b). Indeed, survival of *H. solani* for at least 9 months in soil under laboratory conditions has been shown (Frazier et al., 1998), and low levels of soil inoculum may be present from plant debris (Mérida and Loria, 1994b; Bains et al., 1996; Rodriguez et al., 1996). The primary infections occurs in daughter tubers that are located close to the seed-tuber, especially at the stolon apical part (Jellis and Taylor, 1977; Errampalli et al., 2001b). Tuber infection with *H. solani* starts soon after tuber initiation, and most of the infections occur during plant growth both through enzymatic and mechanical processes, forming or not appressorium (Jellis and Taylor, 1977; Errampalli et al., 2001b; Martinez et al., 2004). However, secondary infections can occur during harvest or storage (Mérida et al., 1994; Errampalli et al., 2001b), and sporulation occurs best at warm temperatures (20°C) and high relative humidity (95%), although sporulation and conidia spread through ventilation can happen in potato storage facilities (Rodriguez et al., 1996). Notably, sporulation of *H. solani* can increase after washing and packaging of potatoes for consumption (Errampalli et al., 2001b).

Conidia or hyphae of *H. solani* are introduced in the field by infected seed-tubers and represent the primary inoculum (Errampalli et al., 2001b). In some fields, especially were low rotation is applied, soil inoculum can also produce primary infections. In the field, infections will occur in daughter tubers from the stolon end (Olivier and Loria, 1998), and will progress during plant growth and, especially, during storage (Errampalli et al., 2001b). Diseased tubers used as seed potatoes will introduce the pathogen in the next generation of potato plants.

1.3.2. The disease

Silver scurf does not usually cause yield losses but has a deleterious impact on tuber quality, although may have an effect on emergence and plant growth, especially in cultivars with low sprouting vigor (Mooi, 1968; Read and Hide, 1984). Furthermore, symptomatic tubers are not appealing, and silver scurf lesions affect tuber quality, especially in the fresh potato industry (Read and Hide, 1984; Secor, 1994), which can lead to downgrading of potato lots heavily infected with *H. solani* (Hunger and McIntyre, 1979). Interestingly, disease symptoms are limited to the tubers, roots and stems do not show silver scurf symptoms (Errampalli et al., 2001b). Tuber symptoms first appear as brown lesions at the stolon end, and can become darker during pathogen sporulation and expansion (Burke, 1938; Jellis and Taylor, 1977; Errampalli et al., 2001b). Older lesions become silvery, due to loss of pigments in the periderm, cell desiccation and suberin accumulation (Frazier et al., 1998). Furthermore, the infection of *H. solani* causes an increase in the permeability of the periderm, leading to water losses and weight loss (Hunger and McIntyre, 1979). *H. solani* hyphae were observed in the periderm and cortical layers of infected tubers, and conidiophores were shown to originate from hyphae beneath the surface (Hunger and McIntyre, 1979; Heiny and McIntyre, 1983).

As for many other diseases, silver scurf control was achieved for long time using fungicides. Silver scurf is believed to be essentially a seedborne disease (Errampalli et al., 2001b; Tsror (Lahkim) and Peretz-Alon, 2004) and fungicide treatments of seed-tubers might reduce silver scurf incidence. In 1968, thiobendazole (TBZ), a broad-spectrum fungicide, was shown to be effective against several fungal plant pathogens, including *H. solani* (Hide et al., 1969), and became widely used for the post-harvest treatment of seed tubers (Errampalli et al., 2001b). However, resistant isolates began to appear in 1977, and in 10 years, resistance to TBZ fungicide was widespread and led to an increase in disease incidence (Hide et al., 1988; Mérida and Loria, 1994a; Errampalli et al., 2001b). Furthermore, resistance to TBZ relies on a single-base mutation, and one single application of the fungicide is sufficient to obtain resistant strains (Errampalli et al., 2001b). Other fungicides have since been studied for their efficacy in controlling silver scurf, especially on seed tubers. Imazalil, alone or in combination with TBZ, was efficient in controlling silver scurf, and treatments of both imazalil and TBZ together did not result in emergence of resistance to TBZ (Hide et al., 1988, 1994c, 1994a; Errampalli et al., 2001b; Tsror (Lahkim) and Peretz-Alon, 2004). Treating seed tubers with prochloraz, a sterol biosynthesis inhibitor, also decreased significantly silver scurf in progeny tubers (Denner et al., 1997), especially when in combination with the multi-site fungicide mancozeb (Tsror (Lahkim) and Peretz-Alon, 2004). Other fungicides, such as fenpiclonil, fludioxonil, propineb, mancozeb and several combinations of these and other fungicides have been shown effective (as seed-tuber treatments) in controlling silver scurf in daughter tubers (Frazier et al., 1998; Errampalli et al., 2001b; Tsror (Lahkim) and Peretz-Alon, 2004). Notably, seed-tuber treatments with azoxystrobin, the commonly used fungicide against black dot as in-furrow applications, is efficient against silver scurf (Tsror (Lahkim) and Peretz-Alon, 2004). However, other authors found that seed-tuber treatments with fungicides such as azoxystrobin, mancozeb or imazalil did not control silver scurf in progeny tubers (Hervieux et al., 2001), suggesting that application methods or soil type might influence silver scurf development. Interestingly, Adams and coworkers (Adams et al., 1970) found that there was a negative correlation between bacterial number in the soil and silver scurf in daughter tubers, indicating that there might be an antagonistic effect between bacteria and *H. solani*. Indeed, treating diseased seed-tubers with *Pseudomonas corrugata* reduces silver scurf incidence (Chun and Shetty, 1994).

Although several fungicides and biological controls are effective against silver scurf as seed-tuber treatments, disease may still appear in the field and spread during harvest. Thus, post-harvest treatment of consumption potatoes may be useful in reducing the incidence of the disease. However, the application of chemical fungicides before storage in consumption potato is not acceptable by

public, and not authorized in several countries, including Switzerland. Thus, post-harvest treatments often rely on non-chemical treatments, including essential oils, mineral salts or biological controls. Several organic and inorganic salts have been shown to inhibit *H. solani* growth *in vitro* (Olivier et al., 1998) and some of these salts were efficient in controlling silver scurf in naturally diseased tubers (Olivier et al., 1998, 1999; Miller et al., 2011). However, the application of some inorganic salts resulted in higher water losses than control tubers, while treatment with some organic salts resulted in lower sprout vigor (Yaganza et al., 2003). Potassium sorbate salts exhibited the best control of silver scurf without affecting weight losses (Olivier et al., 1998, 1999; Yaganza et al., 2003), suggesting that the applications of these salts might help reduce silver scurf without affecting tuber quality. Other possible post-harvest treatments include the use of essential oils. S-carvone, L-menthone, peppermint oil and spearmint oil have been found to inhibit the *in vitro* growth of *H. solani* (Gorris et al., 1994; Hartmans et al., 1995; Bång, 2007; Al-Mughrabi et al., 2013), and some of these essential oils have been found to reduce silver scurf in diseased tubers (Bång, 2007; Al-Mughrabi et al., 2013). The use of antagonists to control silver scurf during storage has also been studied. Several microorganisms have been shown to inhibit the growth of *H. solani in vitro* (Kurzawińska, 2006; Guyer et al., 2015), and some biological control agents have been shown promising in controlling silver scurf during storage (Secor and Gudmestad, 1999; Martinez et al., 2002; Michaud et al., 2002; Miller et al., 2011). Nonetheless, other studies showed inconsistent results in controlling silver scurf by applying antagonists as post-harvest treatment (Elson et al., 1997).

Controlling silver scurf, as for black dot, may not be achieved by a single control method, but requires instead the use of several measures combined in an IPM strategy. Thus, several measures should be taken from seed selection to top shelf. Silver scurf is regarded as essentially seedborne (Errampalli et al., 2001b), and planting clean seed tubers might be efficient in controlling the disease. However, even low disease severity in seed tubers can result in heavily infected daughter tubers (Firman and Allen, 1995b). Some authors found that heavily infected seed tubers produced daughter tubers with fewer symptoms than seed tubers with low disease severity (Jellis and Taylor, 1977), although this was not consistent in other experiments (Read and Hide, 1984; Firman and Allen, 1995b). Other authors even found a good correlation between seed-tuber infection and daughter tuber disease incidence in a trial where successive generations of potato seeds were planted (Geary and Johnson, 2006). Altogether, these results suggest that disease severity in seed-tubers does not always correlate with silver scurf in daughter tubers, and that other factors might be important in the development of the disease. Planting disease-free seed tubers might reduce silver scurf disease (Errampalli et al., 2001b), and the use of chemical pesticides in seed-tubers helps control the disease (Denner et al., 1997; Frazier et al., 1998; Errampalli et al., 2001b; Tsror (Lahkim) and Peretz-Alon, 2004). However, even planting disease-free seed tubers in naturally infested soils resulted in daughter tubers with silver scurf symptoms (Mérida and Loria, 1994b). Indeed, the survival of *H. solani* in the soil for low periods and its ability to infect senescent tissue of several plant species, including weeds, (Mérida and Loria, 1994b; Frazier et al., 1998) might influence disease progression. Furthermore, the effect of fungicides applied on seed tubers has been shown to be site-dependent (Geary et al., 2000; Hervieux et al., 2001), suggesting that field site also influences silver scurf development. Thus, crop rotation should also be included for the control of silver scurf, although a 3-year crop rotation should be sufficient since potatoes are the main host for *H. solani* (Errampalli et al., 2001b; Peters et al., 2003). Furthermore, soil properties might influence silver scurf development. Indeed, soils with high nitrate (Adams et al., 1970) or high nitrate and iron content (Martinez et al., 2002) showed low levels of silver scurf, suggesting that a good soil nutrient management can help controlling silver scurf. Furthermore, antagonistic bacteria could be isolated from soils in which potatoes showed low levels of silver scurf, suggesting that silver scurf soil suppressiveness relies on antagonistic microorganisms (Martinez et al., 2002).

Other cultural methods can be used to control silver scurf. This disease was found to correlate with seed tuber size (Hide et al., 1994a; Firman and Allen, 1995a), and higher potato plant densities in the field resulted in higher silver scurf incidence (Firman and Allen, 1995a). Thus, planting smaller seed tubers in a low-density field results in lower silver scurf incidence. On the other hand, silver scurf can also be controlled with early harvesting (Firman and Allen, 1993; Mérida et al., 1994), but planting date also has an effect on disease incidence (Firman and Allen, 1995a). It is suggested that the length between tuber initiation and harvest (length of exposure to *H. solani*) determines silver scurf disease severity (Avis et al., 2010). Thus, reducing the time of exposure of tubers to the pathogen is expected to reduce disease severity. Growth conditions may also have an effect on silver scurf. Irrigation was found to be negatively correlated with silver scurf (Adams et al., 1987; Firman and Allen, 1993), but irrigation prior to harvest increased silver scurf severity (Hide et al., 1994b). However, meteorological conditions influencing silver scurf development have not been investigated to date.

Host resistance is another method widely used to control plant diseases. Potato cultivars differ on their susceptibility to silver scurf (Joshi and Pepin, 1991), but cultivars with high resistance to silver scurf have not been identified so far (Mérida et al., 1994; Secor, 1994; Errampalli et al., 2001b; Avis et al., 2010). Most cultivar susceptibility studies have been carried out in North America with potato cultivars that are not commonly used in Europe, such as Yukon Gold or Russet Burbank (Mérida et al., 1994; Rodriguez et al., 1996; Errampalli et al., 2001b). Since no highly resistant cultivars have been found in potato cultivars, and other tuber-bearing *Solanum* species show low sporulation of *H. solani* (Rodriguez et al., 1995), introgression of genes from these species into *S. tuberosum* has been performed (De Jong and Tarn, 1984; Murphy et al., 1999). However, no resistant cultivars to silver scurf have been reported from these crossbreedings (Errampalli et al., 2001b; Avis et al., 2010).

Silver scurf symptoms may be not be visible at harvest, but progress during cold storage conditions. which may affect silver scurf development. Upon harvest, removing soil and plant residues from tubers helps controlling the disease because it removes *H. solani* inoculum (Frazier et al., 1998; Errampalli et al., 2001b). Furthermore, the curing process, that allows the tuber to suberize at high humidity (95%) and 10-21°C, reduces silver scurf symptoms (Hide et al., 1994a, 1994b). Longer curing periods reduced silver scurf incidence (Hide et al., 1994a, 1994b), and reducing the relative humidity to 85% during the curing period also decreased disease severity (Frazier et al., 1998). After the curing period, tubers should be cooled to the final storage temperature. Condensation on the tuber surface is the best conditions for the sporulation of *H. solani* (Jouan et al., 1974; Hardy et al., 1997). Therefore avoiding condensation during curing and cooling periods decrease significantly the development of silver scurf (Hardy et al., 1997; Pringle et al., 1998) which could be achieved through ventilation. However conidia of *H. solani* are spread through the ventilation system and promote secondary infections (Rodriguez et al., 1996). On the other hand, temperature and relative humidity during storage also could affect silver scurf development. Potato tubers are usually stored at different temperatures depending on their use: seed tubers and table stock are stored at 4°C, potatoes for French fries at 8-10°C and for crisps/chips at 10-13°C (Errampalli et al., 2001b). Low temperatures (3°-5°C) reduce the spread and development of silver scurf compared to higher temperatures (8-15°C) (Ogilvy, 1992; Rodriguez et al., 1996; Hardy et al., 1997; Pringle et al., 1998), but this results in lower tuber quality for the frying industry (Cunnington et al., 1992). Reducing the relative humidity during storage from 95% to 85% also decreased silver scurf severity, but increased tuber shrinkage (Frazier et al., 1998). Tubers maintained at 90% RH for a month and at 95% thereafter did not experience tuber shrinkage but reduced silver scurf severity (Secor and Gudmestad, 1999). The factors influencing silver scurf development in potatoes are summarized in Figure 1.8.

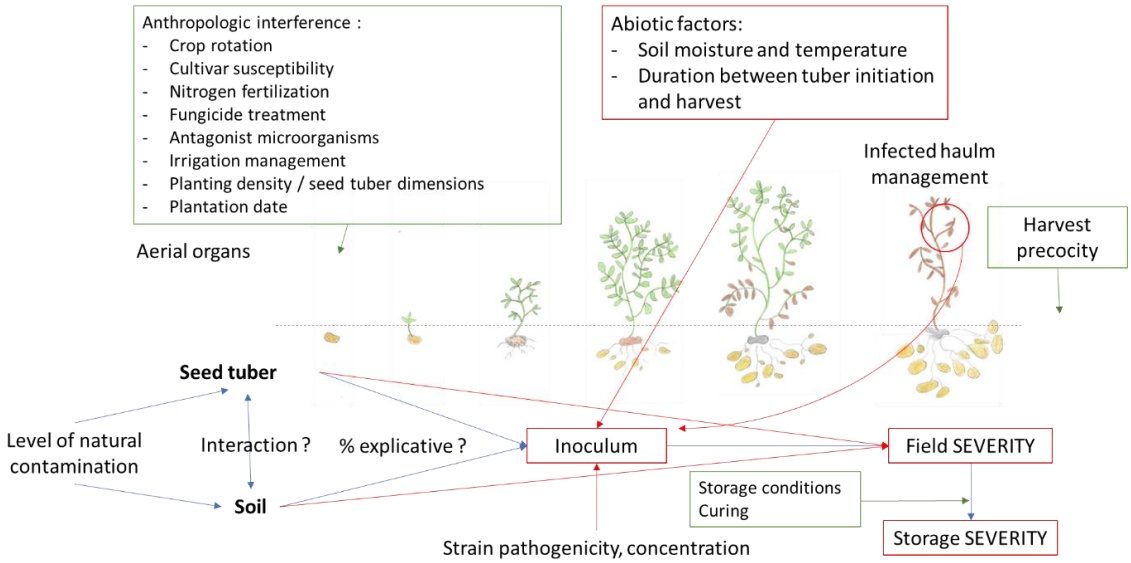

Figure 1.8 Epidemiological parameters involved in the control management of silver scurf. Drawing adapted from the "Crop Stages of potatoes plant" by @Ilyakalinin from Dreamstime.com.

1.4. Comparison of methods to control black dot and silver scurf

Black dot and silver scurf are two blemish diseases of potatoes, with very similar symptoms in the tuber skin, which implies careful microscopic observations of the fungal structures for the correct identification of the disease (Errampalli et al., 2001b; Lees and Hilton, 2003). Thus, they are often not distinguished in most commercial stores. However, downgrading or rejection of tuber lots with high incidence of the disease(s) occur, especially on the fresh consumer's market (Errampalli et al., 2001b; Lees et al., 2010). Controlling both diseases is, then, essential to produce quality tubers. An overview of the methods used to control black dot and silver scurf is presented in Table 1.1, and the fungicides used against black dot and silver scurf are summarized in Table 1.2.

Table 1.1 Comparison of control methods used against black dot and silver scurf

CONTROL METHOD	DISEASE	
CULTURAL METHODS TO REDUCE INOCULUM SOURCE	**Black dot**	**Silver scurf**
Rotation	Efficient	Efficient
Solarization	Efficient	Not studied
Mouldboard ploughing	Efficient	Not studied
Azoxystrobin	Efficient (in-furrow)	Efficient/ambiguous (seed-treatment)
Other fungicides: (mancozeb, imazalil …)	Efficient	Efficient/ambiguous (seed-treatment)
Disease-free seed tubers	Efficient (in clean soils)	Efficient/ambiguous
HOST RESISTANCE	**Black dot**	**Silver scurf**
Full resistance	Unavailable	Unavailable
Differences in susceptibility	Efficient	Efficient
Early maturing cultivars	Efficient	Unknown
OTHER CULTURAL METHODS	**Black dot**	**Silver scurf**
High nitrate and iron soils	Unknown	Efficient
Irrigation	Negative impact	Efficient
Irrigation before harvest	Negative impact	Negative impact
Warm temperatures	Negative impact	Unknown
High bacterial counts	Unknown	Efficient
Early harvesting	Efficient	Efficient
STORAGE	**Black dot**	**Silver scurf**
Short curing	Efficient	Negative impact
Low humidity	Unknown	Efficient
Low temperature	Unknown	Efficient

Table 1.2 Name, fungal target, mode of action and resistance risk in the fungicides used against black dot and silver scurf (adapted from the Fungicide Resistance Action Committee poster).

ACTIVE INGREDIENT	FUNGAL PATHOGEN	MODE OF ACTION	RESISTANCE RISK
Thiabendazole (TBZ)	*H. solani* and *C. coccodes*	Affects cytoskeleton and motor protein	HIGH
Imazalil	*H. solani* and *C. coccodes*	Sterol biosynthesis inhibitor	MEDIUM
Prochloraz	*H. solani* and *C. coccodes*	Sterol biosynthesis inhibitor	MEDIUM
Mancozeb	*H. solani* and *C. coccodes*	Multi-site activity	LOW
Azoxystrobin	*H. solani* and *C. coccodes*	Quinone Outside Inhibitor	HIGH
Fenpiclonil	*H. solani* and *C. coccodes*	MAP/Histidine kinase (Osmotic Signal transduction)	LOW/MEDIUM
Fludioxonil	*H. solani*	MAP/Histidine kinase (Osmotic Signal transduction)	LOW/MEDIUM
Propineb	*H. solani*	Multi-site activity	LOW
Propiconazole	*C. coccodes*	Sterol biosynthesis inhibitor	MEDIUM

1.5. Plant-pathogen interactions

1.5.1. Plant immunity: an overview

Plant diseases are common to all plant species, and they can be caused by multiple pathogens, from viroids to higher plants (Strange and Scott, 2005). They are especially important in crop plants, because they can cause important yield losses that will eventually affect their price or even the availability of food product (Strange and Scott, 2005; Dodds and Rathjen, 2010). Plant pathogens have diverse strategies to successfully infect plant organs. Bacteria usually colonize the apoplast while nematodes possess a stillet that allows them to feed from the plant cells (Jones and Dangl, 2006). Fungi have a particular strategy, since they can penetrate directly plant epidermal cells and extend their hyphae between or through plant cells (Mellersh et al., 2002; Jones and Dangl, 2006). Furthermore, phytopathogenic fungi can be necrogenous saprophytes (they kill the host cell and feed from them), saprotrophic (they usually feed from dead plant organs or substrates, biotrophs (they need a living cell to complete their pathogenic cycle) or hemibiotrophs (they have a biotrophic life style followed by a necrotrophic life style) (Dangl and Jones, 2001). As opposite to animals, which possess mobile defender cells, the plant response to a pathogen relies on local (each cell) immune responses and on signaling molecules that originate from the infected cells and travel to distant cells (Dangl and Jones, 2001; Chisholm et al., 2006). Notably, only specialized parasites can infect plant cells, since plants are usually resistant to most of the pathogens that surround them (Dangl and Jones, 2001). This general resistance relies on the cuticle or suberin from epidermal cells, as well as antimicrobial compounds constitutively present in the host cell (Dangl and Jones, 2001). However, pathogenic microbes are able to enter into the plant tissue and penetrate through the plant cell wall (Chisholm et al., 2006).

Pathogen perception

Upon microbial contact with the extracellular layer of the plasma membrane, the host plant will identify the danger through plant receptors. These plant receptors, called pattern recognition receptors (PRRs), are cell surface proteins possessing an ectodomain facing the extracellular space that recognize pathogen-associated molecular patterns (PAMPs), also called microbial-associated molecular patterns (MAMPs) (Chisholm et al., 2006; Jones and Dangl, 2006; Dodds and Rathjen, 2010; Saijo et al., 2018; van der Burgh and Joosten, 2019). PRRs can also recognize own cell wall degradation products or other host particles from the membrane, also called damage-associated molecular patterns or danger-associated molecular patterns (DAMPs) (Dodds and Rathjen, 2010; Saijo et al., 2018). Several types of ectodomains have been described in plants, the most common being the leucine-rich repeats (LRRs), but also important are the lysin motifs (LysMs), lectin-like motifs and epidermal growth factor (EGF)-like domains (Saijo et al., 2018). Apart from the ectodomain, these receptors have a transmembrane domain, and depending on the presence or absence of a cytosolic kinase domain they can be classified as receptor-like kinases (RLK) or receptor-like proteins (RLP), respectively (Figure 1.9) (Chisholm et al., 2006; Jones and Dangl, 2006; Thomma et al., 2011; Saijo et al., 2018; van der Burgh and Joosten, 2019). RLPs are associated with an adaptor kinase called SOBIR1, and their function is equivalent to the function of the RLKs (Liebrand et al., 2013; Gust and Felix, 2014). The molecular mechanisms triggered by the perception of PAMPs have been largely studied, especially in the model organism *Arabidopsis thaliana* and the bacterial flagellin (Chisholm et al., 2006; Jones and Dangl, 2006; Saijo et al., 2018; van der Burgh and Joosten, 2019). Upon perception, the RLK (or RLP/SOBIR1 complex) will form a complex with other proteins from the CERK (chitin elicitor receptor kinase1) or the SERK (somatic embryogenesis receptor kinase) families (Dodds and Rathjen, 2010; Saijo et al., 2018; van der Burgh and Joosten, 2019). The formation of these complexes leads to the recruitment of another protein in the complex, an intracellular receptor-like cytoplasmic kinases (RLCKs), and phosphorylation (activation) of the proteins of the complex will occur (Dodds and Rathjen, 2010; Saijo et al., 2018). The activation of the RLK or RLP and their complexes will lead to PAMP-triggered immunity (PTI), which include signal transduction activation (MAPK cascade, CDPKs, WRKY transcription factors), calcium influxes, Reactive Oxygen Species (ROS) production, hormone balance, production of defense compounds and metabolic changes, among others (Figure 1.9) (Saijo et al., 2018).

Signal transduction

Quickly upon pathogen perception, an influx of calcium (Ca^{2+}) from the apoplast into the cell occurs, which leads to the activation of Calcium-dependent protein kinases (CDPKs) (Saijo et al., 2018). At the same time, phosphorylation of H^+-ATPases inhibits H^+ effluxes that, in combination with Cl^- and K^+ effluxes, contribute to the alkalinization of the apoplast (Saijo et al., 2018). On the other hand, the phosphorylation of the intracellular RLCK that occurs upon pathogen recognition also triggers the mitogen-activated protein kinase (MAPK) cascade, which includes MAPK, MAPK kinases (MAPKK) and MAPKK kinases (MAPKKK). Different PRR might activate the same MAPK cascades, although some specificity exists between receptors and MAPK activation (Dodds and Rathjen, 2010; Saijo et al., 2018). The MAPK cascade and the CDPKs can act independently or synergistically to regulate transcriptional changes, usually through the de-repression of WRKY transcription factors (Figure 1.9) (Dodds and Rathjen, 2010; Saijo et al., 2018). The regulation of phytohormones, through specific well known metabolic pathways, such as salicylic acid, jasmonic acid and ethylene, is another important aspect associated to plant resistance. Salicylic acid is a local and systemic signal for resistance to biotrophs, while jasmonic acid and ethylene accumulate in order to prevent necrotrophs from colonizing tissues (Jones and Dangl, 2006; Dodds and Rathjen, 2010). Interestingly, these two pathways are coregulated,

and the balance between the two will be used to trigger transcriptomic changes that will give specific resistance responses with the production of different metabolites (Jones and Dangl, 2006).

Defense response

The perception of the pathogen and its signal transduction leads to specific defense reactions, from ROS homeostasis to phytoalexin production. Extracellular reactive oxygen species (ROS) production upon pathogen recognition depends on the NADPH oxidase RBOHD, which is activated by both RLCKs and CDPKs (Figure 1.9) (Saijo et al., 2018). ROS can produce oxidative stress on the pathogen, and if not detoxified, they can affect pathogenesis (Lehmann et al., 2015). However, pathogens usually possess antioxidant compounds that allow them to detoxify host-produced ROS, and thus, they may not be considered as antimicrobial compounds. Instead, they can be regarded as signaling molecules involved in diverse plant responses (Torres, 2010). Their chemical nature allows them to be quickly produced and scavenged, they can be compartmentalized in specific organelles such as the vacuoles and they are transported through cells to interact with multiple specific targets (Lehmann et al., 2015). For example, ROS are involved, together with reactive nitrogen species (RNS), in the hypersensitive response (HR) that leads to programmed cell death (PCD). Furthermore, they can regulate the activation or repression of transcription factors through redox reactions, as well as the post-transcriptional modification of proteins through oxidation or sulfenylation of residues (Lehmann et al., 2015). Notably, an important role of ROS production during pathogen attack is the reinforcement of the cell wall. Upon pathogen perception, peroxidases will be synthesized and secreted to the cell wall, where they will mediate the ROS-dependent cross-linkage of cell wall compounds, such as suberin or lignin components (Almagro et al., 2009). Ultimately, all reactions that take place in an infected cell, including ion effluxes, ROS production, activation of MAPKs and CDPKs and transcriptional changes, will lead to the biosynthesis of defense metabolites, such as phytoalexins or cell wall reinforcing compounds (Figure 1.9) (Saijo et al., 2018).

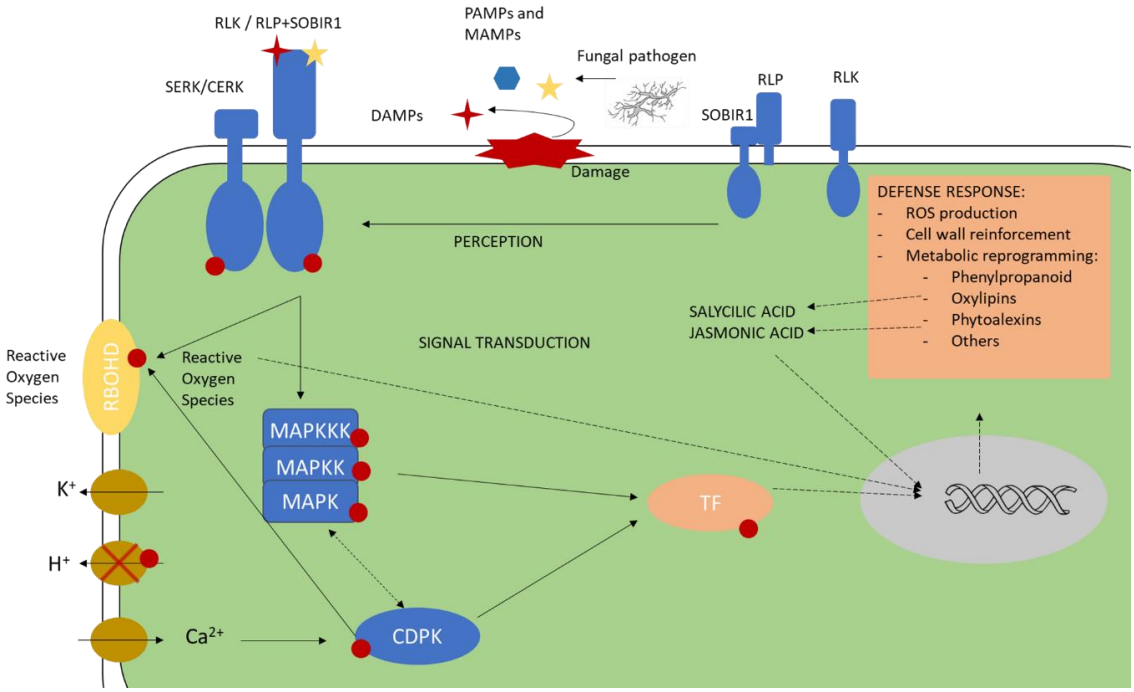

Figure 1.9 An overview of plant-pathogen interactions. Microbe-/Damage/Pathogen-associated molecular patterns (MAMPs, DMPs and PAMPs) are recognized by pattern recognition receptors (PRRs) that leads to the association of RLKs (and RLP/SOBIR1 complexes) and SERKs/CERKs and transphosphorylation of the complexes that start the signal transduction. Signal transduction involves the mitogen-activated protein kinases (MAPK) cascade, calcium-dependent protein kinases (CDPKs) and transcriptional factors (TFs) that leads to the defense response which includes Reactive Oxygen Species (ROS)

production, cell wall reinforcement and metabolic reprogramming. Adapted from *(Dodds and Rathjen, 2010; Corwin and Kliebenstein, 2017; Saijo et al., 2018)*.

Pathogen effectors

Notably, some pathogens have evolved and in order to overcome PTI, they have developed microbial effectors (Dangl and Jones, 2001; Chisholm et al., 2006; Jones and Dangl, 2006; Dodds and Rathjen, 2010; Saijo et al., 2018). Pathogen effectors are molecules synthesized and secreted from the pathogen into the plant cell in order to prevent PTI, and thus result in effector-triggered susceptibility (ETS). Unlike PAMPs, which are conserved among species, effectors are usually species-specific and have diverse functions (Jones and Dangl, 2006; van der Burgh and Joosten, 2019). Gram-negative bacteria deliver their effectors inside the plant cell through the type III secretion system (TTSS), and interfere with PTI at several levels (Jones and Dangl, 2006). On the other hand, fungi do not possess TTSS and their effectors are probably secreted into the apoplast (Chisholm et al., 2006), acting as effectors in the intercellular space or being imported into the plant cell by unknown mechanisms (Jones and Dangl, 2006). In its turn, plants can recognize these effectors through specific receptors, either intracellular receptors for effectors secreted inside the cell, or through cell-surface receptors for apoplastic effectors (Chisholm et al., 2006; Thomma et al., 2011; Saijo et al., 2018). Effectors that are recognized by the host are called avirulence factors (*avr*), and the specific receptors *R* (resistance) proteins (coded by *R* genes) (Jones and Dangl, 2006). The recognition of effectors by plant cells result in a new response called effector-triggered immunity (ETI). PTI and ETI usually involve the same responses, but the response in ETI is stronger and leads to resistance or even local programmed cell death in the hypersensitive response (HR) (Jones and Dangl, 2006), and the interaction is described as incompatible (Desender et al., 2007). Plants and microbial pathogens evolve continuously, triggering respectively new effectors and further receptors that recognize these microbial effectors (Jones and Dangl, 2006). These two types of immunity led to the construction of a zigzag model to explain the plant immune system, in which successive PTI or ETI are triggered by the plant to avoid pathogen colonization, and the delivery of pathogen effectors by the microbes in order to avoid this triggered immunity (Jones and Dangl, 2006; Thomma et al., 2011). An efficient plant response (PTI and/or ETI) that limits the microbial propagation results in plant resistance, which can be categorized as qualitative resistance or quantitative resistance.

1.5.2. Qualitative resistance (gene-for-gene resistance)

Qualitative resistance is defined at the genetic level, in which there are only two classes of individuals (resistant and susceptible) that segregate as simple Mendelian loci (Corwin and Kliebenstein, 2017). Notably, most molecular studies on plant-pathogen interactions have focused on qualitative differences between susceptible and resistant genotypes, unraveling genes implicated in the detection of pathogens and/or effectors. The duality between microbial effectors and plant receptors that specifically recognize the effector, and its genetic characterization, are called gene-for-gene resistance (Flor, 1971). The genes identified in these molecular studies (*R* genes) can directly affect the growth of pathogens, as observed for PR-1 in *Arabidopsis thaliana*, a sterol-binding protein that sequesters sterols from the pathogen in order to limit their growth (Gamir et al., 2017). However, they usually code for proteins that recognize microbial effectors (directly or indirectly), and can be divided as cytosolic nucleotide-binding leucine-rich repeat (NB-LRR) proteins and cell-surface LRR proteins (Chisholm et al., 2006). The recognition of the pathogen leads to expression changes during ETI. These expression changes can lead to programmed cell death (PCR) in the hypersensitive response (HR) or to the accumulation of defense metabolites (i.e. phytoalexins) or hormones involved in the local and systemic disease response, such as salicylic acid (Nawrath and Métraux, 1999). However, resistance conferred by the *R* genes is not durable, because pathogens quickly evolve leading to the emergence of races insensitive to the *R* proteins, resulting in defeated *R* genes (Tan et al., 2008). Stacking of *R*

genes ("functional gene stacking") has been proposed as a tool to avoid this problem (Zhu et al., 2012). However, some *R* genes may be transferred without transferring the trait, if they need related genes (regulatory elements) to express their function (Kushalappa and Gunnaiah, 2013). In potatoes, *R* genes against late blight have been identified (Aguilera-Galvez et al., 2018), but the possession of a single *R* gene is not a sustainable strategy because pathogens quickly evolve to overcome qualitative resistance. For example, the oomycete *Phytophthora infestans* delivers an RXLR effector (Avr2) which interacts with the BSL1 protein of the host cell in order to indirectly suppress immunity by inducing brassinosteroid signaling (Turnbull et al., 2017). An NB-LRR protein (R2) from *Solanum demissum* recognizes the Avr2 effector-BSL1 association (Saunders et al., 2012), and potatoes containing R2 elicit ETI upon *P. infestans* infection leading to the HR, thus controlling infection (Gilroy et al., 2011). However, some *P. infestans* isolates can infect potatoes containing the R2 gene due to the presence of a modified Avr2 effector (Avr2-like), which does still interact with BSL1 but is no longer recognized by R2, thus not triggering ETI (Saunders et al., 2012). This is an example of the evolutionary race between plants and pathogens, and illustrates that qualitative resistance based on a single gene is not a long-term viable approach. Furthermore, introgression of a single gene in potato cultivars is relatively long and affects other characteristics of the plant that are important for potato production (such as yield, tuber quality or starch content.

Plant defense can be considered as a fight between the microbial pathogen and the host plant, in which the latter responds to infection (PTI and ETI) while the former tries to overcome triggered immunity through microbial effectors. As synthesized in the zigzag model, this can result in effector triggered susceptibility (ETS) and disease progression or in effector-triggered immunity (ETI) and hypersensitive response (HR) (Jones and Dangl, 2006). The gene-for-gene resistance focuses on loci that explain the HR in resistant genotypes, and thus, genes involved in resistance are often plant receptors that recognize pathogen effectors (perception of the pathogen). However, the amplitude of the PTI and ETI response depends on both the host and the pathogen (Jones and Dangl, 2006; Kröner et al., 2011), and intermediate disease scenarios can be found between host susceptibility and the HR.

1.5.3. Quantitative resistance

On the contrary to qualitative resistance (gene-for-gene resistance) and incompatible interactions, quantitative resistance results in successful infection of the pathogen (compatible interaction), but its growth and symptoms develop at a lower rate than in interactions with a susceptible host (Kröner et al., 2011). Quantitative resistance is characterized by several genes with small or moderate effect on plant resistance and thus, they may be involved in the signal transduction or the defense response itself rather than the perception of the pathogen (Corwin and Kliebenstein, 2017). It is more durable than qualitative resistance, because it does not rely on a single gene, but their loci are more difficult to identify and to transfer from resistant to susceptible hosts (Ballvora et al., 2002; Bollina et al., 2010). Analysis either by transcriptomics, proteomics or metabolomics, or even a combination of them, help understand the cascade of events that control biochemical processes occurring during plant-pathogen interactions and quantitative resistance (Fiehn et al., 2000). Indeed, transcriptomic analysis has been used to highlight genes upregulated during pathogen attack, especially in the phenylpropanoid pathway, a key metabolic pathway of plants leading to the production of a large panel of metabolites (Fritzemeier et al., 1987; Felix et al., 1991; Schmidt et al., 1998, 1999; Muroi et al., 2009). However, the accumulation of individual metabolites and their correlation with pathogenesis and disease resistance requires other approaches, such as non-targeted metabolomics (Kushalappa and Gunnaiah, 2013). Indeed, untargeted metabolomics approaches has led to the detection of pathogenesis-related (PR) metabolites in different pathosystems, some of them being more abundant in resistant genotypes (resistance-related (RR) metabolites) (Bollina et al., 2010, 2011; Kumaraswamy et al., 2011; Gunnaiah et al., 2012; Pushpa et al., 2014; Yogendra et al., 2015). The use of metabolomics to explain plant

resistance will be detailed in section VI of the introduction of this thesis (1.6: METHODS FOR THE STUDY OF FUNGAL DISEASES IN PLANTS).

1.5.4. Resistance of potatoes to different pathogens

As mentioned, *Solanum tuberosum* L. is a worldwide-cultivated crop with multiple microbial pathogens that cause diseases. The intraspecies genetic diversity (cultivars) allows for differences in quantitative resistance against pathogens, while for qualitative resistant traits, *R* genes found in wild potato species are often introgressed into potato cultivars by classical breeding techniques (Ballvora et al., 2002; Marla, 2017).

Qualitative resistance in potatoes (R genes)

The most important disease of potatoes is late blight, caused by the oomycete *Phytophthora infestans*. More than 20 *R* genes have been identified that confer resistance to this disease in wild potato species, which have been then introgressed to produce potato cultivars with one or more *R genes* (Marla, 2017). These include 11 *R genes* from *Solanum demissum* (R1-11), the first identified source of resistance, but also others from *S. bulbocastanum* (*Rpi-blb1* to *Rpi-blb3*), *S. chacoense* (*Rpi-chc1*) or *S. microdontum* (*Rpi-mcd1*), among others (Tan et al., 2008; Marla, 2017; Aguilera-Galvez et al., 2018). All of the *R genes* against late blight that have been characterized are NB-LRR coding genes that recognize avirulence proteins (effectors) of the pathogen, but resistance-breaking to these genes has appeared in most of them, especially the ones from *S. demissum*, which were the first to be used in agriculture (Marla, 2017). Interestingly, genomic studies have shown that *R genes* and loci involved in quantitative resistance are closely linked (Marla, 2017). *R gene* stacking has been performed in potatoes, and the potato cultivar Sarpo mira contains 5 *R genes* that confers qualitative and quantitative resistance against late blight, being the cultivar with the most durable resistance in the market (Marla, 2017). Resistance to other diseases through *R genes* from wild species has also been described. *R genes* from *S. andigena*, *S. stoloniferum*, *S. phureja* and *S. chacoense* that confer resistance to the most important viral disease of potatoes (PVY) have been introduced to cultivated potatoes (Ry genes), and combining resistance to PVY and late blight in the same cultivar may be an important strategy to control both diseases (Bhardwaj et al., 2007).

Quantitative resistance of potatoes to biotic stresses

The downstream reactions that occur upon pathogen recognition have also been studied in potatoes and related species. Notably, the early defense responses between compatible (susceptibility) and incompatible (qualitative resistance) interactions in the *Solanaceae* genera do not substantially differ (Desender et al., 2007). Indeed, early responses are the same in both type of interactions, regardless of the pathogen or the host species. The differences observed between resistant and susceptible hosts to a pathogen rely on the later responses, which are faster and stronger in incompatible interactions that lead to cell death (HR) (Desender et al., 2007). Notably, this is in accordance with ETI being stronger than PTI (Jones and Dangl, 2006). In quantitative resistance, which involves large sets of genes, resistant hosts will likely have a stronger and faster response than susceptible ones, but the response will probably involve the same reactions, such as transcriptomic and metabolic changes (Kröner et al., 2011). These changes lead to the production of specialized (secondary) metabolites, which are compounds that are restricted to a certain taxonomic group, not essential for growth and produced through varied biosynthetic pathways (Verpoorte, 2000). This is illustrated in the case of the accumulation of individual phenolic compounds upon pathogen detection. Total phenolics, as well as individual phenolic compounds, were induced upon elicitation to different degrees in different cultivars, but production of new metabolites was not detected when potato plants were challenged with necrotrophic or hemibiotrophic pathogens (Kröner et al., 2012). These results suggest that quantitative resistance depends on the accumulation of preexisting phenolic compounds and that

resistance to the bacterial pathogen depends on the final concentration of these molecules (Kröner et al., 2012). It is worth noting that a correlation between defense responses and quantitative resistance was shown for the bacterial pathogen *Pectobacterium atrosepticum* but not for the oomycete *P. infestans*, where defense response and resistance to *P. infestans* negatively correlated (Kröner et al., 2011). Thus, some pathogens are able to progress in host cells with activated defense responses. This observation has led to the hypothesis that these microbial pathogens "escape" from host cells where the defense mechanisms are activated towards neighboring cells without an activated defense response (Kröner et al., 2011). Alternatively, other defense mechanisms than the ones studied on those interactions (activation of the phenylpropanoid pathway) might be involved in the resistance to *P. infestans*. Indeed, metabolomics approaches have identified resistance-related metabolites that can help elucidate quantitative resistance in potatoes, including compounds from the phenylpropanoid pathway, but also others, such as the steroid alkaloids that derive from cholesterol or cycloartenol, or terpenoids or fatty acids from the mevalonate or the MEP pathway (Pushpa et al., 2014; Yogendra et al., 2014, 2015).

Secondary metabolites in the potato tuber and their role in quantitative resistance to biotic stresses

The potato tuber is composed by the periderm (or skin) and the flesh. The flesh of the potato tuber is composed of storage cells that contain high amounts of starch. On the other hand, the potato periderm is richer in secondary metabolites, some of which have an important role in plant protection against biotic and abiotic stresses. The periderm is composed of the phellem, the phellogen (meristematic tissue) and the phelloderm. Phellem cells are surrounded by suberin, a polymer of polyaliphatic and polyaromatic domains that accumulate between the plasma membrane and the primary cell wall (Kolattukudy, 2001; Lulai, 2007). The aliphatic component is a polyester formed by long chain dicarboxylic acids, hydroxy acids, fatty acids and alcohols, and the polyaromatic domain is composed of hydroxycinnamic acid derivatives and glycerol (Kolattukudy and Agrawal, 1974; Graça and Pereira, 2000; Schreiber et al., 2005; Järvinen et al., 2009; Graça, 2015). Furthermore, suberized cell walls also present other materials in their tertiary structure, which are often called "waxes" (Graça, 2015). In the potato periderm, these deposits of waxy layer accounts for 20 % of the tissue weight (Graça and Pereira, 2000). The macrostructure of suberin and the linkage of its monomers is rather controversial because of the lack of technical tools to study the suberin polymer. Despite its complex structure, which protects the plant from most biotic and abiotic stresses, some pathogens have evolved mechanisms to use it as a carbon source (Martins et al., 2014). Chemical studies of suberin need a depolymeryzation step and the study of its monomers or fragments of the suberin polymer from partial depolymeryzation (Wang et al., 2010). Several studies have found that suberin accounts for approximately 25 % of the extractive-free periderm, being 15-20 % of the periderm's dry weight (Kolattukudy and Agrawal, 1974; Graça and Pereira, 2000). The long-chain aliphatic acids are the major monomers found in the suberin macromolecule, and they usually account for 75-90 % of the total suberin content (Graça, 2015). These long-chain aliphatic acids are mostly α,ω-diacids and ω-hydroxyacids, with lower amounts of alkanoic acids and alkanols (Graça and Pereira, 2000; Graça, 2015). In addition, glycerol has been found to account from 5 to 20 % of the suberin monomers. (Graça, 2015). The aromatic domain, which is covalently bound to the primary cell wall, is composed of guaiacyl-monolignols, p-hydroxycinnamic acids and hydroxycinnamic acid amides (Bernards and Lewis, 1998; Mattinen et al., 2009; Macoy et al., 2015). Although present in low quantities, ferulic acid might be important because of its ability to link ω-hydroxyacids and glycerol to other polyaromatics (Graça and Pereira, 2000; Graça, 2015). Similarly, hydroxycinnamic acid amides (HCAAs) are synthesized in the cytosol and delivered to the plasma membrane, possibly through vesicles (Macoy et al., 2015). Interestingly, these HCAAs accumulate in methanol-soluble granules in the inner face of the cell wall outside the plasma membrane, and will be polymerized into the cell wall by the activity of a peroxidase

(Iiyama et al., 1994; Negrel et al., 1996; Macoy et al., 2015). HCAAs are formed by the conjugation of the most abundant hydroxycinnamic acids (feruloyl, caffeoyl, coumaroyl) to aminoacid derived amides such as tyramine, octopamine or putrescine, among others (Macoy et al., 2015; Yogendra et al., 2015): putrescine derivatives found in potato tubers include mainly caffeoylputrescine and feruloylputrescine, as well as low amounts of diferuloylputrescine (Leubner-Metzger and Amrhein, 1993). These compounds have been shown to play a role in the formation of the periderm (Kim et al., 2008), and were increased in leaves upon infection with *Phytophthora infestans* (Keller et al., 1996). Putrescine, which derives from the aminoacid ornithine, is the precursor of spermidine and spermine, two polyamines with several roles in plant growth, protection and development (Takahashi and Kakehi, 2010; Yaakoubi et al., 2014). The conjugation of hydroxycinnamic acids to spermine (also called kukoamines) was first described in *Lycium chinense*, which belongs to the *Solanaceae* family (Funayama et al., 1980, 1995). Interestingly, these kukoamines had a medicinal interest, since they were shown to have hypotensive effects (Funayama et al., 1980) and antitrypanosomal activity (Ponasik et al., 1995). More recently, caffeoyl (or dihydrocaffeoyl) spermine (and spermidine) have been detected in potato tubers (Parr et al., 2005; Huang et al., 2017), but their biological activity *in planta* has not been studied. On the other hand, polyamines derived from the aminoacid tyrosine (mainly tyramine and octopamine conjugated to hydroxycinnamic acids) have also been found in potato, as well as in other crop plants (Yogendra et al., 2014; Huang et al., 2017). Feruloyltyramine and feruloyloctopamine have been found to be more abundant in russeted skins and in scab-infected potato tubers (King and Calhoun, 2005; Huang et al., 2017), and they play a role in periderm formation after wounding (Huang et al., 2017). In general, HCAAs are believed to play a role in cell wall thickening, but the production rate of HCAAs during pathogen infection exceeds the rate of incorporation to the cell wall, indicating that free HCAAs might have a different role during pathogen infection (Macoy et al., 2015). As soluble components, the most abundant secondary metabolites found in the potato skin are phenolic compounds, a very heterogenous class of metabolites, which can be divided into phenolic acids (C_6-C_1 and C_6-C_3 structures) and flavonoids (C_6-C_3-C_6 structures) (Schieber and Saldaña, 2008). Phenolic acids include hydroxycinnamic acids (HCAs) and hydroxybenzoic acids, which share part of their biosynthetic pathway. Indeed, phenylpropanoid biosynthesis starts with the conversion of phenylalanine into cinnamic acid through the phenylalanine ammonia-lyase (PAL) enzyme. Cinnamic acid is the precursor of p-coumaric acid, caffeic acid, ferulic acid and sinapic acid, through the action of hydroxylases and methyltransferases. All these hydroxycinnamic acids can be conjugated to a CoA, which will be the precursors of the most abundant HCAs, but also the HCAAs. Coumaroyl-CoA, Feruloyl-CoA and Caffeoyl-CoA can be conjugated to quinic acid to produce caffeoylquinic acid, coumaroylquinic acid and feruloylquinic acid. The most abundant phenolic compound in potato tubers is 5-O-caffeoylquinic acid, also called chlorogenic acid, which represents up to 90% of the total phenolic content (Friedman et al., 1997). Other two isomers of chlorogenic acid, neochlorogenic acid (3-O-caffeoylquinic acid) and cryptochlorogenic acid (4-O-caffeoylquinic acid) have been found in potato tubers, although in lower quantities (Griffiths and Bain, 1997). Furthermore, caffeoylquinic acids can form homodimers (Huang et al., 2017), and dicaffeoylquinic acid and feruloylcaffeoylquinic acids have also been detected in potato tubers (Yogendra et al., 2014, 2015). Other hydroxycinnamic derivatives detected in potato include glycoside conjugates of caffeic acid, sinapic acid and ferulic acid, as well as other hydroxycinnamic acid conjugates (Yogendra et al., 2014, 2015). Furthermore, coumaroyl-, sinapoyl- and coniferyl-alcohols, which are the monomers of lignin, but that are also precursors of coniferin and syringin, among others, have been found in potatoes (Yogendra et al., 2014, 2015). Moreover, coumaroyl-CoA and feruloyl-CoA are precursors of the coumarins, which are secondary metabolites produced in a wide range of plant species (Yang et al., 2016). The hydroxycoumarin umbelliferone was detected in wild potato species with resistance to Colorado Potato Beetle (Tai et al., 2014), while the coumarin scopoletin and two coumarin glycosides (scopolin and fraxin), were

found in tetraploid or diploid potatoes of advanced breeding programs and were identified as resistance-related compounds against late blight (Yogendra et al., 2014, 2015). Hydroxybenzoic acids have also been found in potato plants. Salicylic acid, an important plant metabolite involved in disease resistance, is produced from cinnamic acid and benzoic acid in tobacco and potato (Yalpani et al., 1993; Coquoz et al., 1998). Furthermore, healthy potato tissues contain high amounts of salicylic acid glycoside, and salicylic acid accumulates upon the biotic elicitor arachidonic acid treatment (Coquoz et al., 1995). The other hydroxybenzoic acids, such as the vanillic acid, protocatechuic acid and syringic acid probably derive from the removal of a 2-carbon fragment of the corresponding hydroxycinnamic acid, although methylation and hydroxylation of protocatechuic acid to form vanillic acid and gallic acid, respectively, occur in some species (el-Basyouni et al., 1964). Alternatively, gallic acid is produced through the oxidation of 3-dehydroshikimate (Tejeda et al., 2014). These hydroxybenzoic acids have been detected in potato tubers, although usually in low amounts (Schieber and Saldaña, 2008). On the other hand, coumaroyl-CoA is the precursor of all flavonoids through the production of naringenin chalcone. A chalcone isomerase transforms naringenin chalcone in naringenin, which is the precursor of flavones, flavonols, flavanones and anthocyanins. In potatoes, the flavanones naringenin, hesperitin and eriodyctiol, as well as their conjugates, have been detected (Lewis et al., 1998; Yogendra et al., 2015). Naringenin is also the precursor of the flavone apigenin, which can be hydroxylated to produce luteolin or glycosylated to produce vitexin. Vitexin and luteolin and their glycoside conjugates have been detected in potato leaves, and been involved in resistance to late blight caused by *Phytophthora infestans* (Yogendra et al., 2014, 2015). Hydroxylation of naringenin produces dihydrokaempferol, which can be further hydroxylated to produce dihydroquercetin and dihydromyricetin; all three molecules are the precursors of other important flavonoids. Both apigenin and dihydrokaempferol are precursors of kaempferol, which can be conjugated to sugar moieties to produce kaempferol glycosides. Among them, kaempferol-3-rutinoside, also called nicotiflorin, has been detected in potato tubers (Lewis et al., 1998; Kröner et al., 2012) and other kaempferol glycosides have been identified in potato leaves (Yogendra et al., 2014, 2015). Quercetin can be produced from kaempferol or dihydroquercetin, and quercetin glycosides have been found in potatoes. The most abundant flavonoid glycoside in potatoes is quercetin-3-rutinoside (also called rutin), but other quercetin glycosides have been also detected (Kröner et al., 2012; Yogendra et al., 2014, 2015; Hamzehzarghani et al., 2016; Huang et al., 2017). On the other hand, myricetin glycosides have not been detected in potatoes so far. Rutin, but not nicotiflorin, was shown to possess antimicrobial activity against the bacterial pathogen *P. atrosepticum* but not against the oomycete *P. infestans in vitro* (Kröner et al., 2012). The dihydroflavonols are also the precursors of anthocyanidins, the aglycones of anthocyanins, which are the responsible of the tuber color. Dihydrokaempferol is the precursor of pelargonidin, dihydroquercetin is the precursor of cyanidin and peonidin, and dihydromyricetin is the precursor of delphinidin, petunidin and malvidin. The most common anthocyaninidins in coloured potatoes are peonidin, malvidin, petunidin and pelargonidin, which are conjugated to sugars and that are often acylated with a hydroxycinnamic acid (Lewis et al., 1998). Red tubers mainly contain pelargonidin and peonidin glycosides, light blue tubers contain petunidin and small amounts of malvidin glycosides, and dark blue tubers contain petunidin and high amounts of malvidin glycosides (Lewis et al., 1998). On the other hand, dihydroquercetin is the precursor of catechin and epicatechin gallate, and dihydromyricetin is the precursor of gallocatechin and epigallocatechin gallate. These flavonoids have been detected in potato leaves and been involved in resistance to *Phytophthora infestans* (Lewis et al., 1998; Henriquez et al., 2012; Yogendra et al., 2014, 2015). Cultivated potatoes also contain low amounts of glycoalkaloids, mainly α-chaconine and α-solanine, which represent at least 95% of the total glycoalkaloid content in commercial potatoes (Friedman et al., 1997). These two glycoalkaloids share the same aglycone, solanidine, which is produced from cholesterol through the cycloartenol precursor. The difference between α-chaconine and α-solanine relies on the sugar moiety attached to

the aglycone. α-chaconine possesses a β-chacotriose (bis-α-L-rhamnopyranosyl-β-D-glucopyranose) side chain attached to the 3-OH group of the solanidine aglycone, while α-solanine possesses a β-solatriose (α-L-rhamnopyranosyl-β-D-glucopyranosyl-β-galactopyranose) at the same position of the solanidine aglycone (Friedman, 2006). The degradation of these glycoalkaloids occurs through acid hydrolysis or enzymatic cleavage of the sugar moieties, and produce β- and γ-chaconines and solanines, and finally, the aglycone solanidine (Ripperger, 1998). These degradation products may be present in low amounts in potato tissues (Friedman, 2006). Total glycoalkaloid content varies among potato cultivars, plant tissues and environmental conditions (Friedman et al., 1997; Friedman, 2006; Krits et al., 2007; Mariot et al., 2016). Leaves can accumulate high amounts of glycoalkaloids, especially upon pathogen attack, but also upon other abiotic stresses (Mariot et al., 2016). However, highest amounts of glycoalkaloids in potato plants are found in flowers and unripe fruits (Friedman, 2006). In tubers, glycoalkaloids are mainly present in the phelloderm, and only lower amounts are found in the parenchyma of cultivated potatoes (Friedman et al., 1997; Friedman, 2006; Krits et al., 2007). Furthermore, total glycoalkaloid content in potato tubers must be lower than 20mg/100 g FW due to its toxicity (Valkonen et al., 1996). Indeed, rabbits fed on high-glycoalkaloid potatoes experienced diarrhea, weight loss and hemolytic anemia (Azim et al., 1982, 1983, 1984), and glycoalkaloid poisoning in humans results in gastrointestinal disorders, confusion, convulsions, coma and even death (Smith et al., 1996). Thus, the production of commercial potato tubers has driven the selection towards cultivars with low solanidine glycoalkaloid content (Ramsay et al., 2005). On the other hand, leaves of wild potato species (*Solanum chacoense*) also contain commersonine and demissine (which contain the demissidine aglycone attached to a commertetraose or a lycotetraose, respectively) and dehydrocommersonine (the aglycone dehydrodemissidine attached to a commertetraose) (Friedman, 2006). However, these glycoalkaloids are not found in cultivated potato tubers (Friedman, 2006). The unsaturated aglycone solanidine is produced from cholesterol, while the saturated aglycone demissidine is produced from cholesteranol. Other potato glycoalkaloid are found in wild species, but not in the cultivated *Solanum tuberosum L*. These glycoalkaloids include the leptines (I and II) and leptininines (I and II), which possess the chacotriose and solatriose moieties attached to the aglycone leptinidine (23-hydroxysolanine) or 23-acetylleptinidine (Friedman et al., 1997; Friedman, 2006; Krits et al., 2007). Furthermore, related species of the *Solanaceae* family contain other glycoalkaloids, such as α-tomatine or dehydrotomatine in *Solanum lycopersicum* or solasonine and solamargine in eggplant (Friedman, 2006). Cycloartenol, a precursor of solanidine alkaloids, is also the precursor of furastanol and spirostanol-type saponins. These molecules contain several glycosidic moieties attached to a furastanol (or furostenol) or spirostanol (or spirostenol) backbone, often hydroxylated in several positions. This is the case of protodioscin, a trisaccharide attached to a 26-(beta-D-glucopyranosyloxy)-3beta,22-dihydroxyfurost-5-ene backbone, found in several plant species, most notably in *Tribulus terrestris*, a medicinal plant found in Southeast Europe and Asia (Dinchev et al., 2008). Furthermore, protodioscin and methylprotodioscin have recently been found in potato peel extracts (Huang et al., 2017).

1.6. Methods for the study of fungal diseases in plants

1.6.1. Methods for pathogen detection

Detecting a plant pathogen that may cause important food losses is essential for agriculture, since early detection can help preventing the onset of the disease (Lau and Botella, 2017). In order to detect pathogens from field samples, several techniques are currently used, including immunofluorescence, fluorescence *in-situ* hybridization (FISH), enzyme-linked immunosorbent assay (ELISA), gas chromatography-mass spectrometry (GC-MS) or flow cytometry (FCM) (Fang and Ramasamy, 2015). Furthermore, other indirect methods using imaging techniques may be used in the future to detect plant diseases, which would be useful due to the rapid data analysis and the unnecessity of trained

laboratory personnel (Fang and Ramasamy, 2015). However, the most used method to detect plant pathogens is polymerase chain reaction (PCR)-based analysis, which is highly sensitive and specific (Mullis et al., 1986). Furthermore, quantification of DNA can be performed by real-time PCR assays, that have been developed for a number of plant pathogens, including several soil-borne potato pathogens (Brierley et al., 2009). Although this is usually the method of choice for quantifying plant pathogens in the field, it requires laboratory equipment and specialized personnel. Thus, other methods based on the PCR principle are being adapted for their use in the field (Lau and Botella, 2017).

In research, sensitive detection of the pathogen causing a disease is essential. Symptoms of the disease can be visually evaluated in order to determine the incidence and severity of the disease. However, identification of the pathogen causing the disease needs molecular diagnosis techniques, mostly PCR-based analysis. PCR analysis relies on the amplification of DNA sequences and thus, it is very sensitive and can be extremely specific if the designed primers are specific to the pathogen species. In some cases, PCR detection can discriminate amongst isolates of the same pathogen species, such as in the case of thiobendazole-resistant and thiobendazole-sensitive isolates of *H. solani* (Errampalli et al., 2001b). Indeed, specific primers to detect *Colletotrichum coccodes* (causing black dot in potatoes) and *Helminthosporium solani* (causing silver scurf in potatoes) have been developed for both conventional and real-time PCR (Olivier and Loria, 1998; Cullen et al., 2001, 2002; Errampalli et al., 2001a; Brierley et al., 2009). Both PCR methods are based on nested PCRs to ensure specificity, with two successive PCRs amplifying a 350 – 500 base pairs of the ITS1/ITS2 region (Errampalli et al., 2001a; Cullen et al., 2002).

1.6.2. Methods for the study of the infection process

Fungal pathogens that cause diseases on plants need to penetrate from the surface into the plant tissue. In general, plants have cuticle or suberin on the surface of their tissues that prevent the infection of most pathogens (Dangl and Jones, 2001). Nonetheless, specific pathogens will be able to successfully penetrate through the host physical and chemical barriers and further develop in host plant cells. The fungal infection process consists of three phases: fungal spores that are transported through wind, water or are present in the soil get in contact with the plant surface and germinate; subsequently, there is an enzymatic or mechanical penetration into the plant tissue, or an entrance through natural orifices (stomata or wounds); finally, penetration into the host cells and intracellular or extracellular progression through the plant tissue (Struck, 2006). The infection process can be evaluated at the different stages using different methods, including morphological, biochemical and molecular methods (Hardham, 2007). Recently, molecular genetics have been used to identify the tools used by fungal pathogens to penetrate and infect plant tissues (Struck, 2006). However, the most used technique to describe infection processes are morphological and cytological studies using optic microscopy, confocal microscopy or electron microscopy (Hardham, 2007, 2012). These techniques allow the visualization of the fungal structures (spores, hyphae), the fungal hyphae in the plant cells and the impact on the host (Read, 1991a; Zeyen, 1991; Magliano and Kikot, 2010; Minker et al., 2018). In potato skins, light and electron microscopy were used to detail the germination process, appressorium formation and periderm penetration of *H. solani* (Heiny and McIntyre, 1983; Martinez et al., 2004). Furthermore, the microscopic study of plant-pathogen interactions has been used to describe the infection process of fungal pathogens at different physiological stages or between susceptible and resistant genotypes, such as for the case of downy mildew in grapevine (Alonso-Villaverde et al., 2011; Gindro et al., 2012b).

1.6.3. Methods to study the epidemiology of plant fungal diseases

Knowledge of the life cycle and the epidemiology of diseases in crops is often essential to develop an integrated pest management strategy. The epidemiological study of fungal plant diseases include

several topics, such as diagnosis, infection process, pathogen population dynamics or disease resistance, among others (Cooke et al., 2006). In order to describe the disease cycle, the most important phases are inoculation (infection), colonization (invasion), reproduction and dissemination of the pathogen (Agrios, 2005). The study of these phases, as well as the conditions that favor each of them are the primary interest of epidemiological studies of plant diseases.

Source of inoculum

Infection of plants with pathogens can occur virtually at any time of the plant cycle, even after harvest. In general, pathogens can be classified according their origin as soilborne, seedborne, airborne or insect-borne, among others. At a given time, the pathogen will encounter the host and initiate the infection. In fungal pathogens, spores, sclerotia or mycelial fragments can initiate infection, and are called the *inoculum* (Agrios, 2005). The source of the primary inoculum is the most important phase, because limiting the primary inoculum can prevent the disease in the field. Determining the importance of the different possible origins of the primary inoculum is usually achieved through field or greenhouse experiments, in which naturally present inoculum or artificially added inoculum in the different sources is used. The visual evaluation of the disease incidence is normally used to determine the importance of each source of inoculum, but molecular biology techniques can be used in order to quantify the source of inoculum and correlate it to the disease severity (Denner et al., 1998; Nitzan et al., 2005, 2008; Rennie and Cokerell, 2006; Lees et al., 2010; Dung et al., 2012).

Climatic and pedoclimatic conditions and cultural control methods

The climatic and pedoclimatic conditions during plant growth have an important effect on plant development, but also in disease development. These conditions are important throughout the disease life cycle, and can affect the infection process, the colonization or the dissemination of the pathogen. Fungal pathogens usually require high humidity for the germination process, as well as the production of spores for its dissemination. Meteorological data collected near field sites were disease symptoms are regularly evaluated can be used to highlight conditions that favor the distinct phases of the disease life cycle. Furthermore, they can be integrated in mathematic models that can be used to forecast the development of the disease and prevent its development and dispersal (Pinzón et al., 2009; Gusberti et al., 2015; Jarroudi et al., 2018; Newlands, 2018). Furthermore, controlled greenhouse experiments in which a single factor is altered can be used to highlight the importance of these factors, such as temperature or irrigation (Lees et al., 2010).

1.6.4. Metabolomics to study plant resistance to fungal pathogens

Metabolomics is the detection and quantification of the observable metabolome from a living organism; practically, it intends to detect and quantify a maximum of small molecules in a given biological sample (Wolfender et al., 2013). These small molecules are, essentially, secondary metabolites (also called specialized metabolites), organic compounds synthesized by living organisms that are not essential for growth, development or reproduction (unlike primary metabolites) but that play an important role in mediating the ecological interactions of the organism (Li et al., 2018). Metabolomic studies are nowadays routinely used to assess chemical diversity of plants or assess their growth (Schauer and Fernie, 2006; De Vos et al., 2007). However, its use in plant-pathogen interactions has only recently emerged (Aliferis et al., 2014). Nonetheless, it has already been successfully used to highlight metabolites involved in the response to pathogens in both compatible and incompatible interactions (Gindro et al., 2012a; Marti et al., 2014; Castro-Moretti et al., 2020). Metabolic profiling of fungal pathogen-plant interactions has also been used, mostly in the past decade, to determine the infection mechanism of the pathogen and the response of the plant host (Chen et al., 2019).

Metabolomics studies can be divided into untargeted and targeted approaches (Castro-Moretti et al., 2020). Untargeted metabolomics is a qualitative approach to perform a global profile of the plant-

pathogen interaction, potentially identifying novel defense compounds, such as has been shown in canola roots infected with *Plasmodiophora brassicae* (Pedras et al., 2008). The analytical method used for untargeted metabolomics needs to be able to detect and quantify a wide range of metabolic classes while showing high sensitivity, resolution and repeatability (Wolfender et al., 2013). The most common approaches used in plant metabolomics are based on Nuclear Magnetic Resonance (NMR) and Mass Spectrometry (MS) detection. NMR is the method of choice in order to chemically characterize a pure compound, because it allows the accurate elucidation of the physicochemical and spectroscopic properties of the metabolite (Wolfender et al., 2019). However, this approach requires the previous isolation of the compound of interest from the crude extract, which can be highly time-consuming and expensive. NMR metabolomics can also be used directly on crude extracts, resulting in a metabolic fringerprint, a reproducible method that allows quantification of the detected metabolites. However, this method has low resolution and sensitivity, and is therefore less used than other analytical methods (i.e. MS-based metabolomics) (Wolfender et al., 2013). MS relies on the ionization of molecular species at the ion source and the separation and detection of the ions based on their mass-to-charge ratio (*m/z*). Additionally, tandem mass spectrometry (MS/MS) can be used to gain structural information of the metabolites by studying their fragmentation pattern upon collision induced dissociation (CID) (Wolfender et al., 2013). High sensitivity can be obtained with MS methods are, specially using high-resolution mass analyzers (HRMS), which can be used directly in crude extracts or without sample extraction (Wolfender et al., 2019). However, MS-based metabolomics are most often found coupled to a separation system, such as Gas Chromatography (GC) for volatile organic compounds and semi-volatile compounds (often derivatized primary metabolites) or Liquid Chromatography (LC) for non-volatile compounds. These hyphenated systems allow the detection, quantification and identification of a broad range of compounds, and their main advantages are the separation of isomers and the diminution of ion suppression (Wolfender et al., 2013).

Metabolomics studies are often untargeted in order to cover the largest possible group of metabolites from a specific plant species, or to highlight metabolites upregulated in a specific situation. However, in some cases, the study of a known metabolite (or group of metabolites) may be of interest, in which case the use of targeted metabolomics is selected because of its higher sensitivity. Targeted metabolomics analysis is a quantitative approach, where a limited number of known compounds are quantified in a given situation (i.e. plant-pathogen interaction). For example, this strategy is used to quantify known phytoalexins, defense compounds that are produced upon pathogen infection, such as for the case of camalexin and indole glucosinolates, which are produced in *Arabidopsis thaliana* against *Phytophthora brassicae* (Schlaeppi and Mauch, 2010).

Experimental design

A critical aspect of metabolomics in plant-pathogen interactions is the experimental design. Factors such as host genotype(s), pathogen isolate, plant tissue or time are crucial factors to consider. Different genotypes of the same host species can be used to determine different host reactions, either using wildtype and mutants in model plants to study a single gene (qualitative resistance), or cultivars of the same plant species with a more complex genetic diversity to study aspects related to quantitative resistance. On the other hand, using different isolates of a pathogen with different virulence levels can be used to unravel pathogenesis-related pathogen metabolites. Similarly, a dynamic evaluation of the metabolome of the host plant following pathogen inoculation might be useful to identify metabolites involved in the plant-pathogen interactions at different stages. In any case, a sufficient number of replicates is necessary to obtain significant data, a number that depends on the experimental design. In controlled conditions, less than five replicates result in inaccurate statistical results (Chen et al., 2019), but this number must be increased when some factors are not fully controlled (i.e. in field

experiments) (Wolfender et al., 2013). Altogether, all these factors need to be considered for a successful use of metabolomics in studying plant-pathogen interactions.

Sample preparation

The validation of the experimental design should include a morphological assessment to confirm the absence or presence of the disease (depending on the experimental design) in the biological samples that will be used for the metabolomics study. Once this is established, sample preparation is the next step to consider. Upon sample collection at the desired time point, samples should be immediately frozen in liquid nitrogen to quench all enzymatic reactions and be kept at temperatures lower than -60 °C (Wolfender et al., 2013; Chen et al., 2019). Furthermore, a step to remove degrading enzymes should be used to prevent metabolite degradation, such as grinding under liquid nitrogen or lyophilizing. The choice of solvent for the metabolomics extraction is also important, since extracting all metabolites with a single extraction procedure is practically impossible (Choi and Verpoorte, 2014). Thus, the extraction method(s) should be designed depending on the purpose of the project. Furthermore, the use of a molecule not present in the biological sample as an internal standard is useful to calculate the losses that may occur during sample preparation. Furthermore, one or multiple Quality Control (QC) sample(s) (consisting of a pool of all samples) should be included in the analysis to detect the instrument's intrinsic variability (Wolfender et al., 2013).

Data acquisition

Once extracted with the adequate sample preparation, metabolites can be separated and detected using different strategies. Among them, the gold standard for metabolite profiling are those hyphenated to mass spectrometry (MS), especially GC-MS and LC-MS (Wolfender et al., 2013, 2019). GC-MS methods are often used to detect volatile organic compounds, and have been successful in identifying antifungal metabolites from various microorganisms (Azzollini et al., 2018; Chinchilla et al., 2019). Alternatively, GC-MS can also be used to detect (previously derivatized) primary metabolites, such as fatty acids or suberin monomers (including fatty acids, diacids and hydroxyacids, among others) (Company-Arumí et al., 2016). On the other hand, LC-MS methods are the most commonly used for metabolite profiling of a wide panel of secondary metabolites (Wolfender et al., 2019). The state-of-the-art profiling method is that using ultrahigh-pressure liquid chromatography (UHPLC) hyphenated to a high resolution mass spectrometer (HRMS) that provides MS and MS/MS spectra (Wolfender et al., 2019). The hyphenated LC-MS systems requires the optimization of the LC conditions, which can increase the number of metabolites detected in the analysis. Optimization of the separation includes the choice of the stationary phase and the mobile phase. In general, LC-MS plant metabolomics use C18 reverse phase (RP) columns and broad organic – aqueous gradients (i.e. methanol – water or acetonitrile – water) with acidic modifiers (such as formic acid) to ensure good separation and/or ionization(Wolfender et al., 2013). Using UHPLC and sub-2 µm particle size short columns, metabolomics analysis with less than 10 min runtime can achieve acceptable chromatographic resolution of plant extracts, allowing the high-throughput analysis of large batches of samples (Wolfender et al., 2019). On the other hand, the MS conditions will also determine the detection of the metabolites separated during the LC, since MS detection is not a universal detection system. Ionization of the compounds is usually achieved by electrospray ionization (ESI), which can be run in positive ionization (PI) and negative ionization (NI) modes. In PI mode, metabolites are protonated at low pH ($[M+H]^+$), while metabolites are deprotonated in NI mode ($[M-H]^-$). Some compounds are better ionized in positive ion (PI) mode (i.e. alkaloids) while others are better ionized in negative ion (NI) mode (i.e. phenolics), and thus, a comprehensive metabolomics study should include both PI and NI modes to ensure the widest detection of metabolites in a biological sample (Wolfender et al., 2013). Moreover, the use of HRMS mass analyzers (i.e. Orbitrap) that combine high mass accuracy with a high frequency of acquisition is essential to detect the largest number of metabolites possible (Wolfender

et al., 2019). Furthermore, the acquisition of MS/MS spectra of the detected molecules is a useful tool, since it provides structural information which can be used for metabolite annotation (Wolfender et al., 2019).

Data processing and analysis

Untargeted metabolomics analysis yields complex and large amount of data, and metabolite profiling data need to be pre-processed to provide the information required for data analysis. This pre-processing step include baseline correction, noise filtering, peak detection, deconvolution and peak alignment, among others (Chen et al., 2019; Wolfender et al., 2019). These steps can be performed with multiple software platforms, including free-software such as MzMine (Katajamaa et al., 2006; Pluskal et al., 2010). The pre-processed data sets ultimately lead to peak-picking of all features that form a matrix which can then be subjected to multivariate data analysis. These include the use of unsupervised models, such as principal component analysis (PCA) or hierarchical cluster analysis (HCA), and supervised models, such as partials least-squares discriminant analysis (PLS-DA), for example (Chen et al., 2019). Unsupervised methods try to find patterns among the analyzed samples without *a priori* information about them, such as genotype or pathogen infection. They are usually the first-choice on metabolomics data because they give an overview of the dataset and allow to detect outliers or confirm the robustness by observing the stability of Quality Control (QC) samples regularly injected during the analysis (Wolfender et al., 2013). Furthermore, they can be useful in detecting biomarkers in some conditions in which biomarkers arise from these unsupervised methods. However, unsupervised methods may also result in groupings that do not fit the experimental design. Supervised methods, in which the knowledge of the dataset (i.e. genotype or infection status) is included in the analysis, may be of help in these cases. Among them, partial least squares (PLS)-based methods are the most commonly used in metabolomics studies, and include PLS discriminant analysis (PLS-DA) and orthogonal PLS (OPLS) algorithms (Wolfender et al., 2013). Recently, a method that combines the ANOVA-based partitioning of the variance in submatrices and the supervised multivariate analysis of these matrices has been described as the ANOVA Multiblock Orthogonal Partial Least Squares (AMOPLS) (Boccard and Rudaz, 2016). This statistical tool allows the use of a single model to analyze a complex dataset and identify the effect of each factor, as well as highlight biomarkers, specific of each condition. Notably, it has been used both in human metabolism studies (González-Ruiz et al., 2017; Gagnebin et al., 2020) and in the analysis of fungal metabolite production (Azzollini et al., 2018), and its use in plant metabolism is foreseen in the near future, especially in plant-pathogen interactions, since it applies perfectly to the experimental design of these multifactorial experiments. Altogether, these methods are used to detect biomarkers that correlate with a factor of the statistical model (i.e. fungal infection or resistance). In plant-pathogen interactions, biomarkers are usually divided in those that indicate the presence of the disease (pathogenesis-related metabolites) and those that correlate with disease resistance (resistance-related metabolites).

Metabolite annotation and identification

Unambiguous identification of the features detected in a metabolomics study can be achieved *via* comparison of the retention time, MS and MS/MS data of a reference standard (Schymanski et al., 2014), or *via* isolation and *de novo* characterization of the metabolites of interest. However, untargeted metabolomics studies are often designed to monitor a high number of metabolites, and unambiguous identification of all these metabolites is an issue. On the other hand, the rapid identification of already known metabolites from a natural sample is called “dereplication” (Hubert et al., 2017), which results in the “annotation” of metabolites. Even without unambiguous identification, metabolite annotation is still a challenging aspect in untargeted metabolomics experiments where thousands of metabolites are potentially detected (da Silva et al., 2015). Depending on the available information, different confidence levels of identification can be proposed (Table 1.3) (Schymanski et

al., 2014). The lowest level of confidence (Level 5) is the exact mass, which is recorded by high resolution mass spectrometry instruments. With additional information, such as the isotopic pattern, the correct molecular formula can be filtered by using the seven golden rules for heuristic filtering of molecular formulas (Kind and Fiehn, 2007), yielding a higher level of confidence (Level 4). Comparing the MS/MS spectral information to spectral databases can strengthen the confidence in the annotation, either to a probable structure (Level 2) if the spectrum data unambiguously matches a structure from an experimental database, or a tentative candidate (Level 3) if the possible structure(s) is not unambiguously referred to a single structure. As already mentioned, the confirmed structure level of confidence (Level 1) is only achieved *via* a reference standard (Schymanski et al., 2014). Level 2 requires the MS/MS spectral match with an experimental database, but there is limited experimental information available, which often leads to a small number of Level 2 identified compounds (Allard et al., 2017). Alternatively, mass spectra can be compared to *in silico* databases, which increase the annotation coverage (Allard et al., 2016). However, these annotations remain as tentative candidates ("putative annotations"), often with several putative structures for each feature. Multiple subclassifications that can be made in this class (Schymanski et al., 2014), by using additional information to increase the confidence of the annotation. For example, taxonomical information of the extract analyzed can increase the confidence in the annotation (Rutz et al., 2019). Recently, a method to cluster features with similar MS/MS spectra, called molecular networking (MN), has been developed (Watrous et al., 2012). The different features of a crude extract are linked in the network depending on their MS/MS spectral similarity, yielding clusters of metabolites with similar fragmentation patterns. The use of *in silico* fragmentation methods coupled with MN has been proposed to further propagate metabolite annotation (Silva et al., 2018). These tools are mainly used in metabolomics studies of plant extracts with pharmacological interest (Raheem et al., 2019; Zhou et al., 2019). However, combining all the currently available methods can increase the confidence in metabolite annotation in all metabolomics experiments, including in studies of plant-pathogen interactions, which will help unravel the biological reactions that occur during plant pathogenesis.

Table 1.3 Proposed identification confidence levels in high resolution mass spectrometry according to *(Schymanski et al., 2014)*.

LEVEL	IDENTIFICATION CONFIDENCE	MINIMUM DATA REQUIREMENTS
Level 1	Confirmed structure (by reference standards)	MS, MS^2, RT, Reference Std
Level 2	Probable structure	MS, MS^2, Library MS^2 or exp. MS^2
Level 3	Tentative candidate(s)	MS, MS^2, exp. MS^2
Level 4	Unequivocal molecular formula	MS isotope/adduct
Level 5	Exact mass of interest	MS

Identification and validation of pathogenesis biomarkers

Multivariate data analysis, molecular networking, and metabolite annotation are tools to highlight and identify biomarkers of biological relevance. In the study of plant-pathogen interactions, the interest relies in identifying pathogenesis-related compounds. The concept of pathogenesis-related metabolites is similar to the concept of pathogenesis-related proteins (PR proteins), which accumulate upon pathogen infection or abiotic stress and are essential for the immune response (Jain and Khurana, 2018). However, the term resistance-related metabolite (*RR* metabolites) is often used, similarly to the concept resistance-related genes or simply, resistance genes (*R* genes). However, the concepts of *R* genes and *PR* proteins define proteins and genes involved in qualitative resistance, and are usually involved in the recognition of the pathogen (Jones and Dangl, 2006). On the other hand, *RR* metabolites can be involved in the downstream process of plant defense (Corwin and Kliebenstein, 2017), in both qualitative and quantitative resistance responses. A general definition for *RR*

metabolites is “a metabolite with higher abundance in resistant genotypes than in susceptible cultivars” (Bollina et al., 2010), and is calculated as the ratio between a resistant genotype and a susceptible genotype. However, in a multifactorial experiment with at least two factors (genotype and inoculation), several *RR* values can be calculated. In a simple model with two genotypes (resistant and susceptible) and a pathogen inoculation (mock or pathogen inoculated), four values can be calculated: resistant mock-inoculated (RM), susceptible mock-inoculated (SM), resistant pathogen-inoculated (RP), and susceptible pathogen-inoculated (SP). The ratio of abundances between genotypes and conditions gives an *RR* score. The Resistance-Related Constitutive metabolites (RRC) are those metabolites with higher abundance in the resistant genotype than in the susceptible genotype under mock-inoculated conditions (RM/SM) (Hamzehzarghani et al., 2008, 2016; Bollina et al., 2010). The ratio of abundances between inoculated and non-inoculated samples of the same genotype can be calculated to form Pathogenesis-Related (PR) metabolites in resistant (PRr = RP/RM) or susceptible cultivars (PRs = SP/SM) (Bollina et al., 2010). These metabolites are involved in the reaction of the plant to the pathogen in a specific genotype background. Finally, the resistance-related induced (RRI) metabolites can also be highlighted in induced conditions. In this case, several scores can be calculated: some authors distinguish quantitative RRI (RP/SP) from qualitative RRI ((RP/RM)/(SP/SM)) (Pushpa et al., 2014). The former does not take into consideration the induction of the metabolite upon pathogen inoculation, but rather the final concentration of the compound on infected tissues. The latter takes into consideration the induction, but not the final concentration of the metabolite. Thus, it is possible that metabolites that are less abundant in inoculated samples than in mock-inoculated samples in the resistant genotype are RRI metabolites (Figure 1.10). Similarly, metabolites identified as quantitative RRI might be less abundant in the resistant genotype than in the susceptible genotype. In order to avoid these possible incongruences, the RRI is often required to possess two characteristics (RRI = RP > RM and RP > SP) (Bollina et al., 2010). Some authors use statistical models, such as student’s *t-test*, to identify those metabolites with significantly higher abundance in the resistant cultivars (Hamzehzarghani et al., 2008; Bollina et al., 2010; Pushpa et al., 2014). The RRC and RRI metabolites are biomarkers that can unravel components important for plant protection, and eventually be used in breeding programs of crop plants.

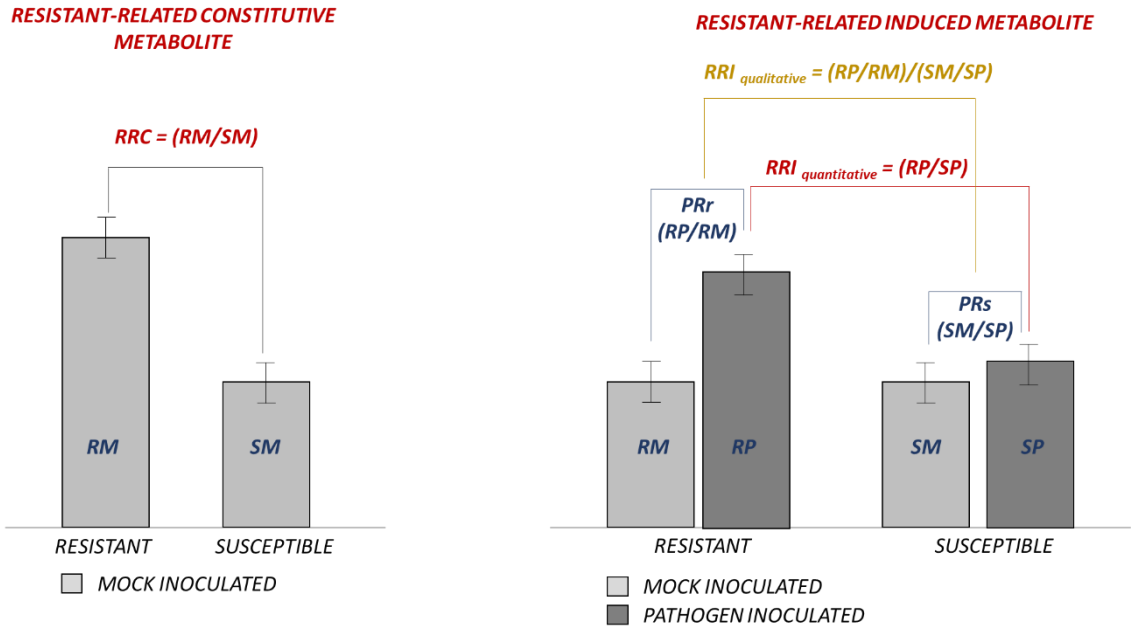

Figure 1.10 Schematic overview of Resistance-Related (*RR*) metabolites. RM = Resistant mock inoculated, SM = susceptible mock inoculated, RP = resistant pathogen inoculated, SP = susceptible pathogen inoculated. Bars represent hypothetical abundance of a metabolite.

1.7. Strategies to treat fungal diseases of agronomic interest

Crops are affected by multiple biotic and abiotic stresses, which affect the quantity (yield) and quality of food production worldwide. Fungal diseases are one of the main biotic stresses of crops, causing food losses of approximately a third of the worldwide crop production, especially in the main crops rice, wheat, maize, potatoes and soybean (Fisher et al., 2012). If these losses were mitigated, the additional crop production would be sufficient to feed 8.5% of the 7 billion world's population in 2011 (Fisher et al., 2012). For this reason, fungal diseases in agriculture have been fought since ancient times, even before the idea that diseases were caused by germs during the nineteenth century.

1.7.1. Chemical fungicides

During the nineteenth century and beginning of the twentieth century, the first chemical treatments against plant pathogens appeared. They included dusting Sulphur, a preparation of lime and Sulphur, copper sulphate, or copper carbonate, and several mixtures containing these and other products (Russell, 2005). However, it was from 1940s that the chemical industry for crop protection appeared, with broad spectrum pesticides such as dithiocarmbamate and phtalimide fungicides, some of which are still used today (Russell, 2005). From the 1970s on, a great number of fungicides for crop production appeared, but with the broad and repetitive fungicide applications that were used in the second half of the twentieth century, microbial resistance to pesticides appeared. In 1966, resistance to organomercury seed treatments was described, although fungicide resistance was not perceived as a major threat at that moment (Noble et al., 1966). However, main fungicides such as Methyl Benzimidazole Carbamides (MBC fungicides) used in vines also developed resistance, as well as the dicarboximides, the products that replaced MBC fungicides (Russell, 1995). Thus, the mode of action of fungicides started to be a main subject of study in order to understand the biological activity of these compounds (Russell, 2005). Nowadays, the Fungicide Resistance Action Committee (FRAC) classifies the available fungicides according to their mode of action (and resistance pattern) in thirteen classes (Table 1.4).

Table 1.4 Mode of action (class) of chemical fungicides and examples of groups and molecules of each class according to the Fungicide Resistance Action Committee (FRAC)

Class (mode of action)	*Example group(s)*	*Example molecule(s)*
A: Nucleic acids metabolism	**Phenylamides**	Metalaxyl
B: Cytoskeleton and motor proteins	**MBC** fungicides (Methyl Benzimidazole Carbamides)	Thiabendazole
C: Respiration	**SDHI** (Succinate DeHydrogenase Inhibitors), **QoI** (Quinone outisde Inhibitors)	Flutolanil, Azoxystrobin
D: Amino acid and protein synthesis	**AP** fungicides (Anilino-Pyrimidines)	Cyprodinil
E: Signal transduction	**PP** fungicides (PhenylPyrroles), **dicarboximides**	Fludioxonil, iprodione
F: Lipid synthesis or transport/Membrane Integrity or function	**Aromatic hydrocarbons & heteroaromatics, carbamates**	Etridiazole, propamocarb
G: Sterol Biosynthesis in Membranes	**DMI** fungicides (DiMethylation Inhibitors), **amines** (morpholines)	Ipconazole, tetraconazole, imazalil, prochloraz, piperalin

H: Cell wall biosynthesis *I: Melanin synthesis in cell wall* *P: Host plant defence induction* *M: Chemicals with multi-site activity* *Unknown mode of action* *BM: Biologicals with multiple mode of action*	**CAA** fungicides (Carboxylic Acid Amides)	Iprovalicarb
	MBI fungicides (Melanin Biosynthesis Inhibitors)	Fenoxanil
	Salicylate related, phosphonates	Isotianil, phosphorous acid
	Inorganic, dithiocarbamate, pthalimide	Sulphur, mancozeb, folpet
	Benzotiazines, pyridazinones	Triazoxide, diclomezine
	Microbes, plant extracts	*Streptomyces spp.,* lupine plantlets extract

Several chemical fungicides have been shown to be efficient in reducing black dot and silver scurf. Azoxystrobin is used as in-furrow application during planting and has been shown to reduce black dot severity in progeny tubers (Nitzan et al., 2005; Pasche et al., 2010; Brierley et al., 2015), and treating seed-tubers with prochloraz also reduced black dot (Denner et al., 1997). Thiobendazole (TBZ) was used to control silver scurf until resistant isolates appeared (Hide et al., 1969, 1988), and other fungicides have been shown to be efficient in controlling silver scurf, including imazalil, prochloraz, mancozeb and several combinations of these and other compounds (Denner et al., 1997; Frazier et al., 1998; Tsror (Lahkim) and Peretz-Alon, 2004).

Fungicide research continues in order to discover new fungicide chemical diversity, although other technologies are being used to reduce the impact of fungal diseases in crops (Hewitt, 2004). Indeed, the FRAC recommends certain guidelines to register new fungicides, which should lead to chemicals with no resistance development or, at least, delay in time for these resistances to appear (Russell, 2005). Multi-site fungicides are obviously more difficult to overcome, and resistance to these chemicals is thus less probable than for the other chemicals. However, these molecules are often cytotoxic compounds, and may not be accepted for registration due to their broad toxicity. Furthermore, other multi-site chemical fungicides that are commercially available today may be left out in regulatory reviews (Russell, 2005). Thus, discovery of new safe antifungal compounds that may not develop resistance are an incredible challenge. In recent years, Integrated Pest (IPM) Management strategies that combine several methods to control fungal diseases have been proposed, in which chemical application of fungicides is the last step. Other preventive measures, as well as mathematical models that determine the best moment for application, or the use of non-chemical fungicides, help reduce chemical fungicide applications worldwide.

1.7.2. Natural extracts

Natural products, including plant extracts, were used in ancient civilizations to treat cankers and mildews, although the exact diseases for which these treatments were applied are not known (Russell, 2005). During the twentieth century, however, the use of chemical fungicides was widespread and natural extracts were less often used in agriculture. In recent years, the study of natural compounds that can help reduce the application of chemical fungicides has gained attention. However, very few natural extracts are commonly used in agriculture due to lower efficacy than chemical pesticides and difficult homologation procedures, as well as higher price/efficiency ratios. Nonetheless, several crude extracts or essential oil preparations have been shown to possess antifungal activities against phytopathogenic fungi. Some plant extracts have been shown to be antifungal against agriculturally important phytopathogens *in vitro*, such in the case of an ethanolic extract of *Agave scabra* against

Botrytis cinerea and *Mucor sp.* (González-Álvarez et al., 2016), the extract of *Lupinus albescens* against *Fusarium oxysporum* and *Fusarium vericilloides* (Confortin et al., 2019), or the extracts of *Curcuma aromatica* and *Garcinia indica* against *Botrytis cinerea*, *Rhizopus stolonifera* and *Colletotrichum coccodes* (Bhagwat and Datar, 2014). Furthermore, the antifungal activity of certain plant extracts has been evaluated *in planta*. Garlic juice, which contains mostly allicin, shows antifungal activity against several important plant phytopahtogens *in vitro* and is able to control *Alternaria spp.* in carrots, *Phytophthora* blight in tomato and potato, *Magnaporthe* on rice and downy mildew in *Arabidopsis* (Bianchi et al., 1997; Slusarenko et al., 2008). Crude extracts of waste materials in agriculture have been investigated because their availability and relatively low cost. Ethanolic extracts of neem cake (the by-product of neem cold pressing), orange peels and rice straw were shown to inhibit *Puccinia triticina* germination (causing leaf rust in wheat) in the greenhouse and in field assays (Ahmed et al., 2019), while methanolic and ethanolic extracts of *Vitis vinifera* canes were shown to be fungitoxic against the three most important vine pathogens *Plasmopara viticola*, *Erysiphe necator* and *Botrytis cinerea* (Schnee et al., 2013). Several methanolic plant extracts were shown to possess antifungal activity against various plant fungal pathogens *in vivo*, including the economically damaging *Botrytis cinerea* or *Phytophthora infestans* (Kim et al., 2004). Among them, the extracts of *Achyranthes japonica* and *Rumex crispus*, as well as the main components of the latter (crysophanol, parietin and nepodin), were shown to be very efficient in controlling powdery mildews in barley and cucumber (Choi et al., 2004; Kim et al., 2004). Cucumber powdery mildew has also been controlled in the field using ethanolic extracts of *Rheum officinale* (Yang et al., 2009), and recently, both *Rumex* and *Rheum* extracts have been shown to protect barley against powdery mildew and wheat against brown rust in the field (Gillmeister et al., 2019). Furthermore, these extracts showed antifungal activity to several plant pathogens *in vitro*, but also induced disease resistance in host plants (Gillmeister et al., 2019). Indeed, most plant extracts likely involve multiple mode of actions due to their chemical diversity, including the induction of host plant defenses. Fusarium head blight in wheat has been controlled by a crude extract of *Frangula alnus*, although the extract did not possess antifungal activity *in vitro*, suggesting that it elicits resistance in host plants (Forrer et al., 2014), as observed in grapevines (Gindro et al., 2007). Diverse plant extracts have been shown to reduce leaf rust disease (caused by *Puccinia triticina*) in wheat, and the efficiency of these compounds pre-infection suggests that they also elicit host defenses (Abd El-Malik and Abbas, 2017; Shabana et al., 2017; Draz et al., 2019). Seaweed extracts, which have been used for a long time in agriculture as biofertilizers, also protect crops through stimulation of defenses (Mukherjee and Patel, 2020). In potato, controlling late blight disease with crude plant extracts has also been attempted. Extracts of *Rheum rhabarbarum*, *Galla chinensis* and *Sophora flavescens* controlled late blight in leaves and seedlings under control conditions, but did not reduce infection or sporangia formation of *Phytophthora infestans* in tubers (Wang et al., 2007). Root extracts of rhubarb and bark extracts of buckthorn also controlled late blight in greenhouse conditions, but these results were not observed under field conditions (Krebs et al., 2006). In field trials, aqueous extracts of *Whitania somnifera*, *Xanthium strumarium* and, especially, *Podophyllum hexandrum* reduced disease incidence of late blight and increased tuber yield (Majeed et al., 2011), and black poplar extracts containing high amounts of populin also controlled late blight under field conditions (Turóczi et al., 2020).

Controlling fungal diseases using plant extracts during storage has also been studied, especially in fruits and vegetables. Post-harvest treatments with agrochemicals is currently being questioned worldwide due to possible toxicity and environmental concerns, and the use of plant extracts or essential oils with antifungal and host resistance inducing properties has potential in the post-harvest industry (Gurjar et al., 2012; Cruz et al., 2013). Ethanolic extracts of neem, chili and pong-pong showed antifungal activity against *Penicillium digitatum in vitro* and controlled green mold of *Citrus* during storage (Al_Samarrai

et al., 2012). Anthracnose of banana fruits was controlled during storage by immersing diseased berries in neem or citric extracts (Cruz et al., 2013), papaya anthracnose was controlled using soapberry hydroethanolic extracts for at least 7 days at 28°C and aqueous extracts of garlic, mallow and ginger showed a very good control of anthracnose in bell peppers as post-harvest treatments (Alves et al., 2015). Yum tubers are also affected by several pathogens during storage, which cause important yield losses, and neem, black pepper and ginger extracts were shown to reduce decay of yam tubers after five months of storage (Gwa et al., 2018). In potatoes, soft rot caused by *Erwinia carotovora* is an important disease both in the field and during storage. Jute leaf and cheerota plant extracts have been shown to reduce soft rot in 40 to 70% after 22 weeks of storage at room temperature (Rahman et al., 2012), aqueous neem extracts reduced 50% of soft rot severity after three weeks at 27°C (Bdliya and Dahiru, 2006) and *Datura stramonium* reduced disease severity in 75% after six days at 30°C (Viswanath et al., 2018).

Storage of fruits and vegetables usually take place in chambers with controlled temperature and humidity that provide the best conditions for keeping the quality of these food products. Furthermore, these installations provide an excellent environment for the use of volatile compounds, such as essential oils, to control post-harvest diseases. Indeed, essential oils are not easily applied in the field, but have been used efficiently against plant pathogens during storage (Gurjar et al., 2012; Jiménez-Reyes et al., 2019). The lemongrass essential oil has been shown to possess antifungal activity *in vitro* against pathogens causing important post-harvest diseases, such as *Colletotrichum coccodes*, *Botrytis cinerea*, *Cladosporium herbarum*, *Rhizopus stolonifer* and *Colletotrichum gloeosporioides* (Palhano et al., 2004; Tzortzakis and Economakis, 2007), and *Illicium verum* and *Schizonepeta tenuifolia* essential oils also showed antifungal activity against *B. cinerea* and *C. gloeosporioides in vitro* (Lee et al., 2007). *In vivo*, good level of disease control has also been achieved with the use of essential oils. For example, treating grapes with essential oils of *Ocimum sanctum* (holi basil), *Prunus persica* (peach) or *Zingiber officinale* (ginger) increased their storage life between 4 and 6 days (Tripathi et al., 2008). Similarly, anthracnose could be controlled with the use of *Cymbopogon citratus* (lemon grass) essential oils in yellow passion fruit (Anaruma et al., 2010) and with *Allium sativum* (garlic) and *Copaifera langsdorfii* (copaiba) essential oils in banana fruits (Cruz et al., 2013), while essential oils of *Cinnamomum zeylanicum* (Ceylon cinnamon tree) and *Syzygium aromaticum* (clove) were fungicidal to crown rot and anthracnose pathogens from banana (Ranasinghe et al., 2002). *Alternaria alternata* control in infected tomatoes was also achieved by nettle and thyme oil as post-harvest treatments (Hadizadeh et al., 2009). Several essential oils have been found to be fungicidal *in vitro* to potato pathogens, and application of *Allium sativum* essential oil reduced the severity of diseases caused by *Fusarium solani*, *Phoma foveate* and *Helminthosporium solani* in potatoes during storage (Bång, 2007). Spearmint oil, peppermint oil, and their main terpenoids S-carvone and L-menthone have also been shown to be fungicidal to several potato pathogens, including *Phytophthora sp.*, *Fusarium sp.*, *Rhizoctonia solani* and *Helminthosporium solani* (Bång, 2007; Al-Mughrabi et al., 2013), and mint oil containing L-carvone is currently commercialized as a sprout inhibitor and fungicide (Xeda International, France). Clove oil and its main component eugenol have been shown to be fungicidal to several plant phytopathogens *in vitro* and controlled crown rot in peanuts (Kishore et al., 2007; Thobunluepop, 2009), and is also commercialized as *biofungicide* for seed treatments and post-harvest treatments of vegetables, fruits and potatoes (Xeda International, France).

1.7.3. Natural Products

Natural Products (NPs) are chemical compounds synthesized by living organisms, and thus, all molecules present in natural extracts. The use of NPs as source of antifungal compounds has been largely used in the past years (Newman and Cragg, 2012) and identification of the NPs responsible for the antifungal activity in crude extracts against phytopathogenic fungi has been reported.

The anthraquinones chrysophanol and parietin, as well as the naphtol nepodin, were isolated from *Rumex crispus* and showed antifungal activity against *Blumeria graminis* f. sp. *hordei* and *Podospharea xanthii,* which cause powdery mildew in barley and cucumber, respectively (Choi et al., 2004). Flavonoids and stilbenes from *Rheum rhabarbarum* were shown to also possess activity against *Blumeria graminis* f. sp. *hordei*, and among them, the falvon-3-ol epicatechin gallate and the stilbene resveratrol were found to be the main responsible of the antifungal activity (Gillmeister et al., 2019). Interestingly, the combination of epicatechin gallate and resveratrol, as well as another combination of a procyanidin (procyanidin B2) and a stilbene (rhaponticin), exhibited better control than the expected accumulated, indicating synergistic effects of the antifungal compounds of the *Rheum rhabarbarum* extract (Gillmeister et al., 2019). Stilbenes from *Vitis vinifera*, including resveratrol, hopeaphenol, *E*-vitisin B and ε-viniferin, also showed strong antifungal activity against the fungal phytopathogen *Plasmopara viticola* (Schnee et al., 2013).

Non-plant organisms, such as actinomycetes, which are Gram-positive mycelial bacteria, also produce antifungal compounds (Kodzius and Gojobori, 2015). Indeed, several antifungal peptides produced by actinomycetes have been shown to be efficient against phytopathogenic fungi, such as for valinomycin against *Botrytis cinerea* and *Magnaporthe grisea* or Cyclothiazomycin B1 against several *Fusarium* species (Zhang et al., 2020). Several bacteria used as biocontrol also possess antifungal compounds, such as bacillomycin L, fengycin or surfactin, produced by *Bacillus amyloliqquefaciens* SYBC H47, which showed antifungal activity against several plant pathogens (Li et al., 2016). Furthermoe, harzianic acid and isoharzianic acid isolated from the fungal organism *Trichoderma harzianum* are antifungal against the tomato (and potato) pathogens *Sclerotinia sclerotiorum* and *Rhizoctonia solani*, and promote growth and induce resistance in tomato (Vinale et al., 2014).

Fungal pathogens of potatoes have also been controlled by the use of NPs. The unusual fatty acid (E)-4-oxohexadec-2-enoic acid was isolated from *Hygrophorus ebumeus* and reported to possess antifungal activity against the cucumber pathogen *Cladosporium cucumerinum* and the potato pathogens *Colletotrichum coccodes* and *Phytophthora infestans in vitro* (Teichert et al., 2005; Eschen-Lippold et al., 2009). Furthermore, the application of the sodium salt of (E)-4-oxohexadec-2-enoic acid prevented *P. infestans* infection in potato leaves (Eschen-Lippold et al., 2009). Late blight caused by *Phytophthora infestans* was also efficiently controlled by populin (benzoyl-salicin) from poplar bud extracts (Turóczi et al., 2020).

1.7.4. Biocontrol (microorganisms)

The reduction of chemical fungicides is a priority in most countries around the world, and, in Switzerland, the market of active ingredients used in organic agriculture has experienced a 40% growth in the past ten years, an increase that was accompanied by a 30% reduction of all other phytosanitary products in the same period, most of which are fungicides (OFAG, 2019a, 2019b). Although plant-based fungicides or plant defence inductors are considered active ingredients that can be used in organic farming, the term biological control or *biocontrol* is often referred to the use of antagonistic microorganisms to control plant diseases. The mode of action of these biocontrol agents is diverse, from direct antibiosis to competition for site and nutrients, parasitism or induced defense (Heydari and Pessarakli, 2010). One of the most studied microorganisms are *Bacillus* species, which possess multiple antifungal compounds and have been used against plant pathogens, especially against *Fusarium sp.* (Li et al., 2016; Lee et al., 2017; Khan et al., 2018). Other studies have shown that compost water extracts were efficient in controlling anthracnose in pepper and cucumber, and in preventing germination of their fungal agents, *Colletotrichum coccodes* and *Colletotrichum orbiculare* (Sang and Kim, 2011). In potatoes, several bacterial strains isolated from their rhizosphere or from shoots showed antifungal activity against five plant pathogens *in vitro*, and protected potato plants against late blight in greenhouse and field experiments (Guyer et al., 2015). Furthermore, three of the *Pseudomonas* strains were shown to possess antifungal activity against several *Phytophthora infestans* strains, and combining two or three of the most active strains results in a better control of late blight in potato leaves (De Vrieze et al., 2018, 2019). Antagonist microorganisms have also been shown to protect

potato tubers during storage, especially against silver scurf caused by *Helminthosporium solani*. Antifungal activity of several *Pseudomonas* strains against *H. solani* was demonstrated *in vitro* (Guyer et al., 2015), and applying *Pseudomonas corrugata* on silver scurf symptomatic potato tubers reduced disease during storage and, especially, when applied as seed-tuber treatment (Chun and Shetty, 1994). Similarly, *Muscodor albus* iosalte CZ-620 produces volatile organic compounds with antimicrobial activity against the potato tuber pathogens *Pectobacteium atrosepticum*, *Fusarium sambucinum* and *Helminthosporium solani*), and showed good control of soft rot, dry rot and silver scurf caused by these pathogens during storage (Corcuff et al., 2011). There are currently few available biopesticides for the control of silver scurf in potatoes: Serenade ASO is a formulation of *Bacillus subtilis* that has been shown to reduce silver scurf incidence and severity (Johnson, 2007), and Bio-Save is a formulation of *Pseudomonas syringae* with good efficacy against silver scurf (Stockwell and Stack, 2007). In Switzerland, a post-harvest treatment of potato tubers with a product based on *Pseudomonas sp. DSMZ 13134* is authorized for the control of silver scurf during storage.

1.7.5. Fungicides as post-harvest treatments in agriculture

The use of protecting agents against fungal diseases in agriculture depends on a cost-efficiency evaluation, as well as the safety in public health and environment of the use of these products. Organic farming practices have increased around the world in the past years despite having, in general, lower yields and higher yield variability than conventional agriculture (Knapp and van der Heijden, 2018). The lower yield of organic practices is, among other factors, due to a lower efficiency of the biopesticides than chemical pesticides, which involves that the former will have a higher cost/efficiency ratio. However, post-harvest chemical treatments of fruits and vegetables are usually more restricted than during plant growth, mainly due to residues on the food products, and some traditionally used compounds are being banned. For example, post-harvest treatment of potatoes with the herbicide chlorpropham (CIPC), traditionally used as a sprout inhibitor in consumption potatoes, is no longer approved in the European Union since January 8th 2020 (European Commission, 2019). Thus, new strategies to control post-harvest diseases in fruits and vegetables need to be directed into using safe phytosanitary products (Dubey et al., 2020). Natural extracts and the Natural Products contained in them are a good source of antifungal compounds and may be safer than traditional chemical fungicides. Similarly, essential oils applied in storage chambers are easily diffused and could provide a good control as post-harvest treatments, and some are already commercialized in Europe to control, among others, storage disease of potatoes. The use of antagonistic microorganisms in storage may also be interesting, and some phytosanitary products are also available to control silver scurf in potatoes. Altogether, despite their higher cost/efficiency ratio, *biofungicides* may be the most important or only solution for the control of storage diseases in fruits and vegetables in the future.

Aim and framework of the thesis

As mentioned, plant diseases are an important constraint for growers around the world. Potatoes, which are the fourth crop in the world, are also attacked by a number of pathogens, which can have an important impact on potato yield. Nonetheless, few of these pathogens do not produce important yield losses, but rather affect the quality of the tubers, especially during storage. Notably, food loss from harvest to distribution was recently estimated at 25% in root and tuber-bearing crops. Among these diseases, black dot, caused by the fungal pathogen *C. coccodes*, and silver scurf, caused by the fungal pathogen *H. solani*, are important tuber diseases of potatoes with very similar symptoms. As reviewed in the introduction, there are no studies that have addressed the factors that influence both diseases at the same time. Thus, the overall aim of this thesis is to better understand the factors that influence the epidemiology of black dot and silver scurf under the same conditions, and to suggest an integrated pest management strategy to reduce the risks of both diseases. To this end, molecular biology techniques, combined with microscopic and biochemical analysis will be used.

In order to understand the pathogenicity and dynamics of infection of the two fungal pathogens, seed-tuber lots showing different severity of symptoms will be planted in different field sites in a three-year field trial. In addition, plant samples will be collected throughout the season and analyzed for the presence of the pathogen. Altogether, these experiments are designed to highlight the importance of the seed-tuber and the environment on each disease, and to describe the dynamics of infection of both diseases.

The second aim of the thesis is to define a strategy to reduce the risk of high disease severity of black dot and silver scurf. One of the most sustainable strategies to defy crop diseases is the selection of cultivars with high quantitative resistance to the pathogen. Quantitative resistance is characterized by the reduction, but not absence, of disease symptoms, and is the result of several genes with small to medium effects. A screening of the level of resistance will be performed on 16 cultivars, currently being marketed as table potato cultivars in Switzerland. To understand quantitative resistance, genetic studies focus on several loci that underpin quantitative resistance, although highlighting these QTLs require populations of great size. Alternative methods to characterize quantitative resistance include the use of plant metabolomics. Metabolomics studies have been used to highlight metabolites involved in quantitative resistance, including in *Solanum tuberosum*. However, quantitative resistance to black dot or silver scurf has not been studied in potatoes. Based on the results obtained in the field, a metabolomics study will be performed on a selection of potato cultivars and potentially highlight biomarkers associated with resistance. Thus, the second aim of this thesis is to identify commercially available potato cultivars with high quantitative resistance to black dot and silver scurf, and to characterize the metabolome associated with this quantitative resistance.

Quantitative resistance of selected potato cultivars might help producers to reduce the risk of black dot and silver scurf in the potato industry. Nonetheless, other potato characteristics such as organoleptic or cooking type, differ among potato cultivars. Thus, it is possible that some cultivars with high susceptibility to blemish diseases are selected by producers because of these properties. In this cases, a strategy to reduce the risk of disease development during storage is necessary. To date, little post-harvest treatments against black dot and silver scurf of consumption potatoes are used, and, in Switzerland, only one bacteria-based product is commercially available. Chemical fungicide treatment in potato tubers stored for human consumption must be done with precaution, since the threshold of chemical residues on food products is established by authorities. The use of plant extracts to control the development of these diseases during storage arises as an interesting approach. This thesis aims at screening plant extracts with antifungal activity to be used as post-harvest treatments of diseased tubers, and to isolate and characterize the potential active antifungal molecules.

The overall aim of this thesis is to characterize the factors that influence the development of black dot and silver scurf in potatoes, and to propose several measures that may be combined in an Integrated Pest Management Strategy.

2. Influence of abiotic factors, inoculum source and cultivar susceptibility on the potato tuber blemish diseases black dot (*Colletotrichum coccodes*) and silver scurf (*Helminthosporium solani*)

Josep Massana-Codina, Sylvain Schnee, Nicole Lecoultre, Eric Droz, Brice Dupuis, Andreas Keiser, Patrice de Werra, Jean-Luc Wolfender, Katia Gindro and Stéphanie Schürch

This chapter is based on a research article submitted to Plant Pathology and accepted following major revisions. The chapter has been reformatted upon the reviewers' suggestions. Furthermore, the figures originally submitted as supplementary are now included in the main text. All references are compiled in a common list at the end of the thesis.

Author's contributions: JM-C, KG, BD, StS and J-LW conceived and designed the study. JM-C and NL performed the DNA extraction and PCR fungal detection. PdW and AK performed the DNA extraction and inoculum quantification in soil. ED conducted the cultivar genotyping. All authors participated in the disease severity determination. JM-C, SyS, StS, and KG analyzed and interpreted the results. JM-C, StS, SyS, KG and JL-W wrote the manuscript. All authors discussed the results and reviewed the final manuscript.

2.1. Abstract

Black dot and silver scurf are two potato blemish diseases that have been garnering increased amounts of attention in recent years. Their symptomatology on tubers is very similar, and microscopic observation of fungal structures is required to identify the pathogens. The epidemiology of both diseases has been studied to some extent, but comparative studies of both diseases at the epidemiological and cultivar-susceptibility levels have not yet been carried out. The influence of cultivar, source of inoculum and climatic conditions on both diseases was studied in field trials during a three-year period (2016-2018) in Switzerland. These trials were complemented by a greenhouse experiment and by disease assessments within the Swiss seed-tuber certification program. *Colletotrichum coccodes* soil inoculum was found to be relatively low at all field sites and had a small influence on disease severity, while *Helminthosporium solani* soil inoculum was not detected at any field site. Furthermore, planting *C. coccodes*-free or *H. solani*-free seed tubers did not prevent disease in daughter tubers. Interestingly, *H. solani* was detected for the first time in stolons. Furthermore, stolon and tuber infections usually appeared late in the season. Black dot severity was relatively high after growing seasons characterized by high humidity, while silver scurf severity was high under warm and dry conditions. Table potato cultivars commonly grown in Switzerland exhibited considerable differences in susceptibility to both diseases. These results will contribute to developing an integrated pest management strategy to control both diseases simultaneously.

2.2. Introduction

Black dot (caused by *Colletotrichum coccodes*) and silver scurf (caused by *Helminthosporium solani*) are two potato blemish diseases that affect the quality of tubers and cause water loss during storage; changes in the marketing of fresh tubers, particularly with respect to the increased demand for washed potatoes, have led to an increased economic impact of these two diseases once considered of minor importance. The effect of blemishes on tuber appearance is more visible on washed potatoes than on unwashed ones and therefore degrades tuber quality and reduces price.

Black dot is caused by *Colletotrichum coccodes* (Wallr.) S. Hughues, a fungal pathogen that has several hosts, including tomato, onion, carrot, and other crop species, and in potatoes, infects all belowground organs as well as stems and leaves (Johnson, 1994; Andrivon et al., 1998). Roots, stolons and daughter tubers are quickly colonized by *C. coccodes,* showing symptoms of black dot soon after their emergence, while stems show disease symptoms only 7 – 10 weeks after inoculation (Andrivon et al., 1998). Black dot disease was higher at 22°C than at 18°C in greenhouse conditions, indicating that high temperatures are conducive of the disease (Lees et al., 2010), and several studies have shown that irrigation results in higher disease levels (Adams et al., 1987; Hide et al., 1994b; Lees et al., 2010; Olanya et al., 2010; Brierley et al., 2015). Long cultivation periods correlate with black dot disease severity, indicating that early harvest may be an efficient management strategy (Brierley et al., 2015). Fungicide application, the use of less susceptible cultivars and short curing periods are other strategies to reduce the impact of black dot on potatoes (Read, 1991b; Hide et al., 1994b; Read and Hide, 1995b; Andrivon et al., 1997, 1998; Olanya et al., 2010; Brierley et al., 2015). Soil inoculum was found to be the primary source of *C. coccodes* inoculum in the UK, and to be an important factor determining the incidence of black dot on daughter tubers (Lees et al., 2010). Short rotations between potato crops and rotations involving other host plant species of *C. coccodes* seem to increase the risk for a higher soil inoculum, indicating that long roations should be included on the management of this disease (Hide and Read, 1991). Infected seed tubers planted in disease-free soils produce progeny tubers that can develop black dot symptoms (Denner et al., 1998), indicating that seed-inoculum is also a source of inocula in the field. However, it is suggested that soil inoculum is the main source of *C. coccodes* in the field (Lees and Hilton, 2003).

Silver scurf is caused by *Helminthosporium solani* Dur. & Mont (Errampalli et al., 2001b). Its only known host is the potato plant, where it causes a blemish disease on tubers. Planting infected seed-tubers in the field is the primary origin of *H. solani* in the soil (Secor and Gudmestad, 1999; Geary and Johnson, 2006; Avis et al., 2010). However, *H. solani* has been found in decaying material, which, together with volunteer potatoes, can be a source of inoculum (Mérida and Loria, 1994b). A study using successive seed generations showed that silver scurf disease increases at each seed generation, and that using nuclear seed tubers generally results in disease control (Geary and Johnson, 2006). However, other authors have found that the use of nuclear seed tubers is not sufficient to prevent silver scurf symptoms in progeny tubers, especially in rotations of less than three years between crops (Mérida and Loria, 1994b; Bains et al., 1996). Silver scurf does not usually cause any yield losses at harvest, but it does increase the permeability of the tuber's skin, which leads to water losses and shrinkage during storage, leading to weight losses reaching 17% (Read and Hide, 1984). Similar to black dot, this disease affects the quality of the tubers, leading to the downgrading or rejection of tuber lots, especially in the fresh potato market (Errampalli et al., 2001b; Lees and Hilton, 2003).

Black dot and silver scurf cause important losses in potato production, and their occurrence has been highlighted worldwide, for instance, in Israel (Tsror (Lahkim) et al., 1999; Tsror (Lahkim) and Peretz-Alon, 2004), North America (Hunger and McIntyre, 1979; Rodriguez et al., 1996), Australia (Harrison, 1963) and especially in Europe (Read and Hide, 1984, 1995a; Hardy et al., 1997; Andrivon et al., 1998; Lees et al., 2010; Brierley et al., 2015). Although these diseases are caused by two unrelated phytopathogenic fungi with different host ranges and life cycles, the symptoms of these two diseases are very similar in appearance, and observation of their microscopic structures (microsclerotia for *C. coccodes* and conidiophores for *H. solani*) is needed to determine the pathogen causing the disease (Errampalli et al., 2001b; Lees and Hilton, 2003). For commercial purposes, these pathogens are often scored together (as blemish diseases), and the level of acceptable incidence of these blemish diseases does not specify which fungus is responsible for the disease. Furthermore, both diseases often appear simultaneously not only in a tuber stock but also on the same tuber. Several studies have focused on the epidemiology or control measures of black dot in potato (Andrivon et al., 1998; Lees et al., 2010; Brierley et al., 2015) or silver scurf (Hide and Read, 1991; Mérida and Loria, 1994a, 1994b; Mérida et al., 1994; Bains et al., 1996; Geary and Johnson, 2006). However, there are no studies either on black dot and silver scurf joint infection or on the control measures and the conditions favoring these two blemish diseases in the same tuber lots.

Differences in black dot susceptibility have been observed in cultivars grown in the UK (Read, 1991b; Brierley et al., 2015), in Israel (Tsror (Lahkim) et al., 1999) and in the USA (Hunger and McIntyre, 1979). Russet-type cultivars have been shown to be more resistant to black dot than thin-skin cultivars (Hunger and McIntyre, 1979), and early-maturing cultivars were more resistant than late-maturing cultivars to black dot in field trials (Read, 1991b; Andrivon et al., 1998). Susceptibility to silver scurf also differs among potato cultivars (Joshi and Pepin, 1991), but cultivars with high levels of resistance to silver scurf have not been identified (Secor, 1994; Errampalli et al., 2001b; Avis et al., 2010; Sedláková et al., 2013). Introgression of resistance traits from wild *Solanum* species into potato cultivars has been attempted (Murphy et al., 1999) since some wild potato species have shown low sporulation of *H. solani* (Rodriguez et al., 1995). However, no resistant cultivars have been reported from these crosses (Avis et al., 2010). Furthermore, most susceptibility studies of potato cultivars to silver scurf have been performed in the USA (Mérida et al., 1994; Rodriguez et al., 1996; Errampalli et al., 2001b) and have not included cultivars commonly used in Europe. Little is known about the genetic basis of resistance to black dot and silver scurf, and information on the susceptibility of cultivars grown in Europe for fresh markets is also lacking.

In the present study, 1) we evaluated the effects of the inoculum source on black dot and silver scurf severity in daughter tubers and studied whether the use of disease-free minitubers was sufficient to prevent either disease; 2) we studied the climatic conditions that affect the development of both diseases in field trials; 3) we investigated the susceptibility of cultivars used in the fresh potato market in Switzerland to both diseases; and 4) using molecular detection techniques, we monitored the development of both diseases on belowground organs sampled during plant growth in controlled and field conditions.

2.3. Material and methods

Disease assessment of seed and daughter tubers

A sample of 50 tubers of each seed-tuber lot was assessed for black dot and silver scurf severity before planting (following approximately 6 months of storage). Daughter tubers (42.5-60 mm diameter) were stored for three months (experiment 1) or four months (experiments 2 and 3) in cold chambers at 6°C after a period of curing. The tubers were then washed and incubated at room temperature and high relative humidity by placing them in closed plastic bags containing wet tissues for two weeks to induce sporulation of fungal pathogens. One hundred individual tubers (experiment 1) or 50 individual tubers (experiments 2 and 3) of each lot were individually observed under a binocular microscope for the presence of microsclerotia of *C. coccodes* (for black dot) or conidiophores of *H. solani* (for silver scurf). Depending on its affected tuber surface area, each tuber was then classified into one of the following classes: 0 (absence of the fungus), 1 (less than 15%), 2 (between 15 and 33%), 3 (between 33 and 66%) and 4 (more than 66%). Disease incidence was calculated as the percentage of tubers showing symptoms, and disease severity was calculated by multiplying the number of tubers in each class by the median value of the class (% affected area). For experiment 1, the commercially available seed-tuber lots always showed black dot and silver scurf symptoms, but the severity differed among lots and years. Efforts were made to select a seed-tuber lot showing low levels of black dot (below 15% disease severity) and silver scurf (below 25% disease severity) and a second seed-tuber lot with relatively high black dot (above 15% disease severity) and silver scurf (above 30% disease severity).

Seed stock

Certified seed tubers for use in experiments 1 and 2 were purchased in the fall and maintained in a cold chamber at 4–6°C over winter. No seed tubers were treated with fungicide. Four to six weeks before planting, all tubers were placed in a chamber with permanent light to induce germination. Cultivar genotype was verified by microstaellite genotyping and comparison with information in the Agrospcope database using previously publushed methods (Milbourne et al., 1998; Moisan-Thiery et al., 2005; Ghislain et al., 2009). Minitubers used in experiment 1 were produced in the greenhouse, and fungal DNA of *H. solani* or *C. coccodes* was not amplified from these minitubers.

Experiment 1: Relationship between source of inoculum of C. coccodes *and* H. solani *and environmental conditions on a) disease severity and b) the extent of fungal colonization, under field conditions*

Three potato seed-tuber lots of the widely grown cultivar Charlotte (two naturally infected lots and a minituber seed-lot) were selected each year and planted at six field sites in three consecutive years (2016-2018): Changins (46°23'52.9"N 6°14'19.4"E), Goumoens (46°38'54.2"N 6°35'46.8"E), Moudon (46°40'51.5"N 6°49'16.3"E), Düdingen (46°50'22.8"N 7°12'53.5"E), Zollikofen (46°59'29.5"N 7°27'43.1"E) and Riedholz (47°13'15.9"N 7°34'09.4"E). The specific field plot differed every year to ensure a minimum of four years since the previous potato crop. Each seed-tuber lot was planted in two rows of 25 plants, each row was separated by 75 cm, and each plant was separated by 33 cm, without replicates. The fields were cultivated according to standard agricultural practices for seed-tuber production. The disease severity of the three seed-tuber lots was determined each year before

planting. To monitor the progression of the infections, daughter tubers were harvested from the initiation of tuberization (which took place between 50 and 70 days after planting) until harvest (which took place between 123 and 135 days after planting) every 2 weeks at the Changins field site (2016-2018). Additionally, in 2017, roots and stolons were harvested from emergence (30 days after planing) until haulm destruction (118 days after planting) in the Changins field site. DNA of *C. coccodes* or *H. solani* was detected by nested PCR as described below. Samples from 10 plants of each seed-tuber lot were analyzed per time point.

Experiment 2: Cultivar susceptibility under field conditions

Sixteen cultivars commonly used for Swiss fresh market production (Agata, Amandine, Annabelle, Celtiane, Charlotte, Cheyenne, Ditta, Erika, Gourmandine, Gwenne, Jazzy, Lady Christl, Lady Felicia, Laura, Venezia and Vitabella) were planted for three consecutive years (from 2016 to 2018) at three different locations in Switzerland: Changins (46°23'52.9"N 6°14'19.4"E) and Reckenholz (47°26'02.6"N 8°30'47.6"E), where conventional practices were used, and Unterstammheim (47°38'35.8"N, 8°46'43.2"E), where organic practices were followed. Each cultivar was planted in four plots (repetitions) of two rows of 25 plants each, each row was separated by 75 cm, and each plant was separated by 33 cm. Daughter tubers were harvested and disease severity assessed after four months of storage at 6°C.

Experiment 3: Assessment of disease severity in tubers from a wide-scale monitoring of commercial potato stocks

Within the framework of the Swiss seed potato propagating program, tubers received for certification as seed stock for the following season were assessed for black dot and silver scurf severity after four months of storage. Several stocks of the cultivars Agata, Amandine, Annabelle, Celtiane, Charlotte, Ditta, Erika, Gourmandine, Lady Christl, Lady Felicia, Laura and Venezia, which had been grown in different field sites across the potato-growing regions of Switzerland, were used. The number of stocks assessed was 166 in 2016 (between 7 and 15 stocks per cultivar), 159 in 2017 (between 7 and 15 stocks per cultivar) and 166 in 2018 (between 10 and 15 stocks per cultivar).

An overview of the four experiments is shown in Table 2.1.

Table 2.1 Overview of the three experiments carried out and the factors evaluated in each of them

	EXPERIMENT 1	EXPERIMENT 2	EXPERIMENT 3
OBJECTIVE	Relationship between source of inoculum and meteorological conditions on disease severity and development of fungal colonization under field conditions	Cultivar susceptibility under field conditions	Assessment of disease severity from a wide-scale monitoring of commercial stocks
FACTORS INVESTIGATED	- Soil inoculum - Seed-tuber inoculum - Climatic conditions	- Soil inoculum - Seed-tuber inoculum - Climatic conditions - Cultivar susceptibility	- Cultivar susceptibility
SEED-LOTS (PER YEAR)	3	16 (1 per cultivar)	159-166 (7-15 per cultivar)
YEARS	2016 to 2018	2016 to 2018	2016 to 2018
CULTIVAR	Charlotte	16 (See Seed stock)	12 (see Seed stock)
FIELD SITES	6	2 conventional + 1 organic	>50
SEVERITY ASSESSMENT BEFORE PLANTING	✓	✓	
SOIL SAMPLING	2017, 2018	2016, 2017, 2018	
PLANT SAMPLING FOR DISEASE INCIDENCE	10 plants/time point		
ASSESSED ORGANS	daughter tubers (2016 to 2018) roots and stolons (2017)	Daughter tubers	Daughter tubers
STORAGE TIME	3 months	4 months	4 months
SEVERITY ASSESSMENT AFTER STORAGE	✓	✓	✓

Production of disease-free minitubers

Plantlets of *Solanum tuberosum* L. cultivar Charlotte were grown for four weeks in sterile conditions as described by Lê & Collet (1985). After 24 hours of reconditioning in a high-humidity environment, potato plants were transferred to 4 liters (18x18x18 cm) square pots containing an autoclaved substrate consisting of brown and blond peat (Gebr. Brill substrate, Georgsdorf, Germany). Potato plants were grown for four months, haulms were mechanically killed, and daughter tubers were left in the soil for an additional four-week period until harvest (to allow the skin to set). After harvest, minitubers were maintained at 4°C in isolation from other tubers and plant parts to avoid contamination with fungal pathogens until planting. Fungal DNA of *H. solani* or *C. coccodes* was not amplified for these minitubers.

Plant and soil sampling and DNA purification

DNA from *in vitro* plantlets for microsatellite genotyping was purified using a DNeasy Plant Mini Kit (Qiagen, Hilden, Germany) according to the manufacturer's protocol. Soil samples were collected from each field plot before planting (experiment 1: 2017 and 2018; experiment 2: 2016, 2017 and 2018). The soil samples were taken from the top 20 cm across the field site in a W-shape as described elsewhere (Lees et al., 2010) and were air dried prior to DNA extraction. Four subsamples (60 g each) for each field plot were processed for DNA extraction, and three aliquots were taken per subsample, thus resulting in twelve samples to be quantified for each soil. The method used for DNA precipitation and purification was that published by Cullen *et al.* (2001, 2002); however, the first steps of lysis and supernatant collection were modified according to the method described by Lees *et al.* (2010) using a Retsch PM100 milling bowl (Retsch, Haan, Germany). Briefly, lysis of fungal cells occurred in a milling bowl containing 60 g of dried soil in 120 ml of preheated (50°C) SPCB buffer (120 mM sodium phosphate (NaH_2PO_4, Na_2HPO_4), 2% CTAB (cetyltrimethylammonium bromide), 1.5 M NaCl; pH 8.0).

Three aliquots of 1.8 ml of this soil suspension were used for DNA extraction. The supernatant of the soil suspension was extracted with one volume of chloroform:isoamyl alcohol (24:1, v/v). DNA in the resulting aqueous phase was then precipitated with one volume of ice-cold isopropanol (-20°C), washed twice with ice-cold 70% ethanol and suspended in 75 µl of TE buffer (10 mM Tris-HCl, 1 mM EDTA; pH 8.0). Before their use in quantitative PCR, DNA extracts were purified through Sephadex G-75 and polyvinylpyrrolidone (PVPP) minicolumns to remove any PCR inhibitors.

Belowground plant organs (roots, stolons and daughter tubers) for the development of fungal colonization (experiment 1) were collected on the date of emergence (90% of plants emerged), followed by sample collection approximately every two weeks during plant growth, including at haulm destruction and at harvest. Ten individual plants (experiment 1) were collected at each time point. The roots, stolons and tubers were washed and maintained at 4°C for a maximum of 24 hours. Roots and stolons were cut, flash frozen and then ground, after which they were maintained at -80°C until DNA extraction. Similarly, whole tubers were pealed, and 500 µl of the juice of the tuber peel was stored at -80°C until DNA extraction. DNA extraction was performed using the CTAB method (Doyle, 1990). Briefly, 500 µl of CTAB buffer (0.2 M Tris, 2.8 M NaCl, 40 mM EDTA, 4% cetyltrimethylammonium bromide; pH 8.0) was added to each sample, which was then vigorously shaken. Afterward, 500 µl of phenol:chloroform:isoamyl alcohol (25:24:1, v/v/v) was added. The contents were then mixed and then centrifuged for 10 minutes at 13,000 rpm. Five hundred microliters of the supernatant was transferred to a new tube, and 280 µl of cold (-20°C) isopropanol was added. The samples were then incubated at -20°C for at least 15 minutes until the DNA precipitated. Following centrifugation at 13,000 rpm for 5 minutes, the supernatants were discarded, and the remaining contents were washed twice with cold 70% ethanol (v/v). The DNA samples were dried in a Speedvac device for 30 minutes. Afterward, 100 µl of TE buffer (10 mM Tris-HCl, 1 mM EDTA; pH 8.0) was added to dried DNA samples, and then they were resuspended and stored at -20°C until PCR analysis.

Cultivar confirmation by microsatellite genotyping

The identity of the varieties was confirmed by microsatellite genotyping and comparison with information in the Agroscope database. The forward primers were marked with DY-682 for Lernalx, STM1097 and STM2005 (Moisan-Thiery et al., 2005) and DY-782 for STM0030, STM5114 and SSR1 (Milbourne et al., 1998; Moisan-Thiery et al., 2005; Ghislain et al., 2009) (Eurofins Genomics, Ebersberg, Germany). PCR amplification of the markers was carried out with a TProfessional Thermocycler (Biometra, Labgene Scientific SA, Chatel-Saint-Denis, Switzerland) in a total volume of 25 µl, which consisted of 1.25 U of Eurobiotaq polymerase (Eurobio Scientific, Les Ulis, France), 2.4 mM $MgCl_2$, each dNTP at 0.2 mM, each primer at 0.2 mM, 1x buffer and ~50 ng of DNA. The PCR conditions were as follows: initial denaturation for 2 min at 94°C; 25 cycles of denaturation for 30 s at 94°C, annealing for 1 min at the primer-specific temperature and elongation for 1 min at 72°C; and then a final elongation step for 5 min at 72°C. The annealing temperatures were 52°C (Lernalx, STM2005 and SSR1), 54°C (STM1097), 56°C (STM5114) and 62°C (STM0030). The PCR products were separated on a 4300 DNA Analyzer (LI-COR Biosciences, Bad Homburg vor der Höhe, Germany), analyzed using SAGA Generation 2 software (LI-COR Biosciences) and scored manually.

Quantification of pathogen DNA in soil

Inoculum of *C. coccodes* and *H. solani* was quantified according to previously published real-time PCR methods (Cullen et al., 2001, 2002).Considering that each 75 µl DNA extract tested contained the DNA from approximately 0.75 g of soil and knowing that 1 µl was quantified, the resulting starting quantity of target DNA (pg) was multiplied by a hundred to obtain the quantity present in 1 g of soil (pg DNA g^{-1}). Three qPCR repetitions were carried out for each subsample (60 g of soil), and the mean of the

twelve values was calculated. Aberrant values of the nonexponential qPCR amplification curve were eliminated from the analysis.

Detection of C. coccodes and H. solani in plant organs

Detection of the fungal pathogens in plant organs was carried out by conventional nested PCR as described previously (Cullen et al., 2001, 2002). For *H. solani* amplification, an initial round of PCR was carried out on diluted (1/10) or undiluted samples using Hs1F1 and Hs2R1 specific primers followed by nested PCR using Hs1NF1 and Hs2NR1 (Cullen et al., 2001). For *C. coccodes*, diluted samples (1/10 or 1/100) were subjected to an initial round of PCR using primers Cc1F1 and Cc2R1 followed by nested PCR using primers Cc1NF1 and Cc2NR1 (Cullen et al., 2002). PCR amplification was carried out with a TProfessional Thermocycler (Biometra Labgene Scientific SA) in a total volume of 20 µl or 25 µl (first-round *C. coccodes* and *H. solani*, respectively) or 15 µl (second-round), which consisted of 0.625 U of Taq DNA polymerase (Qiagen), 2.4 mM $MgCl_2$, each dNTP at 0.2 mM, each primer at 0.2 mM, 1x Qiagen PCR buffer and diluted or undiluted DNA samples (first-round PCR) or PCR product (second-round PCR). The PCR conditions were as follows: initial denaturation for 2 min at 94°C; 30 cycles of denaturation for 45 s at 94°C, annealing for 1 min at a primer-specific temperature and elongation for 1 min at 72°C; and then a final elongation step for 5 min at 72°C. The annealing temperatures were 61°C (first-round *C. coccodes*), 66°C (first-round *H. solani*), 72°C (second-round *C. coccodes*) and 60°C (second-round *H. solani*). The PCR products were separated on a 1% agarose gel stained with ethidium bromide and viewed under UV light. The samples were considered positive if at least one of the dilutions resulted in amplified PCR products.

Statistical analysis

Data on disease severity expressed as a percentage were transformed (arc sin or Johnson's transformations) to meet the assumptions of normality and heteroscedasticity. A three-way analysis of variance (ANOVA) was performed on the overall transformed data with two (experiment 1)- or three (experiment 2)-level interactions. The post hoc Tukey's range test was used for multiple pairwise comparisons. Furthermore, two-way analysis of variance (ANOVA) with (experiment 2) or without (experiment 1) interactions was carried out for year. In experiment 1, the field site Moudon was not included in the analysis of variance since harvest did not take place in this field site in 2017 because of technical problems. Meteorological data from the field sites were downloaded from the publicly available site Agrometeo (http://www.agrometeo.ch/fr/meteorology/datas). Mean temperature and relative humidity data and total precipitation data were calculated per month or for two-week periods. Principal component analysis (PCA) and Pearson's correlation coefficients were analyzed between meteorological parameters and severity data. All the data were analyzed using XLSTAT software.

2.4. Results

Impact of inoculum source on black dot disease severity at harvest

Soil samples of field trials (experiments 1 and 2, Table 2.1) exhibited levels of *C. coccodes* inoculum that ranged from undetectable to 948 pg/g DNA soil. Half of the soil samples contained less than 100 pg DNA/g soil and 80% of the samples less than 250 pg DNA/g soil (Figure 2.1). Linear regression analysis showed no correlation between soil inoculum and disease incidence, severity, or percentage of unmarketable tubers. However, black dot severity at harvest was below 10% in all but two field sites with less than 50 pg DNA/g soil (Figure 2.1).

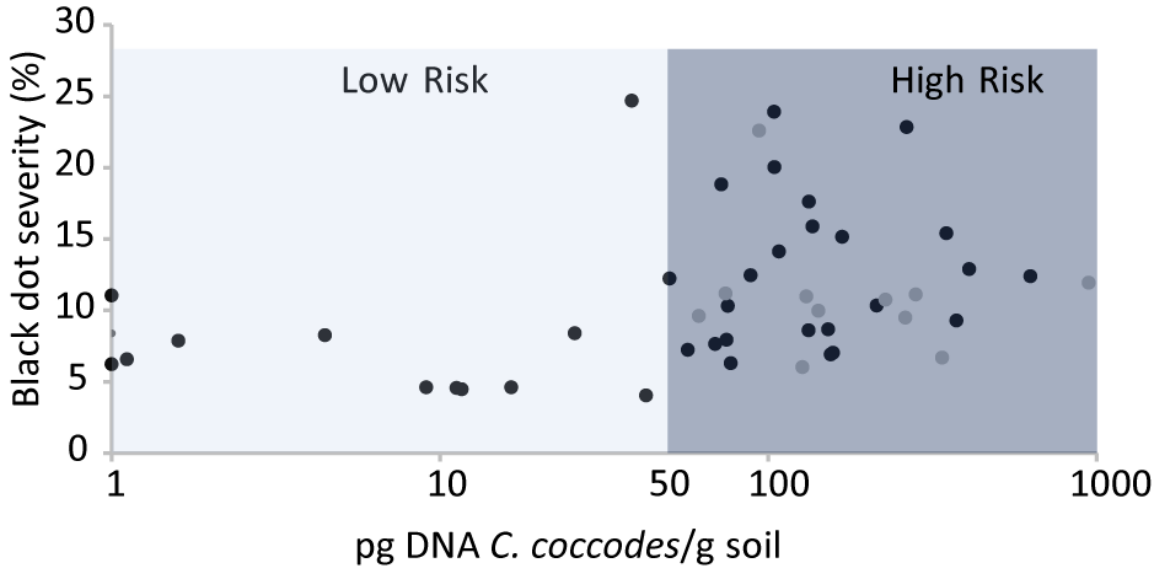

Figure 2.1 Relationship between soilborne inoculum concentration (pg DNA g-1 soil in log scale) and black dot severity (percentage of surface area with symptoms) from experiments 1 (grey dots) and 2 (black dots). The threshold separating low and high risk set at 50 pg DNA g-1 soil is shown.

Black dot incidence on seed tubers did not correlate with black dot severity in daughter tubers (Figure 2.2a). No significant difference in black dot severity at harvest was observed between the two commercially available seed-tuber lots used in experiment 1 (low or high infection) (Figure 2.2b). However, the use of disease-free minitubers resulted in daughter tubers with 35% lower disease severity than using commercial seed-tubers (Figure 2.2b), making the effect of the seed-tuber statistically significant (Table 2.2).

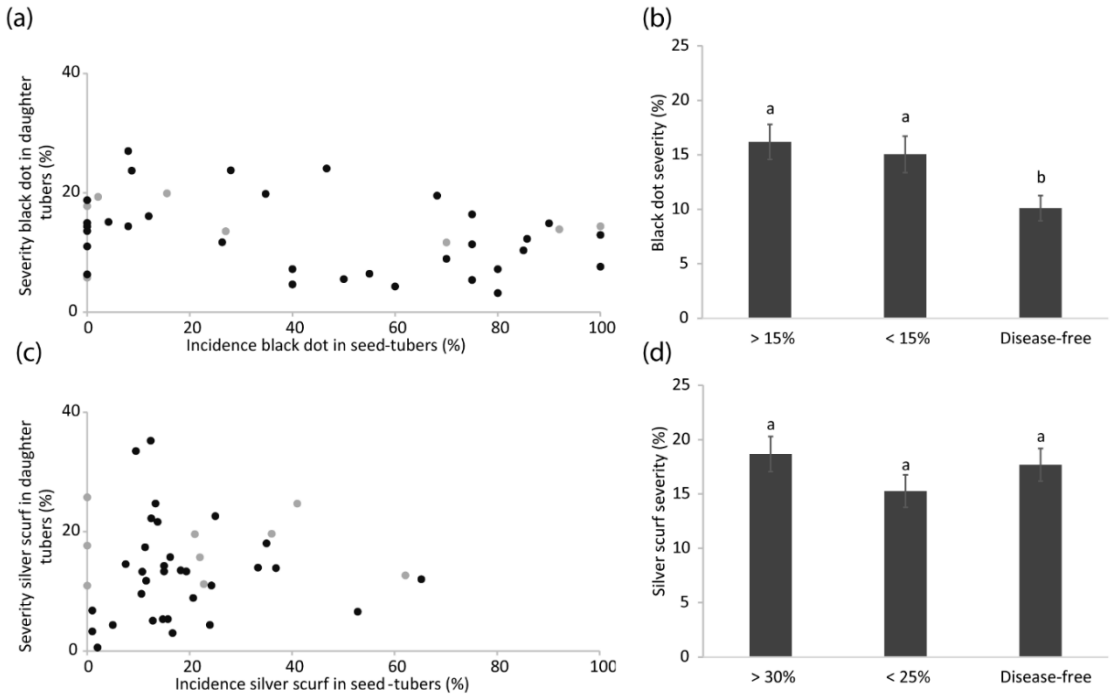

Figure 2.2 Relationship between seed-tuber inoculum and disease severity at harvest. (a) Relationship between black dot incidence in seed-tubers and black dot severity in daughter tubers (experiment 1, grey dots, and experiment 2, black dots); (b) black dot disease severity in daughter tubers from highly infected (>15% disease severity), mildly-infected (<15% disease severity) and disease-free seed-tubers (experiment 1, cv. Charlotte); (c) Relationship between silver scurf incidence in seed-tubers and silver scurf severity in daughter tubers (experiment 1, grey dots, and experiment 2, black dots); and d) silver scurf disease severity in daughter tubers from highly infected (>30% disease severity), mildly-infected (<25% disease severity) and

disease-free seed-tubers (experiment 1, cv. Charlotte). Values in (b) and (d) are means of 17 field trials. Vertical bars represent standard error of means. Different letters indicate statistically significant differences (p<0.01, Tukey's test).

Impact of climatic conditions on black dot severity at harvest

In experiment 1 (Table 2.1), analysis of variance revealed that the main effect « year » was more important than the main effect « field site » in influencing black dot severity, the latter not being statistically significant (Table 2.2). Furthermore, the interaction between these two main effects was not statistically significant (*p*=0.057) (Table 2.2).

Table 2.2 Three-way Analysis of variances (experiment 1) of the main effects seed-tuber lot, field site and year (and their interactions) for black dot and silver scurf disease severity. *df = degrees of freedom, MS = Means of squares, effect size = η2*. *p < 0.05. †p < 0.01. ‡p < 0.001.

		BLACK DOT				SILVER SCURF			
Source	*df*	MS	*F*	*p*	Effect Size	MS	*F*	*p*	Effect Size
Main effects									
Seed-tuber lot (A)	2	202,63	11,46	**< 0.001‡**	0,23	27,54	2,91	0,084	0,02
Field site (B)	4	37,89	2,14	0,122	0,09	106,02	11,19	**< 0.001‡**	0,15
Year (C)	2	153,90	8,71	**0,003†**	0,18	660,03	69,69	**< 0.001‡**	0,46
Interaction									
A x B	8	7,34	0,42	0,895	0,03	16,46	1,74	0,165	0,05
A x C	4	43,27	2,45	0,089	0,10	7,24	0,76	0,563	0,01
B x C	8	44,20	2,50	0,057	0,20	91,02	9,61	**< 0.001‡**	0,26
Model	28	51,79	2,93	**0,014***	0,84	96,00	10,14	**< 0.001‡**	0,95
Residuals	16	17,68				9,47			

Meteorological data recorded in the different field sites were used to study the effects of temperature, precipitation, and relative humidity on black dot severity (Table 2.3). By the use of two-week intervals, principal component analysis (PCA) showed that climatic conditions differed more between years than between field sites (Figure 2.3). These results are in line with those of the analysis of variance where the main effect « year » contributed more than the main effect of « field site » did to the total variability (Table 2.2). The Changins field location had the highest temperatures and the lowest precipitation every year, and the Düdingen location always had the lowest temperature and the highest precipitation (Figure 2.3). PCA suggested that black dot severity was positively correlated with relative humidity and negatively correlated with temperature. Pearson's correlation analysis confirmed a negative trend between black dot severity and season-average temperature, especially in the samples collected during the period from 76 to 120 days after planting (dap) (Table 2.3). Similarly, a positive trend between black dot severity and season-average precipitation and relative humidity was observed. Positive correlations between precipitation and disease severity were observed between 31 and 75 dap, and relative humidity was positively correlated with black dot severity from 46 to 105 dap (Table 2.3). Interestingly, temperature, precipitation and relative humidity between 0 and 15 dap (from planting to emergence) were significantly correlated with black dot severity.

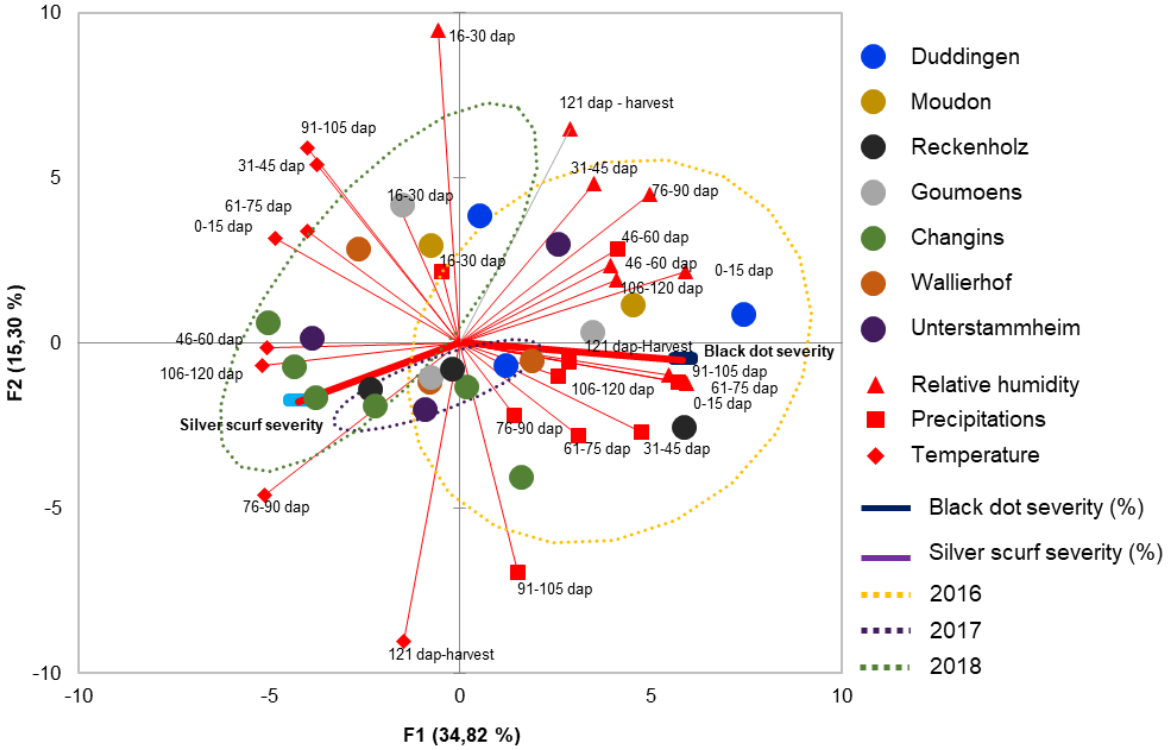

Figure 2.3 Biplot of the principal component analysis (PCA) for meteorological data and the severity of blemish diseases (experiments 1 and 2) in the different field sites. The two first components (PC1 and PC2) explain 50.12% of the total variation. Colored circles represent observations (field sites), ellipses indicate 95% of confidence of each year's observations, red arrows indicate variables (meteorological parameters and disease severity).

Table 2.3 Pearson's correlation values between black dot or silver scurf severity and temperature (temp), relative humidity (RH) or precipitations (Prec) in two-weak intervals from planting to harvest and season-averages. Values in bold indicate significant effects (p<0.05).

Temperature	Black dot	Silver scurf	Precipitations	Black dot	Silver scurf	Relative Humidity	Black dot	Silver scurf
temp_0-15 dap	**-0,590**	0,385	Prec_0-15 dap	**0,778**	**-0,450**	RH_0-15 dap	**0,711**	**-0,445**
temp_16-30 dap	-0,023	0,393	Prec_16-30 dap	0,041	**-0,446**	RH_16-30 dap	-0,207	-0,186
temp_31-45 dap	-0,404	**0,416**	Prec_31-45 dap	**0,620**	-0,283	RH_31-45 dap	0,375	-0,357
temp_46-60 dap	**-0,659**	**0,470**	Prec_46-60 dap	**0,676**	**-0,469**	RH_46-60 dap	**0,541**	-0,262
temp_61-75 dap	-0,395	0,126	Prec_61-75 dap	**0,432**	-0,145	RH_61-75 dap	**0,702**	-0,380
temp_76-90 dap	**-0,675**	0,385	Prec_76-90 dap	0,114	-0,213	RH_76-90 dap	**0,505**	**-0,437**
temp_91-105 dap	**-0,441**	0,128	Prec_91-105 dap	0,222	-0,126	RH_91-105 dap	**0,658**	**-0,420**
temp_106-120 dap	**-0,598**	**0,556**	Prec_106-120 dap	0,240	-0,218	RH_106-120 dap	0,323	**-0,504**
temp_121-harvest	-0,078	0,277	Prec_121-harvest	0,198	-0,351	RH_121-harvest	0,141	-0,312
Seasonal	**-0,664**	**0,583**	Seasonal	**0,737**	**-0,588**	Seasonal	**0,615**	**-0,526**

Monitoring of C. coccodes infections during plant growth

The monitoring of *C. coccodes* infections on potato plant tissues indicated that all belowground tissues were colonized by *Colletotrichum coccodes*. Furthermore, the infection of *C. coccodes* in the roots and stolons appeared very early in the season: more than 60% of the roots were infected 5 days after emergence (34 days after planting) and more than 70% of stolons were infected as soon as they were observed (47 dap) (Figure 2.4a and 2.4b). More than 60% of root samples and more than 70% of stolon samples contained *C. coccodes* fungal DNA at all time points until haulm destruction, which took place at 118 dap. Daughter tubers were infected with *C. coccodes* early upon tuberization, with at least 40% of the tubers infected from 70 dap. Colonization of daughter tubers progressed during plant growth, with more than 75% of samples being infected at 100 dap (except at haulm destruction in 2017 and at harvest in 2016) (Figure 2.4c).

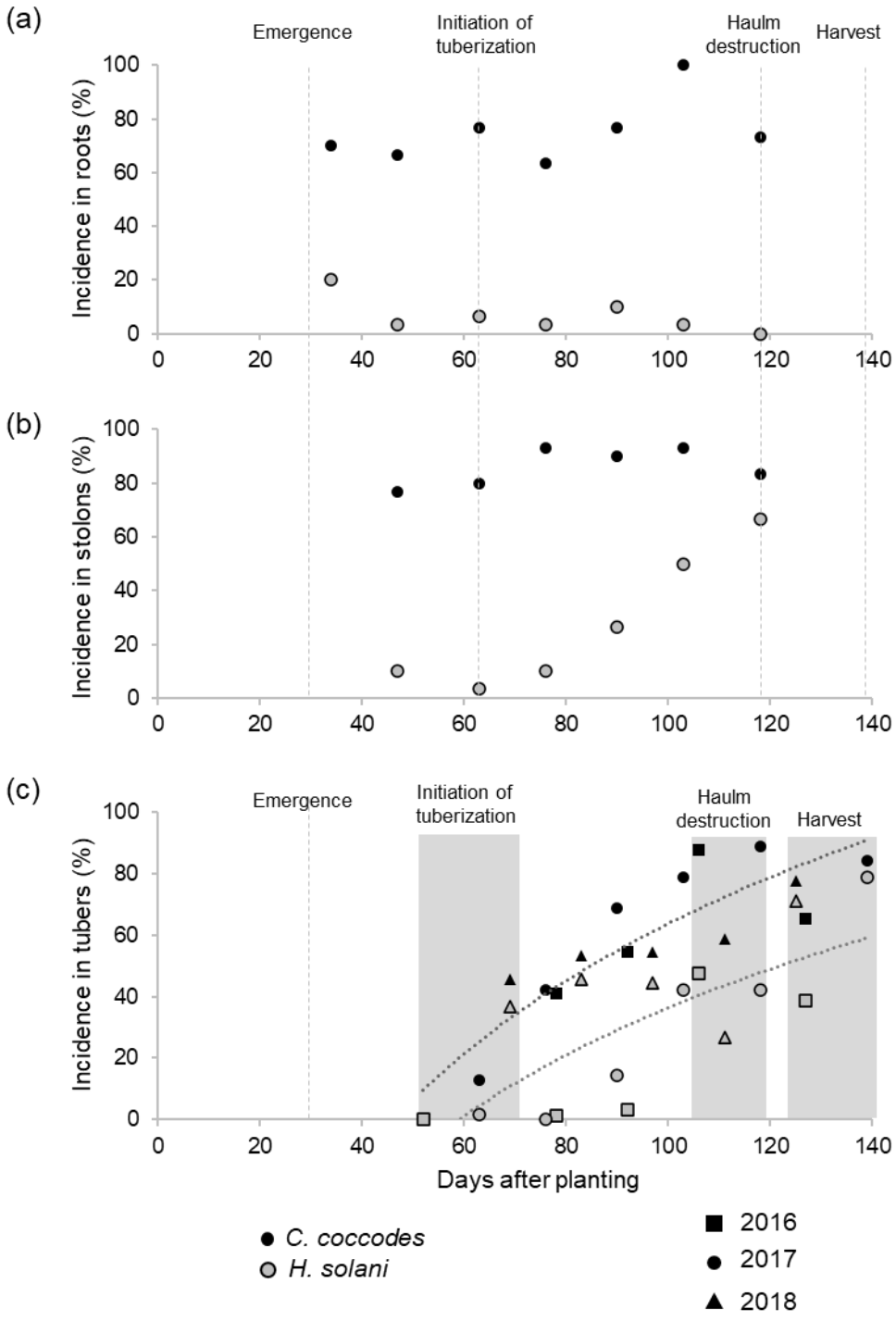

Figure 2.4 Incidence of *C. coccodes* (black) and *H. solani* (light grey) infections detected by PCR in (a) roots, (b) stolons and (c) daughter tubers recorded at 2-week intervals at the Changins field site in 2017 (roots and stolons, n=30/time point) or 2016-2018 (daughter tubers, n=90/time point). Emergence (2016: 25 dap; 2017: 34 dap; 2018: 27 dap), initation of tuberization (2016: 52 dap, 2017: 63 dap, 2018: 69 dap), haulm destruction (2016: 106 dap, 2017: 118 dap, 2018: 111 dap) and harvest (2016: 127 dap, 2017: 139 dap, 2018: 125 dap) are shown. In (c), lines fitted by logarithmic regression.

Susceptibility of potato cultivars to black dot

Disease severity ranged from 4.5% (Changins in 2018) to 23% (Reckenholz in 2016) (Figure 2.5). Significant differences in black dot susceptibility of the different cultivars were observed (Table 2.4, Figure 2.6a). Overall, the main effect « cultivar » accounted for 26% of the total variance observed for black dot severity (Table 2.4). Moreover, the main effect « year » contributed to 25% of the variance observed, the main effect « field site » contributed to 8% of the variance, and the interaction among both contributed to 5% (Table 2.4), indicating that the cultivar contributes as much as the environmental factors did to black dot severity. Furthermore, with respect to the analysis of variance of individual years, the main effect « cultivar » was always more important than the main effect « field site » (data not shown).

Table 2.4 Three-way Analysis of variances (experiment 2) of the main effects cultivar, field site and year (and their interactions) for black dot and silver scurf disease severity. *df = degrees of freedom, MS = Means of squares, effect size = η2*. †p < 0.01. ‡p < 0.001.

		BLACK DOT				SILVER SCURF			
Source	*df*	MS	*F*	*p*	Effect Size	MS	*F*	*p*	Effect Size
Main effects									
Cultivar (A)	15	10,03	29,19	**< 0.001‡**	0,26	21,15	127,77	**< 0.001‡**	0,48
Field site (B)	2	24,29	70,68	**< 0.001‡**	0,08	14,77	89,25	**< 0.001‡**	0,04
Year (C)	2	72,66	211,44	**< 0.001‡**	0,25	59,13	357,30	**< 0.001‡**	0,18
Interaction									
A x B	30	0,79	2,31	**< 0.001‡**	0,04	0,30	1,80	**0,007†**	0,01
A x C	30	0,79	2,30	**< 0.001‡**	0,04	1,50	9,03	**< 0.001‡**	0,07
A x B	4	7,50	21,84	**< 0.001‡**	0,05	13,25	80,06	**< 0.001‡**	0,08
A x B x C	60	0,53	1,54	**0,008†**	0,06	0,26	1,56	**0,007†**	0,02
Model	143	3,17	9,23	**< 0.001‡**	0,79	4,11	24,81	**< 0.001‡**	0,89
Residuals	432	0,34				0,17			

Overall, the mean black dot disease severity ranged from 5% in the most resistance cultivar (Erika) to 19% in the most susceptible cultivar (Celtiane) (Figure 2.6a). The interactions between the maieffect « cultivar » and the main effects « year » and « field site » were statistically significant (p<0.001), but their contribution to the total variance was less than 6% in all cases (Table 2.4). Furthermore, these interactions could be mainly explained by a single potato cultivar (Ditta), which showed high susceptibility in 2018 and especially high susceptibility in 2016 but very low susceptibility in 2017. Notably, there was a strong correlation of black dot severity between field sites (not shown) and years for the other cultivars (Table 2.5).

Table 2.5 Black dot and silver scurf relative susceptibility values (from 0 to 1) in 2016, 2017 and 2018 over all field sites. Relative values are calculated as the ratio between the disease severity of a cultivar and the highest disease severity observed (for each year).

	Black dot relative severity				Silver scurf relative severity		
Cultivar/Year	2016	2017	2018	**Cultivar/Year**	2016	2017	2018
Lady Felicia	0,89	1,00	0,60	Lady Christl	1,00	1,00	1,00
Celtiane	1,00	0,91	1,00	Gourmandine	0,51	0,67	0,56
Charlotte	0,88	0,79	0,87	Venezia	0,38	0,66	0,62
Agata	0,73	0,75	0,63	Lady Felicia	0,70	0,65	0,75
Jazzy	0,60	0,69	0,58	Erika	0,39	0,43	0,60
Amandine	0,70	0,63	0,55	Agata	0,49	0,40	0,72
Vitabella	0,72	0,55	0,47	Amandine	0,41	0,40	0,73
Gourmandine	0,53	0,47	0,41	Charlotte	0,34	0,40	0,33
Venezia	0,50	0,44	0,27	Celtiane	0,19	0,35	0,28
Annabelle	0,56	0,44	0,40	Vitabella	0,25	0,33	0,48
Lady Christl	0,53	0,39	0,30	Laura	0,27	0,20	0,24
Gwenne	0,43	0,34	0,15	Annabelle	0,40	0,16	0,47
Erika	0,23	0,33	0,24	Jazzy	0,14	0,16	0,48
Cheyenne	0,55	0,28	0,35	Ditta	0,45	0,13	0,48
Ditta	0,88	0,26	0,57	Gwenne	0,12	0,10	0,10
Laura	0,41	0,20	0,19	Cheyenne	0,09	0,02	0,13

Thus, the response of potato cultivars to black dot might differ slightly in different environments, but these specific differences are quantitatively less important than the general susceptibility of each cultivar to black dot. Even though the disease severity of black dot was very low in certified tubers (below 3%), a correlation between data from the field experiment (experiment 2) and from certified tubers (experiment 3) was observed for the incidence (data not shown) and the severity of black dot (r^2=0.44, p<0.05) (Figure 2.7a). However, only one cultivar (Celtiane) showed low susceptibility of tubers issued from the certification program (experiment 3) and high susceptibility in the cultivar susceptibility field trials (experiment 2) (Figure 2.8a, red dot). After removal of this cultivar from the analysis, the relationship between black dot severity in both trials (experiment 2 and experiment 3) for the remaining 11 cultivars improved (r^2=0.72, p<0.001); Figure 2.7a). Black dot severity did not correlate with maturity, dormancy, or starch content of the cultivars, suggesting that these physiological parameters do not influence black dot severity, and the year of registration did not significantly correlate with disease severity, indicating that recently developed cultivars are not more resistant than older potato cultivars (Table 2.6). It is worth noting that the cultivars were not genealogically closely related (data not shown).

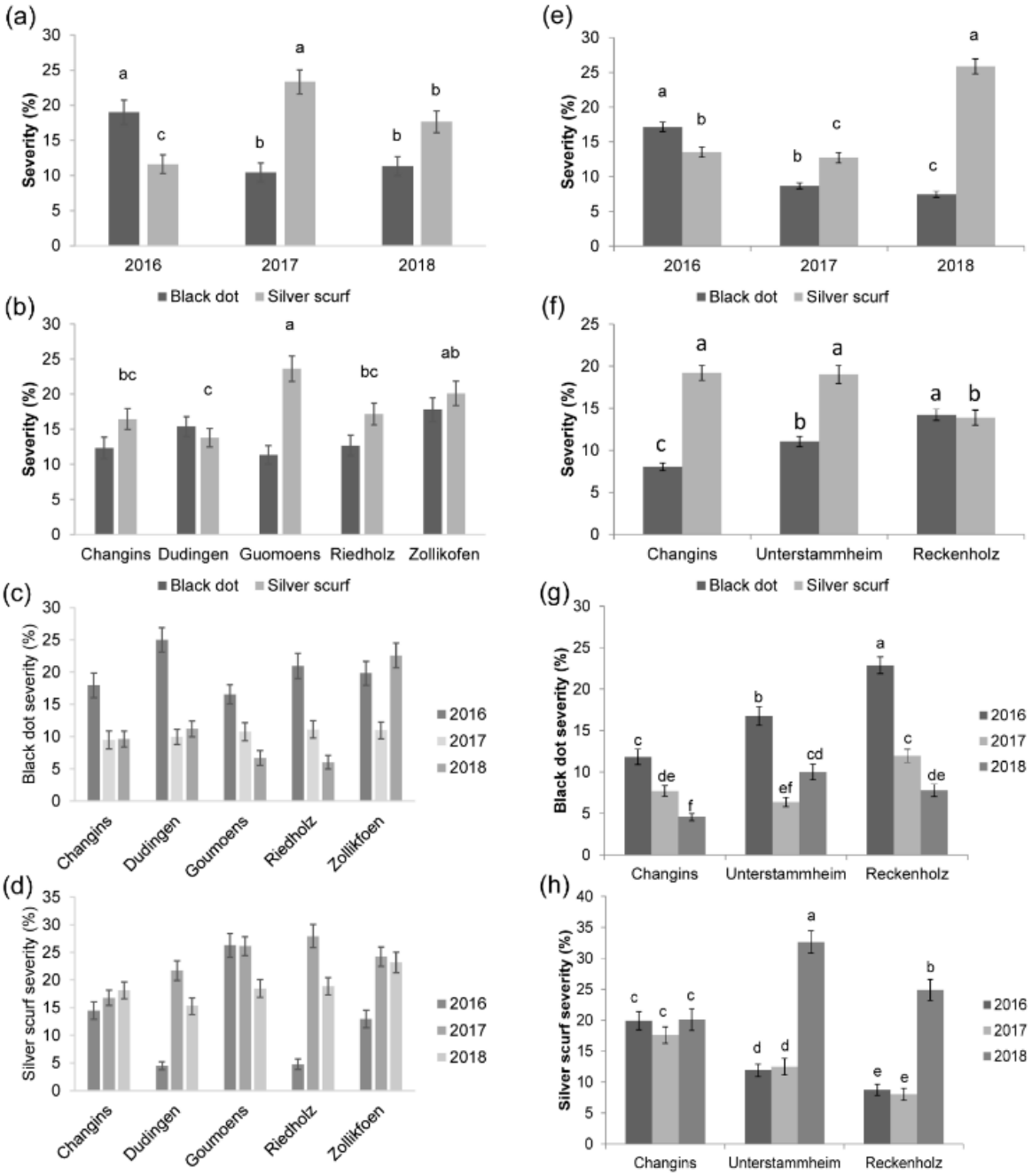

Figure 2.5 Overall black dot and silver scurf severity in experiment 1 (a, b, c and d) or experiment 2 (e, f, g and h) by year (a and e) and field site (b and f) or their combination (c, d, g and h). Different letters indicate statistically significant differences (p<0.01). No letters indicate no significant differences.

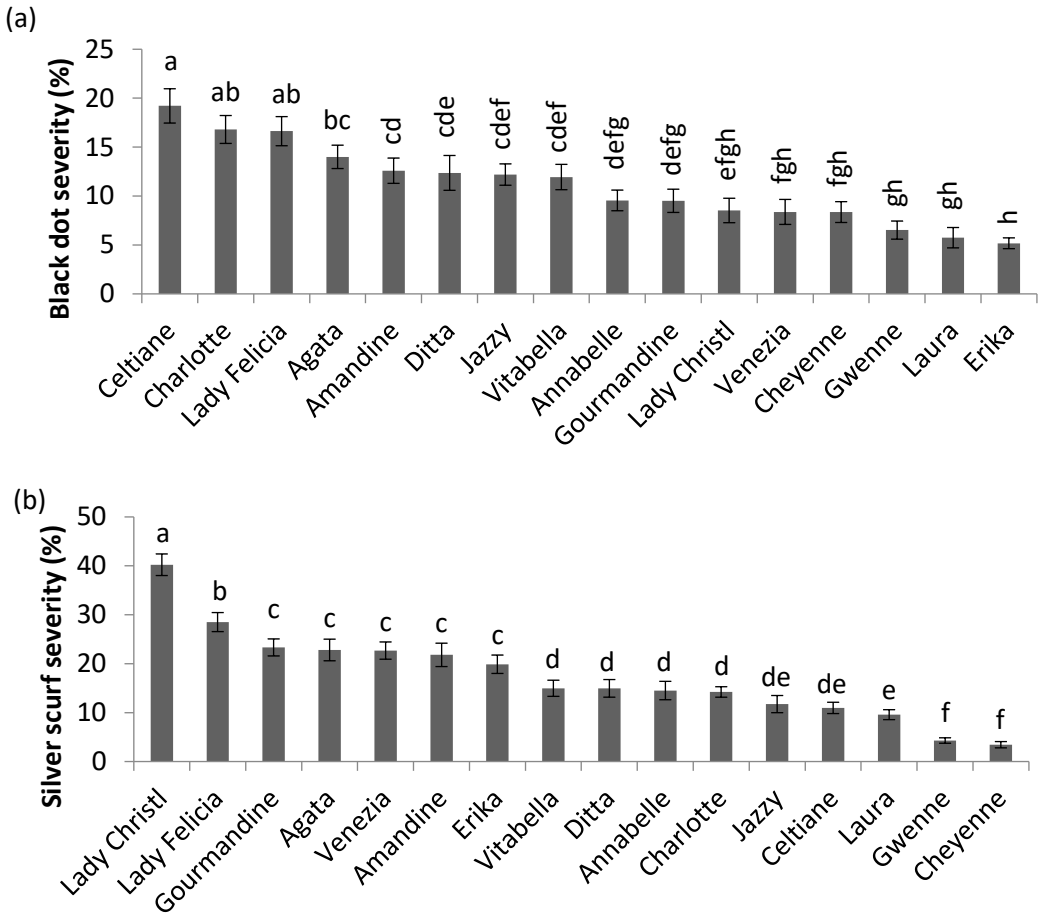

Figure 2.6 a) Black dot and b) silver scurf disease severity among the 16 cultivars in the field trials (2016-2018). Values are means of the three years field trials in randomized plots (n=36). Vertical bars represent standard error of means. Different letters indicate statistically significant differences (p<0.01, Tukey's test).

Impact of inoculum source on silver scurf disease severity at harvest

H. solani soil inoculum was not detected at any field site for either experiment (1 or 2, Table 2.1). However, the limit of detection for this pathogen in the field was found to be higher than that for *C. coccodes* (LOD of *H. solani*: 500 pg DNA/g soil; LOD of *C. coccodes*: 1 pg DNA/g soil). Nonetheless, it is worth noting that the main effect « field site » and its interactions with the main effect « year », which involve both the source of inoculum and climatic conditions, were significant in both experiments (Tables 2.2 and 2.4). Silver scurf disease severity of seed tubers did not influence disease severity at harvest, planting disease-free seed tubers did not prevent the emergence of disease symptoms in daughter tubers, and no differences in silver scurf severity between the various seed-tuber lots were observed (Figure 2.2c and 2.2d, Table 2.2).

Impact of climatic conditions on silver scurf severity at harvest

In experiment 1 (Table 2.1), the main effects « field site » and « year », as well as their interaction, were significant (Table 2.2). The main effect « year » presented the highest contribution to the total variability (46%), the main effect « field site » contributed to 15%, and the interaction between them explained 26% of the total variability (Table 2.2). In experiment 2, the main effect « year » contributed to 18% of the total variability, while the main effect « field site » and their interaction explained 4% and 8% of the total variability, respectively (Table 2.4). PCA of the meteorological data suggested that temperature, precipitation and relative humidity had an effect on silver scurf disease severity (Table

2.3). Notably, a trend between silver scurf and high season-average temperatures was observed (Figure 2.3). However, the correlation was found to be significant only between 31 and 60 dap and between 106 and 120 dap (Table 2.3). Furthermore, a negative trend between precipitation (or relative humidity) and silver scurf severity was found. Precipitation was negatively correlated with disease severity at the beginning of the season (0-30 dap and 46-60 dap), while relative humidity was negatively correlated with silver scurf symptoms between 0-15 dap and from 76 to 120 dap (Table 2.3).

Monitoring of H. solani infections during plant growth

DNA of *H. solani* was found in less than 10% of root samples except at emergence, where 20% of samples contained *H. solani* DNA (Figure 2.4). Furthermore, less than 10% of stolons showed infection until 76 dap. A linear increase in *H. solani*-infected stolons was observed after that time, with 27% of stolons infected at 90 dap, 50% at 103 dap, and 67% at haulm destruction (118 dap) (Figure 2.4b). Similarly, less than 15% of the tubers were infected with *H. solani* before 92 dap in 2016 and 2017, but this percentage increased to 40% at 100 dap, reaching between 40 and 80% of the tubers infected at harvest (Figure 2.4c). Early contamination of daughter tubers with *H. solani* occurred in 2018, with more than 35% of the tubers infected at 69 dap. During all three years, the number of tubers infected remained below 50% until haulm destruction and increased to 71% at harvest (Figure 2.4c).

Susceptibility of potato cultivars to silver scurf

Silver scurf disease severity in experiment 2 ranged from 33% (Unterstammheim in 2018) to 8% (Reckenholz in 2017) (Figure 2.6). The main effect « cultivar » explained 48% of the total variance of silver scurf severity observed in the field trials (Table 2.4) and, in a separate year analysis, the main effect « cultivar » explained 60% of the variance in 2016, 71% in 2017 and 70% in 2018, at least three times more than the main effect « field site » (data not shown). The highest silver scurf severity was observed in the cultivar Lady Christl in all field trials, with an average of 40% of the tuber surface exhibiting symptoms of the disease (Figure 2.7b). Furthermore, differences between Lady Christl and all the other cultivars were statistically significant. The cultivars Gwenne and Cheyenne showed less than 5% disease severity, while all other cultivars showed disease severity levels between 5% and 40% (Figure 2.7b). The interaction between the main effects « cultivar » and « field site » or « year » were statistically significant but accounted for only 1% and 7% of the total variance observed, respectively (Table 2.4). Indeed, the relative severity of silver scurf was found to be stable throughout the years for most cultivars, although two cultivars (Annabelle and Ditta) showed very low susceptibility to silver scurf only in 2017 (Table 2.5). The severity of silver scurf was found to be lower in daughter tubers from the certification program trials (experiment 3) than in the cultivar susceptibility field trials (experiment 2), but there was a strong correlation between disease severity in both experiments (r^2= 0.76, p<0.001, Figure 2.9b). A negative correlation between maturity and silver scurf disease severity on daughter tubers was observed, suggesting that early-maturing cultivars are more susceptible to silver scurf than are late-maturing cultivars (Table 2.6). However, silver scurf severity did not correlate with dormancy or starch content, suggesting that these physiological parameters do not have an influence on silver scurf disease severity (Table 2.6). Furthermore, disease severity of recently developed cultivars did not differ from that of other cultivars (Table 2.6).

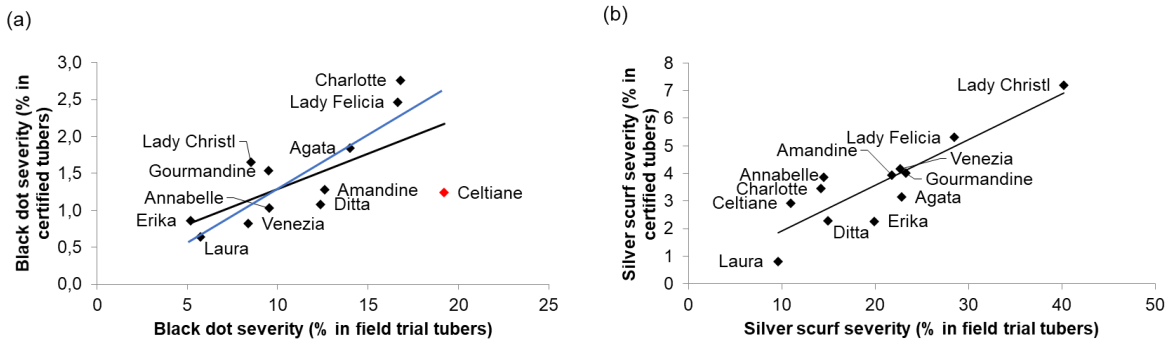

Figure 2.7 Correlation between (a) black dot severity and (b) silver scurf severity of 16 potato cultivars in field assays (experiment 2) and the monitoring of seed-tuber production (experiment 3). In (a) red dot is potato cultivar Celtiane, blue line is linear correlation between all cultivars except Celtiane. Variance accounted for = 44% and 72% for black dot (for all cultivars and all cultivars except Celtiane, respectively) and 76% for silver scurf.

Table 2.6 Pearson's correlation values between black dot or silver scurf severity of cultivars from experiment 2 and maturity, year of inscription, starch content (%) and dormancy. Values in bold indicate significant effects (p<0.05).

Variables	Black dot	Silver scurf
Maturity	-0,19	**-0,69**
Year of inscription	-0,42	-0,15
Starch content (%)	-0,11	-0,34
Dormancy	-0,06	-0,27

2.5. Discussion

Black dot and silver scurf are tuber blemish diseases of potato, with similar visual symptoms. Thus, these diseases are often tagged together during storage, and an efficient pest management strategy should include control of both of them. This study tries to gain new insights into epidemiological factors that drive each disease's development.

Microsclerotia present in the soil have been shown to be an important source of inoculum for black dot (Lees et al., 2010). In the field trials presented here, no correlation was found between the amount of soil inoculum and black dot disease severity, although field sites with low soil inocula usually exhibited low disease severity. The lack of a correlation is probably due not only to the relatively strong impact of other factors on black dot (i.e., cultivar, climatic conditions) but also to the rather low levels of soil inoculum encountered compared to previous studies (Lees et al., 2010). In the UK, thresholds of 100 and 1000 pg DNA/g soil delimiting low, medium and high disease risk have been suggested (Lees et al., 2010). Since soil inocula were rather low in the Swiss trials, we suggest lowering the threshold to 50 pg DNA/g soil for low risk under conditions in Switzerland. Assuming that tubers with more than 10% black dot severity may be unmarketable (Lees et al., 2010), the choice of fields with low soil inocula would have reduced the share of unmarketable tubers from 24% to 16%. In contrast, *H. solani* inoculum was not detected in any of the soils analyzed, suggesting that it might be absent from these field trials. Since the limit of detection of *H. solani* in soils is higher than that for *C. coccodes*, low amounts of *H. solani* cannot be excluded. Potato plants are the only known symptomatic host of *H. solani*, and rotation of three years should be sufficient to control silver scurf (Errampalli et al., 2001b). However, volunteer potato plants often appear in fields where potato crops have been cultivated previously, and *H. solani* has been shown to be saprophytic to a number of crop species that are present in the rotation with potatoes in Switzerlad such as corn and wheat (Mérida and Loria, 1994b), which may also be a reservoir of inocula. Studies conducted in Canada (Bains et al., 1996) showed that

disease-free seed tubers produce diseased daughter tubers even in fields without a known history of potato growth, but other authors have found that the use of clean minitubers reduces silver scurf in the field and that planting disease-free seed tubers generally results in the absence of the disease in daughter tubers (Geary and Johnson, 2006; Miller et al., 2015). In our field trials, planting silver scurf-free minitubers resulted in diseased daughter tubers, suggesting that low amounts of *H. solani* inoculum were indeed present in these fields. However, it cannot be excluded that fungal spores of *H. solani* were transported through water flow from diseased plants towards plants emerged from clean minitubers. Seed-tuber inocula did not influence disease severity at harvest for either disease, as found elsewhere (Read and Hide, 1984; Firman and Allen, 1995b; Denner et al., 1998; Dung et al., 2012). However, disease-free minitubers produced daughter tubers with significantly fewer black dot symptoms (35% reduction). Similar results were observed in South African trials (Denner et al., 1998), although other assays have shown that the use of clean minitubers did not reduce disease severity at harvest (Dung et al., 2012). It is worth noting that plants originating from disease-free minitubers were generally smaller in the field, mostly with a single main stem, and tuberization occurred slightly later in the season. This is probably due to the physiological age of the seed tubers, which were harvested in July for the commercial seed-tuber lots and in late autumn for the minitubers. The delay in tuberization in plants originating from minitubers might explain the lower disease severity, since it has been suggested that early-maturing cultivars are more susceptible to black dot because their tubers are in contact with the soil inoculum for a longer period of time than are those of late-maturing cultivars (Andrivon et al., 1998).). Overall, our results confirm that black dot and silver scurf occur even when disease-free minitubers are planted in the field and indicate that producing disease-free seed tubers is not an effective measure to control these blemish diseases.

The monitoring of fungal infections in the field and in the greenhouse revealed that *C. coccodes* is able to infect all belowground organs of potato plants and that both seed and soil inocula result in early infections, all of which is which in accordance with the results of previous studies (Andrivon et al., 1998; Lees et al., 2010). Notably, we found that *H. solani* DNA was present in stolons and tubers but was very rarely present in the roots. Previous work has shown that roots, stolons and stems do not show silver scurf symptoms (Fahn, 1982), but molecular biology techniques have not been used previously to detect latent *H. solani* infection*s* in belowground organs. Here, we confirmed that *H. solani* does not usually colonize potato roots and also demonstrated that this fungus is able to infect potato stolons, which may transfer the disease from the seed tuber to the daughter tubers. This hypothesis is supported by our observations of stolon infections preceding tuber infections and by previous reports showing that silver scurf lesions appear first at the stolon end of the tuber (Jellis and Taylor, 1977). Furthermore, the presented results showed that potato belowground organs are infected later in the season with *H. solani* than with *C. coccodes*, and even when silver scurf infection appeared early in the season, its epidemiological curve was slower than that of *C. coccodes*.. Since warm temperatures usually occur during the second half of potato production in the climatic conditions of Switzerland, *H. solani* may be more infectious during that period of the season. Notably, higher temperatures at the beginning of the season were recorded in 2018, which correlated with relatively early infections of daughter tubers with *H. solani*, and, in general, warm and dry conditions were associated with increased silver scurf severity. Potato plants grown during humid seasons were more prone to black dot, which is in line with other reports that showed that this disease is favored by irrigation (Hide et al., 1994b; Lees et al., 2010; Olanya et al., 2010; Brierley et al., 2015).

All cultivars showed symptoms of black dot and silver scurf, confirming the lack of full resistance in commercial potato cultivars, as found in other studies (Secor, 1994; Brierley et al., 2015). However, cultivar had a strong impact on disease severity, especially for silver scurf, and disease severity differed on the cultivars studied. Furthermore, a strong correlation between daughter tuberd from field trials

and daughter tubers of the same varieties from the Swiss certification program was found. These results confirm that cultivar choice is a major determinant of the risk of black dot, and it is even more so for silver scurf. Cultivar maturity had been previously suggested to be involved in the susceptibility to black dot (Andrivon et al., 1998), but the results presented here suggest that other genetic characteristics may be more important in determining cultivar susceptibility to black dot under conditions in Switzerland. In contrast, silver scurf severity was higher in the early-maturing cultivars than in the late-maturing cultivars. The basis of quantitative resistance against both diseases remains unknown and may involve several mechanisms.

Taken together, the results presented here can contribute to developing an integrated pest management strategy that can help reduce the risk of black dot and silver scurf in Switzerland. *C. coccodes* soil inoculum can be quantified to determine the risk of tubers developing black dot symptoms, information that can be integrated into the decision making of cultivar selection. Through this work, potato cultivars with different degrees of susceptibility to black dot and silver scurf destined for fresh markets have now been identified, and this information can be integrated into disease-risk management models. Models to predict fungal diseases have been successfully implemented for other diseases, such as downy and powdery mildew of grapevine, by the use of temperature and relative humidity (Dubuis et al., 2019), and monitoring meteorological conditions can help predict the risk of disease development. Since black dot and silver scurf are affected by storage conditions (Hide et al., 1994b; Rodriguez et al., 1996; Peters et al., 2016), the early distribution of tuber lots with high risk (i.e., susceptible cultivars, short rotations) should be prioritized. The present work is part of a Swiss collaborative project including several approaches (disease severity monitoring from planting to distribution, *C. coccodes* host range, chemical and biological treatments during planting and post-harvest) to develop an integrated management strategy to control both diseases.

2.6. Aknowledgements

This work was supported with by a grant from the Commission for Technology and Innovation (CTI) in Switzerland (Grant Number 18536.1 PFLS-LS) and the Swiss potato sector (Swisspatat) to the consortium: School of Agriculture, Forest and Food Sciences, Bern University of Applied Sciences, Agroscope and the Research Institute of Organic Agriculture (FiBL). The authors thank participating growers for the use of the field sites and the potato team of the Varieties and Production Techniques research group of the Plant and Plant Products Division, Agroscope, for field trial management. Susete Ulliel is thankfully aknowledged for assistance in *in vitro* plant production and microsatellite genotyping. All the team of Mycology and Plant Biotechnology of the Plant Protection Division of Agroscope are thankfully aknowledged for assistance in the severity determination of black dot and silver scurf. The authors declare no conflict of interest.

3. Insights on the Structural and Metabolic Resistance of Potato (Solanum tuberosum) Cultivars to Tuber Black Dot (Colletotrichum coccodes)

Josep Massana-Codina, Sylvain Schnee, Pierre-Marie Allard, Adriano Rutz, Julien Boccard, Emilie Michellod, Marilyn Cléroux, Stéphanie Schürch, Katia Gindro, Jean-Luc Wolfender

This chapter is based on an original research article that was published in the journal *Frontiers in Plant Science* (Massana-Codina et al., 2020) (doi: 10.3389/fpls.2020.01287). All references are compiled in a common list at the end of the thesis.

Author's contributions: JM-C, KG, StS and J-LW conceived and designed the study. JM-C performed the experiments in the greenhouse and the in vitro antifungal assays. JM-C and SyS extracted the suberin and specialized metabolites and prepared them for analysis. EM conducted the microscopy analysis of the tuber periderm. MC performed the GC-MS analysis of suberin monomers and analyzed the data. P-MA performed the LCMS analysis of specialized metabolites. JB performed the multivariate data analysis (AMOPLS). JM-C, P-MA and AR analyzed the LCMS data and performed the molecular network analysis. JM-C, SyS, JB, P-MA, AR, KG and JL-W analyzed and interpreted the results. JM-C, KG and JL-W wrote the manuscript. All authors discussed the results and reviewed the final manuscript.

3.1. Abstract

Black dot is a blemish disease of potato tubers caused by the phytopathogenic fungus *Colletotrichum coccodes*. Qualitative resistance (monogenic) that leads to the hypersensitive response has not been reported against black dot, but commercial potato cultivars show different susceptibility levels to the disease, indicating that quantitative resistance (polygenic) mechanisms against this pathogen exist. Cytological studies are essential to decipher pathogen colonization of the plant tissue, and untargeted metabolomics has been shown effective in highlighting resistance-related metabolites in quantitative resistance. In this study, we used five commercial potato cultivars with different susceptibility levels to black dot, and studied the structural and biochemical aspects that correlate with resistance to black dot using cytological and untargeted metabolomics methods. The cytological approach using semithin sections of potato tuber periderm revealed that *C. coccodes* colonizes the tuber periderm, but does not penetrate in cortical cells. Furthermore, skin thickness did not correlate with disease susceptibility, indicating that other factors influence quantitative resistance to black dot. Furthermore, suberin amounts did not correlate with black dot severity, and suberin composition was similar between the five potato cultivars studied. On the other hand, the untargeted metabolomics approach allowed highlighting biomarkers of infection, as well as constitutive and induced resistance-related metabolites. Hydroxycinnamic acids, hydroxycinnamic acid amides and steroidal saponins were found to be biomarkers of resistance under control conditions, while hydroxycoumarins were found to be specifically induced in the resistant cultivars. Notably, some of these biomarkers showed antifungal activity *in vitro* against *C. coccodes*. Altogether, our results show that quantitative resistance of potatoes to black dot involves structural and biochemical mechanisms, including the production of specialized metabolites with antifungal properties.

3.2. Introduction

Colletotrichum coccodes (Wallr.) S. Hughes (Wallroth, 1833; Hughes, 1958) is a ubiquitous phytopathogenic fungus with multiple host plants, including weeds and several crops. It is the responsible for anthracnose in peppers, tomatoes and onions, and causes black dot in potatoes (*Solanum tuberosum* L.). Several Vegetative Compatibility Groups (VCGs) with different morphology and aggressiveness have been isolated from potatoes, indicating a high genetic variability of the fungal species (Nitzan et al., 2002, 2006; Aqeel et al., 2008).Black dot symptoms can be observed in all parts of the plant, and are characterized by the presence of microsclerotia on infected tissue (Read and Hide, 1988). Microsclerotia can survive in the soil for long periods, and high soil inoculum levels result in high disease incidence (Lees et al., 2010). In the field, fungal colonization of roots is followed by colonization of stems, stolons and tubers (Andrivon et al., 1998). Black dot can affect the yield of potato production (Tsror (Lahkim) et al., 1999), and contamination of tubers with *C. coccodes* results in lesions on the skin of potato tubers and water losses during storage (Lees and Hilton, 2003). Qualitative resistance to black dot has not been reported in potatoes, but different susceptibility levels have been observed among commercially available potato cultivars (Read, 1991b; Tsror (Lahkim) et al., 1999; Brierley et al., 2015). Based on disease surveys, it has been suggested that thick-skin cultivars are more resistant to black dot than thin-skin cultivars (Hunger and McIntyre, 1979), and early-maturing cultivars may be less susceptible to the disease because they spend less time in contact with the soil inoculum (Andrivon et al., 1998). Nonetheless, the genetic, morphologic, physiologic and metabolic basis of host resistance to black dot are still poorly understood. The pressure to produce high quality potatoes, together with the limited efficiency of fungicides in controlling black dot, force developing new strategies to reduce the risk of this blemish disease. Among these, the use of existing cultivars with resistance to black dot is of interest, because it does not require chemical fungicide application.

Plant-pathogen interactions have been studied using different model organisms, including several *Solanaceae* plants. Plants' response to pathogen attack localizes to individual cells that are in contact

with the pathogen and systemic signals from the infection sites (Jones and Dangl, 2006). This response results in important changes on the attacked cell, at transcriptomic, proteomic and metabolomics levels. Upon pathogen perception, the host cell activates signaling pathways that i) trigger the transcription of defense genes and ii) mediate ROS production and hormone synthesis (Corwin and Kliebenstein, 2017). Ultimately, the plant cell responds to the pathogen attack through defense mechanisms, which involve the synthesis of compounds and metabolic reprogramming (Saijo et al., 2018). Plant resistance to a pathogen is often provided by genes that code for proteins involved in the recognition of pathogens, in the so-called gene-for-gene plant resistance that leads to programmed cell death (PCD) in the hypersensitive response (HR), avoiding the spread of the pathogen (Jones and Dangl, 2006). The plant resistance that leads to the HR is also called qualitative resistance, because pathogen growth is averted and relies on a single gene. In potatoes, several *R* genes have been identified and introduced in breeding programs. As found in many other crops, *R* genes against late blight (caused by *Phytophthora infestans*) contain a nucleotide binding domain (often NB-LRRs) that recognizes the pathogen and triggers an immune response, such as in the case of *R1* or *R2* (Ballvora et al., 2002; Aguilera-Galvez et al., 2018). However, pathogens evolve to the presence of *R* genes in order to overcome resistance (Aguilera-Galvez et al., 2018), and therefore, the presence of a single *R* gene is not sufficient for long-term resistance. On the other hand, quantitative resistance is characterized by limited pathogen growth and symptom development, and often involves multiple plant defense reactions and genes with small to medium effects (Kröner et al., 2011; Corwin and Kliebenstein, 2017). Quantitative resistance is still poorly understood but might involve different mechanisms and is more durable than qualitative resistance.

Plant response to pathogen attack often involves the generation of metabolites that may act as physical barriers, possess antimicrobial activity, or act as signaling molecules (Desender et al., 2007; Kröner et al., 2012). Interestingly, such metabolites can be present before infection, induced by the pathogen, or both (La Camera et al., 2004; Kröner et al., 2012), suggesting that quantitative resistance may be explained by both constitutive and inducible resistance-related metabolites. Cytological (Thangavel et al., 2016), transcriptomic (Zuluaga et al., 2015) and metabolomics studies (Yogendra et al., 2015) of currently available cultivars might help decipher strategies for the resistance of certain cultivars to plant diseases.

Potato tubers are protected from the outer environment through the potato skin, which contains high amounts of proteins involved in the defense response, including enzymes involved in phenolic acid production and in suberization processes (Barel and Ginzberg, 2008). Fungal infection of potato tubers probably requires the penetration of the pathogen through the suberized phellem tissue. Notably, the number of phellem cells, as well as suberin content, correlate with resistance against common scab, produced by the bacterial pathogen *Streptomyces scabies* (Thangavel et al., 2016). Moreover, the penetration of the fungal hyphae in host cells likely produces non-enzymatic reactions, such as oxidative bursts that will impact the biochemistry of the infected cell (Lehmann et al., 2015). Several metabolomics studies have studied the resistance of cultivars and wild *Solanum* species to a number of pests, highlighting biomarkers of resistance (Aliferis and Jabaji, 2012; Pushpa et al., 2014; Yogendra et al., 2015; Chen et al., 2019). Among the defense-related metabolites present in the potato skin, steroidal glycoalkaloids and calystegines have shown antimicrobial properties (Fewell and Roddick, 1993; Friedman and Levin, 2009), but are also toxic to human consumption and thus, remain in low quantities in commercial cultivars (Petersson et al., 2013; Mariot et al., 2016). On the other hand, the phenylpropanoid pathway leading to the production of various phenolic compounds is activated in potatoes upon microbial infection, and phenolic acids such as the hydroxycinnamic acids (HCA) chlorogenic acid, neochlorogenic acid and cryptochlorogenic acid have been involved in the resistance of tubers against different diseases (Kröner et al., 2012; Yogendra et al., 2014). Furthermore, flavonoid glycosides, such as rutin and nicotiflorin, are important for determining resistance against several plant

pathogens in a number of plants, including potatoes (Bollina et al., 2010; El Hadrami et al., 2011; Henriquez et al., 2012; Kröner et al., 2012; Pushpa et al., 2014). Resistance-related metabolites to late blight have also been identified in potato tubers, and include glucosinolate derivatives, coumarins and organic acids (Hamzehzarghani et al., 2016).

Metabolomics and cytological analysis have been used to highlight pathogenesis related metabolites in several host-pathogen interactions, including interactions between *S. tuberosum* and microbial pathogens. Although recent studies showed the importance of the host variety and pathogen strain on quantitative resistance (Ors et al., 2018; Samain et al., 2019), studies of plant-pathogen interactions often rely on the use of a model using a single susceptible and a single resistant genotype. Furthermore, the effect of the inoculation of *C. coccodes* on the metabolome of potato tubers has not been studied so far.

In this context, the aim of the present study was to investigate the parameters that influence cultivar resistance to black dot both from a cytological and biochemical perspectives. For this, we use five cultivars with a range of quantitative resistance to black dot in a greenhouse experiment under controlled conditions. All cultivars are either mock or fungal inoculated, allowing the comparison of untreated and inoculated samples. A combined cytological and biochemical approach is used to decipher the mechanisms of resistance. Microscopic analyses of the tuber peel of potatoes with different resistance to plant pathogens have been previously used to highlight structural defense responses in the potato tuber (Thangavel et al., 2014, 2016). Here, we combine microscopic observations with a biochemical quantification of the total suberin amount and the composition of this polymer to study the structural differences among potato cultivars and its influence on the resistance to black dot. On the other hand, untargeted metabolomics has been previously used to highlight resistance-related compounds in potatoes against various diseases (Pushpa et al., 2014; Yogendra et al., 2014). Here, we apply an untargeted metabolomics approach (Zhou et al., 2019) combined with multiblock multivariate data analysis (Boccard and Rudaz, 2016) for highlighting features related to the different experimental factors involved. The results are visualized in molecular networks that allow clustering structurally related metabolites with similar fragmentation patterns (Watrous et al., 2012). Furthermore, metabolite annotation is performed using experimental data (www.gnps.ucsd.edu), an *in silico* mass spectral database (Allard et al., 2016) and taxonomical scoring (Rutz et al., 2019) that allow high confidence feature annotation. The cytological studies and the metabolomics analysis reported here could provide insights on the quantitative resistance of potato tubers to black dot, and highlight biomarkers of resistance to this disease.

3.3. Material and methods

Plant Material

Five cultivars of *Solanum tuberosum* L. commonly grown as table potato cultivars in Switzerland were used for all experiments: Cheyenne (a late-maturing cultivar with red skin), Erika (an early-maturing cultivar with yellow skin), Gwenne (a mid-maturing cultivar with yellow skin), Lady Christl (an early-maturing cultivar with yellow skin) and Lady Felicia (an early-maturing cultivar with yellow skin). Twenty plants of each cultivar were grown for four weeks in sterile conditions as described by Lê & Collet (Lê and Collet, 1985). After 24 hours of adaptation to non-sterile conditions in a high humidity environment, potato plants were transferred to 4 liters square pots containing an autoclaved substrate consisting of brown and blond peat (Gebr. Brill substrate, Georgsdorf, Germany). Half of the population was *mock*-inoculated (with sterile water) and half of the population was inoculated with *Colletotrichum coccodes.* For fungal inoculations, ten mL of a conidial suspension (7,5 x 10^5 conidia/mL) containing mycelial fragments of *Colletotrichum coccodes* (strains 456 and 93 from Agroscope, Nyon, Switzerland) in sterile water was sprayed to the root system during the transfer to pots. Potato plants were grown

in a greenhouse for 4 months (from March to July), under a 12-hours photoperiod, 20 – 22 °C and 40 – 60% relative humidity, with weekly watering. Following haulm destruction, tubers were kept in the soil for a further month until harvest. For microscopy analysis, naturally infected field-grown tubers from a field trial carried out in Changins (46°23'52.9"N 6°14'19.4"E) in 2016 were used. Tubers were planted in rows of 25 plants each, each row separated by 75 cm, and each plant separated by 33 cm. Conventional agronomic practices were used during plant growth.

Severity determination

Daughter tubers from the greenhouse experiment were washed and incubated for 2 weeks under high humidity conditions to allow sporulation of fungi prior to severity determination. 30 single tubers were individually observed under a binocular for the presence of microsclerotia of *Colletotrichum coccodes*. Each tuber was then classified in one of the following classes, depending on the affected area of the tuber: 0 (absence of the fungus), 1 (less than 15%), 2 (between 15 and 35%), 3 (between 36 and 65%) and 4 (more than 65%). The number of tubers of each class was multiplied by the median affected area of the class and used to calculate the average affected area (severity).

Microscopy analysis

Tuber peel samples from naturally infected field-grown tubers of all cultivars were harvested and prepared for microscopic analysis after being washed and incubated for 2 weeks under high humidity conditions to allow sporulation of fungi. A black dot symptomatic area and an area free of disease symptoms were selected for each cultivar. Tuber peel samples were prepared as previously described (Hall and Hawes, 1991). Briefly, samples were pre-fixed using a paraformaldehyde (2%) glutaraldehyde (3%) solution at pH 7.0 (0.07 M PIPES buffer) for three hours at room temperature and descending atmospheric pressure. Subsequently, samples were washed three times with PIPES buffer (0.07M, pH 7.0) and post-fixed with 1% OsO_4 in 0.07M PIPES buffer for 90 minutes. Fixed samples were rinsed twice with 0.07M PIPES buffer and stored at 4°C until dehydration and infiltration with the EMbed 812 resin (Electron Microscopy Sciences, Hatfield, PA, USA). Prior to the infiltration with the resin, samples were dehydrated by incubating the samples on growing concentrations of ethanol (30-50-70-95-100% ethanol) for ten minutes and continuous agitation in the tissue processor Leica EM TP (Leica Microsystems, Heerbrugg, Switzerland). The ethanol was then replaced by propylene oxide for 30 minutes and continuous agitation, and the propylene oxide subsequently replaced by the EMbed 812 resin overnight and gentle agitation. To ensure infiltration of the resin, samples were incubated for 2 hours under vacuum (400 bars). Polymerization of the resin took place at 60°C for 48 hours. Infiltrated samples were then thin cut and resulting sections stained with a mixture of methylene blue (1%), sodium tetraborate (1%) and azur II (1%). Pictures were taken on a Leica DMLB Fluorescence Microscope (Leica Microsystems, Heerbrugg, Switzerland), and phellem thickness measured using the ProgResCapturePro 2.9.0.1 software.

Suberin extraction and depolymerization

Suberin extraction was performed using an adapted protocol from Schreiber (Schreiber et al., 2005). Briefly, lyophilized tuber peel tissues from *mock*-inoculated plants of the greenhouse experiment were cut in $1cm^2$ pieces and weighed. Discs were then incubated for 72 hours in a solution of 2% pectinase and 2% cellulose in citric buffer (10 mM, pH 3.0 adjusted with KOH) containing 1 mM of sodium azide to prevent microbial contamination. Subsequently, periderm tissues were washed with a solution of borate buffer for 24 hours, washed again in deionized water, and dried. Waxes were extracted with chloroform (ratio 1 mL $CHCl_3$/5 mg periderm) for 18 hours. The supernatant was recovered in a clean glass tube, and the pellet reextracted twice with chloroform. The supernatants were combined, dried and stored. The suberin contained in the dewaxed periderms was depolymerized using BF_3/MeOH and incubating at 70°C for 18 hours. Subsequently, 10 ug of dotriacontane was added as internal standard.

The methanolysate was transferred to a new vial containing 2 mL of saturated $NaHCO_3$ in water. The residues were washed twice with chloroform, which was then added to the methanolysate. 2 mL of chloroform were added to allow liquid-liquid extraction. The apolar fraction was transferred to a new vial, and the liquid-liquid extraction repeated twice. The extract was washed with milliQ water, and traces of water were removed with the addition of anhydrous sodium sulfate. The extract was then evaporated and stored until analysis.

GC-MS analysis of suberin monomers

Suberin extracts were resuspended in 100 µL of internal standard solution (methyl nonanedecanoate, 1-tricosanol and docontriane at 300 mg/L) before being dried under nitrogen. Subsequently, 50 µL of pyridine and 50 µL of BSTFA + 1% TMCS were added to the dry residues and incubated 30 minutes at 70°C. The sample was dried again under nitrogen before being diluted with 200 µL of dichloromethane and analyzed by GC-MS. GC-MS analysis were performed on a 7890B gas chromatograph (Agilent Technologies, Santa Clara, CA, USA) coupled to a 7010 triple quadrupole mass spectrometer (Agilent Technologies, Santa Clara, CA, USA), equipped with a PAL autosampler MS-2000 (Bruker, Billerica, MA, USA). A split/splitless injector was used in splitless mode with the injector temperature at 250°C. Separation was performed on a DB-5 capillary column (30m x 0.25 mm, 0.25um, film thickness, Agilent Technologies, Santa Clara, CA, USA) and helium as carrier gas was used at 1.2 mL/min in constant flow rate, GC oven was programmed as follow: 100°C hold 2 min followed by 25°C/min increases up to 200°C, hold 1 min, then increased by 3°C/min up to 280 °C and maintained at 280°C for 30 min. MS analysis were carried out with electron impact ionization operating at 70 eV and ion source was set at 230°C. The acquisition was performed in full scan mode, with a scan of 30 to 500 amu. Chromatographic data were analyzed using Masshunter B.08.00 software. The mass spectra were compared with reference spectra from library NIST MS Search 2.2 and derivatized pure standards. Calibration curves were constructed by plotting peak areas versus concentrations of selected standards. The standards used were : mix Supelco 37 for fatty acids, tetracosane, methyl tetracosanoate for alkanoic acids and ω-hydroxy acids, 1-hexacosanol for 1-alkanols, dimethyl tetradecanedioate for α, ω-alkanedioic acids and ferulic acid methyl ester for cis- and trans-ferulic acid. The standards were derivatized as samples. The concentrations of each compound in the extract were calculated by the corresponding calibration curve. The *m/z* used for the quantitation was for alkanoic acids *m/z* 74, for 1-alkanols and ω-hydroxy acids *m/z* 75, for α, ω-alkanedioic acids *m/z* 98 and respectively *m/z* 219, 224, 250 and 250 for methyl caffeate, methyl vanillate, methyl coumarate and methyl ferulate. All solvents were liquid chromatography grade (Carl Roth, Karlsruhe, Germany). Pyridine, BSTFA + 1% TMCS, methyl nonanedecanoate, 1-tricosanol, docontriane, Tetracosane, methyl tetracosanoate, ferulic acid, dimethyl tetradecanedioate, ethyl vanillate and Supelco 37 were purchased from Sigma Aldrich (Sigma Aldrich, Steinheim, Germany).

Extraction of skin specialized metabolites

Mock-inoculated (without black dot symptoms) and *C. coccodes*-inoculated (showing black dot symptoms) tubers from the five different cultivars grown in the greenhouse were used for the untargeted metabolomics approach. Potato skins of single tubers were harvested after severity determination, immediately frozen, and lyophilized (n=10). Approximately 300 mg of dry tissue were extracted with 4 mL HPLC-grade methanol (Fisher Scientific, Hampton, NH, USA) containing 1% acetic acid. After centrifugation for 5 mins at 4000 rpm, the supernatant was recovered, and the pellet re-extracted with 4 mL methanol containing 1% acetic acid. After centrifugation for 5 mins at 4000 rpm, the supernatants were combined, and the solvents were evaporated at 39 mbar of pressure at 40°C (Genevac, SP Scientific, Ipswich, UK). Each extract was dissolved at 5 mg/mL with a 50% methanol aqueous solution and transferred to a vial for UHPLC-MS/MS analysis.

UHPLC-HRMS/MS Analysis

Chromatographic separation was performed on a Waters Acquity UPLC system interfaced to a Q-Exactive Focus mass spectrometer (Thermo Scientific, Bremen, Germany), using a heated electrospray ionization (HESI-II) source. Thermo Scientific Xcalibur 3.1 software was used for instrument control. The LC conditions were as follows: column, Waters BEH C18 50 × 2.1 mm, 1.7 µm; mobile phase, (A) water with 0.1% formic acid; (B) acetonitrile with 0.1% formic acid; flow rate, 600 µL·min^{-1}; injection volume, 2 µL; gradient, linear gradient of 5−100% B over 7 min and isocratic at 100% B for 1 min. The optimized HESI-II parameters were as follows: source voltage, 3.5 kV (pos); sheath gas flow rate (N_2), 55 units; auxiliary gas flow rate, 15 units; spare gas flow rate, 3.0; capillary temperature, 350.00°C, S-Lens RF Level, 45. The mass analyzer was calibrated using a mixture of caffeine, methionine–arginine–phenylalanine–alanine–acetate (MRFA), sodium dodecyl sulfate, sodium taurocholate, and Ultramark 1621 in an acetonitrile/methanol/water solution containing 1% formic acid by direct injection. The data-dependent MS/MS events were performed on the three most intense ions detected in full scan MS (Top3 experiment). The MS/MS isolation window width was 1 Da, and the stepped normalized collision energy (NCE) was set to 15, 30 and 45 units. In data-dependent MS/MS experiments, full scans were acquired at a resolution of 35,000 FWHM (at *m/z* 200) and MS/MS scans at 17,500 FWHM both with an automatically determined maximum injection time. After being acquired in a MS/MS scan, parent ions were placed in a dynamic exclusion list for 2.0 s. Quality Control (QC) samples containing a mixture of all samples were injected every ten samples throughout the analysis.

LC-MS/MS Data processing

LC-MS/MS data files were analyzed by MzMine 2.36 (Pluskal et al., 2010) after converting the ThermoRAW data files to the open MS format (.mzXML) using the MSConvert software from the ProteoWizard package (Chambers et al., 2012). Briefly, masses were detected (both MS1 and MS2 in a single file) using the centroid mass detector with the noise level set at 1.5E5 for MS1 and at 1.0E0 for MS2. Chromatograms were built using the ADAP algorithm, with the minimum group size of scans set at 5, minimum group intensity threshold at 1.0E5, minimum highest intensity was at 1.0E5 and m/z tolerance at 5.0 ppm. For chromatogram deconvolution, the algorithm used was the wavelets (ADAP). The intensity window S/N was used as S/N estimator with a signal to noise ratio set at 25, a minimum feature height at 10,000, a coefficient area threshold at 100, a peak duration ranges from 0.02 to 0.9 min and the RT wavelet range from 0.02 to 0.05 min. Isotopes were detected using the isotopes peaks grouper with a m/z tolerance of 5.0 ppm, a RT tolerance of 0.02 min (absolute), the maximum charge set at 2 and the representative isotope used was the most intense. Peak alignment was performed using the join aligner method (m/z tolerance at 5 ppm), absolute RT tolerance 0.1 min, weight for m/z at 10 and weight for RT at 10. The peak list was gap-filled with the same RT and m/z range gap filler (m/z tolerance at 5 ppm). The resulting aligned peaklist contained 9321 features in negative mode and 10844 features in positive mode. Only variables that appeared in at least 80% of the samples of a group were retained. Furthermore, all variables that were detected in the blanks and represented more than 1% of the average of the samples were eliminated. Finally, only variables that had less than 30% of variation in the Quality Control samples were retained. The application of these filters yielded a total of 5086 variables for negative ionization mode and 6186 variables for ionization positive mode that were subjected to statistical analysis. Only features possessing MS2 spectra were kept to build molecular networks using the peak-list rows filter option from the original peaklist, which yielded 2717 features in negative ionization mode and 2943 in positive ionization mode. The resistance-related constitutive (RRC) and resistance-related induced (RRI) scores were calculated as the ratio of the mean of abundance in the resistant cultivars / the mean of abundance in the susceptible cultivars in control and inoculated conditions, respectively (RRC=RM/SM, RRI=RP/SP, where RP=resistant genotype with pathogen inoculation, RM=resistant genotype with mock inoculation, SP=susceptible genotype with

pathogen inoculation, SM=susceptible genotype with mock inoculation). The qualitative RRI was calculated as the ratio of the induction in the resistant cultivars / induction in the susceptible cultivars (qRRI = (RP/RM)/(SP/SM)).

Multivariate data analysis (AMOPLS)

Analysis of Variance Multiblock Orthogonal Partial Least Squares (AMOPLS) was computed under the MATLAB® 8 environment (TheMathWorks, Natick, MA, United States). The first step of the method is a partition of the data matrix into a series of additive submatrices, each of which is associated with a specific effect of the experimental design. This follows ANOVA principles by computing average values related to each of the factors levels (cultivar, inoculation and their interaction). This allows the relative variability of each main effect or interaction term to be evaluated using the sum of squares of the corresponding submatrix. A multiblock OPLS model is then computed for the joint analysis of the collection of submatrices to predict level barycenters of the experimental factors and their combinations. Further interpretation is carried out following the OPLS framework, using specific predictive components that are associated with the different effects of the experimental design, and orthogonal components summarizing unexplained residual variability. Samples groupings can be investigated on the corresponding score plots (tp and to, respectively), while variables' contributions are analyzed using loading plots (pp and po, respectively). Empirical *p*-values are computed using random permutations of the experimental design to assess the statistical significance of each effect using an effect-to-residuals ratio. A series of 10^4 random permutations was calculated to validate AMOPLS models and evaluate the statistical significance of each main and interaction effect. The interested reader can refer to the original article describing the AMOPLS method for a detailed description (Boccard and Rudaz, 2016).

Molecular networking parameters

A molecular network (MN) was created with the Feature-Based Molecular Networking (FBMN) workflow (Nothias et al., 2019) on GNPS (Wang et al., 2016) (www.gnps.ucsd.edu). The mass spectrometry data were first processed with MZmine (as described above) and the results were exported to GNPS for FBMN analysis. The precursor ion mass tolerance was set to 0.02 Da and the MS/MS fragment ion tolerance to 0.02 Da. A molecular network was then created where edges were filtered to have a cosine score above 0.7 and more than 6 matched peaks. Further, edges between two nodes were kept in the network if and only if each of the nodes appeared in each other's respective top 10 most similar nodes. Finally, the maximum size of a molecular family was set to 100, and the lowest scoring edges were removed from molecular families until the molecular family size was below this threshold. The spectra in the network were then searched against GNPS spectral libraries (Horai et al., 2010; Wang et al., 2016). The library spectra were filtered in the same manner as the input data. All matches kept between network spectra and library spectra were required to have a score above 0.7 and at least 6 matched peaks. The DEREPLICATOR was used to annotate MS/MS spectra (Mohimani et al., 2018). The molecular networks were visualized using Cytoscape 3.6 software (Shannon et al., 2003). The GNPS job parameters and resulting data are available at the following addresses (https://gnps.ucsd.edu/ProteoSAFe/status.jsp?task=d3d5ddbec02d4df9a12bd02b258b6dcc and https://gnps.ucsd.edu/ProteoSAFe/status.jsp?task=fc46d070ee5a4d5d8cfda6abbdb533b8).

Metabolite annotation

The spectral file (.mgf) and attributes metadata (.clustersummary) obtained after the MN step were annotated using the ISDB-DNP (In Silico DataBase—Dictionary of Natural Products), a metabolite annotation workflow that we previously developed (Allard et al., 2016). Annotation was done using the following parameters: parent mass tolerance 0.005 Da, minimum cosine score 0.2, maximal number of returned candidates: 50. Furthermore, taxonomically informed scoring was applied on the

GNPS outputs using *Solanum tuberosum* as species, *Solanum* as genus, and *Solanaceae* as family, returning an attribute table which can be directly loaded in Cytoscape. The taxonomically informed metabolite annotation process has been previously described in detail (Rutz et al., 2019). The scripts are available online (taxo_scorer_user.Rmd) at https://github.com/oolonek/taxo_scorer. The chemical classes of the compounds were described using ClassyFire (http://classyfire.wishartlab.com/) (Djoumbou Feunang et al., 2016).

In vitro Antifungal Bioassay against Colletotrichum coccodes

The *in vitro* antifungal activity of some of the highlighted compounds in the metabolomics analysis was tested using the food-poisoning method in 48-well plates. Briefly, 10 µL of a 1 x 10^6 conidia/mL suspension of *C. coccodes* (fungal strain 456, Agroscope) in water were inoculated in Potato Dextrose Broth (PDB) - Potato Dextrose Agar (PDA) medium (70:30) amended with a range of doses of the following compounds: the glycoalkaloids solanine and chaconine, the saponin protodioscin, the tropane alkaloid calystegine A3, the hydroxycinnamic acid amides feruloyltyramineand kukoamine A, the free polyamines spermine and spermidine, the flavonoid glycosides nicotiflorin and rutin, the coumarins esculetin and scopoletin, and the hydroxycinnamic acid chlorogenic acid. All compounds were solubilized in DMSO (final concentration 3.5%, v/v), except for spermine, spermidine, calystegine A3 and chlorogenic acid, which were soluble in PDB. DMSO (3.5% v/v) in PDB – PDA (70:30) or PDB – PDA (70:30) were used as controls. All compounds were tested at concentrations of 10 – 1000 µM, except for chlorogenic acid, that was tested at concentrations of 150– 15000 µM. Pictures were taken 7 days after inoculation with a Canon EOS 5D and the growth area calculated using the software ImageJ. Growth inhibition was calculated as the percentage of growth reduction respective to the control (100 – (growth area Xi/growth area control *x* 100).

Statistical analysis

Arc sinus transformation was applied to severity data before statistical analysis. One-way ANOVA was applied to severity data, phellem thickness and suberin amounts, followed by the post-hoc Fisher's LSD test for multiple pair-wise comparisons. For the *in vitro* antifungal bioassay data, mycelial growth of each treatment was compared to the untreated control using the Student's T-test.

3.4. Results and discussion

Commercial potato cultivars exhibit different degrees of quantitative resistance to black dot

In order to study resistance to black dot, we used five commercially available potato cultivars that had previously shown different resistance levels to black dot in the field. In a greenhouse experiment under control conditions, mock-inoculated plants produced tubers that did not exhibit symptoms of black dot. On the other hand, the percentage of affected tuber area (severity) of black dot in inoculated plants differed among cultivars, with a cultivar exhibiting very high susceptibility (Lady Felicia), two cultivars exhibiting moderate-to-high susceptibility (Cheyenne and Lady Christl), and two cultivars exhibiting low susceptibility (Erika and Gwenne) (Figure 1). In particular, these results are comparable to those found in field assays for all cultivars except Cheyenne and Lady Christl, which exhibited lower susceptibility to black dot in the field trials. According to additional field trials (data not shown), overall disease severity was higher in the greenhouse experiment than in field trials, suggesting that the artificial inoculation resulted in a disease pressure higher than that found in the field. It is possible that a higher inoculum than that found in the field was applied to the greenhouse experiment, since soil inoculum correlates with disease severity (Lees et al., 2010) Furthermore, inoculum concentration correlation with disease severity is genotype dependent (Alonso-Villaverde et al., 2011), and both the pathogen strain and the plant genotype influence host resistance in other phytopathogenic interactions (Ors et al., 2018; Samain et al., 2019). These results suggest that a high disease pressure as applied in the greenhouse might negatively influence the resistance of Cheyenne and Lady Christl

to black dot. Overall, the cultivars Erika and Gwenne can be considered as resistant to black dot, while Cheyenne, Lady Christl and Lady Felicia are susceptible to black dot and will be regarded as such along this study (Figure 3.1).

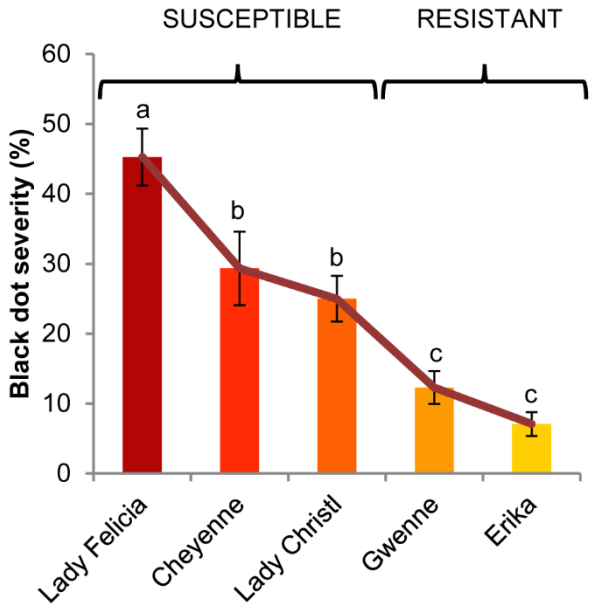

Figure 3.1 Black dot disease severity of five different potato cultivars artificially inoculated with *C. coccodes*. Disease severity is expressed as the percentage of tuber area showing symptoms of black dot (Means ± Standard Error, n=30). Statistically significant differences are indicated by different letters ($p < 0.05$, Fisher's LSD test).

Colletotrichum coccodes colonizes the tuber periderm of the different potato cultivars

Potato tubers are storage organs in which the most abundant compartment is the flesh, which contains large amounts of starch granules (Figure 3.2A, 3.2C). Tuber flesh is separated from the outer environment by the skin, or periderm, formed by suberized phellem cells and unsuberized phellogen cells (Figure 3.2B, 3.2C). Interestingly, *C. coccodes* hyphae were found through the periderm of potato tuber zones showing symptoms of black dot but not in parenchymal tissue, suggesting that *C. coccodes* does not penetrate in these cortical cells (Figure 3.3 B-J).

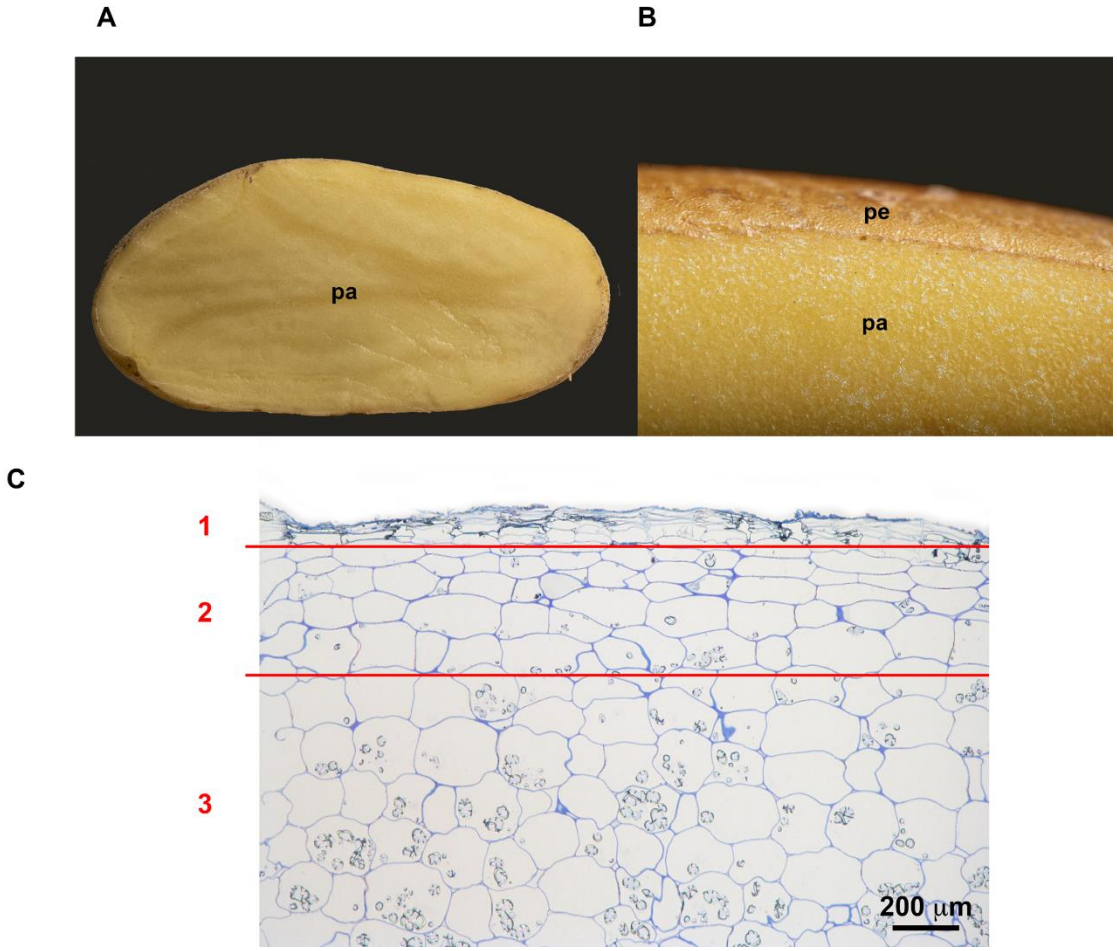

Figure 3.2 Structure of the potato periderm. **(A)** Longitudinal section of a potato tuber. **(B)** Close view of the potato periderm (pe) and parenchyma (pa). **(C)** Microscopic semithin section of the suberized phellem (1), the starch-depleted phelloderm (2) and the starch-containing storage parenchymal cells (3). Bar corresponds to 200 µm

Furthermore, regions of potato tubers with black dot symptoms showed a disorganized and collapsed phellem with microsclerotia of *C. coccodes* forming below the surface (Figure 3.3 B-J). Notably, collapse of the phellem was observed in all cultivars, although to a lesser extent in the resistant ones since symptoms were less abundant (Figure 3.3 B-J). Furthermore, potato cultivars did not respond to *C. coccodes* infection by increasing their periderm layer (Supplementary Figure 3), in opposition to what is observed in response to *Streptomyces scabies* (Khatri et al., 2011). These results suggest that *C. coccodes* induces the collapse of the phellem, which might be responsible for the higher permeability of infected tubers, resulting in water losses during storage. In fungus-free tuber skin regions, the thickness of the phellem ranged from 46 to 84 µm, with between 6 and 10 cellular layers, in the five different cultivars (Figure 3, Figure 4A). Interestingly, phellem thickness was the lowest in the most susceptible cultivar, suggesting that thin-skin cultivars are more susceptible to black dot. That is in accordance with USA surveys, where Russet-type cultivars (thick skin) were more resistant to black dot than thin-skinned cultivars (Hunger and McIntyre, 1979). However, it is worth noting that Russet-type cultivars, which are not commonly used in Europe, possess thicker skins than the cultivars used in our study, with skin thickness of usually more than 150 µm (Artschwager, 1924). Moreover, no correlation between skin thickness and resistance to black dot was found between the other four cultivars, suggesting that other mechanisms are involved in the resistance to black dot.

Phellem cells are surrounded by the polymer suberin, which protects plants from both biotic and abiotic stresses (Vaughn and Lulai, 1991), and potato variants with broad tuber-disease resistance

produce higher amounts of suberin (Thangavel et al., 2016). Total suberin concentrations ranged from 92 to 112 µg/mg periderm in the five cultivars studied, values comparable to those found elsewhere (Company-Arumí et al., 2016). Notably, small differences in the total concentration of suberin were observed among cultivars. Total suberin was higher in the two resistant cultivars than the mid-susceptible cultivars, but no significant differences were observed between the resistant and the most susceptible cultivars (Figure 4B). Furthermore, the composition of the suberin polymer did not strongly differ among potato cultivars, and clear differences were not observed for any of the suberin monomers (Supplementary Table S1). Altogether, these results suggest that thin-skin cultivars such as Lady Felicia are more susceptible to black dot, but that quantitative resistance to black dot cannot be fully explained through the structure of the tuber skin. Furthermore, suberin amount or composition do not explain the differences in the phellem structure and do not correlate with black dot resistance in control conditions. Whether suberin production and accumulation is involved in the reaction of potato tubers to *C. coccodes* infection and to induced resistance to black dot remains to be studied.

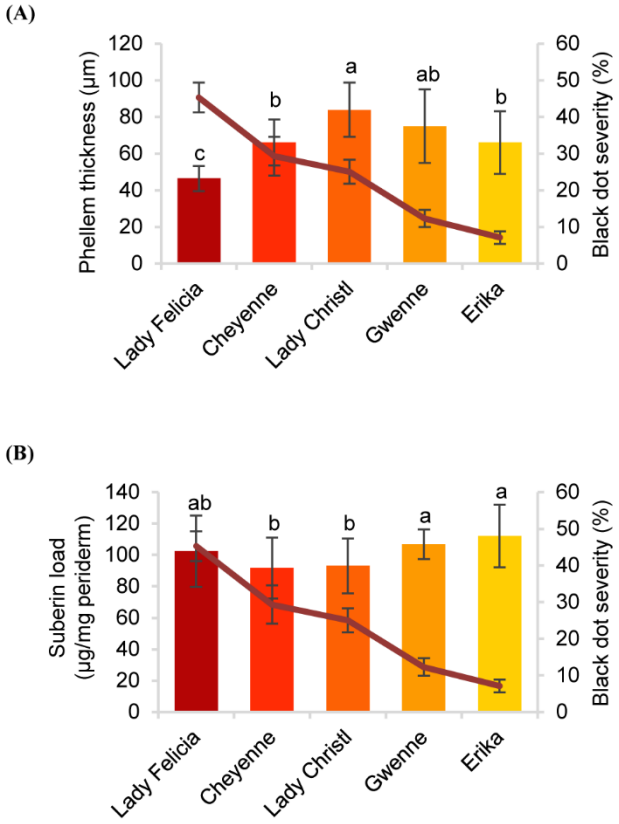

Figure 3.3 Phellem thickness and suberin concentration of five potato cultivars with different quantitative resistance to black dot. **(A)** Phellem thickness (µm) measured in semithin sections of asymptomatic regions of a potato tuber grown in the field of five cultivars (n=12, mean ± Standard Deviation). **(B)** Total suberin amounts (µg/mg periderm) of five potato cultivars grown under controlled conditions in the absence of the fungal pathogen (n=6). Statistically significant differences in phellem thickness or suberin load are indicated by different letters ($p < 0.01$, Fisher's LSD). In all graphs, black dot severity is shown in a red line and its axis on the right.

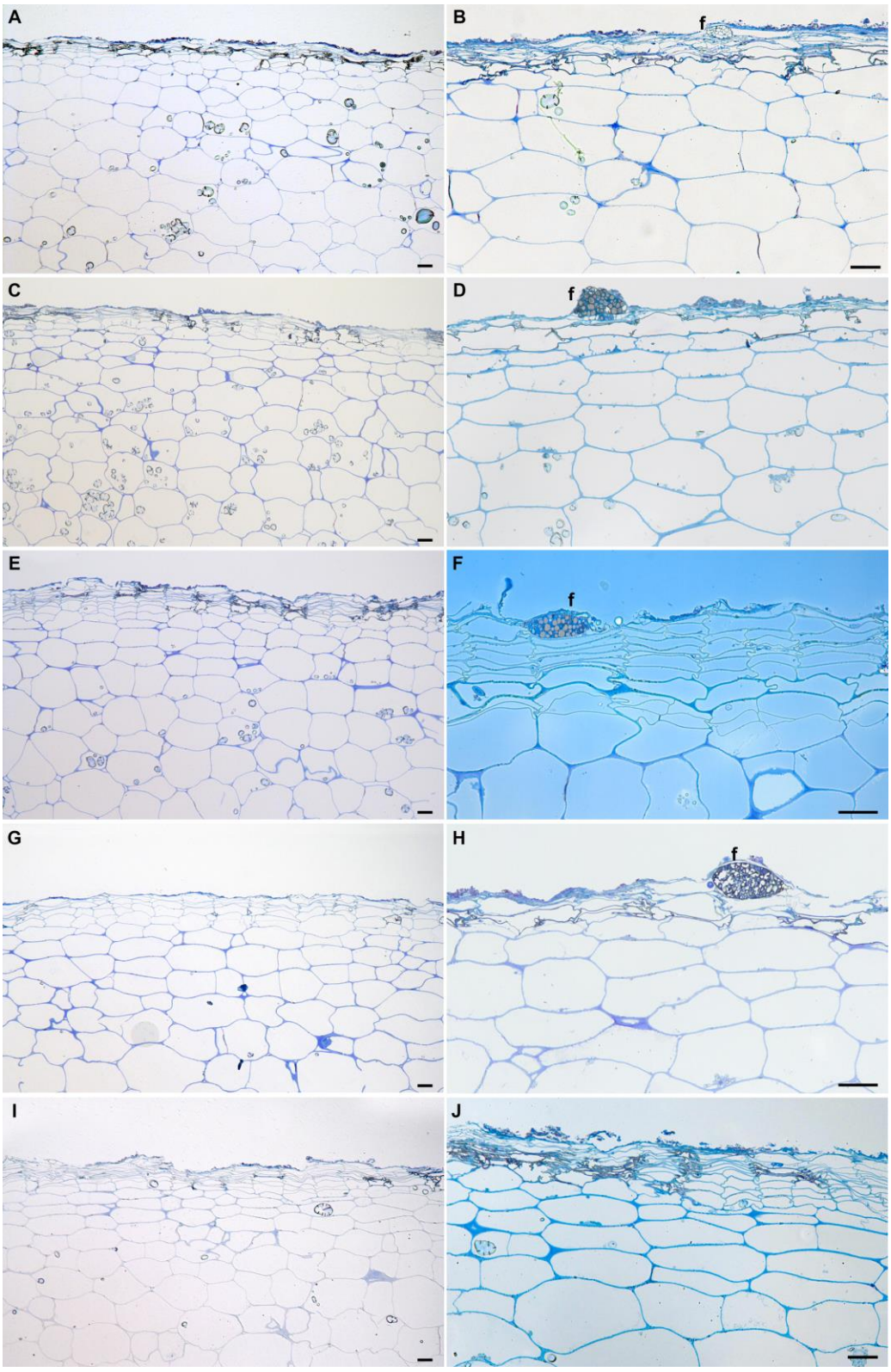

Figure 3.4 Longitudinal semithin sections of the phelloderm of asymptomatic (A, C, E, G and I) and black dot symptomatic (B, D, F, H and J) regions of the potato cultivars Lady Felicia (A and B), Lady Christl (C and D), Cheyenne (E and F), Gwenne (G and H) and Erika (I and J). Bars represent 50 µm. *f*: fungal structures.

Cultivar-specific metabolites are highlighted using untargeted metabolomics

In an attempt to understand the interaction between *S. tuberosum* and *C. coccodes* and, ultimately, decipher quantitative resistance of potatoes to black dot, an untargeted metabolomics approach was carried out on mock and fungal inoculated plants of the five cultivars studied (Figure 5A). Specialized metabolites were extracted with a methanolic solution and profiled by UHPLC-HRMS/MS (Zhou et al., 2019) (Figure 5B). In order to study the complex and large amount of data obtained, a dual method combining statistical multivariate analysis and molecular networking was used (Figure 5C, D). Notably, the full factorial experimental design allowed the study of the genotype effect (cultivar), the effect of the inoculation process, and the interaction of both factors, which can be used to highlight biomarkers. On one hand, the metabolic effects associated with the experimental factors were analyzed in a dedicated supervised statistical model, i.e. AMOPLS, combining ANOVA decomposition of the LC-MS data according to the experimental design, and multiblock orthogonal partial least squares modeling (Figure 5C, Supplementary Table S2) . In addition, metabolite annotation was carried out by a combination of feature based molecular networking (FBMN) (Nothias et al., 2019) and dereplication against experimental data from the GNPS platform (http://gnps.ucsd.edu/) and against an *in-silico* fragmentation database (ISDB) weighted using taxonomical data (Figure 5D) (Allard et al., 2016; Rutz et al., 2019). Furthermore, a selection of the annotated compounds was identified by comparison of the HRMS, MS/MS spectra and RT with authentic standards, which allowed the establishment of experimental anchor points and the confident propagation of annotations through the network. Dereplication through the ISDB of the features that possessed a MS/MS spectrum yielded annotations for 69% and 74% in NI and PI mode, respectively. The most represented metabolic classes in the potato tuber skin were lipid and lipid-like molecules (which include fatty acyls, prenol lipids and steroid derivatives), phenylpropanoids (including cinnamic acids and flavonoids, among others), organic oxygen compounds and organoheterocyclic compounds (including benzopyrans, lactones and indole derivatives) (Supplementary Figure S1). In order to highlight specific biomarkers, the AMOPLS results and the FBMN were combined. Concerning the AMOPLS analysis, the 'cultivar' main effect was the most important in determining the differences among samples in both PI and NI modes, and represented 48% of the total metabolome variability (Supplementary Table S2). These results indicate that the tested commercially available cultivars grown under controlled conditions differ in their biochemical composition, suggesting that this might explain biological or physiological properties. For example, only one of the five cultivars studied has a red skin (Cheyenne), while the other four cultivars have yellow skins. The AMOPLS efficiently highlighted the characteristic features of this cultivar. They were putatively annotated as anthocyanins, the isoflavonoid genistein and the flavanonol dihydrokaempferol, among others (Supplementary Figure S2). These features were also easily highlighted in the corresponding MN (Supplementary Figure S3). Thus, the approach highlighted chemical markers that are very specific to the red skin cultivar Cheyenne, demonstrating that the chosen methodology is efficient to distinguish the different sources of metabolic variations and highlighting biomarkers. This strategy will be used to highlight resistance-related metabolites against black dot and biomarkers of *C. coccodes* inoculation. The main effect 'cultivar' in the AMOPLS model will be used to highlight metabolites that are relatively more abundant in the two resistant cultivars than in the three susceptible cultivars under control conditions (Resistance-Related Constitutive metabolites). The main effect 'inoculation' will be used to highlight biomarkers of the fungal infection (Pathogenesis-Related metabolites). Finally, the 'interaction' between both main effects will be used to highlight metabolites that are specifically induced in the resistant cultivars upon fungal inoculation (Resistance-Related Induced metabolites). Combining the information from the AMOPLS models and the MNs will result in a list of Resistance-Related (RR) compounds (Figure 5E). The biosynthetic pathway of these compounds will be searched to highlight induced biochemical pathways (Figure 5F),

and the antifungal activity of some of these metabolites will be assessed using an *in vitro* bioassay against *C. coccodes* (Figure 5G).

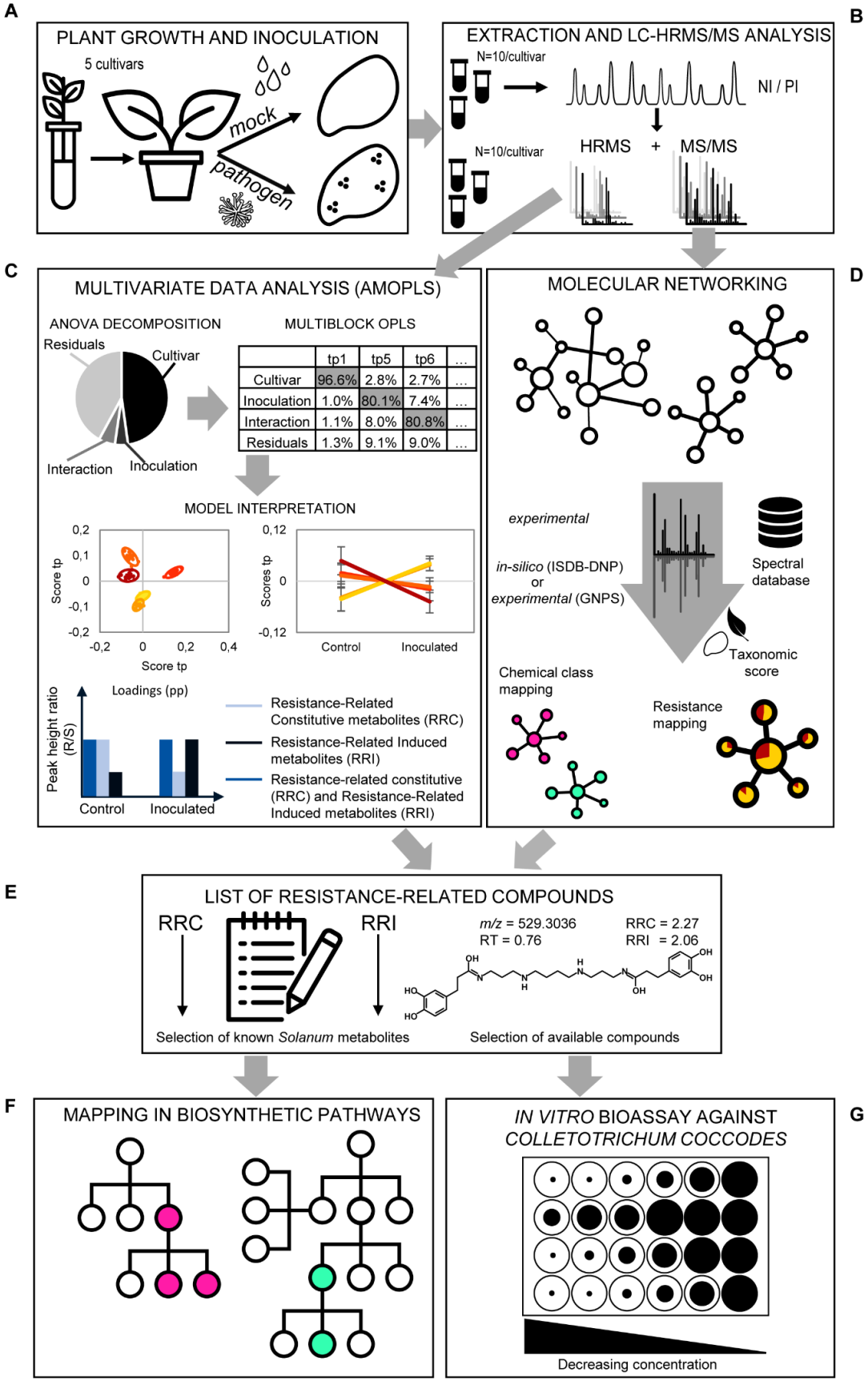

Figure 3.5 (continues)

Figure 3.5 Overview of the metabolomics strategy. **(A)** *Plant growth and inoculation.* Potato plantlets of the five studied cultivars are grown *in vitro* and transferred to the greenhouse in pots using sterilized soil to avoid fungal infection. Half of the population is *mock* inoculated, while the other half is inoculated with *C. coccodes*. **(B)** *Extraction and LC-HRMS/MS analysis.* Methanolic extraction of specialized metabolites is followed by LC-HRMS/MS (data-dependent mode) analysis in both negative ionization (NI) and positive ionization (PI) modes. **(C)** *Multivariate Data Analysis (AMOPLS)*. All features detected in full scan MS are analyzed using an AMOPLS model. ANOVA decomposition of the matrix in submatrices allows assessing the relative variability of each effect (i.e. cultivar, inoculation, interaction and residuals) by computing the sum of squares of the submatrices. This is followed by a multiblock OPLS model, the predictive components of which explain one of the effects (see Supplementary Table 2). AMOPLS separates the sources of variability related to the experimental factors with dedicated predictive score (tp) and loading values (pp) that are used for the model interpretation. Predictive scores (tp) highlight sample groupings (i.e. cultivar, see Figure 3.5)) or trends (i.e. upon inoculation, see Figure 8) and loadings (pp) highlight induced molecules with respect to the different experimental factors to evidence Resistance-Related metabolites. **(D)** *Molecular Networking*. Features possessing MS/MS spectra are used to build a Molecular Network (MN) based on spectral similarity. Features are then annotated by spectral comparison with experimental (GNPS) or *in silico* (ISDB-DNP) spectral databases. *In silico* annotations are re-ranked using taxonomic proximity information. Color of individual clusters of the MN are set according to the most abundant chemical class found in the cluster (consensus chemical class) or the relative intensity in resistant and susceptible cultivars (see Figure 6). **(E)** *List of Resistance-Related compounds.* A combination of the AMOPLS data analysis and the MN visualization is used to build a list of Resistance-Related metabolites, Constitutive (RRC) or Induced (RRI), with their annotations, and sorted according to their RRC or RRI scores (see Supplementary Table 3). **(F)** *Mapping in biosynthetic pathways.* A selection of Resistance-Related annotated metabolites previously reported in the *Solanaceae* family are placed in their biosynthetic pathways according to the Kyoto Encyclopedia of Genes and Genomes (KEGG) for *Solanum tuberosum* (or related plant species, if not available for *S. tuberosum*) to highlight putatively induced or repressed biochemical pathways (see Figure S7). **(G)** *In vitro* bioassay against *Colletotrichum coccodes*. A selection of highlighted Resistance-Related metabolites, commercially available pure compounds, are tested in an *in vitro* bioassay against *C. coccodes* using the food-poisoning method at decreasing concentrations from 1000 µM to 10 µM (see Figure 7 and Figure S6).

Black dot resistance is associated with high constitutive levels of steroidal saponins, hydroxycinnamic acids and hydroxycinnamic acid amides

Differences between the two resistant and the three susceptible cultivars were highlighted by visualizing the second predictive component of the AMOPLS model in both PI and NI modes (Figure 6, Supplementary Figure S2). Resistance-Related Constitutive (RRC) metabolites are described as those being more abundant in the resistant cultivars than in the susceptible cultivars under control conditions, and the RRC ratio (Resistant Mock/Susceptible Mock) was used to highlight biomarkers in the MN (Figure 7). Notably, several clusters of steroid derivatives were evidenced in both PI and NI modes, including the furostanol saponin protodioscin (identified by comparison of MS/MS to a pure standard) and related compounds (cluster 1 in Figure 7). Most features in this cluster were putatively identified through comparison with the ISDB to furostanol and spirostanol saponins. In addition, several clusters of lipid and lipid-like molecules, putatively annotated as spirostanol saponins, were also found to be qualitatively more abundant in the resistant cultivars in PI mode (Supplementary Table 3 and Supplementary Figure S4). Notably, these steroidal saponins showed high RRC values and were also highlighted using AMOPLS (Figure 6, Supplementary Figure S2). Altogether, these results suggest that potato tubers with constitutively high amounts of steroidal saponins, including furostanol and spirostanol saponins, are more resistant to black dot. Steroidal saponins are mainly found in *Liliaceae* and *Agavaceae* plants, but they also have been identified in members of the family *Solanaceae* (Faizal and Geelen, 2013). Their role in plant defense has been proposed as phytoanticipins, because they are produced independently from pathogen detection (Faizal and Geelen, 2013). In order to study whether these compounds might have antifungal activity against *C. coccodes*, an *in vitro* bioassay based on the food-poisoning method was used (Figure 5G). Protodioscin was found to strongly inhibit *C. coccodes* growth at 500 µM (Figure 8). To the best of our knowledge, steroidal saponins have not been quantified in potato commercial cultivars, but steroidal saponins in wild *Solanum* species are found at concentrations of 100 µM or less (Caruso et al., 2013), a concentration that resulted in 30% growth inhibition of *C. coccodes* (Supplementary Figure S5). On the other hand, the most abundant steroidal glycoalkaloids, alpha-chaconine and alpha-solanine, showed RRC values of 1.40 and 1.16, respectively (Supplementary Table S3). These steroidal derivatives, which are found in potatoes and other wild

Solanum species, have been implicated in plant defense, especially against herbivores (Friedman, 2006). Interestingly, alpha-chaconine has been shown to have higher antifungal activity than alpha-solanine (Fewell and Roddick, 1993), and is usually found at higher concentrations (i.e. 500 µM in the cultivar Snowden) than alpha-solanine (i.e. 250 µM in the cultivar Snowden) in the potato peel (Friedman, 2006). At 500 µM, alpha-chaconine showed higher inhibition of *C. coccodes* mycelial growth than alpha-solanine (Figure 8). Furthermore, no significant inhibition was observed by alpha-solanine at 250 µM (Supplementary Figure S5). Altogether, these results suggest that high amounts of alpha-chaconine might be fungitoxic to *C. coccodes in planta*. Nevertheless, it is worth noting that the most susceptible cultivar to black dot exhibits higher amounts of these SGAs than the other susceptible cultivars, suggesting that relatively high SGA amounts might contribute to the resistance phenotype, but they are not sufficient *per se*. Alpha-chaconine and alpha-solanine are glycoalkaloids with a solanidine backbone, and, together with the furostanol and spirostanol saponins, derive from squalene (Supplementary Figure S6). It is worth noting that brassinosteroids (BRs), which are also steroid derivatives, are plant growth hormones, and that a trade-off between BR signaling and plant defense is often observed (Yu et al., 2018). Indeed, some pathogens overcome plant resistance in potato by inducing the BR pathway (Turnbull et al., 2017). Although BRs were not detected in our untargeted analysis, our results suggest that the balance between plant defense and BR signaling may differ between resistant and susceptible cultivars.

Several phenylpropanoids were found to be more abundant in the resistant cultivars than the susceptible ones in control conditions. This is the case of the hydroxycinnamic acids (HCAs) chlorogenic acid, neochlorogenic acid and cryptochlorogenic acid, which were ca. 20% more abundant in the resistant cultivars (Supplementary Table S2). Interestingly, the dimers of these compounds are even more abundant in the resistant cultivars (40 – 84%) and suggests that chlorogenic acid and its isomers and dimers may be associated with quantitative resistance against black dot. Accumulation of HCAs upon pathogen infection has also been described in other plant-pathogen systems, including anthracnose in sweet pepper caused by *C. coccodes* (Mikulič Petkovšek et al., 2009; Mikulic-Petkovsek et al., 2013). Chlorogenic acid is the most abundant HCA in potato tubers (Navarre et al., 2011) and it has been shown to have a direct antimicrobial effect against *Phytophthora infestans* and, especially, *Pectobacterium atrosepticum*, suggesting a stronger activity against bacteria than to fungi-like oomycetes (Kröner et al., 2011, 2012). In our bioassays, chlorogenic acid did not to inhibit *C. coccodes* growth at concentrations as high as 7.5 mM (Supplementary Figure S5), suggesting that this resistance-related metabolite does not possess direct antifungal activity against *C. coccodes in vitro*.

Other clusters highlighted as RRC include a cluster of flavonoid glycosides (cluster 2 in Figure 7). Interestingly, flavonoid glycosides more abundant in resistant cultivars included nicotiflorin (RRC of 1.55) and the most abundant flavonoid glycoside rutin (RRC of 1.41), which have been involved in the resistance of potato tubers to soft rot caused by *P. atrosepticum* (Kröner et al., 2012) and, the latter, has shown antifungal activity (Báidez et al., 2007; Pereira et al., 2008). At 500 µM, rutin showed stronger antifungal activity than nicotiflorin (Figure 8). However, previous studies have quantified rutin and nicotiflorin at ca. 100 and 50 µM in the potato skin, respectively (Kröner et al., 2012), concentrations that did not inhibit the growth of *C. coccodes in vitro* (Supplementary Figure S5). It is worth noting that some of these flavonoid glycosides were abundant in the most resistant (Erika) cultivar but not in the second most resistant one (Gwenne) (Supplementary Table S3), suggesting that flavonoid glycosides might be involved in the resistance of potato tubers against black dot especially in the cultivar Erika.

Interestingly, a cluster of compounds highlighted as abundant in the resistant cultivars included *N*1,*N*12-bis(dihydrocaffeoyl) spermine (kukoamine A) (identified by comparison of MS/MS to a pure standard) (cluster 3a in Figure 7), which has been previously identified in potato tubers (Parr et al., 2005). This cluster also includes other features putatively annotated as dihydrocaffeoyl spermines and

dihydrocaffeoyl spermidines. Furthermore, another cluster with features putatively annotated as caffeoyl, dihydrocaffeoyl spermines and spermidines was highlighted as an RRC cluster (cluster 3b in Figure 7). Notably, spermine derivatives were abundant in one of the resistant cultivars (Gwenne), and spermidine derivatives were most abundant in the other resistant cultivar (Erika) (Supplementary Table S3). On the other hand, the most substituted spermine and spermidine derivatives were found to be more abundant in the susceptible cultivars (Supplementary Table S3). Altogether, these results suggest that cultivars resistant to black dot accumulate spermine (Erika) or spermidine (Gwenne) derivatives, except the most substituted forms. Free spermine has been suggested to play a role in the hypersensitive response of tobacco to Tobacco Mosaic Virus (TMV) (Walters, 2003), but free polyamines were not unambiguously detected in our analysis. Furthermore, no antifungal activity against *C. coccodes* was recorded for these two polyamines at concentrations as high as 1 mM. Notably, *N*-feruloyloctopamine and *N*-feruloyltyramine, other hydroxycinnamic acid amides (HCAAs), were also found to be more abundant in the resistant cultivars (cluster 3c in Figure 7, Supplementary Table S3). The role of HCAAs in plant-pathogen interactions has been studied in several models, such as in *Arabidopsis thaliana*, where they accumulate upon inoculation with *Alternaria brassicicola*, and are required for the defense response against this pathogen (Muroi et al., 2009). HCAAs are synthesized in the cytoplasm and translocated to the plasma membrane through glutathione S-transferases, possibly upon pathogen infection, accumulating in methanol soluble granules in the inner face of the cell wall (Macoy et al., 2015). Peroxidase polymerization of HCAAs in the cell wall results in the integration of HCAAs in the suberin polymer reinforcing the cell wall and providing resistance against pathogen infection (Macoy et al., 2015). HCAAs have also been found to accumulate in potato tubers upon fungal inoculation (Clarke, 1982; Keller et al., 1996), and have been highlighted as resistance-related compounds against late blight (Yogendra et al., 2014). Our results suggest that constitutively enhanced HCAA amounts are a biomarker of black dot resistance in potato tubers. Polyphenolic amides have been found to be more abundant in the potato cultivar Russet Burbank than in other cultivars (Huang et al., 2017), and Russet-type cultivars are more resistant to black dot than thin-skinned cultivars (Hunger and McIntyre, 1979), reinforcing the hypothesis that HCAAs might be involved in the resistance to black dot. Interestingly, the HCAA production rate is higher than its incorporation in the cell wall (Macoy et al., 2015). Since the metabolomics analysis was carried on non-polymerized specialized metabolites, it can be assumed that HCAAs detected are found in the cytosol or in the cell wall before polymerization, indicating that they play a role independently of suberin in the resistance to black dot. Furthermore, suberin levels in non-inoculated samples did not differ among the five cultivars studied, suggesting that constitutively high amounts of HCAAs, but not constitutively high amounts of suberin, correlate with black dot resistance. Notably, *N*1,*N*12-bis(dihydrocaffeoyl) spermine and, especially *N*-feruloyltyramine, were found to strongly inhibit *C. coccodes* growth *in vitro* at 500 µM (Figure 8). Moreover, both compounds showed antifungal activity at 50 µM (Supplementary Figure S5), the estimated concentration of *N*1,*N*12-bis(dihydrocaffeoyl) spermine in potato tubers (Parr et al., 2005) and *N*-feruloyltyramine in healing potato tuber discs (Negrel et al., 1996). Altogether, our results show that non-polymerized HCAAs are relatively more abundant in potato cultivars resistant to black dot, suggesting that free HCAAs, probably in the inner face of the cell wall, play a role in the defense against *C. coccodes* infection.

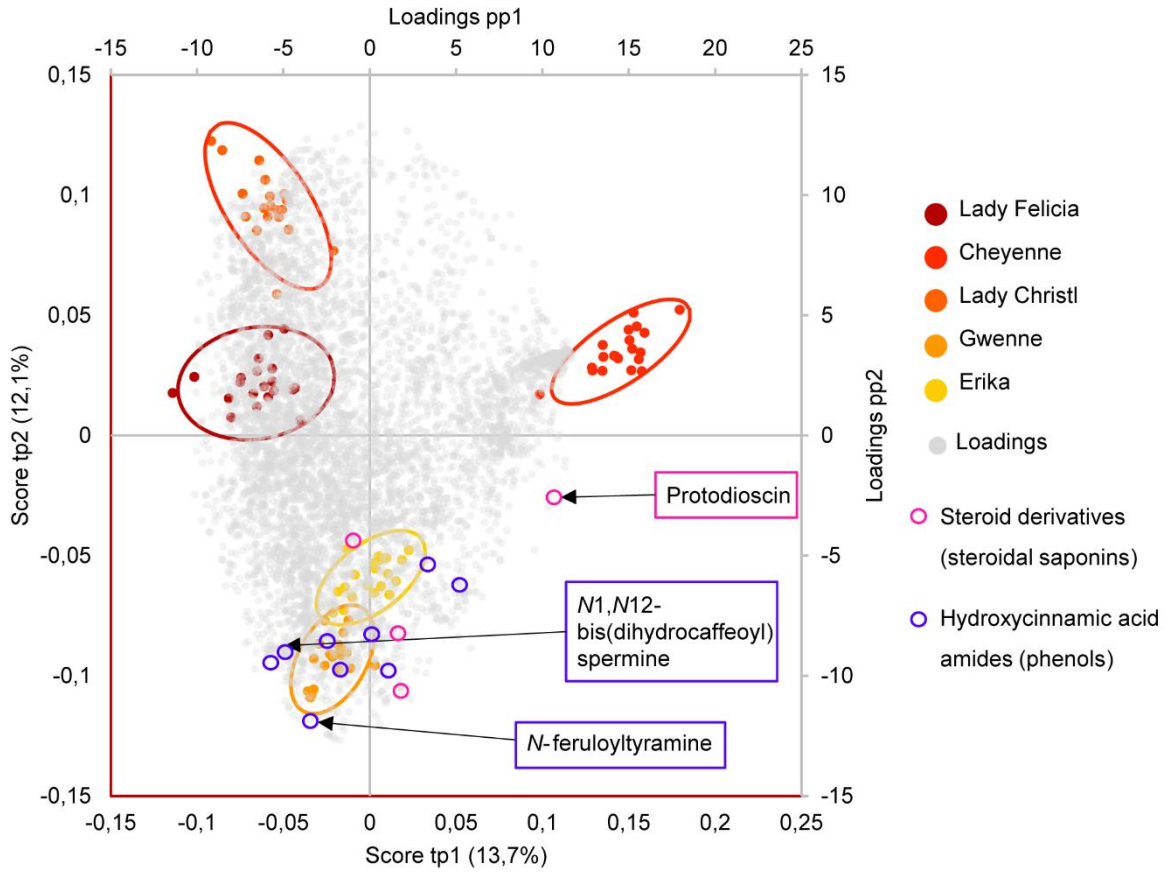

Figure 3.6 Biplot representation of the two first predictive components of the AMOPLS model in negative ion mode explaining 25,9% of the total variance. Observations are color-coded as cultivars (n=20) with 95% confidence ellipses and positioned according to the left and below axis. Loadings are colored in grey and positioned according to the right and above axis. Resistant cultivars (Erika and Gwenne) have negative scores of tp2, while susceptible cultivars (Lady Felicia, Cheyenne and Lady Christl) have positive scores of tp2. The loadings of highlighted resistance-related metabolites annotated as hydroxycinnamic acid amides (including *N*-feruloyltyramine and *N*1,*N*12-bis(dihydrocaffeoyl) spermine) and as steroid derivatives (including protodioscin) are indicated in blue and pink, respectively.

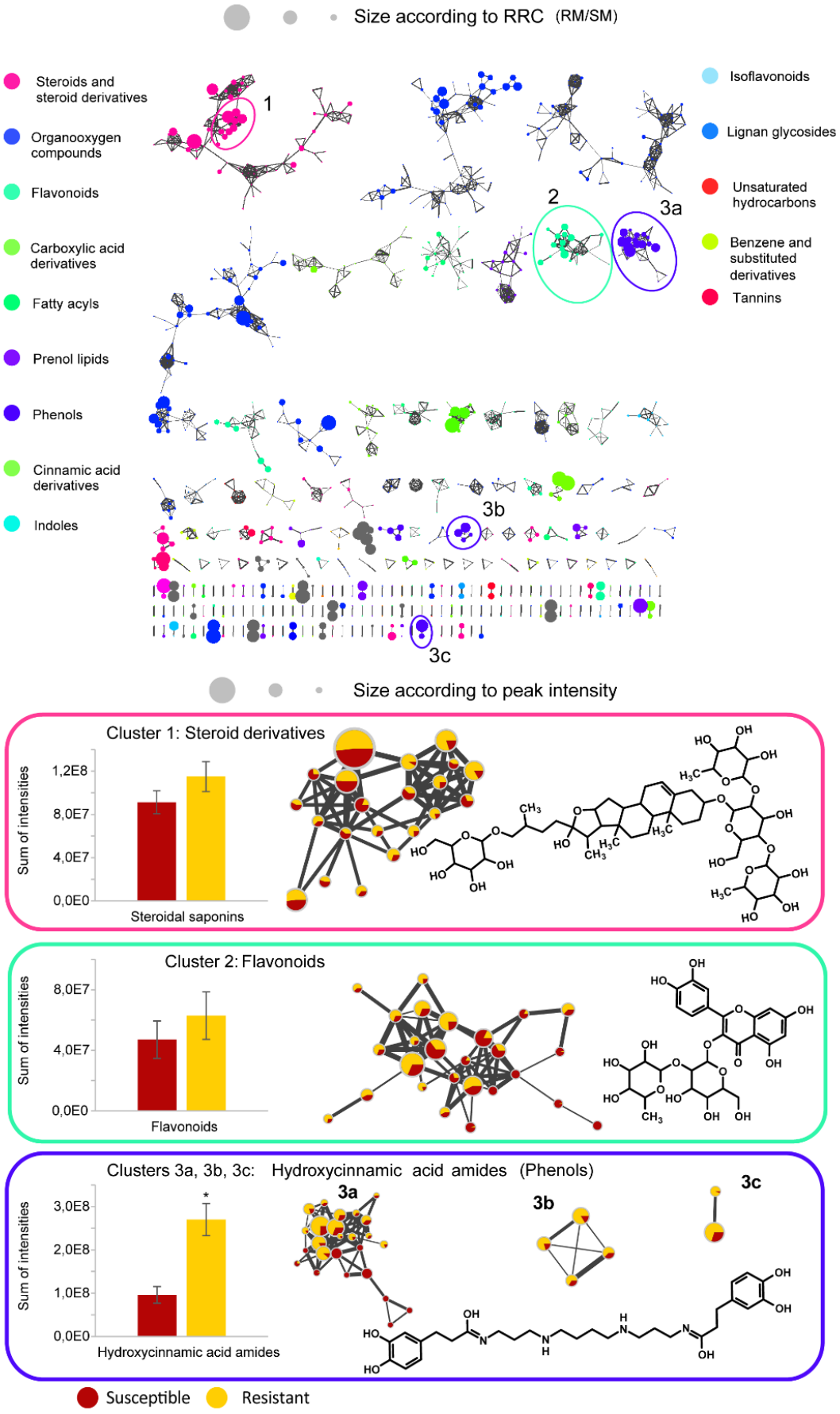

Figure 3.7 (continues)

Figure 3.8 Global Molecular Networks (MNs) in negative ion mode of the five potato cultivars. In the global Molecular Network, color of the node is set according to the consensus chemical class across the cluster, node size is set according to the ratio of intensities between resistant and susceptible cultivars in control conditions (RRC). Molecular families of interest that include compounds confirmed by an analytical standard are highlighted in a cluster, with the structure of the standard displayed, size of the node set according to the average peak intensity (among all samples) and color of the node set as a pie-chart with the relative abundance of the metabolite in the resistant cultivars (yellow) and the susceptible cultivars (red) in control conditions. The average detected intensity (of all features in a cluster) in susceptible and resistant cultivars is shown as a histogram. The average cluster intensity ratio (resistant vs susceptible) provides an estimation of the contribution of the compound class to resistance, the ratio in each node highlights if specific metabolites only are involved. Asterisks indicate significant differences between resistant and susceptible cultivars ($p < 0,05$, T-test). Only clusters containing at least two nodes are shown, self-loop nodes are not displayed.

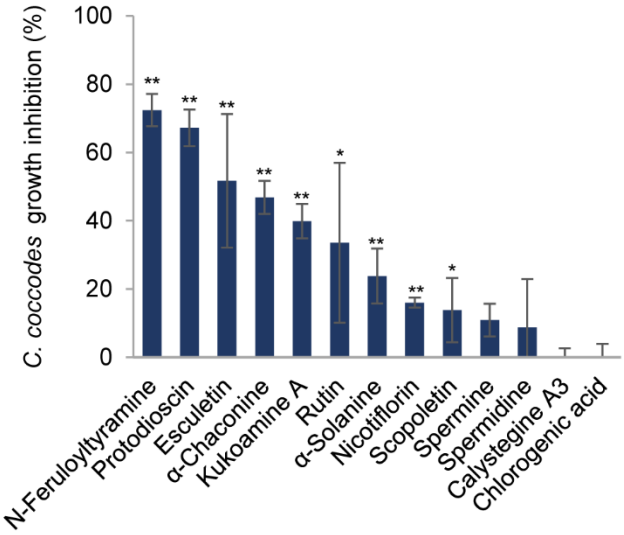

Figure 3.9 Inhibition of *C. coccodes* growth (%) *in vitro* at 750 µM for chlorogenic acid and at 500 µM for the rest of the compounds (n=3, Mean ± Standard Deviation). Kukoamine A = *N*1,*N*12-bis(dihydrocaffeoyl) spermine. Asterisks indicate significant differences compared to the untreated control (*$p < 0,05$, **$p < 0,01$, Student's T-test).

Higher hydroxycinnamic acid and hydroxycoumarin levels and lower levels of flavonoid glycosides are observed in C. coccodes inoculated potato tubers

The ANOVA decomposition step of the multivariate data analysis (i.e. AMOPLS) showed that the inoculation of *C. coccodes* had a statistically significant impact on the potato skin metabolome. The main effect 'inoculation' was found to be responsible of 5% of the total variability observed in the analysis (Supplementary Table 2). One single component of the AMOPLS models in both PI and NI modes explained the contribution of the fungal inoculation to the total variability (Supplementary Table S2), and the loadings of this component were used to detect metabolites exhibiting intensity fold changes upon fungal inoculation. Several phenylpropanoids, including features putatively annotated as HCAs (feruloylquinic acid) and HCAAs (*N*-caffeoylputrescine and *N*-dihydrocaffeoylputrescine), were relatively more abundant upon *C. coccodes* inoculation. Interestingly, even the most abundant HCA (chlorogenic acid) and its dimer showed a significant positive intensity fold-change in inoculated samples (Supplementary Table S3). This is in line with other studies that have shown that total phenolics increase in potato leaves upon bacterial infection (Poiatti et al., 2009) and in potato tubers upon inoculation of the oomycete pathogen *P. infestans* (Kröner et al., 2011, 2012). Moreover, an important increase was observed in *N*-dihydrocaffeoylputrescine and *N*-caffeoylputrescine, but not in other HCAAs. Putrescine HCAAs have been shown to accumulate in rust-infected wheat (Samborski and Rohringer, 1970) and in *Nicotiana tabacum* cells upon inoculation of *P. syringae* (Baker et al.,

2005). Altogether these results suggest that HCA and putrescine derivative production are enhanced in potato tubers infected by *C. coccodes* during growth (Supplementary Figure S6). A group of hydroxycoumarins, including scopoletin (identified by comparison of MS/MS to a pure standard), isofraxidin and dimethylfraxetin showed a positive intensity fold-change upon inoculation (Supplementary Figure S7A). Coumarins have been shown to accumulate upon pathogen attack in several plant species, especially in *Arabidopsis thaliana* and in *Nicotiana tabacum* (Stringlis et al., 2019) and, in potatoes, they have been detected in tubers infected with *Phoma exigua* var. *foveata* (Malmberg and Theander, 1980). Our results suggest that hydroxycoumarins accumulate in potato tubers upon *C. coccodes* infection.

It was noted that different features exhibited lower intensity in potatoes after inoculation, suggesting a degradation or downmodulation of the corresponding metabolites upon fungal inoculation. Quercetin and kaempferol glycosides were found in lower ratios in inoculated samples of all cultivars except for the red-skin cultivar Cheyenne (Supplementary Table 3). Nonetheless, kaempferol glycosides were more abundant in Cheyenne than in the rest of the cultivars, making the visualization of the decrease in kaempferol derivatives less obvious (Supplementary Table S3, Supplementary Figure S7B). Interestingly, quercetin-3-O-rutinoside, but not kaempferol-3-O-rutinoside, has been shown to possess antimicrobial activity against plant pathogens (El Hadrami et al., 2011; Kröner et al., 2012). Altogether, these results suggest a direct or indirect degradation of flavonoid glycosides by *C. coccodes.* This could in turn limit the antimicrobial properties of the potato tuber skin. It is worth noting that coumaric acid is the precursor of all metabolites affected by the inoculation of *C. coccodes* (HCAs, HCAAs, coumarins and flavonoids), and the different pathways involving coumaric acid may be affected during pathogen infection (Supplementary Figure S6).

Hydroxycoumarins and steroid derivatives are specifically induced upon C. coccodes inoculation in resistant cultivars

The AMOPLS models (NI and PI modes) showed that the interaction between cultivar and inoculation had a statistically significant effect on the metabolomic profile of potato tubers (Supplementary Table S2). The interaction effect was responsible for 6% of the total variability observed in this study (Supplementary Table 2). This result indicates that the cultivars respond differently to the inoculation of tubers with *C. coccodes* and suggest that resistance-related induced (RRI) biomarkers could be identified. The 8th predictive component of the AMOPLS model indicates that some metabolites are differentially induced in the resistant versus the susceptible cultivars (Figure 9)..It has been previously suggested that the response to pathogen attack in plants from the *Solanum* genera do not differ between compatible and incompatible interactions (Desender et al., 2007). However, our results suggest that potato cultivars with different susceptibility levels to black dot have different metabolic responses Nonetheless, this component highlights trends upon inoculation but does not take into account the constitutive amount of these metabolites. Quantitative resistance to bacterial and oomycete pathogens in potatoes has been defined by the final content of the target molecules rather than their inducibility by the pathogen (Kröner et al., 2012). Thus, two Resistance-Related Induced ratios were calculated: the relative induction ratio (qualitative RRI = (RP/RM)/(SP/SM)) and the relative concentration in inoculated tubers between resistant and susceptible cultivars (quantitative RRI=RP/SP) (Supplementary Table 3). Some clusters of the molecular network in PI mode highlighted steroid derivatives as quantitative RRIs (Supplementary Figure S4), with some features with positive fold changes in resistant cultivars and negative fold changes in susceptible cultivars upon inoculation (Supplementary Table S3). Interestingly, several hydroxycoumarins, which had been highlighted as induced metabolites upon *C. coccodes* inoculation, were found to be induced at higher levels in the resistant cultivars (Supplementary Table S3). Scopoletin has been shown to correlate with plant resistance against several pathogen in tobacco, and to possess antifungal activity (El Oirdi et al., 2010; Sun et al., 2014; Yang et al., 2018b). Furthermore, several hydroxycoumarins have been associated

with resistance to late blight in potato leaves and tubers (Yogendra et al., 2014, 2015; Hamzehzarghani et al., 2016). In our antifungal bioassay, scopoletin, and especially esculetin (which showed both high RRC and RRI scores), exhibited antifungal activity against *C. coccodes* at 500 µM (Figure 8). These results suggest that hydroxycoumarins are specifically induced upon fungal inoculation in black dot resistant cultivars and may limit the proliferation of the pathogen *in planta*.

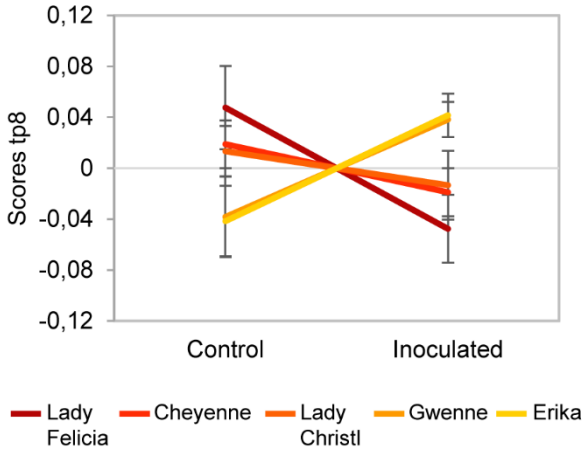

Figure 3.10 Scores of predictive component tp8 associated with the *Cultivar x Inoculation* interaction effect for the negative ion mode dataset. The score value is reported on the vertical axis for control and inoculated conditions (in the horizontal axis). A difference between resistant cultivars (Erika and Gwenne) and susceptible cultivars (Lady Felicia, Cheyenne and Lady Christl) can be observed.

3.5. Conclusion

Quantitative resistance to plant pathogens is the result of several mechanisms that limit the progress of the pathogenic infection. Since it involves different processes, breaking this resistance is more complicated for the pathogen than in qualitative resistance, where a single mutation may be sufficient to overcome resistance. However, studying quantitative resistance involves complementary approaches to the traditional genetic screening for *R* genes. In this work, we studied both structural and biochemical mechanisms of potato cultivars with different degrees of quantitative resistance to black dot disease and we found that both mechanisms seem to be involved at different degrees in quantitative resistance. From a structural point of view, we could clearly highlight across the selected cultivars that in general, phellem thickness does not correlate with black dot resistance. However, the potato cultivar with the thinnest skin, Lady Felicia, was the most susceptible suggesting that a minimum skin thickness may be required for quantitative resistance. This hypothesis is in accordance with previous studies in American cultivars but should be verified across a larger number of European cultivars. In addition, the skin suberin amounts or composition did not correlate with black dot resistance contrarily to that observed with other potato pathogens, such as *Streptomyces scabies.* On the other hand, the metabolite composition of the five cultivars were found to differ significantly, and possible biomarkers of black dot resistance in potato tubers were identified as Resistant-Related Constitutive (RRC) metabolites. Among them, the glycoalkaloid alpha-chaconine, which had been previously shown to possess antifungal activities *in vitro* and to confer resistance to different potato diseases, seems to be involved in resistance to black dot. Other highlighted RRC were the HCAAs, which were previously found to be involved in cell wall fortification. In addition, we found that some HCAAs possess antifungal activities against *C. coccodes in vitro*, indicating a larger role of these metabolites in plant-pathogen interactions. Moreover, inoculation of *C. coccodes* induced the accumulation of RRI metabolites, particularly antifungal hydroxycoumarins, which were more prominent in all resistant cultivars. Altogether, our results suggest that metabolite composition is the main determinant of

resistance of potato cultivars to black dot. The approach used could be applied to a wider panel of potato cultivars in order to confirm the trends observed in the cultivars investigated in this study. Since most of the highlighted biomarkers were found to be constitutively more abundant in the resistant cultivars, their role in resistance to other fungal diseases may be worth investigating. Potentially, these compounds could be used for Marker Assisted Selection within breeding programs and contribute to a sustainable production of table potatoes.

3.6. Aknowledgements

The authors thank Susete Ulliel and Jean-Pierre de Joffrey for installing and producing potato *in vitro* plantlets, and Eric Remolif for assistance during plant development. Figure 3.4 contains modified icons by Irman Firmansyah, Ben Davis, Fredrik Edfors, @daosme, Meaghan Hendricks, Three Six Five, Justiconnic, Guilherme Furtado, Ton, Creative Stall, Julie Ko and Alexchan from thenounproject.com.

3.7. Supplementary material

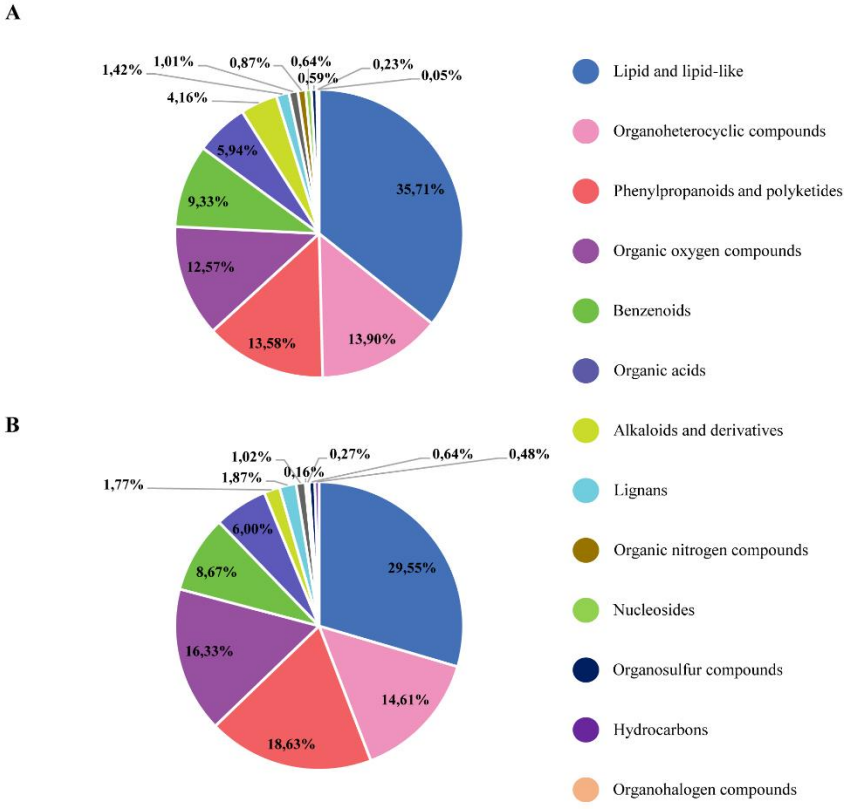

Supplementary Figure 3.1 Pie-chart of the chemical classes of compouds detected in potato periderms in positive (A) and negative (B) ionization modes as annotated by the ISDB-DNP and classified using ClassyFire.

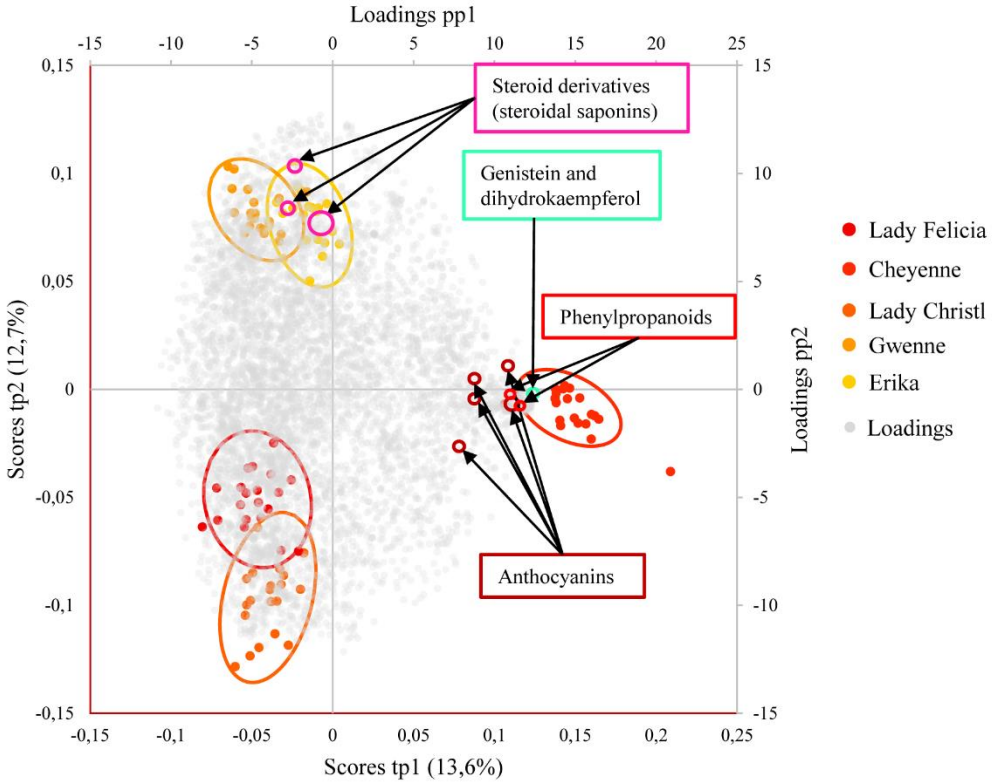

Supplementary Figure 3.2 Biplot representation of the two first predictive components of the AMOPLS model in positive ion mode explaining 26,4% of the total variance. Observations are positioned according to the left and below axis. Loadings are according to the right and above axis. Observations are color-coded as cultivars (n=20) with 95% confidence ellipses. The first component of the model (tp1) separates the red-skin cultivar (Cheyenne, positive scores) from the rest of the cultivars (negative scores). Resistant cultivars (Erika and Gwenne) have positive scores of tp2, while susceptible cultivars (Lady Felicia, Cheyenne and Lady Christl) have negative scores of tp2. The loadings of Cheyenne-specific metabolites annotated as anthocyanins, phenylpropanoids or the isoflavonoid genistein and the flavononol dihydrokaempferol are indicated. The loadings of highlighted resistance-related metabolites annotated as steroid derivatives are also indicated.

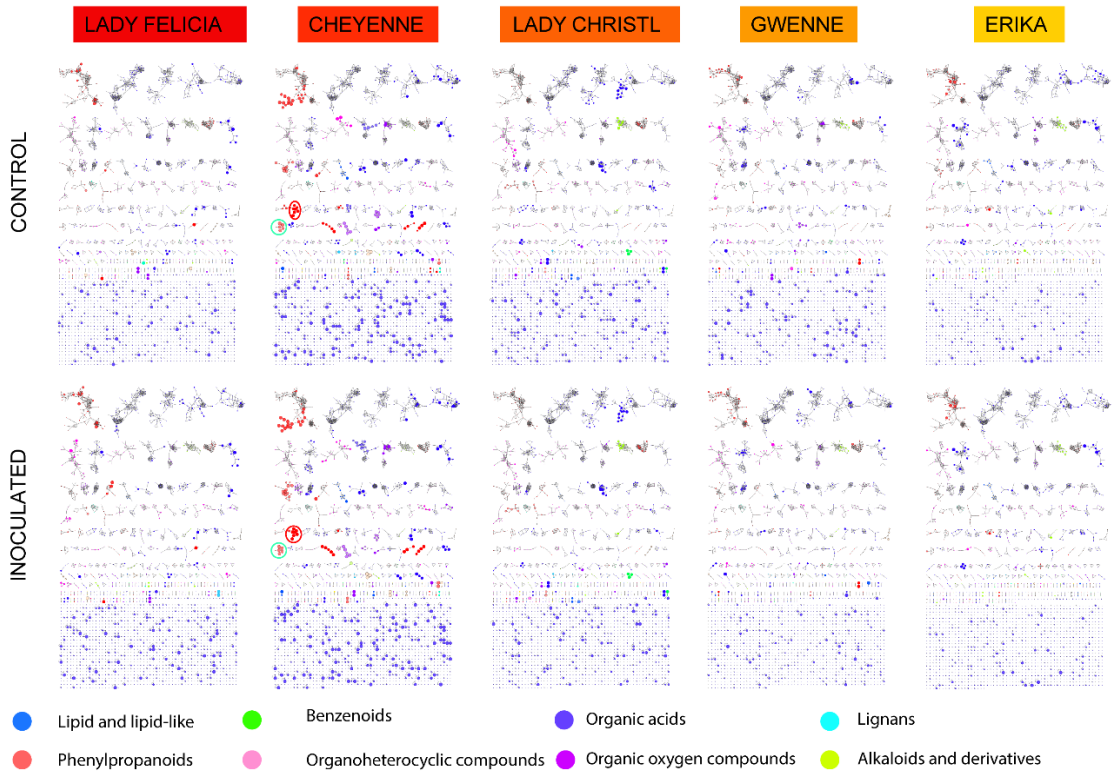

Supplementary Figure 3.3 Individual Molecular Networks in positive ion mode of the five potato cultivars in control and inoculated samples. Color of the node according to consensus chemical class, transparency according to consistency of the chemical class, node size according to relative signal intensity of the respective cultivar. The red-skin cultivar appears to have the most abundant number of specific metabolites, including the isoflavonoid genistein and the flavononol dihydrokaempferol (in the cluster highlighted in light-blue), and a cluster of phenylpropanoids (the cluster highlighted in red) that was also highlighted in the AMOPLS model.

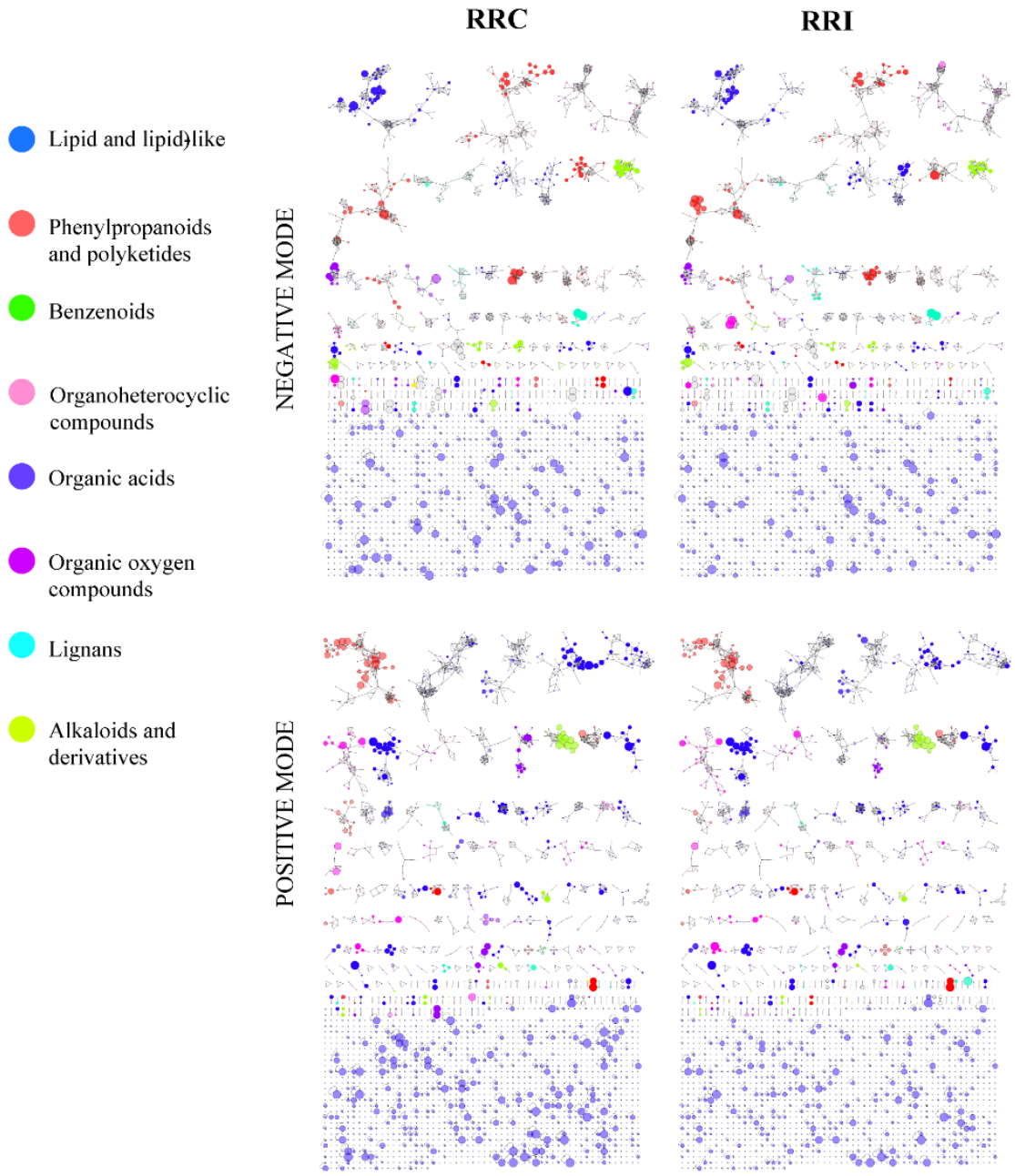

Supplementary Figure 3.4 Global Molecular Networks in positive (A and C) and negative (B and D) ion modes of the five potato cultivars. Color of the node according to consensus chemical class, transparency according to consistency of the chemical class, node size according to the ratio of intensities between resistant and susceptible cultivars in control conditions (RRC) (A and B) or in inoculated samples (RRI) (C and D).

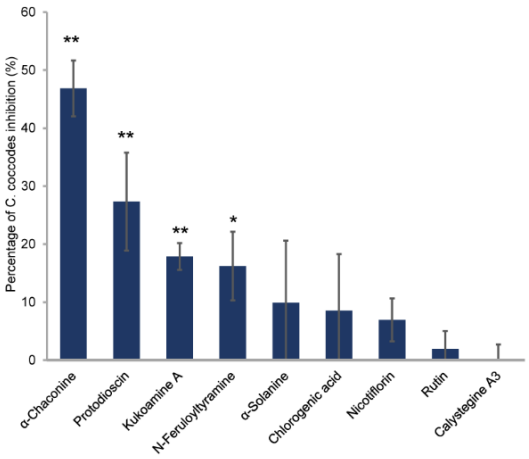

Supplementary Figure 3.5 Growth inhibition percentage of *C. coccodes* growth *in vitro* of the selected compounds at the highest estimated concentration in potato tubers (n=3, Mean ± Standard Deviation): Chlorogenic acid 7,5 mM, alpha-chaconine and calystegine A_3 500 µM, alpha-solanine 250 µM, rutin and protodioscin 100 µM, *N*-feruloyltyramine, *N*1,*N*12-bis(dihydrocaffeoyl) spermine and nicotiflorin at 50 µM. Asterisks indicate significant differences between resistant and susceptible cultivars (p-value<0.05, T-test).

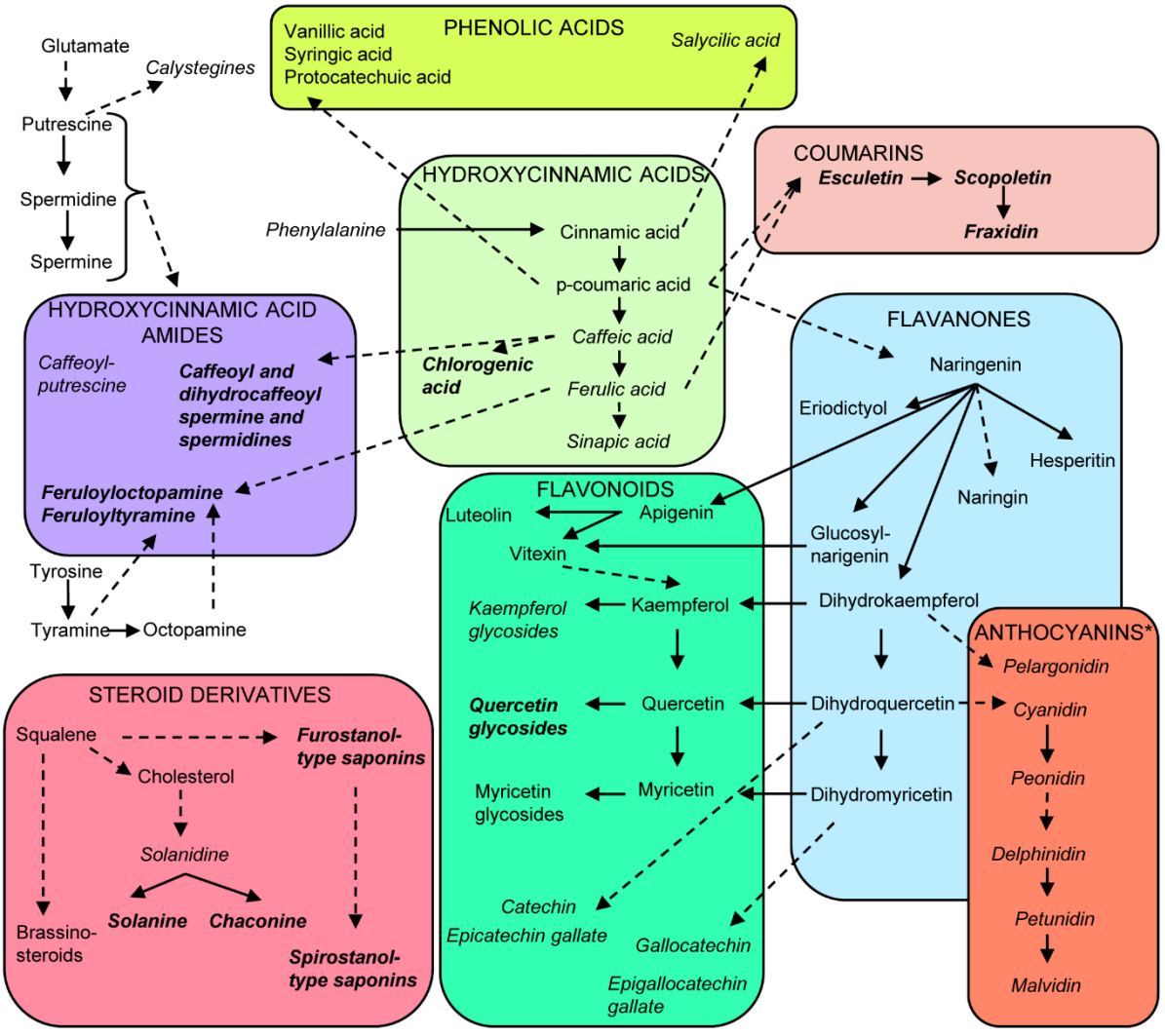

Supplementary Figure 3.6 Metabolic pathways involved in the interaction between *Solanum tuberosum* and *Colletotrichum coccodes*. The central cluster is formed by the hydroxycinnamic acids (HCAs) that derive from phenylalanine.

Hydroxycinnamic acid amides (HCAAs) that derive from HCAs and amino acid derivatives form the cluster in the left. Cinnamic acid and *p*-coumaric acid are precursors of phenolic acids such as salycilic acid. Coumarins derive from *p*-coumaric acid or ferulic acid. Naringenin, produced from *p*-coumaric acid, is the precursor of flavonoids and anthocyanins. Steroidal glycosides (i.e. alpha-chaconine and alpha-solanine), steroidal saponins and brassinosteroids derive from squalene. *For anthocyanins, only the aglycone (anthocyanidin) is shown. Detected metabolites in this study are shown in italics. Dotted lines indicate that more than one step is required for the conversion shown in the figure. Biosynthetic pathways according to the Kyoto Encyclopedia of Genes and Genomes (KEGG) of *Solanum tuberosum* (or related species, if not available for *S. Tubersosum*).

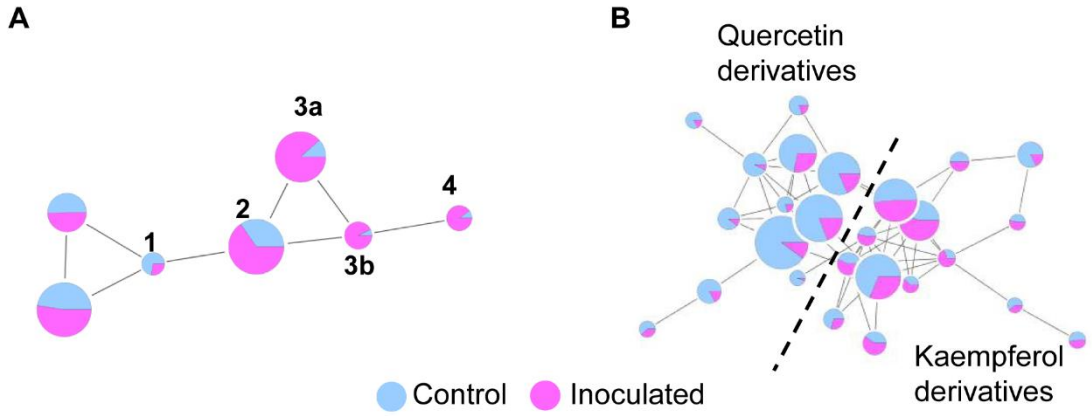

Supplementary Figure 3.7 Molecular Network clusters of hydroxycoumarins (A) and flavonoid glycosides (B) ; size of the node corresponds to mean peak intensity. The color of each node is set as a pie-chart with the relative abundance of the metabolite in control conditions (light blue) or inoculated (pink) conditions. In A: 1. Esculetin, 2. Scopoletin, 3a and 3b. Isofraxidin, 4. Dmethylfraxidin. In B: dotted line separates quercetin glycosides (left) and kaempferol glycosides (right).

Supplementary Table 3.1 Suberin monomeric composition in tuber periderm (µg/mg periderm) of the five potato cultivars studied (n=6, mean ± Standard deviation). [a] In brackets, percentage of each monomers class.

Compound	Periderm (µg/mg)				
Aromatics	**Lady Felicia**	**Cheyenne**	**Lady Christl**	**Gwenne**	**Erika**
Citric acid	0,40 ± 0,06	0,44 ± 0,22	0,42 ± 0,23	0,71 ± 0,24	0,83 ± 0,34
Vanillic acid	0,76 ± 0,26	0,65 ± 0,08	0,43 ± 0,26	0,48 ± 0,09	0,76 ± 0,18
p-coumaric acid	0,14 ± 0,11	1,06 ± 0,54	0,11 ± 0,05	0,15 ± 0,07	0,16 ± 0,03
Ferulic acid	9,84 ± 1,18	9,89 ± 2,17	7,29 ± 1,6	8,25 ± 0,51	10,73 ± 2,04
Caffeic acide	1,26 ± 0,68	1,57 ± 0,83	1,17 ± 1,07	0,87 ± 0,51	1,61 ± 0,42
TOTAL Aromatics[a]	**12,39 ± 1,75 (12,1%)**	**13,61 ± 3,32 (14,8%)**	**9,42 ± 2,94 (10,1%)**	**10,47 ± 0,62 (9,8%)**	**14,10 ± 2,3 (12,6%)**
Alkanoic acids					
Hexadecanoic acid (C16:0)	0,44 ± 0,06	0,35 ± 0,05	0,29 ± 0,06	0,38 ± 0,05	0,53 ± 0,07
Octadecanoic acid (C18:0)	0,08 ± 0,02	0,07 ± 0,04	0,08 ± 0,01	0,06 ± 0,01	0,06 ± 0,01
Docosanoic acid (C22:0)	0,14 ± 0,09	0,28 ± 0,06	0,31 ± 0,04	0,36 ± 0,06	0,19 ± 0,02
Tetracosanoic acid (C24:0)	1,18 ± 0,34	1,05 ± 0,29	1,49 ± 0,2	1,66 ± 0,21	1,58 ± 0,31
Pentacosanoic acid (C25:0)	0,52 ± 0,11	0,48 ± 0,28	0,59 ± 0,05	0,64 ± 0,07	0,33 ± 0,07
Hexacosanoic acid (C26:0)	3,32 ± 0,31	2,81 ± 0,7	3,45 ± 0,34	3,15 ± 0,3	3,35 ± 0,41
Heptacosanoic acid (C27:0)	0,21 ± 0,14	0,18 ± 0,06	0,26 ± 0,03	0,08 ± 0,02	0,14 ± 0,04
Octacosanoic acid (C28:0)	16,09 ± 1,97	9,78 ± 2,15	10,40 ± 1,62	7,10 ± 0,76	9,95 ± 0,92
Nonacosanoaic acid (C29:0)	4,09 ± 0,48	2,75 ± 0,6	2,52 ± 0,43	1,47 ± 0,23	2,56 ± 0,59
Triacontanoic acid (C30:0)	11,77 ± 1,99	7,94 ± 1,68	5,98 ± 0,96	12,50 ± 1,94	10,87 ± 0,75
TOTAL Alkanoic acids[a]	**37,83 ± 5,17 (36,9%)**	**25,68 ± 5,35 (28,0%)**	**25,36 ± 3,25 (27,3%)**	**27,41 ± 3,56 (25,7%)**	**29,55 ± 2,36 (26,4%)**
1-alkanols					
Octadecanol	0,17 ± 0,05	0,22 ± 0,1	0,17 ± 0,08	0,15 ± 0,03	0,11 ± 0,11
Eicosanol	0,04 ± 0,01	0,10 ± 0,03	0,08 ± 0,04	0,06 ± 0,01	0,11 ± 0,04
Heneicosanol	0,67 ± 0,23	0,90 ± 0,25	0,66 ± 0,07	0,81 ± 0,05	0,70 ± 0,17
Docosanol	0,42 ± 0,11	0,69 ± 0,22	0,48 ± 0,2	0,53 ± 0,03	0,25 ± 0,09
Tetracosanol	0,57 ± 0,1	0,55 ± 0,14	0,60 ± 0,19	0,84 ± 0,05	0,68 ± 0,39
Hexacosanol	1,48 ± 0,54	1,26 ± 0,28	1,64 ± 0,4	1,79 ± 0,12	2,02 ± 0,25
Octacosanol	4,75 ± 1,92	3,89 ± 1,02	4,05 ± 0,91	4,39 ± 0,37	4,36 ± 0,88
Tricontanol	0,38 ± 0,14	0,51 ± 0,11	0,41 ± 0,24	0,75 ± 0,11	0,59 ± 0,09
TOTAL 1-alkanols[a]	**8,48 ± 2,81 (8,3%)**	**8,11 ± 1,83 (8,8%)**	**8,09 ± 1,49 8,7%)**	**9,31 ± 0,66 (7,7%)**	**8,80 ± 1,25 (7,8%)**
α,ω-Diacids					
Hexadecanedioic acid	0,93 ± 0,26	1,42 ± 0,42	1,02 ± 0,16	1,27 ± 0,13	1,07 ± 0,24
Octadecanedioic acid	1,43 ± 0,42	1,34 ± 0,42	1,81 ± 0,27	2,10 ± 0,15	1,55 ± 0,35
Octadec-9-enedioic acid	15,02 ± 3,99	15,07 ± 1,68	17,99 ± 3,91	22,14 ± 1,87	19,54 ± 4,27
Eicosanedioic acid	0,42 ± 0,18	0,33 ± 0,14	0,54 ± 0,14	0,57 ± 0,03	0,42 ± 0,11
Docosanedioic acid	0,50 ± 0,28	0,79 ± 0,45	0,87 ± 0,34	0,96 ± 0,07	0,70 ± 0,32
Tetracosanedioic acid	1,01 ± 0,25	1,17 ± 0,43	1,46 ± 0,41	1,64 ± 0,27	1,55 ± 0,26
Hexacosanedioic acid	0,71 ± 0,14	0,61 ± 0,28	1,04 ± 0,34	1,20 ± 0,15	1,22 ± 0,24
Total α,ω-Diacids[a]	**20,04 ± 4,59 (19,6%)**	**20,73 ± 3,19 (22,6%)**	**24,72 ± 4,46 (26,6%)**	**29,86 ± 1,94 (27,9%)**	**26,05 ± 4,56 (23,2%)**
Hydroxyacids					

2-Hydroxyhexadecanoic acid	0,11 ± 0,05	0,11 ± 0,04	0,14 ± 0,05	0,14 ± 0,02	0,17 ± 0,05
16-Hydroxyhexadecanoic acid	0,60 ± 0,2	0,91 ± 0,28	0,71 ± 0,15	1,08 ± 0,17	0,92 ± 0,22
18-Hydroxyoctadecanoic acid	0,02 ± 0,01	0,03 ± 0,01	0,03 ± 0,01	0,03 ± 0,01	0,03 ± 0,01
18-Hydroxy-octadec-9-enoate	16,68 ± 5,96	16,04 ± 4,74	16,19 ± 2,75	18,27 ± 1,31	23,21 ± 7,29
20-Hydroxyeicosanoic acid	0,14 ± 0,24	0,03 ± 0,02	0,06 ± 0,05	0,03 ± 0,02	0,12 ± 0,13
22-Hydroxydocosanoic acid	0,82 ± 0,25	1,43 ± 0,4	1,02 ± 0,44	1,39 ± 0,2	0,75 ± 0,47
24-Hydroxytetracosanoic acid	2,33 ± 1,14	1,83 ± 0,97	3,01 ± 0,89	4,15 ± 0,72	3,16 ± 1,19
26-Hydroxyhexacosanoic acid	2,04 ± 0,81	1,85 ± 0,49	2,83 ± 0,62	3,08 ± 0,27	2,87 ± 0,51
28-Hydroxyoctacosanoic acid	1,02 ± 0,48	1,39 ± 0,44	1,43 ± 0,44	1,65 ± 0,17	1,29 ± 0,6
Total Hydroxyacids[a]	**23,76 ± 7,86 (23,2%)**	**23,61 ± 5,15 (25,7%)**	**25,43 ± 5,02 (27,3%)**	**29,82 ± 1,89 (27,9%)**	**33,61 ± 8,81 (30,0%)**
TOTAL SUBERIN	**102,50 ± 22,72**	**91,74 ± 19,38**	**93,03 ± 17,43**	**106,86 ± 9,48**	**112,11 ± 19,99**

Supplementary Table 3.2 ANOVA decomposition and AMOPLS predictive components (*tp1* to *to*, first row) related to the specific effects of the experimental design (*Cultivar, Inoculation or Cultivar × Inoculation*), for the LC-HRMS/MS dataset (Positive and Negative Ionization, respectively). The predictive components associated with each specific effect are highlighted.

ANOVA decomposition (PI)	**Cultivar**				**Inno-culation**	**Interaction**				**Residuals**
Relative Sum of Squares	48,3%				4,8%	5,5%				41,5%
Predictive components	tp1	tp2	tp3	tp4	tp5	tp6	tp7	tp8	tp9	to
Cultivar	**96,10%**	**96,90%**	**97,40%**	**91,50%**	1,60%	2,90%	5,80%	6,10%	7,20%	10,00%
Inoculation	1,20%	0,90%	0,80%	2,50%	**87,90%**	7,90%	15,80%	16,40%	19,60%	27,00%
Cultivar × Inoculation	1,30%	1,00%	0,90%	2,80%	4,90%	**79,50%**	**58,90%**	**57,20%**	**49,00%**	29,60%
Residuals	1,40%	1,20%	1,00%	3,10%	5,50%	9,70%	19,50%	20,30%	24,20%	33,40%
ANOVA decomposition (NI)	**Cultivar**				**Inno-culation**	**Interaction**				**Residuals**
Relative Sum of Squares	48,3%				4,8%	5,5%				41,5%
Predictive components	tp1	tp2	tp3	tp4	tp5	tp6	tp7	tp8	tp9	to
Cultivar	**96,10%**	**96,90%**	**97,40%**	**91,50%**	1,60%	2,90%	5,80%	6,10%	7,20%	10,00%
Inoculation	1,20%	0,90%	0,80%	2,50%	**87,90%**	7,90%	15,80%	16,40%	19,60%	27,00%
Cultivar × Inoculation	1,30%	1,00%	0,90%	2,80%	4,90%	**79,50%**	**58,90%**	**57,20%**	**49,00%**	29,60%
Residuals	1,40%	1,20%	1,00%	3,10%	5,50%	9,70%	19,50%	20,30%	24,20%	33,40%

Supplementary Table 3.3 List of metabolites detected in the untargeted metabolomics approach and highlighted as resistance-related metabolites or cultivar-specific metabolites. NI Negative ionization mode; PI Positive Ionization mode. RT: Retention Time. Chemical class according to ClassyFyre (Subclass or parent). The values of each feature are standardized to the lowest intensity peak of the feature. RRC=RM/SM, RRI=RP/SP, qualitativeRRI =(RP/RM)/(SP/SM). RRC resistance-related constitutive, RRI resistance-related induced, RP resistant genotype with pathogen inoculation, RM resistant genotype with mock inoculation, SP susceptible genotype with pathogen inoculation, SM susceptible genotype with mock inoculation. Annotation: 1: pure standard (HRMS, MS/MS, RT); 2a: GNPS experimental data; 2b: in silico database (ISDB) with taxonomic ponderation; 3: comparison with published data (anthocyanins (Ieri et al. 2011), steroidal saponins and HCAAs (Parr et al. 2005; Huang et al. 2017); 4: Unannotated features from an annotated MN cluster; 5: HRMS (no MS/MS data available).

m/z ratio	Mode	RT	Putative idendity	Chemical Class	Lady Felicia		Cheyenne		Lady Christl		Gwenne		Erika		RRC	RRI	qRRI	Anno-tation
					C	I	C	I	C	I	C	I	C	I				
164,0708	NI	0,54	Phenylalanine	Aminoacid	2,64	1,94	1,05	1,00	4,91	2,57	4,26	3,75	1,53	1,39	**1,01**	**1,40**	**1,38**	**1**
801,2946	PI	1,75	mal 3-O-rut-5-O-glu	Antho-cyanins	3,79	4,12	1,00	1,93	7,19	7,24	6,18	6,30	5,02	3,64	**1,40**	**1,12**	**0,80**	**2b**
963,2770	PI	1,38	pet 3-O-ferul -rut-5-O-glu	Antho-cyanins	6,46	1,00	nd	nd	nd	nd	nd	nd	nd	nd	**0,00**	**0,00**		**2b**
933,2650	PI	1,31	pet 3-O-p-coum -rut-5-O-glu	Antho-cyanins	220,67	13,06	33,88	106,60	5,27	1,00	nd	nd	49,64	14,56	**0,29**	**0,18**	**0,63**	**3**
741,2236	PI	0,70	pel 3-O-rut -5-O-glu	Antho-cyanins	nd	nd	18,81	35,50	nd	nd	nd	nd	1,29	1,00	**0,10**	**0,04**	**0,41**	**2b**
579,1690	PI	1,05	pel 3-O-rut	Antho-cyanins	7,50	5,69	6,49	29,14	5,05	4,90	1,00	1,48	4,05	3,31	**0,40**	**0,18**	**0,45**	**3**
903,2545	PI	1,27	pel 3-O-caf-rut-5-O-glu	Antho-cyanins	7,49	nd	85,49	316,97	3,91	1,00	nd	nd	18,74	2,52	**0,29**	**0,01**	**0,04**	**3**
887,2606	PI	1,39	pel 3-O-cis-p-coum-rut-5-O-glu	Antho-cyanins	1,05	nd	1153,57	3784,59	3,88	1,00	nd	nd	13,54	4,34	**0,02**	**0,00**	**0,10**	**3**
887,2605	PI	1,68	pel 3-O-p-coum-rut-5-O-glu	Antho-cyanins	nd	nd	1,00	2,05	nd	nd	nd	nd	nd	nd	**0,00**	**0,00**		**3**
917,2705	PI	1,44	pel 3-O-ferul rut-5-O-glu	Antho-cyanins	137,06	1,00	4080,06	#######	90,94	24,45	14,95	15,67	578,56	79,46	**0,21**	**0,01**	**0,06**	**3**
947,2810	PI	1,49	peo 3-O-ferul rut-5-O-glu	Antho-cyanins	18,48	1,00	128,53	246,35	18,16	5,63	6,18	7,92	78,53	34,48	**0,77**	**0,25**	**0,33**	**2b**
725,2069	PI	1,55	pel 3-O-p-coum -rut	Antho-cyanins	nd	nd	1,00	3,86	nd	nd	nd	nd	nd	nd	**0,00**	**0,00**		**2b**
755,2168	PI	1,62	pel 3-O-ferul -rut	Antho-cyanins	19,81	1,00	90,24	296,23	6,23	2,12	1,37	nd	60,30	16,00	**0,80**	**0,08**	**0,10**	**3**
191,0187	NI	0,31	Citric acid	Carboxylic acid	1,43	1,00	1,59	1,55	1,88	1,13	1,92	1,93	1,29	1,71	**1,13**	**1,22**	**1,08**	**2a**
133,0128	NI	0,26	Malic acid	Carboxylic acid	1,52	1,35	1,36	1,73	1,24	1,00	1,59	1,40	1,10	1,17	**0,98**	**0,94**	**0,96**	**2a**

147,0286	NI	0,33	Citramalic acid	Carboxylic acid	1,00	1,27	1,17	2,77	1,56	1,63	1,70	1,14	1,12	1,32	**1,13**	**0,65**	**0,57**	**2a**
299,0775	NI	0,84	Salicylate 2-O-beta-D-glucoside	Carboxylic acid	1,81	2,98	11,05	3,89	1,53	1,00	2,30	1,62	1,11	1,29	**0,35**	**0,56**	**1,57**	**2b**
917,5132	NI	2,72	(1α,3β,7β,8α,9β,24S)-1,3,7,24-Tetrahydroxy-9,19-cyclolanostan-25-yl 4-O-{4-O-[(2S,3R,4R)-3,4-dihydroxy-4-(hydroxymethyl)tetrahydro-2-furanyl]-β-D-xylopyranosyl} -β-D-glucopyranoside	Cyclo-artanols and derivatives	75,78	47,76	1,03	1,25	1,00	nd	5,35	3,21	124,08	82,15	**2,50**	**2,61**	**1,05**	**2b**
447,0932	NI	1,53	kaempferol 3-O-beta-D-galactoside	Flavonoid glycoside	4,08	nd	726,14	1102,10	nd	nd	1,25	1,00	42,06	26,65	**0,09**	**0,04**	**0,42**	**2b**
463,0888	NI	1,41	quercetin-3-O-glucoside (isoquercitrin)	Flavonoid glycoside	19,90	nd	1,43	1,00	8,87	2,67	13,68	3,88	65,35	6,20	**3,92**	**4,12**	**1,05**	**2a/2b**
591,1351	NI	1,69	Kaempferol derivative	Flavonoid glycoside	nd	nd	21,91	12,70	nd	nd	1,00	1,46	nd	nd	**0,07**	**0,17**	**2,53**	**4**
593,1511	NI	1,51	Kaempferol 3-O-Rutinoside	Flavonoid glycoside	55,96	1,00	120,06	130,17	12,14	4,33	10,33	5,00	184,37	19,64	**1,55**	**0,27**	**0,18**	**1**
609,1469	NI	1,31	Quercetin 3-O-Rutinoside	Flavonoid glycoside	135,29	1,00	43,30	50,18	3,10	1,22	3,67	1,82	167,67	5,87	**1,41**	**0,22**	**0,16**	**1**
625,1418	NI	1,16	Quercetin Disaccharide	Flavonoid glycoside	1,00	nd	20,78	17,77	14,98	6,80	30,73	8,75	27,89	2,53	**2,39**	**0,69**	**0,29**	**2b**
739,1891	NI	2,08	Kaempferol-3-O-D-(2-O-trans-coumaroyl)-rutinoside	Flavonoid glycoside	27,26	nd	429,88	780,95	11,50	4,47	5,74	1,00	147,61	15,63	**0,49**	**0,03**	**0,06**	**4**

753,1888	NI	1,43	Kaempferol derivative	Flavonoid glycoside	nd	nd	119,62	101,86	nd	nd	1,00	3,81	nd	nd	**0,01**	**0,06**	**4,47**	**4**
755,1836	NI	1,94	Quercetin 3-O-D-(2-O-trans-coumaroyl)-rutinoside	Flavonoid glycoside	40,98	nd	24,40	40,95	nd	nd	1,00	nd	140,76	5,45	**3,25**	**0,20**	**0,06**	**2b**
755,2052	NI	1,21	Kaempferol 3-O-rutinoside-7-glucoside	Flavonoid glycoside	nd	nd	119,21	129,39	6,48	2,63	10,72	3,07	8,92	1,00	**0,23**	**0,05**	**0,20**	**4**
771,1999	NI	1,10	Quercetin 3-O-Rutinoside-7-glucoside	Flavonoid glycoside	1,00	nd	53,54	27,24	21,00	10,06	84,85	13,80	90,42	2,55	**3,48**	**0,66**	**0,19**	**2a**
785,1934	NI	2,03	Quercetin derivative	Flavonoid glycoside	11,31	nd	1,00	nd	nd	nd	1,97	1,18	36,62	1,33	**4,70**	**∞**	**∞**	**4**
901,2429	NI	1,87	Kaempferol-3-O-D-(2-O-trans-coumaroyl)-rutinoside-7-glucoside	Flavonoid glycoside	nd	nd	1,00	2,39	nd	nd	nd	nd	nd	nd	**0,00**	**0,00**	**0,00**	**4**
931,2531	NI	1,94	Kaempferol triglycosides	Flavonoid glycoside	nd	nd	153,92	238,69	1,00	nd	nd	nd	nd	nd	**0,00**	**0,00**	**0,00**	**4**
477,1042	NI	1,62	(1S)-1,5-Anhydro-1-[3,5,7-trihydroxy-2-(4-hydroxyphenyl)-4-oxo-4H-chromen-8-yl]-D-threo-hexitol	Flavonoid glycoside	1,49	0,00	7,99	8,26	1,00	0,00	1,60	1,61	16,07	7,21	**2,53**	**1,60**	**0,63**	**2b**
623,1619	NI	1,56	isorhamnetin-3-O-rutinoside	Flavonoid glycoside	23,57	1,00	4,88	3,65	3,54	2,52	5,83	2,78	23,38	2,68	**1,37**	**1,14**	**0,83**	**2a/ 2b**

655,1515	NI	1,29	3-[4,5-dihydroxy-6-(hydroxymethyl)-3-[3,4,5-trihydroxy-6-(hydroxymethyl)oxan-2-yl]oxyoxan-2-yl]oxy-5,7-dihydroxy-2-(4-hydroxyphenyl)chromen-4-one	Flavonoid glycoside	0,00	0,00	127,02	153,36	2,54	1,00	3,79	0,00	0,00	0,00	**0,04**	**0,00**	**0,00**	**2a/ 2b**
769,2001	NI	2,14	4',5,7-Trihydroxy-3'-methoxyflavone	Flavonoid glycoside	1,00	0,00	41,46	55,38	0,00	0,00	0,00	0,00	5,95	0,00	**0,21**	**0,00**	**0,00**	**2b**
839,1873	NI	1,09	Quercetin 3-glycosides Trisaccharides, 3-O-[β-D-Glucopyranosyl-(1→2)-[α-L-rhamnopyranosyl-(1→6)]-β-D-glucopyranoside]	Flavonoid glycoside	0,00	0,00	25,96	13,70	10,82	4,65	39,93	7,12	36,66	1,00	**3,12**	**0,66**	**0,21**	**2b**
677,1333	NI	1,36	3',4,4',5',6-Pentahydroxyaurone; (E)-form, 4'-O-[α-L-Rhamnopyranosyl-(1→6)-β-D-glucopyranoside]	Flavonoid glycoside	37,31	0,00	5,00	4,07	2,75	1,00	6,38	1,78	61,12	2,05	**2,25**	**1,14**	**0,51**	**2b**
661,1382	NI	1,52	--	Flavonoid glycoside	14,86	0,00	39,00	35,88	3,59	1,00	2,95	1,26	48,81	6,08	**1,35**	**0,30**	**0,22**	**4**

251,1401	NI	0,50	N-dihydrocaffeoylputrescine	Hydroxy-cinnamic acid amides	3,04	16,81	1,00	2,97	1,48	1,99	2,43	4,69	2,77	3,52	**1,41**	**0,57**	**0,40**	**5**
249,1244	NI	0,61	N-Caffeoylputrescine	Hydroxy-cinnamic acid amides	18,79	41,03	4,41	12,29	7,60	8,54	1,00	12,83	12,32	16,04	**0,65**	**0,70**	**1,08**	**2b**
529,3036	NI	0,76	N1,N12-bis(dihydrocaffeoyl) spermine	Hydroxy-cinnamic acid amides	2,37	2,22	1,00	1,52	3,21	2,16	7,68	5,90	2,27	2,21	**2,27**	**2,06**	**0,91**	**1**
527,2879	NI	0,77	N-(caffeoyl, dihydrocaffeoyl) spermine	Hydroxy-cinnamic acid amides	1,42	1,38	1,00	1,63	4,81	3,17	3,66	3,33	3,37	3,29	**1,46**	**1,61**	**1,10**	**3**
693,3515	NI	1,39	N1,N4,N12-tris(dihydrocaffeoyl) spermine	Hydroxy-cinnamic acid amides	20,05	19,65	6,77	30,63	1,61	1,00	168,73	118,16	3,17	2,19	**9,07**	**3,52**	**0,39**	**3/4**
693,3511	NI	1,54	N1,N9,N12-tris(dihydrocaffeoyl) spermine	Hydroxy-cinnamic acid amides	20,77	18,50	17,57	25,21	3,70	1,00	79,30	61,69	1,03	1,51	**2,87**	**2,12**	**0,74**	**3/4**
691,3356	NI	1,41	Tris(N1-caffeoyl,N4,N12-dihydrocaffeoyl) spermine	Hydroxy-cinnamic acid amides	6,07	5,59	6,17	11,33	2,81	2,19	21,35	17,35	1,38	1,00	**2,27**	**1,44**	**0,64**	**3**
857,3992	NI	1,91	N1,N4,N9,N12-tetra (dihydrocaffeoyl) spermine	Hydroxy-cinnamic acid amides	4,02	2,58	35,93	37,98	7,99	6,61	1,59	1,00	nd	nd	**0,05**	**0,03**	**0,64**	**3/4**
472,2456	NI	1,02	N1,N8-bis(dihydrocaffeoyl) spermidine	Hydroxy-cinnamic acid amides	18,48	19,97	1,00	2,24	1,84	1,25	14,38	9,68	30,83	24,71	**3,18**	**2,20**	**0,69**	**2b**
470,2301	NI	1,10	bis(N1-caffeoyl, N8-dihydrocaffeoyl) spermidine	Hydroxy-cinnamic acid amides	10,12	11,99	1,01	2,13	1,54	1,00	6,97	5,17	39,08	25,09	**5,45**	**3,00**	**0,55**	**2b**

636,2938	NI	1,69	N1,N4,N8-tris(dihydrocaffeoyl) spermidine	Hydroxy-cinnamic acid amides	46,41	29,17	105,33	128,86	151,50	103,31	1,01	1,00	1,27	1,15	**0,01**	**0,01**	**1,09**	**3/4**
328,1193	NI	1,49	N-feruloyl-octopamine	Hydroxy-cinnamic acid amides	1,21	1,00	7,63	3,10	2,53	1,95	4,91	4,80	7,13	6,10	**1,59**	**2,70**	**1,70**	**2b**
328,1194	NI	1,66	N-feruloyl-octopamine	Hydroxy-cinnamic acid amides	1,08	1,00	2,41	1,51	1,34	1,18	2,20	2,03	2,83	2,44	**1,56**	**1,82**	**1,16**	**2b**
328,1194	NI	1,38	N-feruloyl-octopamine	Hydroxy-cinnamic acid amides	3,57	1,00	19,09	5,97	5,25	2,66	65,40	29,83	69,89	22,19	**7,27**	**8,10**	**1,11**	**2b**
312,1246	NI	1,97	N-Feruloylt yramine	Hydroxy-cinnamic acid amides	1,33	2,05	1,82	1,18	1,00	1,24	3,18	3,44	3,48	3,01	**2,41**	**2,17**	**0,90**	**1**
312,1246	NI	1,86	N-Feruloylt yramine	Hydroxy-cinnamic acid amides	1,67	1,00	4,80	5,12	3,90	2,66	46,46	16,72	65,48	14,33	**16,19**	**5,31**	**0,33**	**2a/ 2b**
623,2407	NI	2,76	Grossamide	Hydroxy-cinnamic acid amides	1,00	2,88	2,87	2,63	2,94	2,83	1,27	3,12	2,40	3,50	**0,81**	**1,19**	**1,48**	**2b**
623,2404	NI	2,58	Grossamide	Hydroxy-cinnamic acid amides	1,00	1,77	2,17	1,76	3,34	2,29	1,54	2,68	4,16	2,95	**1,31**	**1,45**	**1,10**	**2b**
282,1139	NI	1,88	p-Coumaroyl-tyramine	Hydroxy-cinnamic acid amides	6,06	1,00	15,98	3,83	3,01	3,04	2,92	2,65	4,33	3,33	**0,43**	**1,14**	**2,62**	**2b**
341,0882	NI	0,83	caffeoyl-glucose	Hydroxy-cinnamic acids	2,74	2,94	1,14	1,66	1,26	1,10	1,44	1,36	1,39	1,00	**0,83**	**0,62**	**0,75**	**2b**

163,0392	NI	1,24	p-coumaric acid	Hydroxy-cinnamic acids	6,10	12,69	31,09	2,07	1,00	22,35	6,30	1,21	9,20	7,16	**0,61**	**0,34**	**0,56**	**1**
163,0392	NI	1,33	p-coumaric acid	Hydroxy-cinnamic acids	52,32	16,04	71,06	26,27	1,00	33,43	4,18	9,09	25,96	11,36	**0,36**	**0,40**	**1,11**	**2b**
179,0342	NI	0,97	Caffeic acid	Hydroxy-cinnamic acids	1,49	1,26	1,00	1,46	1,54	1,63	2,04	2,09	1,97	1,90	**1,49**	**1,38**	**0,92**	**1**
337,0933	NI	1,08	4-coumaroyl quinic acid	Hydroxy-cinnamic acids	4,02	2,53	1,00	1,17	1,64	1,67	2,07	1,44	1,30	1,25	**0,76**	**0,75**	**0,99**	**2b**
335,0777	NI	1,28	4-O-caffeoyl-shikimic acid	Hydroxy-cinnamic acids	1,64	1,23	1,00	1,60	1,09	1,25	1,45	1,42	1,95	1,57	**1,37**	**1,10**	**0,80**	**2b**
335,0778	NI	1,11	3-O-caffeoyl-shikimic acid	Hydroxy-cinnamic acids	3,73	2,93	1,00	1,38	1,36	1,58	6,23	1,73	1,36	1,33	**1,87**	**0,78**	**0,42**	**2b**
335,0777	NI	1,22	5-O-caffeoyl-shikimic acid	Hydroxy-cinnamic acids	1,71	1,54	1,00	1,51	1,42	1,62	1,77	1,62	2,26	1,79	**1,46**	**1,09**	**0,75**	**2b**
353,0881	NI	0,90	4-O-caffeoyl quinic acid	Hydroxy-cinnamic acids	1,49	1,44	1,00	1,33	1,23	1,27	1,52	1,59	1,50	1,41	**1,22**	**1,12**	**0,92**	**1**
707,1838	NI	0,89	4-O-caffeoyl quinic acid dimer	Hydroxy-cinnamic acids	2,59	2,69	1,00	2,04	1,44	1,65	3,62	3,78	2,55	2,58	**1,84**	**1,49**	**0,81**	**1**
353,0880	NI	0,67	3-O-caffeoyl quinic acid	Hydroxy-cinnamic acids	1,63	1,51	1,00	1,41	1,48	1,55	1,53	1,45	1,79	1,42	**1,21**	**0,96**	**0,79**	**5**
707,1838	NI	0,67	3-O-caffeoyl quinic acid dimer	Hydroxy-cinnamic acids	2,67	2,37	1,00	1,74	2,20	2,35	2,35	2,07	3,14	2,21	**1,40**	**0,99**	**0,71**	**4**
353,0880	NI	0,86	5-O-caffeoyl quinic acid	Hydroxy-cinnamic acids	1,30	1,33	1,00	1,25	1,08	1,18	1,42	1,47	1,27	1,35	**1,19**	**1,13**	**0,95**	**2a/ 2b**
707,1838	NI	0,86	5-O-caffeoyl quinic acid dimer	Hydroxy-cinnamic acids	2,41	2,48	1,00	2,09	1,16	1,58	3,14	3,57	2,11	2,30	**1,72**	**1,43**	**0,83**	**4**

515,1199	NI	1,68	3,5-Dicaffeoyl quinic acid	Hydroxy-cinnamic acids	12,73	18,04	1,00	1,59	2,56	2,77	2,91	2,90	4,92	3,65	**0,72**	**0,44**	**0,61**	**2b**
515,1199	NI	1,56	3,4-Dicaffeoyl quinic acid	Hydroxy-cinnamic acids	104,49	133,18	1,00	1,15	2,23	2,15	1,68	1,50	2,71	1,97	**0,06**	**0,04**	**0,62**	**2b**
515,1199	NI	1,74	4,5-Dicaffeoyl quinic acid	Hydroxy-cinnamic acids	16,67	19,01	1,00	2,04	2,57	2,61	2,80	3,64	4,53	4,03	**0,54**	**0,49**	**0,90**	**2b**
193,0499	NI	1,46	Ferulic acid	Hydroxy-cinnamic acids	37,38	31,60	15,48	22,46	14,57	13,29	45,60	42,82	1,25	1,00	**1,04**	**0,98**	**0,94**	**2a/ 2b**
367,1038	NI	1,19	5-O-Feruloyl quinic acid	Hydroxy-cinnamic acids	3,65	2,52	1,51	1,00	2,55	2,70	2,89	3,06	4,31	3,50	**1,40**	**1,58**	**1,13**	**2a/ 2b**
367,1038	NI	0,94	3-O-Feruloyl quinic acid	Hydroxy-cinnamic acids	3,00	2,24	2,19	1,18	4,85	5,19	1,02	1,00	2,21	1,20	**0,48**	**0,38**	**0,79**	**2b**
367,1038	NI	1,32	4-O-Feruloyl quinic acid	Hydroxy-cinnamic acids	1,98	2,87	1,06	2,65	1,00	1,56	2,40	4,05	1,89	2,87	**1,59**	**1,46**	**0,92**	**2b**
223,0610	NI	1,41	Sinapic acid	Hydroxy-cinnamic acids	2,12	2,87	1,00	1,86	2,55	2,39	6,60	5,91	2,13	2,22	**2,31**	**1,71**	**0,74**	**2a/ 4**
385,1145	NI	1,05	Sinapoyl malate	Hydroxy-cinnamic acids	19,25	19,78	1,00	4,45	4,95	6,55	48,01	41,70	1,69	1,24	**2,96**	**2,09**	**0,71**	**2a/ 4**
339,0724	NI	1,47	Sinapoyl glucoside	Hydroxy-cinnamic acids	4,09	9,50	1,00	1,96	2,05	2,46	2,77	1,89	1,84	2,09	**0,97**	**0,43**	**0,44**	**2a/ 4**
575,3570	PI	2,13	24,25-Epoxy-7,22-dihydroxyergosta-1,4-dien-3-one	Steroid derivative	2,49	1,80	1,00	1,08	1,57	1,35	4,04	3,79	5,13	4,46	**2,73**	**2,92**	**1,07**	**2b/ 4**

883,4662	PI	2,46	3,23-Dihydroxy-30-nor-12,20(29) -oleanadien-28-oic acid; 3β-form, 3-O-[β-D-Xylopyranosyl-(1→2)-[β-D-glucopyranosyl-(1→3)]-α-L-arabinopyranoside]	Steroid derivative	1,49	1,00	5,35	4,02	2,24	1,92	5,78	4,16	10,71	10,61	**2,72**	**3,19**	**1,17**	**2b/4**
883,4665	PI	2,11	3,23-Dihydroxy-30-nor-12,20(29)-oleanadien-28-oic acid; 3β-form, 3-O-[β-D-Xylopyranosyl-(1→2)-[β-D-glucopyranosyl-(1→3)]-α-L-arabinopyranoside]	Steroid derivative	9,77	7,17	1,55	1,00	35,98	33,14	109,07	74,22	4,87	4,53	**3,61**	**2,86**	**0,79**	**2b/4**
883,4700	PI	1,85	3,23-Dihydroxy-30-nor-12,20(29)-oleanadien-28-oic acid; 3β-form, 3-O-[β-D-Xylopyranosyl-(1→2)-[β-D-glucopyranosyl-(1→3)]-α-L-arabinopyranoside]	Steroid derivative	8,68	5,90	2,53	1,00	51,63	39,87	85,46	64,54	nd	nd	**2,04**	**2,07**	**1,01**	**2b/4**
398,3413	PI	2,75	Solanidine	Steroidal alkaloid	2,53	19,26	1,00	8,80	1,93	8,27	1,88	6,59	2,47	9,89	**1,19**	**0,68**	**0,57**	**1**
398,3413	PI	2,14	Solanidine	Steroidal alkaloid	3,22	2,46	1,20	1,00	2,52	2,11	2,71	2,57	3,04	2,62	**1,24**	**1,40**	**1,13**	**2b**
400,3560	PI	2,01	Demissidine	Steroidal alkaloid	4,69	2,45	164,00	214,67	2,04	1,00	69,73	82,00	145,33	248,00	**1,90**	**2,27**	**1,20**	**2b/4**

414,3366	PI	1,99	Solasodine	Steroidal alkaloid	1,59	1,00	10,36	9,36	7,37	4,89	2,32	1,61	2,45	1,32	**0,37**	**0,29**	**0,78**	**2a/ 2b/ 4**
706,4516	PI	2,16	beta-chaconine	Steroidal alkaloid	1,88	1,70	1,00	1,06	1,54	1,39	1,95	2,00	2,25	1,99	**1,43**	**1,44**	**1,01**	**2b**
721,4155	PI	2,49	16,23:16,24-Diepoxycycloartane-3,12,15,25-tetrol; (3β,12β,15α,16S,23R,24S)-form, 12-Ac, 3-O-(3-O-acetyl-β-D-xylopyranoside)	Steroidal glycoside	1,86	1,00	5,33	5,56	3,28	2,60	8,97	7,46	24,59	22,54	**4,81**	**4,92**	**1,02**	**2b/ 4**
750,4443	NI	2,20	Solanidine; O-[α-L-Rhamnopyranosyl-(1→4)-β-D-glucopyranoside]	Steroidal glycoside	2,42	3,48	1,37	2,62	1,00	1,66	1,33	1,77	4,65	6,14	**1,87**	**1,53**	**0,82**	**2b/ 4**
986,4983	NI	2,37	3,16-Dihydroxypregn-5-en-20-one; (3β,16β)-form, 16-O-(2-Methoxy-4-methylpyrrolidine-2-carbonyl), 3-O-[α-L-rhamnopyranosyl-(1→2)-[α-L-rhamnopyranosyl-(1→4)]-β-D-glucopyranoside]	Steroidal glycoside	9,90	4,70	1,71	1,00	2,51	3,35	nd	nd	30,07	20,20	**3,19**	**3,35**	**1,05**	**2b/ 4**
771,3459	PI	1,95	--	Steroidal glycoside	nd	nd	1,02	1,00	nd	nd	nd	nd	1,97	1,90	**2,41**	**2,54**	**1,05**	**4**
914,4388	PI	2,26	--	Steroidal glycoside	nd	nd	1,00	1,01	nd	nd	nd	nd	1,87	1,71	**2,80**	**2,54**	**0,91**	**4**
918,4147	PI	2,63	--	Steroidal glycoside	nd	nd	nd	nd	nd	nd	1,35	1,00	nd	nd	**∞**	**∞**	**∞**	**4**

966,4570	PI	2,00	--	Steroidal glycoside	nd	nd	nd	nd	2,19	1,00	85,71	87,58	nd	nd	**59,03**	**131,57**	**2,23**	**4**
987,4357	PI	2,61	--	Steroidal glycoside	nd	nd	1,00	1,18	nd	nd	nd	nd	1,27	1,11	**1,90**	**1,41**	**0,74**	**4**
1049,4836	PI	1,84	--	Steroidal glycoside	nd	nd	1,02	1,00	nd	nd	nd	nd	1,97	1,90	**2,89**	**2,86**	**0,99**	**4**
1065,5651	PI	2,14	--	Steroidal glycoside	1,13	1,06	1,41	1,86	1,14	1,00	1,85	2,24	5,42	5,50	**2,96**	**2,97**	**1,00**	**4**
1196,6059	PI	2,03	--	Steroidal glycoside	2,17	1,00	12,09	3,87	45,40	38,34	322,09	227,30	40,18	48,77	**9,08**	**9,57**	**1,05**	**4**
577,3737	PI	2,69	6-Hydroxyspirostan-3-one; (5α,6α,25S)-form, 6-O-α-L-Rhamnopyranoside	Steroidal Saponin	2,13	1,00	8,30	6,12	1,68	1,65	7,16	4,21	4,13	3,13	**1,40**	**1,25**	**0,90**	**2b/4**
577,3738	PI	2,87	6-Hydroxyspirostan-3-one; (5α,6α,25S)-form, 6-O-α-L-Rhamnopyranoside	Steroidal Saponin	2,10	1,00	2,17	1,84	3,82	1,55	3,09	1,91	3,42	2,19	**1,21**	**1,40**	**1,16**	**2b/4**
721,4158	PI	2,13	16,23:16,24-Diepoxycycloartane -3,12,15,25-tetrol; (3β,12β,15α,16S,23R,24S)-form, 12-Ac, 3-O-(3-O-acetyl-β-D-xylopyranoside)	Steroidal Saponin	2,24	1,65	1,00	1,17	1,50	1,35	4,49	4,12	5,57	5,19	**3,19**	**3,35**	**1,05**	**2b/4**

737,4104	PI	2,11	Spirosta-5,25(27)-diene-1,3-diol; (1β,3β) -form, 3-O-[α-L-Rhamnopyranosyl-(1→4)-β-D-glucopyranoside]	Steroidal Saponin	5,69	3,48	1,32	1,00	15,56	13,24	45,74	31,39	1,99	1,83	**3,17**	**2,81**	**0,89**	**2b/4**
867,4721	PI	2,50	Spirosta-5,25(27)-dien-3-ol; 3β-form, 3-O-[α-L-Rhamnopyranosyl-(1→2)-[α-L-rhamnopyranosyl-(1→4)]-β-D-glucopyranoside]	Steroidal Saponin	1,57	1,00	9,66	10,19	5,40	3,94	14,88	10,94	42,37	39,97	**5,16**	**5,05**	**0,98**	**2b/4**
867,4733	PI	3,60	Spirosta-5,25(27)-dien-3-ol; 3β-form, 3-O-[α-L-Rhamnopyranosyl-(1→2)-[α-L-rhamnopyranosyl-(1→4)]-β-D-glucopyranoside]	Steroidal Saponin	2,01	1,00	8,41	7,63	6,31	5,70	13,52	8,97	41,96	37,39	**4,97**	**4,86**	**0,98**	**2b/4**
885,4833	PI	2,17	Spirost-5-en-3-ol; (3β,25R)-form, 3-O-[α-L-Rhamnopyranosyl-(1→2)-[β-D-glucopyranosyl-(1→3)]-β-D-galactopyranoside]	Steroidal Saponin	2,31	1,00	5,78	5,02	2,60	1,88	7,15	3,88	1,70	1,21	**1,24**	**0,97**	**0,78**	**2b/4**

896,4982	NI	2,11	Solanidine; O-[α-L-Rhamnopyranosyl-(1→2)-O-[α-L-rhamnopyranosyl-(1→4)]-β-D-glucopyanoside]	Steroidal Saponin	8,64	3,27	1,43	1,56	1,40	1,00	4,72	10,93	79,49	4,15	**11,02**	**3,88**	**0,35**	**2b/4**
915,4575	PI	2,08	3,15,23-Trihydroxyspirost-5-en-26-one; (3β,15α,23R,25R)-form, 3-O-[α-L-Rhamnopyranosyl-(1→2)-[α-L-rhamnopyranosyl-(1→4)]-β-D-glucopyranoside]	Steroidal Saponin	10,54	3,96	23,35	16,06	1,31	1,00	118,23	120,20	6,45	6,40	**5,30**	**9,04**	**1,71**	**2b/4**
929,4764	NI	3,60	Spirost-5-ene-3,12-diol; (3β,12β,25R)-form, 3-O-[α-L-Rhamnopyranosyl-(1→2)-[α-L-rhamnopyranosyl-(1→4)]-β-D-glucopyranoside]	Steroidal Saponin	1,47	1,00	5,91	4,73	3,63	3,10	16,93	18,13	8,46	5,70	**3,46**	**4,05**	**1,17**	**2b/4**
929,4769	NI	2,49	Spirost-5-ene-3,12-diol; (3β,12β,25R)-form, 3-O-[α-L-Rhamnopyranosyl-(1→2)-[α-L-rhamnopyranosyl-(1→4)]-β-D-glucopyranoside]	Steroidal Saponin	1,59	1,00	5,50	6,32	3,61	2,80	24,16	21,40	8,19	6,06	**4,53**	**4,07**	**0,90**	**2b/4**

933,5067	NI	2,65	Cholestane-3,16,22,26-tetrol; (3β,5α,16α,25ξ)-form, 22-Ketone, 3-O-[β-D-xylopyranosyl-(1→2)-α-L-rhamnopyranosyl-(1→4)-β-D-glucopyranoside]	Steroidal Saponin	36,95	26,11	2,70	1,23	1,84	1,00	2,76	2,86	40,24	30,34	**1,55**	**1,76**	**1,13**	**2b/4**
945,4715	NI	2,45	Spirost-5-ene-3,12-diol; (3β,12β,25R)-form, 3-O-[α-L-Rhamnopyranosyl-(1→2)-[β-D-glucopyranosyl-(1→3)]-β-D-galactopyranoside]	Steroidal Saponin	1,19	1,00	2,26	1,99	2,08	1,72	4,94	5,41	3,67	2,33	**2,34**	**2,46**	**1,05**	**2b/4**
945,4716	NI	2,11	Spirost-5-ene-3,12,26-triol; (3β,12β,25R,26R)-form, 3-O-[α-L-Rhamnopyranosyl-(1→2)-[α-L-rhamnopyranosyl-(1→4)]-β-D-glucopyranoside]	Steroidal Saponin	2,27	1,20	1,36	1,00	169,03	146,78	2,84	2,76	457,63	365,58	**4,00**	**3,71**	**0,93**	**2b/4**

948,4945	PI	2,40	26-Aminospirost-5-en-3-ol; (3β,25R,26R)-form, N-Ac, 3-O-[α-L-rhamnopyranosyl-(1→2)-[α-L-rhamnopyranosyl-(1→4)]-β-D-glucopyranoside]	Steroidal Saponin	4,48	2,31	2,55	2,23	1,00	1,33	16,19	9,85	nd	nd	**3,02**	**2,52**	**0,83**	**2b/4**
949,4981	NI	2,20	Furostane-3,6,22,26-tetrol; (3β,5α,6α,22ξ,25S)-form, 6-O-[α-L-Rhamnopyranosyl-(1→3)-6-deoxy-β-D-glucopyranoside], 26-O-β-D-glucopyranoside	Steroidal Saponin	4,16	1,00	6,14	4,29	4,57	4,78	12,98	10,92	5,02	3,15	**1,81**	**2,10**	**1,16**	**2b/4**
949,5000	PI	2,40	Furost-5-ene-1,3,22,26-tetrol; (1β,3β,22ξ,25S)-form, 22-Me ether, 3-O-[β-D-glucopyranosyl-(1→4)-β-D-galactopyranoside], 26-O-β-D-glucopyranoside	Steroidal Saponin	4,72	1,50	2,56	2,17	1,00	1,26	14,72	6,90	nd	nd	**2,68**	**2,11**	**0,79**	**2b/4**

970,5031	NI	2,40	26-Aminospirost-5-en-3-ol; (3β,25R,26R)-form, N-Ac, 3-O-[α-L-rhamnopyranosyl-(1→2)-[α-L-rhamnopyranosyl-(1→4)]-β-D-glucopyranoside]	Steroidal Saponin	4,03	1,61	1,73	1,41	1,00	1,03	nd	nd	13,57	9,61	**3,01**	**3,55**	**1,18**	**2b/4**
1031,5413	PI	2,18	beta-D-Glucopyranoside, (3beta,22beta,25R)-26-(beta-D-glucopyranosyloxy)-22-hydroxyfurost-5-en-3-yl O-6-deoxy-alpha-L-mannopyranosyl-(1->2)-O-[6-deoxy-alpha-L-mannopyranosyl-(1->4)]-	Steroidal Saponin	2,42	1,24	8,87	8,15	1,58	1,00	10,39	5,05	2,98	2,76	**1,56**	**1,13**	**0,72**	**2a/2b/4**
1047,5363	PI	1,71	Cholest-5-ene-3,16,22,26-tetrol; (3β,16β,22ξ,25R)-form, 16,22-Diketone, 3-O-[α-L-rhamnopyranosyl-(1→2)-[α-L-rhamnopyranosyl-(1→4)]-β-D-glucopyranoside], 26-O-β-D-glucopyranoside	Steroidal Saponin	131,97	90,16	39,43	26,48	118,85	94,26	511,48	260,66	2,44	1,00	**2,66**	**1,87**	**0,70**	**2b/4**

1048,5677	PI	2,70	Spirosolan-3-ol; (3β,5α,22R,25R)-form, 3-O-[β-D-Glucopyranosyl-(1→2)-β-D-glucopyranosyl-(1→4)-[α-L-rhamnopyranosyl-(1→2)]-β-D-galactopyranoside]	Steroidal Saponin	2,43	1,03	12,89	10,79	1,13	1,00	17,32	8,53	4,86	3,89	**2,03**	**1,45**	**0,72**	**2b/4**
1064,5629	PI	2,13	Leptinidine; 3-O-[β-D-Glucopyranosyl -(1→2)-[β-D-xylopyranosyl-(1→3)]-β-D-glucopyranosyl-(1→4)-β-D-galactopyranoside]	Steroidal Saponin	1,34	1,25	1,21	1,48	1,09	1,00	1,98	2,16	4,69	4,93	**2,75**	**2,85**	**1,04**	**2b/4**
1075,5342	NI	2,69	22,25-Epoxyfurost-5-ene-3,7,26-triol; (3β,7β,22S,25S)-form, 7-Me ether, 3-O-[α-L-rhamnopyranosyl-(1→2)-[α-L-rhamnopyranosyl-(1→4)]-β-D-glucopyranoside], 26-O-β-D-glucopyranoside	Steroidal Saponin	2,52	1,00	8,18	9,00	1,23	1,12	4,70	3,57	9,18	6,23	**1,74**	**1,32**	**0,76**	**2b/4**

1079,5650	NI	2,25	Cholest-5-ene-3,22,26-triol; (3β,22R,25S)-form, 3-O-[α-L-Rhamnopyranosyl-(1→2)-[α-L-rhamnopyranosyl-(1→4)]-β-D-glucopyranoside], 26-O-β-D-glucopyranoside	Steroidal Saponin	191,87	123,68	5,40	6,04	1,63	1,00	8,84	10,00	200,37	160,85	**1,58**	**1,96**	**1,24**	**2b/4**
1091,5293	NI	2,11	Nuatigenin; 3-O-[α-L-Rhamnopyranosyl-(1→2)-[β-D-xylopyranosyl-(1→3)]-β-D-galactopyranoside], 26-O-β-D-glucopyranoside	Steroidal Saponin	2,97	2,75	2,14	2,61	3,11	2,72	7,50	8,53	1,00	2,52	**1,55**	**2,05**	**1,32**	**2b/4**
1093,5438	NI	2,28	Protodioscin/ neoprotodioscin	Steroidal Saponin	2,90	1,76	3,13	3,49	1,16	1,00	2,45	2,97	5,34	4,15	**1,62**	**1,71**	**1,05**	**2b/4**
1093,5438	NI	2,17	Protodioscin/ neoprotodioscin	Steroidal Saponin	1,87	1,03	8,12	7,55	1,39	1,00	2,83	2,69	7,82	4,30	**1,40**	**1,09**	**0,78**	**1**
1107,5245	NI	2,10	Methyl-protodioscin	Steroidal Saponin	7,07	5,62	1,64	1,00	3,60	2,88	4,02	3,88	4,11	4,17	**0,99**	**1,27**	**1,28**	**2b/4**
1107,5246	NI	2,27	Methyl-protodioscin	Steroidal Saponin	1,97	1,42	2,13	1,10	1,35	1,01	1,06	1,04	1,14	1,00	**0,61**	**0,87**	**1,43**	**2b/4**
1109,5395	NI	1,71	Spirostane-3,15-diol; (3β,5α,15α,25R)-form, 3-O-[β-D-Glucopyranosyl-(1→2)-[β-D-xylopyranosyl-(1→3)]-β-D-glucopyranosyl-(1→4)-β-D-galactopyranoside]	Steroidal Saponin	41,47	28,90	8,47	6,23	28,02	22,68	1,00	1,11	113,88	74,30	**2,21**	**1,96**	**0,89**	**2b/4**

1223,5720	NI	2,04	Spirost-5-ene-3,27-diol; (3β,25S)-form, 3-O-[β-D-Xylopyranosyl-(1→2)-α-L-rhamnopyranosyl-(1→4)-[α-L-rhamnopyranosyl-(1→2)]-β-D-glucopyranoside], 27-O-β-D-glucopyranoside	Steroidal Saponin	1,40	1,00	5,91	2,55	21,93	19,13	20,71	25,16	139,26	112,01	**8,21**	**9,08**	**1,11**	**2b/4**
722,4470	PI	2,14	beta-solanine	Steroidal Saponin	4,27	3,36	1,41	1,00	3,22	2,73	3,16	3,12	3,59	3,54	**1,14**	**1,41**	**1,24**	**2b**
852,5091	PI	2,16	alpha-chaconine	Steroidal Saponin	1,94	1,67	1,11	1,00	1,62	1,42	2,13	2,16	2,21	1,87	**1,39**	**1,48**	**1,06**	**1**
866,4891	PI	1,90	7-Hydroxysolanidine; (3β,7β)-form, 7-Ketone, 3-O-[α-L-rhamnopyranosyl-(1→2)-[α-L-rhamnopyranosyl-(1→4)]-β-D-glucopyranoside]	Steroidal Saponin	2,97	1,86	1,56	1,00	2,52	2,06	3,33	3,71	5,24	3,55	**1,82**	**2,21**	**1,21**	**2b/4**
868,5038	PI	2,14	alpha-solanine	Steroidal Saponin	3,40	2,89	1,35	1,00	2,76	2,39	2,55	2,69	3,28	2,87	**1,16**	**1,33**	**1,14**	**1**
868,5043	PI	1,55	alpha-solanine isomer	Steroidal Saponin	1,44	1,00	3,95	1,47	8,38	7,35	1,46	1,19	17,36	12,10	**2,05**	**2,03**	**0,99**	**2b**

882,4846	PI	1,89	7-Hydroxysolanidine; (3β,7β)-form, 7-Ketone, 3-O-[α-L-rhamnopyranosyl-(1→2)-[β-D-glucopyranosyl-(1→3)]-β-D-galactopyranoside]	Steroidal Saponin	3,76	2,36	1,35	1,00	3,22	2,86	2,69	2,96	5,71	4,04	**1,51**	**1,69**	**1,12**	**2b/4**
884,4993	PI	1,97	Spirosol-5-en-3-ol; (3β,16β,22S,25S)-form, 3-O-[α-L-Rhamnopyranosyl-(1→2)-β-D-glucopyranosyl-(1→3)-β-D-galactopyranoside]	Steroidal Saponin	1,57	1,00	6,08	4,45	6,06	3,72	1,81	1,53	2,24	1,33	**0,44**	**0,47**	**1,05**	**2b/4**
910,5153	PI	2,49	Leptinidine; 23-Ac, 3-O-[α-L-rhamnopyranosyl-(1→2)-[α-L-rhamnopyranosyl-(1→4)]-β-D-glucopyranoside]	Steroidal Saponin	4,53	3,43	1,25	1,00	3,18	2,78	3,30	3,77	4,90	4,48	**1,37**	**1,71**	**1,25**	**2b**
910,5158	PI	2,08	Leptinidine; 23-Ac, 3-O-[α-L-rhamnopyranosyl-(1→2)-[α-L-rhamnopyranosyl-(1→4)]-β-D-glucopyranoside]	Steroidal Saponin	24,59	17,87	4,23	2,70	2,87	3,89	36,11	32,03	1,19	1,00	**1,77**	**2,03**	**1,15**	**2b**

547,2403	NI	1,56	9,13-Dihydroxy-4,7-megastigmadien-3-one; (6R,7E,9R)-form, 9,13-Di-O-β-D-glucopyranoside	Terpene glycoside	2,56	4,17	3,57	4,51	2,03	3,65	1,09	1,00	9,35	8,81	**1,92**	**1,19**	**0,62**	**2b/4**
160,1078	PI	0,39	Calystegine A3	Tropane alkaloid	2,81	2,29	nd	4,50	3,00	3,25	2,61	1,00	3,44	3,14	**2,07**	**1,54**	**0,74**	**1**
176,0917	PI	0,25	Calystegine B2	Tropane alkaloid	1,51	2,65	3,82	6,82	5,35	1,00	2,67	4,05	1,00	1,90	**1,40**	**1,16**	**0,83**	**2b/4**
179,0340	PI	0,96	Esculetin	Hydroxy-coumarin	4,19	1,00	4,02	3,17	2,44	1,63	20,48	6,47	17,44	6,24	**5,34**	**3,29**	**0,62**	**1**
191,0342	NI	1,38	Scopoletin	Hydroxy-coumarin	4,13	11,93	24,68	13,58	1,51	1,00	1,80	1,96	6,59	17,67	**0,42**	**1,12**	**2,39**	**1**
223,0601	PI	1,46	Isofraxidin	Hydroxy-coumarin	1,00	15,23	7,58	32,22	1,06	4,64	1,50	10,75	1,34	32,47	**0,44**	**1,24**	**2,81**	**2a**
223,0602	PI	0,99	Isofraxidin	Hydroxy-coumarin	1,82	88,75	24,52	170,21	5,87	17,93	1,00	34,08	2,32	150,96	**0,15**	**1,18**	**6,31**	**2a**

4. Potato (*Solanum tuberosum*) Cultivars with Quantitative Resistance to Silver Scurf (*Helminthosporium solani*) exhibit Different Resistance Strategies

4.1. Abstract

Silver scurf is a potato blemish disease caused by the fungal pathogen *Helminthosporium solani* Durieu & Mont. (1849). The disease, characterized by well-delimited silvery lesions on the potato skin, leads to permeabilization of the tuber periderm and water losses during storage, as well as a reduction on tuber quality. The economic importance of blemish diseases, including silver scurf, has increased in recent years, partially due to a higher demand for washed pre-packed potatoes, which make these diseases more visible. Potato cultivars with different susceptibility to silver scurf have been reported, but the physiological basis of resistance against this disease have not been studied. Here, we analyze the structural and biochemical aspects of potato cultivars with different degrees of susceptibility to silver scurf under field and controlled conditions. Microscopic studies indicate that the number of phellem cells or phellem thickness does not influence disease symptoms. Furthermore, untargeted metabolomics analysis suggest that different resistance traits may be expressed by different potato cultivars with quantitative resistance to silver scurf. Nonetheless, a few conserved resistance-related metabolites could be highlighted. Constitutively high amounts of a cytokinin glycoside and hydroxycoumarins were found to be associated with resistance to silver scurf. Furthermore, gallic acid and protocatechuic acid specifically accumulated in resistant cultivars upon *H. solani* inoculation. The results presented here give new insights on the resistance of potato cultivars to silver scurf. The use of the biochemical markers described in this study in breeding programs and its practical application is discussed.

4.2. Introduction

Silver scurf is a potato tuber blemish disease caused by *Helminthosporium solani* Durieu & Mont. (1849), an ascomycete of the order Pleosporales (Termorshuizen, 2007). The only known host of *H. solani* is the potato plant *Solanum tuberosum* L., although it is also capable of colonizing senescent plant tissues of other crops (Mérida and Loria, 1994b). On potato tubers, it causes silvery lesions that lead to water losses and shrinkage of the tuber during storage and, finally, rejection of tuber lots for commercialization. Wild potato species show resistance to silver scurf, and some of these species have been crossed with commercial cultivars to select for resistance against several diseases, including silver scurf (De Jong and Tarn, 1984; Rodriguez et al., 1995; Murphy et al., 1999; Errampalli et al., 2001b). However, a potato cultivar specifically resistant to silver scurf from these breeding programs has not been reported yet (Avis et al., 2010). Commercial potato cultivars differ on their susceptibility to silver scurf especially in North America (Joshi and Pepin, 1991; Mérida et al., 1994; Rodriguez et al., 1996), indicating that they have different levels of resistance to *H. solani*.

In potato tubers, the plant response to pathogen attack is often observed at the periderm (skin), where the pathogen penetrates and further develops causing infection and symptoms. Potato variants with resistance to several tuber pathogens were shown to produce more skin cell layers and suberize these cells upon pathogen inoculation (Thangavel et al., 2016), and high amounts of proteins involved in phenolic acids production and suberization processes are found in the potato skin (Barel and Ginzberg, 2008). Notably, structural tissue modification upon fungal infection results in a global metabolome change (Yoder and Turgeon, 2001), activating specific biochemical pathways linked to host defense. Plant hosts have co-evolved with fungal pathogens for long periods culminating in constitutive resistance mechanisms (defense metabolites present in absence of the pathogen) but have also developed strategies based on the induction of specific metabolites to circumscribe pathogen development. Phenolic acids are upregulated during pathogenic infection in potato tubers (Kröner et al., 2011), leading to the production of various secondary metabolites involved in quantitative resistance against different phytopathogenic organisms (Kröner et al., 2012; Yogendra et al., 2014, 2015). Furthermore, other secondary metabolites of the potato tuber have been identified as

resistance-related metabolites in potato cultivars or wild *Solanum* species, including glycoalkaloids or hydroxycoumarins, among others (Tai et al., 2014; Yogendra et al., 2014; Hamzehzarghani et al., 2016; Tomita et al., 2017). Because breeding is time-consuming, the study of current commercial cultivars and their susceptibility to different pathogens is getting importance and unraveling the mechanisms of quantitative resistance of these cultivars can highlight critical aspects of plant resistance.

Little information on cultivar susceptibility to silver scurf of potato cultivars commonly grown in Switzerland is available. Furthermore, quantitative resistance to silver scurf has not been studied to date. Identifying cultivars with high resistance to silver scurf in European potato cultivars could help potato growers manage this disease in the field and highlighting biomarkers of resistance may be a long-term sustainable tool for potato breeders. In the present work, we studied the influence of the structural and chemical aspects of the potato skin on silver scurf disease from field grown potato tubers of 16 potato cultivars. Structural analysis of the periderm of these potato cultivars was carried out to determine the effect of the periderm structure on the susceptibility to silver scurf. Furthermore, based on previous field studies (Chapter 3), five cultivars with different susceptibility levels to silver scurf were selected in a greenhouse experiment under controlled conditions for resistance-related metabolite investigation. All cultivars were either mock or fungal inoculated, allowing the comparison of untreated and inoculated samples. An untargeted metabolomic approach was performed on the specialized metabolites of the skin of these five cultivars to study cultivar-specific metabolites and induced compounds upon inoculation, in order to highlight resistance-related metabolites.

4.3. Material and methods

Plant Material

Field trial: Seed-tubers were planted in a split-plot trial with sixteen cultivars of different physiologic properties used as table potato cultivars in Switzerland (Agata, Amandine, Annabelle, Celtiane, Charlotte, Cheyenne, Ditta, Erika, Gourmandine, Gwenne, Jazzy, Lady Christl, Lady Felicia, Laura, Venezia and Vitabella) for three consecutive years (from 2016 to 2018) in three different locations: in Changins (46°23'52.9"N 6°14'19.4"E) and Reckenholz (47°26'02.6"N 8°30'47.6"E) where conventional practices were used; and in Unterstammheim (47°38'35.8"N 8°46'43.2"E), where organic practices were followed. Each cultivar was planted in four plots of two rows of 25 plants each, each row separated by 75 cm, and each plant separated by 33 cm. Seed-tubers were not treated with fungicides.

Greenhouse experiment: Ten plants of five cultivars showing different susceptibility to silver scurf in the field trials (Cheyenne, Gwenne, Erika, Lady Christl and Lady Felicia) were grown for four weeks in sterile conditions as described by Lê & Collet (Lê and Collet, 1985). After 24 hours of adaptation to non-sterile conditions in a high humidity environment, potato plants were transferred to 4 liters square pots containing an autoclaved substrate composed of brown and blond peat (Gebr. Brill substrate, Georgsdorf, Germany). 10 ml of a conidial suspension (7,5 x 10^5 conidia/ml) containing mycelial fragments of *Helminthosporium solani* (strain 73 from Agroscope) was applied at initiation of tuberization. For control plants, sterile water was applied at the same time as the fungal inoculations. Potato plants were grown in a greenhouse for 4 months (from March to July), with regular watering. Haulm destruction was performed after 4 months of growth, and tubers were kept in the soil for a further month until harvest. Upon harvest, tubers were washed and incubated for 2 weeks under high humidity conditions and room temperature in darkness to allow sporulation of fungi.

Severity determination

Single tubers of each cultivar grown under controlled conditions (n=50) or in the field (n=200) were individually observed under a binocular for the presence of conidiophores of *H. solani*. Each tuber was then classified in one of the following classes, depending on the affected area of the tuber: 0 (absence

of the fungus), 1 (less than 15%), 2 (between 15 and 35%), 3 (between 35 and 65%) and 4 (more than 65%). The number of tubers of each class was multiplied by the median affected area of the class and used to calculate the average affected area (severity).

Microscopy analysis

Tuber peel samples of all cultivars were harvested and prepared for microscopic analysis. A silver scurf symptomatic area and an area free of disease symptoms were selected for each cultivar. Tuber peel samples were prepared for TEM as described (Hall and Hawes, 1991). Briefly, samples were pre-fixed using a paraformaldehyde (2%) glutaraldehyde (3%) solution at pH 7.0 (0.07 M PIPES buffer) for three hours at room temperature and descending atmospheric pressure. Subsequently, samples were washed three times with PIPES buffer (0.07M, pH 7.0) and post-fixed with 1% OsO_4 in 0.07M PIPES buffer for 90 minutes. Fixed samples were rinsed twice with 0.07M PIPES buffer and stored at 4°C until dehydration and infiltration with the EMbed 812 resin (Electron Microscopy Sciences, USA). Prior to the infiltration with the resin, samples were dehydrated by incubating the samples on growing concentrations of ethanol (30-50-70-95-100% ethanol) for ten minutes and continuous agitation in the tissue processor Leica EM TP (Leica Microsystems, Switzerland). The ethanol was then replaced by propylene oxide for 30 minutes and continuous agitation, and the propylene oxide subsequently replaced by the EMbed 812 resin overnight and gentle agitation. To ensure infiltration of the resin, samples were incubated for 2 hours under vacuum (400 bars). Polymerization of the resin took place at 60°C for 48 hours. Infiltrated samples were then thin cut and resulting sections stained with a mixture of methylene blue (1%), sodium tetraborate (1%) and azur II (1%). Pictures were taken on a Leica DMLB Fluorescence Microscope (Leica Microsystems, Switzerland), and phellem or cell wall thickness calculated using the ProgResCapturePro 2.9.0.1 software.

Extraction of skin specialized metabolites

Potato skins of single tubers were harvested using a peeler after severity determination, immediately frozen, and lyophilized. Approximately 100 mg of dry tissue was extracted with 4 ml HPLC-grade methanol (Fisher Scientific, Hampton, NH, USA) containing 1% acetic acid. Samples were extracted for 5 mins under agitation. After centrifugation for 5 mins at 4000 rpm, the supernatant was recovered, and the pellet re-extracted with 4 ml methanol containing 1% acetic acid. After centrifugation, the supernatants were combined, and the solvents were evaporated at 39 mbars of pressure at 40°C (Genevac, SP Scientific, Ipswich, UK). Each extract was weighted and stored at -80°C until analysis. Samples were dissolved at 5 mg/mL with a 50% methanol aqueous solution and transferred to a vial for UHPLC-MS/MS analysis.

UHPLC-HRMS/MS Analysis

Chromatographic separation was performed on a Waters Acquity UPLC system interfaced to a Q-Exactive Focus mass spectrometer (Thermo Scientific, Bremen, Germany), using a heated electrospray ionization (HESI-II) source. Thermo Scientific Xcalibur 3.1 software was used for instrument control. The LC conditions were as follows: column, Waters BEH C18 50 × 2.1 mm, 1.7 µm; mobile phase, (A) water with 0.1% formic acid; (B) acetonitrile with 0.1% formic acid; flow rate, 600 µl·min^{-1}; injection volume, 6 µl; linear gradient of 5−100% B over 7 min and isocratic at 100% B for 1 min. The optimized HESI-II parameters were as follows: source voltage, 3.5 kV (pos); sheath gas flow rate (N_2), 55 units; auxiliary gas flow rate, 15 units; spare gas flow rate, 3.0; capillary temperature, 350°C, S-Lens RF Level, 45. The mass analyzer was calibrated using a mixture of caffeine, methionine–arginine–phenylalanine–alanine–acetate (MRFA), sodium dodecyl sulfate, sodium taurocholate, and Ultramark 1621 in an acetonitrile/methanol/water solution containing 1% formic acid by direct injection. The data-dependent MS/MS events were performed on the three most intense ions detected in full scan MS (Top3 experiment). The MS/MS isolation window width was 1 Da, and the stepped normalized collision

energy (NCE) was set to 15, 30 and 45 units. In data-dependent MS/MS experiments, full scans were acquired at a resolution of 35,000 FWHM (at *m/z* 200) and MS/MS scans at 17,500 FWHM both with an automatically determined maximum injection time. After being acquired in a MS/MS scan, parent ions were placed in a dynamic exclusion list for 2.0 s. Quality Control (QC) samples containing a mixture of all samples were injected every ten samples throughout the analysis.

LC-MS/MS Data processing

LC-MS/MS data files were analyzed by MzMine 2.36 (Pluskal et al. 2010) after converting the ThermoRAW data files to the open MS format (.mzXML) using the MSConvert software from the ProteoWizard package (Chambers et al. 2012). Briefly, masses were detected (both MS1 and MS2 in a single file) using the centroid mass detector with the noise level set at 1.5E5 for MS1 and at 1.0E0 for MS2. Chromatograms were built using the ADAP algorithm, with the minimum group size of scans set at 5, minimum group intensity threshold at 1.0E5, minimum highest intensity was at 1.0E5 and m/z tolerance at 5.0 ppm. For chromatogram deconvolution, the algorithm used was the wavelets (ADAP). The intensity window S/N was used as S/N estimator with a signal to noise ratio set at 25, a minimum feature height at 10,000, a coefficient area threshold at 100, a peak duration ranges from 0.02 to 0.9 min and the RT wavelet range from 0.02 to 0.05 min. Isotopes were detected using the isotopes peaks grouper with a m/z tolerance of 5.0 ppm, a RT tolerance of 0.02 min (absolute), the maximum charge set at 2 and the representative isotope used was the most intense. Peak alignment was performed using the join aligner method (m/z tolerance at 5 ppm), absolute RT tolerance 0.1 min, weight for m/z at 10 and weight for RT at 10. The peak list was gap-filled with the same RT and m/z range gap filler (m/z tolerance at 5 ppm). The resulting aligned peak list contained 10358 peaks in negative mode and 12015 features in positive mode. Several filters were applied before multivariate data analysis to investigate only the robust and reliable variables. Only variables that appeared in at least 80% of the samples of a group were retained. Furthermore, all variables that were detected in the blanks and represented more than 1% of the average of the samples were eliminated. Finally, only variables that had less than 30% of variation in the Quality Control samples were retained. The application of these filters yielded a total of 4811 variables for negative mode and 4265 variables for positive mode that were subjected to statistical analysis. Only features possessing MS2 spectra were kept to build molecular networks using the peak-list rows filter option, which yielded 1842 features in negative mode and 3765 in positive mode. The resistance-related constitutive (RRC) and the resistance-related induced (RRI) values were calculated as the ratio of the mean of abundance in the resistant cultivars / the mean of abundance in the susceptible cultivars in control and inoculated conditions, respectively (RRC=RM/SM, RRI=RP/SP, where RP=resistant genotype with pathogen inoculation, RM=resistant genotype with mock inoculation, SP=susceptible genotype with pathogen inoculation, SM=susceptible genotype with mock inoculation). The qualitative qRRI was calculated as the ratio of the induction in the resistant cultivars / induction in the susceptible cultivars (qRRI = (RP/RM)/(SP/SM).

Multivariate data analysis (AMOPLS)

Analysis of Variance Multiblock Orthogonal Partial Least Squares (AMOPLS) was computed under the MATLAB® 8 environment (TheMathWorks, Natick, MA, United States). The first step of the method is a partition of the data matrix into a series of additive submatrices, each of which is associated with a specific effect of the experimental design. This follows ANOVA principles by computing average values related to each of the factors levels. This allows the relative variability of each main effect or interaction term to be evaluated using the sum of squares of the corresponding submatrix. A multiblock OPLS model is then computed for the joint analysis of the collection of submatrices to predict level barycenters of the experimental factors and their combinations. Further interpretation is carried out following the OPLS framework, using specific predictive components that are associated with the different effects of the experimental design, and orthogonal components summarizing

unexplained residual variability. Samples groupings can be investigated on the corresponding score plots (tp and to), while variables' contributions are analyzed using loading plots (pp and po).

Empirical p-values are computed using random permutations of the experimental design to assess the statistical significance of each effect using an effect-to-residuals ratio. A series of 10.000 random permutations was calculated to validate AMOPLS models and evaluate the statistical significance of each main and interaction effects. The interested reader can refer to the original article describing the AMOPLS method for a detailed description (Boccard and Rudaz, 2016).

Molecular networking parameters

A molecular network was created with the Feature-Based Molecular Networking (FBMN) workflow (Nothias et al., 2019) on GNPS (Wang et al., 2016) (www.gnps.ucsd.edu). The mass spectrometry data were first processed with MZMINE2 (as described above) and the results were exported to GNPS for FBMN analysis. The precursor ion mass tolerance was set to 0.02 Da and the MS/MS fragment ion tolerance to 0.02 Da. A molecular network was then created where edges were filtered to have a cosine score above 0.7 and more than 6 matched peaks. Further, edges between two nodes were kept in the network if and only if each of the nodes appeared in each others respective top 10 most similar nodes. Finally, the maximum size of a molecular family was set to 100, and the lowest scoring edges were removed from molecular families until the molecular family size was below this threshold. The spectra in the network were then searched against GNPS spectral libraries (Horai et al., 2010; Wang et al., 2016). The library spectra were filtered in the same manner as the input data. All matches kept between network spectra and library spectra were required to have a score above 0.7 and at least 6 matched peaks. The DEREPLICATOR was used to annotate MS/MS spectra (Mohimani et al., 2018). The molecular networks were visualized using Cytoscape 3.6 software (Shannon et al., 2003). The GNPS job parameters and resulting data are available at the following addresses https://gnps.ucsd.edu/ProteoSAFe/status.jsp?task=50596ad63e8d4402815dbd8356a18500 and https://gnps.ucsd.edu/ProteoSAFe/status.jsp?task=41c5c1b3566c45dbbde657569503c25d for positive and negative ion modes, respectively).

Metabolite annotation

The spectral file (.mgf) and attributes metadata (.clustersummary) obtained after the MN step were annotated using the ISDB-DNP (In Silico DataBase—Dictionary of Natural Products), a metabolite annotation workflow that has been previously developed (Allard et al., 2016). Annotation was done using the following parameters: parent mass tolerance 0.005 Da, minimum cosine score 0.2, maximal number of returned candidates: 50. Furthermore, taxonomically informed scoring was applied on the GNPS outputs, returning an attribute table which can be directly loaded in Cytoscape. The taxonomically informed metabolite annotation process has been previously described in detail (Rutz et al., 2019). The scripts are available online (taxo_scorer_user.Rmd) at https://github.com/oolonek/taxo_scorer. The chemical classes of the compounds were described using ClassyFire (http://classyfire.wishartlab.com/) (Djoumbou Feunang et al., 2016). Identification of a selection of putatively annotated metabolites was confirmed by comparison of retention time, HRMS and MS/MS data with pure standards.

Statistical analysis

Arc sinus transformation was applied to severity data before statistical analysis. One-way ANOVA was applied to severity data and phellem thickness, followed by the post-hoc Tukey's LSD test for multiple pair-wise comparisons.

4.4. Results and discussion

Periderm thickness is not associated with resistance to silver scurf

Silver scurf symptomatic regions of the potato skin of tubers grown in the field were analyzed by microscopy which revealed that *Helminthosporium solani* colonized the periderm of potato tubers but did not penetrate in the cortical cells (Figure 4.1). Other studies have shown that *H. solani* colonizes mainly the periderm, although some hyphae in the cortical cells were previously observed (Martinez et al., 2004). Interestingly, we did not observe appressorium formation of the fungus, in line with recent observations (Martinez et al., 2004), although these specialized structures had been observed in *H. solani* infecting potato tubers in the past (Heiny and Mclntyre, 1983). The use of different cultivars as host plants and different fungal strains in these and our studies may explain these differences, suggesting that the production of appressorium depends on the fungal strain and/or the host cell (Avis et al., 2010). Alternatively, appressorium may be formed during early infection or only in few cells. Thus, a higher number of microscopical analysis may result in appressorium detection. Notably, *H. solani* induces the collapse of the tuber periderm (Figure 4.1), which is likely to be the responsible of the water losses observed during storage in silver scurf diseased potatoes (Errampalli et al., 2001b).

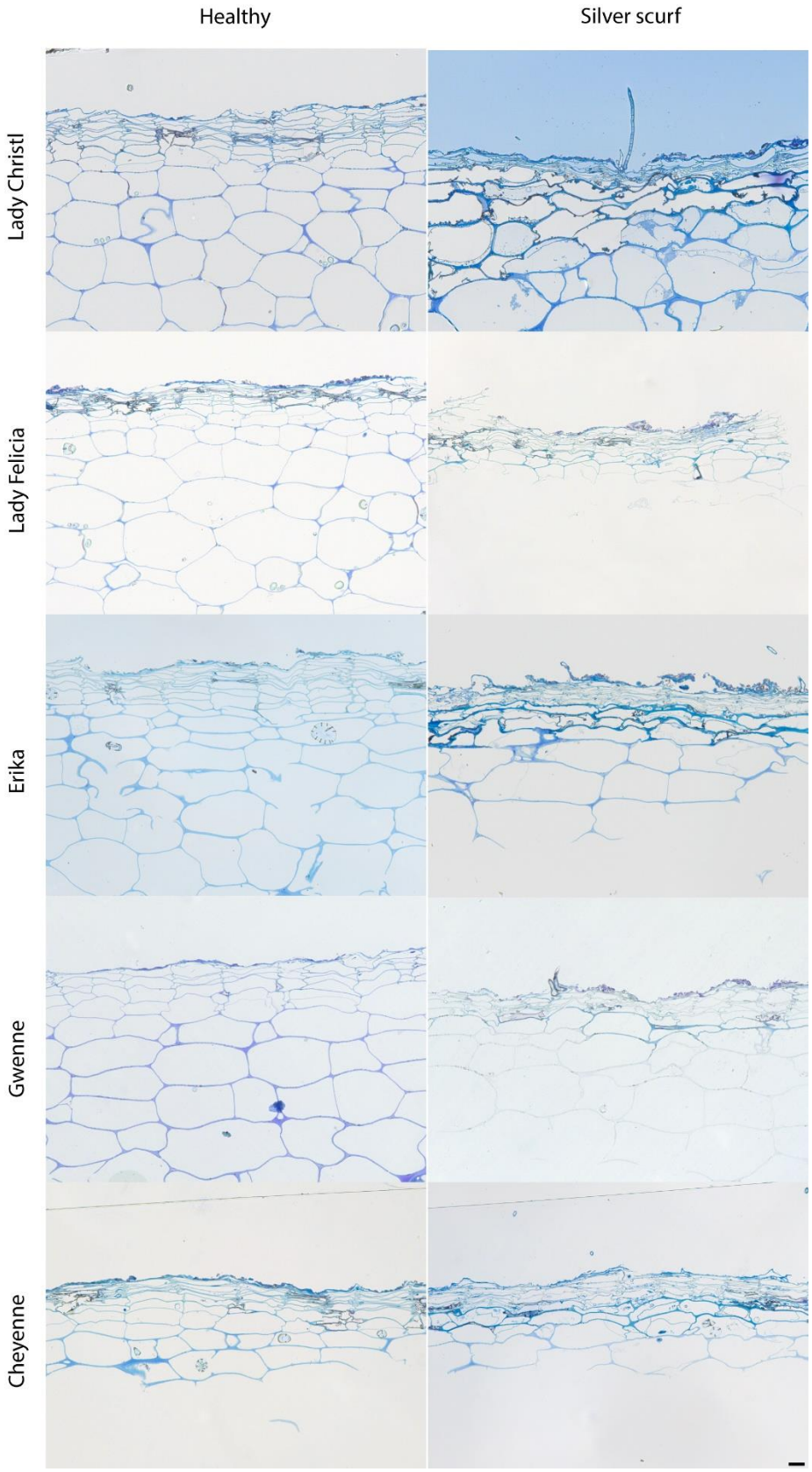

Figure 4.1 Longitudinal sections of the phelloderm of asymptomatic (A, C, E, G and I) and silver scurf symptomatic (B, D, F, H and J) regions of the potato cultivars Lady Felicia (A and B), Lady Christl (C and D), Cheyenne (E and F), Gwenne (G and H) and Erika (I and J). Bars represent 50 µm. f: fungal structures.

The phellem (suberized tissue of the periderm) thickness of the 16 potato cultivars grown in the field was assessed on asymptomatic potato tubers and these studies showed that silver scurf severity is not associated with constitutively thicker phellem tissues. It is worth noting that the second most susceptible cultivar showed very thin skin, suggesting that thin skins are more susceptible to silver scurf (Figure 4.2). This is consistent with the observations on black dot, where highest susceptibility was observed on the cultivar with thinnest skin. Nonetheless, and as observed on black dot disease, no significant correlation between silver scurf disease severity and skin thickness was observed in the other cultivars. Furthermore, suberin accumulation in control conditions is similar among the cultivars studied (Chapter 3). It has been shown that potato tubers with old lesions of silver scurf accumulate suberin (Frazier et al., 1998), and it is to be studied whether suberin accumulation upon *H. solani* inoculation depends on the cultivar and is associated with resistance to silver scurf. Altogether, these results suggest that other mechanisms than the structure of the potato periderm are involved in the resistance of silver scurf in potato tubers.

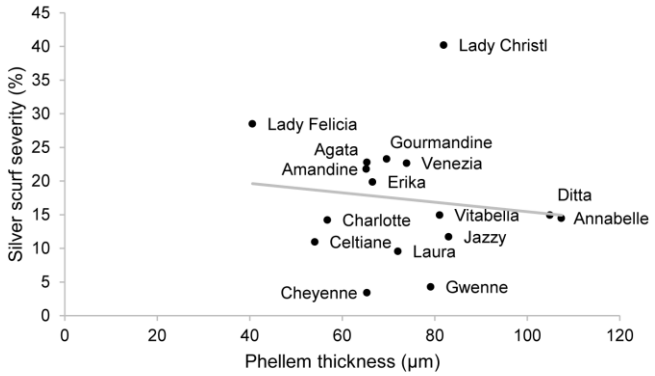

Figure 4.2 Relationship between silver scurf disease severity (in percentage) and phellem thickness (in µm) of 16 potato cultivars grown under field conditions. (n= 12 for phellem thickness, n= 36 for silver scurf severity). Trend in grey represents linear regression (r^2= 0.02).

Cultivar susceptibility to silver scurf is not highly influenced by environmental factors

Potato cultivars with different susceptibility levels in the field were planted in the greenhouse in absence of the pathogen, and half of the population was inoculated with *H. solani* and the other half was *mock* inoculated. Notably, the results on silver scurf disease severity were similar in the greenhouse and the field experiments (Figure 4.3). The two susceptible cultivars (Lady Christl and Lady Felicia) showed high severity in both trials (more than 23%) while the resistant cultivars showed disease severities below 15% in the field and below 10% in the greenhouse. These results suggest that cultivar susceptibility is not highly influenced by environmental factors but rather by intrinsec resistance mechanisms. Thus, the metabolome comparison of these cultivars may be useful to highlight biomarkers of resistance.

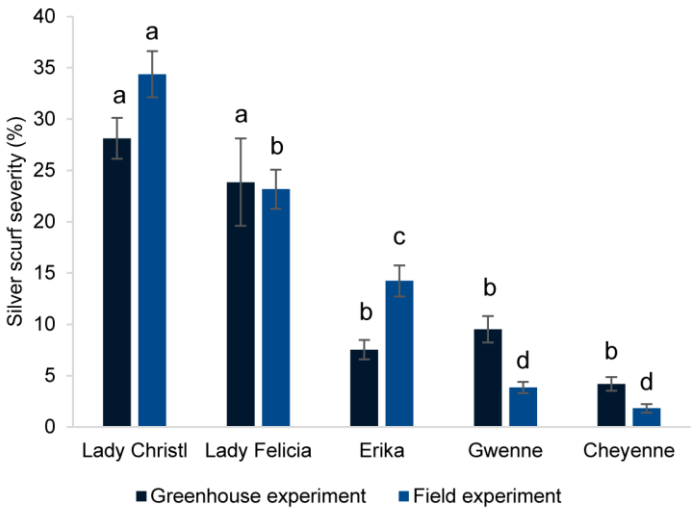

Figure 4.3 Silver scurf severity (percentage of tuber area showing symptoms) under field conditions and in the greenhouse of five selected cultivars. Different letters indicate significantly different severities in the greenhouse *or* in the field (Tukey's test, $p<0.05$).

Cultivars with quantitative resistance to silver scurf use different strategies

The experimental design of the untargeted metabolomics analysis allowed the evaluation of the cultivar and the inoculation main effects, as well as their interaction. This evaluation was carried out using the AMOPLS statistical model and the visualization of the detected features in molecular networks (MNs) (Chapter 3). The AMOPLS model highlighted that the highest contribution to the total variance is carried by the cultivar factor (35%), while the factor of inoculation and the interaction result both in metabolic changes that contribute to 7.4% and 7.6% of the total variance (Table 4.1). Notably, four components are required to explain the differences between potato cultivars, but the observation of the scores using two dimensions does not allow the discrimination of the resistant and the susceptible cultivars (Figure 4.4). These results indicate that different potato cultivars with quantitative resistance to silver scurf may use specific metabolic strategies. Similarly, visualization of the metabolites detected in the LC-HRMS/MS analysis using molecular networks (MNs) showed that potato cultivars differ, but without clear clusters of metabolites being highly abundant in all resistant cultivars (Figure 4.5). Altogether, these results suggest that the studied potato cultivars with quantitative resistance against *H. solani* have different metabolic strategies.

Table 4.1 ANOVA decomposition and AMOPLS predictive components (tp1 to to, first row) related to the specific effect of the experimental design (Cultivar, Inoculation or Cultivar × Inoculation), for the LC-HRMS/MS dataset in negative ionization mode. The predictive components associated with each specific effect are highlighted.

ANOVA decomposition			**Cultivar**		**Innoculation**		**Interaction**		**Residuals**	
Relative Sum of Squares			34.84%		7.37%		7.61%		50.18%	
Predictive components	tp1	tp2	tp3	tp4	tp5	tp6	tp7	tp8	tp9	to
Cultivar	**94.95%**	4.58%	**96.55%**	**95.40%**	**96.54%**	5.53%	8.31%	12.37%	11.02%	17.02%
Inoculation	1.52%	**79.81%**	1.04%	1.39%	1.04%	8.14%	12.23%	18.20%	16.21%	25.03%
Cultivar × Inoculation	1.60%	7.09%	1.09%	1.46%	1.10%	**76.04%**	**64.00%**	**46.44%**	**52.28%**	26.31%
Residuals	1.93%	8.52%	1.31%	1.75%	1.32%	10.29%	15.46%	23.00%	20.49%	31.64%

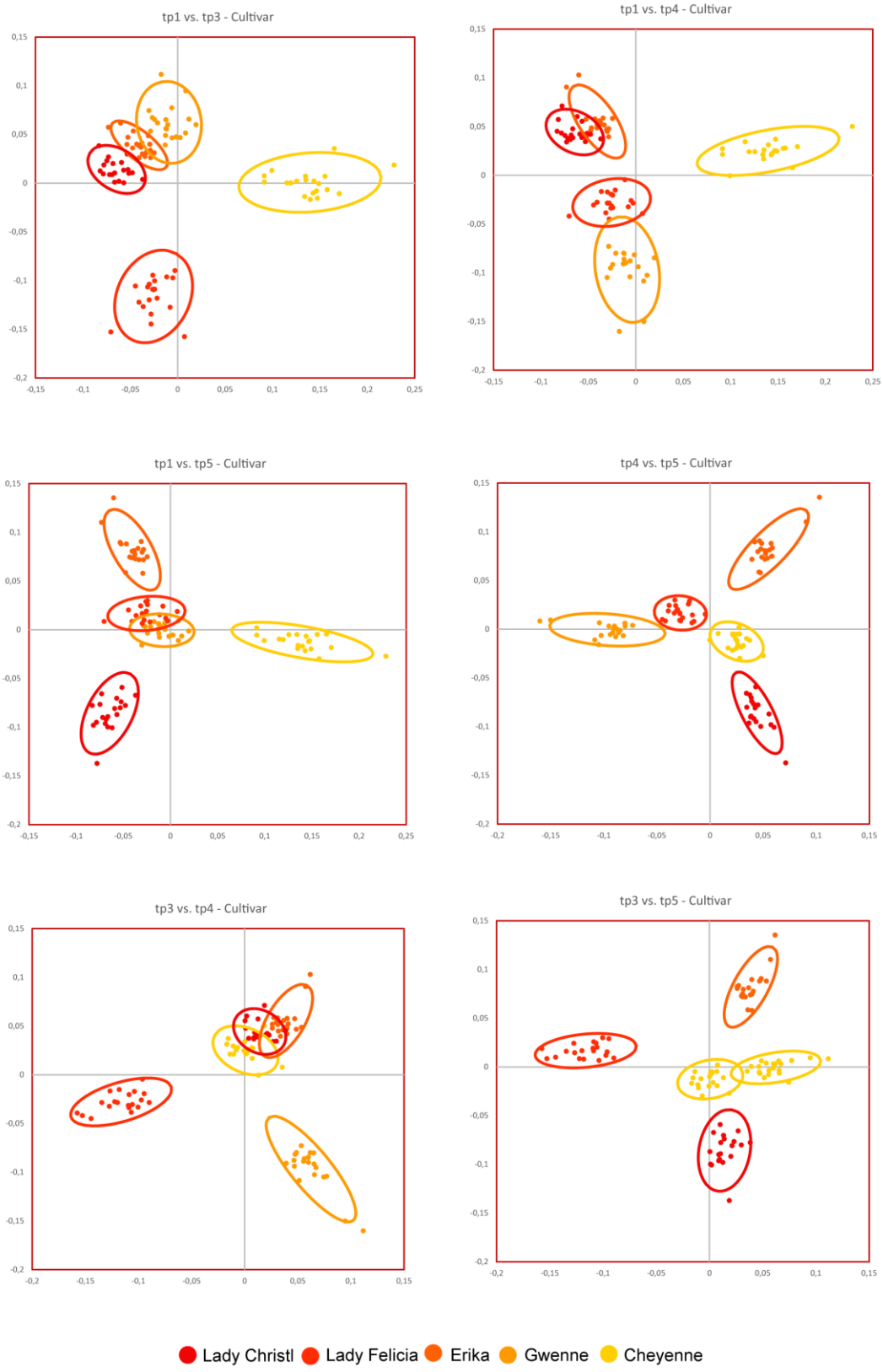

Figure 4.4 Scores plot of the four predictive components of the AMOPLS model in negative ionization mode explaining cultivar differences. Observations are positioned according to the left and below axis. Observations are color-coded as cultivars (n=20) with 95% confidence ellipses.

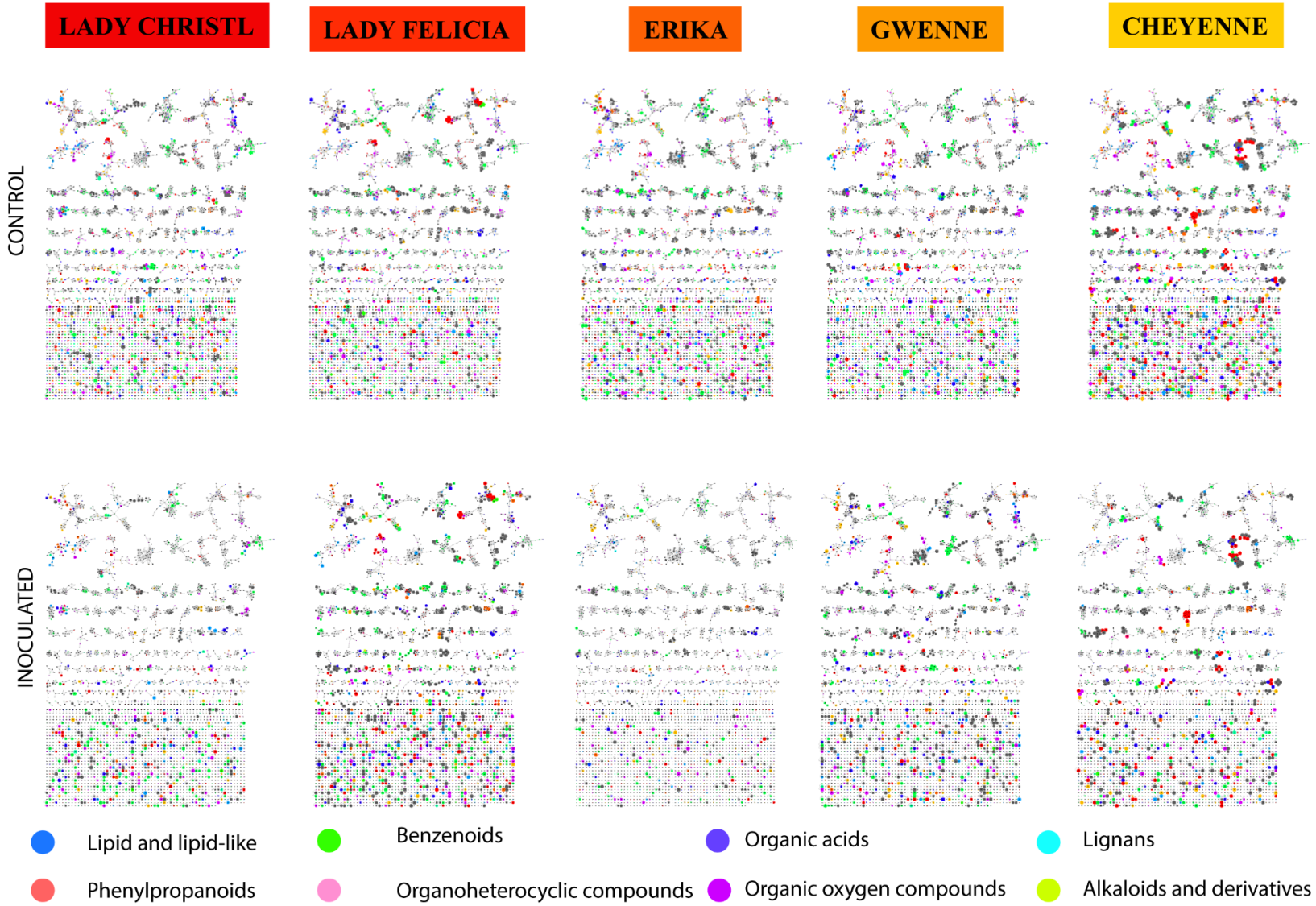

Figure 4.5 Global Molecular Networks in negative ionization mode of the five potato cultivars in control and inoculated conditions. Color of the node according to chemical class (ClassyFire), node size according to signal intensity of the respective cultivar.

In order to annotate the highest possible number of features, a global MN was built (Wang et al., 2016) and all detected features were compared to experimental databases and an *In Silico Data Base (ISDB)* previously developed (Allard et al., 2016). Furthermore, a taxonomical ponderation was used to increse the robustness of the annotations (Rutz et al., 2019). This strategy resulted in the annotation of 60% of the detected features in both positive and negative mode. From these, the most abudant structural classes were lipid and lipid-like metabolites, which represented 22% (negative ion mode) and 26% (positive ion mode) of all anotated features (Figure 4.6). Phenylpropanoids and organic oxygen compounds represented 21% and 18% of the anotated features in negative mode, but only 15% and 11% in positive mode, likely due to their higher ionization in negative mode. Organoheterocyclic compounds represented between 14% and 18% of all anotated features, while benzenoids and organic acids represented between 7% and 10% of all putatively anotated metabolites. Altogether, these results are comparable to those found in potato cultivars inoculated with *C. coccodes* (Chapter 3), and suggest robustness of the methodology.

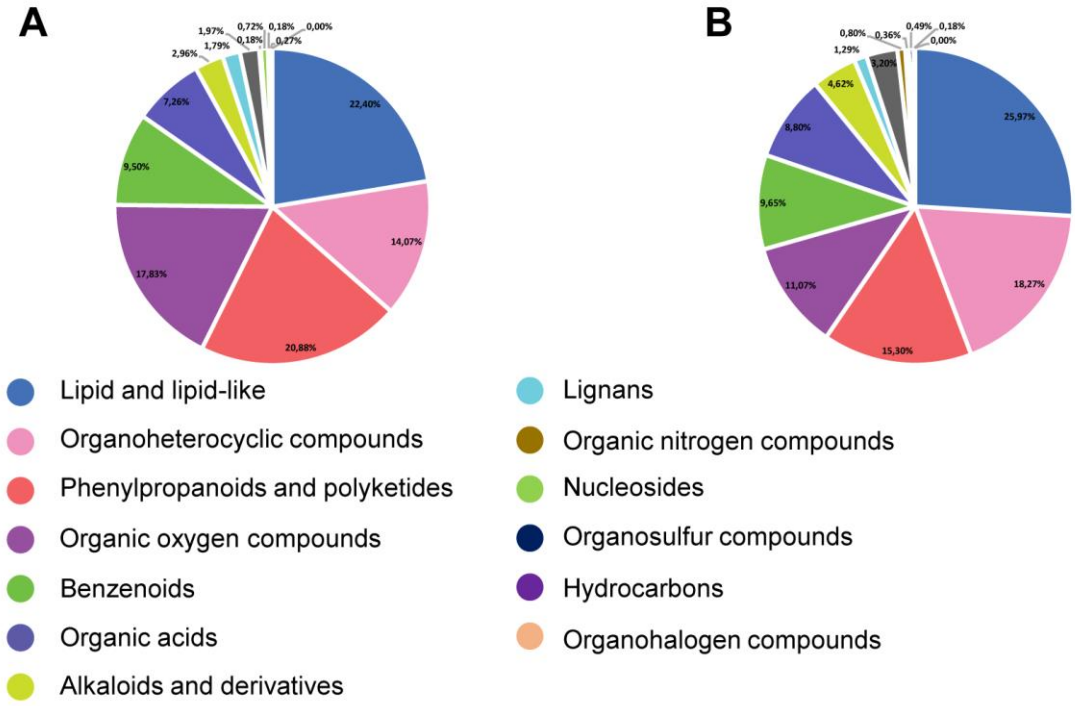

Figure 4.6 Pie-chart of the chemical classes of compounds detected in potato periderms in positive (A) and negative (B) ionization mode as annotated by the ISDB (according to ClassyFire).

Hydroxycoumarins, HCAAs and zeatin glycoside are Resistance-Related Constitutice metabolites

The four components of the AMOPLS model that explained the main effect cultivar were combined in different plots to visualize cultivar groups (Figure 4.4). The red-skin cultivar (Cheyenne) showed the most different metabolome, with higher amounts of anthocyanins and flavonoid glycosides (Figure 4.5), as observed previously (Chapter 3). Nonetheless, a clear grouping of the resistant cultivars (Erika, Gwenne and Cheyenne) and the susceptible cultivars (Lady Felicia and Lady Christl) could not be highlighted in these 2D plots. The most informative biplot using two components was *tp3* and *tp5*, although differences among resistant cultivars were obvious, reinforcing the hypothesis that quantitative resistance to silver scurf in these cultivars may be the result of different plant metabolic strategies. Interestingly, the visualization of the LC-MS/MS data in Molecular Networks (MNs) highlighted some RRC (metabolites more abundant in resistant cultivars than in susceptible cultivars) clusters, suggesting that some metabolite chemical classes are more abundant in the resistant cultivars (Figure 4.7). However, the RRC is calculated as the average intensities of all resistant cultivars versus

all susceptible cultivars, and RRC values were often highly influenced by a single cultivar (Figure 4.7 and Figure 4.5).

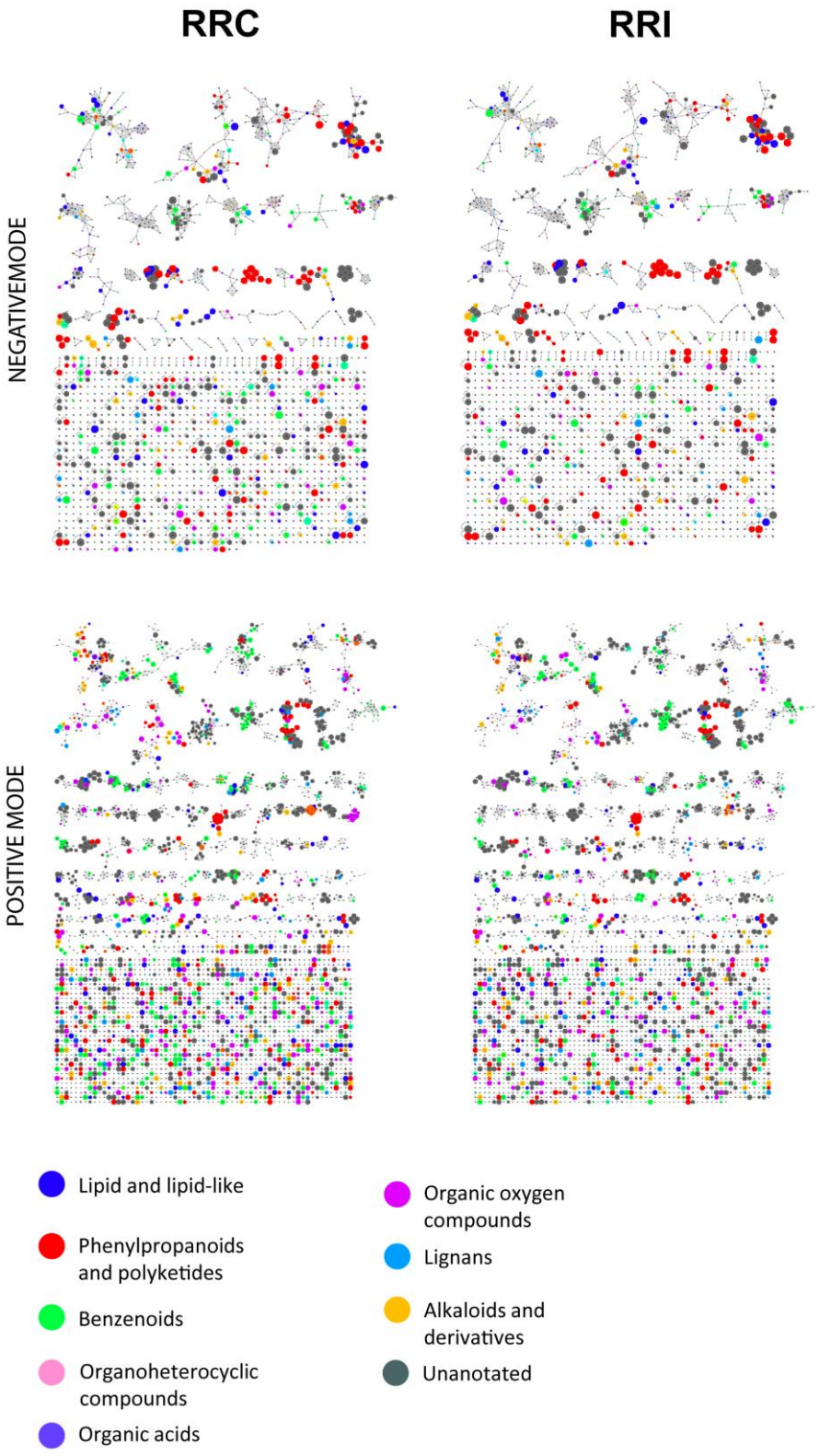

Figure 4.7 Global Molecular Networks in negative and positive ionization mode. Color of the node according to chemical class (ClassyFire), node size according to the ratio of intensities between resistant and susceptible cultivars in control conditions (RRC) or in inoculated samples (RRI).

For example, since the red-skin cultivar Cheyenne is resistant to silver scurf, all Cheyenne-specific metabolites were highlighted as RRC. Among them, anthocyanins and flavonoid glycosides were highlighted as Cheyenne-specific metabolites. However, it is likely that some of the Cheyenne-specific metabolites are not exclusively linked to silver scurf resistance, especially since other red-skinned cultivars are susceptible to silver scurf (Secor, 1994). Other metabolites were more abundant in some but not all resistant cultivars, such as the alkaloids **calystegines**. Calystegine A3 and calystegine B2 were detected in our study, but other calystegines found in potato tubers (such as calystegine B4) could not be unambiguously identified. Interestingly, calystegines were found to be more abundant in the resistant cultivars Cheyenne and Erika than in the other cultivars in control conditions and upon inoculation. However, the other resistant cultivar (Gwenne) contained lower amounts of both calystegines than the susceptible cultivar Lady Felicia. Altogether, these results suggest that calystegines might be involved in the resistance to silver scurf, but high amounts of these metabolites do not confer resistance *per se* (Lady Felicia). Other metabolites that could be highlighted as RRC were hydroxycinnamic acid derivatives, such as the polyamine conjugates **hydroxycinnamic acid amides** (HCAAs). Indeed, feruloyloctopamine, feruloyltyramine and putrescine derivatives were more abundant in all resistant cultivars than in susceptible ones in control conditions (Table 4.2). Furthermore, HCAAs of **spermine derivatives** were found to be more abundant in the resistant cultivars Gwenne and Cheyenne, but relatively low levels of all spermine derivatives were found in the resistant cultivar Erika. Furthermore, the *N*1,*N*4,*N*9,*N*12-tetra(dihydrocaffeoyl) spermine was found to be abundant only in the resistant Cheyenne resistant. On the other hand, **spermidine derivatives** were most abundant in the cultivar Erika, but relatively low in the cultivar Cheyenne. Altogether, these results suggest that high amounts of free HCAAs correlate with resistance to silver scurf, although accumulating spermine or spermidine derivatives depends on the cultivar. Notably, very few metabolites were more abundant in all three resistant cultivars compared to the susceptible cultivars. Illustrating this, only 57 features in positive mode (1.5% of all features) and 25 in negative mode (1.4% of all features) showed an overall RRC of 1.5 or higher and were more abundant in all resistant cultivars than in the susceptible cultivars. Among them, several features were putatively annotated as **carbohydrates and carbohydrate derivatives**, including a glycosylated form of the cytokinin cis-zeatin, which was highlighted as a RRC in both positive and negative ionization modes (Figure 4.8).

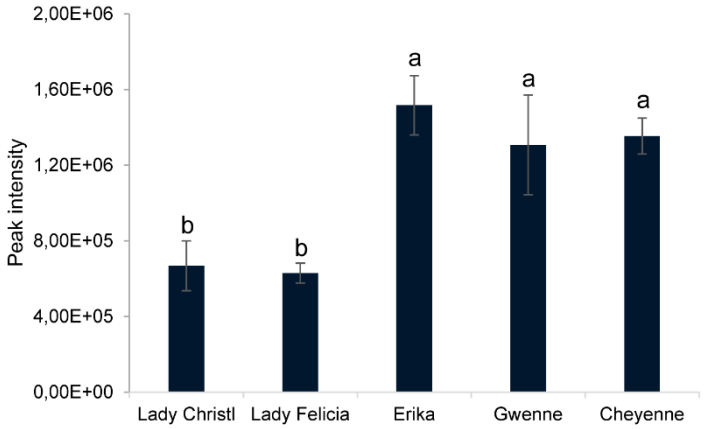

Figure 4.8 Mean peak intensity of feature 1536 with *m/z* 380,1575 (in negative ionization mode) and *RT* = 1,11 putatively annotated as Zeatin(E)-D-Glucopyranosyl by the ISDB-DNP. Data are shown as mean peak intensity (n=10) ± standard error. Different letters indicate statistically significant differences (Tukey's test, p<0,05).

Glycosylated cis-zeatin has been previously detected in potato tuber sprouts (Nicander et al., 1995) and cytokinins are involved in tuber formation and sprouting (Hartmann et al., 2011; Lomin et al., 2018). Our results suggest that **cytokinin** accumulation before fungal inoculation may provide

resistance to silver scurf. Interestingly, plant cytokinins prime salicylic acid and other defense responses (Choi et al., 2011), suggesting that indeed, higher amounts of cytokinins may initiate defense against *H. solani*. Interestingly, three features putatively annotated as **hydroxycoumarins** were highlighted as resistance-related metabolites, with RRC values higher than 3 (Table 4.2). Notably, one of these features was putatively annotated as isofraxidin by comparison of its MS/MS spectra to an experimental database (GNPS) and suggests that hydroxycoumarins are present in the potato tuber and are involved in the resistance against silver scurf. Altogether, our results show that few metabolites are more abundant in all resistant cultivars under control conditions, and these include HCAAs and hydroxycoumarins, as well as a cytokinin glycoside. Notably, HCAAs and hydroxycoumarins were also highlighted as RRC against black dot, suggesting that high constitutive amounts of these metabolites provide resistance to both fungal pathogens. HCAAs have been shown to be involved in the resistance of plants against pathogens, mainly through cell wall reinforcement (Macoy et al., 2015). However, their accumulation as non-bound to the cell wall suggest that they may have additional functions. They have been shown to possess antioxidant activity (Macoy et al., 2015), and we previously showed their antifungal activity against *C. coccodes* (Chapter 3). Their possibly antifungal activity against *H. solani* requires further study. On the other hand, hydroxycoumarins had been involved in resistance against late blight (Yogendra et al., 2015) and Colorado Potato Beetle in potato leaves (Tai et al., 2014). Our results suggest that hydroxycoumarins are present in the potato periderm of commercially available potato cultivars and that they are involved in the resistance against fungal pathogens.

Inoculation of H. solani induces the phenylpropanoid pathway and affects the production of steroid derivatives and flavonoid glycosides

The inoculation of *H. solani* on potato tubers induced changes in the potato metabolome, as highlighted in the second component of the AMOPLS model (Table 4.1, Figure 4.9). The biplot of this predictive component shows that non-inoculated potato tubers of all cultivars have similar scores (positive), while all inoculated potato tubers have the opposite scores (negative) (Figure 4.9).

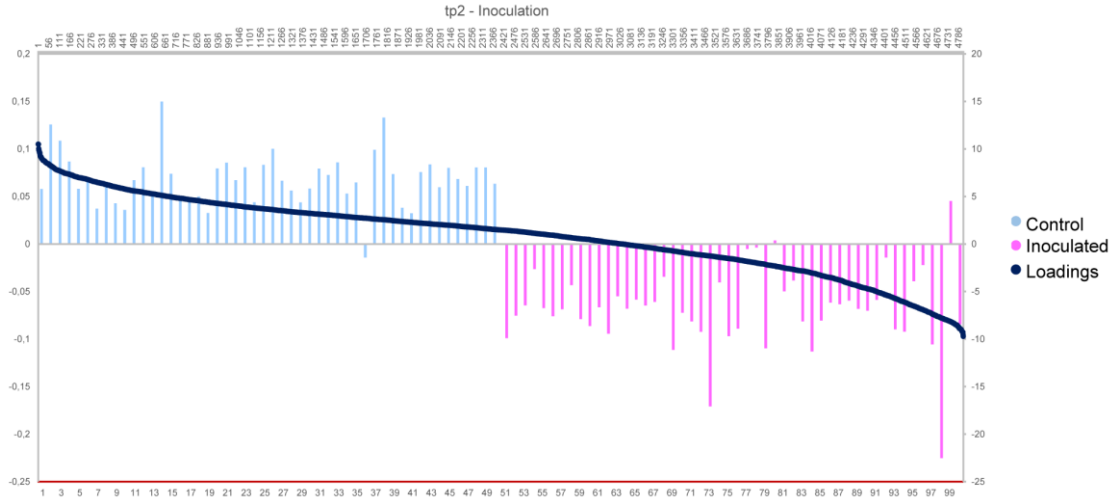

Figure 4.9 Biplot representations of the second predictive components of the AMOPLS model in negative mode explaining inoculation main effect. Observations are positioned according to the left axis (samples 1 – 50 control conditions, 51 – 100 inoculated conditions). Loadings are positioned according to the right axis (ID 1 – 4786).

Plotting the loadings of this component shows that some features are more abundant in control conditions (left side of the graph) or in inoculated samples (right side of the graph). Thus, these results indicate that induction and repression of metabolic pathways may be regulated upon *H. solani* infection. Studies carried out with other microbes revealed that the response upon pathogen

inoculation in potato plants strongly relies on the **phenylpropanoid** pathway activation (Desender et al., 2007; Kröner et al., 2011, 2012). The first step of this pathway is catalyzed by the *Phenylalanine Ammonia-Lyase* (PAL) enzyme, converting phenylalanine in cinnamic acid, an enzyme that is upregulated in potato tubers following treatment with a concentrate filtrate of *Phytophthora infestans* (Kröner et al., 2011). Cinnamic acid is the precursor of several phenylpropanoids, including the highly abundant hydroxycinnamic acids (Figure 4.10). Interestingly, inoculation with *H. solani* resulted in a reduction of ca. 50% on the amounts of phenylalanine and cinnamic acid in all cultivars, suggesting that the production of downstream hydroxycinnamic acids, as well as other cinnamate derivatives, might be induced by the presence of *H. solani*, resulting in relatively lower amounts of their precursors. This is in line with several studies showing the accumulation of phenolic derivatives and the upregulation of the PAL enzyme upon pathogen inoculation (Matsuda et al., 2005; Desender et al., 2007; Kröner et al., 2011, 2012). Nonetheless, the most abundant hydroxycinnamic acids (caffeoylquinic acids), were not more abundant in pathogen-inoculated tubers, suggesting that this specific pathway is not up-regulated during *H. solani* infection and other analogues are synthetized. **Hydroxycinnamic acid amides** (HCAAs) are hydroxycinnamic acids conjugated to an amide such as putrescine, spermine, spermidine, tyramine or octopamine, among others. A specific accumulation of *N*-caffeoylputrescine and *N*-dihydrocaffeoylputrescine was observed in inoculated samples, indicating that *H. solani* specifically induces the production of these phenylpropanoids (HCAAs), which may result from the activation of the *PAL* pathway (Figure 4.10). HCAAs with spermine and spermidine backbones were slightly less abundant in inoculated conditions, suggesting that only the putrescine derivatives are upregulated upon pathogen infection. Alternatively, the fungal inoculation may induce the production and the polymerization of HCAAs into the cell wall (Macoy et al., 2015), where they would be unsoluble and thus, not analyzed in our experiment. Interestingly, MNs highlighting the induction of metabolites upon fungal inoculation revealed that free sugars, such as fructose or sorbose, accumulate upon *H. solani* inoculation. Notably, other pathogens have been shown to induce the accumulation of the sugar mannitol, which is assimilated by the fungus for hyphal growth (Patel and Williamson, 2016), suggesting that *H. solani* may induce the production and accumulation of sugars for their own growth. Some clusters of the MNs showed several features being more abundant in inoculated samples, some of which were putatively annotated as **steroid derivatives**, suggesting that the biochemical pathway that leads to the production of steroidal glycosides, steroid lactones and steroidal saponins may be induced upon *H. solani* infection in potato tubers (Figure 4.10). It is worth noting that the most abundant steroid alkaloids, alpha-chaconine and alpha-solanine, showed a ca. 30% reduction upon fungal inoculation, suggesting that the increased accumulation of other minor steroid derivatives is accompanied by a decrease in the most abundant steroidal glycoside alkaloids (SGA) (Table 4.2). The degradation of the SGAs *alpha*-chaconine and *alpha*-solanine results in the production of *beta* and *gamma*-solanine/chaconine, and finally, the aglycone solanidine. Notably, inoculation with *H. solani* resulted in an increase of *beta*-chaconine, *beta*-solanine and solanidine, an increase that was higher in the susceptible cultivars. Altogether, these results suggest that *H. solani* possess enzymes or detoxification mechanisms that result in the degradation of *alpha*-solanine and *alpha*-chaconine in potato tubers, most especially in those susceptible to silver scurf. However, it is worth noting that the decrease in SGAs is comparable in all cultivars. Thus, a higher production of SGAs in the susceptible cultivars upon inoculation might compensate this increased degradation. Notably, a reduction of the amounts of flavonoid glycosides was observed upon inoculation with *H. solani*. These results confirm our previous observations, where all flavonoid glycosides detected were strongly reduced upon inoculation with *C. coccodes* (Chapter 3). Altogether, our results suggest that flavonoid glycosides may be repressed upon fungal inoculation in potato periderms.

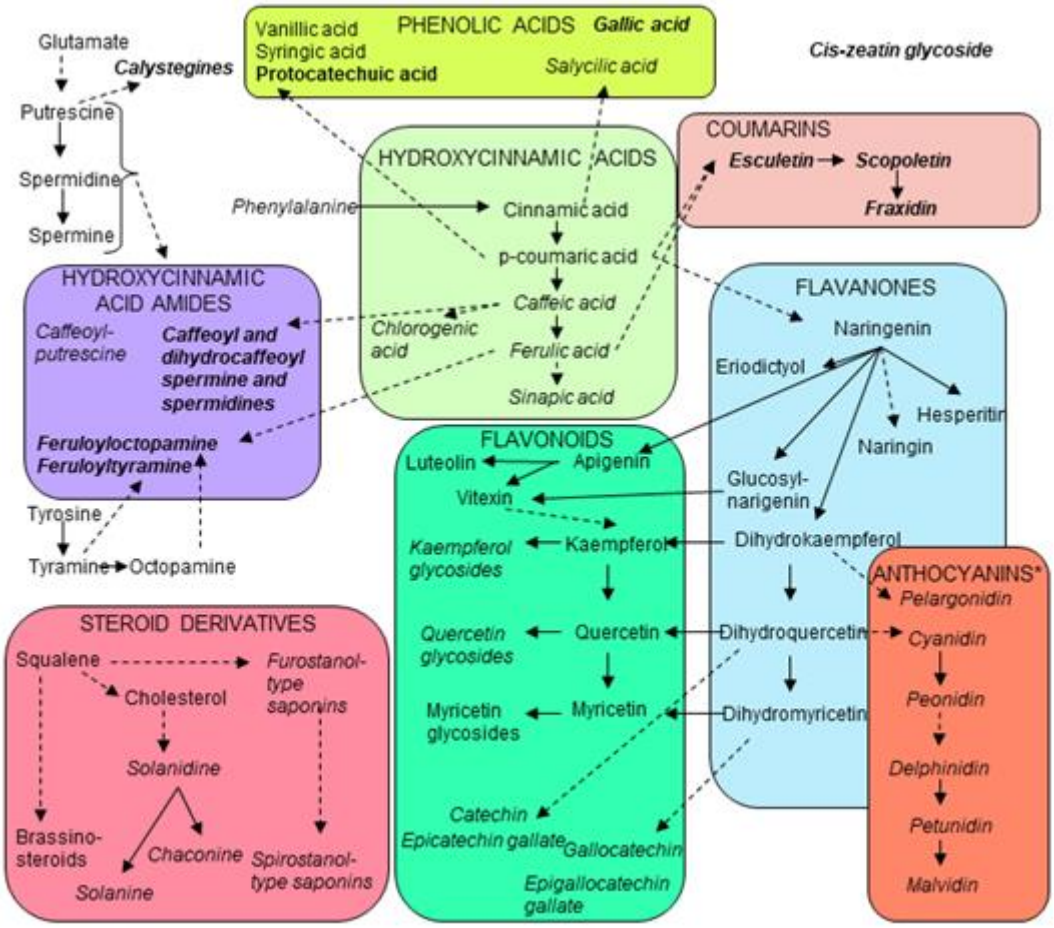

Figure 4.10 Metabolic pathways involved in the interaction between *Solanum tuberosum* and *Helminthosporium solani*. The central cluster is formed by the hydroxycinnamic acids (HCAs) that derive from phenylalanine. Hydroxycinnamic acid amides (HCAAs) that derive from HCAs and amino acid derivatives form the cluster in the left. Cinnamic acid and p-coumaric acid are precursors of phenolic acids such as salicylic acid. Coumarins derive from p-coumaric acid or ferulic acid. Naringenin, produced from p-coumaric acid, is the precursor of flavonoids and anthocyanins. Steroidal glycoalkaloids (i.e. α-chaconine and α-solanine), steroidal saponins and brassinosteroids derive from squalene. *For anthocyanins, only the aglycone (anthocyanidin) is shown. Detected metabolites in this study are shown in italics. Dotted lines indicate that more than one step is required for the conversion shown in the figure. Biosynthetic pathways according to the Kyoto Encyclopedia of Genes and Genomes (KEGG) of *Solanum tuberosum* (or related plant species, if not available for *S. tuberosum*).

Gallic acid and protocatechuic acid are induced in resistant cultivars upon H. solani inoculation

Inoculating *H. solani* in potato tubers induces the production or the degradation of several metabolites, which are cultivar dependent. Four predictive components of the AMOPLS model show this interaction (Table 4.1), and especially relevant information is found in components 6 and 8 (Figure 4.11). In *tp6*, metabolites that are induced in the resistant cultivar Cheyenne are repressed in the susceptible cultivars when inoculated with *H. solani*. In *tp8*, metabolites that are induced in Erika and Gwenne are repressed in the rest of the cultivars. These results suggest that the inoculation of *H. solani* has a different impact among potato cultivars, and that one of the resistant cultivars (Cheyenne) reacts to the fungal infection differently than the other two resistant cultivars. Among the features differentially regulated in **Cheyenne**, flavonoid glycosides were highlighted, since its degradation upon fungal inoculation was less pronounced than in the rest of the cultivars. On the other hand, features upregulated in the resistant cultivars **Erika and Gwenne** included several coumaric acid derivatives and phenolic glycosides, including two caffeoylshikimic acid isomers. The inoculation of *H. solani* resulted in the accumulation of ferulic acid and reduced levels of caffeic acid only in the susceptible cultivars. Furthermore, derivatives of ferulic acid, such as feruloyl quinic acids feruloyl-glucoside were found to

be more abundant in the susceptible cultivars upon fungal inoculation. These results suggest that conversion of caffeic acid into ferulic acid and its derivatives occurs upon *H. solani* inoculation specifically in the susceptible cultivars (Figure 4.10). Interestingly, another ferulic acid derivative, feruloyltyramine, an HCAA that is more abundant in the resistant cultivars under control conditions, specifically accumulates in the susceptible cultivars upon fungal inoculation. On the other hand, feruloyloctopamine is upregulated in all cultivars except the resistant Erika and the susceptible Lady Christl upon fungal inoculation. However, feruloyloctopamine is more abundant in the resistant cultivars under control conditions, but also upon fungal inoculation, highlighting feruloyloctopamine as a resistance-related constitutive and induced (RRC and RRI) metabolite. Interestingly, two features putatively annotated as gallic acid and protocatechuic acid were shown to accumulate specifically in the resistant cultivars upon fungal inoculation (Table 4.2). Interestingly, gallic acid and protocatechuic acid are phenolic acids with antioxidant properties (Asnaashari et al., 2014; Safaeian et al., 2018). Furthermore, gallic acid plays a role in plant defense against insects (Ananthakrishnan, 1997). Our results suggest that accumulation of gallic and protocatechuic acid upon fungal inoculation is specific of resistant cultivars and indicates that they play a role against fungal diseases.

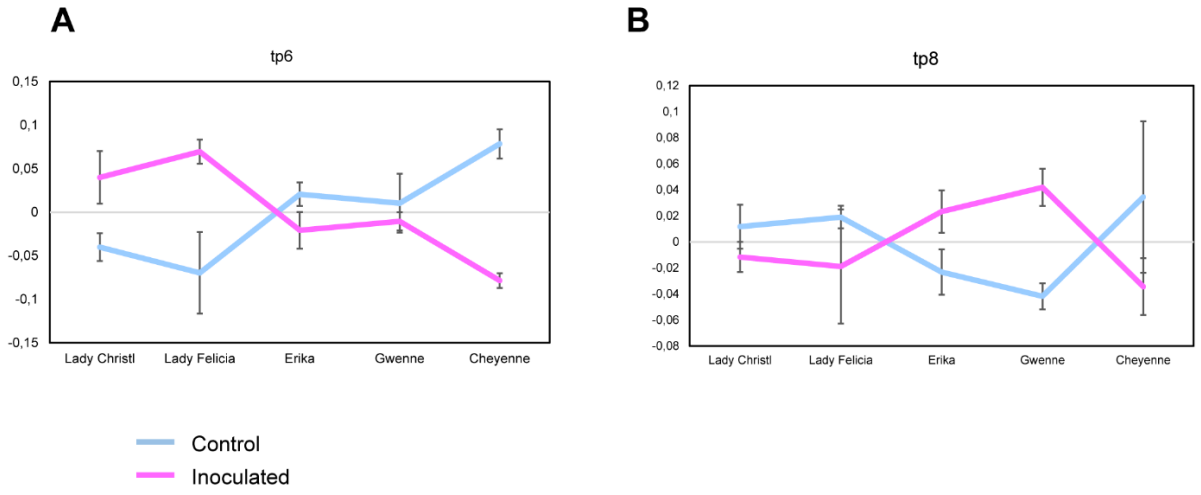

Figure 4.11 Score plots of the sixth (A) and eighth (B) predictive components of the AMOPLS model in negative mode explaining the interaction of the main effects.

4.5. Conclusion

Host qualitative resistance to silver scurf has not been described in commercially potato cultivars, but a gradient of susceptibility to the disease exist among cultivars (Joshi and Pepin, 1991; Mérida et al., 1994; Rodriguez et al., 1996). However, the aspects that control quantitative resistance to silver scurf in potatoes have not been studied to date. Here, we compared the structural and biochemical changes that occur on different potato cultivars upon *H. solani* infection. Notably, the cultivar with the thinnest periderm was highly susceptible to silver scurf, but the periderm thickness of the sixteen cultivars studied did not correlate with silver scurf disease. These results suggest that cultivars with very thin skins are more susceptible to the disease, but that other factors influence the quantitative resistance to *H. solani* infection. Notably, a survey in the USA showed that Russet-type cultivars, which have thick skins, are more resistant to silver scurf than those with thin skins (Heiny and McIntyre, 1983). However, these thick-skin cultivars often have periderms of more than 150 µm (Artschwager, 1924), thicker than the cultivars that we studied. Thus, it is possible that cultivars with thicker skin are more resistant to silver scurf than the ones used in this study, but these cultivars are not appreciated in Europe, and thus, far less cultivated (Lees and Hilton, 2003). Furthermore, we found differences of susceptibility to silver scurf in potato tubers with similar periderm thickness, indicating that other mechanisms are

involved in the quantitative resistance to *H. solani*. Among them, the constitutive or inducible presence of metabolites that act as physical barriers, antioxidants or antimicrobials against the pathogen have been identified in several plant-pathogen interactions (Bollina et al., 2010; Yogendra et al., 2014, 2015). In order to study the metabolome of different potato cultivars upon fungal inoculation, five of the potato cultivars were cultivated in a greenhouse experiment and inoculated with *H. solani* during tuberization. Disease assessment of daughter tubers revealed that susceptibility to silver scurf is strongly related to genotype susceptibility, since similar results of disease severity were observed between the greenhouse experiment and field trials. An untargeted metabolomics approach combining multivariate data analysis (AMOPLS), molecular networking (MN) and annotation based on an *in silico database* was used to highlight biomarkers of the potato-*H. solani* interaction. We found that inoculating *H. solani* on potato plants resulted in reduced levels of phenylalanine and cinnamic acid, suggesting an upregulation of the phenylpropanoid pathway. Indeed, the phenylpropanoid pathway is induced in several plant-pathogen interactions, including in the interaction between potato and the fungal-like oomycete *Phytophthora infestans* (Kröner et al., 2011). However, only specific phenylpropanoid derivatives were found to accumulate upon *H. solani* inoculation and included the putrescine hydroxycinnamic acid amides (HCAAs). On the other hand, the most abundant steroidal glycosides (alpha-chaconine and alpha-solanine) were found to be less abundant in inoculated potatoes, which was accompanied with an increase in their degradation products, suggesting a fungal-induced degradation of these steroidal glycoalkaloids. However, other minor steroid derivatives were more abundant in *H. solani* inoculated potato tubers, suggesting that other pathways are up-regulated. Finally, flavonoid glycosides were less abundant on fungal inoculated tubers, suggesting a degradation of these metabolites upon *H. solani* inoculation. Notably, the same phenomenon was observed when potato plants were inoculated with *C. coccodes* (Chapter 3), suggesting that this is a process that might be conserved in different potato-fungal interactions.

Notably, the metabolomes of the five cultivars differed, but a clear distinction between resistant and susceptible metabolomes could not be highlighted. These results suggest that cultivars resistant to silver scurf may use different metabolic strategies. For example, the cultivar Cheyenne is a red-skin cultivar with strong differences in its metabolome compared to the rest of the cultivars, some of them related to its color (i.e. anthocyanins). Since other red-skin cultivars have been shown to be susceptible to silver scurf (Secor, 1994), comparing the metabolome of susceptible and resistant red-skin cultivars would help highlight resistance-related metabolites in red-skin cultivars. Interestingly, HCAAs, which had been found to be more abundant in resitant cultivars against black dot, were also highlighted in this study. However, differences in the composition of these metabolites were observed among resistant cultivars, suggesting specific HCAA metabolism in the different cultivars.

Despite the differences among cultivars, some metabolites could be highlighted as conserved resistant related (RR) metabolites, being more abundant in all resistant cultivars compared to the susceptible cultivars, both in control conditions (RRC) or in inoculated plants (RRI). The highlighted RRC included a cytokinin glycoside (zeatin glycoside) and hydroxycoumarins. The former has been previously detected in potato sprouts and is believed to play a role in tuber formation and sprouting, (Nicander et al., 1995; Hartmann et al., 2011; Lomin et al., 2018), although the role of cytokinins in priming defense has also been proposed (Choi et al., 2011). Our results indicate that zeatin glycoside is present in higher amounts in the resistant cultivars in absence of the pathogen, suggesting that is plays a role in priming defense against silver scurf. On the other hand, hydroxycoumarins were identifed as resistance-related metabolite against Colorado Potato Beetle in wild potatoes (Tai et al., 2014). Furthermore, the antimicrobial activities of these compounds has been previously demonstrated (Navarro-García et al., 2011; Yang et al., 2016). Interestingly, we previously found that hydroxycoumarins were involved in

the resistance of potatoes against black dot (Chapter 3), and that they have antifungal activity against *C. coccodes*.

Upon fungal inoculation, susceptible cultivars induced the phenylpropanoid pathway towards the production of ferulic acid. On the other hand, gallic acid and protocatechuic acid, two hydroxybenzoic acid derivatives, were shown to be specifically upregulated upon fungal inoculation in the resistant cultivars. These metabolites posses antioxidant (Asnaashari et al., 2014; Safaeian et al., 2018) and antifungal properties (Nguyen et al., 2015; Li et al., 2017), and our results suggest that they play a role in the quantitative resistance against silver scurf. Altogether, we suggest that quantitative resistance of potato cultivars against silver scurf may be the result of different coordonated biochemical pathways expression, with some conserved Resistance-Related metabolites, including hydroxycoumarins and a cytokinin glycoside as RRC, and gallic acid and protocatechuic acid as RRI.

Table 4.2 List of metabolites detected in the untargeted metabolomics approach and highlighted as resistance-related metabolites or cultivar-specific metabolites. NI Negative ionization mode; PI Positive Ionization mode. RT: Retention Time. The values of each feature are standardized to the lowest intensity peak of the feature. RRC=RM/SM, RRI=RP/SP, qualitativeRRI =(RP/RM)/(SP/SM). RRC resistance-related constitutive, RRI resistance-related induced, RP resistant genotype with pathogen inoculation, RM resistant genotype with mock inoculation, SP susceptible genotype with pathogen inoculation, SM susceptible genotype with mock inoculation. Annotation: 1: pure standard (HRMS, MS/MS, RT); 2: GNPS or in silico database (ISDB) mass spectra comparison; 3: comparison with published data (anthocyanins (Ieri et al. 2011), steroidal saponins and HCAAs (Parr et al. 2005; Huang et al. 2017); 4: HRMS (no MS/MS data available).

Ion mode	m/z	RT	Putative identity	Lady Christl		Lady Felicia		Erika		Gwenne		Cheyenne		**RRC**	**RRI**	**qRRI**	**Anno-ta-tions**
				M	P	M	P	M	P	M	P	M	P				
NI	147.0445	0.80	Cinnamic acid	3.21	1.76	2.14	1.04	1.70	1.09	3.66	2.39	2.14	1.00	**0.94**	**1.07**	**1.14**	**1**
NI	310.1092	2.94	trans-cinnamoyl-beta-D-glucoside	1.91	1.21	1.00	1.89	3.56	3.22	3.69	4.40	3.02	4.54	**2.35**	**2.61**	**1.11**	**4**
NI	341.0867	0.91	Caffeic acid 3-glucoside	5.10	9.24	2.33	5.64	10.47	5.22	3.02	3.82	1.00	0.00	**1.30**	**0.41**	**0.31**	**4**
NI	179.0346	1.65	Caffeic acid	3.12	1.00	2.45	1.72	2.51	2.74	3.13	3.07	3.29	2.73	**1.07**	**2.10**	**1.96**	**1**
NI	337.0920	1.42	Coumaroyl quinic acid	1.61	1.14	1.70	1.77	1.57	1.13	1.28	1.15	1.58	1.00	**0.89**	**0.75**	**0.84**	**4**
NI	337.0947	2.32	Coumaroyl quinic acid	1.83	1.18	2.65	2.10	1.92	1.08	2.21	1.36	1.38	1.00	**0.82**	**0.70**	**0.86**	**4**
NI	337.0949	2.42	Coumaroyl quinic acid	2.29	4.46	3.02	2.32	1.97	1.85	2.08	3.35	1.57	1.00	**0.71**	**0.61**	**0.86**	**4**
NI	319.0792	0.39	4-coumaroylshikimate	3.34	3.37	1.00	1.39	5.40	5.22	2.51	1.33	2.09	1.47	**1.54**	**1.12**	**0.73**	**4**
NI	335.0785	2.29	4-O-caffeoylshikimate	1.56	1.07	1.86	1.94	1.20	1.02	1.00	1.48	2.41	2.30	**0.90**	**1.06**	**1.19**	**4**
NI	335.0785	2.45	5-O-caffeoylshikimate	1.84	1.00	2.00	2.35	1.25	1.12	1.16	1.70	3.81	3.11	**1.08**	**1.18**	**1.09**	**4**
NI	353.0887	1.16	3-O-caffeoyl quinic acid	1.96	1.17	2.07	1.57	1.51	1.00	1.35	1.34	2.52	1.52	**0.89**	**0.94**	**1.05**	**2**
NI	707.1849	1.16	3-O-caffeoyl quinic acid dimer	6.13	1.20	6.53	3.81	3.02	1.00	2.26	2.42	10.68	3.16	**0.84**	**0.87**	**1.04**	**2**
NI	353.0887	1.59	5-O-caffeoyl quinic acid	1.40	1.10	1.90	1.90	1.62	1.00	1.80	1.87	2.56	2.10	**1.21**	**1.10**	**0.91**	**1**
NI	707.1849	1.62	5-O-caffeoyl quinic acid dimer	3.83	1.00	5.81	9.05	3.02	1.98	6.81	6.01	6.94	4.03	**1.16**	**0.80**	**0.69**	**2**
NI	353.0889	1.97	4-O-caffeoyl quinic acid	2.01	1.12	2.88	2.98	1.99	1.00	2.78	2.16	3.35	1.71	**1.11**	**0.79**	**0.72**	**2**
NI	515.1210	3.45	3,5-Dicaffeoylquinic acid	3.98	1.00	89.03	30.67	3.02	1.49	2.04	1.11	1.92	1.94	**0.05**	**0.10**	**1.91**	**4**
NI	515.1211	3.14	3,4-Dicaffeoylquinic acid	5.81	1.00	578.52	207.51	6.97	1.51	2.94	1.83	5.09	2.85	**0.02**	**0.02**	**1.15**	**4**
NI	193.0504	2.79	Ferulic acid	5.40	10.03	8.42	15.34	1.51	1.00	12.66	12.63	20.15	7.52	**1.66**	**0.56**	**0.34**	**1**
NI	367.1043	1.70	3-O-Feruloylquinic acid	4.62	4.17	6.44	7.20	1.78	1.18	1.78	1.58	2.63	1.00	**0.37**	**0.22**	**0.59**	**4**
NI	367.1045	2.30	5-O-Feruloylquinic acid	1.02	1.29	3.78	5.63	1.36	1.70	2.11	2.43	1.70	1.00	**0.72**	**0.49**	**0.69**	**4**
NI	367.1045	2.58	4-O-Feruloylquinic acid	1.37	1.00	1.61	2.27	1.56	1.07	1.96	2.82	4.37	3.39	**1.77**	**1.49**	**0.84**	**4**

NI	355.1050	1.49	1-O-Feruloyl-beta-D-glucose;1-O-p-Coumaroylglucoseβ-D-form3'-Methoxy	4.58	3.02	1.02	3.05	1.56	1.00	2.66	2.63	4.08	3.64	**0.99**	**0.80**	**0.81**	**4**
NI	249.1249	1.10	N-Caffeoylputrescine	1.00	24.16	2.15	17.05	5.60	15.57	1.84	13.43	1.72	1.95	**1.94**	**0.50**	**0.26**	**4**
NI	251.1405	0.80	N-dihydrocaffeoylputrescine	1.58	12.75	2.47	30.51	1.43	2.85	1.81	9.79	1.00	1.81	**0.70**	**0.22**	**0.32**	**4**
NI	379.1622	1.25	N,N'-Dicinnamoylputrescine(E,E)-form4''',4''''-Dihydroxy	1.09	1.27	1.00	1.39	1.55	1.02	2.18	1.85	2.63	1.13	**2.03**	**1.00**	**0.50**	**2**
NI	529.3047	1.45	N1,N12-bis(dihydrocaffeoyl) spermine	3.17	1.26	2.82	1.21	2.31	1.00	4.04	3.23	2.67	1.08	**1.00**	**1.43**	**1.43**	**3**
NI	527.2892	1.49	N-(caffeoyl, dihydrocaffeoyl) spermine	7.78	2.09	2.08	1.00	6.40	2.43	2.89	2.19	4.10	1.73	**0.91**	**1.37**	**1.51**	**3**
NI	691.3372	2.82	Tris(N1-caffeoyl,N4,N12-dihydrocaffeoyl) spermine	4.74	2.23	15.24	12.11	2.66	1.00	20.22	28.29	22.35	15.71	**1.51**	**2.09**	**1.39**	**3**
NI	691.3377	2.65	Tris(N1-caffeoyl,N4,N12-dihydrocaffeoyl) spermine	0.00	0.00	4.71	1.00	0.00	0.00	11.42	16.02	14.84	6.81	**3.72**	**15.22**	**4.09**	**3**
NI	693.3522	4.47	N1,N4,N12-tris(dihydrocaffeoyl) spermine	2.00	1.00	16.46	7.53	1.13	0.00	27.03	24.24	18.89	13.36	**1.70**	**2.94**	**1.73**	**3**
NI	693.3527	2.82	N1,N4,N12-tris(dihydrocaffeoyl) spermine	1.74	1.33	23.66	13.95	2.81	1.00	70.64	73.81	63.77	30.93	**3.60**	**4.61**	**1.28**	**3**
NI	857.4008	4.01	N1,N4,N9,N12-tetra(dihydrocaffeoyl) spermine	74.18	27.99	34.97	12.19	1.00	1.36	8.44	3.61	476.17	219.55	**2.97**	**3.72**	**1.26**	**3**
NI	470.2310	2.02	bis(N1-caffeoyl, N8-dihydrocaffeoyl) spermidine	1.29	1.00	4.92	3.40	8.11	4.17	2.94	3.11	1.58	1.34	**1.35**	**1.31**	**0.96**	**3**
NI	472.2466	1.98	N1,N8-bis(dihydrocaffeoyl) spermidine	2.32	1.11	13.76	10.08	17.84	11.25	9.08	8.72	3.33	1.00	**1.25**	**1.25**	**1.00**	**3**
NI	472.2466	2.79	N1,N8-bis(dihydrocaffeoyl) spermidine	2.19	1.30	11.48	8.03	14.23	7.41	5.39	5.64	1.40	1.00	**1.02**	**1.00**	**0.98**	**3**
NI	328.1201	2.93	N-feruloyloctopamine	1.71	1.32	1.00	1.49	2.74	2.62	2.76	3.83	2.63	3.47	**2.00**	**2.36**	**1.18**	**2**
NI	328.1202	3.19	N-feruloyloctopamine	2.02	2.16	1.00	2.10	3.07	3.17	3.24	4.74	2.57	4.03	**1.96**	**1.87**	**0.96**	**2**
NI	312.1253	3.92	N-Feruloyltyramine	1.95	6.80	1.00	5.71	5.79	4.43	8.18	9.65	1.50	1.05	**3.50**	**0.81**	**0.23**	**2**
NI	623.2419	5.77	Grossamide	2.80	4.77	1.00	4.49	3.54	3.70	2.64	4.80	1.12	1.13	**1.28**	**0.69**	**0.54**	**4**
NI	282.1145	3.69	p-Coumaroyltyramine	13.57	3.78	1.00	2.19	3.48	2.02	2.74	2.78	2.93	1.42	**0.42**	**0.69**	**1.66**	**4**
NI	343.1409	3.06	sinapoyltyramine	6.22	6.20	21.10	26.20	9.14	6.22	4.28	2.43	3.33	1.00	**0.41**	**0.20**	**0.49**	**4**
NI	609.1479	2.66	Quercetin 3-O-Rutinoside-	78.81	0.00	26.69	1.00	145.57	16.56	77.26	16.88	784.59	424.35	**305.19**	**47.94**	**0.54**	**2**
NI	771.2016	1.62	Quercetin 3-O-Rutinoside-7-glucoside	8.18	3.38	37.43	84.23	5.51	1.00	27.76	54.96	62.75	29.59	**0.65**	**0.46**	**0.47**	**2**

NI	755.1890	2.93	Quercetin 3-O-D-(2-O-trans-coumaroyl)-rutinoside	6.69	9.15	6.68	12.95	1.00	0.00	9.20	3.88	7.66	1.85	**0.17**	**0.19**	**0.24**	**2**
NI	625.1382	1.80	Quercetin Disaccharide	4.63	4.49	1.27	1.43	1.57	1.32	1.13	1.00	2.04	1.69	**0.45**	**0.84**	**0.83**	**2**
NI	593.1521	3.10	Kaempferol 3-O-Rutinoside	8.74	1.00	3.91	2.00	14.56	4.68	11.76	4.08	819.96	543.85	**122.91**	**2.76**	**0.66**	**2**
NI	755.2066	2.47	Kaempferol 3-O-rutinoside-7-glucoside	70.36	0.00	41.05	0.00	27.08	1.00	201.75	25.32	3177.98	1557.31	**#DIV/0!**	**#DIV/0!**	**0.49**	**2**
NI	447.0943	3.05	kaempferol 3-O-beta-D-galactoside	3.99	0.00	2.64	0.00	1.00	0.00	2.56	0.00	208.32	86.46	**#DIV/0!**	**#DIV/0!**	**0.42**	**2**
NI	739.1905	4.41	Kaempferol-3-O-D-(2-O-trans-coumaroyl)-rutinoside	3.69	0.00	3.01	0.00	2.02	0.00	7.19	1.00	767.71	356.06	**#DIV/0!**	**#DIV/0!**	**0.46**	**2**
NI	901.2439	3.89	Kaempferol-3-O-D-(2-O-trans-coumaroyl)-rutinoside-7-glucoside	6.57	0.00	4.03	0.00	1.00	0.00	8.61	0.00	349.23	265.54	**#DIV/0!**	**#DIV/0!**	**0.76**	**2**
NI	931.2545	4.10	Kaempferol Triglycosides	3.89	0.00	1.15	0.00	1.00	0.00	5.79	0.00	271.18	126.32	**#DIV/0!**	**#DIV/0!**	**0.47**	**4**
NI	591.1364	3.46	Kaempferol derivative	0.00	0.00	0.00	1.57	0.00	0.00	1.00	0.00	176.88	53.16	**22.52**	**#DIV/0!**	**0.30**	**4**
NI	753.1906	2.94	Kaempferol derivative	1.00	0.00	0.00	0.00	0.00	0.00	1.62	0.00	72.95	38.57	**#DIV/0!**	**#DIV/0!**	**0.53**	**4**
NI	1107.5263	4.02	Unknown saponin	132.98	44.48	84.06	80.64	117.50	71.29	4.23	1.00	32.91	14.69	**0.47**	**0.46**	**0.98**	**3**
NI	1107.5263	4.54	Unknown saponin	3.10	2.58	7.95	6.72	3.20	2.15	3.24	2.23	2.55	1.00	**0.54**	**0.39**	**0.71**	**3**
NI	1093.5457	4.70	Protodioscin/neoprotodioscin	1.71	1.00	2.37	1.35	4.72	3.03	4.28	2.48	25.85	10.85	**5.70**	**4.64**	**0.81**	**3**
NI	1079.5674	4.91	Saponin C51H86O21	2.29	0.00	51.76	29.28	36.93	22.38	2.60	1.01	3.15	1.00	**0.53**	**0.56**	**1.06**	**3**
NI	929.4785	7.06	Saponin C45H72O17	4.65	1.00	4.04	1.00	5.99	2.10	17.26	9.97	8.05	5.14	**2.40**	**5.74**	**2.39**	**3**
NI	929.4789	5.31	Saponin C45H72O17	5.77	1.00	4.39	1.06	7.32	2.75	23.94	12.90	18.36	6.62	**3.26**	**7.22**	**2.22**	**3**
NI	933.5029	5.26	C45H76O17 Saponin	24.55	1.00	28.01	4.99	74.22	35.80	82.48	46.42	84.57	45.29	**3.06**	**14.19**	**4.64**	**3**
NI	933.5093	5.67	C45H76O17 Saponin	1.28	0.00	33.29	17.07	33.99	15.56	1.00	0.00	1.04	0.00	**0.69**	**0.61**	**0.87**	**3**
NI	946.4127	4.98	unknonwn saponin	23.92	14.57	29.30	19.83	91.46	33.58	20.97	17.83	1.00	0.00	**1.42**	**1.00**	**0.70**	**3**
NI	917.5149	5.84	C45H76O16 Saponin	10.33	0.00	154.19	91.44	228.88	100.54	10.54	1.00	9.19	0.00	**1.01**	**0.74**	**0.73**	**3**
NI	128.0343	0.39	5-oxo-L-proline	3.01	4.00	1.18	2.92	3.72	3.98	2.37	2.92	1.00	1.04	**1.13**	**0.77**	**0.68**	**4**
NI	130.0864	0.50	Leucine	2.02	2.59	1.00	1.34	1.70	1.12	2.11	1.58	1.94	1.37	**1.27**	**0.69**	**0.55**	**4**
NI	132.0486	0.67	L-asparagine	1.74	1.51	1.68	3.10	2.23	1.76	2.36	2.15	2.03	1.00	**1.29**	**0.71**	**0.55**	**4**
NI	144.0294	0.48	2-oxoglutaramate	2.39	1.94	1.89	1.78	1.36	1.32	1.75	2.00	1.30	1.00	**0.69**	**0.77**	**1.12**	**4**
NI	146.0452	0.27	L-glutamate	2.70	2.20	1.53	1.49	2.40	1.68	1.75	1.81	1.00	1.01	**0.81**	**0.81**	**1.00**	**4**
NI	164.0711	0.80	Phenylalanine	2.80	1.52	2.04	1.08	1.86	1.00	3.13	2.42	1.97	1.02	**0.96**	**1.14**	**1.19**	**4**

NI	154.0616	0.25	Histidine	1.80	1.70	1.11	1.53	2.07	1.76	1.82	1.25	1.02	1.00	**1.13**	**0.83**	**0.73**	**4**
NI	133.0133	0.30	Malic acid	1.00	1.15	1.08	1.40	1.00	1.03	1.22	1.02	1.28	1.21	**1.12**	**0.85**	**0.76**	**4**
NI	147.0292	0.38	Citramalic acid	1.59	1.25	1.55	3.79	1.56	1.50	1.69	1.00	1.63	1.15	**1.04**	**0.48**	**0.47**	**4**
NI	137.0236	2.99	Salicylic acid	1.27	1.36	1.00	1.50	1.60	1.53	3.87	2.67	2.28	3.17	**2.28**	**1.71**	**0.75**	**4**
NI	187.0973	3.33	Azelaic acid	2.35	1.87	1.60	2.43	1.93	1.31	1.97	1.45	2.29	1.00	**1.04**	**0.58**	**0.56**	**4**
NI	299.0781	1.53	Salicylate 2-O-beta-D-glucoside	1.29	1.00	1.53	1.15	1.89	1.28	1.39	1.58	3.69	1.99	**1.65**	**1.51**	**0.91**	**4**
PI	852.5020	4.48	alpha-chaconine	1.65	1.00	1.97	1.57	1.83	1.33	1.85	1.53	1.77	1.00	**1.00**	**1.00**	**1.00**	**1**
PI	868.4966	4.41	alpha-solanine	3.17	2.13	3.40	2.92	3.55	2.68	2.68	2.27	1.00	1.09	**0.73**	**0.80**	**1.09**	**1**
PI	850.4870	4.29	Dehydrochaconine	3.13	1.00	6.09	3.63	10.04	1.98	6.48	2.91	50.82	13.87	**4.87**	**2.70**	**0.55**	**4**
PI	850.4864	3.79	Dehydrochaconine	3.70	1.32	6.19	2.49	4.41	1.40	4.61	1.40	2.96	1.00	**0.81**	**0.67**	**0.83**	**4**
PI	852.5081	5.52	alpha-chaconine isomer	2.04	1.47	2.26	2.35	3.69	2.45	1.85	2.12	1.00	1.53	**1.02**	**1.06**	**1.05**	**2**
PI	852.5092	6.94	alpha-chaconine isomer	1.91	1.44	2.20	2.14	3.28	2.28	1.85	2.11	1.00	1.77	**0.99**	**1.15**	**1.15**	**2**
PI	852.5110	7.23	alpha-chaconine isomer	2.28	1.54	2.72	2.25	3.22	2.63	1.76	2.50	1.00	1.52	**0.80**	**1.17**	**1.47**	**2**
PI	866.4814	4.37	Solanidadienol chacotriose	5.74	1.00	6.76	1.44	9.30	1.73	8.42	1.19	15.04	3.92	**1.75**	**1.87**	**1.07**	**3**
PI	866.4812	3.92	Solanidadienol chacotriose	5.33	1.72	5.45	4.16	8.86	3.08	8.68	3.61	2.90	1.00	**1.26**	**0.87**	**0.69**	**3**
PI	882.4944	4.24	solanidadienol solatriose	4.66	1.00	6.23	1.03	18.37	1.02	12.55	1.27	5.35	1.43	**2.22**	**1.22**	**0.55**	**3**
PI	414.3330	4.21	Solasodine	3.75	4.55	1.00	1.87	1.35	2.31	1.35	1.44	7.84	7.57	**1.48**	**1.18**	**0.79**	**2**
PI	414.3334	5.00	Solasodine	1.09	351.33	1.00	175.28	2.87	162.91	1.04	119.15	1.05	19.68	**1.58**	**0.38**	**0.24**	**2**
PI	910.5152	5.20	Leptine I	1.59	1.68	1.70	3.93	3.47	2.91	1.00	1.64	1.52	1.75	**1.21**	**0.75**	**0.62**	**2**
PI	910.5135	4.61	Leptine I	1.88	2.07	2.17	3.74	3.27	3.01	1.58	1.86	1.00	1.16	**0.96**	**0.69**	**0.72**	**2**
PI	1030.5505	4.24	Solanidene tetraose	7.06	4.77	6.74	6.06	8.80	7.58	4.78	3.18	2.42	1.00	**0.77**	**0.72**	**0.94**	**3**
PI	884.4913	3.95	Leptinine II or solasonine	5.00	2.37	5.03	3.11	10.58	1.92	13.14	1.76	3.06	1.00	**1.78**	**0.57**	**0.32**	**2**
PI	706.4515	4.60	beta-chaconine	1.32	19.26	1.27	6.82	4.58	7.25	1.29	5.42	1.00	1.60	**1.77**	**0.36**	**0.21**	**2**
PI	722.4409	4.38	beta-solanine	2.48	9.20	2.06	5.35	4.03	5.23	3.89	1.74	1.84	1.00	**1.43**	**0.37**	**0.25**	**2**
PI	560.3898	4.61	gamma-solanine/chaconine	1.53	2.51	1.90	1.81	2.53	1.76	1.70	1.88	1.60	1.00	**1.13**	**0.72**	**0.63**	**4**
PI	398.3377	5.55	Solanidine	1.14	8.10	1.00	8.60	2.52	7.32	2.43	3.35	1.12	1.98	**1.89**	**0.51**	**0.27**	**2**
PI	398.3379	4.48	Solanidine	2.89	2.18	4.33	3.31	4.10	3.61	3.03	2.36	1.72	1.00	**0.82**	**0.85**	**1.04**	**2**
PI	400.3519	5.82	Demissidine	5.15	7.13	1.50	7.26	19.25	4.70	23.09	6.37	1.00	1.75	**4.35**	**0.59**	**0.14**	**2**
PI	1047.5289	3.68	Steroidal saponin (C51H82O22)	69.36	27.81	57.19	69.28	270.31	126.52	7.48	1.00	24.26	12.02	**1.59**	**0.96**	**0.60**	**3**

PI	1047.5277	4.66	Steroidal saponin (C51H82O22)	2.50	2.47	2.37	2.30	1.97	1.00	2.23	1.30	9.66	3.92	**1.90**	**0.87**	**0.46**	**3**
PI	885.4950	3.86	Steroidal saponin	8.05	3.80	7.50	3.86	16.65	2.75	19.61	2.21	5.26	1.00	**1.78**	**0.52**	**0.29**	**3**
PI	885.4951	4.11	Steroidal saponin	4.93	4.32	2.29	1.58	3.43	1.40	4.96	1.00	5.45	2.30	**1.28**	**0.53**	**0.42**	**3**
PI	160.0955	0.72	Calystegine A3	1.84	1.54	5.30	2.81	5.81	3.47	1.80	1.00	18.35	16.17	**2.42**	**3.16**	**1.31**	**4**
PI	176.0919	0.49	Calystegine B2	1.77	1.30	4.92	1.87	5.61	3.61	1.22	1.00	8.38	4.09	**1.52**	**1.83**	**1.21**	**4**
PI	741.2172	1.38	pel 3-O-rut-5-O-glu	1.71	0.00	1.00	0.00	8.35	5.70	2.19	0.00	2191.25	1043.97	**541.95**	**#DIV/0!**	**#DIV/0!**	**3**
PI	579.1665	2.08	pel 3-O-rut	2.37	3.13	7.91	10.68	3.10	1.85	1.17	1.00	7.00	11.90	**0.73**	**0.71**	**0.97**	**3**
PI	903.2466	2.58	pel 3-O-caf-rut-5-O-glu	0.00	0.00	0.00	0.00	1.00	0.00	0.00	0.00	463.74	251.80	**#DIV/0!**	**#DIV/0!**	**#DIV/0!**	**3**
PI	887.2510	2.65	pel 3-O-cis-p-coum-rut-5-O-glu	1.00	0.00	0.00	0.00	0.00	0.00	0.00	0.00	1485.30	835.86	**990.20**	**#DIV/0!**	**#DIV/0!**	**3**
PI	887.2522	2.87	pel 3-O-p-coum-rut-5-O-glu	3.45	0.00	1.60	1.53	1.00	1.39	2.52	0.00	8761.31	5739.48	**1157.15**	**2505.97**	**2.17**	**3**
PI	917.2601	3.14	pel 3-O-ferul rut-5-O-glu	1.00	0.00	0.00	0.00	3.68	0.00	0.00	0.00	862.98	645.19	**577.77**	**#DIV/0!**	**#DIV/0!**	**3**
PI	917.2629	2.96	pel 3-O-ferul rut-5-O-glu	1.74	0.00	1.31	0.00	6.23	1.00	2.05	0.00	1798.58	2268.14	**394.95**	**#DIV/0!**	**#DIV/0!**	**3**
PI	947.2738	3.09	peo 3-O-ferul rut-5-O-glu	1.48	0.00	0.00	0.00	110.29	43.43	9.96	1.00	1846.91	814.68	**884.76**	**#DIV/0!**	**#DIV/0!**	**3**
PI	725.1999	3.03	pel 3-O-p-coum-rut	0.00	0.00	0.00	0.00	0.00	0.00	0.00	0.00	1.43	1.00	**#DIV/0!**	**#DIV/0!**	**#DIV/0!**	**3**
PI	755.1949	2.94	pel 3-O-ferul-rut	1.37	0.00	0.00	0.00	1.00	0.00	4.48	0.00	136.09	90.94	**68.93**	**#DIV/0!**	**#DIV/0!**	**3**
NI	221.0459	2.71	Isofraxidin	0.58	0.45	0.47	1.27	1.09	0.71	1.45	2.55	1.63	0.54	**2.22**	**1.28**	**0.58**	**2**
NI	310.1095	4.04	Longifolonine4'-Me ether	0.87	0.72	0.53	0.87	1.49	1.18	1.21	1.09	1.01	1.17	**1.60**	**1.35**	**0.84**	**2**
NI	380.1575	1.11	Zeatin(E)-form7-Î²-D-Glucopyranosyl	0.56	1.32	0.52	0.60	1.53	0.72	1.25	2.28	1.31	0.48	**2.15**	**1.10**	**0.51**	**2**
NI	461.1676	1.31	2-(4-Hydroxyphenyl)ethanolDi-O-Î²-D-glucopyranoside	0.30	0.28	0.43	0.37	1.13	1.50	1.01	2.38	2.81	1.03	**3.36**	**3.82**	**1.14**	**2**
NI	401.2193	5.28	11-Taxene-2,4,5,7,9,10,13,20-octol	0.42	0.77	0.68	0.81	1.11	0.77	1.41	1.28	1.57	1.44	**2.11**	**1.35**	**0.64**	**2**
NI	273.1717	4.20	7,7'-Oxybisheptanoic acid	0.63	5.61	0.43	0.30	1.52	1.15	1.12	0.23	1.50	0.30	**2.20**	**0.35**	**0.16**	**2**
NI	342.1358	4.01	Octopamine(S)-formÎ²-Me ether, N-(4-hydroxy-3-methoxy-E-cinnamoyl)	0.72	0.19	0.28	0.26	2.01	0.96	1.19	2.27	1.11	2.05	**2.38**	**5.63**	**2.37**	**2**
NI	221.0459	1.88	6,7,8-Trihydroxy-2H-1-benzopyran-2-one7,8-Di-Me ether	0.37	0.49	0.26	3.35	1.06	0.43	1.35	1.56	2.57	0.24	**3.89**	**0.51**	**0.13**	**2**
NI	359.0782	1.66	3-(3,4-Dihydroxyphenyl)-2-hydroxypropanoic acid(R)-form2-O-(3,4-Dihydroxy-Z-cinnamoyl)	0.94	0.24	1.17	0.97	0.63	1.13	1.30	1.49	1.02	1.37	**0.93**	**1.98**	**2.12**	**2**

NI	329.0679	2.75	3',4',5,7,8-Pentahydroxyflavone3',8-Di-Me ether	0.68	0.42	1.07	0.81	0.88	1.01	1.04	1.71	1.39	1.23	**1.21**	**1.86**	**1.54**	**2**
NI	153.0187	0.95	protocatechuic acid	0.73	0.28	1.04	0.75	0.92	1.12	0.95	1.73	1.42	1.38	**1.19**	**2.34**	**1.97**	**2**
NI	181.0452	1.71	dihydrocaffeic acid	1.49	0.41	1.32	0.70	0.40	1.22	1.95	1.05	0.26	1.85	**0.62**	**2.08**	**3.38**	**2**
NI	179.0346	1.65	3-(3,5-Dihydroxyphenyl)-2-propenoic acid(E)-form	1.01	0.32	0.83	0.66	0.86	1.35	1.33	1.52	1.00	1.38	**1.12**	**2.41**	**2.16**	**2**
NI	507.1508	3.23	4,7'-Epoxy-3',4',5,9'-tetrahydroxy-8,9-dinor-3,8'-lignan-7-oic acid(7'R,8'S)-form3',5-Di-Me ether, 4'-O-Î²-D-glucopyranoside	0.38	0.32	0.46	0.57	1.60	1.44	0.66	1.07	2.46	1.95	**2.81**	**2.71**	**0.96**	**2**
NI	461.1676	1.31	2-(4-Hydroxyphenyl)ethanolDi-O-Î²-D-glucopyranoside	0.30	0.28	0.43	0.37	1.13	1.50	1.01	2.38	2.81	1.03	**3.36**	**3.82**	**1.14**	**2**
NI	439.0867	0.31	3-Hydroxy-2-methyl-4H-pyran-4-oneO-[3,4,5-Trihydroxybenzoyl-(â†'6)-Î²-D-glucopyranoside]	1.24	0.97	0.34	0.34	1.53	1.36	1.07	1.31	0.98	1.17	**1.45**	**1.77**	**1.22**	**2**
PI	312.1206	2.95	Cularin alkaloid	0.80	0.55	0.23	0.54	1.88	1.32	1.15	1.36	1.24	1.39	**2.78**	**2.49**	**0.90**	**2**
PI	180.1383	0.90	2-(4-Aminophenyl)ethanolMe ether, N,N-di-Me	0.21	0.12	0.00	1.12	2.21	2.00	2.37	2.69	1.14	0.07	**18.58**	**2.57**	**0.14**	**2**
PI	193.1328	1.21	(2-Phenylethyl)ureaN',N'-Di-Me	0.97	0.89	0.31	1.58	1.38	0.54	1.30	1.00	1.20	1.10	**2.02**	**0.71**	**0.35**	**2**
PI	271.1136	1.30	FructoseÎ±-D-Furanose-formBenzyl glycoside	0.48	0.78	0.00	0.00	1.80	1.77	2.21	2.50	1.18	0.68	**7.25**	**4.21**	**0.58**	**2**
PI	382.1695	1.11	Zeatin(Z)-form9-Î²-D-Glucopyranosyl	0.53	0.78	0.38	0.98	1.36	0.92	1.84	2.44	1.17	0.32	**3.17**	**1.39**	**0.44**	**2**
PI	293.1203	4.53	3,4-Dihydro-2-methyl-2H-pyran-3,4-diol(2S,3R,4S)-form4-O-Î²-D-Glucopyranoside	0.53	0.66	0.86	1.15	1.10	1.22	1.01	1.32	1.63	0.73	**1.79**	**1.20**	**0.67**	**2**
PI	223.0941	6.23	3-(4-Hydroxy-3-methoxyphenyl)-2-propenoic acid(E)-formEt ester	0.53	1.20	0.35	4.61	1.89	0.00	1.31	0.82	1.22	0.27	**3.33**	**0.13**	**0.04**	**2**
PI	555.2346	2.94	Citrumarin B7-Me ether	0.41	0.97	0.42	1.71	1.63	0.76	1.39	1.53	1.43	0.30	**3.54**	**0.64**	**0.18**	**2**
PI	323.0716	1.51	3,3',4,4',5,5',7-Heptahydroxyflavan(2Î¾,3Î¾,4Î¾)-form	0.42	0.31	0.43	0.73	1.29	0.38	1.58	3.49	1.56	1.14	**3.49**	**3.22**	**0.92**	**2**
PI	223.0589	2.70	Isofraxidin	0.42	0.68	0.07	1.91	1.69	0.93	2.06	1.50	1.33	0.30	**6.88**	**0.70**	**0.10**	**2**
PI	537.2526	3.31	1,2,4,9-Tetrahydroxydihydro-Î²-agarofuran(1Î±,2Î²,4Î²,9Î²)-form1,9-Dibenzoyl, 2-Ac	0.20	0.00	0.16	1.60	2.63	4.09	1.30	0.83	1.51	0.15	**10.13**	**2.11**	**0.21**	**2**

PI	883.4665	5.19	3,23-Dihydroxy-30-nor-12,20(29)-oleanadien-28-oic acid3Î²-form3-O-[Î²-D-Xylopyranosyl-(1â†'2)-[Î²-D-glucopyranosyl-(1â†'3)]-Î±-L-arabinopyranoside]	0.38	0.00	1.03	0.37	1.11	0.25	1.48	1.91	1.14	4.57	**1.76**	**12.31**	**7.00**	**2**
PI	537.3056	7.26	Ixocarpalactone A2,3-Dihydro, 3Î²-methoxy	0.00	0.00	0.00	5.79	1.62	0.00	1.86	1.23	2.61	0.84	**100.00**	**0.24**	**0.00**	**2**
PI	529.3	1.60	3,13,19-Trihydroxy-1,6,10,14-phytatetraen-16-oic acid(3S,6Z,10E,14E)-formMe ester, 3-O-Î²-D-glucopyranoside	0.31	0.77	0.78	0.24	1.28	2.50	1.04	0.90	1.85	1.09	**2.55**	**2.96**	**1.16**	**2**
PI	272.2568	6.94	2-Amino-4-hexadecene-1,3-diol	1.08	0.77	0.73	0.76	1.07	1.25	1.08	1.14	1.05	1.12	**1.18**	**1.52**	**1.29**	**2**
PI	171.0286	0.72	gallic acid	0.78	0.21	1.40	0.56	1.06	1.31	0.77	2.15	1.03	1.21	**0.88**	**4.04**	**4.59**	**2**
PI	166.0708	0.54	Xylonic acidD-formAmide	0.76	0.73	0.77	0.56	0.99	1.18	1.10	1.02	1.44	1.64	**1.54**	**1.98**	**1.28**	**2**
PI	429.1368	0.73	Xylonic acidD-formAmide	0.86	0.91	1.04	0.51	0.89	1.38	0.50	1.20	1.91	1.09	**1.16**	**1.72**	**1.49**	**2**
PI	217.1552	0.73	4,11-Eudesmadien-3-ol3Î±-form1,2-Didehydro, 3-ketone	0.36	0.00	0.00	0.95	0.53	1.56	6.95	1.67	0.81	1.21	**15.50**	**3.12**	**0.20**	**2**
PI	399.2514	7.37	3-Hydroxy-9(11),15-kauradien-19-oic acid(ent-3Î±)-formTigloyl	0.84	0.63	0.36	0.66	0.88	1.82	2.70	1.04	0.77	1.03	**2.41**	**2.01**	**0.83**	**2**
PI	352.2224	2.63	SpermidineN-(4-Hydroxy-3,5-dimethoxycinnamoyl)	0.00	0.00	0.00	0.00	100.00	2.31	0.00	1.50	0.00	2.26	**100.00**	**100.00**	**#DIV/0!**	**2**

5. Antifungal Natural Products against Colletotrichum coccodes and Helminthosporium solani and post-harvest control of potato blemish diseases by anthraquinone and curcuminoid-rich plant extracts

Josep Massana-Codina, Sylvain Schnee, Emerson Ferreira Queiroz, Laurence Marcourt, Stéphanie Schürch, Katia Gindro and Jean-Luc Wolfender

This chapter is based on an original research article that will be submitted to Journal of Agricultural and Food Science with minor modifications. All references are compiled in a common list at the end of the thesis.

5.1. Abstract

Screening plant extracts for antifungal activity against two phytopathogens causing blemish diseases in potatoes (*Colletotrichum coccodes* and *Helminthosporium solani*) resulted in the selection of the methanolic crude extracts of *Curcuma longa* rhizomes and *Rheum palmatum* roots, and the aqueous extract of *Frangula alnus* bark. Bio-guided isolation of the antifungal compounds was performed on these plant extracts and revealed that frangulin B and curcumin were respectively the main antifungal compounds of *F. alnus* bark and *C. longa* rhizomes, respectively. Furthermore, several anthraquinones and phenylpropanoid derivatives isolated from *R. palmatum* roots exhibited fungicidal activities. Post-harvest treatment of potatoes with *C. longa* and *F. alnus* extracts resulted in the satisfactory control of both diseases under high disease pressure conditions. The potential use of plant extracts as post-harvest treatments of potatoes is discussed.

5.2. Introduction

Black dot and silver scurf are two blemish diseases of potato tubers (*Solanum tuberosum* L., *Solanaceae*) with similar disease symptoms affecting the tuber skin (Errampalli et al., 2001b; Lees and Hilton, 2003). They had been considered minor diseases in the past, but recently, the fresh potato market has shifted to pre-packed washed potato tubers, which provides an excellent environment for the sporulation of the fungal pathogens and blemish diseases become more apparent, reducing tuber quality. Indeed, the economic importance of both diseases has risen, and it has been estimated that they represent £5 million in losses in the UK alone (Lees and Hilton, 2003). Chemical control of seed-tubers or soil fumigation before planting are partially effective in the control of these two diseases (Denner et al., 1997, 2000; Tsror (Lahkim) and Peretz-Alon, 2004), but potato tubers are often contaminated at harvest since these methods do not fully control the diseases. Furthermore, storage of potatoes for several months may result in higher disease severity, and pre-storage and storage conditions influence the development of both diseases (Firman and Allen, 1993; Hide et al., 1994b; Frazier et al., 1998; Peters et al., 2016). Potatoes are usually harvested a few weeks after haulm destruction, a time that allows the potato tuber to adhere the skin to the flesh (a process called skin-set), and a curing step that allows the tuber to suberize and heal from wounds produced at harvest is required to endure storage at low temperatures. Short curing period has been shown to be efficient in controlling black dot (Peters et al., 2016), but silver scurf is better controlled with longer curing periods (Hide et al., 1994b, 1994a). Notably, control measures often result in reduced levels of one disease and increased levels of the other (Lees and Hilton, 2003), i.e. controlling silver scurf with the chemical fungicide imazalil results in higher severity of black dot (Hide and Hall, 1993). Chemical post-harvest treatments of potatoes for the fresh market should be avoided due to possible occurrence of residues with potential health toxicity. To date, no satisfactory method is established to control both diseases during growing season and post-harvest storage and more efficient control strategy must be investigated.

Plant extracts have been previously shown to possess antifungal activity against phytopathogenic fungi (Schnee et al., 2013; Bhagwat and Datar, 2014) and to control plant diseases under field conditions (Krebs et al., 2006; Gillmeister et al., 2019). Crude extracts from diverse plant species possess antifungal activities to numerous plant pathogens *in vitro*, including the causal agent of black dot, *C. coccodes* (Bhagwat and Datar, 2014; González-Álvarez et al., 2016; Confortin et al., 2019). Furthermore, essential oils from various plant species exhibit antifungal activities against *H. solani,* the causal agent of silver scurf (Bång, 2007; Al-Mughrabi et al., 2013). Anthracnose in fruits, which is caused by diverse *Colletotrichum* species, has been controlled with the post-harvest application of plant extracts, such as garlic or ginger aqueous extracts (Cruz et al., 2013; Alves et al., 2015), and post-harvest treatments of plant extracts in potatoes have been used to control soft rot, caused by the

bacterial pathogen *Erwinia carotovora*, with control efficacies of 20 to 80% (Bdliya and Dahiru, 2006; Rahman et al., 2012; Viswanath et al., 2018). However, the antifungal activity of plant extracts and natural products (NPs) against both *C. coccodes* and *H. solani* has not been studied *in vitro* nor *in planta*. Since there might be competition between both fungal pathogens in potato tubers and their symptoms are very similar (Lees and Hilton, 2003), a post-harvest treatment to control both diseases at the same time during storage arises as an interesting approach. Here, we present an antifungal *in vitro* screening against *C. coccodes* and *H. solani* of several plant extracts selected based on several criteria for their potential use as post-harvest application on potato tubers. The screening resulted in the selection of three plant extracts for bio-guided isolation (Schnee et al., 2013) of their active compounds and determination of their antifungal activity. Furthermore, the control of black dot and silver scurf on potato tubers during long period storage with these three plant extracts is studied.

5.3. Material and methods

General experimental procedures

NMR spectroscopic data were recorded on a Bruker Avance III HD 600 MHz NMR spectrometer equipped with a QCI 5 mm Cryoprobe and a SampleJet automated sample changer (Bruker BioSpin, Rheinstetten, Germany). Chemical shifts are reported in parts per million (δ) using the residual CD3OD signal (δH 3.31; δC 49.0) or DMSO-d6 signal (δH 2.50; δC 39.5) as internal standard for 1H and 13C NMR, respectively and coupling constants (J) are reported in Hz. The complete assignment was performed based on two-dimensional experiments (COSY, ROESY, HSQC and HMBC). High-resolution mass spectrometry data were obtained on a Micromass LCT Premier Time-Of-Flight (TOF) mass spectrometer from Waters with an electrospray ionization (ESI) interface (Waters, Milford, MA) or a Q-Exactive Focus mass spectrometer using heated electrospray ionization (HESI-II) source (Thermo Scientific, Bremen, Germany). Analytical reverse-phase analyses were performed on high-performance liquid chromatography (HPLC) Agilent 1260 Infinity II LC system consisting of a degasser, a mixing pump, an autosampler, and a diode array detector (PDA) (Agilent Technologies, Santa Clara, USA) connected to an evaporative light scattering detector (ELSD) Sedex LT-ELSD 85 (Sedere, Oliver, France). Crude extract profiling was carried out on a ultra-high-pressure liquid chromatography (UHPLC) Vanquish Horizon UHPLC System consisting of a degasser, a mixing pump, an autosampler, a diode array detector (PDA) and a Vanquish Charged Aerosol Detector (CAD) (ThermoFisher, Waltham, MA, USA). Flash Chromatography was performed on a preparative chromatographic system using Büchi sepacore system equipment (Büchi, Flawil, Switzerland).

Plant material

Powder-ground material of Aloe vera leaves, Rheum palmatum roots, Frangula alnus bark, Urtica dioica leaves, Salix viminalis plants, Equisetum arvense plants, Epilobium sp. flowers, Hypericum perforatum herbs, Artemisia sp. plants and Curcuma longa rhizomes were purchased from Dixa (St. Gallen, Switzerland). Vitis vinifera canes had been previously collected from the experimental untreated plots of Agroscope ACW (Nyon, Switzerland) (Schnee et al., 2013). All plant material was stored as a powder in sealed plastic boxes at 20 °C in the dark until use.

Extraction

Powder-ground plant tissues were extracted at 20% w/v using three different methods: (1) aqueous extraction in nanopure water by stirring for three hours at room temperature (AE), (2) aqueous extraction in nanopure water at 80-100°C in reflux for 10 minutes (AER) and (3) methanolic extraction by stirring for three hours at room temperature (ME). The resulting extracts were then centrifuged (4000 rpm, 10 min, 20°C) and the supernatants were filtered under vacuum through 9 cm 589/3 cellulose filters (Schleicher & Schuell, Dassel, Germany). The ME was then dried under vacuum on a rotary evaporator, and the resulting extract solubilized in 100 mL nanopure water using an ultrasonic

bath. All aqueous solutions were then freeze-dried. The yields of the different extracts are summarized in Table S1. The dry extracts were stored in sealed plastic boxes at room temperature and darkness.

UHPLC-DAD-CAD analysis

The methanolic extracts of *R. palmatum* and *C. longa*, as well as the aqueous extract of *F. alnus*, were analyzed by reverse phase UHPLC with UV and CAD detection using an XSelect C_{18} column (150 x 3.0 mm i.d., 5 µm particle size; Waters, Milford, MA, USA) using a mobile phase consisting of nanpoure water (A) and acetonitrile (B) with both solvants containing 0.1% formic acid; separation was performed with a step gradient from 5% B to 20% B in 15 minutes, from 20 to 40% B in 15 minutes, from 40% B to 100% B in 5 minutes and held at 100% B for 3 minutes; Flow rate: 0.6 mL/min; injection volume: 4 µL. The extracts were diluted at 5 mg/mL in 50:50 methanol:water. The DAD/UV detection was recorded at 210, 254, 280, 350 and 435 nm. CAD conditions are the following: evaporator temperature set at 35°C and the Data Collection Rate set at 10 Hz.

HPLC-DAD-ELSD analysis

The active extracts and fractions were analyzed by reverse phase HPLC with UV and ELSD detection on a X-Bridge C_{18} column (250 x 4.6 mm i.d., 5 µm; Waters, Milford, MA, USA) using a mobile phase consisting of nanopure water (A) and methanol or acetonitrile (B) with both solvants containing 0.1% formic acid; separation was performed with step gradients specifically determined for each extract as described below; flow rate: 1 mL/min; injection volume: 20 µL. The samples were diluted in methanol at 5 mg/mL. The UV detection was recorded at 210, 254, 280 350 and 435 nm. ELSD conditions were fixed at 55 °C, 3.1 bar N_2 and gain 8.

UHPLC-HRMS/MS analysis

Chromatographic separation was performed on a Waters Acquity UPLC system interfaced to a Q-Exactive Focus mass spectrometer (Thermo Scientific, Bremen, Germany), using heated electrospray ionization (HESI-II) source. Thermo Scientific Xcalibur 3.1 software was used for instrument control. The LC conditions were as follows: column, Waters BEH C18 50 × 2.1 mm, 1.7 µm; mobile phase, (A) water with 0.1% formic acid; (B) acetonitrile with 0.1% formic acid; flow rate, 600 µL·min−1; injection volume, 2 µL; gradient, linear gradient of 5−100% B over 7 min and isocratic at 100% B for 1 min. The optimized HESI-II parameters were as follows: source voltage, 3.5 kV (pos); sheath gas flow rate (N2), 55 units; auxiliary gas flow rate, 15 units; spare gas flow rate, 3.0; capillary temperature, 350.00°C, S-Lens RF Level, 45. The mass analyzer was calibrated using a mixture of caffeine, methionine–arginine–phenylalanine–alanine–acetate (MRFA), sodium dodecyl sulfate, sodium taurocholate, and Ultramark 1621 in an acetonitrile/methanol/water solution containing 1% formic acid by direct injection. The data-dependent MS/MS events were performed on the three most intense ions detected in full-scan MS (Top3 experiment). The MS/MS isolation window width was 1 Da, and the stepped normalized collision energy (NCE) was set to 15, 30 and 45 units. In data-dependent MS/MS experiments, full scans were acquired at a resolution of 35,000 FWHM (at m/z 200) and MS/MS scans at 17,500 FWHM both with an automatically determined maximum injection time. After being acquired in a MS/MS scan, parent ions were placed in a dynamic exclusion list for 2.0 s.

LC-MS/MS Data Processing

LC-MS/MS data files were analyzed by MzMine 2.36 (Pluskal et al., 2010) after converting the ThermoRAW data files to the open MS format (.mzXML) using the MSConvert software from the ProteoWizard package (Chambers et al., 2012). Briefly, masses were detected (both MS1 and MS2 in a single file) using the centroid mass detector with the noise level set at 1.0E6 for MS1 and at 1.0E1 for MS2. Chromatograms were built using the ADAP algorithm, with the minimum group size of scans set at 5, minimum group intensity threshold at 1.0E6, minimum highest intensity was at 1.0E6 and m/z tolerance at 5.0 ppm. For chromatogram deconvolution, the algorithm used was the wavelets (ADAP).

The intensity window S/N was used as S/N estimator with a signal to noise ratio set at 25, a minimum feature height at 100,000, a coefficient area threshold at 100, a peak duration ranges from 0.02 to 0.9 min and the RT wavelet range from 0.02 to 0.05 min. Isotopes were detected using the isotopes peaks grouper with a m/z tolerance of 5.0 ppm, a RT tolerance of 0.02 min (absolute), the maximum charge set at 2 and the representative isotope used was the most intense. Peak alignment was performed using the join aligner method (m/z tolerance at 5 ppm), absolute RT tolerance 0.1 min, weight for m/z at 20 and weight for RT at 20. The peak list was gap-filled with the same RT and m/z range gap filler (m/z tolerance at 5 ppm). Only features possessing MS2 spectra were kept to build molecular networks using the peak-list rows filter option from the original peaklist, which yielded 514 features in negative ionization mode and 1606 in positive ionization mode.

Molecular networking parameters

A molecular network (MN) was created with the Feature-Based Molecular Networking (FBMN) workflow (Nothias et al., 2019) on GNPS (Wang et al., 2016) (www.gnps.ucsd.edu). The mass spectrometry data were first processed with MZmine (as described above) and the results were exported to GNPS for FBMN analysis. The precursor ion mass tolerance was set to 0.02 Da and the MS/MS fragment ion tolerance to 0.02 Da. A molecular network was then created where edges were filtered to have a cosine score above 0.7 and more than 6 matched peaks. Further, edges between two nodes were kept in the network if and only if each of the nodes appeared in each other's respective top 10 most similar nodes. Finally, the maximum size of a molecular family was set to 100, and the lowest scoring edges were removed from molecular families until the molecular family size was below this threshold. The spectra in the network were then searched against GNPS spectral libraries (Horai et al., 2010; Wang et al., 2016). The library spectra were filtered in the same manner as the input data. All matches kept between network spectra and library spectra were required to have a score above 0.7 and at least 6 matched peaks. The DEREPLICATOR was used to annotate MS/MS spectra (Mohimani et al., 2018). The molecular networks were visualized using Cytoscape 3.6 software (Shannon et al., 2003). The GNPS job parameters and resulting data are available at the following addresses: (http://gnps.ucsd.edu/ProteoSAFe/status.jsp?task=45f63d972dfb40529121a7f3f140e492 and http://gnps.ucsd.edu/ProteoSAFe/status.jsp?task=4e255438b1b24a67b03c9759e6e9541f).

UHPLC-TOF-HRMS analysis.

Ultra-high performance liquid chromatography coupled to Time of Flight (UHPLC-TOF) HRMS was used to monitor pure compounds according to standard protocol previously described (Brillatz et al., 2018, 2020).

SPE Fractionation.

Solid Phase Extraction fractionation of crude extracts was carried out using a 70mL/10 grams Chromabond C18 SPE column with 45 µm particle size (Macherey-Nagel, Düren, Germany). The sample deposited in the top of the SPE column. For this, 500 mg of crude extract was mixed with 500 mg of ZEOprep C18 silica (15−25 µm, Zeochem AG, Uetikon am See, Switzerland). This mixture was deposited on the top of the SPE cartridge. A mixture of 0.1% formic acid in H_2O (A) and 0.1% formic acid in MeOH (B) was used as mobile phase. The fractionation of the methanolic extracts of *R. palmatum* roots and *C. longa* rhizomes was performed using the following step gradient: 100 mL at 30% of B resulting in Fraction 1, 100 mL at 50% of B (Fraction 2), 100 mL at 80% of B (Fraction 3) and 100 mL at 100% of B (Fraction 4). After collection, fractions were evaporated and dried under N_2 stream. All fractions were analyzed by UHPLC-PDA/CAD and tested in the antifungal bioassay. The separation of the *F. alnus* bark aqueous extract was performed using a volume of 100 mL of the following step gradient: 10% B (Fraction 1), 30% B (Fraction 2), 50% B (Fraction 3), 65% B (Fraction 4), 80% B (Fraction 5) and 100% B

(Fraction 6). After collection, fractions were evaporated and dried under N_2 stream. All fractions were analyzed by HPLC-PDA and tested in the antifungal bioassay.

Fractionation and purification of the R. palmatum methanolic extract.

The 80% methanol fraction (Fraction 3) of the R. palmatum methanolic extract was first analyzed on an HPLC in analytical scale to determine the optimal conditions of separation using an XBridge C_{18} column (250 x 4.6 mm i.d., 5 µm; Waters, Milford, MA, USA) with 0.1% formic acid in water (A) and 0.1% formic acid in methanol as mobile phase, a flow rate of 1 mL/min and the following gradient: held at 40% B for 6 minutes, 40% B to 55% B in 80 minutes, 55% B to 80% B in 22 mins, 80 to 100% B in 5 mins and held at 100% B for 16 mins. After applying the geometrical gradient transfer (Challal et al., 2015) to the semi-preparative scale, 35 mg of the SPE Fraction 3 was separated using a semi-preparative HPLC system (Shimadzu, Kyoto, Japan) equipped with a LC-20AP preparative pump, UV detector and a fraction collector. The separation was performed using an XBridge C_{18} column (250 x 19 mm i.d., 5 µm; Waters, Milford, MA, USA) with 0.1% formic acid in water (A) and 0.1% formic acid in methanol with a flow rate of 17 mL/min. Only relevant peaks detected on the UV chromatogram were collected in 10 mL aliquots and dried under a GeneVac HT-4X Series II system (Genevac Limited, UK). This separation allowed the isolation of the compounds: **4** (2.6 mg), **5** (1.0 mg), **6** (1.2 mg), **7** (0.60 mg), **8** (0.65 mg), **9** (1.7 mg) and **10** (0.7 mg).

Fractionation and purification of the F. alnus aqueous extract.

The aqueous extract of *F. alnus* bark was first separated at the analytical scale to determine the best conditions for separation of its components using an HPLC C_{18} reverse phase column (250 x 4.6 mm i.d., 15 µm; Interchim, Montluçon Cedex, France) with a gradient of 0.1% formic acid in water (A) and 0.1% formic acid in methanol (B) as mobile phase and the following gradient: 5% B to 50% B in 10 minutes, 50%B to 70% B in 45 minutes, 70% B to 100% B in 5 minutes and held at 100% for 5 minutes. After geometrical gradient transfer (Challal et al., 2015), the *F. alnus* AE (50 g) was separated in a Flash chromatography System (Sepacore Control software) using a twon pump (module C-605) equipped with a UV detector (UV photometer C-640) and a fraction collector (Fraction Collector C-620) (Buchi, Flawil, Switzerland) with a Flash column (60 × 230 mm i.d., 15 µm particle size, Interchim PF-15 C18 HP, Interchim, Montluçon Cedex, France). A dry load (Queiroz et al., 2019) was prepared using 50 grams of crude extract mixed with ZEOprep C18 silica (15−25 µm, Zeochem AG, Uetikon am See, Switzerland) and sand (Sigma-Aldrich, St. Louis, MI, USA), and separated using a mixture of 0.1% formic acid in nanopure water(A) and 0.1% formic acid in methanol (B) at a flow rate of 40 mL/min with the following gradient: held at 5% B for 22 mins, 5 to 50% of B in 57 mins, 50 to 70% of B in 152 mins, 70 to 100% B in 38 mins and 100% B for 38 mins. 48 fractions of 250 mL each were collected and fractions from 13 to 48 tested in the antifungal assay at 5 mg/mL. Fractions 39-41 showed antifungal activity and were further purified by semi-preparative HPLC-UV (100 mg) after optimization on an analytical scale using a semi-preparative HPLC-UV system (Shimadzu, Kyoto, Japan) equipped with a LC-20AP preparative pump, UV detector and a fraction collector. The separation was performed using an XBridge C_{18} column (250 x 19 mm i.d., 5 µm; Waters, Milford, MA, USA) with 0.1% formic acid in water (A) and 0.1% formic acid in acetonitrile with a flow rate of 17 mL/min and the following gradient: 5%B to 20% B in 2 minutes, 20 to 31% B in 8 minutes, held at 31% B for 52 minutes, 31% B to 60% B in 18 minutes, 60% B to 10% B in 5 minutes, 100% B for 15 minutes. Only relevant peaks detected on the UV chromatogram were collected in 10 mL aliquots and dried under a GeneVac HT-4X Series II system (Genevac Limited, UK). This separation allowed the isolation of three pure compounds: **12** (2.5 mg), **13** (2.0 mg), **14** (5.2 mg) and **15** (8.5 mg).

Emodin 8-O-[β-D-glucopyranosyl-(1→5)-O-β-D-apiofuranoside] (**12**). ^{1}H NMR (CD_3OD, 600 MHz) δ 2.46 (3H, s, CH_3-3), 3.25 (1H, dd, *J* = 9.2, 7.8 Hz, Glc-2), 3.37 (3H, m, Glc-3, Glc-4, Glc-5), 3.69 (1H, m, Glc-6''),

3.71 (1H, d, *J* = 10.5 Hz, Api-5''), 3.90 (1H, d, *J* = 12.4 Hz, Glc-6'), 3.97 (1H, d, *J* = 9.9 Hz, Api-4''), 4.02 (1H, d, *J* = 10.5 Hz, Api-5'), 4.19 (1H, d, *J* = 9.9 Hz, Api-4'), 4.34 (1H, d, *J* = 7.8 Hz, Glc-1), 4.41 (1H, d, *J* = 3.2 Hz, Api-2), 5.74 (1H, d, *J* = 3.2 Hz, Api-1), 6.89 (1H, d, *J* = 2.5 Hz, H-7), 7.15 (1H, s, H-2), 7.43 (1H, d, *J* = 2.5 Hz, H-5), 7.64 (1H, s, H-4); ^{13}C NMR (CD_3OD, 151 MHz) δ 22.1 (CH_3-3), 62.7 (Glc-6), 71.6 (Glc-4), 72.1 (Api-5), 75.0 (Glc-2), 76.3 (Api-4), 78.0 (Glc-3), 78.1 (Glc-5), 78.9 (Api-2), 79.5 (Api-3), 104.8 (Glc-1), 108.6 (Api-1), 110.2 (C-5), 110.3 (C-7), 112.1 (C-8a), 114.8 (C-9a), 122.0 (C-4), 125.3 (C-2), 150.2 (C-3), 165.5 (C-6/8), 165.9 (C-6/8), 182.9 (C-10).

6,8-O-β-D-glucopyranoside, O-α-L-rhamnopyranoside emodin dianthrone (**13**). ^{1}H NMR (CD_3OD, 600 MHz) δ 1.27 (3H, d, *J* = 6.2 Hz, Rha-6), 2.20 (3H, s, CH_3-3/3'), 2.21 (3H, s, CH_3-3'/3), 3.45 (2H, m, Glc-3, Glc-5), 3.50 (2H, m, Rha-4, Glc-4), 3.62 (2H, m, Rha-5, Glc-2), 3.78 (1H, dd, *J* = 12.0, 5.2 Hz, Glc-6''), 3.86 (1H, dd, *J* = 9.5, 3.5 Hz, Rha-3), 3.99 (1H, dd, *J* = 12.0, 2.1 Hz, Glc-6'), 4.10 (1H, dd, *J* = 3.5, 1.8 Hz, Rha-2), 4.47 (1H, d, *J* = 3.4 Hz, H-10/10'), 4.56 (1H, d, *J* = 3.4 Hz, H-10/10'), 4.77 (1H, d, *J* = 7.7 Hz, Glc-1), 5.68 (1H, s, Rha-1), 5.85 (1H, s, H-4/4'), 5.92 (1H, s, H-4/4'), 6.28 (1H, d, *J* = 2.2 Hz, H-7'), 6.38 (1H, s, H-5'), 6.58 (1H, s, H-2/H-2'), 6.60 (1H, s, H-2/H-2'), 6.79 (1H, d, *J* = 2.3 Hz, H-5), 7.28 (1H, d, *J* = 2.3 Hz, H-7); ^{13}C NMR (CD_3OD, 151 MHz) δ 30.4 (Rha-6), 56.8 (C-10/10'), 57.7 (C-10'/10), 62.2 (Glc-6), 70.9 (Rha-5, Glc-4), 71.4 (Rha-2), 71.7 (Rha-3), 73.3 (Rha-4), 74.4 (Glc-2), 77.4 (Glc-3), 78.4 (Glc-5), 99.5 (Rha-1), 102.5 (C-7'), 104.4 (Glc-1), 106.2 (C-7), 109.5 (C-5'), 112.9 (C-5), 117.1 (C-2/2'), 117.4 (C-2'/2), 118.7 (C-8a), 121.5 (C-4/4'), 122.2 (C-4'/4), 161.4 (C-8/6), 162.1 (C-6/8).

Di-rhamnoside, mono-glucoside emodin dianthrone (**14**). ^{1}H NMR (CD_3OD, 600 MHz) δ 1.22 (3H, d, *J* = 5.7 Hz, Rha-6'), 1.27 (3H, d, *J* = 6.1 Hz, Rh-a6), 2.29 (3H, s, CH_3-3'), 2.30 (3H, s, CH_3-3), 3.46 (1H, dd, *J* = 9.8, 8.6 Hz, Glc-4), 3.51 (5H, m, Glc-2, Glc-5, Rha-4, Rha-4', Rha-5'), 3.61 (2H, m, Rha-5, Glc-3), 3.77 (1H, dd, *J* = 12.2, 5.2 Hz, Glc-6''), 3.81 (1H, dd, *J* = 9.1, 3.5 Hz, Rha-3'), 3.83 (1H, dd, *J* = 9.5, 3.6 Hz, Rha-3), 3.95 (1H, dd, *J* = 12.2, 2.3 Hz, Glc-6'), 4.02 (1H, dd, *J* = 3.6, 1.8 Hz, Rha-2), 4.12 (1H, dd, *J* = 3.5, 1.8 Hz, Rha-2'), 4.59 (2H, d, *J* = 4.0 Hz, H-10), 4.60 (1H, d, *J* = 4.0 Hz, H-10'), 4.72 (1H, d, *J* = 7.7 Hz, Glc-1), 5.50 (1H, s, Rha-1), 5.66 (1H, d, *J* = 1.8 Hz, Rha-1'), 6.64 (1H, d, *J* = 2.3 Hz, H-7'), 6.69 (1H, s, H-2), 6.69 (1H, s, H-2'), 7.14 (1H, d, *J* = 2.4 Hz, H-7); ^{13}C NMR (CD_3OD, 151 MHz) δ 18.2 (Rha-6'), 18.3 (Rha-6), 21.9 (CH_3-3), 22.0 (CH_3-3'), 56.6 (C-10'), 57.9 (C-10), 62.4 (Glc-6), 71.1 (Glc-4), 71.2 (Rhae5, Rha-5'), 71.7 (Rha-2, Rha-2'), 72.1 (Rha-3, Rha-3'), 73.5 (Rha-4), 73.6 (Rhaee4'), 75.0 (Glc-2), 77.2 (Glc-3), 78.7 (Glc-5), 99.5 (Rha-1, Rha-1'), 103.7 (C-7'), 106.1 (Glc-1), 108.2 (C-7), 111.3 (C-5'), 112.3 (C-5), 113.1 (C-8'a), 115.7 (C-9'a), 117.6 (C-2), 118.0 (C-2'), 118.3 (C-9a), 118.8 (C-8a), 122.1 (C-4), 122.8 (C-4'), 147.9 (C-3), 148.6 (C-3'), 161.5 (C-8), 162.3 (C-1), 163.0 (C-1'), 163.3 (C-8'), 165.3 (C-6'), 188.6 (C-9/9'), 191.6 (C-9/9').

Chemicals.

The anthraquinones emodin, aloe-emodin, rhein, frangulin A and frangulin B were purchased from Carl Roth Gmbh (Carl Roth Gmbh, Karlsruhe, Germany). Curcumin, demethoxycurcumin and bisdemethoxycurcumin were purchased from Sigma-Aldrich (Sigma-Aldrich, St Louis, MO, USA).

In vitro Antifungal assay against Colletotrichum coccodes and Helminthosporium solani.

The fungal pathogens *Colletotrichum coccodes* (Wallr.) S. Hugues and *Helminthosporium solani* Durieu & Mont. were grown in PDA plates for 2 and 4 weeks, respectively, in order to provide mycelial material and conidia for the bioassays. Plant extracts were tested *in vitro* in a poisoned food method (Ali-Shtayeh and Abu Ghdeib, 1999). Briefly, crude extracts were dissolved in ethanol or DMSO (1% and 5% v/v final concentration, respectively) and added to the liquid culture media (PDB, potato dextrose broth, Difco) to obtain final concentrations of 1, 5 and 10 mg/mL. Solutions were then distributed in a 24-well plate in triplicates. Positive control was prepared by mixing an ethanol or DMSO solution to the media culture (1% and 5% v/v, respectively) and negative control by adding the commercially available fungicide Amistar (250g/L azoxystrobin, Syngenta, Basel, Switzerland) to the culture media (final concentration of 5mg/mL azoxystrobin). The addition of a nutrient agar medium (PDA, potato

dextrose agar, Difco) maintained at 45°C at a final concentration of 30% v/v allowed solidification of the nutrient medium. A 4 mm mycelial plug of *Colletotrichum coccodes* or *Helminthosporium solani* was applied upside down to the center of the well; plates were stored at 21°C or 30°C for 7 or 14 days for *C. coccodes* and *H. solani*, respectively, and images recorded. Image treatment with ImageJ was used to calculate mycelial growth respective to the positive control. Plant extracts that inhibited fungal growth at early time points (i.e. 3 days for *C. coccodes* and 7 days for *H. solani*) but not at late time points (i.e. 7 days for *C. coccodes* and 14 days for *H. solani*) were considered fungistatic. Plant extracts that exhibited mycelial growth inhibition at late time points were considered fungitoxic. The 24-well plate antifungal assay was substituted by a 48-well plate antifungal assay for the antifungal analysis of the fractions resulting from the fractionations (at 5 mg/mL) and for the dose-dependent analysis of the individual molecules obtained by preparative HPLC. Furthermore, conidial suspensions (10.000 - 100.000 conidia/well) were applied instead of the mycelial plug in the 48-well-plate assay. EC_{50} values for azoxystrobin against *C. coccodes* were calculated using the XLSTAT software as previously described (Schnee et al., 2013).

In vivo antifungal effect of plant extracts against black dot and silver scurf.

Potato tubers (of the cultivar Charlotte, grown in experimental fields in Agroscope, Nyon, Switzerland) with black dot and silver scurf symptoms at harvest (disease severity assessed on 50 tubers as described below) were treated with water (negative control) and Amistar (250g/L azoxystrobin, Syngenta, Basel, Switzerland) (positive control), or with plant extracts, using a processing robot. Plant extracts were diluted at 10 g/L in 1% ethanol in water. The chemical fungicide Amistar was applied diluted at 2.4 g/L in water (0.6 mg azoxystrobin/mL). The pulverization was fixed at 2,5 mL/kg and 2,25 $\mu L/cm^2$ in 4 passages, turning the tubers after the second passage. Tubers were homogeneously positioned on a plate so that no contact was possible between tubers. This application resulted in a good coverage of the tuber avoiding dumping the tubers. A brief period of drying (2-8 hours) was applied before storing the tubers in the cold chamber at 5°C for four months. To avoid cross-contaminations, each treatment was stored in especially designed individual storage units. These units were developed to contain ca. 5 kg of tubers, had a 30 liters capacity, were hermetically closed, and contained an air pump inside the container with entry and exit tubing that allowed renewal of the air. Full renewal of the air in these containers was assured every 12 hours by placing a rotary vane pump G 6/01-K-LCL 6 (Gardner Denver Schweiz AG, Switzerland) in each barrel with electronic control. The air pump was connected to a timer that activated the pump for two minutes every 96 minutes (flow at 2 L/min), allowing a complete renewal of the air every 12 hours, which was sufficient to maintain levels inferior to the 3000 ppm of carbon dioxide threshold required for potato storage. The individual storage units were placed in a cold chamber maintained at 5°C and >95% relative humidity for 5 months. The experiment was conducted for three consecutive years with a new tuber lot every year (2016-2018).

Disease severity assessment.

After four months of storage, potato tubers were washed and incubated at room temperature and high relative humidity by placing them in closed plastic bags containing wet tissues to induce sporulation of fungal pathogens. Potato tubers were individually observed under a binocular for the presence of microsclerotia of *C. coccodes* (for black dot) or conidiophores of *H. solani* (for silver scurf). Each tuber was then classified in one of the following classes, depending on the affected area of the tuber: 0 (absence of the fungus), 1 (less than 15%), 2 (between 15 and 33%), 3 (between 33 and 66%) and 4 (more than 66%). Incidence was calculated as the percentage of tubers showing symptoms. Disease severity was calculated by multiplying the number of tubers in each class by the median value of the class (% affected area).

Statistical analysis.

One-way ANOVA was performed on black dot and silver scurf severity data from the *in vivo* biotest. The post-hoc Dunett's test was used to compare the different treatments with the negative control (water-treated tubers).

5.4. Results and discussion

Screening of plant extracts for antifungal activities against Colletotrichum coccodes and Helminthosporium solani.

Eleven plant species were selected and their extracts were submitted to an *in vitro* screening of their antifungal activities against *Colletotrichum coccodes* and *Helminthosporium solani* (Table 5.1). The plants were selected based on several criteria: i) previously known fungitoxic activity against plant pathogens (Table 5.1), ii) local availability of the raw material and iii) the potential extractability of active principles in aqueous or alcoholic media. Three simple, cost-effective and environmentally-friendly extraction methods were used for each plant material: i) aqueous extraction at room temperature to extract polar metabolites, ii) aqueous extraction with reflux to potentially increase the extraction of polar metabolites, as done for the decoction of medicinal plants in traditional medicine (Brillatz et al., 2020), and iii) methanolic extraction to extract medium-polarity metabolites. These methods yielded 28 plant extracts (Table 5.1) that could easily be applied in agriculture, directly diluted in water or with relatively simple formulation strategies. The antifungal activity of these plant extracts was screened using a food-poisoning method (Amadioha, 2000), and mycelial growth inhibition was assessed at early and late time points to detect fungistatic (temporary growth inhibition) and fungitoxic activities (complete growth inhibition with potential death of the pathogen) (Table 5.1). Since crude plant extracts usually show antifungal activities at the mg/mL concentrations against plant pathogenic fungi (Schnee et al., 2013; Bhagwat and Datar, 2014; Chen et al., 2018; Gillmeister et al., 2019), the plant extracts were screened at a range of concentrations of 1 – 10 mg/mL. Furthermore, the amount of fungicide applied as post-harvest treatments on tubers depends on the active ingredient, but typically includes concentrations of 5 – 100 mg/mL (Miller et al., 2006). Among the 28 tested plant extracts, 11 showed fungistatic activity against *C. coccodes*, and three of them showed fungitoxic activity. On the other hand, eight plant extracts showed fungistatic activity against *H. solani*, from which seven were fungitoxic. Among them, two plant extracts (the methanolic extract of *Curcuma longa* rhizomes and the methanolic extract of *Rheum palmatum* roots) showed fungitoxic activities against both targeted pathogens. Another plant extract (the aqueous extract of *Frangula alnus* bark) showed fungitoxic activity against *C. coccodes* and fungistatic activity against *H. solani*. The minimum inhibitory concentrations (MIC) of the *C. longa* rhizomes methanolic extract was 10 mg/mL for *C. coccodes* and 10 mg/mL for *H. solani*. The *R. palmatum* roots methanolic extract exhibited a MIC of 10 mg/mL against *C. coccodes* and of 2.5 mg/mL against *H. solani*. At 10 mg/mL, the *F. alnus* bark aqueous extract showed fungitoxic activity against *C. coccodes* and fungistatic activity against *H. solani*. These plant extracts, which exhibited antifungal activity against both pathogens, were studied in more detail to characterize their antifungal compounds.

Table 5.1 Antifungal activity of crude extracts. AER: Aqueous extract with reflux; AE: Aqueous extract; ME: methanolic extract. Fungistatic activity (growth inhibition at early time points: T3 for *C. coccodes* and T7 for *H. solani*) and fungitoxic activity (growth inhibition at late time points: T7 for C. coccodes and T14 for H. solani). "++" fungitoxic activity; "+" fungistatic activity; "-" no significant (<75% growth inhibition) fungistatic or fungitoxic activity; "n.d." Not determined.

Plant material	AER		AE		ME		Literature
	C. coccodes	***H. solani***	***C. coccodes***	***H. solani***	***C. coccodes***	***H. solani***	Target for known antifungal activity
***Aloe vera* leaves**	+	-	+	-	+	-	*Alternaria alternata, Botrytis cinerea* (Saks and Barkai-Golan, 1995)
***Rheum palmatum* roots**	-	++	+	-	++	++	*Blumeria graminis* (Gillmeister et al., 2019), *Phytophthora infestans* (Krebs et al., 2006)
***Frangula alnus* bark**	+	-	++	+	+	-	*Trichoderma viride*, *Mucor mucedo* (Manojlovic et al., 2005), *Phytophthora infestans* (Krebs et al., 2006) *Fusarium graminearum* (Forrer et al., 2014)
***Urtica dioica* leaves**	-	-	-	-	nd	nd	*Alternaria alternate* (Hadizadeh et al., 2009)
***Salix viminalis* bark**	-	-	-	-	nd	nd	*Plasmopara viticola* (Andreu et al., 2018)
***Equisetum arvense* herb**	-	-	-	-	nd	nd	*Aspergillus flavus, Fusarium verticilloides* (Garcia et al., 2013)
***Vitis vinifera* bark**	-	-	-	-	-	++	*Plasmopara viticola, Erysiphae necator* (Schnee et al., 2013)
***Epilobium parviflorum* flowers**	+	-	-	++	-	++	*Candida spp.*, *Trycophyton spp.*(Webster et al., 2008)
***Hypericum perforatum* herb**	-	-	-	-	-	++	*Aspergillus spp., Alternaria alternata* (Fenner et al., 2005; Mašković et al., 2011)
***Artemisia annua* herb**	-	-	-	-	+	-	*Fusarium oxysporum, Fusarium solani* (Ma et al., 2019)
***Curcuma longa* rhizomes**	nd	nd	nd	nd	++	++	*Colletotrichum spp.* (Chen et al., 2018)

Chemical composition of the antifungal plant extracts

The plants that showed antifungal activities against *C. coccodes* and *H. solani* have been extensively studied from a chemical point of view. Curcuminoids (curcumin, detemhoxycurcumin and bisdemethoxycurcumin) are one of the main constituents of *Curcuma sp.* (Inoue et al., 2008), and anthraquinones have been reported in both *F. alnus* and *R. palmatum* as one of the most abundant chemical classes in these plants (van den Berg and Labadie, 1984; Kremer et al., 2012; Gillmeister et al., 2019). The UHPLC-PDA-CAD and UHPLC-HRMS profiles of the *C. longa* rhizome methanolic extract confirmed that the most abundant compounds in this extract were bisdemethoxycurcumin (**1**) (Inoue et al., 2008), demethoxycurcumin (**2**) (Inoue et al., 2008) and curcumin (**3**) (Inoue et al., 2008), which were unambiguously identified based on retention time (Rt), mass spectra (MS) and ultra-violet photo diode array (PDA) spectra comparison with commercial available standards (Figure 5.1A). On the other

hand, the chemical profiles of *F. alnus* bark and *R. palmatum* root extracts showed that several metabolites with the characteristic PDA spectra of anthraquinones chromophores, with a peak of absorbance at 410-450 nm (Anouar et al., 2014), were present in these extracts. Aloe-emodin (**8**) (Danielsen et al., 1992), rhein (**10**) (Danielsen et al., 1992) and emodin (**11**) (Kögl and Postowsky, 1925) were unambiguously identified in the *R. palmatum* methanolic extract by comparison of the Rt, MS and PDA spectra of pure commercial standards (Figure 5.1B). Emodin (**11**), as well as frangulin A (**16**) (Francis et al., 1998) and frangulin B (**15**) (Wagner and Demuth, 1972), were identified in the *F. alnus* aqueous extract by the same means (Figure 5.1C).

The UHPLC-PDA-CAD profiles showed that all extracts contained a relatively high number of primary polar metabolites (most probably sugars) (Figure 5.1). In order to remove these primary metabolites and enrich the extracts in secondary metabolites, a large-scale solid phase extraction (SPE) was performed in all three extracts with four to six fractions of different polarity (Supplementary Table 5.2). The generated SPE fractions obtained (at the tens of mg range) were submitted to a chemical screening using a UHPLC-PDA-CAD, which demonstrated the efficiency of the enrichment procedure, and all fractions were tested in the *in vitro* antifungal bioassay. Using this strategy, it was possible to successfully identify the fractions containing the active compounds in each plant extract. As expected, the most polar fractions of all extracts were not active against the pathogens and, for all extracts, the fraction eluted with 80% of methanol showed the highest antifungal activity against both fungal pathogens (Supplementary Table 5.2).

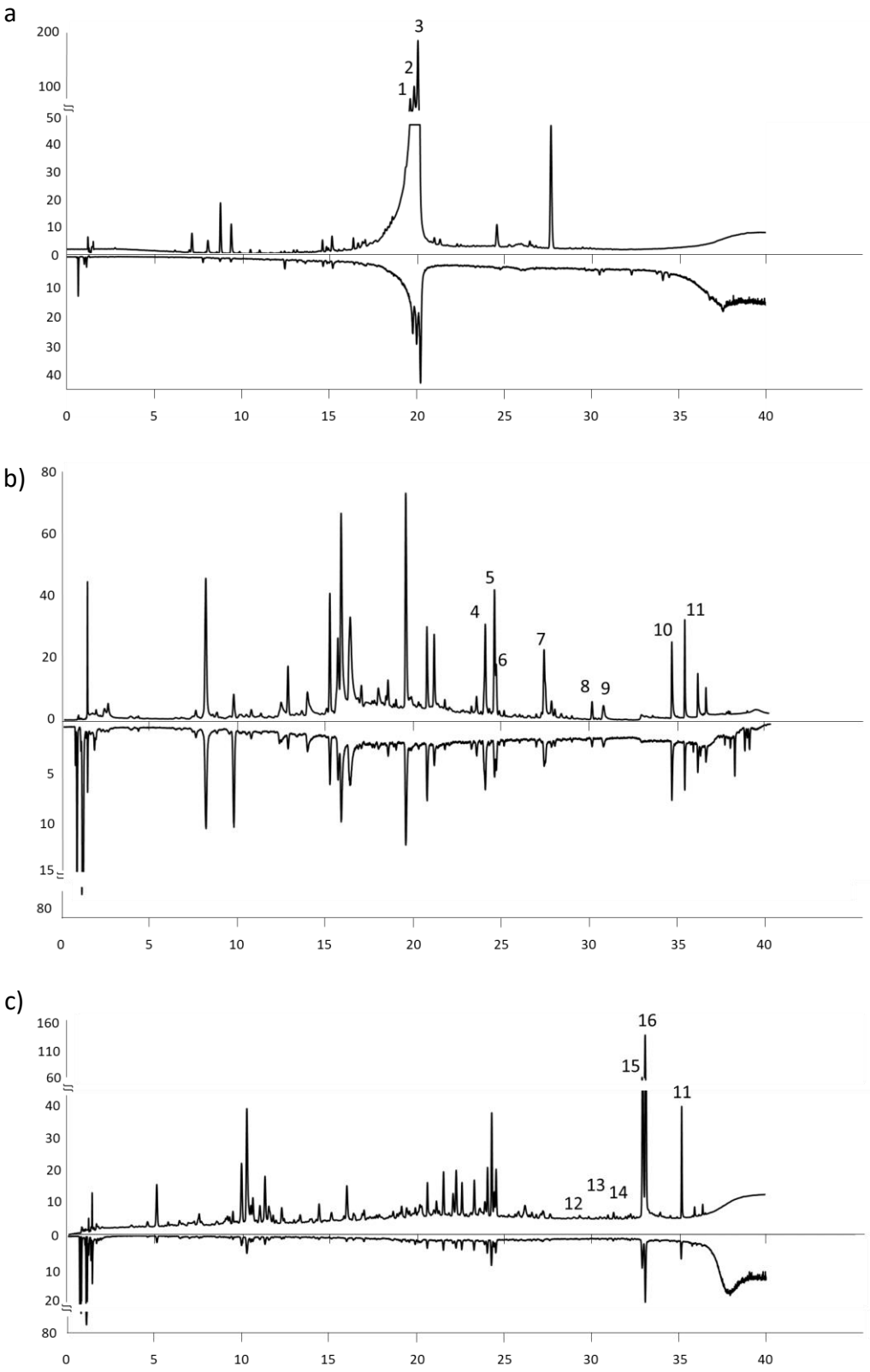

Figure 5.1 : UV at 280 nm (above) and CAD (below) chromatograms of a) *C. longa* rhizomes methanolic extract, b) *R. palmatum* roots methanolic extract and c) *F. alnus* bark aqueous extract. **1**: Bisdemethoxycurcumin, **2**: Demethoxycrucumin, **3**: Curcumin, **4**: chrysophanol 1-O-β-D-glucopyranoside, 5 : emodin-6-O-β-D-glucoside, **6**: chrysophanol 8-O-β-D-glucopyranoside, **7**: 4-[4-[[6-O-[(2E)-3-(4-hydroxyphenyl)-1-oxo-2-propen-1-yl]-2-O-(3,4,5-trihydroxybenzoyl)-β-D-glucopyranosyl]oxy]phenyl]- 2-Butanone , **8**: aloe-emodin, **9**: 4-[4-[[6-O-[(2E)-1-Oxo-3-phenyl-2-propen-1-yl]-2-O-(3,4,5-trihydroxybenzoyl)-ß-D-glucopyranosyl]oxy]phenyl]-2-butanone , **10**: rhein, **11**: emodin, **12**: emodin 8-O-[β-D-glucopyranosyl-(1→5)-O-β-D-apiofuranoside] , **13**: 6,8-O-β-D-glucopyranoside, O-α-L-rhamnopyranoside emodin dianthrone, **14**: di-rhamnoside, mono-glucoside emodin dianthrone, **15**: Frangulin B and **16**: Frangulin A.

Bioassay-guided fractionation of the C. longa methanolic extract.

The 80% methanol fraction (Fraction 3) from the SPE of the *C. longa* methanolic extract (35% of the crude extract) showed fungitoxic activity against *C. coccodes* and *H. solani* at 10 and 5 mg/mL, respectively (Supplementary Table 5.2). In this case, the enrichment allowed a higher antifungal activity than the crude extract against *C. coccodes*. However the MIC of this fraction was the same as the crude extract against *H. solani* (Supplementary Table 5.2). The UHPLC-PDA-CAD analysis showed that this fraction mainly included the main *C. longa* curcuminoids bisdemethoxycurcumin (**1**), demethoxycurcumin (**2**) and curcumin (**3**) (Supplementary Figure 5.1). These three commercially available compounds were selected and tested together with the other isolated compounds of the other active plant extracts for their antifungal activity against *C. coccodes* and *H. solani* (Table 5.2).

Bioassay-guided fractionation of the R. palmatum methanolic extract.

As for the *C. longa* extract, the 80% methanol fraction from the SPE of the *R. palmatum* methanolic extract (Fraction 3, 22% of the crude extract) showed the highest antifungal activity against both pathogens. The enrichment through the SPE allowed a decrease in the MIC for both pathogens, with values of 2.5 mg/mL against *C. coccodes* and of 0.125 mg/mL against *H. solani* (Supplementary Table 5.2). Comparing the UHPLC-PDA-CAD profile of this fraction with the crude extract, several major compounds were present in the active fraction (Supplementary Figure 5.2). Among them, only rhein (**10**) and aloe-emodin (**8**) could be unambiguously identified (based on Rt, MS and PDA spectra comparison with the analytical standard). Since other abundant compounds with similar PDA spectra were present in this active fraction, the fraction was further purified by semi-preparative HPLC to isolate the other compounds. In order to obtain these compounds in pure form to assess antifungal activity (at mg range), a single-step preparative HPLC on 35 mg of the active fraction (Fraction 3) was performed. The optimal separation conditions were established on a HPLC-PDA-ELSD, the gradient was then geometrically transferred (Challal et al., 2015) to a semi-preparative HPLC system using the same stationary phase, and the fraction separated using a dry load to obtain optimal separation performance (Queiroz et al., 2019) (Supplementary Figure 5.3). This efficient procedure allowed the isolation of seven compounds that were identified on the basis of HRMS and NMR data as chrysophanol 1-*O*-β-D-glucopyranoside (**4**) (Kubo et al., 1992), emodin-6-*O*-β-D-glucoside (**5**) (Zhang et al., 2004), chrysophanol 8-*O*-β-D-glucopyranoside (**6**) (Kubo et al., 1992), 4-[4-[[6-O-[(2E)-3-(4-hydroxyphenyl)-1-oxo-2-propen-1-yl]-2-O-(3,4,5-trihydroxybenzoyl)-β-D-glucopyranosyl]oxy]phenyl]- 2-Butanone (**7**) (Kashiwada et al., 1986), aloe-emodin (**8**) (Danielsen et al., 1992), 4-[4-[[6-O-[(2E)-1-Oxo-3-phenyl-2-propen-1-yl]-2-O-(3,4,5-trihydroxybenzoyl)-ß-D-glucopyranosyl]oxy]phenyl]-2-butanone (**9**) (Kashiwada et al., 1986) and rhein (**10**) (Danielsen et al., 1992) (Figure 5.2). The antifungal activity of these compounds was tested using the *in vitro* bioassay together with the isolated compounds of the other plant extracts (Table 5.2).

Bioassay-guided fractionation of the F. alnus aqueous extract

In the case of the aqueous extract of *F. alnus*, the fractions 4 – 6 (65%, 80% and 100% methanol) showed antifungal activity against *C. coccodes*, with fraction 5 being the most active (Supplementary Table 5.2). Similarly, fractions 5 and 6 (80% and 100% methanol, respectively) showed antifungal activity against *H. solani*. However, the enrichment did not allow a strong decrease of the MIC against *C. coccodes* nor *H. solani,* it was similar than that of the crude extract (Supplementary Table 5.2). The UHPLC-PDA-CAD profile of these fractions showed the presence of several compounds, including the anthraquinone glycoside frangulin B (**15**) (Supplementary Figure 5.4). Notably, frangulin B (**15**), as well as other compounds present in the active fractions, were more abundant in the active aqueous extract based on the UHPLC-CAD profiles than in the inactive methanolic or aqueous extract with reflux of *F. alnus* (Table 5.1). This indicated that water at room temperature is more efficient than methanol in extracting frangulins (Supplementary Figure 5.5). The SPE fractionation and UHPLC-PDA-CAD profiles

demonstrated that the antifungal compounds present in fractions 5 and 6 represent less than 10% of the crude extract (Supplementary Table 5.2). In order to generate sufficient material for the isolation of their active metabolites, the process in this case was considerably scaled up and 50 grams of the *F. alnus* aqueous extract were separated by Flash chromatography. To this end, ideal conditions for separation of the crude extract were determined by HPLC-PDA-ELSD and after geometrical transfer (Challal et al., 2015), the crude extract was fractionated using the same stationary phase. Using this approach 59 fractions were obtained. The fractions 1 – 12 contained polar metabolites and were not analyzed further since the antifungal activity was detected in the most apolar fractions of the SPE. Fractions 13 – 59 were tested for their antifungal activity and fractions 39, 40 and 41 showed antifungal activity. These fractions were pooled (100 mg, ca. 1.6% of the original extract) and further purified by semi-preparative HPLC after gradient optimization at the analytical scale (Supplementary Figure 5.6). This approach led to the isolation of four compounds (**12-15**) that were fully identified *de novo* by HRMS and NMR.

The HRMS of compound **12** indicated a molecular formula of $C_{26}H_{28}O_{14}$, as deduced from the peak at m/z 565.1927 $[M+H]^+$. The UV absorption peaks at 278 nm and 418 nm showed that **12** is an anthraquinone of the same type as frangulins. The NMR data showed indeed close similarities with Frangulin B with additional signals corresponding to a glucose moiety. The HMBC correlation from the anomeric proton of the glucose at δ_H 4.34 (1H, d, *J* = 7.8 Hz) to the carbon C-5 of the apiose at δ_C 72.1 indicated that compound **12** is emodin 8-*O*-[β-D-glucopyranosyl-(1→5)-*O*-β-D-apiofuranoside] (Figure 5.2).

The HRMS data of **13** displayed a peak at m/z 819.2477 $[M+H]^+$ from which the molecular formula $C_{42}H_{42}O_{17}$ could be calculated (2.17 ppm mass error) and the MS/MS pattern indicated the loss of a hexose (162 uma) and a deoxy-hexose (146 uma). The MS molecular weight range and the UV spectrum of compound **13** was characteristic of dianthrone derivatives with absorption maxima at 278 and 342 nm (Lemli, 1965; van den Berg and Labadie, 1984; Yang et al., 2018a). The NMR data showed the presence of 8 aromatic protons, 4 of which being broad singlets, 2 anomeric protons at δ_H 4.77 (1H, d, *J* = 7.7 Hz, Glc-1) and 5.68 (1H, s, Rha-1), 2 methine protons at δ_H 4.47 (1H, d, *J* = 3.4 Hz, H-10/10') and 4.56 (1H, d, *J* = 3.4 Hz, H-10/10'), 2 methyl singlets at δ_e 2.20 (3H, s, CH_3-3/3'), 2.21 (3H, s, CH_3-3'/3), a methyl doublet at δ_H 1.27 (3H, d, *J* = 6.2 Hz, Rha-6), and between δ_H 3.45 and 4.10 a series of 8 oxymethines and 1 oxymethylene belonging to the sugars. The ^{13}C chemical shifts and the coupling constants values of carbons and protons of the sugars allowed identifying the presence of a glucose and a rhamnose in **13**. The aromatic protons H-2, H-4 and H-2', H-4' were identified through their HMBC correlations with the methyl in C-3 and C-3'. The ROESY correlations between the aromatic proton H-7 and both the anomeric proton of the glucose and the anomeric proton of the rhamnose made it possible to position the 2 sugars on the same aromatic ring in C-6 and C-8. Despite solubilization tests in different solvents (acetone-d_6, CD_3OD and DMSO- d_6) and the recording of spectra at several temperatures, it was not possible to obtain a better resolution of the aromatic protons H-4, H-5, H-4', and H-5'. Due to the width of these aromatic signals and the lack of HMBC correlations, it was not possible to tell whether glucose was attached to C-6 and rhamnose to C-8 or vice versa. H-5/H-5' (δ_H 6.79 and 6.36, respectively) being more downfield than H-4/H-4' (δ_H 5.85/5.92) suggest that the relative configuration of **13** is a trans H-10/10' dianthrone (Ji et al., 2014). Compound **13** was thus partially identified as 6,8-*O*-β-D-glucopyranoside, *O*-α-L-rhamnopyranoside emodin dianthrone (Figure 5.2).

As for compound **13**, the UV and MS spectra of **14** were characteristic of dianthrone derivatives, with absorption maxima at 280 and 347 nm. The HRMS data of **14** presented a difference of 146 uma compared to **13**. The NMR data confirmed the presence of an additional rhamnose. The ROESY

correlations from H-7 to the anomeric proton of the glucose and to the anomeric proton of the rhamnose and from H-7' to the anomeric proton of the second rhamnose did not allowed to identify compound **14** more precisely than a di-rhamnoside, mono-glucoside emodin dianthrone (Figure 5.2).

Compound **15** was identified as Frangulin B (Wagner and Demuth, 1972) based on retention time (Rt), MS and UV spectra comparison with commercially available standards. Furthermore, NMR analysis confirmed the identity of Frangulin B.

Glucofrangulin B, a molecule with the same molecular formula as **12**, had been previously identified in *R. frangula* (*F. alnus* synonym) bark (Wagner and Demuth, 1974). Emodin dianthrones and heterodianthrones of emodin and crysophanol had been identified in *R. frangula* (Lemli, 1965), and dianthrone glycosides, some of which possess moderate cytotoxic activities, have been reported in other plant species (Yang et al., 2018a). However, to the best of our knowledge, these two dianthrone glycosides, as well as emodin 8-*O*-[β-D-glucopyranosyl-(1→5)-*O*-β-D-apiofuranoside], have not been previously reported in *F. alnus* or other plant species.

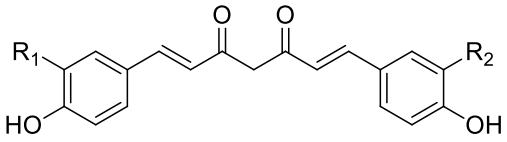

1. **Bisdemethoxycurcumin:** R_1=H, R_2=H
2. **Demethoxycurcumin:** R_1=OCH_3, R_2=H
3. Curcumin: R_1=OCH_3, R_2=OCH_3

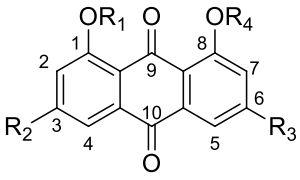

4. **Chrysophanol 1-*O*-β-D-glucopyranoside:** R_1=Glc, R_2=CH_3, R_3=H, R_4=H
5. **Emodin 6-*O*-β-D-glucoside:** R_1=H, R_2=CH_3, R_3=OGlc, R_4=H
6. Chrysophanol 8-*O*-β-D-glucopyranoside: R_1=Glc, R_2=CH_3, R_3=H, R_4=Glc
8. **Aloe emodin:** R_1=H, R_2=CH_2OH, R_3=H, R_4=H
10. **Rhein:** R_1=H, R_2=COOH, R_3=H, R_4=H
11. **Emodin:** R_1=H, R_2=CH_3, R_3=OH, R_4=H
12. R_1=H, R_2=CH_3, R_3=O-Glc-(1->5)-Api, R_4=H
15. **Frangulin B:** R_1=H, R_2=CH_3, R_3=Api, R_4=H
16. **Frangulin A:** R_1=H, R_2=CH_3, R_3=Rha, R_4=H

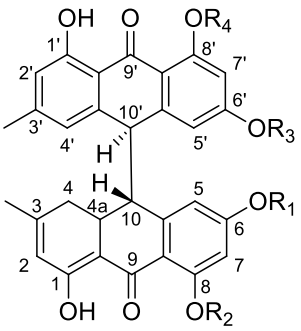

13. R_1,R_2=Glc,Rha, R_3=H, R_4=H
14. R_1,R_2=Glc,Rha, R_3,R_4=Rha,H

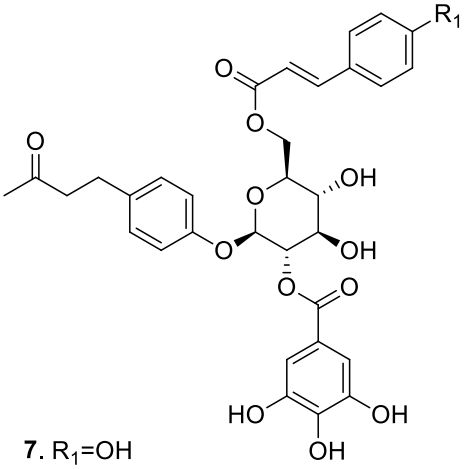

7. R_1=OH
9. R_1=H

Figure 5.2 Chemical structures of the compounds isolated in the aqueous extract of *F. alnus* or the methanolic extracts of *R. palmatum* and *C. longa*. Curcuminoids (**1-3**), anthraquinones (**4-6**, **8**, **10-12**, **15-16**), dianthrones (**13-14**) and phenolic derivatives (**7** and **9**).

In vitro Antifungal Activity of the Isolated Compounds against C. coccodes and H. solani

The antifungal activity of the compounds isolated from *R. palmatum* (**4 – 10**) and *F. alnus* (**12 – 15**), as well as the commercially available curcuminoids identified in *C. longa* (**1 – 3**), and the anthraquinone standards identified in *R. palmatum* (**11**) and *F. alnus* (**11** and **16**) were tested in an *in vitro* bioassay. The Minimum Inhibitory Concentrations (MIC) of all pure compounds (**1 – 16**) was assessed on the conidia germination of both pathogens (Table 2). Highest inhibition of *C. coccodes* conidia germination was produced by frangulin B (**15)** and rhein (**10**), with MIC values below 100 µM (below 30 µg/mL). Furthermore, chrysophanol 1-*O*-β-D-glucopyranoside (**4**), compound **9** and compound **7** showed antigerminative activity against *C. coccodes* at concentrations between 250 and 1000 µM (between 104 and 624 µg/mL). The three curcuminoids, as well as chrysophanol 8-*O*-β-D-glucopyranoside (**6**), exhibited antifungal activity against *C. coccodes* only at 2000 µM (617 - 832 µg/mL). Emodin (**11**), aloe-emodin (**8**), emodin-6-*O*-β-D-glucoside (**5**), emodin 8-*O*-[β-D-glucopyranosyl-(1→5)-*O*-β-D-apiofuranoside (**12**), compound **13** and frangulin A (**16**) did not show antifungal activity against *C. coccodes* at any of the tested concentrations. It is worth noting that the reference fungicide azoxystrobin has been shown to exhibit EC_{50} values of 0.5-5 µg/mL against *Colletotrichum* species (Queiroz et al., 2012; Baggio et al., 2018). In our study, the EC_{50} of azoxystrobin against *C. coccodes* was 3.8 µg/mL, while the MIC was found to be between 250 - 500 µM (101 - 202 µg/mL). Thus, the antifungal activity against *C. coccodes* of some of the isolated compounds showed similar values than the reference commercially available fungicide azoxystrobin.

The phenolic glycoside **7** showed the highest antifungal activity of all isolated compounds against *H. solani*, with a MIC value of 100 µM (62 µg/mL) (Table 5.2). Furthermore, the anthraquinones rhein (**10**) and chrysophanol 1-*O*-β-D-glucopyranoside (**4**), as well as the phenolic glycoside compound **9** exhibited a MIC value of 250 µM against this pathogen. Aloe-emodin (**8**), chrysophanol 8-*O*-β-D-glucopyranoside (**6**), frangulin B (**15**), emodin-6-B-D-glucoside (**5**) and compound **12** exhibited antigerminative activity against *H. solani* at concentrations between 750 and 1000 µM, while frangulin A (**16**) and the three curcuminoids (**1**-**3**) only inhibited *H. solani* at 2000 µM (617 - 833 µg/mL). Emodin (**11**) and compound **13** were found not to inhibit *H. solani* conidia germination at the concentrations tested (Table 5.2). The reference fungicide azoxystrobin showed strong antifungal activity against *H. solani*, with a MIC value below 50 µM (<20 µg/mL).

It is worth noting that only rhein (**10**), chrysophanol 1-*O*-β-D-glucopyranoside (**4**) and compound **9** showed antifungal activity against both phytopathogens at MIC below 500 µM, values comparable to the reference fungicide azoxystrobin (Table 5.2). Other compounds, such as frangulin B (**15**) or compound **7**, showed strong antifungal activity however only against one of the pathogens.

Table 5.2 Minimum Inhibitory concentration (MIC, in µg/ml and µM) of isolated compounds from the different plant extracts after seven days (*C. coccodes*) or fourteen days (*H. solani*) of growth.

	MIC (µg/mL)		MIC (µM)	
Compounds	*C. coccodes*	*H. solani*	*C. coccodes*	*H. solani*
Bisdemethoxycurcumin (1)	**617**	**617**	**2000**	**2000**
Demethoxycurcumin (2)	**677**	**677**	**2000**	**2000**
Curcumin (3)	**737**	**737**	**2000**	**2000**
chrysophanol 1-O-β-D-glucopyranoside (4)	**104**	**104**	**250**	**250**
emodin-6-O-β-D-glucoside (5)	**>864**	**432**	**>2000**	**1000**
chrysophanol 8-O-β-D-glucopyranoside (6)	**832**	**312**	**2000**	**750**
Compound 7	**624**	**62**	**1000**	**100**
Aloe-emodin (8)	**>540**	**203**	**>2000**	**750**
Compound 9	**304**	**152**	**500**	**250**
Rhein (10)	**28**	**71**	**100**	**250**
Emodin (11)	**>564**	**>565**	**>2000**	**>2000**
Compound 12	**>564**	**565**	**>1000**	**1000**
Compound 13	**>964**	**>964**	**>2000**	**>2000**
Compound 14	**n.d.**	**n.d.**	**n.d**	**n.d**
Frangulin B (15)	**20**	**402**	**50**	**1000**
Frangulin A (16)	**>833**	**833**	**>2000**	**2000**
Azoxystrobin	**202**	**<20**	**500**	**<50**

In-depth chemical characterization of the antifungal plant extracts

The bio-guided fractionation of the three antifungal plant extracts showed that curcuminoids, anthraquinones and phenolic derivatives were the main antifungal compounds present in those extracts.

In order to determine whether non-isolated analogs of these antifungal compounds were present in the crude extracts, we took advantage of the generic UHPLC-HRMS/MS metabolite profile performed

for dereplication for a more detailed metabolome composition analysis. For this, all MS/MS data of the active extracts were organized as a single molecular network (MN). Indeed, highlighting chemically related compounds can indeed be achieved by MN (Watrous et al., 2012). As expected, the global MN showed that the *F. alnus* aqueous extract, the *R. palmatum* methanolic extract and the *C. longa* methanolic extract possess specific secondary metabolites, and only share primary metabolites such as sugars or amino acids (putatively annotated based on experimental MS/MS fragmentation patterns). The features detected in the *C. longa* methanolic extract were usually found in clusters specific of this extract (Figure 5.3). Curcumin (**1**) ($C_{21}H_{20}O_6$, 0.64 ppm mass error) was found in a cluster with other features detected in the *C. longa* extract. From these features, several had the same *m/z* ratio than curcumin, but eluted at different retention times, indicating that several isomers of curcumin exist in the *C. longa* extract (10 features at different retention times). Furthermore, curcumin derivatives with higher *m/z ratios* were observed (calculated molecular formulas $C_{36}H_{42}O_6$, 0.10 ppm mass error and $C_{36}H_{44}O_7$, 0.98 ppm mass error). Another feature present in the cluster exhibited higher *m/z* ratios, with a peak at 735.2431 $[M+H]^+$, suggesting a dimerization of curcumin (calculated molecular formula $C_{42}H_{38}O_{12,}$ 0.68 ppm mass error). Furthermore, other features from the three plant extracts were present in this cluster, including the phenolic derivatives compound 7 and compound 9 isolated from *R. palmatum.* Ferulic acid was found in all three plant extracts, being the link between the phenolic derivatives from *R. palmatum* and the curcumin from *C. longa* (also known as diferuloylmethane) (Figure 5.3, cluster 3). Demethoxycurcumin (**2**) was found on another cluster with features from the *C. longa* extract. In this cluster, the features possessed *m/z* ratios of 339.1231 (demethoxycurcumin, $C_{20}H_{18}O_5$, 1.18 ppm mass error), 325.1067 ($C_{19}H_{16}O_5$, 1.08 ppm mass error) and 355.1177 ($C_{20}H_{18}O_6$, 0.24 ppm mass error), suggesting the loss of a CH_2 and the addition of an oxygen atom from demethoxycurcumin in these compounds. Bisdemethoxycurcumin (**3**) ($C_{19}H_{16}O_4$, 0.21 ppm mass error) was found in another cluster with features detected in the *C. longa* extract that possessed higher *m/z* ratios. Interestingly, features that possessed *m/z* ratios with the same difference from the curcuminoids curcumin and bisdemethoxycurcumin (calculated molecular formulas $C_{34}H_{38}O_4$, 3.55 ppm mass error and $C_{34}H_{40}O_5$, 0.09 ppm mass error) were observed in each cluster, suggesting that these compounds may be conjugated to the same moieties. Based on MS only, no putative structure for such minor derivatives can be proposed and the targeted isolated would be needed to assess their structure and their possible antifungal activity. Whether these curcuminoid derivatives possess antifungal activities against *C. coccodes* needs to be further studied.

The anthraquinones isolated from *R. palmatum* and *F. alnus* were clustered together (Figure 5.3, cluster 1). This cluster contained mainly the anthraquinone aglycones emodin (**11**), aloe-emodin (**8**) and rhein (**10**), but also the anthraquinone glycosides frangulin A (**16**) and B (**15)**. Furthermore, the non-isolated anthraquinone chrysophanol aglycone was putatively identified by comparison of the MS/MS spectra to an experimental database from the *R. palmatum* extract (GNPS). Its presence was expected since crysophanol glycosides were isolated from *R. palmatum*. In addition, flavonoids (kaempferol and datiscetin) were putatively identified in this cluster. The chrysophanol glycosides (**4** and **6**) and the *de novo* identified anthraquinone glycoside (**12**) were found in another anthraquinone glycoside cluster, with the features clearly divided between each plant species (Figure 5.3, cluster 2). The analysis of the anthraquinone clusters demonstrate that they were linked through their MS/MS spectra patterns, but that both plants exhibited distinct anthraquinone composition (with the exception of the emodin aglycone and three minor anthraquinone derivatives). This allowed to highlight ca. 30 minor anthraquinone derivatives from each plant extract (*R. palmatum* and *F. alnus*).

Finally, the isolated dianthrones (**13** and **14**) were found in a cluster of *F. alnus* compounds with *m/z* ratio ranges between 643.1782 and 1144.3885 (Figure 5.3, cluster 4). The MS/MS spectra indicate the losses of sugar moieties from emodin (*m/z* 271.0599) or chrysophanol (255.0699), suggesting that ca.

20 other dianthrone glycosides are present in the *F. alnus* aqueous extract. The MN also clearly indicated no dianthrones were found in *R. palmatum*. Whether the non-isolated anthraquinone derivatives and phenolic glycosides are fungitoxic to *C. coccodes* and *H. solani* remains to be studied.

The MN analysis highlighted the presence of at least 50 minor analogs of the active compounds. Working with higher quantities of plant extract to obtain large collection of anthraquinone derivatives would allow to study the structure-activity relationship between the active compounds and their antifungal activity against *C. coccodes* and *H. solani*.

Interestingly, three features detected in the *R. palmatum* and *F. alnus* extracts were putatively identified as the flavan-3-ols catechin, epicatechin gallate and afzelechin, some of which have shown antifungal or eliciting activities against other fungal phytopathogens (Gillmeister et al., 2019) (Figure 5.3, cluster 5). These compounds were not isolated during the bioguided fractionation since they eluted in the polar fractions, which did not show *in vitro* antifungal activity. However, the elicitation properties of the compounds was not tested in our antifungal bioassay. Whether these non-isolated compounds can elicite defenses against black dot and silver scurf remains to be determined.

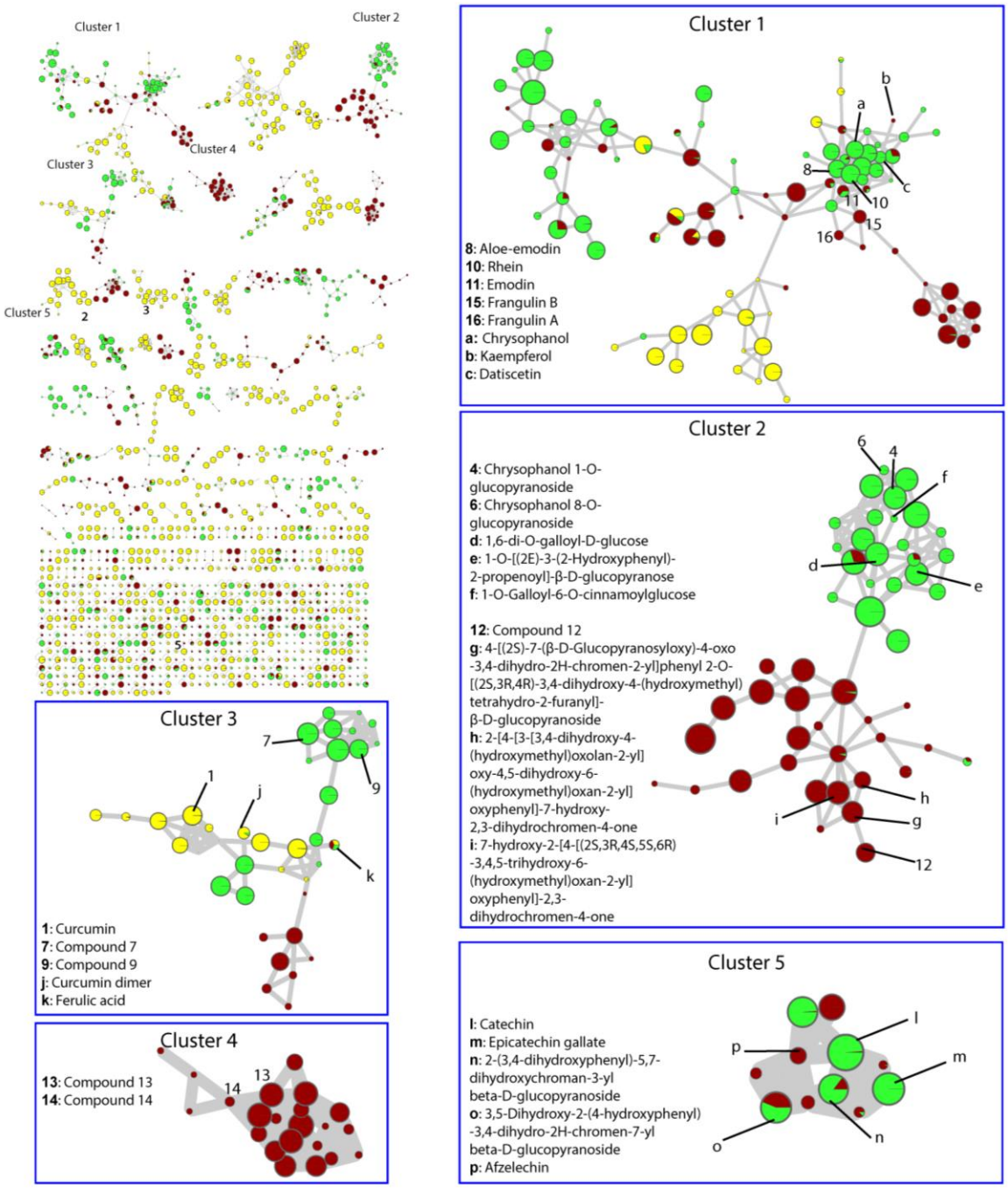

Figure 5.3 Molecular Network (MN) of the crude extracts of *Curcuma longa* (ME), *Frangula alnus* (AE) and *Rheum palmatum* (ME). Color of the node set as a pie-chart with the relative abundance of the feature in the different plant extracts. Cluster 1 includes putatively annotated anthraquinones. Cluster 2 includes anthraquinone glycosides and putatively annotated phenylpropanoids detected in *R. palmatum* and *F. alnus*. Cluster 3 contains curcumin, curcumin derivatives and phenolic glycosides. Cluster 4 is formed by dianthrones found exclusively in *F. alnus.* Cluster 5 contains putatively annotated catechins detected in *R. palmatum* and *F. alnus*.

Post-harvest application of plant extracts on potato tubers

The *in vitro* bioassay screening allowed the identification of three plant extracts with antifungal activities against *C. coccodes* and *H. solani*, and their bio-guided fractionation showed that these extracts contain antifungal compounds including curcuminoids (*C. longa*), anthraquinones (in *R. palmatum* and *F. alnus*), dianthrone derivatives (*F. alnus*) and phenolic glycosides (*R. palmatum*). Furthermore, other compounds highlighted by MN analysis in these extracts (i.e. catechins in *R. palmatum*) may be elicitors of potato defenses, as has been shown for other crops (Gillmeister et al., 2019). Altogether, these results suggest that the plant extracts of *F. alnus, R. palmatum* and *C. longa* may be used as a post-harvest treatment to control black dot (caused by *C. coccodes*) and silver scurf (caused by *H. solani*) in potatoes. To that end, a bioassay was developed to assess the control of these diseases using individual storage units in a laboratory-scale storage room (Supplementary Figure 5.7). Potato tubers with black dot and silver scurf symptoms at harvest were treated with water (positive control) or the chemical fungicide Amistar (250g/L azoxystrobin, Syngenta, Basel, Switzerland) diluted at 2.4 g/L (corresponding to 0.6 mg/mL azoxystrobin) (negative control). The plant extracts were diluted at 10 g/L, which, would correspond to the active concentration observed *in vitro* if full coverage of the tuber surface. To study the control efficiency of these plant-based products on the development of blemish diseases during storage, treated tubers were stored in individual storage units at 5°C and 95% relative humidity for 5 months. The experiment was conducted for three consecutive years (2016 – 2018), with a new tuber lot every year.

Silver scurf disease control on potato tubers with plant extracts during storage

In 2016, silver scurf severity was of 12% on the water-treated tubers after storage. Statistically significant differences were not observed between the water-treated control and any of the products applied, including the chemical fungicide Amistar, possibly due to a relatively low disease pressure (Ojiambo et al., 2010) (Figure 5.4A). In 2017, water-treated potato tubers showed much higher disease severity (52%). The chemical fungicide Amistar showed an efficacy of 35% in controlling silver scurf, and the plant extracts of *C. longa* and *F. alnus* exhibited a 43% and 31% reduction in silver scurf symptoms, respectively (Figure 5.4A). In 2018, silver scurf severity was 31% in the water-treated control. The chemical fungicide showed 43% disease reduction. The *C. longa* extract reduced in 23% the silver scurf symptoms, but differences in silver scurf severity between the water-treated control and the *C. longa*-treated tubers were not statistically significant in 2018 (Figure 5.4A). Surprisingly, the *F. alnus* aqueous extract did not show a reduction of siver scurf disease in 2018, and the *R. palmatum* extract did not show significant disease control in any of the years tested. The results obtained in 2017 suggest that the post-harvest application of the methanolic extract of *C. longa* and the aqueous extract of *F. alnus* may be efficient in controlling silver scurf, especially in seasons with very high disease pressure.

Black dot disease control on potato tubers with plant extracts during storage

In 2016, black dot severity in the water-treated control was 14%. The application of the fungicide Amistar and the *F. alnus* extract resulted in 45% and 36% disease reduction, although these differences were not statistically significant (Figure 5.4B). In 2017, the high disease pressure of silver scurf did not allow to precisely determine black dot severity, since its symptoms were masked by those of silver scurf. In 2018, the water-treated tubers exhibited 8% black dot severity. The chemical fungicide Amistar and the plant extracts of *F. alnus* and *R. palmatum* showed 30 – 35% disease reduction, but differences in disease severity with the water-treated control were not significant. The *C. longa* extract showed 47% efficacy in controlling black dot in 2018, with only 4% disease severity, significantly less than the water-treated control (Figure 5.4B). Altogether, these results suggest that the post-harvest application of the *C. longa* extract on black dot symptomatic potato tubers may be used to control disease during storage.

Notably, statistically significant differences between the water-treated tubers and the application of the chemical fungicide (containing azoxystrobin) were not observed for black dot; however, black dot disease was lower in the chemical fungicide-treated tubers every year, suggesting there is a trend of reduction in disease severity. Azoxystrobin was shown to have a higher MIC value against *C. coccodes* than against *H. solani in vitro*, indicating that the dose applied in potato tubers was sufficient to prevent the growth of *H. solani* but not (or only partially) of *C. coccodes*. Low disease pressure is associated with higher variability, and fungicide application may result in no disease control in low disease pressure conditions (Ojiambo et al., 2010). This may also explain the lack of statistically significant disease control in 2016 for both diseases, and in 2018 for black dot.

It is worth noting that full solubilization of the methanolic extracts of *R. palmatum* and *C. longa* in water for spraying was not totally achieved which may have lowered the applied dose. An adapted formulation of these crude extracts to preserve the antifungal activity and increase solubility may enhance the control of blemish diseases of potato during storage. Moreover, the concentration used in the storage bioassays was equivalent to the *in vitro* bioassays (10 g/L). The control of silver scurf using mineral salts, such as potassium sorbate, was shown to be efficient at 0.2M, equivalent to 30 g/L (Olivier et al., 1998), and phosphite was used at 335 g/metric ton of tubers (equivalent to 161 g/L) to control late blight and pink rot diseases in potato tubers (Miller et al., 2006). Thus, a higher dose of the plant extracts on potato tubers may be used to increase the efficacy of these treatments.

The bioguided isolation and characterization of the antifungal compounds present in these extracts allows now to monitor the stability of these compounds after treatment and during storage. Indeed, quantifying the antifungal compounds present on the tuber surface after treatment and during the storage time would allow to understand the dynamics of these active principles, information that could be used to include formulating agents that may preserve their activity if necessary.

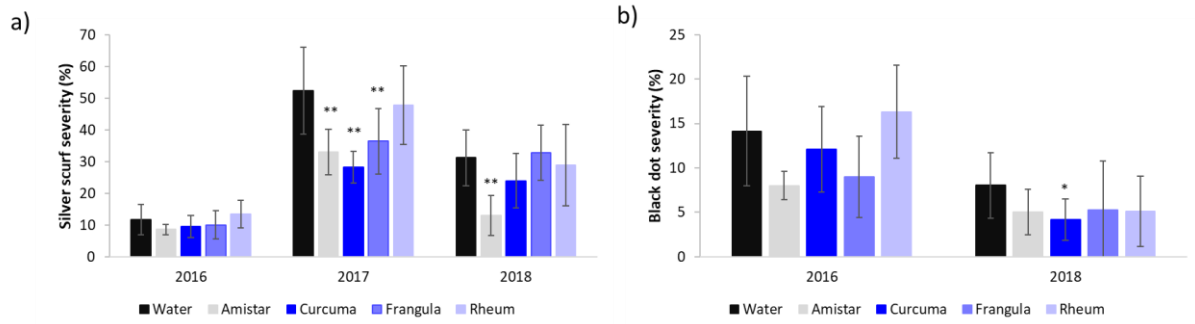

Figure 5.4 Silver scurf severity (A) and black dot severity (B) in potato tubers treated with water (negative control), the fungicide Amistar (positive control), C. longa ME, F. alnus AE or R. palmatum ME. Data represent the mean ± SD (n>3). Statistical analysis was performed by one-way ANOVA with the post-hoc Dunett's test compared to the negative control (*p <0,05 ; **p<0,01).

5.5. Conclusion

The post-harvest application of fungicides on potato tubers for human consumption need to result in residue levels below the fixed threshold by authorities, which are usually very low. In practice, chemical fungicides are not usually applied as post-harvest treatments because of residue concerns. An alternative method to control plant diseases during storage is the use of natural plant extracts or essential oils, methods that have been shown efficient in post-harvest diseases of several crops (Tripathi et al., 2008; Cruz et al., 2013; Malik A and Ahmed, 2016). The *in vitro* screening of plant extracts against *C. coccodes* and *H. solani* and the chemical characterization of their antifungal

compounds demonstrated that three plant extracts possess antifungal compounds against both diseases (curcuminoids in *C. longa* and anthraquinones and phenolic derivatives in *R. palmatum* and *F. alnus*). The three curcuminoids identified in *C. longa* have previously been shown to inhibit several phytopathogenic fungi, including *Colletotrichum* species and potato pathogens (*Phytophtora infestans*), *in vitro* (Kim et al., 2003; Radwan et al., 2014). Our results show that curcuminoids are also fungicidal to *C. coccodes* and *H. solani*, and the *in vivo* bioassay suggests that the *C. longa* methanolic extract, which is rich in these curcuminoids, could be an efficient tool to control black dot and silver scurf during storage.

Plant extracts of the *Rheum* genus have been shown to possess antifungal activity against several phytopathogens *in vitro* and to protect plants in the field, showing both antifungal and elicitation properties (Krebs et al., 2006; Gindro et al., 2007; Gillmeister et al., 2019). Our results show that the *R. palmatum* extract contains several antifungal compounds, including anthraquinones (i.e. rhein) and phenolic glycosides, which are fungicidal to *C. coccodes* and *H. solani*. However, the post-harvest application of the *R. palmatum* methanolic extract on potato tubers did not control black dot or silver scurf during storage in any of the three years. A higher dose than that used in the assays (10 g/L), or the use of an enriched fraction of the extract, should be tested for the control of both diseases in potato tubers. Furthermore, quantifying the active principles on potato tubers after treatment and throughout storage could be performed in order to understand the stability of these compounds, and specific formulations could be designed to ensure stability throughout storage. Furthermore, residue analysis after storage could be analyzed in order to determine whether residual anthraquinones or other compounds are still present in potato tubers at commercialization. If necessary, a washing of the tubers before commercialization could be recommended, as it is for *Deposan®*-treated (bacterial-based product) potato tubers.

The *F. alnus* bark extract had previously been shown to possess antifungal activity against several phytopathogens, including the potato pathogen *Alternaria alternata* (Manojlovic et al., 2005). Furthermore, controlling fusarium head blight in wheat and downy mildew in grapewine by *F. alnus* extracts is achieved by the elicitation of host defenses (Gindro et al., 2007; Forrer et al., 2014). Our results showed that frangulin B (**15**) is fungicidal to *C. coccodes,* with a MIC value comparable to a reference fungicide. However, all compounds isolated from *F. alnus* showed relatively high MIC values against *H. solani*. Nonetheless, the *F. alnus* aqueous extract showed control of silver scurf, caused by *H. solani*, *in planta*. These results suggest that *F. alnus* may contain other antifungal compounds or compounds that prime defenses in potato tubers, especially against silver scurf.

Altogether, our results show that the crude plant extracts of *F. alnus*, *R. palmatum* and *C. longa* are a source of antifungal compounds against phytopathogenic fungi, especially anthraquinones and curcuminoids, but also phenolic derivatives. Furthermore the potential of using plants to treat post-harvest potato diseases is shown. The post-harvest treatment of potato tubers with these extracts to control blemish diseases has potential, an approach that could be used for both organic and conventional farming.

The isolation and characterization of the bioactive compounds in this study allows their detection on potato tubers after treatment and during storage, which allows to determine their evolution using the *in vivo* bioassays. These informations can then be used to establish treatment protocols, formulation strategies and residue persistence for the post-harvest treatment of black dot and silver scurf-infected potato tubers. Efforts in formulating these extracts to preserve the antifungal activity and increasing stability, adhesion and solubility need to be adressed for the successful use of these products.

5.6. Aknowledgements

The authors are thankful to the Commission for Technology and Innovation (Switzerland) for providing financial support for this project. The School of Pharmaceutical Sciences of the University of Geneva (J-L. Wolfender) is thankful to the Swiss National Science Foundation for the support in the acquisition of the NMR 600 MHz (SNF R'Equip grant 316030_164095).

5.7. Supplementary material

Supplementary Table 5.1 Yield (g/100 g of dry material) of the different extraction methods in the plant extracts used for the screening of antifungal compounds

	Yield (g/100 g)		
Plant material	**AER**	**AE**	**ME**
Aloe vera	10,35	11,24	31,02
Rheum palmatum roots	19,40	11,62	21,69
Frangula alnus bark	12,41	15,24	19,41
Urtica dioica leaves	10,41	12,34	n.a.
Salix viminalis	9,65	11,47	n.a.
Equisetum arvense	11,65	10,85	n.a.
Vitis vinifera bark	10,48	15,95	6,95
Epilobium sp. Flowers	11,44	22,61	7,65
Hypericum perforatum herb	15,50	12,14	14,66
Artemisia sp.	19,97	17,25	21,05
Curcuma longa rhizomes	n.a.	n.a.	13,50

Supplementary Table 5.2 Yield (percentage, %) and MIC (in mg/mL) of the crude extract and the SPE fractions of the *C. longa* methanolic extract (ME), *R. palmatum* methanolic extract (ME) and *F. alnus* aqueous extract (AE). * Indicates fungistatic activity.

			Yield (%)	MIC (mg/mL)	
				C. coccodes	*H. solani*
C. longa rhizomes	Crude extract			10	10
	F1	30%	31,27	>10	>10
	F2	50%	20,86	>10	10
	F3	80%	34,98	10	5
	F4	100%	10,96	>10	>10
R. palmatum roots	Crude extract			10	2,5
	F1	30%	44,27	>10	>10
	F2	50%	24,05	>10	>10
	F3	80%	22,32	2,5	0,125
	F4	100%	9,36	10	1
F. alnus bark	Crude extract			10	10*
	F1	10%	40,15	>10	>10
	F2	30%	12,12	>10	>10
	F3	50%	16,21	>10	>10
	F4	65%	23,24	10	>10
	F5	80%	4,75	8	10
	F6	100%	3,53	10	10

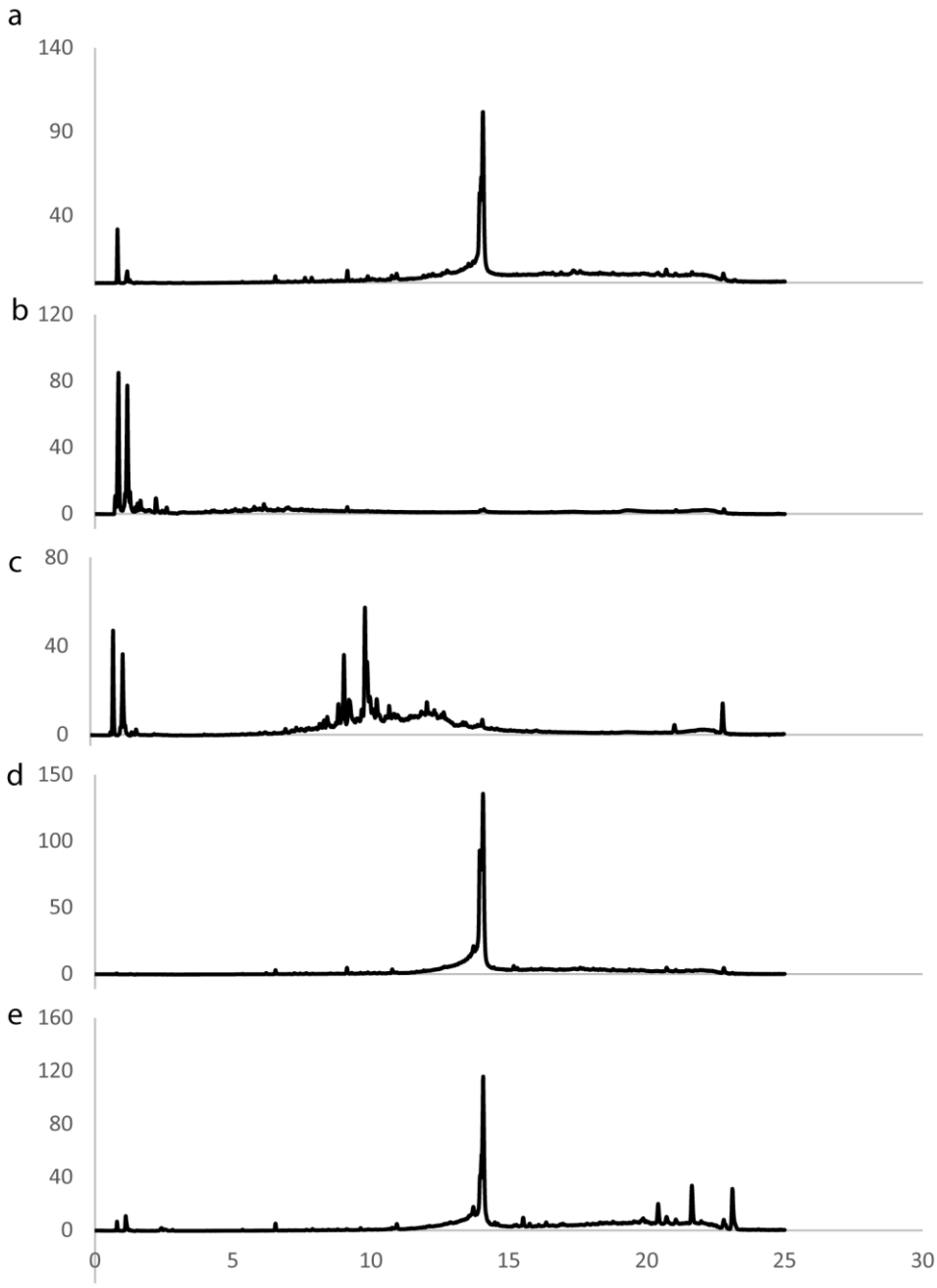

Supplementary Figure 5.1 CAD chromatograms of the methanolic extract of *C. longa* and its SPE Fractions. a) UHPLC chromatogram of the methanolic extract of *C. longa* exhibiting a main central peak corresponding to the curcuminoids. b) UHPLC chromatograms of Fraction 1 (30% methanol) of the SPE exhibiting mainly polar metabolites, c) UHPLC chromatograms of Fraction 2 (50% methanol) of the SPE exhibiting mainly polar and mid-polar metabolites, d) UHPLC chromatograms of Fraction 3 (80% methanol) of the SPE exhibiting mainly the curcuminoids, e) UHPLC chromatograms of Fraction 4 (100% methanol) of the SPE exhibiting mainly curcuminoids and other apolar compounds.

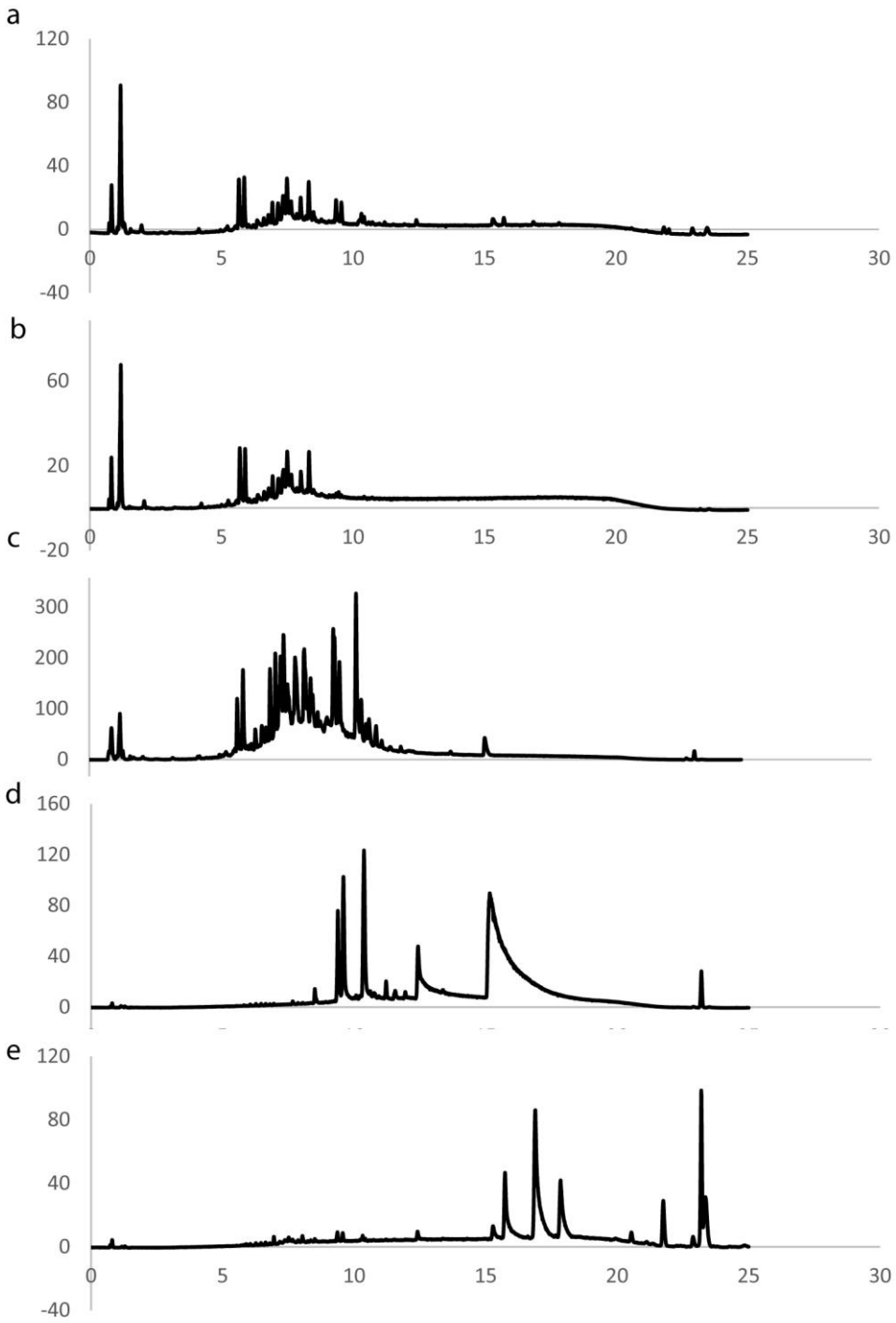

Supplementary Figure 5.2 CAD chromatograms of the methanolic extract of *R. palmatum* and its SPE Fractions. a) UHPLC chromatogram of the methanolic extract of *R. palmatum* exhibiting mainly polar compounds. b) UHPLC chromatograms of Fraction 1 (30% methanol) of the SPE exhibiting mainly polar metabolites, c) UHPLC chromatograms of Fraction 2 (50% methanol) of the SPE exhibiting mainly polar and mid-polar metabolites, d) UHPLC chromatograms of Fraction 3 (80% methanol) of the SPE exhibiting mid-polar compounds, including anthraquinones (i.e. rhein), e) UHPLC chromatograms of Fraction 4 (100% methanol) of the SPE exhibiting mainly apolar compounds.

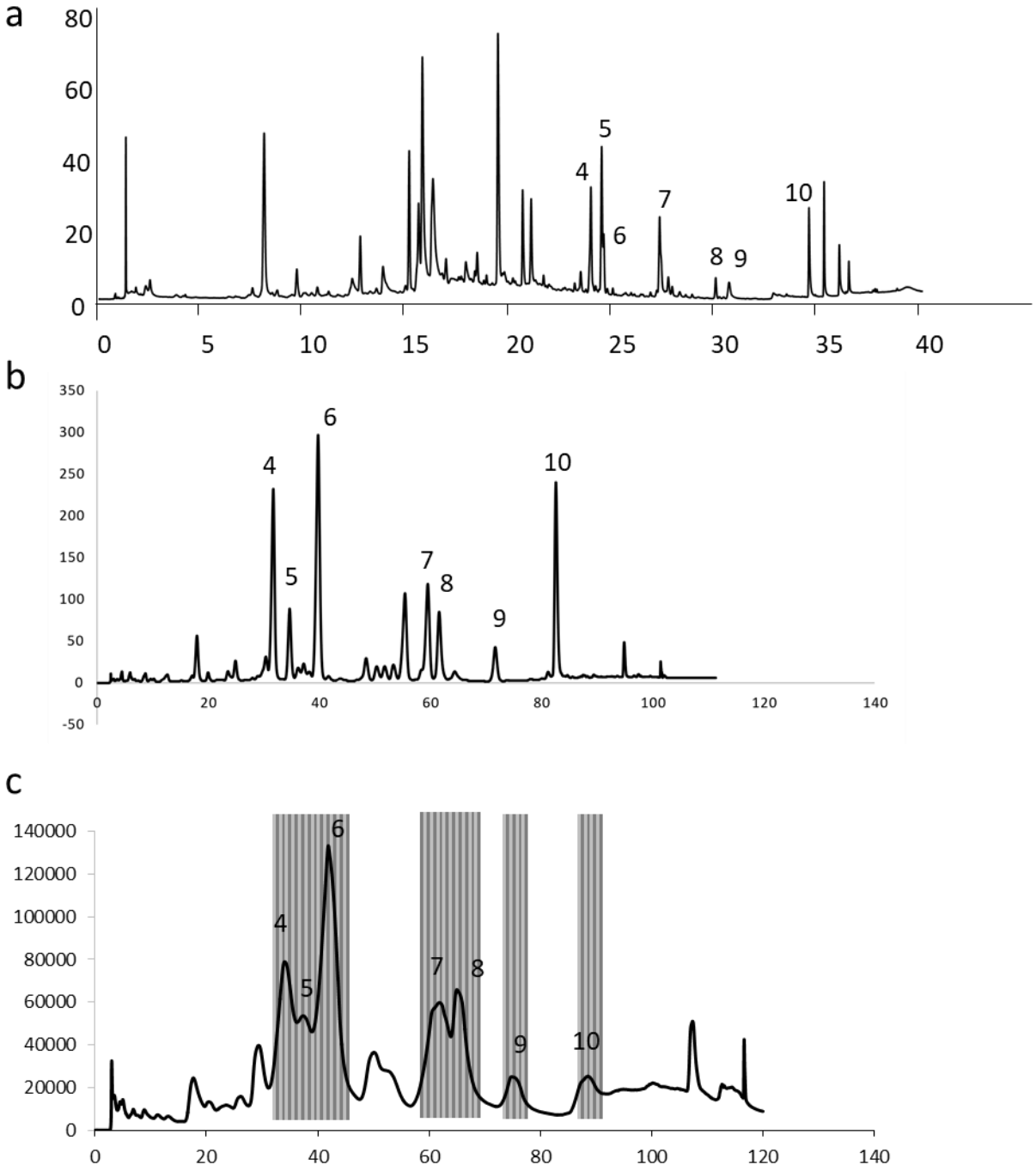

Supplementary Figure 5.3 UV chromatograms of the aqueous extract of *R. palmatum* and its fractionation by preparative chromatography. a) UHPLC metabolite profiling of the methanolic crude extract of *R. palmatum*. b) HPLC metabolite profiling of Fraction 3 of the SPE (optimized gradient in analytical conditions). c) Semi-preparative chromatography for the fractionation of fractions 3 (35 mg). All chromatograms show UV at 280 nm. Compounds 4 – 10 are the isolated compounds from *R. palmatum.*

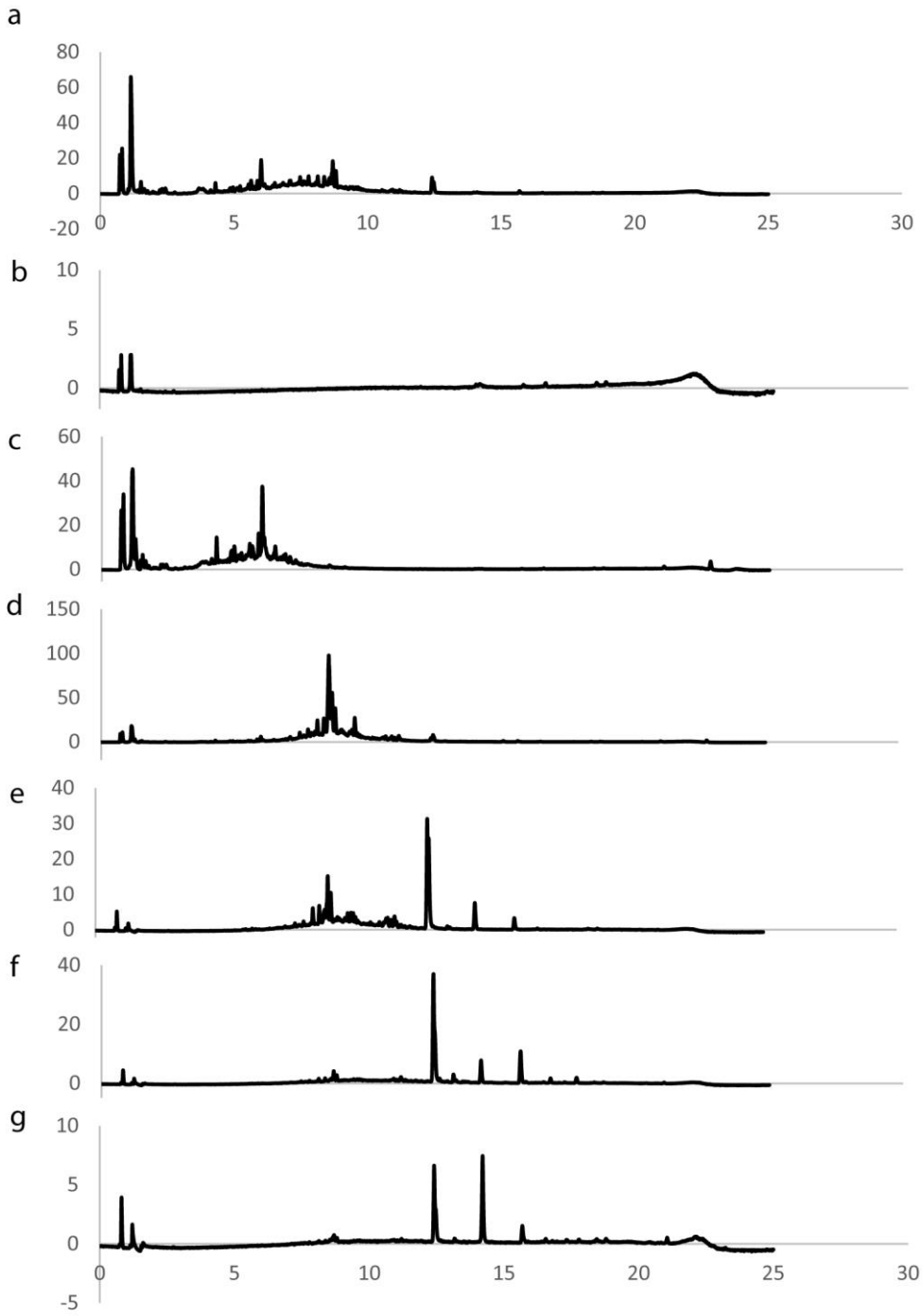

Supplementary Figure 5.4 CAD chromatograms of the aqueous extract of *F. alnus* and its SPE Fractions. a) UHPLC chromatogram of the aqueous extract of *F. alnus* exhibiting mainly polar compounds. b) UHPLC chromatograms of Fraction 1 (10% methanol) of the SPE exhibiting mainly polar metabolites, c) UHPLC chromatograms of Fraction 2 (30% methanol) of the SPE exhibiting mainly polar metabolites, d) UHPLC chromatograms of Fraction 3 (50% methanol) of the SPE exhibiting mid-polar compounds, e) UHPLC chromatograms of Fraction 4 (65% methanol) of the SPE exhibiting mid-polar compounds including anthraquinone glycosides (frangulins), f) UHPLC chromatograms of Fraction 5 (80% methanol) of the SPE exhibiting mid-polar compounds including anthraquinones, g) UHPLC chromatograms of Fraction 6 (100% methanol) of the SPE exhibiting mid-polar compounds including anthraquinones.

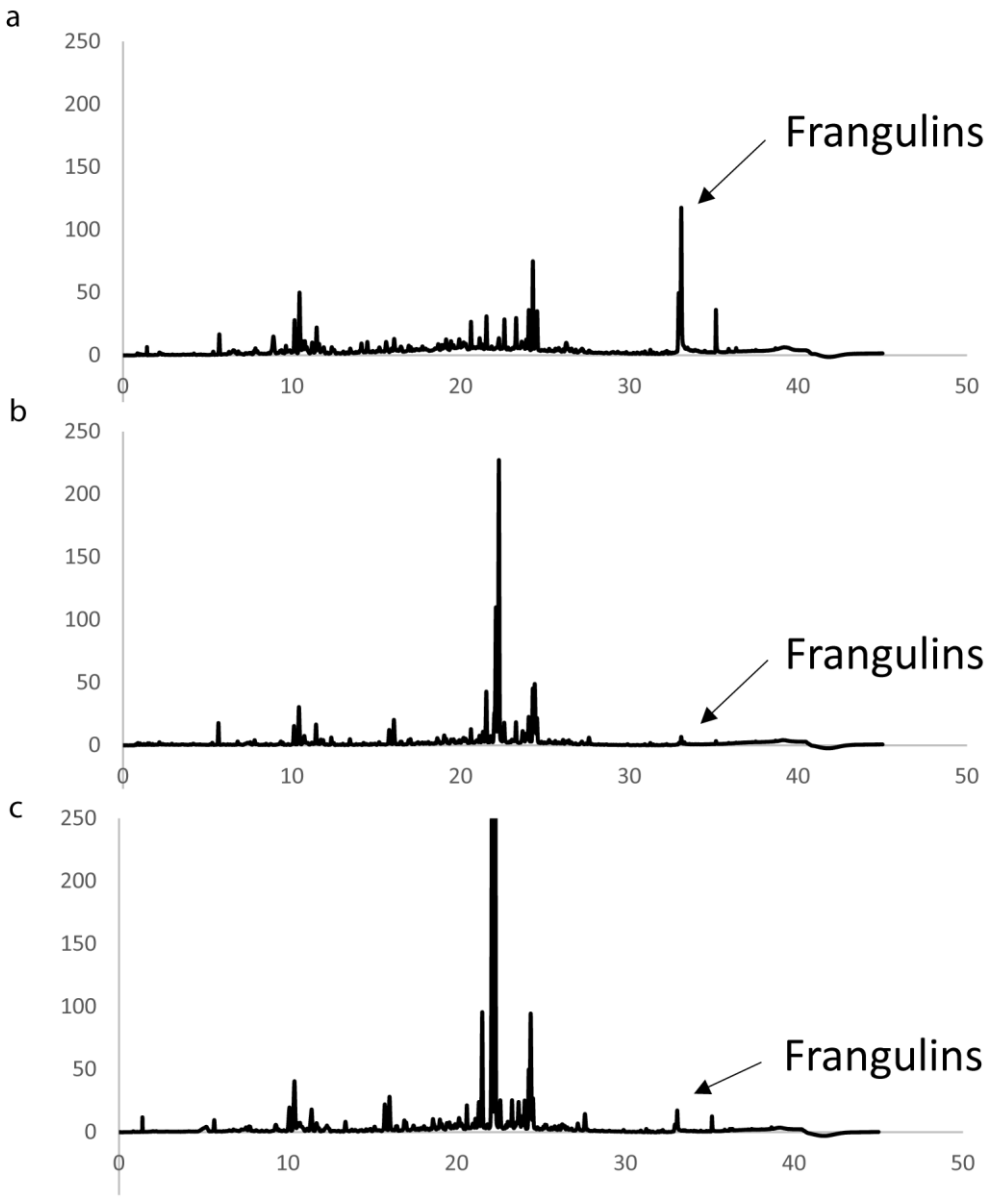

Supplementary Figure 5.5 UV (435 nm) chromatograms of the a) aqueous extract, b) aqueous extract with reflux and c) methanolic extract of *F. alnus*. Frangulin A and B (coeluting) are indicated with an arrow.

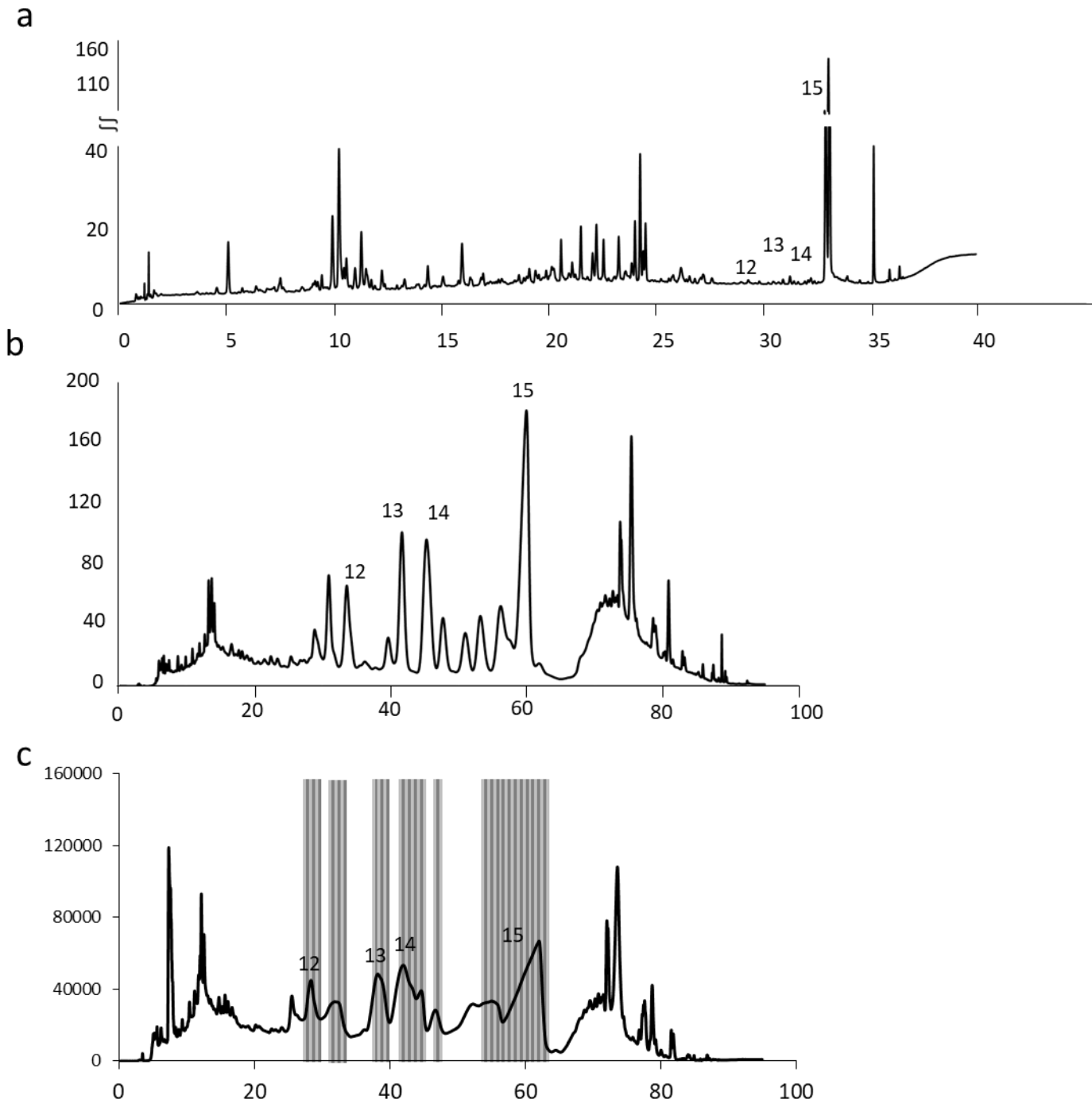

Supplementary Figure 5.6 UV chromatograms of the aqueous extract of *F. alnus* and its fractionation by preparative chromatography. a) UHPLC metabolite profiling of the aqueous crude extract of *F. alnus*. b) HPLC metabolite profiling of Fractions 39-41 (optimized gradient in analytical conditions). c) Semi-preparative chromatography for the fractionation of fractions 39-41 (35 mg). All chromatograms show UV at 280 nm. Compounds 12 – 15 are the isolated compounds from *F. alnus*.

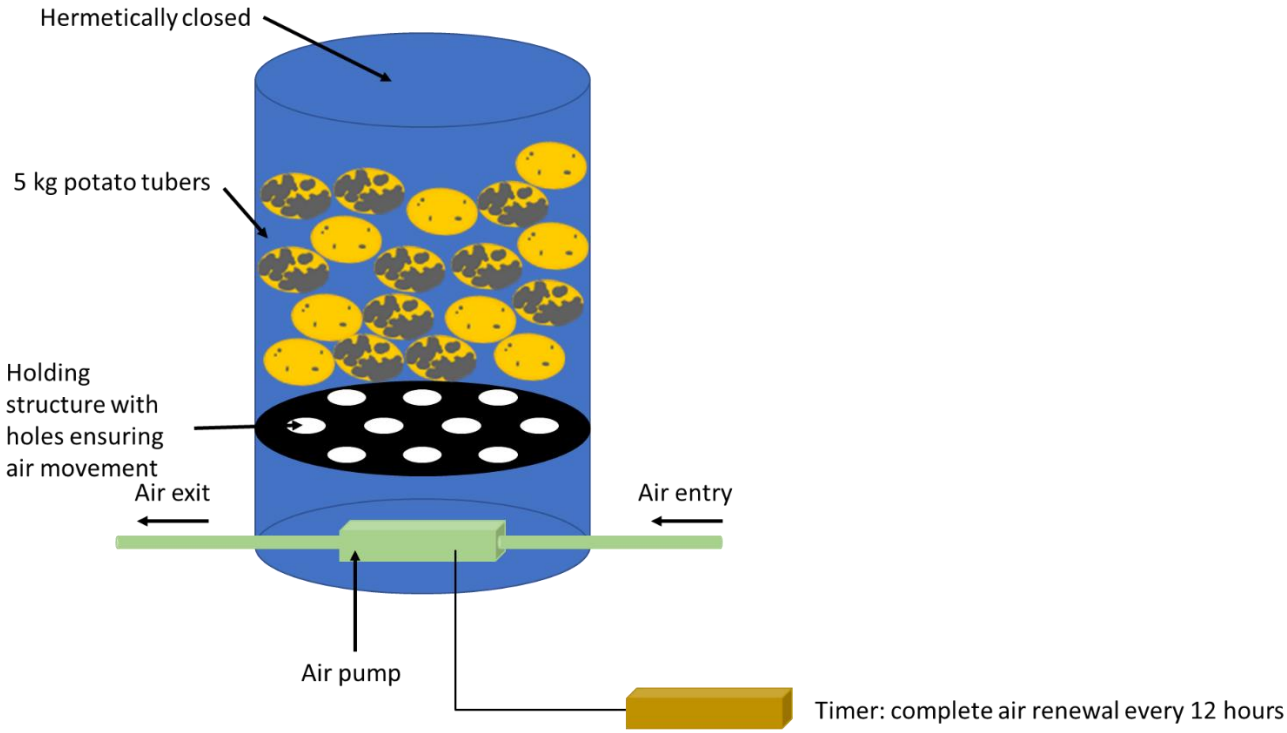

Supplementary Figure 5.7 Design of the prototypes used for potato storage in the *in vivo* bioassay of plant extracts against black dot and silver scurf. 30 liters containers, hermetically closed, contain 5 kg of potato tubers (approximately 80 tubers) laying on a holding structure. Beneath the holding structure, an air pump controlled with a timer ensures renewal of the air every 12 hours to avoid concentration of CO_2 above 3000 ppm.

NMR data of known compounds:

Chrysophanol 1-O-β-D-glucopyranoside (**4**) ^{1}H NMR (CD_3OD, 600 MHz) δ 2.52 (3H, s, CH_3-3), 3.43 (1H, t, *J* = 9.2 Hz, H-4'), 3.54 (1H, t, *J* = 9.2 Hz, H-3'), 3.57 (1H, m, H-5'), 3.69 (1H, dd, *J* = 9.2, 7.7 Hz, H-2'), 3.72 (1H, dd, *J* = 12.1, 6.2 Hz, H-6'b), 3.95 (1H, dd, *J* = 12.1, 2.3 Hz, H-6'a), 5.09 (1H, d, *J* = 7.7 Hz, H-1'), 7.31 (1H, dd, *J* = 7.9, 1.2 Hz, H-7), 7.62 (1H, s, H-2), 7.69 (1H, t, *J* = 7.9 Hz, H-6), 7.74 (1H, dd, *J* = 7.9, 1.2 Hz, H-5), 7.86 (1H, s, H-4); ^{13}C NMR (CD_3OD, 151 MHz) δ 22.2 (CH_3-3), 62.6 (C-6'), 71.4 (C-4'), 74.9 (C-2'), 77.6 (C-3'), 78.7 (C-5'), 103.5 (C-1'), 118.3 (C-8a), 119.8 (C-5), 120.6 (C-9a), 123.7 (C-4), 125.3 (C-2), 125.5 (C-7), 134.3 (C-10a), 136.3 (C-4a), 137.3 (C-6), 149.4 (C-3), 160.2 (C-1), 163.5 (C-8), 183.7 (C-10), 190.1 (C-9).

Emodin 6-O-β-D-glucoside (**5**) ^{1}H NMR (DMSO-d_6, 600 MHz) δ 2.36 (3H, s, CH_3-3), 3.21 (1H, t, *J* = 9.3 Hz, H-4'), 3.30 (1H, t, *J* = 9.3 Hz, H-3'), 3.34 (2H, m, H-2', H-5'), 3.51 (1H, dd, *J* = 11.9, 5.6 Hz, H-6'b), 3.72 (1H, dd, *J* = 11.9, 1.7 Hz, H-6'a), 4.79 (1H, d, *J* = 7.6 Hz, H-1'), 6.50 (1H, d, *J* = 2.3 Hz, H-7), 6.84 (1H, d, *J* = 2.3 Hz, H-5), 7.04 (1H, d, *J* = 1.7 Hz, H-2), 7.37 (1H, d, *J* = 1.7 Hz, H-4), 14.03 (1H, s, OH-1); ^{13}C NMR (DMSO-d_6, 151 MHz) δ 21.3 (CH_3-3), 60.7 (C-6'), 69.7 (C-4'), 73.5 (C-2'), 75.9 (C-3'), 77.4 (C-5'), 102.6 (C-1'), 106.9 (C-8a), 110.7 (C-7), 114.9 (C-5), 115.3 (C-9a), 118.5 (C-4), 123.8 (C-2), 145.1 (C-3), 161.7 (C-1), 162.9 (C-8), 183.9 (C-10).

Chrysophanol 8-O-β-D-glucopyranoside (**6**) ^{1}H NMR (CD_3OD, 600 MHz) δ 2.46 (3H, s, CH_3-3), 3.45 (1H, t, *J* = 9.3 Hz, H-4'), 3.54 (2H, m, H-3', H-5'), 3.69 (1H, dd, *J* = 9.3, 7.7 Hz, H-2'), 3.73 (1H, dd, *J* = 12.1, 5.9 Hz, H-6'b), 3.94 (1H, dd, *J* = 12.1, 2.3 Hz, H-6'a), 5.09 (1H, d, *J* = 7.7 Hz, H-1'), 7.15 (1H, s, H-2), 7.60 (1H, s, H-4), 7.79 (1H, dd, *J* = 8.5, 1.6 Hz, H-7), 7.82 (1H, t, *J* = 8.5, 7.2 Hz, H-6), 8.02 (1H, dd, *J* = 7.2, 1.6 Hz, H-5); ^{13}C NMR (CD_3OD, 151 MHz) δ 21.6 (CH_3-3), 62.3 (C-6'), 70.9 (C-4'), 74.6 (C-2'), 77.3 (C-3'), 78.3 (C-

5'), 103.2 (C-1'), 116.0 (C-9a), 120.6 (C-4), 122.6 (C-5), 124.7 (C-7), 125.0 (C-2), 136.2 (C-10a), 136.6 (C-6), 149.2 (C-3), 159.8 (C-8), 183.4 (C-10).

4-[4-[[6-O-[(2E)-3-(4-hydroxyphenyl)-1-oxo-2-propen-1-yl]-2-O-(3,4,5-trihydroxybenzoyl)-β-D-glucopyranosyl]oxy]phenyl]- 2-Butanone (**7**) ^{1}H NMR (CD_3OD, 600 MHz) δ 2.05 (3H, s, H-1), 2.58 (2H, m, H-4), 2.66 (2H, m, H-3), 3.54 (1H, t, *J* = 9.9, 9.1 Hz, Glc-4), 3.76 (1H, t, *J* = 9.1 Hz, Glc-3), 3.81 (1H, ddd, *J* = 9.8, 7.3, 2.3 Hz, Glc-5), 4.44 (1H, dd, *J* = 11.8, 7.3 Hz, Glc-6''), 4.58 (1H, dd, *J* = 11.8, 2.3 Hz, Glc-6'), 5.09 (1H, d, *J* = 8.0 Hz, Glc-1), 5.16 (1H, t, *J* = 9.1, 8.0 Hz, Glc-2), 6.39 (1H, d, *J* = 16.0 Hz, pC-8), 6.84 (2H, d, *J* = 8.7 Hz, pC-3, pC-5), 6.85 (2H, d, *J* = 8.7 Hz, H-3', H-5'), 6.96 (2H, d, *J* = 8.7 Hz, H-2', H-6'), 7.09 (2H, s, G-3, G-7), 7.50 (2H, d, *J* = 8.7 Hz, pC-2, pC-6), 7.66 (1H, d, *J* = 16.0 Hz, pC-7); ^{13}C NMR (CD_3OD, 151 MHz) δ 29.5 (C-1, C-3), 45.4 (C-4), 64.2 (Glc-6), 71.9 (Glc-4), 74.9 (Glc-2), 75.4 (Glc-5), 76.0 (Glc-3), 100.8 (Glc-1), 109.8 (G-3, G-7), 114.8 (pC-8), 116.6 (pC-3, pC-5), 117.8 (C-3', C-5'), 127.1 (pC-1), 129.9 (C-2', C-6'), 131.0 (pC-2, pC-6), 136.5 (C-1'), 139.7 (G-5), 146.2 (G-4, G-6), 146.5 (pC-7), 157.0 (C-4'), 161.2 (pC-4), 167.3 (G-1), 168.7 (pC-9), 210.7 (C-2).

Aloe emodin (**8**) : ^{1}H NMR (CD_3OD, 600 MHz) δ 4.72 (2H, s, H-11), 7.34 (1H, d, *J* = 1.5 Hz, H-2), 7.34 (1H, dd, *J* = 8.3, 1.2 Hz, H-7), 7.76 (2H, t, *J* = 8.3, 7.5 Hz, H-6), 7.81 (1H, d, *J* = 1.5 Hz, H-4), 7.82 (1H, dd, *J* = 7.5, 1.2 Hz, H-5); ^{13}C NMR (CD_3OD, 151 MHz) δ 63.8 (C-11), 115.5 (C-9a), 116.9 (C8a), 118.3 (C-4), 120.5 (C-5), 121.9 (C-2), 125.2 (C-7), 134.9 (C-10a), 138.0 (C-6), 153.9 (C-3), 163.4 (C-8).

4-[4-[[6-O-[(2E)-1-Oxo-3-phenyl-2-propen-1-yl]-2-O-(3,4,5-trihydroxybenzoyl)-ß-D-glucopyranosyl]oxy]phenyl]-2-butanone (**9**) ^{1}H NMR (CD_3OD, 600 MHz) δ 2.04 (3H, s, H-1), 2.59 (2H, m, H-4), 2.65 (2H, m, H-3), 3.55 (1H, t, *J* = 9.6, 8.9 Hz, Glc-4), 3.76 (1H, t, *J* = 9.4, 8.9 Hz, Glc-3), 3.83 (1H, ddd, *J* = 9.6, 7.2, 2.3 Hz, Glc-5), 4.46 (1H, dd, *J* = 11.9, 7.2 Hz, Glc-6''), 4.60 (1H, dd, *J* = 11.9, 2.3 Hz, Glc-6'), 5.11 (1H, d, *J* = 8.0 Hz, Glc-1), 5.16 (1H, dd, *J* = 9.4, 8.0 Hz, Glc-2), 6.59 (1H, d, *J* = 16.0 Hz, cin-8), 6.85 (2H, d, *J* = 8.8 Hz, H-3', H-5'), 6.97 (2H, d, *J* = 8.8 Hz, H-2', H-6'), 7.09 (2H, s, G-3, G-7), 7.44 (3H, m, cin-3, cin-4, cin-5), 7.65 (2H, m, cin-2, cin-6), 7.74 (1H, d, *J* = 16.0 Hz, cin-7); ^{13}C NMR (CD_3OD, 151 MHz) δ 29.5 (C-1, C-3), 45.5 (C-4), 64.4 (Glc-6), 71.7 (Glc-4), 74.9 (Glc-2), 75.3 (Glc-5), 75.8 (Glc-3), 100.9 (Glc-1), 109.8 (G-3, G-7), 117.8 (C-3', C-5'), 118.5 (cin-8), 120.9 (G-2), 129.0 (cin-2, cin-6), 129.8 (cin-3, cin-5), 129.9 (C-2', C-6'), 131.3 (cin-4), 135.5 (cin-1), 136.6 (C-1'), 139.8 (G-5), 146.1 (G-4, G-6), 146.3 (cin-7), 156.8 (C-4'), 167.4 (G-1), 167.9 (cin-9), 210.5 (C-2).

Rhein (**10**) ^{1}H NMR (CD_3OD, 600 MHz) δ 7.34 (1H, dd, *J* = 8.3, 1.2 Hz, H-7), 7.77 (1H, dd, *J* = 8.3, 7.5 Hz, H-6), 7.82 (1H, d, *J* = 1.6 Hz, H-2), 7.83 (1H, dd, *J* = 7.5, 1.2 Hz, H-5), 8.35 (1H, d, *J* = 1.6 Hz, H-4); ^{13}C NMR (CD_3OD, 151 MHz) δ 117.3 (C-8a), 118.3 (C-9a), 120.8 (C-5), 121.2 (C-4), 125.4 (C-2), 125.5 (C-7), 134.9 (C-4a), 135.3 (C-10a), 138.5 (C-6), 163.6 (C-1), 163.7 (C-8), 170.8 (C-11), 182.8 (C-10), 194.3 (C-9).

NMR spectra of new compounds:

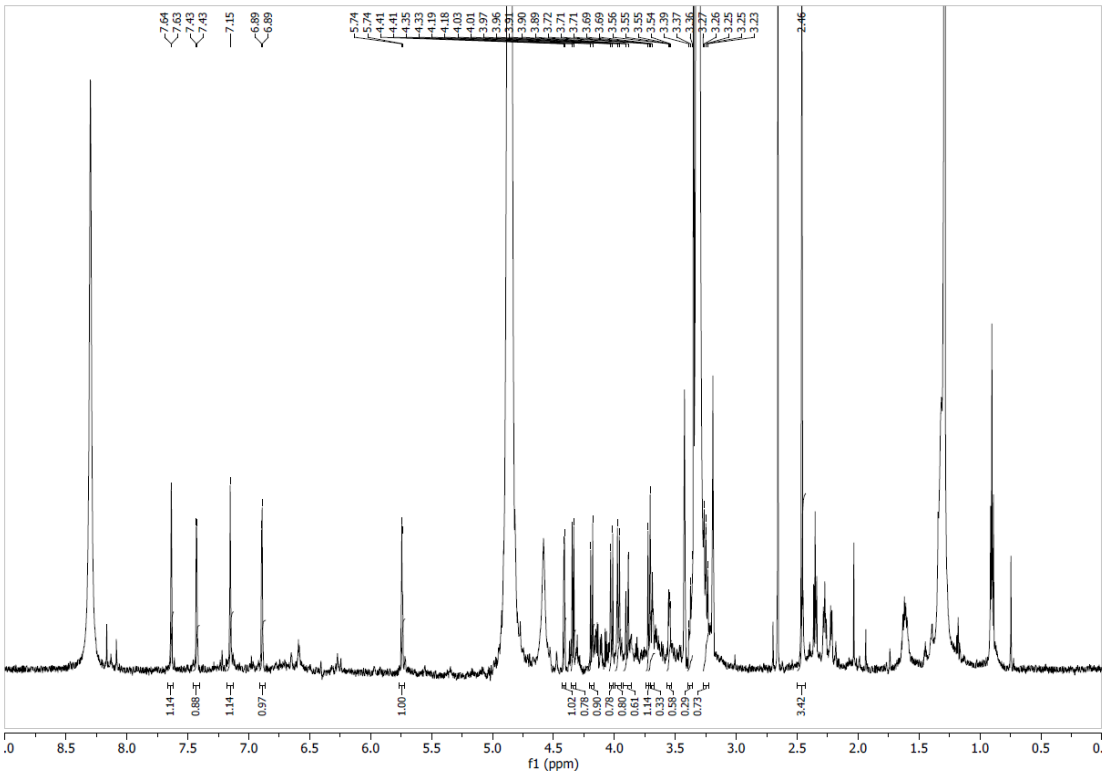

Supplementary Figure 5.8 ^{1}H NMR spectrum of compound **12** in CD_3OD at 600 MHz

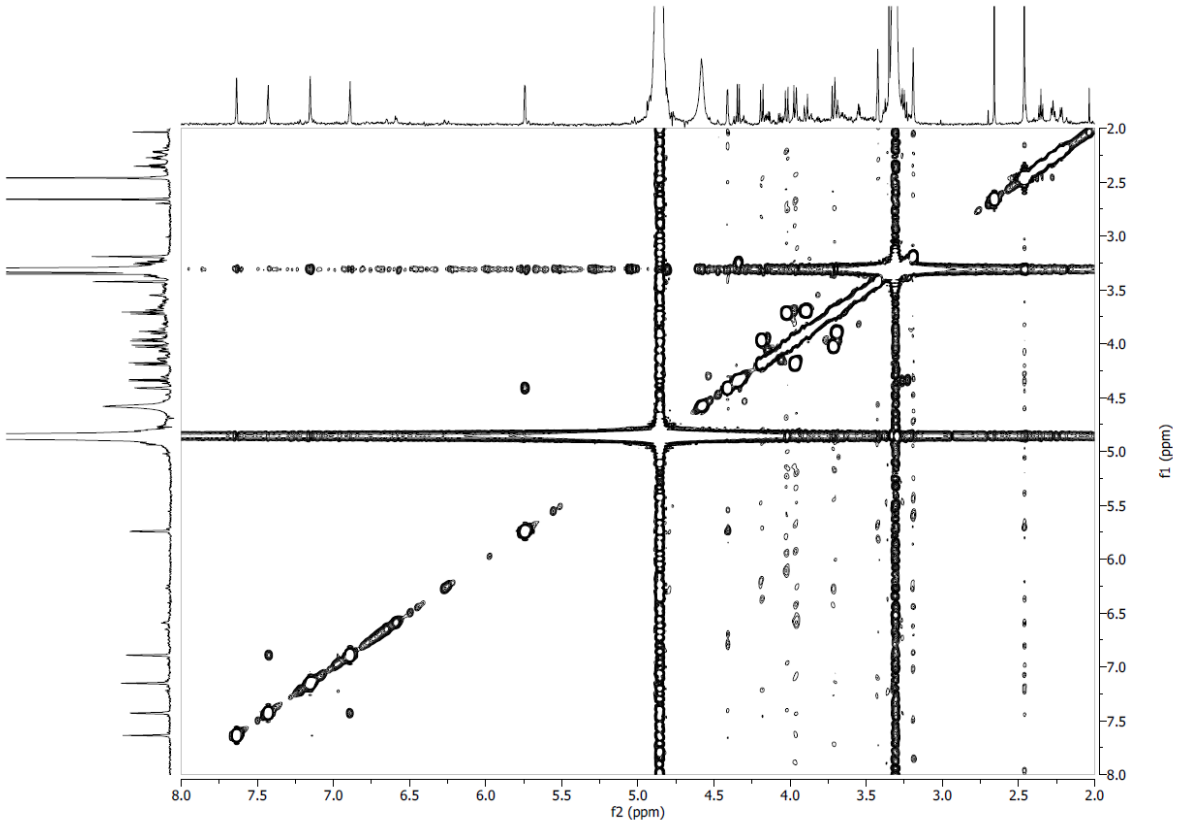

Supplementary Figure 5.9 COSY NMR spectrum of compound **12** in CD_3OD

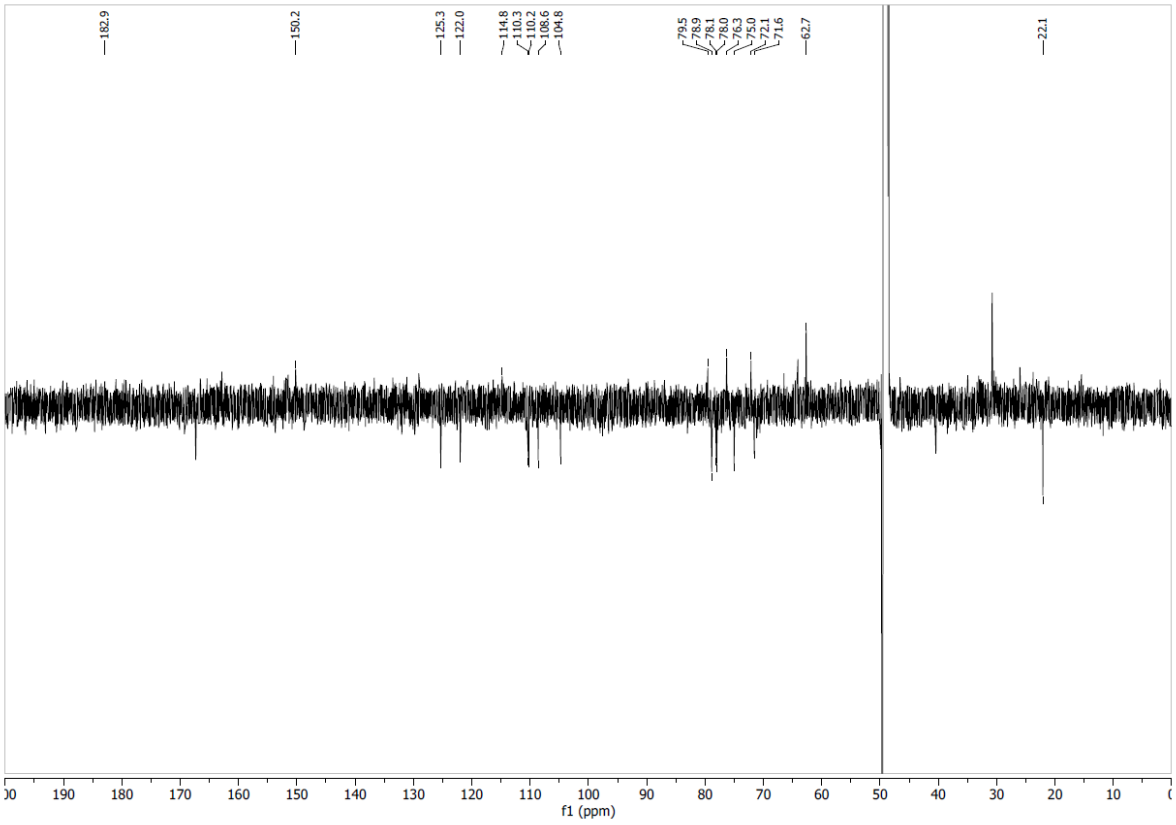

Supplementary Figure 5.10 ^{13}C-DEPTQ NMR spectrum of compound **12** in CD_3OD at 151 MHz

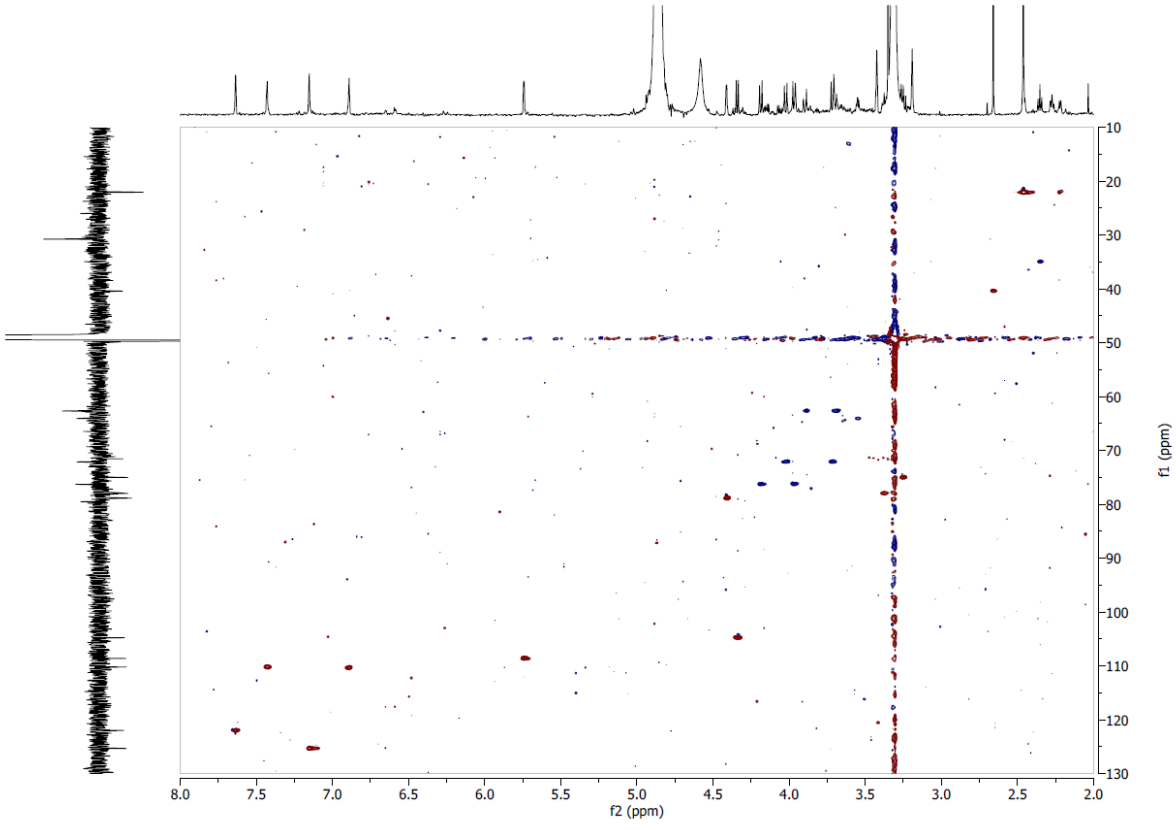

Supplementary Figure 5.11 Edited-HSQC NMR spectrum of compound **12** in CD_3OD

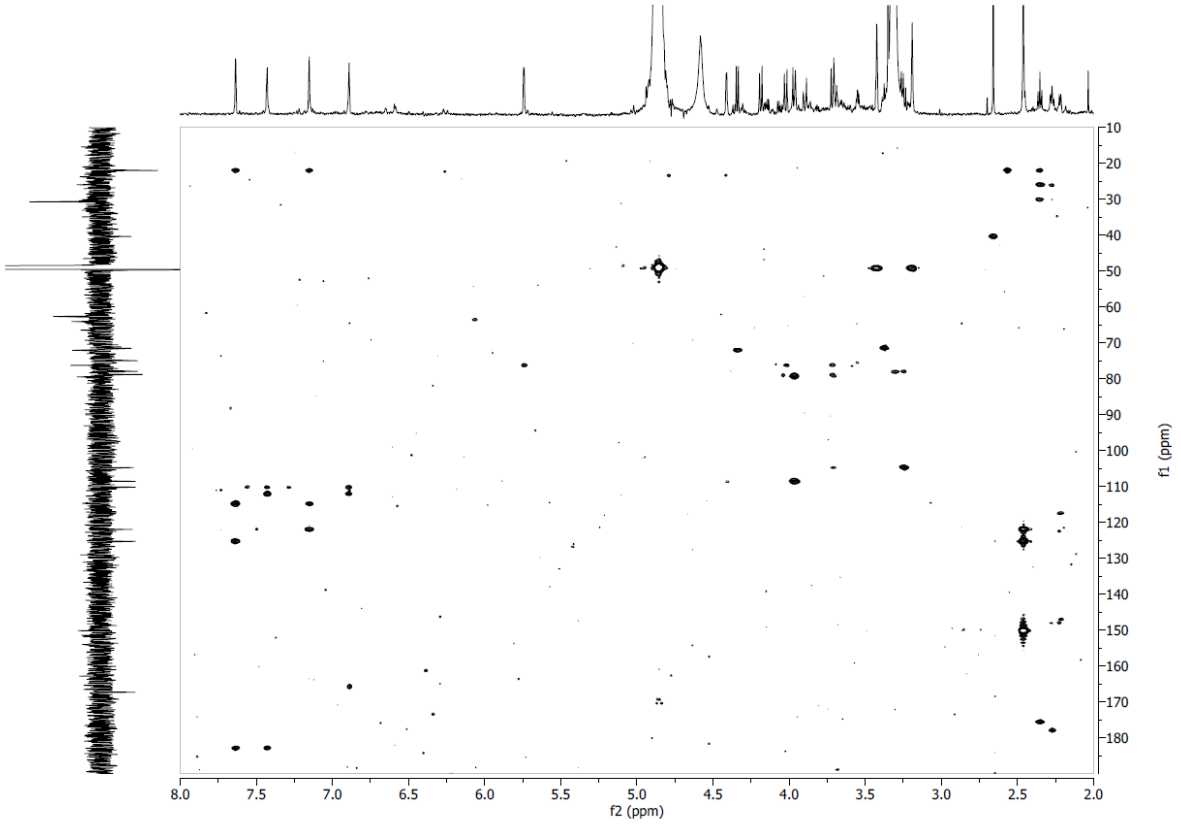

Supplementary Figure 5.12 HMBC NMR spectrum of compound **12** in CD_3OD

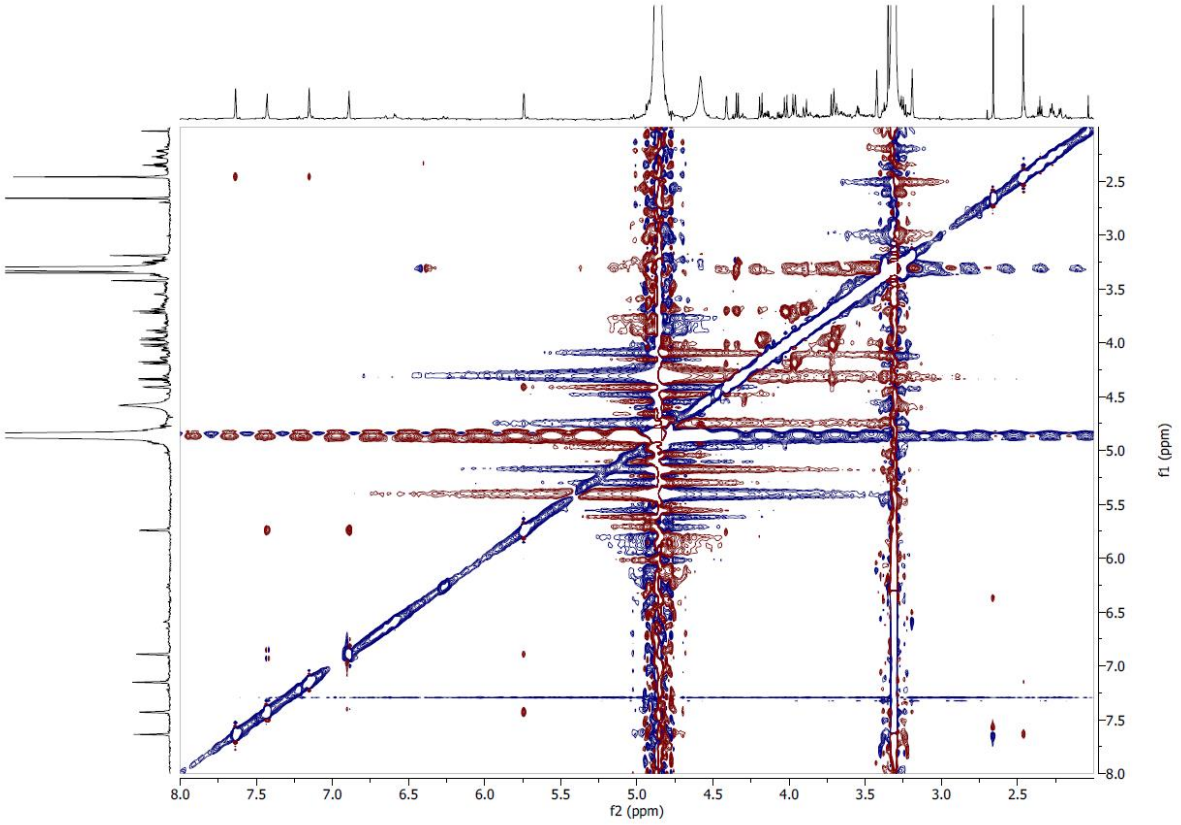

Supplementary Figure 5.13 ROESY NMR spectrum of compound **12** in CD_3OD

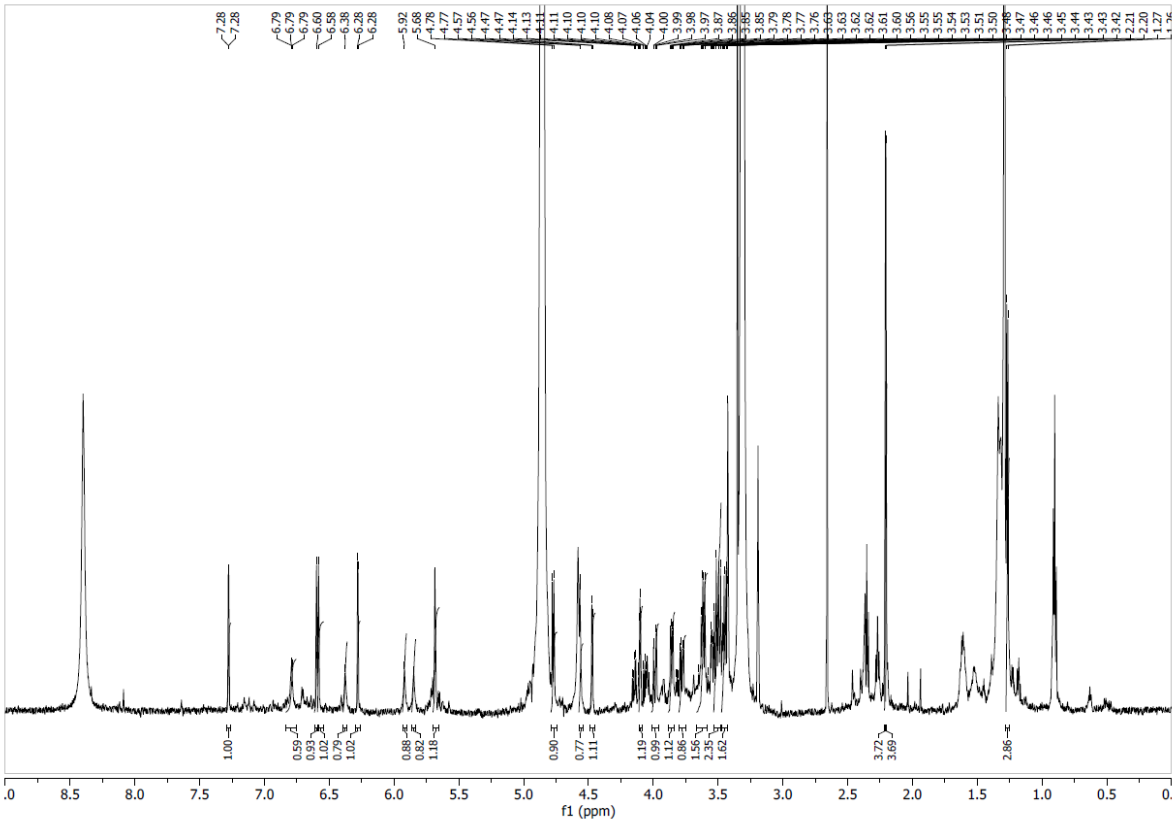

Supplementary Figure 5.14 ^{1}H NMR spectrum of compound **13** in CD_3OD at 600 MHz

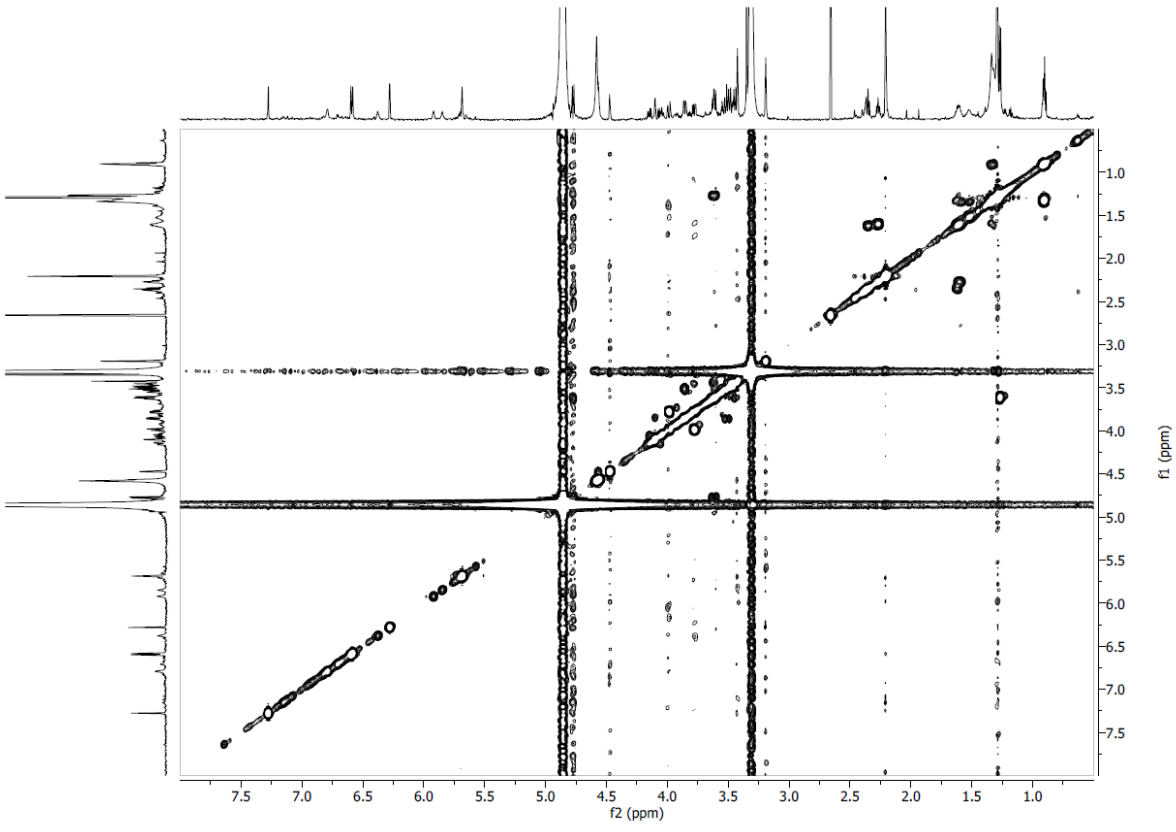

Supplementary Figure 5.15 COSY NMR spectrum of compound **13** in CD_3OD

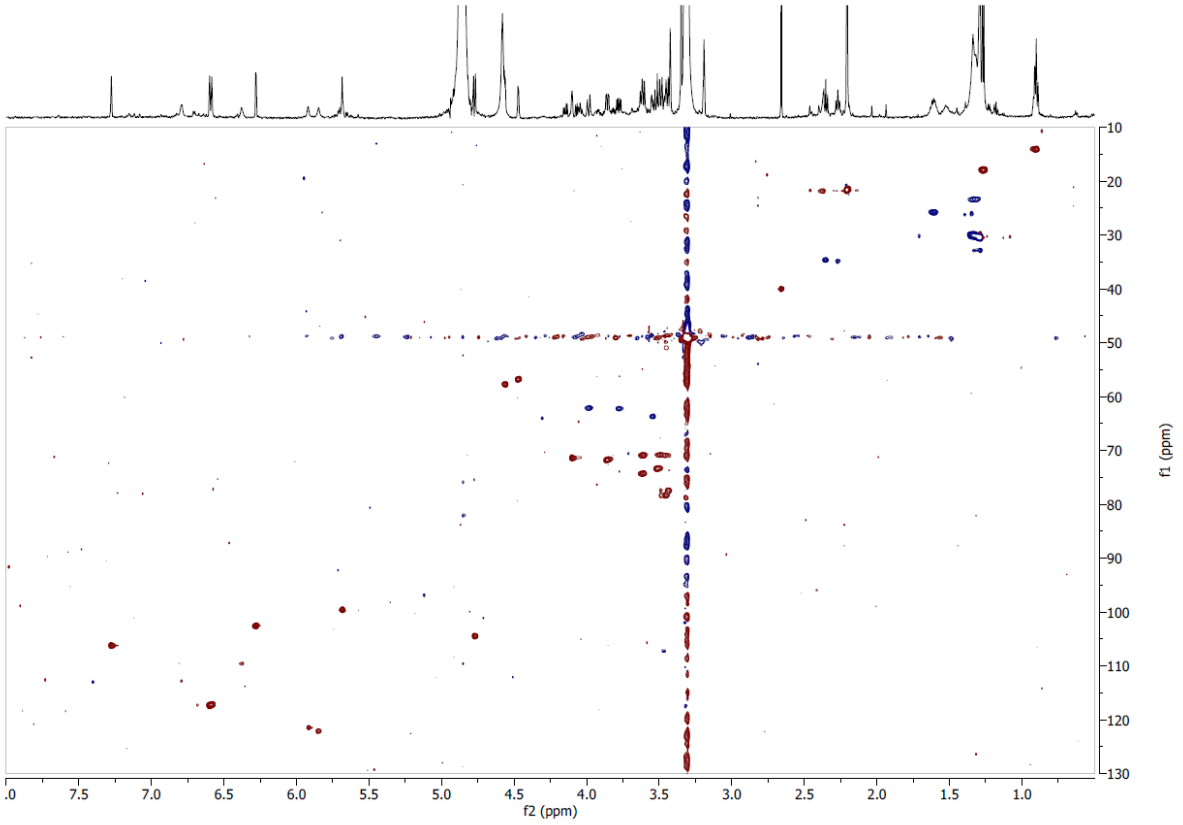

Supplementary Figure 5.16 Edited-HSQC NMR spectrum of compound **13** in CD_3OD

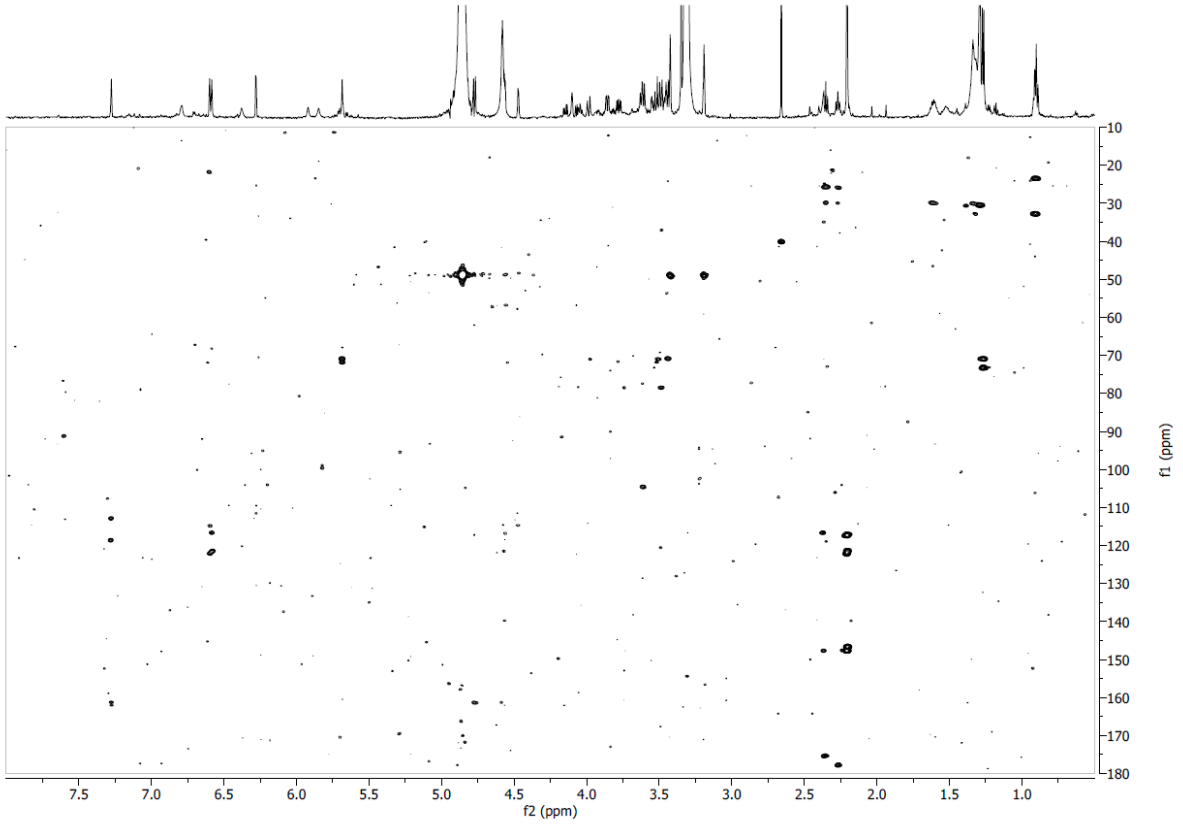

Supplementary Figure 5.17 HMBC NMR spectrum of compound **13** in CD_3OD

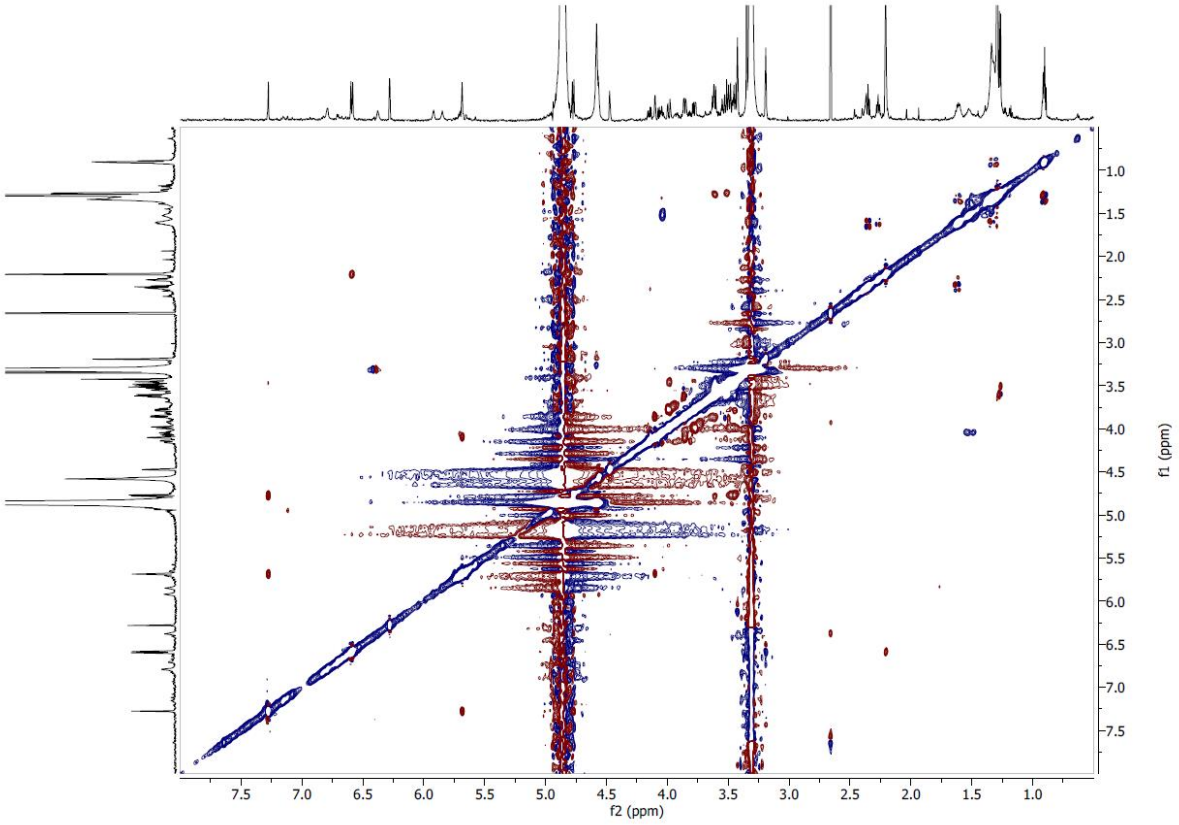

Supplementary Figure 5.18 ROESY NMR spectrum of compound **13** in CD_3OD

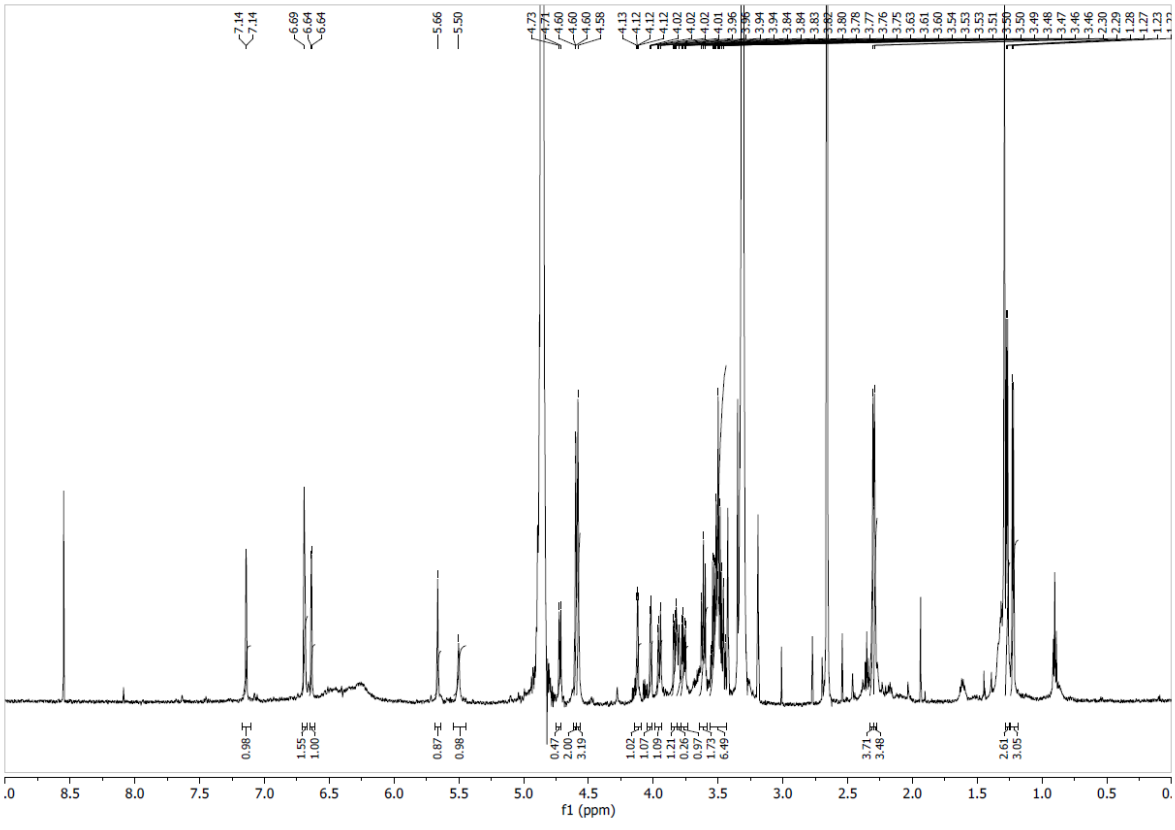

Supplementary Figure 5.19 ^1H NMR spectrum of compound **14** in CD_3OD at 600 MHz

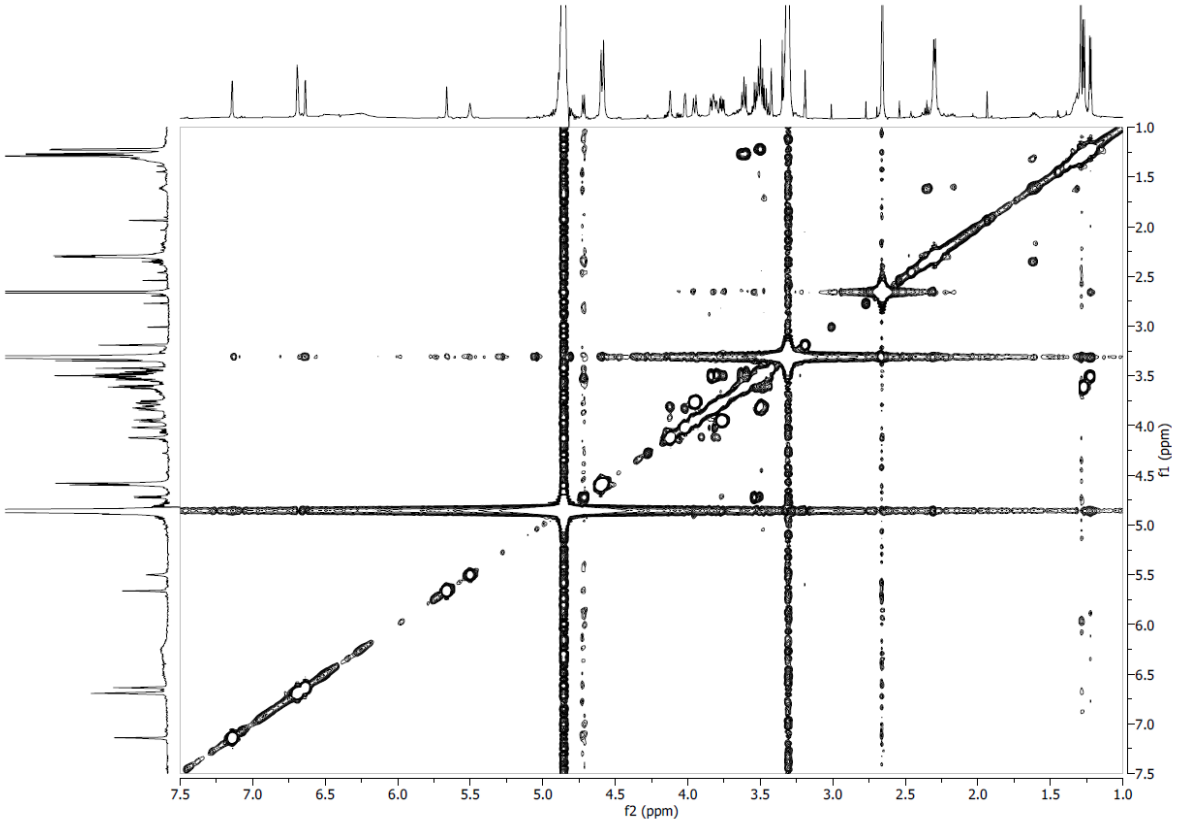

Supplementary Figure 5.20 COSY NMR spectrum of compound **14** in CD_3OD

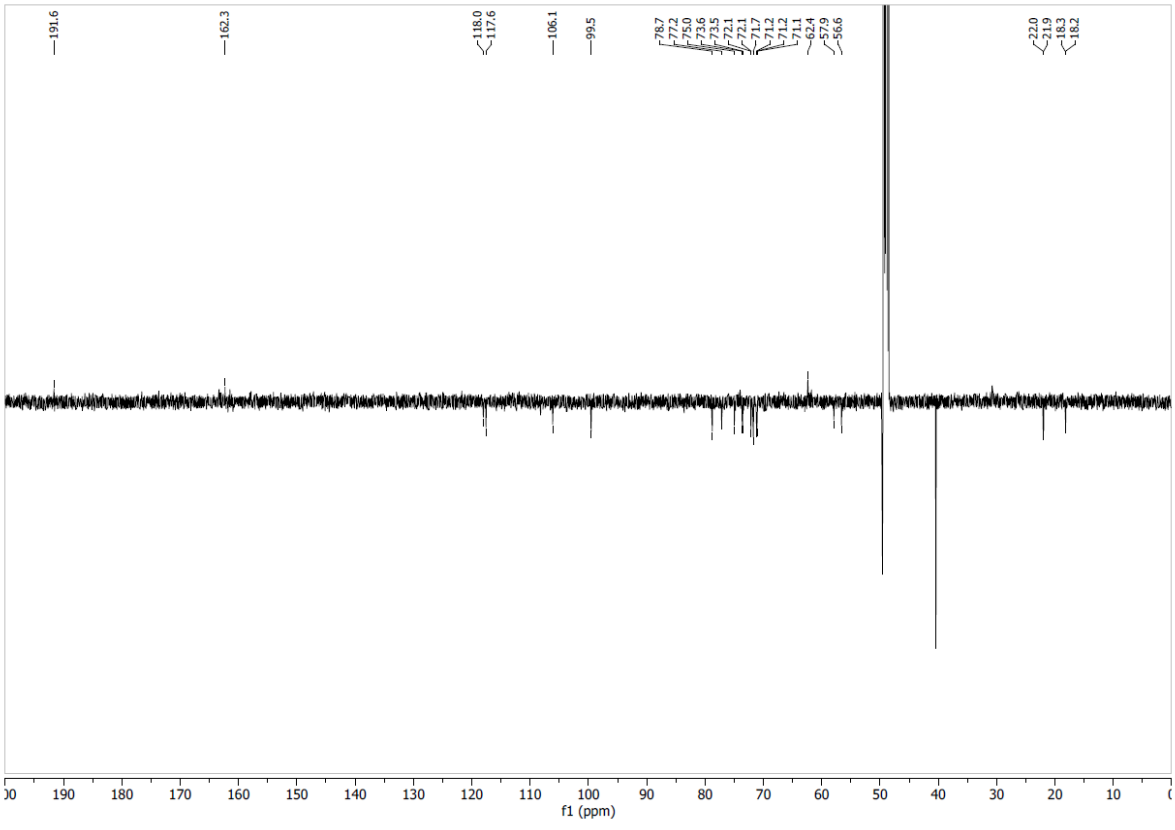

Supplementary Figure 5.21 ^{13}C-DEPTQ NMR spectrum of compound **14** in CD_3OD at 151 MHz

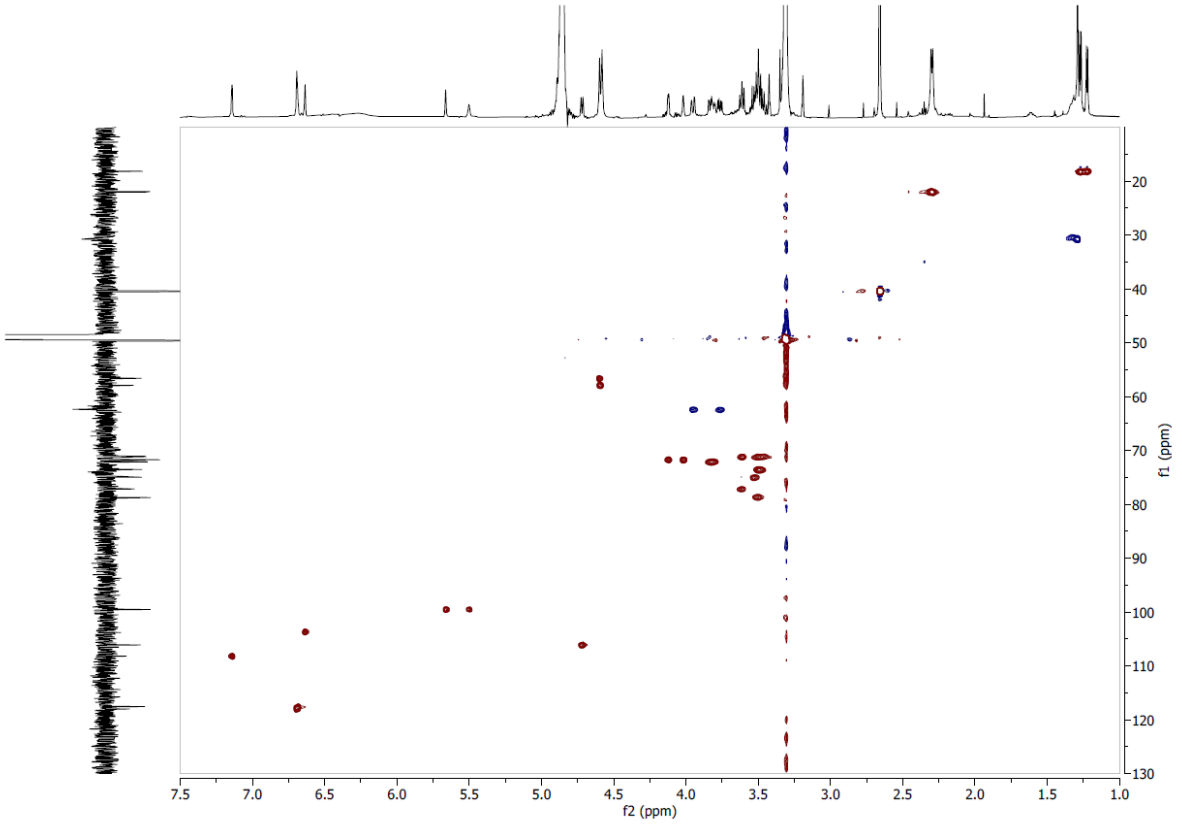

Supplementary Figure 5.22 Edited-HSQC NMR spectrum of compound **14** in CD_3OD

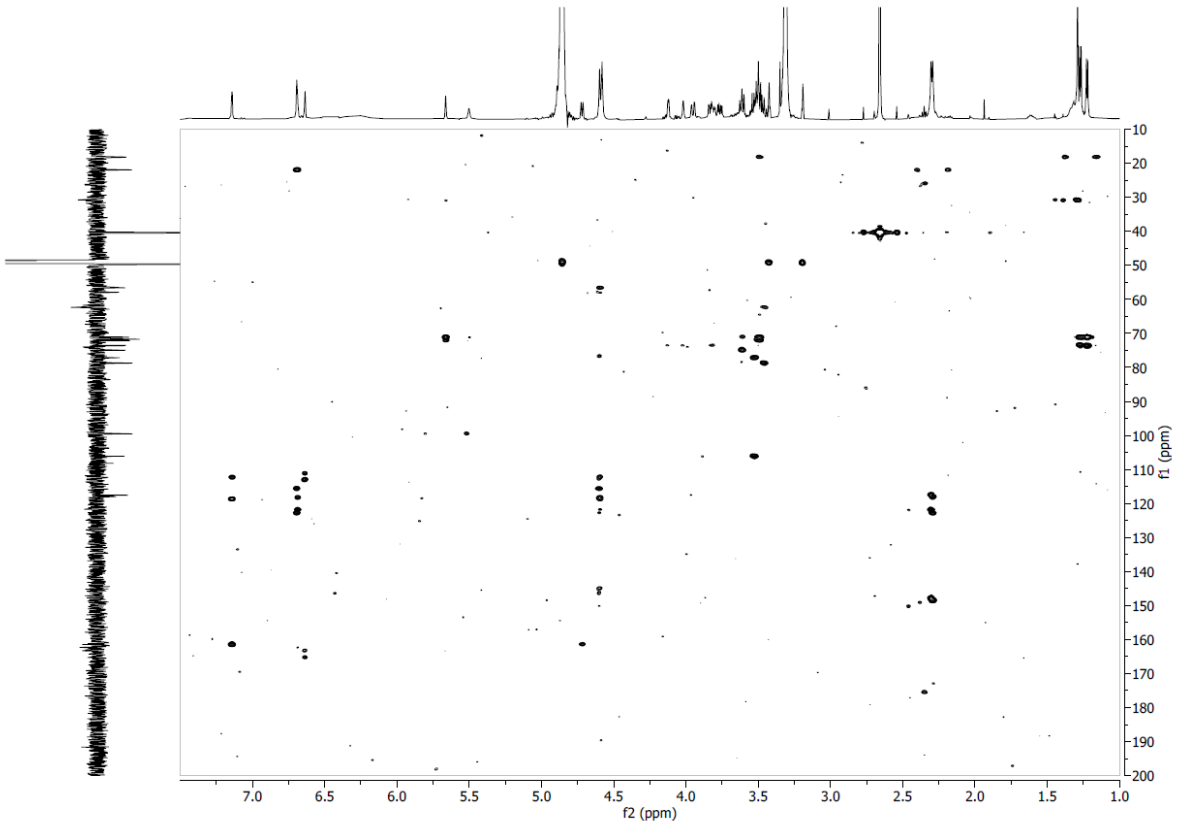

Supplementary Figure 5.23 HMBC NMR spectrum of compound **14** in CD_3OD

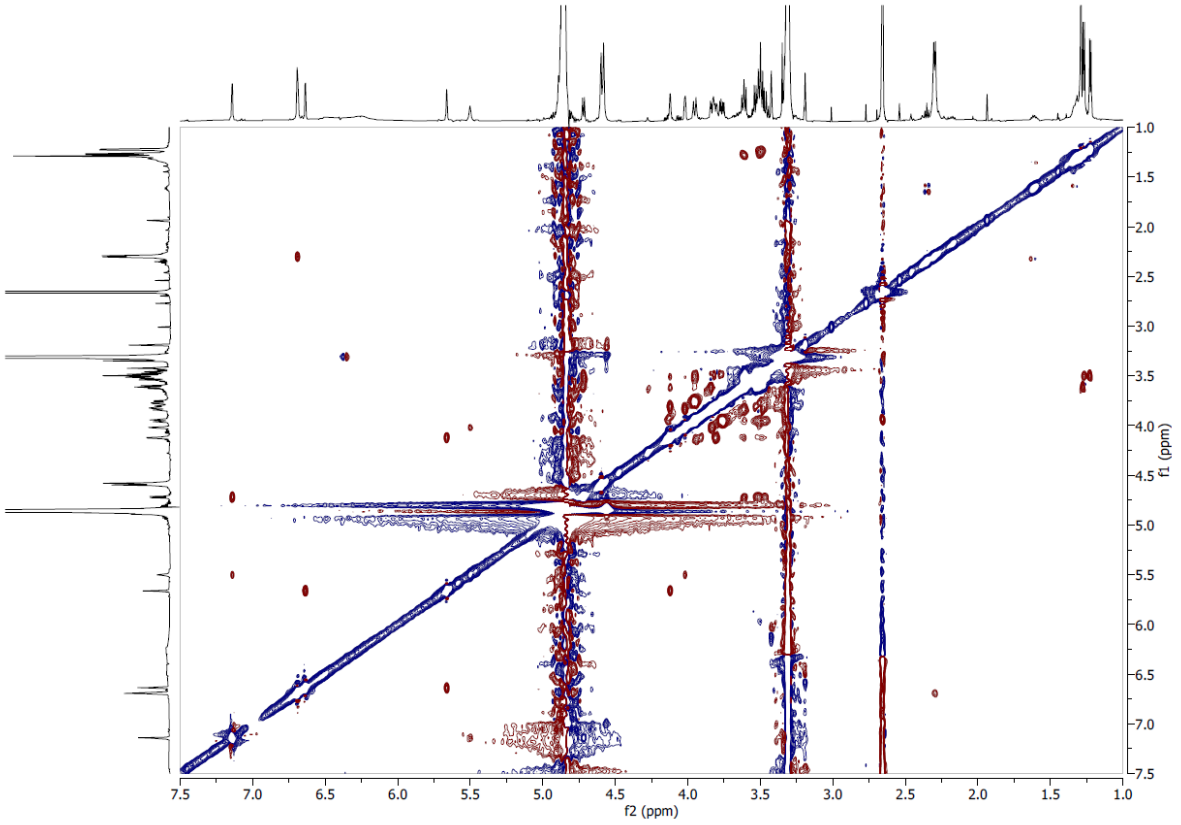

Supplementary Figure 5.24 ROESY NMR spectrum of compound **14** in CD_3OD

6. Conclusions and perspectives

Black dot (caused by *Colletotrichum coccodes*) and silver scurf (caused by *Helminthosporium solani*) are two blemish diseases of potato tubers that cause important economic losses on table potato production in Switzerland. The general aim of this thesis was to understand the factors that affect these diseases, the epidemiology of the fungal pathogens and the host-pathogen interaction of both diseases and to develop an integrated and sustainable pest management strategy (both in the field and during storage). To that end, this thesis was structured in three main pillars: 1) studying the main factors that influence disease incidence in the field, 2) investigating resistance mechanisms of potato cultivars to black dot and silver scurf and 3) evaluating the antifungal activity of plant extracts that may be used to control both diseases during storage.

6.1. Influence of abiotic factors, soil inoculum and cultivar susceptibility on the potato tuber blemish diseases black dot (*Colletotrichum coccodes*) and silver scurf (*Helminthosporium solani*)

Potato plants are cultivated through vegetative propagation using seed-tubers. In western countries, a certification program of seed-tuber production is used to reduce the incidence of several diseases that are transmitted *via* seed inoculum. Several diseases, such as PVY or blackleg, respectively a viral and a bacterial disease, can be controlled by planting seed-tuber lots with low disease incidence (Czajkowski et al., 2011; Lindner et al., 2015). On the other hand, soilborne diseases are usually controlled by other methods, such as crop rotation or soil treatments that reduce the soil inoculum. Potato diseases can also be transmitted through wind (airborne), water, or vectors such as aphids. Knowing the transmission of the pathogen is important in order to determine efficient strategies to control the disease. However, pathogens may be seed and soilborne at the same time, and identifying the most relevant inoculum source may depend on other factors, such as cultivar genotype, soil type or pedoclimatic conditions. In earlier studies, *C. coccodes* has often been regarded as, essentially, a soilborne pathogen (Tsror (Lahkim) et al., 1999; Lees and Hilton, 2003; Johnson et al., 2018), while *H. solani* is suggested to be mainly a seedborne pathogen (Errampalli et al., 2001b; Geary and Johnson, 2006). In our field trials, we found that planting disease-free minitubers as seed stock results in silver scurf and black dot symptomatic daughter tubers and indicates that producing disease-free seed stock is not sufficient to eradicate these diseases in the field. Furthermore, correlations between seed-stock and daughter tubers disease severity were not observed for either disease. Thus, efforts of the seed-tuber production industry should not focus on producing black dot nor silver scurf-free material since this will not heavily impact disease severity at harvest. Furthermore, we found that soil inoculum of *C. coccodes* was relatively low in Swiss field trials compared to studies in the UK (Lees et al., 2010) and we did not observe a correlation between soil inoculum and disease at harvest. However, field sites that contained less than 50 pg DNA *C. coccodes* / g soil resulted in low incidence of black dot, and this threshold may be used by potato growers to infer a risk of their potatoes to develop black dot (low risk vs high risk), and adapt additional measures. Nonetheless, it is worth noting that soil inoculum tests are not commercially available to date in Switzerland. Until these tests are available, cultural control methods that reduce soil inoculum should be used by all potato producers. Moreover, we did not detect *H. solani* soil inoculum in any field site, but planting disease-free seed tubers resulted in daughter tubers with similar silver scurf incidence than commercial seed stock, indicating that i) *H. solani* inoculum may be present in the soil and/or ii) *H. solani* inoculum may travel through water (irrigation, rainfall) from diseased to healthy plants. We found that the limit of detection of *H. solani* inoculum in the soil by quantitative PCR was higher than for *C. coccodes*, and the sensitivity of detection must be improved for accurate detection of soil inoculum. Since *H. solani* develops saprophytically on several crops and reveals only pathogenic on potatoes (Mérida and Loria, 1994b),

efforts should be focused on reducing voluntary potatoes and dead plant material during crop rotation. Altogether, our results show that reducing soil inoculum (crop rotation, haulm destruction management) should be prioritized before reducing seed inoculum for both diseases.

Another aspect revealed in our field trials was that climatic conditions have an influence on black dot and silver scurf diseases. Previous studies had shown that black dot severity is higher in highly irrigated fields or under damp conditions (Lees et al., 2010; Brierley et al., 2015). Precipitations (including irrigation) and relative humidity positively correlated with black dot disease severity in our field trials, suggesting that humid conditions are optimal for *C. coccodes* successful infections. These results indicate that black dot severity will be higher in humid seasons, and additional control measures should be applied in years with these circumstances. Aerial temperatures during plant growth correlated negatively with disease severity, which would suggest that black dot severity is higher in colder periods. Nonetheless, temperatures and precipitations negatively correlated in the field (as seen often in field conditions) and thus, the correlation between temperatures and disease severity might be influenced by that. Notably, *C. coccodes* growth *in vitro* is faster at temperatures of 20-27°C than 15°C (Glais-Varlet et al., 2004) and higher disease incidence was found in potatoes grown at 22°C than at 18°C (Lees et al., 2010). Altogether, these results suggest that the negative correlation between temperature and black dot severity is due to the negative correlation between precipitations and temperatures, and it suggests that humidity influences more than temperature the development of black dot. Silver scurf severity correlated positively with temperatures and negatively with precipitations or relative humidity. As observed for *C. coccodes*, *H. solani* grows faster at higher temperatures, indicating that high temperatures are favorable for the development of silver scurf. Our observations indicate that the development of black dot will be more important under humid (and relatively fresh) conditions and silver scurf severity will be higher in warm (and not so humid) seasons. Disease severity of black dot and silver scurf severity were negatively correlated in the field trials. This indicates that both fungal pathogens might compete for space or nutrients, which was already suggested (Hide and Hall, 1993; Lees and Hilton, 2003). Despite this possible competition, both diseases are often found in the same tuber. As previously observed (Andrivon et al., 1998), we found that *C. coccodes* infections occur in all underground parts of the potato plant and appear early after emergence. However, *H. solani* had been only observed on potato tubers and no other plant parts, since potato stems, roots or stolons do not show any symptoms of silver scurf (Fahn, 1982). Using molecular detection techniques, we confirmed that potato stolons are colonized by *H. solani*. Furthermore, these infections occur later than *C. coccodes* infections in the field. Since potatoes are planted in early spring in Switzerland (as soon as freezing does not occur), the influence of temperature and precipitations on silver scurf disease might be more important at the end of the season, when temperatures are usually higher and precipitations lower.

Altogether, our results could be used as a basic predictive model in order to prioritize control measures depending on the specific climatic conditions of each field. However, this model needs to be adapted and refined using local climatic data of multiple field sites in order to gain robustness and determine fixed thresholds for disease incidence.

One of the control methods that can be applied to numerous plant pests is to discover natural host resistance mechanisms in order to exploit them as a tool for crop breeding or varietal evaluation of natural susceptibiity of cultivars. This approach allows to have a better control of the disease while reducing substantially the use of phytosanitary products. In crop plants, high genetic variability occur among cultivars planted worldwide that provide certain levels of resistance to various phytopathogens. More than 5’000 potato cultivars are cultivated around the world, although most of them are only cultivated in South America, essentially in the Andes (Hijmans and Spooner, 2001). Since

different levels of susceptibility to black dot (Andrivon et al., 1998; Brierley et al., 2015) and silver scurf (Mérida et al., 1994; Secor, 1994; Rodriguez et al., 1995) have been observed on commercial potato cultivars, we decided to study cultivar susceptibility to both diseases on Swiss table potato cultivars. The results obtained indicate that cultivar choice has a great effect on black dot and on silver scurf disease severity. Thus, the susceptibility to each disease should be the first criterion to consider when choosing the potato cultivars to be grown in specific field sites. However, several other criteria must be taken in consideration before selecting a specific cultivar, such as resistance to other diseases (e.g. late blight, PVY, blackleg), yield, or organoleptic properties. Indeed, growers may choose the cultivars through these other criteria. In this case, cultivar susceptibility data may be used to prioritize storage and commercialization processes. Since both diseases are influenced by storage conditions and disease symptoms progress during storage (Andrivon et al., 1998; Errampalli et al., 2001b; Lees and Hilton, 2003; Avis et al., 2010; Johnson et al., 2018), most susceptible cultivars should be commercialized with higher priority. Altogether, the results obtained in our field trials and greenhouse experiments can be used to indicate the factors of risk on the development of black dot and silver scurf that can help create an Integrated Pest Management (IPM) strategy that involves both blemish diseases.

6.2. Quantitative resistance to black dot and silver scurf

Using host resistance data to further control fungal diseases is a sustainable way to reduce the use of phytosanitary products in many plant diseases models. Understanding the basis of the resistance patterns can help elucidating plant-pathogenic interactions but also serves as providing biomarkers of resistance that can be integrated in cultivar breeding (Gindro et al., 2012a). In order to gain more insights into the physiological resistance strategies of potato plants against black dot and silver scurf, we analzyed potato cultivars with different degrees of quantitative resistance to both diseases under light microscopy. Potato variants with high resistance to various tuber diseases have been shown to possess and produce more suberized periderm cells (Thangavel et al., 2016). We found that neither silver scurf nor black dot severity correlate with skin thickness, indicating that this marker is not pertinent to discriminate resistance against these two diseases. However, none of the potato cultivars analyzed in this study showed periderms thicker than 110 µm, while other thick-skinned cultivars (Russet-type) often possess periderms of more than 150 µm (Artschwager, 1924). Thus, it is possible that very thick-skin cultivars may be resistant to both blemish diseases, but those are not used as table potato cultivars in Europe (Lees and Hilton, 2003).

In our greenhouse experiments, suberin content and composition did not strongly differ among the tested cultivars under control conditions, suggesting that constitutive high levels of suberin do not provide resistance to black dot and silver scurf. Nonetheless, we did not study the impact of the inoculation of both fungal pathogens on the suberin accumulation. Potato tubers infected with *Streptomyces scabies* produce more periderm cells and suberize them (Thangavel et al., 2016). The symptoms of silver scurf, with well-delimited silvery lesions, are possibly due to cell dessication and suberin accumulation (Frazier et al., 1998), suggesting that *H. solani* may indeed trigger the production of suberin. It would be interesting to study whether *H. solani* and *C. coccodes* infection induces the production of this polymer, and if this correlates with disease resistance.

Since the structure of the periderm did not fully explain plant resistance to black dot and silver scurf, an untargeted metabolomics approach was carried out in *mock* or fungal inoculated potato tubers of five cultivars with different susceptibility to black dot and silver scurf. To that end, secondary metabolites of the potato skin were analyzed by LC-HRMS/MS in positive and negative ionization modes to detect the greatest amount of produced metabolites. In order to process and analyze the dataset from these analyses, a dual method combining multivariate statistical analysis and molecular networking (MN) (Watrous et al., 2012) were applied. We showed that the use of AMOPLS and MN

was useful in highlighting differences between potato cultivars, i.e. a red-skin cultivar (Cheyenne). In addition, the factor cultivar had a strong impact on the metabolome, being the factor that contributes the most to the AMOPLS model in both potato-pathogen interactions. This result indicates that metabolic differences among commercial potato cultivars can be highlighted using this method. Furthermore, the effect of the inoculation of the fungal pathogen could be evidenced using this method, and appeared that inoculating *H. solani* had a stronger impact on the metabolome than inoculating *C. coccodes* (contributing to 7.5% and 5% of the variability, respectively). Interestingly, some metabolites showed the same tendency in both potato-fungal interactions. For example, and as observed in other *Solanaceae*-pathogen interactions (Desender et al., 2007; Kröner et al., 2011), we showed that hydroxycinnamic acids deriving from the *Phenylalanine Lyase* (PAL) pathway were induced in fungal-inoculated samples. On the other hand, most flavonoid glycosides detected in our study, including rutin -which possess antimicrobial activity (Kröner et al., 2012)-, were strongly reduced in potato tubers inoculated with *C. coccodes* or *H. solani*. Our results suggest that the studied fungal pathogens are able to induce the repression or the degradation of these compounds potentially involved in resistance mechanisms. Moreover, potato tubers inoculated with *H. solani* accumulated fructose and sorbose. Other photoassimilates have been shown to be consumed by phytopathogenic fungi during infection (Patel and Williamson, 2016), and our results suggest that *H. solani* induces the production of these metabolites for its own growth.

Highlighting biomarkers of resistance against black dot was achieved with the workflow that uses both multivariate data analysis (i.e. AMOPLS) and global vizualization of metabolite relationships within the potato metabolome (i.e. Molecular Networks). Among the resistance-related constitutive (RRC) metabolites detected, there were several hydroxycinnamic acid amides (HCAAs), which have been shown to accumulate upon pathogen infection in several plant hosts (Macoy et al., 2015). The role of HCAAs in plant-pathogenic interactions is believed to be mainly related to cell wall fortification, since they are part of the aromatic domain of the suberin polymer. However, the rate of HCAA synthesis is higher than its incorporation into the cell wall (Macoy et al., 2015), indicating that free HCAAs (not bound to the cell wall) have other roles in the plant-pathogen interactions. Our results suggest that HCAAs do indeed play a role as free monomers, since differences in suberin content were not observed between potato cultivars. HCAAs possess antioxidant (Bouchereau et al., 1999) and antifungal properties (Kyselka et al., 2018), and we found that *N*-feruloyltyramine and kukoamine A, two HCAAs that were more abundant in resistent cultivars towards black dot, are fungitoxic against *C. coccodes*. These results suggest that HCAAs may play a role in quantitative resistance to black dot as direct antifungal compounds. On the other hand, hydroxycoumarins were also highlighted as biomarkers of resistance against black dot, either constitutively or specifically induced upon fungal infection. These metabolites have been previously detected in diploid potato plants with resistance against late blight (Yogendra et al., 2015). Notably, hydroxycoumarins are involved in resistance against *Botrytis cinerea* in the *Solanaceae* tobacco plant, and scopoletin shows antifungal activity against *B. cinerea* (El Oirdi et al., 2010) and *C. coccodes* (Chapter 3). Highlighted constitutive biomarkers of resistance against black dot also included steroidal saponins, some of which were shown to possess antifungal activity against *C. coccodes*. Furthermore, some of these saponins, as well as HCAAs and hydroxycoumarins, were specifically induced in resistant cultivars upon fungal infection. Altogether, our results highlight resistance-related markers against black dot in commercially available potato cultivars that i) give insights into the plant-pathogenic interaction and ii) may be used as biomakers for potato breeding.

Discovering resistance-related markers against silver scurf revealed to be more challenging: using AMOPLS, a clear clustering of resistant cultivars against silver scurf was not observed. Furthermore, the MNs of the resistant cultivars studied showed very different metabolomes, suggesting that different metabolic strategies are used by these potato cultivars against *H. solani* infection. For

example, flavonoid glycosides and anthocyanins are specific of the resistant cultivar Cheyenne, but not abundant in other resistant cultivars. Nonetheless, some constitutive biomarkers can be highlighted in all resistant cultivars against silver scurf. HCAAs and hydroxycoumarins, which have been highlighted as *RR* metabolites againt black dot, are also more abundant in silver scurf resistant potato cultivars. However, some resistant cultivars preferentially accumulate spermine HCAAs, while others accumulate spermidine HCAAs, and all resistant cultivars accumulate feruloyloctopamine and feruloyltyramine. Moreover, a cytokinin glucoside (zeatin glucoside) previously reported in potato and involved in sprouting (Nicander et al., 1995; Lomin et al., 2018) is abundant in cultivars resistant to silver scurf. Since cytokinins have been shown to prime defense responses in plants (Choi et al., 2011), our results suggest that high amounts of cytokinin glycosides may trigger defense against *H. solani*. Upon *H. solani* inoculation, a specific induction of gallic and protocatechuic acids in the resistant cultivars was observed. These phenolic acids have been shown to possess antioxidant (Asnaashari et al., 2014; Safaeian et al., 2018) as well as antifungal activities (Nguyen et al., 2015; Li et al., 2017), and our results suggest that they may be related to resistance against silver scurf.

Overall, our studies on potato cultivars with quantitative resistance to black dot and silver scurf revealed some common features in both fungal infections. Both fungal pathogens were found in the periderm of potato tubers, but not in parenchymal cells, indicating that they only infect the periderm. Furthermore, very thin-skin potato cultivars are more susceptible to black dot and silver scurf, but differences in resistance are observed among cultivars with similar skin thickness. Resistance-Related metabolites were found for both diseases, some of which were common. HCAAs and hydroxycoumarins were revealed as constitutive or induced resistance-related metabolites against black dot and silver scurf, suggesting that they may indeed be used as resistance-related markers against these two blemish diseases in potatoes. The correlation of these metabolites with resistance against other tuber diseases has to be investigated.

6.3. Post-harvest treatments of potato tubers to reduce the impact of black dot and silver scurf

Several control measures can be used in order to limit black dot and silver scurf disease severities (i.e. cultivar choice, field selection). However, growers might select susceptible cultivars due to organoleptic or commercial purposes and may not have the choice of selecting a field in which conditions of disease development are unfavorable. In such cases, the post-harvest treatment of diseased potatoes may become a control measure applicable, especially if long storage is required. Post-harvest control of potatoes against rot diseases using plant extracts has been previously shown effective (Bdliya and Dahiru, 2006; Rahman et al., 2012; Viswanath et al., 2018), and plant extracts with antifungal properties against *Colletotrichum coccodes* and *Helminthosporium solani* have been reported (Bång, 2007; Bhagwat and Datar, 2014; Confortin et al., 2019). In this context, our screening of plant extracts for antifungal activity against *C. coccodes* and *H. solani* resulted in three plant extracts with fungistatic or fungitoxic activity against both pathogens. Bio-guided fractionation of all three extracts resulted in the isolation and characterization of the active metabolites, mainly curcuminoids and anthraquinones, but also phenylpropanoid derivatives. Extracts of *Curcuma spp.* had already been shown to possess antifungal activities against *Colletotichum* species (Imtiaj et al., 2005; Bhagwat and Datar, 2014), but not against *H. solani*. Furthermore, *Rheum palmatum* and *Frangula alnus* plant extracts have been used against several phytopathogens, including potato fungal pathogens (Manojlovic et al., 2005; Krebs et al., 2006; Forrer et al., 2014; Gillmeister et al., 2019), but never against the causal agents of black dot and silver scurf. Our results have shown that *F. alnus*, *R. palmatum* and *C. longa* possess curcuminoids, anthraquinones and phenylpropanoid derivatives with antifungal activities against *C. coccodes* and *H. solani in vitro*.

We found that applying the *C. longa* and the *F. alnus* extracts on diseased potato tubers before storage resulted in black dot and silver scurf disease control under high disease pressure conditions. However, a high variability in the disease incidence and a relatively low disease pressure was observed in several *in vivo* experiments, which resulted in non-significant differences between the untreated control and the post-harvest treatments in several experiments. Furthermore, the post-harvest application of the *R. palmatum* plant extract did not result in the control of black dot nor silver scurf in any trial.

In our post-harvest treatments, plant extracts were directly applied without formulation on potato tubers at a concentration of 10 g/L, corresponding to the concentration used in the *in vitro* bioassays. The post-harvest application of fungicides in potato tubers often exceeds that, i.e. potassium sorbate is applied at 30 g/L to control late blight, and phosphite is applied at 161 g/L to control pink rot. Thus, additional *in vivo* bioassays with a higher concentration of the plant extracts should be performed to highlight the dose required for an efficient control of these diseases. Moreover, the identification of the antifungal compounds through the bioguided isolation allows now to detect these molecules throughout the experiment, and assess the stability of these compounds under storage conditions. If the active principles show a relatively low stability during storage, the formulation of these extracts should be performed to solve this issue. Furthermore, this formulation should ensure the adhesion of the extracts on the tuber skin upon treatment. The formulated plant extracts should be tested at different concentrations, as well as with a higher number of potato tubers, possibly from different cultivars, in order to determine whether these plant extracts may be used as post-harvest treatments of potato tubers to control blemish diseases.

Altogether, the results presented in this thesis can be used to determine the factors of risk for the development of the potato blemish diseases black dot and silver scurf and to give agronomical advices that mitigate their impact in a sustainable integrated pest management (IPM) strategy. To that end, several aspects need still further study. The quantification of the soil inoculum by quantitative PCR should be optimized to detect lower inoculum amounts of *H. solani*, and the quantification of *C. coccodes* and *H. solani* in soil should be made accessible to potato producers for an integration of these informations to the IPM strategy. Meteorological data from numerous field sites in Switzerland is publicly available, and correlations between precipitations or temperature with disease severity should be studied with a larger dataset to confirm the trends observed in our study. Host resistance against both diseases was observed in the table potato cultivars used in Switzerland during the 2016-2018 period. New cultivars could now be tested for their resistance to black dot and silver scurf, and compared to the resistance level found in our studies. Furthermore, the resistance-related compounds highlighted in our study could be quantified in different potato cultivars, which could be then correlated to their resistance against the fungal pathogen. It would be very interesting to study the correlation of these highlighted resistance-related metabolites with other fungal diseases, in potato or in other related species. Finally, the application of plant extracts as post-harvest treatment against black dot and silver scurf was only observed under high disease pressure conditions. Additional experiments with higher concentrations of these plant extracts may enhance disease control. The stability of the antifungal compounds (which were identified in our study) on potato tubers should be assessed by quantifying them during potato storage to determine how these extracts should be formulated. The formulation and application procedures of these plant extracts need to be optimized for a practical application of the plant extracts as post-harvest antifungal products.

HIGH RISK	FACTOR	ACTION
SUSCEPTIBLE CULTIVARS	CULTIVAR	Choose resistant cultivars especially in conditions that favor the disease.
SOIL CONTAMINATION	FIELD SITE	Crop rotation, haulm management, volunteer potatoes management.
INFECTED SEED IN CLEAN SOIL	SEED HEALTH	Plant clean seed (if available) or fungicide treatment on contaminated seed only in clean soil to avoid introduction of the pathogen.
WET SOIL (black dot) / HIGH TEMPERATURES (silver scurf)	CLIMATIC CONDITIONS	Limit irrigation on black dot susceptible cultivars. Monitor the climatic conditions to estimate the risk of disease severity.
LONG STORAGE	STORAGE	Do not store susceptible cultivars for long periods. Post-harvest treatments of susceptible cultivars for long-term storage.
STORAGE OF UNTREATED TUBERS	STORAGE	Apply post-harvest treatments of antifungal plant extracts especially on high disease pressure seasons.

Table 6.1 Factors of risk for the development of black dot and silver scurf and actions to mitigate their impact.

7. References

Abd El-Malik, N., I., and Abbas, I., K. (2017). Evaluation of certain plant extracts for the control of wheat leaf rust disease. *Egypt. J. Biol. Pest Control* 27, 23–33.

Adams, A., Sander, N., and Nelson, D. C. (1970). Some properties of soils affecting russet scab and silver scurf of potatoes. *Am. Potato J.* 47, 49–57.

Adams, M. J., Read, P. J., Lapwood, D. H., Cayley, G. R., and Hide, G. A. (1987). The effect of irrigation on powdery scab and other tuber diseases of potatoes. *Ann. Appl. Biol.* 110, 287–294. doi:10.1111/j.1744-7348.1987.tb03258.x.

Agrios, G. N. (2005). *Plant pathology*. 5th ed. Amsterdam ; Boston: Elsevier Academic Press.

Aguilera-Galvez, C., Champouret, N., Rietman, H., Lin, X., Wouters, D., Chu, Z., et al. (2018). Two different R gene loci co-evolved with Avr2 of Phytophthora infestans and confer distinct resistance specificities in potato. *Stud. Mycol.* 89, 105–115. doi:10.1016/j.simyco.2018.01.002.

Ahmed, S. S., Abd El-Aziz, G. H., Abou-Zeid, M. A., and Fahmy, A. H. (2019). Environmental Impact of The Use of Some Eco-friendly Natural Fungicides to Resist Rust Disease in Wheat. *Catrina-Int. J. Environ. Sci.* 18, 87–95.

Aliferis, K. A., Faubert, D., and Jabaji, S. (2014). A Metabolic Profiling Strategy for the Dissection of Plant Defense against Fungal Pathogens. *PLOS ONE* 9, e111930. doi:10.1371/journal.pone.0111930.

Aliferis, K. A., and Jabaji, S. (2012). Deciphering plant–pathogen interactions applying metabolomics: principles and applications. *Can. J. Plant Pathol.* 34, 29–33. doi:10.1080/07060661.2012.665388.

Ali-Shtayeh, M. S., and Abu Ghdeib, S. I. (1999). Antifungal activity of plant extracts against dermatophytes. *Mycoses* 42, 665–672. doi:10.1046/j.1439-0507.1999.00499.x.

Allard, P.-M., Genta-Jouve, G., and Wolfender, J.-L. (2017). Deep metabolome annotation in natural products research: towards a virtuous cycle in metabolite identification. *Curr. Opin. Chem. Biol.* 36, 40–49. doi:10.1016/j.cbpa.2016.12.022.

Allard, P.-M., Péresse, T., Bisson, J., Gindro, K., Marcourt, L., Pham, V. C., et al. (2016). Integration of Molecular Networking and *In-Silico* MS/MS Fragmentation for Natural Products Dereplication. *Anal. Chem.* 88, 3317–3323. doi:10.1021/acs.analchem.5b04804.

Almagro, L., Gómez Ros, L. V., Belchi-Navarro, S., Bru, R., Ros Barceló, A., and Pedreño, M. A. (2009). Class III peroxidases in plant defence reactions. *J. Exp. Bot.* 60, 377–390. doi:10.1093/jxb/ern277.

Al-Mughrabi, K. I., Coleman, W. K., Vikram, A., Poirier, R., and Jayasuriya, K. E. (2013). Effectiveness of Essential Oils and Their Combinations with Aluminum Starch Octenylsuccinate on Potato Storage Pathogens. *J. Essent. Oil Bear. Plants* 16, 23–31. doi:10.1080/0972060X.2013.764201.

Alonso-Villaverde, V., Voinesco, F., Viret, O., Spring, J.-L., and Gindro, K. (2011). The effectiveness of stilbenes in resistant Vitaceae: Ultrastructural and biochemical events during Plasmopara

viticola infection process. *Plant Physiol. Biochem.* 49, 265–274. doi:10.1016/j.plaphy.2010.12.010.

Al_Samarrai, G., Singh, H., and Syarhabil, M. (2012). Evaluating eco-friendly botanicals (natural plant extracts) as alternatives to synthetic fungicides. *Ann. Agric. Environ. Med.* 19, 673–676.

Alves, K. F., Laranjeira, D., Câmara, M. P., Câmara, C. A., and Michereff, S. J. (2015). Efficacy of plant extracts for anthracnose control in bell pepper fruits under controlled conditions. *Hortic. Bras.* 33, 332–338. doi:10.1590/S0102-053620150000300009.

Alyokhin, A., Vincent, C., and Giordanego, P. eds. (2013). *Insect Pests of Potato*. Elsevier doi:10.1016/C2010-0-67998-3.

Amadioha, A. C. (2000). Controlling rice blast in vitro and in vivo with extracts of Azadirachta indica. *Crop Prot.* 19, 287–290. doi:10.1016/S0261-2194(99)00080-0.

Ananthakrishnan, T. N. (1997). Gallic and salicylic acids: Sentinels of plant defence against insects. *Curr. Sci.* 73, 576–579.

Anaruma, N. D., Schmidt, F. L., Duarte, M. C. T., Figueira, G. M., Delarmelina, C., Benato, L. A., et al. (2010). Control of Colletotrichum gloeosporioides (penz.) Sacc. In yellow passion fruit using Cymbopogon citratus essential oil. *Braz. J. Microbiol. Publ. Braz. Soc. Microbiol.* 41, 66–73. doi:10.1590/S1517-838220100001000012.

Andreu, V., Levert, A., Amiot, A., Cousin, A., Aveline, N., and Bertrand, C. (2018). Chemical composition and antifungal activity of plant extracts traditionally used in organic and biodynamic farming. *Environ. Sci. Pollut. Res. Int.* 25, 29971–29982. doi:10.1007/s11356-018-1320-z.

Andrivon, D., Lucas, J. -M., Guérin, C., and Jouan, B. (1998). Colonization of roots, stolons, tubers and stems of various potato (*Solanum tuberosum*) cultivars by the black-dot fungus *Colletotrichum coccodes*. *Plant Pathol.* 47, 440–445. doi:10.1046/j.1365-3059.1998.00267.x.

Andrivon, D., Ramage, K., Guérin, C., Lucas, J. M., and Jouan, B. (1997). Distribution and fungicide sensitivity of Colletotrichum coccodes in French potato-producing areas. *Plant Pathol.* 46, 722–728. doi:10.1046/j.1365-3059.1997.d01-60.x.

Anouar, E. H., Osman, C. P., Weber, J.-F. F., and Ismail, N. H. (2014). UV/Visible spectra of a series of natural and synthesised anthraquinones: experimental and quantum chemical approaches. *SpringerPlus* 3. doi:10.1186/2193-1801-3-233.

Aqeel, A. M., Pasche, J. S., and Gudmestad, N. C. (2008). Variability in Morphology and Aggressiveness Among North American Vegetative Compatibility Groups of *Colletotrichum coccodes*. *Phytopathology* 98, 901–909. doi:10.1094/PHYTO-98-8-0901.

Arora, R. K., and Khurana, S. M. P. (2004). “Major Fungal and Bacterial Diseases of Potato and their Management,” in *Fruit and Vegetable Diseases* Disease Management of Fruits and Vegetables., ed. K. G. Mukerji (Dordrecht: Springer Netherlands), 189–231. doi:10.1007/0-306-48575-3_6.

Artschwager, E. (1924). “Studies on the potato tuber,” in *Journal of Agricultural Research* (Washington, USA: U.S. Government Printing Office), 809–836.

Asnaashari, M., Farhoosh, R., and Sharif, A. (2014). Antioxidant activity of gallic acid and methyl gallate in triacylglycerols of Kilka fish oil and its oil-in-water emulsion. *Food Chem.* 159, 439–444. doi:10.1016/j.foodchem.2014.03.038.

Avis, T. J., Martinez, C., and Tweddell, R. J. (2010). Minireview/Minisynthèse Integrated management of potato silver scurf (*Helminthosporium solani*). *Can. J. Plant Pathol.* 32, 287–297. doi:10.1080/07060661.2010.508627.

Azim, A., Shaikh, H. A., and Ahmad, R. (1982). Effect of feeding greened potatoes on different visceral organs and blood plasma of rabbits. *J. Sci. Food Agric.* 33, 1275–1279. doi:https://doi.org/10.1002/jsfa.2740331214.

Azim, A., Shaikh, H. A., and Ahmad, R. (1983). Toxic effects of high glycoalkaloid [greened potatoes] feeding on the protein digestibility and growth of rabbits. *J. Pharm. Pak.* 2, 15–24.

Azim, A., Shaikh, H. A., and Ahmad, R. (1984). Toxic effects of high glycoalkaloid feeding on the red blood cell counts and haemoglobin concentration of rabbit blood. *J. Pharm. Pak.* 3, 43–49.

Azzollini, A., Boggia, L., Boccard, J., Sgorbini, B., Lecoultre, N., Allard, P.-M., et al. (2018). Dynamics of Metabolite Induction in Fungal Co-cultures by Metabolomics at Both Volatile and Non-volatile Levels. *Front. Microbiol.* 9, 72. doi:10.3389/fmicb.2018.00072.

Baggio, J. S., Wang, N.-Y., Peres, N. A., and Amorim, L. (2018). Baseline sensitivity of Colletotrichum acutatum isolates from Brazilian strawberry fields to azoxystrobin, difenoconazole, and thiophanate-methyl. *Trop. Plant Pathol.* 43, 533–542. doi:10.1007/s40858-018-0232-2.

Báidez, A. G., Gómez, P., Del Río, J. A., and Ortuño, A. (2007). Dysfunctionality of the Xylem in *Olea europaea* L. Plants Associated with the Infection Process by *Verticillium dahliae* Kleb. Role of Phenolic Compounds in Plant Defense Mechanism. *J. Agric. Food Chem.* 55, 3373–3377. doi:10.1021/jf063166d.

Bains, P. S., Bisht, V. S., and Benard, D. A. (1996). Soil survival and thiabendazole sensitivity of Helminthosporium solani isolates from Alberta, Canada. *Potato Res.* 39, 23–29. doi:10.1007/BF02358203.

Baker, C. J., Whitaker, B. D., Roberts, D. P., Mock, N. M., Rice, C. P., Deahl, K. L., et al. (2005). Induction of redox sensitive extracellular phenolics during plant–bacterial interactions. *Physiol. Mol. Plant Pathol.* 66, 90–98. doi:10.1016/j.pmpp.2005.05.002.

Ballvora, A., Ercolano, M. R., Weiss, J., Meksem, K., Bormann, C. A., Oberhagemann, P., et al. (2002). The R1 gene for potato resistance to late blight (Phytophthora infestans) belongs to the leucine zipper/NBS/LRR class of plant resistance genes. *Plant J. Cell Mol. Biol.* 30, 361–371. doi:10.1046/j.1365-313x.2001.01292.x.

Bång, U. (2007). Screening of Natural Plant Volatiles to Control the Potato (Solanum tuberosum) Pathogens Helminthosporium solani, Fusarium solani, Phoma foveata and Rhizoctonia solani. *Potato Res.* 50, 185–203. doi:10.1007/s11540-008-9044-y.

Barel, G., and Ginzberg, I. (2008). Potato skin proteome is enriched with plant defence components. *J. Exp. Bot.* 59, 3347–3357. doi:10.1093/jxb/ern184.

Barkdoll, A. W., and Davis, J. R. (1992). Distribution of Colletotrichum coccodes in Idaho and variation in pathogenicity on potato. *Plant Dis.* 76, 131–135.

Barnett, H. L., and Hunter, B. B. (1998). "Helminthosporium," in *Illustrated Genera of Imperfect Fungi*, eds. H. L. Barnett and B. B. Hunter (St Paul, MN, USA: American Phytopathological Society Press).

Bdliya, B. S., and Dahiru, B. (2006). Efficacy of some plant extracts on the control of potato tuber soft rot caused by Erwinia carotovora ssp. Carotovora. *J. Plant Prot. Res.* 46, 285–294.

Bernards, M. A., and Lewis, N. G. (1998). The macromolecular aromatic domain in suberized tissue: A changing paradigm. *Phytochemistry* 47, 915–933. doi:10.1016/S0031-9422(98)80052-6.

Bhagwat, M. K., and Datar, A. G. (2014). Antifungal activity of herbal extracts against plant pathogenic fungi. *Arch. Phytopathol. Plant Prot.* 47, 959–965. doi:10.1080/03235408.2013.826857.

Bhardwaj, V., Kaushik, S. K., Chakrabarti, S. K., Pandey, S. K., Singh, P. H., Manivel, P., et al. (2007). Combining resistance to late blight and PVY in potato. *Potato J.* 34, 41–42.

Bianchi, A., Zambonelli, A., D'Aulerio, A. Z., and Bellesia, F. (1997). Ultrastructural Studies of the Effects of Allium sativum on Phytopathogenic Fungi in vitro. *Plant Dis.* 81, 1241–1246. doi:10.1094/PDIS.1997.81.11.1241.

Blancard, D. (2012). "2 - Diagnosis of Parasitic and Nonparasitic Diseases," in *Tomato Diseases (Second Edition)*, ed. D. Blancard (San Diego: Academic Press), 35–411. doi:10.1016/B978-0-12-387737-6.50002-9.

Boccard, J., and Rudaz, S. (2016). Exploring Omics data from designed experiments using analysis of variance multiblock Orthogonal Partial Least Squares. *Anal. Chim. Acta* 920, 18–28. doi:10.1016/j.aca.2016.03.042.

Bollina, V., Kumaraswamy, G. K., Kushalappa, A. C., Choo, T. M., Dion, Y., Rioux, S., et al. (2010). Mass spectrometry-based metabolomics application to identify quantitative resistance-related metabolites in barley against Fusarium head blight. *Mol. Plant Pathol.* 11, 769–782. doi:10.1111/j.1364-3703.2010.00643.x.

Bollina, V., Kushalappa, A. C., Choo, T. M., Dion, Y., and Rioux, S. (2011). Identification of metabolites related to mechanisms of resistance in barley against Fusarium graminearum, based on mass spectrometry. *Plant Mol. Biol.* 77, 355–370. doi:10.1007/s11103-011-9815-8.

Bouchereau, A., Aziz, A., Larher, F., and Martin-Tanguy, J. (1999). Polyamines and environmental challenges: recent development. *Plant Sci.* 140, 103–125. doi:10.1016/S0168-9452(98)00218-0.

Bradshaw, J. E., Bryan, G. J., and Ramsay, G. (2006). Genetic Resources (Including Wild and Cultivated Solanum Species) and Progress in their Utilisation in Potato Breeding. *Potato Res.* 49, 49–65. doi:10.1007/s11540-006-9002-5.

Bradshaw, J. E., and Ramsay, G. (2009). "Potato Origin and production," in *Advances in Potato Chemistry and Technology* (Elsevier), 1–26.

Brierley, J. L., Hilton, A. J., Wale, S. J., Peters, J. C., Gladders, P., Bradshaw, N. J., et al. (2015). Factors affecting the development and control of black dot on potato tubers. *Plant Pathol.* 64, 167–177. doi:10.1111/ppa.12238.

Brierley, J. L., Stewart, J. A., and Lees, A. K. (2009). Quantifying potato pathogen DNA in soil. *Appl. Soil Ecol.* 41, 234–238. doi:10.1016/j.apsoil.2008.11.004.

Brillatz, T., Jacmin, M., Queiroz, E. F., Marcourt, L., Slacanin, I., Petit, C., et al. (2020). Zebrafish bioassay-guided isolation of antiseizure compounds from the Cameroonian medicinal plant Cyperus articulatus L. *Phytomedicine* 70, 153175. doi:10.1016/j.phymed.2020.153175.

Brillatz, T., Lauritano, C., Jacmin, M., Khamma, S., Marcourt, L., Righi, D., et al. (2018). Zebrafish-based identification of the antiseizure nucleoside inosine from the marine diatom Skeletonema marinoi. *PLOS ONE* 13, e0196195. doi:10.1371/journal.pone.0196195.

Brush, S. B., Carney, H. J., and Huamán, Z. (1981). Dynamics of Andean Potato Agriculture. *Econ. Bot.* 35, 70–88.

Burke, O. D. (1938). The silver scurf disease of potatoes. *Bull. Cornell Univ. Agric. Exp. Stn.* 692, 1–30.

Byrne, J. M., Hausbeck, M. K., and Hammerschmidt, R. (1997). Conidial Germination and Appressorium Formation of *Colletotrichum coccodes* on Tomato Foliage. *Plant Dis.* 81, 715–718. doi:10.1094/PDIS.1997.81.7.715.

Cannon, P. F., Damm, U., Johnston, P. R., and Weir, B. S. (2012). Colletotrichum – current status and future directions. *Stud. Mycol.* 73, 181–213. doi:10.3114/sim0014.

Caruso, I., Dal Piaz, F., Malafronte, N., De Tommasi, N., Aversano, R., Zottele, C. W., et al. (2013). Impact of Ploidy Change on Secondary Metabolites and Photochemical Efficiency in *Solanum Bulbocastanum*. *Nat. Prod. Commun.* 8, 1934578X1300801. doi:10.1177/1934578X1300801011.

Castro-Moretti, F. R., Gentzel, I. N., Mackey, D., and Alonso, A. P. (2020). Metabolomics as an Emerging Tool for the Study of Plant–Pathogen Interactions. *Metabolites* 10, 52. doi:10.3390/metabo10020052.

Chailakhyan, M. K., Yanina, L. I., Devedzhyan, A. G., and Lotova, G. N. (1981). Photoperiodism and tuberization with grafting of tobacco on potato. *Dokl. Akad. Nauk SSSR* 257, 1276–1280.

Challal, S., Queiroz, E. F., Debrus, B., Kloeti, W., Guillarme, D., Gupta, M. P., et al. (2015). Rational and Efficient Preparative Isolation of Natural Products by MPLC-UV-ELSD based on HPLC to MPLC Gradient Transfer. *Planta Med.* 81, 1636–1643. doi:10.1055/s-0035-1545912.

Chambers, M. C., Maclean, B., Burke, R., Amodei, D., Ruderman, D. L., Neumann, S., et al. (2012). A cross-platform toolkit for mass spectrometry and proteomics. *Nat. Biotechnol.* 30, 918–920. doi:10.1038/nbt.2377.

Charkowski, A., Sharma, K., Parker, M. L., Secor, G. A., and Elphinstone, J. (2020). “Bacterial Diseases of Potato,” in *The Potato Crop: Its Agricultural, Nutritional and Social Contribution to Humankind*, eds. H. Campos and O. Ortiz (Cham: Springer International Publishing), 351–388. doi:10.1007/978-3-030-28683-5_10.

Chen, C., Long, L., Zhang, F., Chen, Q., Chen, C., Yu, X., et al. (2018). Antifungal activity, main active components and mechanism of Curcuma longa extract against Fusarium graminearum. *PLoS ONE* 13. doi:10.1371/journal.pone.0194284.

Chen, F., Ma, R., and Chen, X.-L. (2019). Advances of Metabolomics in Fungal Pathogen–Plant Interactions. *Metabolites* 9. doi:10.3390/metabo9080169.

Chinchilla, D., Bruisson, S., Meyer, S., Zühlke, D., Hirschfeld, C., Joller, C., et al. (2019). A sulfur-containing volatile emitted by potato-associated bacteria confers protection against late blight through direct anti-oomycete activity. *Sci. Rep.* 9, 18778. doi:10.1038/s41598-019-55218-3.

Chisholm, S. T., Coaker, G., Day, B., and Staskawicz, B. J. (2006). Host-Microbe Interactions: Shaping the Evolution of the Plant Immune Response. *Cell* 124, 803–814. doi:10.1016/j.cell.2006.02.008.

Choi, G. J., Lee, S.-W., Jang, K. S., Kim, J.-S., Cho, K. Y., and Kim, J.-C. (2004). Effects of chrysophanol, parietin, and nepodin of Rumex crispus on barley and cucumber powdery mildews. *Crop Prot.* 23, 1215–1221. doi:10.1016/j.cropro.2004.05.005.

Choi, J., Choi, D., Lee, S., Ryu, C.-M., and Hwang, I. (2011). Cytokinins and plant immunity: old foes or new friends? *Trends Plant Sci.* 16, 388–394. doi:10.1016/j.tplants.2011.03.003.

Choi, Y. H., and Verpoorte, R. (2014). Metabolomics: What You See is What You Extract. *Phytochem. Anal.* 25, 289–290. doi:10.1002/pca.2513.

Chun, W. W. C., and Shetty, K. K. (1994). Control of silver scurf disease of potatoes caused by Helminthosporium solani Dur. & Mont. with Pseudomonas corrugata. *Phytopathology* 84, 1090.

Clarke, D. D. (1982). The accumulation of cinnamic acid amides in the cell walls of potato tissue as an early response to fungal attack. *Act. Def. Mech. Plants* 37, 321–322.

Company-Arumí, D., Figueras, M., Salvadó, V., Molinas, M., Serra, O., and Anticó, E. (2016). The Identification and Quantification of Suberin Monomers of Root and Tuber Periderm from Potato (*Solanum tuberosum*) as Fatty Acyl *tert* -Butyldimethylsilyl Derivatives: Monomeric Composition of Potato Root and Tuber Suberins By Mtbstfa. *Phytochem. Anal.* 27, 326–335. doi:10.1002/pca.2625.

Confortin, T. C., Todero, I., Soares, J. F., Luft, L., Brun, T., Rabuske, J. E., et al. (2019). Extracts from Lupinus albescens: antioxidant power and antifungal activity in vitro against phytopathogenic fungi. *Environ. Technol.* 40, 1668–1675. doi:10.1080/09593330.2018.1427800.

Cooke, B. M., Jones, D. G., and Kaye, B. eds. (2006). *The Epidemiology of Plant Diseases*. Dordrecht: Springer Netherlands.

Coquoz, J. L., Buchala, A., Meuwly, P., and Metraux, J. P. (1995). Arachidonic acid induces local but not systemic synthesis of salicylic acid and confers systemic resistance in potato plants to Phytophthora infestans and Alternaria solani. *Phytopathology*. Available at: http://agris.fao.org/agris-search/search.do?recordID=US19970020736 [Accessed February 12, 2020].

Coquoz, J.-L., Buchala, A., and Métraux, J.-P. (1998). The Biosynthesis of Salicylic Acid in Potato Plants. *Plant Physiol.* 117, 1095–1101. doi:10.1104/pp.117.3.1095.

Corcuff, R., Mercier, J., Tweddell, R., and Arul, J. (2011). Effect of water activity on the production of volatile organic compounds by Muscodor albus and their effect on three pathogens in stored potato. *Fungal Biol.* 115, 220–227. doi:10.1016/j.funbio.2010.12.005.

Corwin, J. A., and Kliebenstein, D. J. (2017). Quantitative Resistance: More Than Just Perception of a Pathogen. *Plant Cell* 29, 655–665. doi:10.1105/tpc.16.00915.

Cruz, M. E. S., Schwan-Estrada, K. R. F., Clemente, E., Itako, A. T., Stangarlin, J. R., and Cruz, M. J. S. (2013). Plant extracts for controlling the post-harvest anthracnose of banana fruit. *Rev. Bras. Plantas Med.* 15, 727–733. doi:10.1590/S1516-05722013000500013.

Cullen, D. W., Lees, A. K., Toth, I. K., and Duncan, J. M. (2001). Conventional PCR and Real-time Quantitative PCR Detection of Helminthosporium Solani in Soil and on Potato Tubers. *Eur. J. Plant Pathol.* 107, 387–398.

Cullen, D. W., Lees, A. K., Toth, I. K., and Duncan, J. M. (2002). Detection of Colletotrichum coccodes from soil and potato tubers by conventional and quantitative real-time PCR. *Plant Pathol.* 51, 281–292. doi:10.1046/j.1365-3059.2002.00690.x.

Cunnington, A. C., Mawson, K., and Briddon, A. (1992). Low temperature storage for quality crops. *Asp. Appl. Biol.* 33, 205–212.

Czajkowski, R., Pérombelon, M. C. M., Jafra, S., Lojkowska, E., Potrykus, M., van der Wolf, J. M., et al. (2015). Detection, identification and differentiation of *Pectobacterium* and *Dickeya* species causing potato blackleg and tuber soft rot: a review: Detection of soft rot *Enterobacteriaceae*. *Ann. Appl. Biol.* 166, 18–38. doi:10.1111/aab.12166.

Czajkowski, R., Pérombelon, M. C. M., Veen, J. A. van, and Wolf, J. M. van der (2011). Control of blackleg and tuber soft rot of potato caused by Pectobacterium and Dickeya species: a review. *Plant Pathol.* 60, 999–1013. doi:10.1111/j.1365-3059.2011.02470.x.

da Silva, R. R., Dorrestein, P. C., and Quinn, R. A. (2015). Illuminating the dark matter in metabolomics. *Proc. Natl. Acad. Sci. U. S. A.* 112, 12549–12550. doi:10.1073/pnas.1516878112.

Dangl, J. L., and Jones, J. D. G. (2001). Plant pathogens and integrated defence responses to infection. *Nature* 411, 826–833. doi:10.1038/35081161.

Danielsen, K., Aksnes, D. W., and Francis, G. W. (1992). NMR study of some anthraquinones from rhubarb. *Magn. Reson. Chem.* 30, 359–360. doi:10.1002/mrc.1260300414.

Dashwood, E. P., Fox, R. A., and Perry, D. A. (1992). Effect of inoculum source on root and tuber infection by potato blemish disease fungi. *Plant Pathol.* 41, 215–223. doi:10.1111/j.1365-3059.1992.tb02340.x.

Dauch, A. L., and Jabaji-Hare, S. H. (2006). Metallothionein and bZIP Transcription Factor Genes from Velvetleaf and Their Differential Expression Following Colletotrichum coccodes Infection. *Phytopathology™* 96, 1116–1123. doi:10.1094/PHYTO-96-1116.

De Jong, H., and Tarn, T. R. (1984). Using germplasm in potato breeding in Canada. *Can. Agric.* 30, 12–14.

De Vos, R. C., De Vos, R. C. H., de Vos, R. C. H., Moco, S., Lommen, A., Keurentjes, J. J. B., et al. (2007). Untargeted large-scale plant metabolomics using liquid chromatography coupled to mass spectrometry. Available at: https://www.scienceopen.com/document?vid=ac56428e-7aee-42a4-ac3e-6546980df964 [Accessed March 12, 2020].

de Vries, H. (1878). Beitrage zur speciellen Physiologie landwirtschaftlicher Kulturpflanzen. V. Wachsthamsgeschichte der Kartoffelpflanze. *Landwirtsch. Jahrb. Schweiz* 1, 591–682.

De Vrieze, M., Germanier, F., Vuille, N., and Weisskopf, L. (2018). Combining Different Potato-Associated Pseudomonas Strains for Improved Biocontrol of Phytophthora infestans. *Front. Microbiol.* 9. doi:10.3389/fmicb.2018.02573.

De Vrieze, M., Gloor, R., Massana Codina, J., Torriani, S., Gindro, K., L'Haridon, F., et al. (2019). Biocontrol Activity of Three Pseudomonas in a Newly Assembled Collection of Phytophthora infestans Isolates. *Phytopathology™* 109, 1555–1565. doi:10.1094/PHYTO-12-18-0487-R.

Dean, R., Kan, J. a. L. V., Pretorius, Z. A., Hammond-Kosack, K. E., Pietro, A. D., Spanu, P. D., et al. (2012). The Top 10 fungal pathogens in molecular plant pathology. *Mol. Plant Pathol.* 13, 414–430. doi:10.1111/j.1364-3703.2011.00783.x.

Denner, F. D. N., Millard, C., Geldenhuys, A., and Wehner, F. C. (1997). Treatment of seed potatoes with prochloraz for simultaneous control of silver scurf and black dot on progeny tubers. *Potato Res.* 40, 221–227. doi:10.1007/BF02358247.

Denner, F. D. N., Millard, C. P., and Wehner, F. C. (1998). The effect of seed-and soilborne inoculum ofColletotrichum coccodes on the incidence of black dot on potatoes. *Potato Res.* 41, 51–56. doi:10.1007/BF02360261.

Denner, F. D. N., Millard, C. P., and Wehner, F. C. (2000). Effect of soil solarisation and mouldboard ploughing on black dot of potato, caused byColletotrichum coccodes. *Potato Res.* 43, 195–201. doi:10.1007/BF02358079.

Desender, S., Andrivon, D., and Val, F. (2007). Activation of defence reactions in Solanaceae: where is the specificity? *Cell. Microbiol.* 9, 21–30. doi:10.1111/j.1462-5822.2006.00831.x.

Dickson, B. T. (1926). The "black dot" disease of the potato. *Phytopathology* 16, 23–40.

Dillard, H. R., and Cobb, A. C. (1998). Survival of *Colletotrichum coccodes* in Infected Tomato Tissue and in Soil. *Plant Dis.* 82, 235–238. doi:10.1094/PDIS.1998.82.2.235.

Dinchev, D., Janda, B., Evstatieva, L., Oleszek, W., Aslani, M. R., and Kostova, I. (2008). Distribution of steroidal saponins in Tribulus terrestris from different geographical regions. *Phytochemistry* 69, 176–186. doi:10.1016/j.phytochem.2007.07.003.

Djoumbou Feunang, Y., Eisner, R., Knox, C., Chepelev, L., Hastings, J., Owen, G., et al. (2016). ClassyFire: automated chemical classification with a comprehensive, computable taxonomy. *J. Cheminformatics* 8, 61. doi:10.1186/s13321-016-0174-y.

Dodds, P. N., and Rathjen, J. P. (2010). Plant immunity: towards an integrated view of plant-pathogen interactions. *Nat. Rev. Genet.* 11, 539–548. doi:10.1038/nrg2812.

Doyle, J. J. (1990). Isolation of Plant DNA from Fresh Tissue. *Focus* 12, 13–15.

Draz, I. S., Elkhwaga, A. A., Elzaawely, A. A., El-Zahaby, H. M., and Ismail, A.-W. A. (2019). Application of plant extracts as inducers to challenge leaf rust of wheat. *Egypt. J. Biol. Pest Control* 29, 6. doi:10.1186/s41938-019-0109-9.

Dubey, O., Dubey, S., Schnee, S., Glauser, G., Nawrath, C., Gindro, K., et al. (2020). Plant surface metabolites as potent antifungal agents. *Plant Physiol. Biochem.* 150, 39–48. doi:10.1016/j.plaphy.2020.02.026.

Dubuis, P. H., Bleyer, G., Krause, R., Viret, O., Fabre, A.-L., Werder, M., et al. (2019). VitiMeteo and Agrometeo: Two platforms for plant protection management based on an international collaboration. in *BIO Web of Conferences* (EDP Sciences), 01036. doi:10.1051/bioconf/20191501036.

Ducomet, V. (1908). Une nouvelle maladie de la pomme de terre: Dartrose. *Annu. Iecole Natl. Agric. Rennes*, 24–47.

Dung, J. K. S., Ingram, J. T., Cummings, T. F., and Johnson, D. A. (2012). Impact of Seed Lot Infection on the Development of Black Dot and Verticillium Wilt of Potato in Washington. *Plant Dis.* 96, 1179–1184. doi:10.1094/PDIS-01-12-0061-RE.

el-Basyouni, S. Z., Chen, D., Ibrahim, R. K., Neish, A. C., and Towers, G. H. N. (1964). The biosynthesis of hydroxybenzoic acids in higher plants. *Phytochemistry* 3, 485–492. doi:10.1016/S0031-9422(00)88025-5.

El Hadrami, A., Adam, L. R., and Daayf, F. (2011). Biocontrol Treatments Confer Protection Against *Verticillium dahliae* Infection of Potato by Inducing Antimicrobial Metabolites. *Mol. Plant. Microbe Interact.* 24, 328–335. doi:10.1094/MPMI-04-10-0098.

El Oirdi, M., Trapani, A., and Bouarab, K. (2010). The nature of tobacco resistance against *Botrytis cinerea* depends on the infection structures of the pathogen. *Environ. Microbiol.* 12, 239–253. doi:10.1111/j.1462-2920.2009.02063.x.

Elson, M. K., Schisler, D. A., and Bothast, R. J. (1997). Selection of Microorganisms for Biological Control of Silver Scurf (*Helminthosporium solani*) of Potato Tubers. *Plant Dis.* 81, 647–652. doi:10.1094/PDIS.1997.81.6.647.

Errampalli, D., Saunders, J., and Cullen, D. (2001a). A PCR-based method for detection of potato pathogen, Helminthosporium solani, in silver scurf infected tuber tissue and soils. *J. Microbiol. Methods* 44, 59–68. doi:10.1016/S0167-7012(00)00240-2.

Errampalli, D., Saunders, J. M., and Holley, J. D. (2001b). Emergence of silver scurf (Helminthosporium solani) as an economically important disease of potato. *Plant Pathol.* 50, 141–153. doi:10.1046/j.1365-3059.2001.00555.x.

Eschen-Lippold, L., Draeger, T., Teichert, A., Wessjohann, L., Westermann, B., Rosahl, S., et al. (2009). Antioomycete Activity of γ-Oxocrotonate Fatty Acids against *P. infestans*. *J. Agric. Food Chem.* 57, 9607–9612. doi:10.1021/jf902067k.

European Commission (2019). COMMISSION IMPLEMENTING REGULATION (EU) 2019/ 989 - of 17 June 2019 - concerning the non-renewal of approval of the active substance chlorpropham, in accordance with Regulation (EC) No 1107 / 2009 of the European Parliament and of the Council concerning the placing of plant protection products on

the market, and amending the Annex to Commission Implementing Regulation (EU) No 540 / 2011. *Off. J. Eur. Union*, 3.

Fahn, A. (1982). *Plant anatomy*. 3rd ed. Oxford, UK: Pergamon Press Available at: https://onlinelibrary.wiley.com/doi/abs/10.1111/j.1756-1051.1983.tb01458.x [Accessed March 19, 2020].

Faizal, A., and Geelen, D. (2013). Saponins and their role in biological processes in plants. *Phytochem. Rev.* 12, 877–893. doi:10.1007/s11101-013-9322-4.

Fang, Y., and Ramasamy, R. P. (2015). Current and Prospective Methods for Plant Disease Detection. *Biosensors* 5, 537–561. doi:10.3390/bios5030537.

Fehr, W. (1987). *Principles of Cultivar Development: Crop Species*. New York, NY: Agronomy Books Available at: https://lib.dr.iastate.edu/agron_books/2.

Felix, G., Grosskopf, D. G., Regenass, M., Basse, C. W., and Boller, T. (1991). Elicitor-induced ethylene biosynthesis in tomato cells: characterization and use as a bioassay for elicitor action. *Plant Physiol.* 97, 19–25. doi:10.1104/pp.97.1.19.

Fenner, R., Sortino, M., Rates, S. M. K., Dall'Agnol, R., Ferraz, A., Bernardi, A. P., et al. (2005). Antifungal activity of some Brazilian Hypericum species. *Phytomedicine Int. J. Phytother. Phytopharm.* 12, 236–240. doi:10.1016/j.phymed.2003.11.004.

Fewell, A. M., and Roddick, J. G. (1993). Interactive antifungal activity of the glycoalkaloids α-solanine and α-chaconine. *Phytochemistry* 33, 323–328. doi:10.1016/0031-9422(93)85511-O.

Fiehn, O., Kopka, J., Dörmann, P., Altmann, T., Trethewey, R. N., and Willmitzer, L. (2000). Metabolite profiling for plant functional genomics. *Nat. Biotechnol.* 18, 1157–1161. doi:10.1038/81137.

Firman, D. M., and Allen, E. J. (1993). Effects of windrowing, irrigation and defoliation of potatoes on silver scurf (Helminthosporium solani) disease. *J. Agric. Sci.* 121, 47–53. doi:10.1017/S0021859600076784.

Firman, D. M., and Allen, E. J. (1995a). Effects of seed size, planting density and planting pattern on the severity of silver scurf (Helminthosporium solani) and black scurf (Rhizoctonia solani) diseases of potatoes. *Ann. Appl. Biol.* 127, 73–85. doi:10.1111/j.1744-7348.1995.tb06652.x.

Firman, D. M., and Allen, E. J. (1995b). Transmission of *Helminthosporium solani* from potato seed tubers and effects of soil conditions, seed inoculum and seed physiology on silver scurf disease. *J. Agric. Sci.* 124, 219–234. doi:10.1017/S0021859600072890.

Fisher, M. C., Henk, D. A., Briggs, C. J., Brownstein, J. S., Madoff, L. C., McCraw, S. L., et al. (2012). Emerging fungal threats to animal, plant and ecosystem health. *Nature* 484, 186–194. doi:10.1038/nature10947.

Flor, H. H. (1971). Current status of the gene-for-gene concept. *Annu. Rev. Phytopathol.* 9, 275–296.

Food and Agriculture Organization of the United Nations (2008). Why potato? - International Year of the Potato 2008. *Why Potato - Int. Year Potato 2008*. Available at: http://www.fao.org/potato-2008/en/aboutiyp/index.html [Accessed March 31, 2020].

Forrer, H. R., Hecker, A., and Steenblock, T. (2000). Hot water treatment of potato seed tubers - a practicable means to prevent primary foci and delay epidemics of potato late blight? *IFOAM 2000 World Grows Org. Proc. 13th Int. IFOAM Sci. Conf. Basel Switz. 28 31 August 2000*. Available at: https://www.cabdirect.org/cabdirect/abstract/20001009821 [Accessed February 14, 2020].

Forrer, H.-R., Musa, T., Schwab, F., Jenny, E., Bucheli, T. D., Wettstein, F. E., et al. (2014). Fusarium Head Blight Control and Prevention of Mycotoxin Contamination in Wheat with Botanicals and Tannic Acid. *Toxins* 6, 830–849. doi:10.3390/toxins6030830.

Francis, G. W., Aksnes, D. W., and Holt, Ø. (1998). Assignment of the 1H and 13C NMR spectra of anthraquinone glycosides from Rhamnus frangula. *Magn. Reson. Chem.* 36, 769–772. doi:10.1002/(SICI)1097-458X(1998100)36:10<769::AID-OMR361>3.0.CO;2-E.

Frazier, M. J., Shetty, K. K., Kleinkopf, G. E., and Nolte, P. (1998). Management of silver scurf (Helminthosporium solani) with fungicide seed treatments and storage practices. *Am. J. Potato Res.* 75, 129–135. doi:10.1007/BF02895847.

Friedman, M. (2006). Potato Glycoalkaloids and Metabolites: Roles in the Plant and in the Diet. *J. Agric. Food Chem.* 54, 8655–8681. doi:10.1021/jf061471t.

Friedman, M., and Levin, C. E. (2009). "Analysis and Biological Activities of Potato Glycoalkaloids, Calystegine Alkaloids, Phenolic Compounds, and Anthocyanins," in *Advances in Potato Chemistry and Technology* (Elsevier), 127–161. doi:10.1016/B978-0-12-374349-7.00006-4.

Friedman, M., McDonald, G. M., and Filadelfi-Keszi, P. M. (1997). Potato Glycoalkaloids: Chemistry, Analysis, Safety, and Plant Physiology. *Crit. Rev. Plant Sci.* 16, 55–132. doi:10.1080/07352689709701946.

Fritzemeier, K. H., Cretin, C., Kombrink, E., Rohwer, F., Taylor, J., Scheel, D., et al. (1987). Transient Induction of Phenylalanine Ammonia-Lyase and 4-Coumarate: CoA Ligase mRNAs in Potato Leaves Infected with Virulent or Avirulent Races of Phytophthora infestans. *Plant Physiol.* 85, 34–41. doi:10.1104/pp.85.1.34.

Frost, K., Groves, R., and Charkowski, A. (2013). Integrated Control of Potato Pathogens Through Seed Potato Certification and Provision of Clean Seed Potatoes. *Plant Dis.* 97, 1268–1280. doi:10.1094/PDIS-05-13-0477-FE.

Funayama, S., Yoshida, K., Konno, C., and Hikino, H. (1980). Structure of kukoamine A, a hypotensive principle of Lycium chinense root barks1. *Tetrahedron Lett.* 21, 1355–1356. doi:10.1016/S0040-4039(00)74574-6.

Funayama, S., Zhang, G.-R., and Nozoe, S. (1995). Kukoamine B, a spermine alkaloid from Lycium chinense. *Phytochemistry* 38, 1529–1531. doi:10.1016/0031-9422(94)00826-F.

Gagnebin, Y., Pezzatti, J., Lescuyer, P., Boccard, J., Ponte, B., and Rudaz, S. (2020). Combining the advantages of multilevel and orthogonal partial least squares data analysis for longitudinal metabolomics: Application to kidney transplantation. *Anal. Chim. Acta* 1099, 26–38. doi:10.1016/j.aca.2019.11.050.

Gamir, J., Darwiche, R., van't Hof, P., Choudhary, V., Stumpe, M., Schneiter, R., et al. (2017). The sterol-binding activity of PATHOGENESIS-RELATED PROTEIN 1 reveals the mode of action of an antimicrobial protein. *Plant J.* 89, 502–509. doi:10.1111/tpj.13398.

Garcia, D., Ramos, A. J., Sanchis, V., and Marín, S. (2013). Equisetum arvense hydro-alcoholic extract: phenolic composition and antifungal and antimycotoxigenic effect against Aspergillus flavus and Fusarium verticillioides in stored maize. *J. Sci. Food Agric.* 93, 2248–2253. doi:10.1002/jsfa.6033.

Garner, W., and Allard, H. (1920). Effect of the relative length of day and night and other factors of the environment on growth and reproduction in plants. *J. Agric. Res.* 18, 553.

Garner, W., and Allard, H. (1923). Localization of the response in plant to relative length of day and night. *J. Agric. Res.* 23, 871.

Gau, R. D., Merz, U., Falloon, R. E., and Brunner, P. C. (2013). Global Genetics and Invasion History of the Potato Powdery Scab Pathogen, Spongospora subterranea f.sp. subterranea. *PLOS ONE* 8, e67944. doi:10.1371/journal.pone.0067944.

Geary, B., Hamm, P. B., Johnson, D. A., James, S. R., and Rykbost, K. A. (2000). Effects of fungicides and location on development of silver scurf. *Am. J. Potato Res.* 77, 399.

Geary, B., and Johnson, D. A. (2006). Relationship between silver scurf levels on seed and progeny tubers from successive generations of potato seed. *Am. J. Potato Res.* 83, 447–453. doi:10.1007/BF02883505.

Ghislain, M., Núñez, J., del Rosario Herrera, M., Pignataro, J., Guzman, F., Bonierbale, M., et al. (2009). Robust and highly informative microsatellite-based genetic identity kit for potato. *Mol. Breed.* 23, 377–388. doi:10.1007/s11032-008-9240-0.

Gillmeister, M., Ballert, S., Raschke, A., Geistlinger, J., Kabrodt, K., Baltruschat, H., et al. (2019). Polyphenols from Rheum Roots Inhibit Growth of Fungal and Oomycete Phytopathogens and Induce Plant Disease Resistance. *Plant Dis.* 103, 1674–1684. doi:10.1094/PDIS-07-18-1168-RE.

Gilroy, E. M., Breen, S., Whisson, S. C., Squires, J., Hein, I., Kaczmarek, M., et al. (2011). Presence/absence, differential expression and sequence polymorphisms between PiAVR2 and PiAVR2-like in Phytophthora infestans determine virulence on R2 plants. *New Phytol.* 191, 763–776. doi:10.1111/j.1469-8137.2011.03736.x.

Gindro, K., Alonso-Villaverde, V., Viret, O., Spring, J.-L., Marti, G., Wolfender, J.-L., et al. (2012a). "Stilbenes: Biomarkers of Grapevine Resistance to Disease of High Relevance for Agronomy, Oenology and Human Health," in *Plant Defence: Biological Control* Progress in Biological Control., eds. J. M. Mérillon and K. G. Ramawat (Dordrecht: Springer Netherlands), 25–54. doi:10.1007/978-94-007-1933-0_2.

Gindro, K., Alonso-Villaverde, V., Voinesco, F., Spring, J.-L., Viret, O., and Dubuis, P.-H. (2012b). Susceptibility to downy mildew in grape clusters: New microscopical and biochemical insights. *Plant Physiol. Biochem.* 52, 140–146. doi:10.1016/j.plaphy.2011.12.009.

Gindro, K., Godard, S., De Groote, I., Viret, O., Forrer, H. R., and Dorn, B. (2007). Is it possible to induce grapevine defence mechanisms? A new method to evaluate the potential of elicitors. *Rev. Suisse Vitic. Arboric. Hortic.* 39, 377–383.

Glais-Varlet, I., Bouchek-Mechiche, K., and Andrivon, D. (2004). Growth in vitro and infectivity of Colletotrichum coccodes on potato tubers at different temperatures. *Plant Pathol.* 53, 398–404. doi:10.1111/j.1365-3059.2004.01045.x.

González-Álvarez, M., Moreno-Limón, S., Salcedo-Martínez, S. M., and Pérez-Rodríguez, E. C. (2016). In vitro evaluation of antifungal activity of Agave (Agave scabra, Salm Dyck) extracts against post-harvest mushrooms. *Phyton Int. J. Exp. Bot.* 84, 427-434–434.

González-Ruiz, V., Pezzatti, J., Roux, A., Stoppini, L., Boccard, J., and Rudaz, S. (2017). Unravelling the effects of multiple experimental factors in metabolomics, analysis of human neural cells with hydrophilic interaction liquid chromatography hyphenated to high resolution mass spectrometry. *J. Chromatogr. A* 1527, 53–60. doi:10.1016/j.chroma.2017.10.055.

Gorris, L. G. M., Oosterhaven, K., Hartmans, K. J., de Witte, Y., Smid, E. J., and DeWitte, Y. (1994). Control of fungal storage diseases of potato by use of plant essential oil components. in *Proceedings of the Brighton Crop Protection Conference, Pests and Diseases* (Farnham, UK: British Crop Protection Council), 307–312.

Goss, E. M., Tabima, J. F., Cooke, D. E. L., Restrepo, S., Fry, W. E., Forbes, G. A., et al. (2014). The Irish potato famine pathogen Phytophthora infestans originated in central Mexico rather than the Andes. *Proc. Natl. Acad. Sci.* 111, 8791–8796. doi:10.1073/pnas.1401884111.

Graça, J. (2015). Suberin: the biopolyester at the frontier of plants. *Front. Chem.* 3. doi:10.3389/fchem.2015.00062.

Graça, J., and Pereira, H. (2000). Suberin Structure in Potato Periderm: Glycerol, Long-Chain Monomers, and Glyceryl and Feruloyl Dimers. *J. Agric. Food Chem.* 48, 5476–5483. doi:10.1021/jf0006123.

Griffiths, D. W., and Bain, H. (1997). Photo-induced changes in the concentrations of individual chlorogenic acid isomers in potato (Solanum tuberosum) tubers and their complexation with ferric ions. *Potato Res.* 40, 307–315. doi:10.1007/BF02358012.

Gunnaiah, R., Kushalappa, A. C., Duggavathi, R., Fox, S., and Somers, D. J. (2012). Integrated Metabolo-Proteomic Approach to Decipher the Mechanisms by Which Wheat QTL (Fhb1) Contributes to Resistance against Fusarium graminearum. *PLOS ONE* 7, e40695. doi:10.1371/journal.pone.0040695.

Gurjar, M. S., Ali, S., Akhtar, M., and Singh, K. S. (2012). Efficacy of plant extracts in plant disease management. *Agric. Sci.* 03, 425–433. doi:10.4236/as.2012.33050.

Gusberti, M., Klemm, U., Meier, M. S., Maurhofer, M., and Hunger-Glaser, I. (2015). Fire Blight Control: The Struggle Goes On. A Comparison of Different Fire Blight Control Methods in Switzerland with Respect to Biosafety, Efficacy and Durability. *Int. J. Environ. Res. Public. Health* 12, 11422–11447. doi:10.3390/ijerph120911422.

Gust, A. A., and Felix, G. (2014). Receptor like proteins associate with SOBIR1-type of adaptors to form bimolecular receptor kinases. *Curr. Opin. Plant Biol.* 21, 104–111. doi:10.1016/j.pbi.2014.07.007.

Guyer, A., De Vrieze, M., Bönisch, D., Gloor, R., Musa, T., Bodenhausen, N., et al. (2015). The Anti-Phytophthora Effect of Selected Potato-Associated Pseudomonas Strains: From the Laboratory to the Field. *Front. Microbiol.* 6. doi:10.3389/fmicb.2015.01309.

Gwa, V., Nwankiti, A. O., and Hamzat, O. T. H. (2018). Antimicrobial Activity of Five Plant Extracts and Synthetic Fungicide in the Management of Postharvest Pathogens of Yam (Dioscorea

Rotundata Poir) in Storage. *Open Access J. Microbiol. Biotechnol.* 3. doi:10.23880/OAJMB-16000128.

Hadizadeh, I., Peivastegan, B., and Hamzehzarghani, H. (2009). Antifungal Activity of Essential Oils from Some Medicinal Plants of Iran against Alternaria alternate. *Am. J. Appl. Sci.* 6, 857–861. doi:10.3844/ajassp.2009.857.861.

Hall, J. L., and Hawes, C. (1991). *Electron Microscopy of Plant Cells*. Academic Press doi:10.1016/B978-0-12-318880-9.X5001-7.

Hameed, A., Mehmood, M. A., Shahid, M., Fatma, S., Khan, A., and Ali, S. (2019). Prospects for potato genome editing to engineer resistance against viruses and cold-induced sweetening. *GM Crops Food* 0, 1–21. doi:10.1080/21645698.2019.1631115.

Hamzehzarghani, H., Paranidharan, V., Abu-Nada, Y., Kushalappa, A. C., Dion, Y., Rioux, S., et al. (2008). Metabolite profiling coupled with statistical analyses for potential high-throughput screening of quantitative resistance to Fusarium head blight in wheat. *Can. J. Plant Pathol.-Rev. Can. Phytopathol. - CAN J PLANT PATHOL* 30, 24–36. doi:10.1080/07060660809507493.

Hamzehzarghani, H., Vikram, A., Abu-Nada, Y., and Kushalappa, A. C. (2016). Tuber metabolic profiling of resistant and susceptible potato varieties challenged with Phytophthora infestans. *Eur. J. Plant Pathol.* 145, 277–287. doi:10.1007/s10658-015-0840-3.

Hannapel, D. (2007). "Signalling the induction of tuber formation," in *Potato biology and biotechnology : advances and perspectives*, ed. D. Vreugdenhil (Amsterdam: Elsevier).

Hardham, A. R. (2007). "Cell Biology of Fungal and Oomycete Infection of Plants," in *Biology of the Fungal Cell* The Mycota., eds. R. J. Howard and N. A. R. Gow (Berlin, Heidelberg: Springer), 251–289. doi:10.1007/978-3-540-70618-2_11.

Hardham, A. R. (2012). Confocal microscopy in plant-pathogen interactions. *Methods Mol. Biol. Clifton NJ* 835, 295–309. doi:10.1007/978-1-61779-501-5_18.

Hardigan, M., Laimbeer, P., Newton, L., Crisovan, E., Hamilton, J., Vaillancourt, B., et al. (2017). Genome diversity of tuber-bearing Solanum uncovers complex evolutionary history and targets of domestication in the cultivated potato. *Proc. Natl. Acad. Sci.* 114, 201714380. doi:10.1073/pnas.1714380114.

Hardy, C. E., Burgess, P. J., and Pringle, R. T. (1997). The effect of condensation on sporulation ofHelminthosporium solani on potato tubers infected with silver scurf and held in simulated store conditions. *Potato Res.* 40, 169–180. doi:10.1007/BF02358243.

Harrison, D. E. (1963). Black dot disease of potato. *J. Dep. Agric. Vic.* 61, 573–6.

Hartmann, A., Senning, M., Hedden, P., Sonnewald, U., and Sonnewald, S. (2011). Reactivation of Meristem Activity and Sprout Growth in Potato Tubers Require Both Cytokinin and Gibberellin. *Plant Physiol.* 155, 776–796. doi:10.1104/pp.110.168252.

Hartmans, K. J., Diepenhorst, P., Bakker, W., and Gorris, L. G. M. (1995). The use of carvone in agriculture: sprout suppression of potatoes and antifungal activity against potato tuber and other plant diseases. *Ind. Crops Prod.* 4, 3–13. doi:10.1016/0926-6690(95)00005-W.

Heiny, D. K., and McIntyre, G. A. (1983). Helminthosporium solani Dur. & Mont. development on potato periderm. *Am. Potato J.* 60, 773–789. doi:10.1007/BF02856896.

Henriquez, M. A., Adam, L. R., and Daayf, F. (2012). Alteration of secondary metabolites' profiles in potato leaves in response to weakly and highly aggressive isolates of Phytophthora infestans. *Plant Physiol. Biochem.* 57, 8–14. doi:10.1016/j.plaphy.2012.04.013.

Hervieux, V., Chabot, R., Arul, J., and Tweddell, R. J. (2001). Evaluation of different fungicides applied as seed tuber treatments for the control of potato silver scurf. *Phytoprotection* 82, 41–48.

Hewitt, H. G. (2004). Do we need new fungicides? *Outlooks Pest Manag.* 15, 90–95. doi:info:doi/10.1564/15apl13.

Heydari, A., and Pessarakli, M. (2010). A Review on Biological Control of Fungal Plant Pathogens Using Microbial Antagonists. *J. Biol. Sci.* 10, 273–290. doi:10.3923/jbs.2010.273.290.

Hide, G. A., and Boorer, K. J. (1991). Effects of drying potatoes (Solanum tuberosum L.) after harvest on the incidence of disease after storage. *Potato Res.* 34, 133–137. doi:10.1007/BF02358034.

Hide, G. A., Boorer, K. J., and Hall, S. M. (1994a). Controlling potato tuber blemish diseases on cv. Estima with chemical and non-chemical methods. *Ann. Appl. Biol.* 124, 253–265. doi:10.1111/j.1744-7348.1994.tb04132.x.

Hide, G. A., Boorer, K. J., and Hall, S. M. (1994b). Effects of watering potato plants before harvest and of curing conditions on development of tuber diseases during storage. *Potato Res.* 37, 169–172. doi:10.1007/BF02358718.

Hide, G. A., and Hall, S. M. (1993). Development of resistance to thiabendazole in Helminthosporium solani (silver scurf) as a result of potato seed tuber treatment. *Plant Pathol.* 42, 707–714. doi:10.1111/j.1365-3059.1993.tb01556.x.

Hide, G. A., Hall, S. M., and Boorer, K. J. (1988). Resistance to thiabendazole in isolates of Helminthosporium solani, the cause of silver scurf disease of potatoes. *Plant Pathol.* 37, 377–380. doi:10.1111/j.1365-3059.1988.tb02088.x.

Hide, G. A., Hall, S. M., and Read, P. J. (1994c). Control of skin spot and silver scurf on stored cv. King Edward potatoes by chemical and non-chemical methods. *Ann. Appl. Biol.* 125, 87–96. doi:10.1111/j.1744-7348.1994.tb04949.x.

Hide, G. A., Hirst, J. M., and Griffith, R. L. (1969). Control of potato tuber diseases with systemic fungicides. in *Proceedings of the Fifth British Insecticide and Fungicide Conference* (Brighton, UK: British Crop Protection Council).

Hide, G. A., and Read, P. J. (1991). Effects of rotation length, fungicide treatment of seed tubers and nematicide on diseases and the quality of potato tubers. *Ann. Appl. Biol.* 119, 77–87. doi:10.1111/j.1744-7348.1991.tb04845.x.

Hijmans, R. J., and Spooner, D. M. (2001). Geographic distribution of wild potato species. *Am. J. Bot.* 88, 2101–2112.

Horai, H., Arita, M., Kanaya, S., Nihei, Y., Ikeda, T., Suwa, K., et al. (2010). MassBank: a public repository for sharing mass spectral data for life sciences. *J. Mass Spectrom.* 45, 703–714. doi:10.1002/jms.1777.

Huang, W., Serra, O., Dastmalchi, K., Jin, L., Yang, L., and Stark, R. E. (2017). Comprehensive MS and Solid-State NMR Metabolomic Profiling Reveals Molecular Variations in Native Periderms from Four *Solanum tuberosum* Potato Cultivars. *J. Agric. Food Chem.* 65, 2258–2274. doi:10.1021/acs.jafc.6b05179.

Hubert, J., Nuzillard, J.-M., and Renault, J.-H. (2017). Dereplication strategies in natural product research: How many tools and methodologies behind the same concept? *Phytochem. Rev.* 16, 55–95. doi:10.1007/s11101-015-9448-7.

Hughes, S. J. (1958). Revisiones hyphomycetum aliquot cum appendice de nominibus rejiciendis. *Can. J. Bot.* 36, 727–836. doi:10.1139/b58-067.

Hunger, R. M., and McIntyre, G. A. (1979). Occurrence, development, and losses associated with silver scurf and black dot on Colorado potatoes. *Am. Potato J.* 56, 289–306. doi:10.1007/BF02855598.

Iiyama, K., Lam, TBT., and Stone, B. A. (1994). Covalent Cross-Links in the Cell Wall. *Plant Physiol.* 104, 315–320.

Imtiaj, A., Rahman, S. A., Alam, S., Parvin, R., Farhana, K. M., Kim, S.-B., et al. (2005). Effect of Fungicides and Plant Extracts on the Conidial Germination of Colletotrichum gloeosporioides Causing Mango Anthracnose. *Mycobiology* 33, 200–205. doi:10.4489/MYCO.2005.33.4.200.

Index Fungorum Available at: http://www.indexfungorum.org/Names/NamesRecord.asp?RecordID=295323 [Accessed February 19, 2020].

Ingram, J., and Johnson, D. A. (2010). Colonization of Potato Roots and Stolons by Colletotrichum coccodes from Tuberborne Inoculum. *Am. J. Potato Res.* 87, 382–389. doi:10.1007/s12230-010-9144-5.

Inoue, K., Nomura, C., Ito, S., Nagatsu, A., Hino, T., and Oka, H. (2008). Purification of Curcumin, Demethoxycurcumin, and Bisdemethoxycurcumin by High-Speed Countercurrent Chromatography. *J. Agric. Food Chem.* 56, 9328–9336. doi:10.1021/jf801815n.

Jain, D., and Khurana, J. P. (2018). "Role of Pathogenesis-Related (PR) Proteins in Plant Defense Mechanism," in *Molecular Aspects of Plant-Pathogen Interaction*, eds. A. Singh and I. K. Singh (Singapore: Springer), 265–281. doi:10.1007/978-981-10-7371-7_12.

Jansen, G., Flamme, W., Schüler, K., and Vandrey, M. (2001). Tuber and starch quality of wild and cultivated potato species and cultivars. *Potato Res.* 44, 137–146. doi:10.1007/BF02410100.

Jarroudi, M. E., Kouadio, L., Tychon, B., ElJarroudi, M., Junk, J., Bock, C., et al. (2018). Modeling the Main Fungal Diseases of Winter Wheat: Constraints and Possible Solutions. *Adv. Plant Pathol.* doi:10.5772/intechopen.75983.

Järvinen, R., Silvestre, A. J. D., Holopainen, U., Kaimainen, M., Nyyssölä, A., Gil, A. M., et al. (2009). Suberin of Potato (Solanum tuberosum Var. Nikola): Comparison of the Effect of Cutinase CcCut1 with Chemical Depolymerization. *J. Agric. Food Chem.* 57, 9016–9027. doi:10.1021/jf9008907.

Jellis, G. J., and Taylor, G. S. (1977). The development of silver scurf (Helminthosporium solani) disease of potato. *Ann. Appl. Biol.* 86, 19–28. doi:10.1111/j.1744-7348.1977.tb01811.x.

Ji, N.-Y., Liang, X.-R., Sun, R.-R., and Miao, F.-P. (2014). A rule to distinguish diastereomeric bianthrones by 1H NMR. *RSC Adv.* 4, 7710–7715. doi:10.1039/C3RA47055E.

Jiménez-Reyes, M. F., Carrasco, H., Olea, A. F., Silva-Moreno, E., Jiménez-Reyes, M. F., Carrasco, H., et al. (2019). NATURAL COMPOUNDS: A SUSTAINABLE ALTERNATIVE TO THE PHYTOPATHOGENS CONTROL. *J. Chil. Chem. Soc.* 64, 4459–4465. doi:10.4067/S0717-97072019000204459.

Johns, T., and Alonso, J. G. (1990). Glycoalkaloid change during the domestication of the potato, Solanum Section Petota. *Euphytica* 50, 203–210. doi:10.1007/BF00023646.

Johnson, D. A. (1994). Effect of foliar infection caused by Colletotrichum coccodes on yield of Russet Burbank potato. *Plant Dis.* 78, 1075–1078.

Johnson, D. A., and Cummings, T. F. (2015). Effect of Extended Crop Rotations on Incidence of Black Dot, Silver Scurf, and Verticillium Wilt of Potato. *Plant Dis.* 99, 257–262. doi:10.1094/PDIS-03-14-0271-RE.

Johnson, D. A., Geary, B., and (Lahkim) Tsror, L. (2018). Potato Black Dot – The Elusive Pathogen, Disease Development and Management. *Am. J. Potato Res.* 95, 340–350. doi:10.1007/s12230-018-9633-5.

Johnson, S. B. (2007). Evaluation of a Biological Agent for Control of Helminthosporium solani. *Plant Pathol. J.* 6, 99–101.

Jones, J. D. G., and Dangl, J. L. (2006). The plant immune system. *Nature* 444, 323–329. doi:10.1038/nature05286.

Joshi, P. K., and Pepin, H. S. (1991). A survey of silver scurf disease (Helminthosporium solani) of potatoes in Lower Fraser Valley and Pemberton area of B.C. *Can. Plant Dis. Surv.* 71, 115.

Jouan, B., Lemaire, J. M., Perennec, P., and Sailly, M. (1974). Études sur la gale argentée de la pomme de terre Helminthosporium solani Dur. et Mont. *Ann. Phytopathol.* 6, 407–423.

Kamara, A. M., and Hugelet, J. E. (1972). Host range and overwintering of Helminthosporium solani. *Am. Potato J.* 49, 365.

Kashiwada, Y., Nonaka, G., and Nishioka, I. (1986). Tannins and related compounds. XLVII: Rhubarb. Isolation and characterication of new p-hydroxyphenylbutanones, stilbenes and gallic acid glucosides. *Chem. Pharm. Bull. (Tokyo)* 34, 3237–3243.

Katajamaa, M., Miettinen, J., and Orešič, M. (2006). MZmine: toolbox for processing and visualization of mass spectrometry based molecular profile data. *Bioinformatics* 22, 634–636. doi:10.1093/bioinformatics/btk039.

Keller, H., Hohlfeld, H., Wray, V., Hahlbrock, K., Scheel, D., and Strack, D. (1996). Changes in the accumulation of soluble and cell wall-bound phenolics in elicitor-treated cell suspension cultures and fungus-infected leaves of Solanum tuberosum. *Phytochemistry* 42, 389–396. doi:10.1016/0031-9422(95)00866-7.

Khan, N., Martínez-Hidalgo, P., Ice, T. A., Maymon, M., Humm, E. A., Nejat, N., et al. (2018). Antifungal Activity of Bacillus Species Against Fusarium and Analysis of the Potential Mechanisms Used in Biocontrol. *Front. Microbiol.* 9. doi:10.3389/fmicb.2018.02363.

Khatri, B. B., Tegg, R. S., Brown, P. H., and Wilson, C. R. (2011). Temporal association of potato tuber development with susceptibility to common scab and Streptomyces scabiei-induced responses in the potato periderm. *Plant Pathol.* 60, 776–786. doi:10.1111/j.1365-3059.2011.02435.x.

Kim, J. H., Kim, H. S., Lee, Y. H., Kim, Y. S., Oh, H. W., Joung, H., et al. (2008). Polyamine Biosynthesis Regulated by StARD Expression Plays an Important Role in Potato Wound Periderm Formation. *Plant Cell Physiol.* 49, 1627–1632. doi:10.1093/pcp/pcn115.

Kim, J.-C., Choi, G. J., Lee, S.-W., Kim, J.-S., Chung, K. Y., and Cho, K. Y. (2004). Screening extracts of Achyranthes japonica and Rumex crispus for activity against various plant pathogenic fungi and control of powdery mildew. *Pest Manag. Sci.* 60, 803–808. doi:10.1002/ps.811.

Kim, M., Choi, G., and Lee, H. (2003). Fungicidal Property of Curcuma longa L. Rhizome-Derived Curcumin against Phytopathogenic Fungi in a Greenhouse. *J. Agric. Food Chem.* 51, 1578–1581. doi:10.1021/jf0210369.

Kind, T., and Fiehn, O. (2007). Seven Golden Rules for heuristic filtering of molecular formulas obtained by accurate mass spectrometry. *BMC Bioinformatics* 8, 105. doi:10.1186/1471-2105-8-105.

King, R. R., and Calhoun, L. A. (2005). Characterization of cross-linked hydroxycinnamic acid amides isolated from potato common scab lesions. *Phytochemistry* 66, 2468–2473. doi:10.1016/j.phytochem.2005.07.014.

Kishore, G. K., Pande, S., and Harish, S. (2007). Evaluation of Essential Oils and Their Components for Broad-Spectrum Antifungal Activity and Control of Late Leaf Spot and Crown Rot Diseases in Peanut. *Plant Dis.* 91, 375–379. doi:10.1094/PDIS-91-4-0375.

Knapp, S., and van der Heijden, M. G. A. (2018). A global meta-analysis of yield stability in organic and conservation agriculture. *Nat. Commun.* 9, 1–9. doi:10.1038/s41467-018-05956-1.

Kodzius, R., and Gojobori, T. (2015). Marine metagenomics as a source for bioprospecting. *Mar. Genomics* 24, 21–30. doi:10.1016/j.margen.2015.07.001.

Kögl, F., and Postowsky, J. J. (1925). Untersuchungen über Pilzfarbstoffe. II. Über die Farbstoffe des blutroten Hautkopfes (Dermocybe sanguinea Wulf.). *Justus Liebigs Ann. Chem.* 444, 1–7. doi:10.1002/jlac.19254440102.

Kolattukudy, P. E. (2001). “Suberin from plants,” in *Biopolymers*, eds. A. Steinbüchel and Y. Doi (Weinheim: Wiley-VCH Verlag GmbH & Co. KGaA), 41–73.

Kolattukudy, P. E., and Agrawal, V. P. (1974). Structure and composition of aliphatic constituents of potato tuber skin (suberin). *Lipids* 9, 682–691. doi:10.1007/BF02532176.

Krebs, H., Dorn, B., and Forrer, H.-R. (Agroscope F. R. (2006). Control of late blight of potato with medicinal plant suspensions. *Agrar. Switz.* 13, 16–21.

Kremer, D., Kosalec, I., Locatelli, M., Epifano, F., Genovese, S., Carlucci, G., et al. (2012). Anthraquinone profiles, antioxidant and antimicrobial properties of Frangula rupestris (Scop.) Schur and Frangula alnus Mill. bark. *Food Chem.* 131, 1174–1180. doi:10.1016/j.foodchem.2011.09.094.

Krits, P., Fogelman, E., and Ginzberg, I. (2007). Potato steroidal glycoalkaloid levels and the expression of key isoprenoid metabolic genes. *Planta* 227, 143–150. doi:10.1007/s00425-007-0602-3.

Kröner, A., Hamelin, G., Andrivon, D., and Val, F. (2011). Quantitative Resistance of Potato to Pectobacterium atrosepticum and Phytophthora infestans: Integrating PAMP-Triggered Response and Pathogen Growth. *PLoS ONE* 6, e23331. doi:10.1371/journal.pone.0023331.

Kröner, A., Marnet, N., Andrivon, D., and Val, F. (2012). Nicotiflorin, rutin and chlorogenic acid: phenylpropanoids involved differently in quantitative resistance of potato tubers to biotrophic and necrotrophic pathogens. *Plant Physiol. Biochem.* 57, 23–31. doi:10.1016/j.plaphy.2012.05.006.

Kubo, I., Murai, Y., Soediro, I., Soetarno, S., and Sastrodihardjo, S. (1992). Cytotoxic anthraquinones from Rheum pulmatum. *Phytochemistry* 31, 1063–1065. doi:10.1016/0031-9422(92)80078-S.

Kumaraswamy, K. G., Kushalappa, A. C., Choo, T. M., Dion, Y., and Rioux, S. (2011). Mass spectrometry based metabolomics to identify potential biomarkers for resistance in barley against fusarium head blight (Fusarium graminearum). *J. Chem. Ecol.* 37, 846–856. doi:10.1007/s10886-011-9989-1.

Kurzawińska, H. (2006). An interaction of potato crop soil fungi population on fungi responsible for tuber superficial diseases. *J. Plant Prot. Res.* 46, 339–346.

Kushalappa, A. C., and Gunnaiah, R. (2013). Metabolo-proteomics to discover plant biotic stress resistance genes. *Trends Plant Sci.* 18, 522–531. doi:10.1016/j.tplants.2013.05.002.

Kyselka, J., Bleha, R., Dragoun, M., Bialasová, K., Horáčková, Š., Schätz, M., et al. (2018). Antifungal Polyamides of Hydroxycinnamic Acids from Sunflower Bee Pollen. *J. Agric. Food Chem.* 66, 11018–11026. doi:10.1021/acs.jafc.8b03976.

La Camera, S., Gouzerh, G., Dhondt, S., Hoffmann, L., Fritig, B., Legrand, M., et al. (2004). Metabolic reprogramming in plant innate immunity: the contributions of phenylpropanoid and oxylipin pathways. *Immunol. Rev.* 198, 267–284. doi:10.1111/j.0105-2896.2004.0129.x.

Lau, H. Y., and Botella, J. R. (2017). Advanced DNA-Based Point-of-Care Diagnostic Methods for Plant Diseases Detection. *Front. Plant Sci.* 8, 2016. doi:10.3389/fpls.2017.02016.

Lê, C. L., and Collet, G. F. (1985). Assainissement de la variété de pomme de terre Sangema. Méthode combinant la thermothérapie in vitro et la culture de méristèmes. Premiers résultats. *Rev. Suisse Agric.* 17, 221–225.

Lee, S. O., Park, I.-K., Choi, G. J., Lim, H. K., Jang, K. S., Cho, K. Y., et al. (2007). Fumigant activity of essential oils and components of Illicium verum and Schizonepeta tenuifolia against Botrytis cinerea and Colletotrichum gloeosporioides. *J. Microbiol. Biotechnol.* 17, 1568–1572.

Lee, T., Park, D., Kim, K., Lim, S. M., Yu, N. H., Kim, S., et al. (2017). Characterization of Bacillus amyloliquefaciens DA12 Showing Potent Antifungal Activity against Mycotoxigenic Fusarium Species. *Plant Pathol. J.* 33, 499–507. doi:10.5423/PPJ.FT.06.2017.0126.

Lees, A. K., Brierley, J. L., Stewart, J. A., Hilton, A. J., Wale, S. J., Gladders, P., et al. (2010). Relative importance of seed-tuber and soilborne inoculum in causing black dot disease of potato:

Black dot disease of potato. *Plant Pathol.* 59, 693–702. doi:10.1111/j.1365-3059.2010.02284.x.

Lees, A. K., and Hilton, A. J. (2003). Black dot (Colletotrichum coccodes): an increasingly important disease of potato. *Plant Pathol.* 52, 3–12. doi:10.1046/j.1365-3059.2003.00793.x.

Lehmann, S., Serrano, M., L'Haridon, F., Tjamos, S. E., and Metraux, J.-P. (2015). Reactive oxygen species and plant resistance to fungal pathogens. *Phytochemistry* 112, 54–62. doi:10.1016/j.phytochem.2014.08.027.

Lemli, J. (1965). Anthraquinones and dianthrones from Rhamnus frangula. *Lloydia* 28, 63–67.

Leubner-Metzger, G., and Amrhein, N. (1993). DIFFERENT ORGANS OF SOLANUM TUBEROSUM AND OTHER SOLANACEOUS SPECIES. *Phytochemistry* 32, 551–556.

Lewis, C. E., Walker, J. R. L., Lancaster, J. E., and Sutton, K. H. (1998). Determination of anthocyanins, flavonoids and phenolic acids in potatoes. I: Coloured cultivars of Solanum tuberosum L. *J. Sci. Food Agric.* 77, 45–57. doi:10.1002/(SICI)1097-0010(199805)77:1<45::AID-JSFA1>3.0.CO;2-S.

Li, J., Schuman, M. C., Halitschke, R., Li, X., Guo, H., Grabe, V., et al. (2018). The decoration of specialized metabolites influences stylar development. *eLife* 7, e38611. doi:10.7554/eLife.38611.

Li, X., Zhang, Y., Wei, Z., Guan, Z., Cai, Y., and Liao, X. (2016). Antifungal Activity of Isolated Bacillus amyloliquefaciens SYBC H47 for the Biocontrol of Peach Gummosis. *PLoS ONE* 11. doi:10.1371/journal.pone.0162125.

Li, Z.-J., Liu, M., Dawuti, G., Dou, Q., Ma, Y., Liu, H.-G., et al. (2017). Antifungal Activity of Gallic Acid In Vitro and In Vivo. *Phytother. Res. PTR* 31, 1039–1045. doi:10.1002/ptr.5823.

Liebrand, T. W. H., Berg, G. C. M. van den, Zhang, Z., Smit, P., Cordewener, J. H. G., America, A. H. P., et al. (2013). Receptor-like kinase SOBIR1/EVR interacts with receptor-like proteins in plant immunity against fungal infection. *Proc. Natl. Acad. Sci.* 110, 10010–10015. doi:10.1073/pnas.1220015110.

Lindner, K., Trautwein, F., Kellermann, A., and Bauch, G. (2015). Potato virus Y (PVY) in seed potato certification. *J. Plant Dis. Prot.* 122, 109–119.

Liu, Y., Gao, M., Luo, Q. Y., Zhang, Q., and He, W. M. (2015). Analysis on the basic situation and characteristics of world potatoes consumption. *World Agric.* 5, 119–124.

Lomin, S. N., Myakushina, Y. A., Kolachevskaya, O. O., Getman, I. A., Arkhipov, D. V., Savelieva, E. M., et al. (2018). Cytokinin perception in potato: new features of canonical players. *J. Exp. Bot.* 69, 3839–3853. doi:10.1093/jxb/ery199.

Lulai, E. C. (2007). "Skin-set, wound healing and related defects," in *Potato biology and biotechnology : advances and perspectives*, ed. D. Vreugdenhil (Amsterdam: Elsevier), 471–500.

Luttrell, E. S. (1964). Systematics of Helminthosporium and Related Genera. *Mycologia* 56, 119–132. doi:doi.org/10.1080/00275514.1964.12018090.

Ma, Y.-N., Chen, C.-J., Li, Q.-Q., Xu, F.-R., Cheng, Y.-X., and Dong, X. (2019). Monitoring Antifungal Agents of Artemisia annua against Fusarium oxysporum and Fusarium solani, Associated with Panax notoginseng Root-Rot Disease. *Mol. Basel Switz.* 24. doi:10.3390/molecules24010213.

Macoy, D. M., Kim, W.-Y., Lee, S. Y., and Kim, M. G. (2015). Biotic stress related functions of hydroxycinnamic acid amide in plants. *J. Plant Biol.* 58, 156–163. doi:10.1007/s12374-015-0104-y.

Magliano, T. M. A., and Kikot, G. E. (2010). Microscopy techniques to analyse plant-pathogen interaction: Fusarium graminearum as pathogen of wheat. 8.

Majeed, A., Ahmad, H., Chaudhry, Z., Jan, G., Alam, J., and Muhammad, Z. (2011). Assessment of leaf extracts of three medicinal plants against late blight of potato in Kaghan valley, Pakistan. *J. Agric. Technol.* 7, 1155–1161.

Malik A, A., and Ahmed, N. (2016). Plant Extracts in Post-Harvest Disease Management of Fruits and Vegetables-A Review. *J. Food Process. Technol.* 7. doi:10.4172/2157-7110.1000592.

Malmberg, A. G., and Theander, O. (1980). Two phytoalexin glycosides from potato tubers infected with Phoma. *Phytochemistry* 19, 1739–1742. doi:10.1016/S0031-9422(00)83805-4.

Manojlovic, N. T., Solujic, S., Sukdolak, S., and Milosev, M. (2005). Antifungal activity of Rubia tinctorum, Rhamnus frangula and Caloplaca cerina. *Fitoterapia* 76, 244–246. doi:10.1016/j.fitote.2004.12.002.

Mariot, R. F., de Oliveira, L. A., Voorhuijzen, M. M., Staats, M., Hutten, R. C. B., van Dijk, J. P., et al. (2016). Characterization and Transcriptional Profile of Genes Involved in Glycoalkaloid Biosynthesis in New Varieties of *Solanum tuberosum* L. *J. Agric. Food Chem.* 64, 988–996. doi:10.1021/acs.jafc.5b05519.

Marla, S. S. (2017). "Structural Analysis of Resistance (R) Genes in Potato (Solanum Species) Genome," in *The Potato Genome* Compendium of Plant Genomes., eds. S. Kumar Chakrabarti, C. Xie, and J. Kumar Tiwari (Cham: Springer International Publishing), 269–281. doi:10.1007/978-3-319-66135-3_14.

Marti, G., Schnee, S., Andrey, Y., Simoes-Pires, C., Carrupt, P.-A., Wolfender, J.-L., et al. (2014). Study of leaf metabolome modifications induced by UV-C radiations in representative Vitis, Cissus and Cannabis species by LC-MS based metabolomics and antioxidant assays. *Mol. Basel Switz.* 19, 14004–14021. doi:10.3390/molecules190914004.

Martinez, C., Michaud, M., Bélanger, R. R., and Tweddell, R. J. (2002). Identification of soils suppressive against Helminthosporium solani, the causal agent of potato silver scurf. *Soil Biol. Biochem.* 34, 1861–1868. doi:10.1016/S0038-0717(02)00199-2.

Martinez, C., Rioux, D., and Tweddell, R. J. (2004). Ultrastructure of the infection process of potato tuber by Helminthosporium solani, causal agent of potato silver scurf. *Mycol. Res.* 108, 828–836. doi:10.1017/s0953756204000589.

Martins, I., Hartmann, D. O., Alves, P. C., Martins, C., Garcia, H., Leclercq, C. C., et al. (2014). Elucidating how the saprophytic fungus Aspergillus nidulans uses the plant polyester suberin as carbon source. *BMC Genomics* 15, 613. doi:10.1186/1471-2164-15-613.

Mašković, P. Z., Mladenović, J. D., Cvijović, M. S., Aćamović-Đoković, G., Solujić, S. R., and Radojković, M. M. (2011). Phenolic content, antioxidant and antifungal activities of acetonic, ethanolic and petroleum ether extracts of Hypericum perforatum L. *Hem. Ind.* 65, 159–164.

Massana-Codina, J., Schnee, S., Allard, P.-M., Rutz, A., Boccard, J., Michellod, E., et al. (2020). Insights on the Structural and Metabolic Resistance of Potato (Solanum tuberosum) Cultivars to Tuber Black Dot (Colletotrichum coccodes). *Front. Plant Sci.* 11, 1287. doi:10.3389/fpls.2020.01287.

Matsuda, F., Morino, K., Ano, R., Kuzawa, M., Wakasa, K., and Miyagawa, H. (2005). Metabolic Flux Analysis of the Phenylpropanoid Pathway in Elicitor-treated Potato Tuber Tissue. *Plant Cell Physiol.* 46, 454–466. doi:10.1093/pcp/pci042.

Mattinen, M.-L., Filpponen, I., Järvinen, R., Li, B., Kallio, H., Lehtinen, P., et al. (2009). Structure of the Polyphenolic Component of Suberin Isolated from Potato (Solanum tuberosum var. Nikola). *J. Agric. Food Chem.* 57, 9747–9753. doi:10.1021/jf9020834.

Mellersh, D. G., Foulds, I. V., Higgins, V. J., and Heath, M. C. (2002). H2O2 plays different roles in determining penetration failure in three diverse plant–fungal interactions. *Plant J.* 29, 257–268. doi:10.1046/j.0960-7412.2001.01215.x.

Mérida, C. L., and Loria, R. (1994a). Comparison of thiabendazole-sensitive and -resistant Helminthosporium solani isolates from New York. *Plant Dis. USA*. Available at: http://agris.fao.org/agris-search/search.do?recordID=US9439171 [Accessed November 15, 2019].

Mérida, C. L., and Loria, R. (1994b). Survival of Helminthosporium solani in soil and in vitro colonization of senescent plant tissue. *Am. Potato J.* 71, 591–598. doi:10.1007/BF02851524.

Mérida, C. L., Loria, R., and Halseth, D. E. (1994). Effects of potato cultivar and time of harvest on the severity of silver scurf. *Plant Dis. USA*. Available at: http://agris.fao.org/agris-search/search.do?recordID=US9439142 [Accessed November 15, 2019].

Michaud, M., Martinez, C., Simao-Beaunoir, A.-M., Bélanger, R. R., and Tweddell, R. J. (2002). Selection of Antagonist Microorganisms Against Helminthosporium solani, Causal Agent of Potato Silver Scurf. *Plant Dis.* 86, 717–720. doi:10.1094/PDIS.2002.86.7.717.

Mikulič Petkovšek, M., Štampar, F., and Veberič, R. (2009). Accumulation of phenolic compounds in apple in response to infection by the scab pathogen, Venturia inaequalis. *Physiol. Mol. Plant Pathol.* 74, 60–67. doi:10.1016/j.pmpp.2009.09.003.

Mikulic-Petkovsek, M., Schmitzer, V., Jakopic, J., Cunja, V., Veberic, R., Munda, A., et al. (2013). Phenolic compounds as defence response of pepper fruits to Colletotrichum coccodes. *Physiol. Mol. Plant Pathol.* 84, 138–145. doi:10.1016/j.pmpp.2013.09.003.

Milbourne, D., Meyer, R. C., Collins, A. J., Ramsay, L. D., Gebhardt, C., and Waugh, R. (1998). Isolation, characterisation and mapping of simple sequence repeat loci in potato. *Mol. Gen. Genet. MGG* 259, 233–245. doi:10.1007/s004380050809.

Miller, J. S., Hamm, P. B., Dung, J. K. S., Geary, B. D., James, S. R., Johnson, D. A., et al. (2015). Influence of Location, Year, Potato Rotation, and Chemical Seed Treatment on Incidence and Severity of Silver Scurf on Progeny Tubers. *Am. J. Potato Res.* 92, 62–70. doi:10.1007/s12230-014-9412-x.

Miller, J. S., Hamm, P. B., Olsen, N., Geary, B. D., and Johnson, D. A. (2011). Effect of Post-Harvest Fungicides and Disinfestants on the Suppression of Silver Scurf on Potatoes in Storage. *Am. J. Potato Res.* 88, 413–423. doi:10.1007/s12230-011-9207-2.

Miller, J. S., Olsen, N., Woodell, L., Porter, L. D., and Clayson, S. (2006). Post-harvest applications of zoxamide and phosphite for control of potato tuber rots caused by oomycetes at harvest. *Am. J. Potato Res.* 83, 269–278. doi:10.1007/BF02872163.

Minker, K. R., Biedrzycki, M. L., Kolagunda, A., Rhein, S., Perina, F. J., Jacobs, S. S., et al. (2018). Semi-automated confocal imaging of fungal pathogenesis on plants: microscopic analysis of macroscopic specimens. *Microsc. Res. Tech.* 81, 141–152. doi:10.1002/jemt.22709.

Mohimani, H., Gurevich, A., Shlemov, A., Mikheenko, A., Korobeynikov, A., Cao, L., et al. (2018). Dereplication of microbial metabolites through database search of mass spectra. *Nat. Commun.* 9, 1–12. doi:10.1038/s41467-018-06082-8.

Moisan-Thiery, M., Marhadour, S., Kerlan, M. C., Dessenne, N., Perramant, M., Gokelaere, T., et al. (2005). Potato cultivar identification using simple sequence repeats markers (SSR). *Potato Res.* 48, 191–200. doi:10.1007/BF02742376.

Money, N. P. (2016). "Fungal Cell Biology and Development," in *The Fungi*, eds. S. C. Watkinson, L. Boddy, and N. P. Money (Boston: Academic Press), 37–66. doi:10.1016/B978-0-12-382034-1.00002-5.

Mooi, J. C. (1968). The silver scurf disease of the potato. *Meded. Van Het Instituute Voor Plantenzeiktenkundig Onderz.* 482, 1–62.

Mukherjee, A., and Patel, J. S. (2020). Seaweed extract: biostimulator of plant defense and plant productivity. *Int. J. Environ. Sci. Technol.* 17, 553–558. doi:10.1007/s13762-019-02442-z.

Mullis, K., Faloona, F., Scharf, S., Saiki, R., Horn, G., and Erlich, H. (1986). Specific enzymatic amplification of DNA in vitro: the polymerase chain reaction. *Cold Spring Harb. Symp. Quant. Biol.* 51 Pt 1, 263–273. doi:10.1101/sqb.1986.051.01.032.

Muroi, A., Ishihara, A., Tanaka, C., Ishizuka, A., Takabayashi, J., Miyoshi, H., et al. (2009). Accumulation of hydroxycinnamic acid amides induced by pathogen infection and identification of agmatine coumaroyltransferase in Arabidopsis thaliana. *Planta* 230, 517–527. doi:10.1007/s00425-009-0960-0.

Murphy, A. M., Jong, H. D., Proudfoot, K. G., and Proudfoot, K. G. (1999). A multiple disease resistant potato clone developed with classical breeding methodology. *Can. J. Plant Pathol.* 21, 207–212. doi:10.1080/07060669909501183.

Navarre, D. A., Pillai, S. S., Shakya, R., and Holden, M. J. (2011). HPLC profiling of phenolics in diverse potato genotypes. *Food Chem.* 127, 34–41. doi:10.1016/j.foodchem.2010.12.080.

Navarro-García, V. M., Rojas, G., Avilés, M., Fuentes, M., and Zepeda, G. (2011). In vitro antifungal activity of coumarin extracted from Loeselia mexicana Brand. *Mycoses* 54, e569-571. doi:10.1111/j.1439-0507.2010.01993.x.

Nawrath, C., and Métraux, J.-P. (1999). Salicylic Acid Induction–Deficient Mutants of Arabidopsis Express PR-2 and PR-5 and Accumulate High Levels of Camalexin after Pathogen Inoculation. *Plant Cell*, 1393–1404.

Negrel, J., Pollet, B., and Lapierre, C. (1996). Ether-linked ferulic acid amides in natural and wound periderms of potato tuber. *Phytochemistry* 43, 1195–1199. doi:10.1016/S0031-9422(96)00500-6.

Newlands, N. K. (2018). Model-Based Forecasting of Agricultural Crop Disease Risk at the Regional Scale, Integrating Airborne Inoculum, Environmental, and Satellite-Based Monitoring Data. *Front. Environ. Sci.* 6. doi:10.3389/fenvs.2018.00063.

Newman, D. J., and Cragg, G. M. (2012). Natural Products As Sources of New Drugs over the 30 Years from 1981 to 2010. *J. Nat. Prod.* 75, 311–335. doi:10.1021/np200906s.

Nguyen, X. H., Naing, K. W., Lee, Y. S., Moon, J. H., Lee, J. H., and Kim, K. Y. (2015). Isolation and characteristics of protocatechuic acid from Paenibacillus elgii HOA73 against Botrytis cinerea on strawberry fruits. *J. Basic Microbiol.* 55, 625–634. doi:10.1002/jobm.201400041.

Nicander, B., Bjorkman, P. O., and Tillberg, E. (1995). Identification of an N-Glucoside of cis-Zeatin from Potato Tuber Sprouts. *Plant Physiol.* 109, 513–516. doi:10.1104/pp.109.2.513.

Nitzan, N., Cummings, T. F., and Johnson, D. A. (2005). Effect of Seed-Tuber Generation, Soilborne Inoculum, and Azoxystrobin Application on Development of Potato Black Dot Caused by Colletotrichum coccodes. *Plant Dis.* 89, 1181–1185. doi:10.1094/PD-89-1181.

Nitzan, N., Cummings, T. F., and Johnson, D. A. (2008). Disease Potential of Soil- and Tuberborne Inocula of Colletotrichum coccodes and Black Dot Severity on Potato. *Plant Dis.* 92, 1497–1502. doi:10.1094/PDIS-92-11-1497.

Nitzan, N., Hazanovsky, M., Tal, M., and Tsror(Lahkim), L. (2002). Vegetative Compatibility Groups in *Colletotrichum coccodes* , the Causal Agent of Black Dot on Potato. *Phytopathology* 92, 827–832. doi:10.1094/PHYTO.2002.92.8.827.

Nitzan, N., and Lahkim, L. T. (2003). Effect of temperature and pH onin vitro growth rate and sclerotial density ofColletotrichum coccodes isolates from different VCGs. *Am. J. Potato Res.* 80, 335–339. doi:10.1007/BF02854318.

Nitzan, N., Tsror (Lahkim), L., and Johnson, D. A. (2006). Vegetative Compatibility Groups and Aggressiveness of North American Isolates of *Colletotrichum coccodes* , the Causal Agent of Potato Black Dot. *Plant Dis.* 90, 1287–1292. doi:10.1094/PD-90-1287.

Noble, M., Macgarvie, Q. D., Hams, A. F., and Leafe, E. L. (1966). Resistance to Mercury of Pyrenophora Avenae in Scottish Seed Oats. *Plant Pathol.* 15, 23–28. doi:10.1111/j.1365-3059.1966.tb00316.x.

Nothias, L. F., Petras, D., Schmid, R., Dührkop, K., Rainer, J., Sarvepalli, A., et al. (2019). Feature-based Molecular Networking in the GNPS Analysis Environment. Bioinformatics doi:10.1101/812404.

OFAG, O. fédéral de l'agriculture (2019a). Volumes de vente des substance actives de produits phytosanitaires par catégorie. Available at: https://www.blw.admin.ch/blw/fr/home/nachhaltige-produktion/pflanzenschutz/pflanzenschutzmittel/verkaufsmengen-der-pflanzenschutzmittel-wirkstoffe.html [Accessed April 1, 2020].

OFAG, O. fédéral de l'agriculture (2019b). Volumes de vente des substances actives de produits phytosanitaires par type d'utilisation. Available at: https://www.blw.admin.ch/blw/fr/home/nachhaltige-produktion/pflanzenschutz/pflanzenschutzmittel/verkaufsmengen-der-pflanzenschutzmittel-wirkstoffe.html [Accessed April 1, 2020].

Ogilvy, S. E. (1992). The use of pre-planting and post-harvest fungicides and storage temperatures for the control of silver scurf in ware potatoes. *Asp. Appl. Biol.* 33, 151–158.

Ojiambo, P. S., Paul, P. A., and Holmes, G. J. (2010). A Quantitative Review of Fungicide Efficacy for Managing Downy Mildew in Cucurbits. *Phytopathology®* 100, 1066–1076. doi:10.1094/PHYTO-12-09-0348.

Okhovat, M., and Zafari, D. (1996). Evaluation of antagonistic effects of trichoderma spp. on Colletotrichum coccodes (Wallr) hughes isolated from potato. *Iran. J. Plant Pathol.* Available at: http://agris.fao.org/agris-search/search.do?recordID=IR9700544 [Accessed February 20, 2020].

Olanya, O. M., Porter, G., and Lambert, D. (2010). Supplemental irrigation and cultivar effects on potato tuber diseases. *Aust. J. Crop Sci.* 4.

Olivier, C., Halseth, D. E., Mizubuti, E. S. G., and Loria, R. (1998). Postharvest Application of Organic and Inorganic Salts for Suppression of Silver Scurf on Potato Tubers. *Plant Dis.* 82, 213–217. doi:10.1094/PDIS.1998.82.2.213.

Olivier, C., and Loria, R. (1998). Detection of *Helminthosporium solani* from soil and plant tissue with species-specific PCR primers. *FEMS Microbiol. Lett.* 168, 235–241. doi:10.1111/j.1574-6968.1998.tb13279.x.

Olivier, C., MacNeil, C. R., and Loria, R. (1999). Application of Organic and Inorganic Salts to Field-Grown Potato Tubers Can Suppress Silver Scurf During Potato Storage. *Plant Dis.* 83, 814–818. doi:10.1094/PDIS.1999.83.9.814.

Ors, M. E., Randoux, B., Selim, S., Siah, A., Couleaud, G., Maumené, C., et al. (2018). Cultivar-dependent partial resistance and associated defence mechanisms in wheat against Zymoseptoria tritici. *Plant Pathol.* 67, 561–572. doi:10.1111/ppa.12760.

Palaniyandi, S. A., Yang, S. H., and Suh, J.-W. (2013). Extracellular proteases from Streptomyces phaeopurpureus ExPro138 inhibit spore adhesion, germination and appressorium formation in Colletotrichum coccodes. *J. Appl. Microbiol.* 115, 207–217. doi:10.1111/jam.12212.

Palhano, F. L., Vilches, T. T. B., Santos, R. B., Orlando, M. T. D., Ventura, J. A., and Fernandes, P. M. B. (2004). Inactivation of Colletotrichum gloeosporioides spores by high hydrostatic pressure combined with citral or lemongrass essential oil. *Int. J. Food Microbiol.* 95, 61–66. doi:10.1016/j.ijfoodmicro.2004.02.002.

Parr, A. J., Mellon, F. A., Colquhoun, I. J., and Davies, H. V. (2005). Dihydrocaffeoyl Polyamines (Kukoamine and Allies) in Potato (Solanum tuberosum) Tubers Detected during Metabolite Profiling. *J. Agric. Food Chem.* 53, 5461–5466. doi:10.1021/jf050298i.

Pasche, J. S., Taylor, R. J., and Gudmestad, N. C. (2010). Colonization of Potato by Colletotrichum coccodes: Effect of Soil Infestation and Seed Tuber and Foliar Inoculation. *Plant Dis.* 94, 905–914. doi:10.1094/PDIS-94-7-0905.

Patel, T. K., and Williamson, J. D. (2016). Mannitol in Plants, Fungi, and Plant-Fungal Interactions. *Trends Plant Sci.* 21, 486–497. doi:10.1016/j.tplants.2016.01.006.

Pearsall, D. M. (2008). "Plant Domestication and the Shift to Agriculture in the Andes," in *The Handbook of South American Archaeology*, eds. H. Silverman and W. H. Isbell (New York, NY: Springer), 105–120. doi:10.1007/978-0-387-74907-5_7.

Pedras, M. S. C., Zheng, Q.-A., and Strelkov, S. (2008). Metabolic Changes in Roots of the Oilseed Canola Infected with the Biotroph Plasmodiophora brassicae: Phytoalexins and Phytoanticipins. *J. Agric. Food Chem.* 56, 9949–9961. doi:10.1021/jf802192f.

Peeters, N., Guidot, A., Vailleau, F., and Valls, M. (2013). Ralstonia solanacearum, a widespread bacterial plant pathogen in the post-genomic era. *Mol. Plant Pathol.* 14, 651–662. doi:10.1111/mpp.12038.

Pereira, A. C., Oliveira, D. F., Silva, G. H., Figueiredo, H. C. P., Cavalheiro, A. J., Carvalho, D. A., et al. (2008). Identification of the antimicrobial substances produced by Solanum palinacanthum (Solanaceae). *An. Acad. Bras. Cienc.* 80, 427–432. doi:10.1590/s0001-37652008000300004.

Peters, J. C., Harper, G., Brierley, J. L., Lees, A. K., Wale, S. J., Hilton, A. J., et al. (2016). The effect of post-harvest storage conditions on the development of black dot (*Colletotrichum coccodes*) on potato in crops grown for different durations. *Plant Pathol.* 65, 1484–1491. doi:10.1111/ppa.12535.

Peters, R. D., Sturz, A. V., Carter, M. R., and Sanderson, J. B. (2003). Developing disease-suppressive soils through crop rotation and tillage management practices. *Soil Tillage Res.* 72, 181–192. doi:10.1016/S0167-1987(03)00087-4.

Peters, R. D., Sturz, A. V., Carter, M. R., and Sanderson, J. B. (2004). Influence of crop rotation and conservation tillage practices on the severity of soil-borne potato diseases in temperate humid agriculture. *Can. J. Soil Sci.* 84, 397–402. doi:10.4141/S03-060.

Peterson, R. L., Barker, W. G., and Howarth, M. J. (1985). "Development and Structure of Tubers," in *Potato Physiology*, ed. P. H. Li (Orlando: Elsevier), 124–153.

Petersson, E. V., Arif, U., Schulzova, V., Krtková, V., Hajšlová, J., Meijer, J., et al. (2013). Glycoalkaloid and Calystegine Levels in Table Potato Cultivars Subjected to Wounding, Light, and Heat Treatments. *J. Agric. Food Chem.* 61, 5893–5902. doi:10.1021/jf400318p.

Pinzón, A., Barreto, E., Bernal, A., Achenie, L., González Barrios, A. F., Isea, R., et al. (2009). Computational models in plant-pathogen interactions: the case of Phytophthora infestans. *Theor. Biol. Med. Model.* 6, 24. doi:10.1186/1742-4682-6-24.

Pluskal, T., Castillo, S., Villar-Briones, A., and Orešič, M. (2010). MZmine 2: Modular framework for processing, visualizing, and analyzing mass spectrometry-based molecular profile data. *BMC Bioinformatics* 11, 395. doi:10.1186/1471-2105-11-395.

Poiatti, V. A. D., Dalmas, F. R., and Astarita, L. V. (2009). Defense mechanisms of Solanum tuberosum L. in response to attack by plant-pathogenic bacteria. *Biol. Res.* 42, 205–215. doi:/S0716-97602009000200009.

Ponasik, J. A., Strickland, C., Faerman, C., Savvides, S., Karplus, P. A., and Ganem, B. (1995). Kukoamine A and other hydrophobic acylpolyamines: potent and selective inhibitors of

Crithidia fasciculata trypanothione reductase. *Biochem. J.* 311, 371–375. doi:10.1042/bj3110371.

Pringle, R. T., Hardy, C. E., Clayton, R., McGovern, R., and Potter, K. (1998). Chemical free storage of potatoes. *Scott. Agric. Coll. Inf. Bull.*

Pushpa, D., Yogendra, K. N., Gunnaiah, R., Kushalappa, A. C., and Murphy, A. (2014). Identification of Late Blight Resistance-Related Metabolites and Genes in Potato through Nontargeted Metabolomics. *Plant Mol. Biol. Report.* 32, 584–595. doi:10.1007/s11105-013-0665-1.

Queiroz, E. F., Alfattani, A., Afzan, A., Marcourt, L., Guillarme, D., and Wolfender, J.-L. (2019). Utility of dry load injection for an efficient natural products isolation at the semi-preparative chromatographic scale. *J. Chromatogr. A* 1598, 85–91. doi:10.1016/j.chroma.2019.03.042.

Queiroz, S. C. N., Cantrell, C. L., Duke, S. O., Wedge, D. E., Nandula, V. K., Moraes, R. M., et al. (2012). Bioassay-directed isolation and identification of phytotoxic and fungitoxic acetylenes from Conyza canadensis. *J. Agric. Food Chem.* 60, 5893–5898. doi:10.1021/jf3010367.

Radcliffe, E. B., and Lagnaoui, A. (2007). "Insect Pests in Potato," in *Potato Biology and Biotechnology*, eds. D. Vreugdenhil, J. Bradshaw, C. Gebhardt, F. Govers, D. K. L. Mackerron, M. A. Taylor, et al. (Amsterdam: Elsevier Science B.V.), 543–567. doi:10.1016/B978-044451018-1/50067-1.

Radwan, M. M., Tabanca, N., Wedge, D. E., Tarawneh, A. H., and Cutler, S. J. (2014). Antifungal compounds from turmeric and nutmeg with activity against plant pathogens. *Fitoterapia* 99, 341–346. doi:10.1016/j.fitote.2014.08.021.

Raheem, D. J., Tawfike, A. F., Abdelmohsen, U. R., Edrada-Ebel, R., and Fitzsimmons-Thoss, V. (2019). Application of metabolomics and molecular networking in investigating the chemical profile and antitrypanosomal activity of British bluebells (Hyacinthoides non-scripta). *Sci. Rep.* 9, 1–13. doi:10.1038/s41598-019-38940-w.

Rahman, M. M., Khan, A. A., Ali, M. E., Mian, I. H., Akanda, A. M., and Abd Hamid, S. B. (2012). Botanicals to Control Soft Rot Bacteria of Potato. *Sci. World J.* 2012. doi:10.1100/2012/796472.

Raid, R. N., and Pennypacker, S. P. (1987). Weeds as Hosts for Colletotrichum coccodes. *Plant Dis.* 71, 643. doi:10.1094/PD-71-0643.

Ramsay, G., Griffiths, D. W., and Deighton, N. (2005). Patterns of solanidine glycoalkaloid variation in four gene pools of the cultivated potato. *Genet. Resour. Crop Evol.* 51, 805–813. doi:10.1007/s10722-005-0004-y.

Ranasinghe, L., Jayawardena, B., and Abeywickrama, K. (2002). Fungicidal activity of essential oils of Cinnamomum zeylanicum (L.) and Syzygium aromaticum (L.) Merr et L.M.Perry against crown rot and anthracnose pathogens isolated from banana. *Lett. Appl. Microbiol.* 35, 208–211. doi:10.1046/j.1472-765X.2002.01165.x.

Read, N. D. (1991a). "Low-Temperature Scanning Electron Microscopy of Fungi and Fungus-Plant Interactions," in *Electron Microscopy of Plant Pathogens*, eds. K. Mendgen and D.-E. Lesemann (Berlin, Heidelberg: Springer), 17–29. doi:10.1007/978-3-642-75818-8_2.

Read, P. J. (1991b). The susceptibility of tubers of potato cultivars to black dot (Colletotrichum coccodes (Walk.) Hughes). *Ann. Appl. Biol.* 119, 475–482. doi:10.1111/j.1744-7348.1991.tb04887.x.

Read, P. J., and Hide, G. A. (1984). Effects of silver scurf (Helminthosporium solani) on seed potatoes. *Potato Res.* 27, 145–154. doi:10.1007/BF02357459.

Read, P. J., and Hide, G. A. (1988). Effects of inoculum source and irrigation on black dot disease of potatoes (Colletotrichum coccodes (Wallr.) Hughes) and its development during storage. *Potato Res.* 31, 493–500. doi:10.1007/BF02357887.

Read, P. J., and Hide, G. A. (1995a). Development of black dot disease (Colletotrichum coccodes (Wallr.) Hughes) and its effects on the growth and yield of potato plants. *Ann. Appl. Biol.* 127, 57–72. doi:10.1111/j.1744-7348.1995.tb06651.x.

Read, P. J., and Hide, G. A. (1995b). Effects of fungicides on the growth and conidial germination of Colletotrichum coccodes and on the development of black dot disease of potatoes. *Ann. Appl. Biol.* 126, 437–447. doi:10.1111/j.1744-7348.1995.tb05378.x.

Reeve, R. M., Hautala, E., and Weaver, M. L. (1969). Anatomy and compositional variation within potatoes. *Am. Potato J.* 46, 361–373. doi:10.1007/BF02869557.

Rennie, W. J., and Cokerell, V. (2006). "Seedborne diseases," in *The Epidemiology of Plant Diseases*, eds. B. M. COOKE, D. G. JONES, and B. KAYE (Dordrecht: Springer Netherlands), 357–372. doi:10.1007/1-4020-4581-6_13.

Ripperger, H. (1998). "Solanum Steroid Alkaloids - an Update," in *Alkaloids: Chemical and Biological Perspectives*, ed. S. W. Pelletier (Pergamon), 103–185. doi:10.1016/S0735-8210(98)80004-6.

Rodriguez, D. A. (North D. S. U., Secor, G. A., Gudmestad, N. C., and Francl, L. J. (1996). Sporulation of Helminthosporium solani and infection of potato tubers in seed and commercial storages. *Plant Dis. USA*. Available at: http://agris.fao.org/agris-search/search.do?recordID=US9632735 [Accessed November 15, 2019].

Rodriguez, D. A., Secor, G. A., Gudmestad, N. C., and Grafton, K. (1995). Screening tuber-bearing Solanum species for resistance to Helminthosporium solani. *Am. Potato J.* 72, 669–679. doi:10.1007/BF02849176.

Rodriguez-Salamanca, L. M., Enzenbacher, T. B., Derie, M. L., du Toit, L. J., Feng, C., Correll, J. C., et al. (2012). First Report of Colletotrichum coccodes Causing Leaf and Neck Anthracnose on Onions (Allium cepa) in Michigan and the United States. *Plant Dis.* 96, 769–769. doi:10.1094/PDIS-01-12-0022-PDN.

Russell, P. E. (1995). Fungicide resistance: occurrence and management. *J. Agric. Sci.* 124, 317–323. doi:10.1017/S0021859600073275.

Russell, P. E. (2005). A century of fungicide evolution. *J. Agric. Sci.* 143, 11–25. doi:10.1017/S0021859605004971.

Rutz, A., Dounoue-Kubo, M., Ollivier, S., Bisson, J., Bagheri, M., Saesong, T., et al. (2019). Taxonomically Informed Scoring Enhances Confidence in Natural Products Annotation. *Front. Plant Sci.* 10, 1329. doi:10.3389/fpls.2019.01329.

Safaeian, L., Emami, R., Hajhashemi, V., and Haghighatian, Z. (2018). Antihypertensive and antioxidant effects of protocatechuic acid in deoxycorticosterone acetate-salt hypertensive rats. *Biomed. Pharmacother. Biomedecine Pharmacother.* 100, 147–155. doi:10.1016/j.biopha.2018.01.107.

Saijo, Y., Loo, E. P., and Yasuda, S. (2018). Pattern recognition receptors and signaling in plant–microbe interactions. *Plant J.* 93, 592–613. doi:10.1111/tpj.13808.

Saks, Y., and Barkai-Golan, R. (1995). Aloe vera gel activity against plant pathogenic fungi. *Postharvest Biol. Technol.* 6, 159–165. doi:10.1016/0925-5214(94)00051-S.

Salazar, L. F. (1996). *Potato viruses and their control*. Lima (Peru): International Potato Center Available at: http://agris.fao.org/agris-search/search.do?recordID=QP9600002 [Accessed February 14, 2020].

Samain, E., Aussenac, T., and Selim, S. (2019). The Effect of Plant Genotype, Growth Stage, and Mycosphaerella graminicola Strains on the Efficiency and Durability of Wheat-Induced Resistance by Paenibacillus sp. Strain B2. *Front. Plant Sci.* 10. doi:10.3389/fpls.2019.00587.

Samborski, D. J., and Rohringer, R. (1970). Abnormal metabolites of wheat: Occurrence, isolation and biogenesis of 2-hydroxyputrescine amides. *Phytochemistry* 9, 1939–1945. doi:10.1016/S0031-9422(00)85343-1.

Sang, M. K., and Kim, K. D. (2011). Biocontrol Activity and Primed Systemic Resistance by Compost Water Extracts Against Anthracnoses of Pepper and Cucumber. 9.

Saunders, D. G. O., Breen, S., Win, J., Schornack, S., Hein, I., Bozkurt, T. O., et al. (2012). Host Protein BSL1 Associates with Phytophthora infestans RXLR Effector AVR2 and the Solanum demissum Immune Receptor R2 to Mediate Disease Resistance. *Plant Cell* 24, 3420–3434. doi:10.1105/tpc.112.099861.

Schauer, N., and Fernie, A. R. (2006). Plant metabolomics: towards biological function and mechanism. *Trends Plant Sci.* 11, 508–516. doi:10.1016/j.tplants.2006.08.007.

Schieber, A., and Saldaña, M. D. A. (2008). Potato Peels: A Source of Nutritionally and Pharmacologically Interesting Compounds – A Review. *Food* 3, 23–29.

Schlaeppi, K., and Mauch, F. (2010). Indolic secondary metabolites protect Arabidopsis from the oomycete pathogen Phytophthora brassicae. *Plant Signal. Behav.* 5, 1099–1101. doi:10.4161/psb.5.9.12410.

Schmidt, A., Grimm, R., Schmidt, J., Scheel, D., Strack, D., and Rosahl, S. (1999). Cloning and expression of a potato cDNA encoding hydroxycinnamoyl-CoA:tyramine N-(hydroxycinnamoyl)transferase. *J. Biol. Chem.* 274, 4273–4280. doi:10.1074/jbc.274.7.4273.

Schmidt, A., Scheel, D., and Strack, D. (1998). Elicitor-stimulated biosynthesis of hydroxycinnamoyltyramines in cell suspension cultures of Solanum tuberosum. *Planta* 205, 51–55. doi:10.1007/s004250050295.

Schnee, S., Queiroz, E. F., Voinesco, F., Marcourt, L., Dubuis, P.-H., Wolfender, J.-L., et al. (2013). *Vitis vinifera* Canes, a New Source of Antifungal Compounds against *Plasmopara viticola, Erysiphe necator* , and *Botrytis cinerea*. *J. Agric. Food Chem.* 61, 5459–5467. doi:10.1021/jf4010252.

Schreiber, L., Franke, R., and Hartmann, K. (2005). Wax and suberin development of native and wound periderm of potato (Solanum tuberosum L.) and its relation to peridermal transpiration. *Planta* 220, 520–530. doi:10.1007/s00425-004-1364-9.

Schymanski, E. L., Jeon, J., Gulde, R., Fenner, K., Ruff, M., Singer, H. P., et al. (2014). Identifying Small Molecules via High Resolution Mass Spectrometry: Communicating Confidence. *Environ. Sci. Technol.* 48, 2097–2098. doi:10.1021/es5002105.

Secor, G. A. (1994). "Management strategies for fungal diseases of tubers," in *Advances in Potato Pest Biology and Management*, eds. G. W. Zhender, M. L. Powelson, R. K. Jansson, and K. V. Raman (St. Paul, USA: American Phytopathological Society Press,), 155–7.

Secor, G. A., and Gudmestad, N. C. (1999). Managing fungal diseases of potato. *Can. J. Plant Pathol.* 21, 213–221. doi:10.1080/07060669909501184.

Sedláková, V., Dejmalová, J., Doležal, P., Hausvater, E., Sedlák, P., and Baštová, P. (2013). Characterization of forty-four potato varieties for resistance to common scab, black scurf and silver scurf. *Crop Prot.* 48, 82–87. doi:10.1016/j.cropro.2013.02.014.

Shabana, Y. M., Abdalla, M. E., Shahin, A. A., El-Sawy, M. M., Draz, I. S., and Youssif, A. W. (2017). Efficacy of plant extracts in controlling wheat leaf rust disease caused by Puccinia triticina. *Egypt. J. Basic Appl. Sci.* 4, 67–73. doi:10.1016/j.ejbas.2016.09.002.

Shannon, P., Markiel, A., Ozier, O., Baliga, N. S., Wang, J. T., Ramage, D., et al. (2003). Cytoscape: A Software Environment for Integrated Models of Biomolecular Interaction Networks. *Genome Res.* 13, 2498–2504. doi:10.1101/gr.1239303.

Shcolnick, S., Dinoor, A., and Tsror (Lahkim), L. (2007). Additional Vegetative Compatibility Groups in *Colletotrichum coccodes* Subpopulations from Europe and Israel. *Plant Dis.* 91, 805–808. doi:10.1094/PDIS-91-7-0805.

Silva, R. R. da, Wang, M., Nothias, L.-F., Hooft, J. J. J. van der, Caraballo-Rodríguez, A. M., Fox, E., et al. (2018). Propagating annotations of molecular networks using in silico fragmentation. *PLOS Comput. Biol.* 14, e1006089. doi:10.1371/journal.pcbi.1006089.

Slusarenko, A. J., Patel, A., and Portz, D. (2008). Control of plant diseases by natural products: Allicin from garlic as a case study. *Eur. J. Plant Pathol.* 121, 313–322. doi:10.1007/s10658-007-9232-7.

Smith, D. B., Roddick, J. G., and Jones, J. L. (1996). Potato glycoalkaloids: Some unanswered questions. *Trends Food Sci. Technol.* 7, 126–131. doi:10.1016/0924-2244(96)10013-3.

Smith, O. E., and Palmer, C. E. (1969). Cytokinins and Tuber Initiation in the Potato Solanum tuberosum L. *Nature* 221, 279–280.

Smith, O. E., and Palmer, C. E. (1970). Cytokinin-cytokinin-Induced tuber formation Tuber Formation on Stolons of Solanum tuberosum. *Physiol. Plant.* 23, 599–606. doi:10.1111/j.1399-3054.1970.tb06452.x.

Spooner, D. M., McLean, K., Ramsay, G., Waugh, R., and Bryan, G. J. (2005). A single domestication for potato based on multilocus amplified fragment length polymorphism genotyping. *Proc. Natl. Acad. Sci.* 102, 14694–14699. doi:10.1073/pnas.0507400102.

Stead, D. (1999). Bacterial diseases of potato: relevance to in vitro potato seed production. *Potato Res.* 42, 449–456. doi:10.1007/BF02358161.

Steckel, J. R. A., and Gray, D. (1979). Drought tolerance in potatoes. *J. Agric. Sci.* 92, 375–381. doi:10.1017/S0021859600062900.

Stockwell, V. O., and Stack, J. P. (2007). Using Pseudomonas spp. for Integrated Biological Control. *Phytopathology* 97, 244–249. doi:10.1094/PHYTO-97-2-0244.

Strange, R. N., and Scott, P. R. (2005). Plant Disease: A Threat to Global Food Security. *Annu. Rev. Phytopathol.* 43, 83–116. doi:10.1146/annurev.phyto.43.113004.133839.

Stringlis, I. A., de Jonge, R., and Pieterse, C. M. J. (2019). The Age of Coumarins in Plant–Microbe Interactions. *Plant Cell Physiol.* 60, 1405–1419. doi:10.1093/pcp/pcz076.

Struck, C. (2006). "Infection strategies of plant parasitic fungi," in *The Epidemiology of Plant Diseases*, eds. B. M. COOKE, D. G. JONES, and B. KAYE (Dordrecht: Springer Netherlands), 117–137. doi:10.1007/1-4020-4581-6_4.

Struik, P. C. (2007). "Above-ground and below-ground plant development," in *Potato biology and biotechnology : advances and perspectives*, ed. D. Vreugdenhil (Amsterdam: Elsevier), 219–236. Available at: https://library.wur.nl/WebQuery/wurpubs/357509 [Accessed November 25, 2019].

Sun, H., Wang, L., Zhang, B., Ma, J., Hettenhausen, C., Cao, G., et al. (2014). Scopoletin is a phytoalexin against Alternaria alternata in wild tobacco dependent on jasmonate signalling. *J. Exp. Bot.* 65, 4305–4315. doi:10.1093/jxb/eru203.

Sutton, B. C. (1992). "The genus Glomerella and its anamorph Colletotrichum," in *Colletotrichum: Biology, Pathology and Control*, eds. J. A. Bailey and M. J. Jeger (Wallingford, UK: CAB International), 1–26.

Tai, H. H., Worrall, K., Pelletier, Y., De Koeyer, D., and Calhoun, L. A. (2014). Comparative Metabolite Profiling of *Solanum tuberosum* against Six Wild *Solanum* Species with Colorado Potato Beetle Resistance. *J. Agric. Food Chem.* 62, 9043–9055. doi:10.1021/jf502508y.

Takahashi, T., and Kakehi, J.-I. (2010). Polyamines: ubiquitous polycations with unique roles in growth and stress responses. *Ann. Bot.* 105, 1–6. doi:10.1093/aob/mcp259.

Tan, M. Y. A., Hutten, R. C. B., Celis, C., Park, T.-H., Niks, R. E., Visser, R. G. F., et al. (2008). The RPi-mcd1 Locus from Solanum microdontum Involved in Resistance to Phytophthora infestans, Causing a Delay in Infection, Maps on Potato Chromosome 4 in a Cluster of NBS-LRR Genes. *Mol. Plant-Microbe Interactions®* 21, 909–918. doi:10.1094/MPMI-21-7-0909.

Teichert, A., Lübken, T., Schmidt, J., Porzel, A., Arnold, N., and Wessjohann, L. (2005). Unusual Bioactive 4-Oxo-2-alkenoic Fatty Acids from Hygrophorus eburneus. *Z. Für Naturforschung B* 60, 25–32. doi:10.1515/znb-2005-0105.

Tejeda, L., Alvarado, J. A., Dębiec, M., Peñarrieta, J. M., Cárdenas, O., Alvarez, M. T., et al. (2014). Relating genes in the biosynthesis of the polyphenol composition of Andean colored potato collection. *Food Sci. Nutr.* 2, 46–57. doi:10.1002/fsn3.69.

Termorshuizen, A. J. (2007). “Fungal and Fungus-Like Pathogens of Potato,” in *Potato Biology and Biotechnology*, eds. D. Vreugdenhil, J. Bradshaw, C. Gebhardt, F. Govers, D. K. L. Mackerron, M. A. Taylor, et al. (Amsterdam: Elsevier Science B.V.), 643–665. doi:10.1016/B978-044451018-1/50071-3.

Thangavel, T., Steven Tegg, R., and Wilson, C. R. (2014). Resistance to Multiple Tuber Diseases Expressed in Somaclonal Variants of the Potato Cultivar Russet Burbank. *Sci. World J.* 2014, 1–8. doi:10.1155/2014/417697.

Thangavel, T., Tegg, R. S., and Wilson, C. R. (2016). Toughing It Out—Disease-Resistant Potato Mutants Have Enhanced Tuber Skin Defenses. *Phytopathology* 106, 474–483. doi:10.1094/PHYTO-08-15-0191-R.

Thobunluepop, P. (2009). Implementation of bio-fungicides and seed treatment in organic rice cv. KDML 105 farming. *Pak. J. Biol. Sci.* 12, 1119–26. doi:10.3923/pjbs.2009.1119.1126.

Thomma, B. P. H. J., Nürnberger, T., and Joosten, M. H. A. J. (2011). Of PAMPs and Effectors: The Blurred PTI-ETI Dichotomy. *Plant Cell* 23, 4–15. doi:10.1105/tpc.110.082602.

Tomita, S., Ikeda, S., Tsuda, S., Someya, N., Asano, K., Kikuchi, J., et al. (2017). A survey of metabolic changes in potato leaves by NMR-based metabolic profiling in relation to resistance to late blight disease under field conditions: NMR metabolic profiling for predicting potato late blight resistance. *Magn. Reson. Chem.* 55, 120–127. doi:10.1002/mrc.4506.

Torrance, L., Cowan, G. H., McLean, K., MacFarlane, S., Al-Abedy, A. N., Armstrong, M., et al. (2020). Natural resistance to Potato virus Y in Solanum tuberosum Group Phureja. *Theor. Appl. Genet.* doi:10.1007/s00122-019-03521-y.

Torres, M. A. (2010). ROS in biotic interactions. *Physiol. Plant.* 138, 414–429. doi:10.1111/j.1399-3054.2009.01326.x.

Tripathi, P., Dubey, N. K., and Shukla, A. K. (2008). Use of some essential oils as post-harvest botanical fungicides in the management of grey mould of grapes caused by Botrytis cinerea. *World J. Microbiol. Biotechnol.* 24, 39–46. doi:10.1007/s11274-007-9435-2.

Tsror (Lahkim), L., Erlich, O., and Hazanovsky, M. (1999). Effect of *Colletotrichum coccodes* on Potato Yield, Tuber Quality, and Stem Colonization During Spring and Autumn. *Plant Dis.* 83, 561–565. doi:10.1094/PDIS.1999.83.6.561.

Tsror (Lahkim), L., and Peretz-Alon, I. (2004). Control of silver scurf on potato by dusting or spraying seed tubers with fungicides before planting. *Am. J. Potato Res.* 81, 291–294. doi:10.1007/BF02871771.

Turnbull, D., Yang, L., Naqvi, S., Breen, S., Welsh, L., Stephens, J., et al. (2017). RXLR Effector AVR2 Up-Regulates a Brassinosteroid-Responsive bHLH Transcription Factor to Suppress Immunity. *Plant Physiol.* 174, 356–369. doi:10.1104/pp.16.01804.

Turóczi, B., Bakonyi, J., Szabó, K.-A., Bálint, J., Máthé, I., Lányi, S., et al. (2020). In Vitro and In Vivo Effect of Poplar Bud Extracts on Phytophthora infestans: A New Effective Biological Method in Potato Late Blight Control. *Plants* 9, 217. doi:10.3390/plants9020217.

Tzortzakis, N. G., and Economakis, C. D. (2007). Antifungal activity of lemongrass (Cympopogon citratus L.) essential oil against key postharvest pathogens. *Innov. Food Sci. Emerg. Technol.* 8, 253–258. doi:10.1016/j.ifset.2007.01.002.

Valkonen, J. P. T., Keskitalo, M., Vasara, T., Pietilä, L., and Raman, D. K. V. (1996). Potato Glycoalkaloids: A Burden or a Blessing? *Crit. Rev. Plant Sci.* 15, 1–20. doi:10.1080/07352689609701934.

van den Berg, A. J., and Labadie, R. P. (1984). Anthraquinones, Anthrones and Dianthrones in Callus Cultures of Rhamnus frangula and Rhamnus purshiana. *Planta Med.* 50, 449–451. doi:10.1055/s-2007-969765.

van der Burgh, A. M., and Joosten, M. H. A. J. (2019). Plant Immunity: Thinking Outside and Inside the Box. *Trends Plant Sci.* 24, 587–601. doi:10.1016/j.tplants.2019.04.009.

Vaughn, S. F., and Lulai, E. C. (1991). The involvement of mechanical barriers in the resistance response of a field-resistant and a field-susceptible potato cultivar to Verticillium dahliae. *Physiol. Mol. Plant Pathol.* 38, 455–465. doi:10.1016/S0885-5765(05)80113-4.

Verpoorte, R. (2000). "Secondary Metabolism," in *Metabolic Engineering of Plant Secondary Metabolism*, eds. R. Verpoorte and A. W. Alfermann (Dordrecht: Springer Netherlands), 1–29. doi:10.1007/978-94-015-9423-3_1.

Vinale, F., Manganiello, G., Nigro, M., Mazzei, P., Piccolo, A., Pascale, A., et al. (2014). A Novel Fungal Metabolite with Beneficial Properties for Agricultural Applications. *Molecules* 19, 9760–9772. doi:10.3390/molecules19079760.

Viswanath, H. S., Bhat, K. A., Bhat, N. A., Wani, T. A., and Mughal, M. N. (2018). Antibacterial Efficacy of Aqueous Plant Extracts against Storage Soft Rot of Potato Caused by Erwinia carotovora. *Int. J. Curr. Microbiol. Appl. Sci.* 7, 2630–2639. doi:10.20546/ijcmas.2018.701.314.

Vos, J., and Biemond, H. (1992). Effects of Nitrogen on the Development and Growth of the Potato Plant. 1. Leaf Appearance, Expansion Growth, Life Spans of Leaves and Stem Branching. *Ann. Bot.* 70, 27–35. doi:10.1093/oxfordjournals.aob.a088435.

Vreugdenhil, D., Xu, X., Jung, C. S., van LAMMEREN, A. a. M., and Ewing, E. E. (1999). Initial Anatomical Changes Associated with Tuber Formation on Single-node Potato (Solanum tuberosum L.) Cuttings: A Re-evaluation. *Ann. Bot.* 84, 675–680. doi:10.1006/anbo.1999.0950.

Vulavala, V. K. R., Fogelman, E., Faigenboim, A., Shoseyov, O., and Ginzberg, I. (2019). The transcriptome of potato tuber phellogen reveals cellular functions of cork cambium and genes involved in periderm formation and maturation. *Sci. Rep.* 9, 10216. doi:10.1038/s41598-019-46681-z.

Vulavala, V. K. R., Fogelman, E., Rozental, L., Faigenboim, A., Tanami, Z., Shoseyov, O., et al. (2017). Identification of genes related to skin development in potato. *Plant Mol. Biol.* 94, 481–494. doi:10.1007/s11103-017-0619-3.

Wagner, H., and Demuth, G. (1972). 76-O-(d-Apiofuranosyl)-1,6,8-Trihydroxy-3-Methylanthraquinone, New Glycoside (frangulin B) from Bark of Rhamnus-Frangula L. *Tetrahedron Lett.*, 5013-.

Wagner, H., and Demuth, G. (1974). [Investigations of the anthrachinone-glycosides from Rhamnus frangula L. 3. 6-O (D-apiofuranosyl)-1,6,8-trihydroxy-3-methyl-anthrachinone, a new glycoside (frangulin B) from the bark of Rhamnus frangula L (author's transl)]. *Z. Naturforsch. [C]* 29, 204–208.

Wallroth, C. F. W. (1833). *Flora Cryptogamica Germaniae*. Nürnberg (Germany): J.L. Schrag.

Walters, D. R. (2003). Polyamines and plant disease. *Phytochemistry* 64, 97–107. doi:10.1016/s0031-9422(03)00329-7.

Wang, M., Carver, J. J., Phelan, V. V., Sanchez, L. M., Garg, N., Peng, Y., et al. (2016). Sharing and community curation of mass spectrometry data with Global Natural Products Social Molecular Networking. *Nat. Biotechnol.* 34, 828–837. doi:10.1038/nbt.3597.

Wang, S., Hu, T., Zhang, F., Forrer, H. R., and Cao, K. (2007). Screening for plant extracts to control potato late blight. *Front. Agric. China* 1, 43–46. doi:10.1007/s11703-007-0007-x.

Wang, W., Tian, S., and Stark, R. E. (2010). Isolation and Identification of Triglycerides and Ester Oligomers from Partial Degradation of Potato Suberin. *J. Agric. Food Chem.* 58, 1040–1045. doi:10.1021/jf902854y.

Watrous, J., Roach, P., Alexandrov, T., Heath, B. S., Yang, J. Y., Kersten, R. D., et al. (2012). Mass spectral molecular networking of living microbial colonies. *Proc. Natl. Acad. Sci.* 109, E1743–E1752. doi:10.1073/pnas.1203689109.

Webster, D., Taschereau, P., Belland, R. J., Sand, C., and Rennie, R. P. (2008). Antifungal activity of medicinal plant extracts; preliminary screening studies. *J. Ethnopharmacol.* 115, 140–146. doi:10.1016/j.jep.2007.09.014.

Whitworth, J. L., Nolte, P., McIntosh, C., and Davidson, R. (2006). Effect of Potato virus Y on Yield of Three Potato Cultivars Grown Under Different Nitrogen Levels. *Plant Dis.* 90, 73–76. doi:10.1094/PD-90-0073.

Wolfender, J.-L., Nuzillard, J.-M., van der Hooft, J. J. J., Renault, J.-H., and Bertrand, S. (2019). Accelerating Metabolite Identification in Natural Product Research: Toward an Ideal Combination of Liquid Chromatography–High-Resolution Tandem Mass Spectrometry and NMR Profiling, in Silico Databases, and Chemometrics. *Anal. Chem.* 91, 704–742. doi:10.1021/acs.analchem.8b05112.

Wolfender, J.-L., Rudaz, S., Choi, Y. H., and Kim, H. K. (2013). Plant metabolomics: from holistic data to relevant biomarkers. *Curr. Med. Chem.* 20, 1056–1090.

Xu, X., AA, van, Vermeer, E., and Vreugdenhil, D. (1998a). The Role of Gibberellin, Abscisic Acid, and Sucrose in the Regulation of Potato Tuber Formation in Vitro. *Plant Physiol.* 117, 575–84.

Xu, X., Vreugdenhil, D., and Lammeren, A. A. M. van (1998b). Cell division and cell enlargement during potato tuber formation. *J. Exp. Bot.* 49, 573–582. doi:10.1093/jxb/49.320.573.

Yaakoubi, H., Hamdani, S., Bekalé, L., and Carpentier, R. (2014). Protective Action of Spermine and Spermidine against Photoinhibition of Photosystem I in Isolated Thylakoid Membranes. *PLoS ONE* 9. doi:10.1371/journal.pone.0112893.

Yaganza, E.-S., Arul, J., and Tweddell, R. J. (2003). Effect of pre-storage application of different organic and inorganic salts on stored potato quality. *Potato Res.* 46, 167–178. doi:10.1007/BF02736086.

Yalpani, N., Leon, J., Lawton, M. A., and Raskin, I. (1993). Pathway of Salicylic Acid Biosynthesis in Healthy and Virus-Inoculated Tobacco. *Plant Physiol.* 103, 315–321. doi:10.1104/pp.103.2.315.

Yang, J., Yan, Z., Ren, J., Dai, Z., Ma, S., Wang, A., et al. (2018a). Polygonumnolides A1–B3, minor dianthrone derivatives from the roots of Polygonum multiflorum Thunb. *Arch. Pharm. Res.* 41, 617–624. doi:10.1007/s12272-016-0816-7.

Yang, L., Ding, W., Xu, Y., Wu, D., Li, S., Chen, J., et al. (2016). New Insights into the Antibacterial Activity of Hydroxycoumarins against Ralstonia solanacearum. *Molecules* 21, 468. doi:10.3390/molecules21040468.

Yang, L., Wu, L., Yao, X., Zhao, S., Wang, J., Li, S., et al. (2018b). Hydroxycoumarins: New, effective plant-derived compounds reduce Ralstonia pseudosolanacearum populations and control tobacco bacterial wilt. *Microbiol. Res.* 215, 15–21. doi:10.1016/j.micres.2018.05.011.

Yang, X., Ma, X., Yang, L., Yu, D., Qian, Y., and Ni, H. (2009). Efficacy of Rheum officinale liquid formulation on cucumber powdery mildew. *Crop Prot.* 28, 1031–1035. doi:10.1016/j.cropro.2009.08.004.

Yoder, O. C., and Turgeon, B. G. (2001). Fungal genomics and pathogenicity. *Curr. Opin. Plant Biol.* 4, 315–321. doi:10.1016/S1369-5266(00)00179-5.

Yogendra, K. N., Kushalappa, A. C., Sarmiento, F., Rodriguez, E., and Mosquera, T. (2015). Metabolomics deciphers quantitative resistance mechanisms in diploid potato clones against late blight. *Funct. Plant Biol.* 42, 284. doi:10.1071/FP14177.

Yogendra, K. N., Pushpa, D., Mosa, K. A., Kushalappa, A. C., Murphy, A., and Mosquera, T. (2014). Quantitative resistance in potato leaves to late blight associated with induced hydroxycinnamic acid amides. *Funct. Integr. Genomics* 14, 285–298. doi:10.1007/s10142-013-0358-8.

Yu, M.-H., Zhao, Z.-Z., and He, J.-X. (2018). Brassinosteroid Signaling in Plant–Microbe Interactions. *Int. J. Mol. Sci.* 19. doi:10.3390/ijms19124091.

Zeyen, R. J. (1991). "Analytical Electron Microscopy in Plant Pathology: X-Ray Microanalysis and Energy Loss Spectroscopy," in *Electron Microscopy of Plant Pathogens*, eds. K. Mendgen and D.-E. Lesemann (Berlin, Heidelberg: Springer), 59–71. doi:10.1007/978-3-642-75818-8_5.

Zhang, D., Lu, Y., Chen, H., Wu, C., Zhang, H., Chen, L., et al. (2020). Antifungal peptides produced by actinomycetes and their biological activities against plant diseases. *J. Antibiot. (Tokyo)*, 1–18. doi:10.1038/s41429-020-0287-4.

Zhang, W., Ye, M., Zhan, J., Chen, Y., and Guo, D. (2004). Microbial glycosylation of four free anthraquinones by Absidia coerulea. *Biotechnol. Lett.* 26, 127–131. doi:10.1023/b:bile.0000012890.46665.02.

Zhou, S., Allard, P.-M., Wolfrum, C., Ke, C., Tang, C., Ye, Y., et al. (2019). Identification of chemotypes in bitter melon by metabolomics: a plant with potential benefit for management of diabetes in traditional Chinese medicine. *Metabolomics* 15, 104. doi:10.1007/s11306-019-1565-7.

Zhu, S., Li, Y., Vossen, J. H., Visser, R. G. F., and Jacobsen, E. (2012). Functional stacking of three resistance genes against Phytophthora infestans in potato. *Transgenic Res.* 21, 89–99. doi:10.1007/s11248-011-9510-1.

Zuluaga, A. P., Solé, M., Lu, H., Góngora-Castillo, E., Vaillancourt, B., Coll, N., et al. (2015). Transcriptome responses to Ralstonia solanacearum infection in the roots of the wild potato Solanum commersonii. *BMC Genomics* 16. doi:10.1186/s12864-015-1460-1.

Remerciements

J’aimerais remercier La Commission pour la technologie et l'innovation CTI Suisse, qui a financé ce projet. Spécifiquement, Dr. Stéphanie Schürch et Dr. Brice Dupuis à Agroscope, mais aussi Dr. Andreas Keiser à HAFL, pour avoir conçu, préparé et supervisé le projet collaboratif “Integrierte Bekämpfung von Colletotrichum coccodes und Helminthosporium solani in der Kartoffelwirtschaft”.

Le travail présenté dans cette thèse qui fait partie du projet cité ci-dessus, est un véritable projet collaboratif, dans lequel plusieurs personnes ont eu un rôle important : je tiens à remercier le groupe d'Andreas Keiser à HAFL pour avoir effectué les analyses qPCR sur des échantillons de sol et leurs idées et commentaires sur le projet lui-même et la rédaction d'un des articles. Je tiens également à remercier Marilyn Cléroux, de la Haute Ecole de Viticulture et Oenologie de Changins, qui m'a aidé avec l'analyse de la subérine par GC. Cette thèse n'aurait pas pu se faire sans la production, la récolte et le stockage des pommes de terre sur le terrain. Je remercie donc tout le groupe de recherche travaillant sur la pomme de terre (groupe de Variétés et techniques culturales) d’Agroscope, dirigé par Brice Dupuis. Je tenais aussi à remercier tout le groupe de Phytochimie et Produits Naturels Bioactifs de l’Université de Genève, qui m’ont accueilli à bras ouverts à chaque fois que j’avais besoin de leur laboratoire ou de leur expertise. J’aimerais également remercier tout particulièrement tout le groupe de Mycologie et Biotechnologie d’Agroscope à Changins : Nicole, Emilie, Francine, Anne-Lise, Pierre-Henri, Aurélie, Jean-Pierre, Corinne et Susete pour leur aide aux taxations, au laboratoire et spécialement pour leur soutien pendant toute la thèse. Je remercie tout particulièrement Stéphanie, qui a toujours été une référence pour le projet dans sa globalité. Finalement, j’aimerais remercier Sylvain Schnee, qui s’est toujours pris le temps pour m’apprendre une procédure, discuter des réactions hôte-pathogène des plantes ou encore pour parler de la performance de Griezmann au sein du FC Barcelona.

Je voudrais terminer en remerciant les membres du Jury, pour leurs bons commentaires et suggestions déjà lors du Thesis Advisory Committee à la fin de la première année de Thèse. Je voudrais également remercier tout particulièrement le directeur de ma thèse, le professeur Jean-Luc Wolfender, pour son aide, son soutien et pour avoir su garder la vision d’ensemble dans toutes les situations. Enfin et surtout, j’aimerais remercier ma co-directrice de thèse, Dr. Katia Gindro, pour son soutien inconditionnel, sa confiance en mon travail et son implication dans le projet.